
**THE ROLE OF CANONICAL WNT SIGNALLING IN NORMAL
HAEMATOPOIESIS AND IN ACUTE MYELOID LEUKAEMIA**

A thesis submitted to Cardiff University in candidature
for the degree of Doctor of Philosophy



Adam Matthew Leckenby

Department of Haematology,
Division of Cancer and Genetics,
School of Medicine,
Cardiff University
September 2022

ABSTRACT

Acute myeloid leukaemia (AML) is a heterogeneous haematological malignancy which presents with the clonal expansion of immature myeloid lineage cells that are incapable of terminal differentiation. AML cells accumulate, resulting in a dysfunctional bone marrow. Induction chemotherapy is often applied as a treatment, but relapse of AML is frequent, possibly due to a quiescent population of leukaemic stem cells.

WNT/ β -catenin signalling is critical to normal developmental processes in adults. Without an external WNT agonist, the pathway remains in a state of active suppression through constitutive degradation of the central mediator, β -catenin (*CTNNB1*). When stimulated, the destruction complex becomes disrupted and stabilised β -catenin translocates to the nucleus. Here, β -catenin binds transcription factors of the TCF family which form a transcription complex promoting the expression of target genes involved in cell proliferation and other roles. WNT/ β -catenin signalling is active in haematopoiesis, with WNT genes influencing proliferation and differentiation.

Self-renewal is a fundamental characteristic of haematopoietic stem cells and leukaemic stem cells. WNT/ β -catenin signalling represents an important pathway for roles in disease onset and progression as it can confer self-renewal, proliferative, and survival effects. β -catenin is found to be overexpressed in approximately 60% of AML patients, regardless of genotype. Further, it has been shown to be a good prognostic marker for poor prognosis patients. *In vitro* studies in cell lines suggest that β -catenin enhances proliferation whilst decreasing apoptosis and differentiation, though *in vitro* studies in primary haematopoietic cells have failed to reproduce this. A close homolog, γ -catenin, is also overexpressed in AML. Directly, γ -catenin has the capacity to induce *TCF*-dependent transcription in some contexts. γ -catenin may also indirectly promote *TCF*-dependent transcription through β -catenin stabilisation as a consequence of destruction complex saturation. If β -catenin is critical to AML maintenance or leukaemic stem cell self-renewal, it would represent an attractive induction or maintenance therapeutic target.

By utilising CRISPR-Cas9 to derive complete knockout clones, this study has revealed that β -catenin is dispensable for normal haematopoietic functions. Deletion of β -catenin and γ -catenin had no consequence for AML maintenance, sensitivity to standard chemotherapeutics, or differentiation status; however, knockout of β -catenin was incompatible with clonal expansion in AML cell lines with active WNT/ β -catenin signalling and in primary AML samples. γ -catenin had no compensative capacity for β -catenin loss and was not required for the translocation of β -catenin into the nuclear compartment. Transcriptomic analysis by RNA-sequencing of WNT/ β -catenin signalling active and knockout clones revealed that WNT/ β -catenin signalling activated the RAP1 signalling pathway in AML. Re-activation of RAP1 signalling was able to rescue clonal expansion capacity in β -catenin knockout cells. Further investigation using CRISPR-mediated activation revealed that the WNT/ β -catenin target gene and activator of RAP1, *RAPGEF4*, was able to restore clonal growth significantly, whilst CRISPR-mediated inhibition of *SIPA1L1*, an inhibitor of RAP1 signalling increased clonogenicity modestly. Applied together, activation of *RAPGEF4* and inhibition of *SIPA1L1* elevated clonogenicity above scrambled controls. Whilst these studies, alongside recent *in vivo* literature, revealed WNT/ β -catenin signalling is dispensable for AML, further investigation of the unexplored downstream RAP1 signalling pathway represents a promising opportunity with potential clinical benefits.

ACKNOWLEDGEMENTS

I would like to express my immense gratitude to Prof. Richard Darley and Prof. Alex Tonks for the invaluable mentorship and expertise they have provided during the course of this research project. This gratitude is particularly emphasised for their support during the extraordinary times of late which have borne unique challenges. Thanks to your encouraging words and guidance, I have been able to grow as a scientist these past few years.

Within the haematology department, I would like to thank Amanda Gilkes for assisting with the genomics aspects of this project, and for her incredible efforts to manage the department both before and throughout the reopening of the laboratories within the hospital following the pandemic closures. I would also like to thank Dr. Ann Kift-Morgan from the Central Biotechnology Service at Cardiff University for providing guidance on the flow cytometry and sequencing facets of this project. Further, I wish to extend thanks to Dr. Amanda Tonks, director of PGR, for assisting in securing additional funding for this project, and for her constant support throughout the project. I am sincerely grateful to the School of Medicine at Cardiff University for providing the scholarship funding necessary for this project to proceed.

Special thanks are owed to friends and family that supported me throughout the course of this research. I would like to especially thank my colleague Dr Rachael Nicholson for being there to celebrate the victories, troubleshoot the issues, and provide a positive lift day to day. I am endlessly grateful to my parents and brothers for their constant praise and encouragement.

Aleksandra, I owe you infinite thanks for your incredible patience and tireless help throughout this project. Without you and your support, this success would not have been possible.

This research is dedicated to my friend Robert Brown, who sadly passed from leukaemia.

(1994-2016)

PUBLICATIONS AND PRESENTATIONS

Publications:

Abstract: Canonical Wnt Signalling-Responsive Acute Myeloid Leukaemia Cells Are Dependent On Beta-Catenin But Not Gamma-Catenin For Clonal Growth; A. Leckenby, A. Tonks, R. Darley; EHA2021 Virtual Congress Abstract Book; EHA Library. June 2021; Volume 5; Issue p e566; 06/09/21; 325147; EP393

Oral Presentations:

2018-2021 – Department of Haematology Seminar Series, Cardiff University, UK

2019 – Division of Cancer and Genetics PGR Research Symposium, Cardiff University, UK

2020 – Division of Cancer and Genetics PGR Research Symposium, Cardiff University, UK

2021 – Division of Cancer and Genetics Seminar Series, Cardiff University, UK

Poster Presentations:

2021 – European Haematology Association; Virtual

ABBREVIATIONS

ABC	ATP-binding Cassette
ALL	Acute Lymphoblastic Leukaemia
aMEM	Minimum Essential Medium Eagle - Alpha
AML	Acute Myeloid Leukaemia
ANG	Angiopoietin
ANXA	Annexin
APC	Adenomatous Polyposis Coli
APC^F	Allophycocyanin
APL	Acute Promyelocytic Leukaemia
Ara-C	Cytarabine
ATCC	American Type Culture Collection
ATO	Arsenic Trioxide
ATRA	All-Trans Retinoic Acid
AXIN	Axis Inhibition Protein
BC	Biocarta
β-ME	Beta-mercaptoethanol
BIO	6-Bromoindirubin-3'-Oxime
BM	Bone Marrow
BSA	Bovine Serum Albumin
BstR	Blasticidin Resistance Gene
Ca²⁺	Calcium
CAMK	Calcium/calmodulin-dependent Protein Kinase
CAR-T	Chimeric Antigen Receptor T-cell based Therapies
Cas9	CRISPR-associated 9
CB	Human Umbilical Cord Blood
CBP	CREB-binding Protein
CBS	Cardiff University Central Biotechnology Service
CBW	Cord Blood Wash
CCLE	Cancer Cell Line Encyclopaedia
CD	Cluster Of Differentiation
CDC	Catenin Destruction Complex
cDNA	Complementary DNA
CEB	Cytosolic Extraction Buffer
CEBP	CCAAT Enhancer-binding Protein
CHIP	Clonal Haematopoiesis of Indeterminate Potential
CHIR	CHIR99021
CK1	Casein Kinase 1
cKIT	Tyrosine-Protein Kinase KIT
CLL	Chronic Lymphocytic Leukaemia
CLP	Common Lymphoid Progenitors
CM	Conditioned Media
CML	Chronic Myeloid Leukaemia

CMP	Common Myeloid Progenitors
CR	Complete Remission
CRC	Colorectal Cancer
CRi	Incomplete Haematological Recovery
CRISPR	Clustered Regularly Interspaced Short Palindromic Repeats
CRISPRa	CRISPR Activation
CRISPRi	CRISPR Inactivation
CRISPR-KO	CRISPR Knockout
CSF	Colony Stimulating Factor
CtBP	C-terminal Binding Protein
CTNNB1	β -Catenin (Gene)
CXCL	CXC-Chemokine Ligand
DACT	Dishevelled Binding Antagonist of Beta-catenin
DAG	Diacylglycerol
DC	Dendritic Cell
dCas9	Deactivated Cas9
DEPMAP	Cancer Dependency Map Project Portal
DET	Differentially Expressed Transcripts
DFS	Disease Free Survival
DGCA	Differential Gene Correlation Analysis
DIXDC	Dishevelled-Axin Domain Containing
DKK	Dickkopf-related Protein
dKO	Dual Knockout
DMEM	Dulbecco's Modified Eagles Medium
DMSO	Dimethyl Sulfoxide
DNA-seq	DNA-sequencing
DNR	Daunorubicin
DSB	Double-strand Break
DSMZ	Deutsche Sammlung Von Mikroorganismen Und Zellkulturen
DsRED	Discosoma Sp. Red Fluorescent Protein
DVL	Dishevelled
ECACC	European Collection of Cell Cultures
ECL	Enhanced Chemiluminescence
ECM	Extracellular Matrix
EDTA	Ethylenediamine Tetraacetic Acid
EFS	Event-Free Survival
EGTA	Ethylene Glycol-Bis (B-Aminoethyl Ether)-N-N-N'-N'-Tetra Acetic Acid
ELN	European Leukaemia Net
EMP	Erythro-myeloid Progenitors
EPO	Erythropoietin
ERK	Extracellular Signal-Regulated Kinases
FAB	French American-British
FACS	Fluorescence Activated Cell Sorting
FBS	Foetal Bovine Serum
FDA	Food and Drug Administration

FDR	False Discovery Rate
FITC	Fluorescein Isothiocyanate
FLT3	FMS-Like Tyrosine Kinase 3
FLT3-ITD	FLT3 Internal Tandem Duplicates
FLT3-TKD	FLT3 Tyrosine Kinase Domain
FPKM	Fragments per Kilobase of Exon per Million Mapped Fragments
FSC	Forward Scatter
FZD	Frizzled
GAP	GTPase Activating Protein
GAPDH	Glyceraldehyde-3-Phosphate Dehydrogenase
GATA	Globin Transcription Factor
G-CSF	Granulocyte Colony Stimulating Factor
GEF	Guanine Nucleotide Exchange Factor
GEO	Gene Expression Omnibus
GFI	Growth Factor Independence
GFP	Green Fluorescent Protein
GI50	Growth Inhibition Fifty
GM-CSF	Granulocyte-Macrophage Colony Stimulating Factor
GMP	Granulocyte-Monocyte Progenitors
GO	Gene Ontology
gRNA	Guide-RNA
GSEA	Gene-Set Enrichment Analysis
GSK	Glycogen Synthase Kinase
GSVA	Gene-Set Variance Analysis
HBSS	Hanks Balanced Salt Solution
HCC	Hepatocellular Carcinoma
HDAC	Histone Deacetylases
HDR	Homology Directed Repair
HEPES	4-(2-Hydroxyethyl)-1-Piperazine-Ethanesulfonic Acid
HGNC	Hugo Gene Nomenclature Committee
HiDAC	High-dose Ara-C
HMA	Hypomethylating Agents
HR	Hazard Ratio
HRP	Horseradish Peroxidase
HSC	Haematopoietic Stem Cell
HSPC	Haematopoietic Stem Progenitor Cell
ICAT	Beta-catenin Interacting Protein
ICE	Inference of CRISPR Edits
IDH	Isocitrate Dehydrogenase (NADP(+))
IF	Interferon
IL	Interleukin
IL1RAP	Interleukin Receptor Accessory Protein
IMDM	Iscove's Modified Dulbecco's Medium
InDel	Insertion or Deletion
Inv	Inversion

IRF	Interferon-regulatory Factor
IT-HSC	Intermediate-Term HSC
JNK	C-Jun N-terminal Kinase
JUN	JUN Proto-oncogene
JUP	γ -Catenin (Gene)
KD	Knockdown
KEGG	Kyoto Encyclopaedia of Genes and Genomes
KO	Knockout
LB	Luria Bertani
LDAC	Low-dose Ara-C
LDS	Lithium Dodecyl Sulphate
LEF	Lymphoid Enhancer-Binding Factor
LIC	Leukaemia Initiating Cells
LIF	Leukaemia Inhibitory Factor
LIN	Lineage Marker
LPC	Lymphoid Progenitor Cell
LRP	LDL Receptor-related Protein
LSC	Leukaemic Stem Cell
LT-HSC	Long-Term HSC
MACS	Magnetic-Antibody Cell Sorting
MAPK	Mitogen-Activated Protein Kinase
MCA	Module Co-Expression Analysis
M-CSF	Macrophage - Colony Stimulating Factor
MDP	Monocyte-Dendritic Progenitor
MDR	Multi-drug Resistance
MDS	Myelodysplastic Syndrome
MEP	Megakaryocyte-Erythrocyte Progenitors
MFI	Mean Fluorescence Intensity
MgCL₂	Magnesium Chloride
miRNA	Micro-RNA
MLL	Mixed Lineage Leukaemia
MM	Mismatch
MNC	Mononuclear Cells
MPA	Mechanistic Pathway Analysis
MPC	Multipotent Progenitor Cell
MPP	Multi-Potent Progenitor
MRC	Medical Research Council
MRP1	Multidrug Resistance Related Protein-1
MSC	Mesenchymal Stem Cell
MSIG	Hallmark Molecular Signatures
MYC	Myelocytomatosis Oncogene
NCBI	National Centre for Biotechnology Information
NCRI	National Cancer Research Institute
NEB	New England Biolabs
NeoR	Neomycin Resistance Gene

NES	Nuclear Export Sequence
NF-AT	Nuclear Factor of Activated T-cells
NF-κB	Nuclear Factor Kappa-light-chain-enhancer of Activated B-cells
NGS	Next Generation Sequencing
NH2	Amino (Terminus)
NHEJ	Non-homologous End Joining
NK	Natural Killer Cell
NMD	Nonsense Mediated Decay
NPM	Nucleophosmin
NSAID	Non-steroidal Anti-inflammatory Drugs
OPN	Osteopontin
ORA	Overrepresentation Analysis
OS	Overall Survival
PAM	Protospacer Adjacent Motif
pBARV	β -Catenin Activated Reporter Venus
PBS	Phosphate-buffered Saline
PCA	Principle Component Analysis
PE	Phycoerythrin
pegRNA	Prime Editing guide RNA
PerCP	Peridinin Chlorophyll Protein Complex
PerCP-Cy5.5	Peridinin Chlorophyll Protein - Cyanine5.5
pfuBARV	β -Catenin Found Unresponsive Activated Reporter Venus
PGP	P-glycoprotein
PI	Propidium Iodide
PIP	Peroxisome Proliferation Transcriptional Regulator
PK	Protein Kinase
PLC	Phospholipase C
PORCN	Porcupine-O-Acyltransferase
PRL	Phosphate of Regenerating Liver
PTA	Pathway Topology Analysis
PTH	Parathyroid Hormone
PuroR	Puromycin Resistance Gene
PVDF	Polyvinylidene Fluoride
QC	Quality Control
qRT-PCR	Quantitative Reverse Transcriptase - Polymerase Chain Reaction
RAC	RAS-related C3 Botulinum Toxin Substrate
RAP	RAS-Associated Protein
RAPGEF	Rap Guanine Nucleotide Exchange Factor
REAC	Reactome
RFP	Red Fluorescence Protein
RHO	Ras-homolog Family Member
RIN	RNA Integrity Number
RNA-seq	RNA-sequencing
ROCK	RHO-associated Coiled-coil Containing Protein Kinase
ROI	Region Of Interest

ROS	Reactive Oxygen Species
RPKM	Reads per Kilobase Million
RPM	Revolutions Per Minute
RPMI	Roswell Park Memorial Institute
RPPA	CCLE Reverse Phase Protein Array
RR	Relapse Risk
RSEM	RNA-seq by Expectation-Maximisation
RUNX	Runt-related Transcription Factor
SA-PerCP	Streptavidin-Peridinin Chlorophyll Protein
SB	Staining Buffer
SCF	Stem Cell Factor
SCL	Stem Cell Leukaemia
SCR	Scrambled
scRNA-seq	Single cell RNA Sequencing
SDS-Page	Sodium Dodecyl Sulphate Polyacrylamide Gel Electrophoresis
SF	Serum-Free
sFRP	Soluble Frizzled-Related Protein
shRNA	Short Hairpin RNA
siRNA	Small Interfering RNA
SIRP	Signal Regulatory Protein
SNP	Single Nucleotide Polymorphism
SPIA	Signalling Pathway Impact Analysis
SSC	Side Scatter
STAR	Spliced Transcripts Alignment to a Reference
STAT	Signal Transducer and Activator of Transcription
ST-HSC	Short-Term HSC
t-AML	Therapy-related Acute Myeloid Leukaemia
TBE	Tris-borate-EDTA
TBS	Tris-buffered Saline
TBS-T	Tris-buffered Saline Tween
TCF	T-Cell Factor
TCGA	The Cancer Genome Atlas
TCR	T-Cell Antigen Receptor
TF	Transcription Factor
TFRA	Transcription Factor Regulator Analysis
TLE	Transducin-like Enhancer Protein
TMM	Trimmed Mean of M-values
TPM	Transcripts Per Million
TPO	Thrombopoietin
TRAIL	Tumour Necrosis Factor-Related Apoptosis-Inducing Ligand
WHO	World Health Organisation
WIF	WNT Inhibitory Factor
WNT	Wingless-Related Integration Site
WP	Wikipathways
WT	Wild Type

Table of Contents

ABSTRACT	I
ACKNOWLEDGEMENTS	II
PUBLICATIONS AND PRESENTATIONS	III
ABBREVIATIONS.....	IV
Table of Contents	X
List of Figures	XVI
List of Tables.....	XXI
Chapter 1	1
1.1 The Haematopoietic System.....	2
1.1.1 An Overview of Normal Haematopoiesis	2
1.1.2 Haemopoietic Stem Cell Characteristics	3
1.1.3 The Bone Marrow Niche	5
1.1.4 Regulation of Haematopoiesis.....	8
1.2 Acute Myeloid Leukaemia.....	10
1.2.1 Overview	10
1.2.2 Aetiology of Acute Myeloid Leukaemia	10
1.2.3 Leukaemogenesis and Clonal Cancer Evolution	12
1.2.4 The Leukaemic Stem Cell	15
1.2.5 Epidemiology and Clinical Diagnosis of AML.....	16
1.2.6 Disease Subtyping and Prognostic Stratification.....	17
1.2.7 Treatment for Acute Myeloid Leukaemia	21
1.3 WNT Signalling	26
1.3.1 Overview of the WNT Pathways.....	26
1.3.2 The Catenin Family	29
1.3.3 Regulation of the Canonical WNT/ β -catenin Pathway	34
1.3.4 WNT/ β -catenin in Haematopoiesis	36
1.3.5 WNT/ β -catenin Activity in Acute Myeloid Leukaemia.....	38
1.3.6 WNT/ β -catenin-derived Resistance to Standard Chemotherapeutic Agents	40
1.3.7 Therapeutic Targeting of WNT/ β -catenin.....	42
1.4 CRISPR/Cas9 Genetic Engineering.....	47
1.5 Aims and Objectives	51
Chapter 2.....	53
2.1 Cell Culture	54

2.1.1	Culture of Cell Lines in Suspension	54
2.1.2	Culture of Adherent Cell Lines	54
2.1.3	Quantification of Live/Dead Cells.....	54
2.1.4	Cryopreservation and Recovery of Cells.....	56
2.2	Primary Cell Culture: Haematopoietic Model	56
2.2.1	Isolation Of Mononuclear Cells from Human Neonatal Cord Blood.....	56
2.2.2	Isolation of CD34 ⁺ HSPC from Mononuclear Cells.....	57
2.2.3	<i>In Vitro</i> Culture of CD34 ⁺ HSPC	58
2.3	Primary Cell Culture: Primary AML	58
2.3.1	<i>In Vitro</i> Culture of Primary AML.....	58
2.3.2	Assessment of Cell Morphology	60
2.4	Limiting Dilution Cloning.....	60
2.5	Molecular Biology.....	64
2.5.1	Plating and liquid growth of <i>Escherichia coli</i> bacteria	64
2.5.2	Isolation of Plasmid DNA	64
2.6	Viral Transfection	65
2.6.1	Transfection of HEK293T Cells.....	65
2.6.2	Harvesting of Lentiviral Virions.....	65
2.7	Lentiviral Transduction	66
2.7.1	Lentiviral Transduction of Suspension Cell Lines	66
2.7.2	Lentiviral Transduction of Adherent Cell Lines.....	66
2.7.3	Lentiviral Transduction of CD34 ⁺ HSPC.....	67
2.7.4	Lentiviral Transduction of Primary AML	67
2.8	CRISPR-Cas9.....	67
2.8.1	<i>In Silico</i> Generation of guide-RNA	67
2.8.2	Selection of Transduced Cells	68
2.9	Modulating and Quantifying WNT Signalling	72
2.9.1	Stabilisation of β -catenin.....	72
2.9.2	Generating WNT3a Conditioned Media.....	72
2.9.3	pBARV and pfuBARV TCF Reporters	73
2.10	Protein Analysis by Western Blotting.....	73
2.10.1	Whole Protein Extraction	73
2.10.2	Cytosolic and Nuclear Cell Protein Fractionation	74
2.10.3	Determining Protein Concentration by Bradford Assay.....	74
2.10.4	Polyacrylamide Gel Electrophoresis and Electroblothing.....	75
2.10.5	Protein Detection Methods	76

2.10.6	Densitometric Quantification of Protein.....	77
2.11	Flow Cytometry.....	79
2.11.1	Estimation of CD34 ⁺ HSPC Cell Proportion	79
2.11.2	Fluorescence Activated Cell Sorting of Transduced CD34 ⁺ HSPC	82
2.11.3	Sorting Populations for pBARV and pfuBARV Construct Incorporation	82
2.11.4	Immunophenotyping of Transduced CD34 ⁺ HSPC.....	84
2.11.5	Measuring the pBARV Response.....	87
2.11.6	Monitoring Cell Viability	87
2.11.7	Proliferation and Viability Assay	87
2.11.8	DNA Content Assay	87
2.11.9	Annexin V Assay.....	88
2.11.10	Migration Assay	88
2.11.11	Immunophenotyping Assay	89
2.11.12	Drug Sensitivity Assay	92
2.11.13	Stress-induction Assays.....	92
2.12	Genomics.....	93
2.12.1	Cleavage Detection by Polymerase Chain Reaction	93
2.12.2	Quantifying DNA by Capillary Electrophoresis	96
2.12.3	DNA Sequencing.....	96
2.13	Transcriptomics.....	99
2.13.1	Total RNA Extraction.....	99
2.13.2	Generation of Data.....	100
2.13.3	RNA-Sequencing Bioinformatic Analysis	102
2.13.4	Publicly Available Data.....	106
2.14	Statistical Analyses	110
Chapter 3	112
3.1	Introduction	113
3.2	Aims	113
3.3	Results.....	115
3.3.1	Examination of WNT/ β -catenin Gene Expression in Haematopoiesis and AML.....	115
3.3.2	<i>CTNNB1</i> and <i>JUP</i> Expression do not Significantly Impact Clinical Outcome in AML.....	116
3.3.3	Characterising WNT/ β -catenin Activity in AML.....	120
3.3.4	WNT/ β -catenin Signalling Response is Heterogeneous in AML Cell Lines...	121
3.3.5	Validating β -catenin Translocation in AML Cell Lines by Western Blot	126

3.3.6	Validating γ -catenin Expression in AML Cell Lines by Western Blot	126
3.4	CRISPR-Cas9 Knockout Method Development	130
3.4.1	Evaluation of <i>CTNNB1</i> CRISPR-Cas9 gRNA in K562	130
3.4.2	Genetic Cleavage Assay Verifies DNA-level Presence of InDels	130
3.5	Selection of AML Cell Lines for Knockout.....	134
3.5.1	Establishment of AML Cell Lines for Knockout Studies.....	134
3.6	Single β -catenin Knockout in AML.....	136
3.6.1	WNT Signalling was Significantly Reduced in Responder Lines with Knockout.....	136
3.6.2	β -catenin Protein Levels are Substantially Reduced by CRISPR-Cas9 KO ...	136
3.6.3	β -catenin Knockout Does Not Perturb General Characteristics	139
3.6.4	Clonogenicity is Significantly Reduced for Responder Lines with β -catenin Knockout	141
3.7	Single γ -catenin Knockout in AML	143
3.7.1	WNT Signalling was Unaffected by γ -catenin Knockout in Responder Lines	143
3.7.2	γ -catenin Protein Levels are Substantially Reduced by CRISPR-Cas9 KO.....	143
3.7.3	Clonogenicity and Proliferation are Unaffected by γ -catenin Knockout.....	143
3.8	Dual β -catenin and γ -catenin Knockout in AML Cell Lines	147
3.8.1	Generation of Dual Knockout Cell Lines	147
3.8.2	WNT Reporter Activity was Reduced Significantly by Dual KO in Responder Lines.....	147
3.8.3	β -catenin and γ -catenin were Reduced by CRISPR-Cas9 Mediated Knockout	147
3.8.4	Combined Knockout of β -catenin and γ -catenin Does Not affect Growth and Viability of the Bulk Population.....	147
3.9	Knockout Clones from Responder Lines are Lost During Clonal Expansion	151
3.10	β -catenin KO in HSPC is Inconsequential for Differentiation and Self-renewal ...	154
3.10.1	Generation of <i>CTNNB1</i> Knockout in CD34 ⁺ HSPC.....	154
3.10.2	β -catenin Knockout in HSPC Does Not Impact Proliferation or Lineage Development.....	157
3.10.3	β -catenin Knockout has no Impact on Colony Formation, Apoptosis, and Cell Cycle.....	157
3.11	Discussion	160
Chapter 4	169
4.1	Introduction	170
4.1.1	Canonical WNT/ β -catenin Signalling in AML	170
4.1.2	Deductions from Chapter 3.....	171
4.2	Aims	172

4.3	Results	174
4.3.1	Generating Complete Knockout Clones	174
4.3.2	Generation and Isolation of Putative Knockout Clones	175
4.3.3	Sequence Validation of Complete Knockout AML Responder Clones	176
4.3.4	Characterisation of Complete Dual Knockout Clones	187
4.3.5	Characterising WNT/ β -catenin Activity in Primary AML Cultures	200
4.4	Discussion	214
Chapter 5		223
5.1	Introduction	224
5.2	Aims	224
5.3	Results	226
5.3.1	Preparation of samples for RNA-Sequencing	226
5.3.2	Differential Expression Analysis Reveals WNT-Active and Knockout Profile.....	241
5.3.3	Mechanistic Pathway Analysis Suggests RAP1 is a Target of WNT/ β -catenin Signalling.....	252
5.3.4	Differential Expression based on LEF1 in Patient Data.....	260
5.3.5	Patient Analysis – Survival Delimitation	265
5.3.6	Perturbed Genes Convey Prognostic Value.....	269
5.3.7	RAP1 Signalling Affects AML Growth and Modulates Clonogenicity	273
5.3.8	<i>RAPGEF4</i> and <i>SIPAIL1</i> Regulate Clonogenicity in AML	276
5.4	Discussion	278
5.4.1	Identifying a WNT/ β -catenin/RAP1 Signalling Axis in AML	279
5.4.2	Validating the WNT/RAP Signalling Axis Modulates Clonogenicity	285
Chapter 6		290
6.1	Background	291
6.2	WNT/ β -catenin Signalling Activity is Heterogenous in AML and Reveals an Expression Profile of Stemness and Chemoresistance Traits	292
6.3	β -catenin and γ -catenin are Dispensable for AML Maintenance and Chemoresistance, but β -catenin is Absolutely Required for Clonogenicity in Responder AML cell lines.....	293
6.4	WNT/ β -catenin is Dispensable for Myeloid Lineage Development in Normal Haematopoiesis and for HSC Self-Renewal	295
6.5	Dual catenin Knockout Perturbs the AML Transcriptome and RAP1 Signalling ..	295
6.6	Restoration of RAP1 Signalling Activity in β -catenin Knockout AML Restores Responder Clonogenicity and Enhances Non-responder AML Clonogenicity	296
6.7	Future Directions and Limitations.....	298

Appendix.....	302
S1. Examining β -catenin and γ -catenin in Human Haematopoiesis	302
S2. Examining the Transcriptomic Profile of Responder AML.....	306
S3. Public Pooled CRISPR Data Suggests No Requirement for β -catenin or γ -catenin.....	312
S4. Master Regulator Analysis Identifies Factors of Interest.....	314
S5. Examining the rWNT3a-induced WNT-active Transcriptomic Profile.....	317
S6. Examining the Effect of Dual Knockout Transcriptomic Profile	321
S7. LEF1 Patient Context.....	326
S8. Integrating Datasets.....	326
References.....	329

List of Figures

Figure 1-1: Haematopoiesis in the Classical Lineage Tree Model	4
Figure 1-2: The Bone Marrow Microenvironment	7
Figure 1-3: The Canonical WNT/ β -catenin Pathway, and the Classical Non-canonical WNT/ Ca^{2+} and WNT/PCP Pathways	28
Figure 1-4: The Structure of Beta-catenin and Gamma-catenin	31
Figure 1-5: Involvement of WNT/ β -catenin Signalling in AML	43
Figure 1-6: Molecular Targets of Therapeutics in WNT/ β -catenin Signalling	45
Figure 1-7: Mechanisms of Genetic Knockout, Inhibition, and Activation with CRISPR-Cas9	50
Figure 2-1: The CRISPR-CTNNB1-2 gRNA Target Site	71
Figure 2-2: Gating Strategy used to Estimate CD34 ⁺ HSPC Percentage by Flow Cytometry	81
Figure 2-3: Flow Cytometry Gating Strategy applied to Sort Transduced CD34 ⁺ HSPC.....	83
Figure 2-4: Immunophenotyping Gating Strategy for Lineage Determination	86
Figure 2-5: Cell Cycle Strategy	91
Figure 2-6: Apoptosis Gating Strategy	91
Figure 2-7: RNA-Sequencing Overview	101
Figure 2-8: A Flowchart of the RNA-Sequencing Analysis Plan.....	108
Figure 2-9: XCell Cell Type Contributions to Total RNA Profile Identifies T-Cell Contaminated Samples.....	111
Figure 3-1: Expression of <i>CTNNB1</i> and <i>JUP</i> in Haematopoiesis and AML Subtypes.....	117
Figure 3-2: <i>CTNNB1</i> and <i>JUP</i> Expression are Indicative of Clinical Characteristics.....	118
Figure 3-3: Overall Survival Analysis of Central WNT/ β -catenin Members.....	119
Figure 3-4: Expression of pBARV and pfuBARV in AML cell lines.....	122
Figure 3-5: CHIR Induces WNT/ β -catenin Signalling in K562 pBARV	123
Figure 3-6: Relative Viability Changes over 72-hours with CHIR and BIO GSK3 β Treatment	124

Figure 3-7: AML Cell Line WNT Reporter Assessment Following Treatment with GSK3 β Inhibitors	125
Figure 3-8: β -catenin Expression in AML Cell Lines	127
Figure 3-9: γ -catenin Expression in AML Cell Lines.....	128
Figure 3-10: CRISPR-Cas9 Knockout Rapidly and Stably Reduces WNT Reporter Activity	131
Figure 3-11: Genetic Cleavage Assay Reveals InDel Rate and Stability	132
Figure 3-12: Protein Analysis of β -catenin and γ -catenin Following Knockout	133
Figure 3-13: WNT Signalling Activity Delineates AML Cell Lines in Knockout Panel.....	135
Figure 3-14: β -catenin Knockout Significantly Reduces WNT Reporter Activity	137
Figure 3-15: Establishing Levels of β -catenin Knockout in Single <i>CTNNB1</i> Knockout Cells	138
Figure 3-16: Partial Knockout of <i>CTNNB1</i> Does Not Perturb General Characteristics of AML in a Bulk Population Setting	140
Figure 3-17: Clonogenicity is Significantly Reduced in β -catenin Knockout Responder Lines	142
Figure 3-18: γ -catenin Knockout Does Not Influence WNT/ β -catenin Signalling	144
Figure 3-19: γ -catenin Knockout in Single <i>JUP</i> Target Cell Lines.....	145
Figure 3-20: Clonogenicity is Unaffected by γ -catenin Knockout	146
Figure 3-21: Dual-catenin Knockout Significantly Reduces WNT Reporter Activity.....	148
Figure 3-22: Levels of β -catenin and γ -catenin Knockout in Dual gRNA Target Model	149
Figure 3-23: Dual Knockout Has No Influence on Proliferation, Apoptosis, and Cell Cycle	150
Figure 3-24: Loss of Knockout Clones During Limiting Dilution Cloning	152
Figure 3-25: THP1 Clones Retained a Functional <i>CTNNB1</i> Allele and Protein Expression	153
Figure 3-26: β -catenin and γ -catenin Expression Reduces During Haematopoiesis	155
Figure 3-27: Infection Efficiency of CRISPR-Cas9-gRNA-GFP.....	156

Figure 3-28: β -catenin Knockout Does Not Perturb Lineage Development and Proliferation During Haematopoiesis.....	158
Figure 3-29: β -catenin Knockout Does Not Impact Normal Cell Cycle, Apoptosis, or Self-renewal.....	159
Figure 4-1: Soluble Rescue Conditions Do Not Rescue Clonal Growth of Dual Knockout Responder AML Cells	177
Figure 4-2: Parental Co-culture Improves Clonal Growth of Dual Knockout Responder AML Cells	178
Figure 4-3: Co-culture with Dual Knockout U937 cells Rescues Clonal Growth of Dual Knockout Responder HEL Cells.....	179
Figure 4-4: Screening for Non-Responsive Clones using the WNT Reporter Assay.....	180
Figure 4-5: Representative Histograms Illustrating Purification of Putative Knockout Clones by FACS.....	181
Figure 4-6: Absence of β -catenin and γ -catenin in Recovered Putative Dual Knockout Clones Generated by Parental Co-culture.....	182
Figure 4-7: Absence of β -catenin and γ -catenin in Putative Dual Knockout Clones	183
Figure 4-8: Dual Knockout Has No Impact on Cell Characteristics of HEL	188
Figure 4-9: Dual Knockout Has No Impact on Cell Characteristics of THP1.....	189
Figure 4-10: Dual Knockout Has No Impact on Cell Characteristics of U937	190
Figure 4-11: Dual Knockout Has No Impact on Cell Characteristics of MV4;11.....	191
Figure 4-12: WNT Reporter Activity is β -catenin Dependent in Responder AML Cells.....	192
Figure 4-13: Responder AML Cell Lines Retain Dependence on β -catenin for Clonal Growth	193
Figure 4-14: Responder Knockout Cells are Not Sensitised to Chemotherapeutics	196
Figure 4-15: Non-responder Knockout Cells are Not Sensitised to Chemotherapeutics.....	197
Figure 4-16: Dual Knockout Has No Effect on Response to Serum-depletion Conditions...	198
Figure 4-17: Dual Knockout Has No Effect on Growth at Low-density	199
Figure 4-18: Analysis of Primary AML Cultures for WNT/ β -catenin Mediators.....	201

Figure 4-19: Frequency of Lentiviral CRISPR-Cas9 Transduction in Primary AML Cultures	203
Figure 4-20: Growth of CRISPR-Cas9 Transduced Primary AML Cultures is Unaffected by β -catenin Knockout.....	204
Figure 4-21: Quantification of β -catenin Knockout in Primary AML Samples by Western Blot.....	205
Figure 4-22: Knockout of β -catenin Reduces Colony Forming Efficiency of WNT Active Primary AML Cultures	207
Figure 4-23: Optimising WNT/ β -catenin Inhibitors in AML Cell Lines	211
Figure 4-24: β -catenin Inhibitors are Inconsequential to Proliferation and Viability in Primary AML.....	212
Figure 4-25: WNT/ β -catenin Inhibitors Reduce the Clonogenicity of Primary AML	213
Figure 5-1: RNA-Sequencing Experimental Design	228
Figure 5-2: rWNT3a Stimulates WNT Signalling in THP1	229
Figure 5-3: Pre-filtering of Low Abundance Genes	233
Figure 5-4: Normalisation of Filtered RNA-Seq Counts.....	234
Figure 5-5: Pearson Correlation Matrix Demonstrating the Similarity Between Cell Lines.	236
Figure 5-6: PCA Biplots Showing the Separation of Scrambled and Knockout Clones	237
Figure 5-7: <i>CTNNB1</i> and <i>JUP</i> are Ablated at the mRNA Level	239
Figure 5-8: WNT/ β -catenin Signalling is Not Perturbed as a Whole Pathway	240
Figure 5-9: Volcano Plots and p-value Distribution Histograms for THP1 Comparisons	244
Figure 5-10: Heatmap of Differentially Expressed Transcripts in THP1	245
Figure 5-11: Volcano Plot for Scrambled <i>versus</i> Knockout.....	248
Figure 5-12: Heatmap of Differential Transcripts between Scrambled and Knockout	249
Figure 5-13: Transcripts Changed in Both HEL and THP1 Cell Lines Arising from Dual Knockout of β -catenin and γ -catenin	250
Figure 5-14: Pathway Analysis for THP1 Scrambled with rWNT3a Treatment.....	254
Figure 5-15: GSEA Barcode Plot for Significant Terms with rWNT3a Treatment	255

Figure 5-16: Pathway Analysis Results for Knockout <i>versus</i> Scrambled Contrast.....	256
Figure 5-17: GSEA Barcode Plot for Significant Terms with Knockout	257
Figure 5-18: SPIA of rWNT3a Treated and Knockout Comparisons.....	259
Figure 5-19: Pathway Analysis Results for <i>LEF1</i> ^{HIGH} <i>versus</i> <i>LEF1</i> ^{LOW} Contrast.....	262
Figure 5-20: GSVA Heatmap of Perturbed Terms Between LEF1 Expression Levels.....	263
Figure 5-21: Gene-set Enrichment Analysis Results for 5-year Survival Contrast.....	266
Figure 5-22: GSEA Barcode Plots for Top Enriched Terms Relating to 5-year Survival.....	267
Figure 5-23: Genes Perturbed by WNT-activation Convey Prognostic Value.....	270
Figure 5-24: Genes Perturbed by Knockout Convey Prognostic Consequence	272
Figure 5-25: Constitutive RAP1 Signalling Activity Affects AML Expansion Variably	274
Figure 5-26: RAP1 ^{E63} Restores Responder AML Clonogenicity	275
Figure 5-27: <i>RAPGEF4</i> and <i>SIPA1L1</i> Restore and Enhance Clonogenicity in AML.....	277
Figure 5-28: Summary of the WNT and RAP1 Signalling Pathways	280
Figure 5-29: Hypothetical Crosstalk Between WNT/ β -catenin and RAP1 Signalling Pathways	284
Figure S-6-1: <i>CTNNB1</i> Poorly Indicative for HSC in the Continuum of Haematopoiesis ...	303
Figure S-6-2: β -catenin and γ -catenin Expression Reduces During Haematopoiesis	304
Figure S-6-3: Expression Patterns of <i>CTNNB1</i> and <i>JUP</i> in TCGA Patients.....	305
Figure S-6-4: Transcriptomic Profile Reveals Mechanisms of WNT/ β -catenin Activation and Prognostic Indicators	310
Figure S-6-5: Pathway Analysis Reveals Pathways Associated with Responder AML.....	311
Figure S-6-6: β -catenin and γ -catenin Are Not Essential in AML.	313
Figure S-6-7: Identified Master Regulator Transcription Factors Perturbed Within Generated Dataset.....	315
Figure S-6-8: Identified Master Regulator Transcription Factors Perturbed with <i>LEF1</i> ^{HIGH} vs <i>LEF1</i> ^{LOW} and five-year survival	316
Figure S-6-9: Heatmap Demonstrating Transcript Expression Differences Between <i>LEF1</i> ^{HIGH} and <i>LEF1</i> ^{LOW}	327

List of Tables

Table 1-1: Frequent Mutations in AML.....	14
Table 1-2: French-American-British Classification System for AML	18
Table 1-3: The World Health Organisation 2016 AML Classification System.....	19
Table 1-4: The European LeukemiaNet 2017 AML Prognostic Classifications	20
Table 1-5: Targeted Therapies for WNT/ β -catenin in Preclinical or Clinical Trials	44
Table 2-1: The List of Cell Lines Used for Studies	55
Table 2-2: Cell Culture Medium Used for Growth and Development of CD34 ⁺ HSPC.....	59
Table 2-3: Patient-derived Primary AML Samples	59
Table 2-4: Patient-derived Primary AML Culture Medium	59
Table 2-5: Single Cell Supplemented Media Conditions for Rescue	63
Table 2-6: Co-culture Conditions for Rescue of Dual Knockout AML Responder Lines	63
Table 2-7: The Determined Antibiotic Minimum Lethal Concentrations After Seven Days..	69
Table 2-8: Plasmid Vectors used within this Study	70
Table 2-9: Western Blot Antibodies used within Study	78
Table 2-10: Technical Specifications of the Accuri C6 Plus.....	80
Table 2-11: Flow Cytometry Antibodies used for Cord Blood HSPC Estimation.....	80
Table 2-12: Flow Cytometry Antibody Panel used for CD34 ⁺ HSPC Immunophenotyping .	85
Table 2-13: Cell Line Immunophenotyping Marker Antibody Panel.....	90
Table 2-14: Primer Design for Cleavage Detection.....	95
Table 2-15: Mastermix Composition for PCR.....	98
Table 2-16: PCR Cycle Conditions.....	98
Table 2-17: Samples Preparation for RNA-Seq.....	101
Table 2-18: The Statistical Pathway Analysis Methods Applied	107
Table 3-1: Summary Table of β -catenin and γ -catenin Expression.....	129
Table 4-1: <i>CTNNB1</i> DNA-Sequencing Reveals InDel Events	184

Table 4-2: <i>JUP</i> DNA-Sequencing Reveals InDel Events.....	185
Table 4-3: Summary Table of Generated Knockout Clones.....	186
Table 4-4: Summary Data for CRISPR-Cas9 Transduced Primary AML samples.....	208
Table 5-1: Quantification and Quality Control of Total RNA Isolate Samples	230
Table 5-2: Pre-filtering of Poor-Quality Sequence Reads	231
Table 5-3: STAR Alignment Results to the GRCh38.p13 Genome	232
Table 5-4: Comparisons Applied For RNA-Sequencing	243
Table 5-5: Top Differentially Expressed Transcripts in THP1 Scrambled Treated with rWNT3a	246
Table 5-6: Top Differentially Expressed Transcripts between THP1 knockout and scrambled	247
Table 5-7: Top Differentially Expressed Transcripts Between Knockout and Scrambled....	251
Table 5-8: Top Pathways Identified by Minepath Based on <i>LEF1</i> Expression Levels	264
Table 5-9: Top Pathways Identified by Minepath Relating to 5-year Survival.....	268
Table 5-10: Significantly Perturbed Genes with Knockout Convey Prognostic Influence ...	271
Table S-1: Integration of Patient and Cell Line Data Reveals Novel Insight into Directionally Changing Genes	328

Chapter 1

Introduction

1.1 The Haematopoietic System

1.1.1 An Overview of Normal Haematopoiesis

The continuous replenishment of blood cells occurs through a process known as haematopoiesis, in which haematopoietic stem cells (HSC) terminally differentiate into myriad mature blood cells with specialised functions. Continual production is essential, as constituent cell types provide essential functions including oxygen transport, immune response, and coagulation, yet often have short lifespans (Orkin *et al.*, 2008). Haematopoiesis is initiated by the HSC, which are characterised by their pluripotent and self-renewal capacity, having the ability to generate progeny which have differentiation potential, whilst maintaining undifferentiated properties. Haematopoiesis is segregated into a lymphoid arm, with progeny involved in adaptive immunity, and a myeloid arm which generates diversely functioning cells.

Prenatally, haematopoiesis progresses in a highly orchestrated process in which spatiotemporal regulation results in the development of haematopoietic progenitor cells. Initially, the aorta–gonad–mesonephros region is the hematopoietic site for an embryo. Later within early embryonic development, the yolk sac produces blood cells in a primitive form of haematopoiesis with a preference for red blood cells (Ivanovs *et al.*, 2017). A second, definitive stage of embryonic haematopoiesis is characterised by the development of erythro-myeloid progenitors (EMP) which generate erythrocyte and myeloid lineages, in addition to early T- and B-cell progenitors, from the aorta-gonad-mesonephros, before later in the placenta, spleen, liver, and bone marrow (BM) (Ivanovs *et al.*, 2017).

Postnatally, haematopoiesis is restricted to the BM within which HSC constitute ~10,000 cells (<0.01%) (Catlin *et al.*, 2011). However, limited haematopoietic capacity can be recruited from the spleen and liver in response to trauma (Kim, 2010). Classically, differentiation was considered hierarchical through a lineage tree with discrete, terminal commitment. HSC would differentiate into oligopotent progenitor cells, advancing to unipotent progenitor cells, and finally terminally differentiated cells (**Figure 1-1**) (Medvinsky *et al.*, 1999). However, research utilising mass cytometry and single-cell RNA-sequencing (scRNA-seq) has challenged this model (Giebel *et al.*, 2008), with evidence suggesting lineage development exists dynamically with cells, previously deemed unipotent, displaying oligopotent capacities (Hirschi *et al.*, 2017; Velten *et al.*, 2017). In fact, Cheng *et al.* recently proposed a new continuous haematopoietic model (Cheng *et al.*, 2020). Regardless of mechanism, increased differentiation is associated with the loss of self-renewal capacity (Seita *et al.*, 2010).

1.1.2 Haemopoietic Stem Cell Characteristics

HSC are characterised by the capability to differentiate into any haematopoietic cell, alongside self-renewal capacity to maintain the HSC pool throughout life (Ng *et al.*, 2017). HSC can remain in a quiescent state for extended periods of up to twenty years (Bernitz *et al.*, 2016). Historically, much of the research on HSC was performed in murine transplantation models, in which the capacity of transplanted cells was scored upon the ability to restore the haematopoietic system. In humans, the transmembrane phosphoglycoprotein CD34 was identified as the primary positive selection marker for HSC (Bhatia *et al.*, 1997). However, as CD34⁻ HSC are recognised in addition to CD34⁺ non-haematopoietic progenitor cells (Sidney *et al.*, 2014), there was a requirement for the identification of additional markers for HSC such as CD90, as well as CD45RA, CD49f, and CD38 for progenitor cells; this has resulted in the current classification of HSC as Lin⁻CD34⁺CD38⁻CD90⁺CD45RA⁻ (Lansdorp *et al.*, 1990; Baum *et al.*, 1992; Majeti *et al.*, 2007; Notta *et al.*, 2011). HSC can divide by asymmetric or symmetric means, producing one differentiated and one stem daughter cell, or two stem daughter cells, respectively (Shahriyari *et al.*, 2013).

In the classical model derived from research in *in vivo* murine models, HSC are sub-classified into long-term HSC (LT-HSC) which reconstitute the HSC pool throughout life, and short-term HSC (ST-HSC) which sustain haematopoiesis for several months, due to significantly reduced self-renewal capability (Frelin *et al.*, 2013). Within the mature adult BM, 1% of HSC are LT-HSC, with recent research suggesting HSC can modulate self-renewal divisions with LT-HSC dividing merely four times symmetrically throughout life (Bernitz *et al.*, 2016). Recent research using human models of HSC alongside mass cytometry and scRNA-seq have provided evidence for similar classifications, alongside the existence of an intermediate-term HSC (IT-HSC) group, suggesting further plasticity rather than definitive subtypes (Benveniste *et al.*, 2010; Knapp *et al.*, 2018).

The process through which the self-renewal properties of HSC are lost as lineage programming and resulting differentiation progresses represents an incompletely understood process. It is likely that a transcriptional profile maintains stemness traits and studies have suggested that the majority of transcriptional alterations between HSC and early progenitor cells are independent of lineage fate (Laurenti *et al.*, 2018).

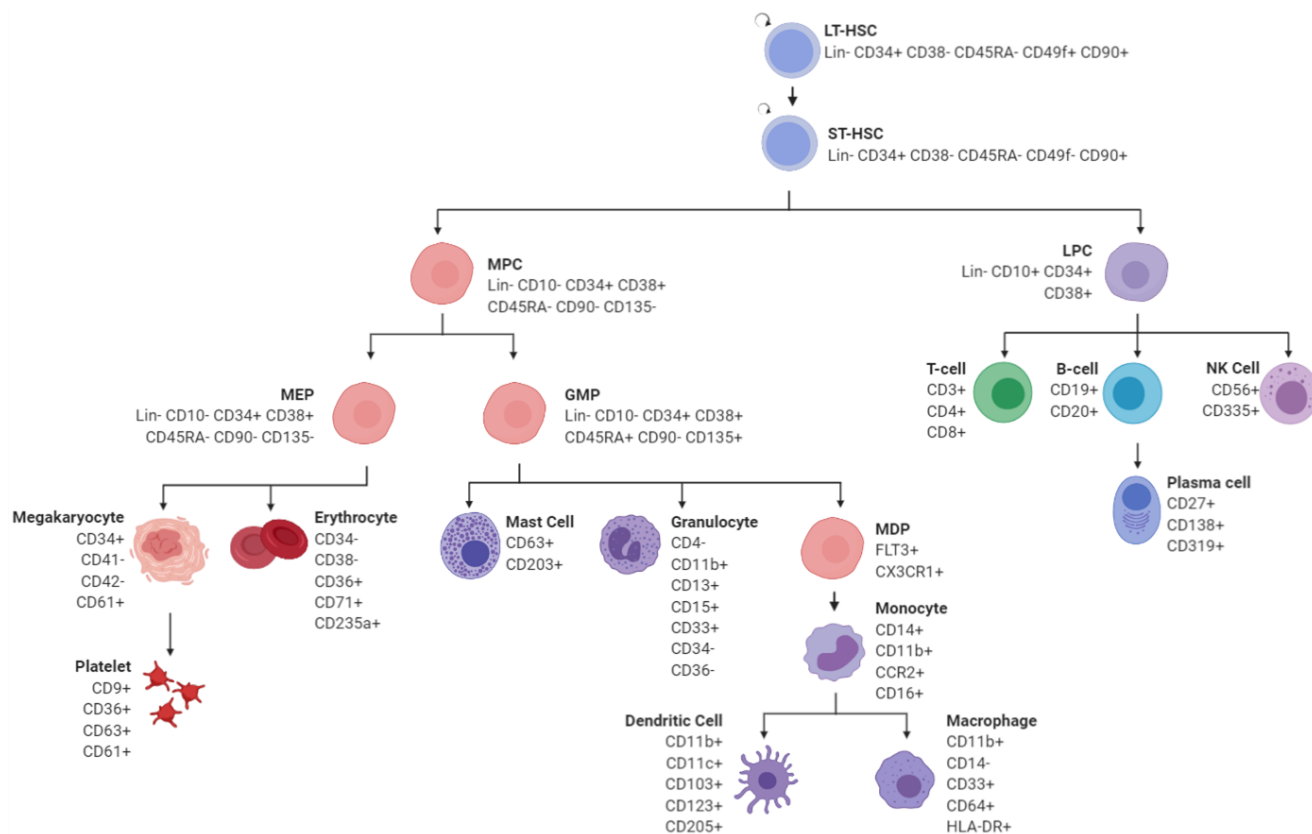


Figure 1-1: Haematopoiesis in the Classical Lineage Tree Model

The classic lineage tree details how a haematopoietic stem cell with self-renewal capacity leads to the generation of differentiated cells supported by cytokines, resulting in the production of specific daughter cells. The process proceeds branch wise, with no capacity to return to an alternate progenitor state. As an example, addition of IL-3, GM-CSF, and M-CSF will cause an HSC to differentiate into a common myeloid progenitor. Through addition of IL-3, SCF, and TPO it will develop into a megakaryocyte erythroid progenitor. Functional erythrocytes can be generated through addition of EPO, or alternatively these progenitors can become platelets through TPO. The balance of cytokines determines the generated daughter cells.

LT-HSC – Long-term Haematopoietic Stem Cell; **ST-HSC** – Short-term Haematopoietic Stem Cell; **MPC** – Multipotent Progenitor Cell; **LPC** – Lymphoid Progenitor Cell; **MEP** – Megakaryocytic-Erythroid Progenitor Cell; **GMP** – Granulocyte-Monocyte Progenitor Cell; **MDP** – Monocyte-Dendritic Progenitor Cell; **NK cell** – Natural Killer Cell; **Lin** – Lineage markers. **CD** – Cluster of Differentiation Marker (Presence or absence for cell type indicated above); Circular arrow represents self-renewal characteristics.

HSC are characterised by a resulting profile of attenuated mitochondrial activity, heightened glycolytic activity, and reduced metabolic activity, with strict regulation of protein synthesis, suggesting a unique set of characteristics permits long-term self-renewal (Takubo *et al.*, 2010; Signer *et al.*, 2014; Vannini *et al.*, 2016; Laurenti *et al.*, 2018). In contrast, progenitor cells present with a highly proliferative profile and enhanced metabolic activity (Laurenti *et al.*, 2018). Recent scRNA-seq and other *in silico* studies have enabled the delimitation of further cellular subtypes between branching points with primed characteristics, however, no consensus has yet been reached within the field as *in vitro* and *in vivo* validation is necessary and variation in age confounds definitions (Velten *et al.*, 2017; Anjos-Afonso *et al.*, 2022; Mitchell *et al.*, 2022; Monga *et al.*, 2022; Zhang *et al.*, 2022).

1.1.3 The Bone Marrow Niche

The concept of a BM niche was first proposed by Schofield in 1978, with the full appreciation of a supportive niche realised in subsequent research (Schofield, 1978). The BM niche provides cellular and acellular factors which facilitate quiescence and modulate activity of HSC, such as self-renewal, differentiation, and proliferation (Morrison *et al.*, 2014). Haematopoiesis can be modulated by numerous aspects, including growth factors and cytokines which associate with cell surface receptors to activate transcription factors. In turn, these modulate signalling pathways which regulate HSC maintenance and activity (Zon, 2008). The quiescence, self-renewal, and terminal differentiation of HSC can be regulated by these extrinsic factors which are tightly regulated.

The BM is sub-divided into endosteal and perivascular niches, which harbour quiescent LT-HSC and active ST-HSC, respectively, in humans (Szade *et al.*, 2018; Kulkarni *et al.*, 2020). The endosteal niche exists at the outer edge of the marrow containing osteocytes, which enable HSC chemotactic homing by producing calcium ions that are detected by HSC (Adams *et al.*, 2006). Moreover, it is a region of hypoxia which stabilises LT-HSC quiescence (Takubo *et al.*, 2010). The perivascular niche, on the other hand, is located within the inner core of the BM with ST-HSC localising to the sinusoidal endothelium. The endosteal niche is also occupied by a heterogenous population of mesenchymal-derived osteoblasts, osteoclasts, osteocytes, bone lining cells, fibroblasts, amongst others. The two central mediators of bone homeostasis are osteoblasts and osteoclasts, which synthesise bone tissue and reabsorb bone tissue respectively. Osteoblasts are well recognised for excreting cytokines which contribute to the regulation and maintenance of HSC, most notably osteopontin (OPN), thrombopoietin (TPO), angiopoietin-1 (ANG1), annexin 2 (ANXA2), granulocyte colony-stimulating factor

(G-CSF), stem-cell factor (SCF), and CXC-chemokine ligand 12 (CXCL12) (Taichman *et al.*, 1994; Ponomaryov *et al.*, 2000; Calvi *et al.*, 2003; Arai *et al.*, 2004; Stier *et al.*, 2005; Jung *et al.*, 2007; Yoshihara *et al.*, 2007). Other cell types within the region provide signals which support HSC, such as TGF- β from macrophages (Garbe *et al.*, 1997). Functionally, CXCL12 influences HSC repopulation and migration, SCF affects HSC maintenance, OPN affects HSC differentiation, ANXA2 changes HSC migration, G-CSF promotes myelopoiesis, and ANG1 and TPO both regulate LT-HSC quiescence (Taichman *et al.*, 1994; Ponomaryov *et al.*, 2000; Calvi *et al.*, 2003; Arai *et al.*, 2004; Stier *et al.*, 2005; Jung *et al.*, 2007; Yoshihara *et al.*, 2007). The bone microenvironment is represented in **Figure 1-2**.

Further to cytokines, many cells of the endosteal niche express membrane-bound ligands and receptors which contribute to HSC maintenance. Whilst it remains contentious, research has demonstrated that the Notch ligand, Jagged, maintains HSC (Varnum-Finney *et al.*, 2000; Paik *et al.*, 2010; Poulos *et al.*, 2015).

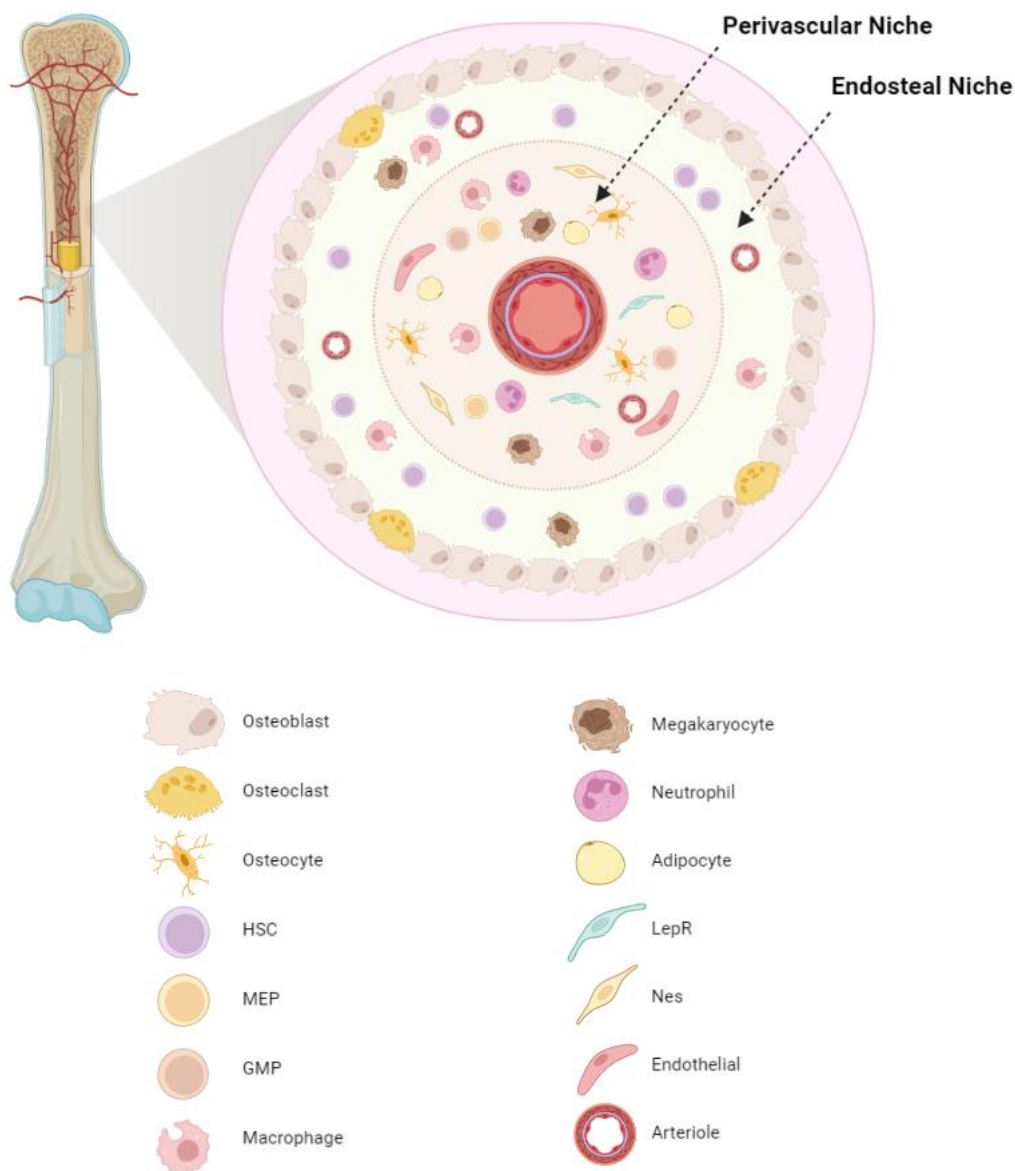


Figure 1-2: The Bone Marrow Microenvironment

The BM microenvironment is subset into two main areas: the endosteal, and the perivascular. In this diagram, a cross section of the BM demonstrates the perivascular niche which covers the central region between the core arteriole and the dashed perimeter, whilst the endosteal niche presents between the dashed perimeter of the perivascular niche and the osteoblast lining.

HSC – Haematopoietic Stem cell; **MEP** – Megakaryocytic-erythroid Progenitor Cell; **GMP** – Granulocyte-monocyte Progenitor Cell.

1.1.4 Regulation of Haematopoiesis

Haematopoiesis is a closely regulated process controlled by numerous interactions between cytokines, transcription factors (TF), and signalling pathways which are regulated by HSC and by communication with the cells within the stroma microenvironment. The resulting production of differentiated cells is lineage-dependent, with the current consensus built upon the classical hierarchical model. However, it is widely acknowledged that this model represents a generalisation of biological events and requires further derivation (Velten *et al.*, 2017).

The production of blood cells is influenced by haematopoietic cytokines. Cytokines are extracellular glycoproteins which bind and activate cytokine receptors, enabling their function to be applied in an auto-, para-, or endocrine manner. Principle cytokines include colony stimulating factor (CSF), interferons (IF), interleukins (IL), erythropoietin (EPO), thrombopoietin (TPO), and FMS-like tyrosine kinase 3 (FLT3). Cytokines are incorporated into the hierarchical model of haematopoiesis as the instructive model of fate determination, with select cytokines responsible for definitively driving specific cell fate determination (Rieger *et al.*, 2009), such as EPO in the context of erythroid production. However, other cytokines, such as IL-3, are known to promote proliferation in a lineage agnostic manner suggesting some cytokines are pleiotropic (Ihle, 1992).

EPO drives late-stage erythropoiesis by promoting the expression of GATA-1, an erythroid-associated transcription factor (Koury *et al.*, 1990; Zhao *et al.*, 2006). Genetic ablation of EPO induced anaemia and resulting gestational death *in vivo* in a mouse model, despite the presence of erythroid progenitor cells with the BM, demonstrating the necessity of EPO in late-stage differentiation (Wu *et al.*, 1995; Lin *et al.*, 1996). The detection of early erythroid progenitors has demonstrated that the current instruction model requires further adaption, with speculations that TPO provides the needed stimuli to drive these early erythroid progenitors. Genetic ablation of TPO resulted in a substantial reduction in erythroid progenitors in addition to platelets, megakaryocytes, and notably HSC, suggesting a common dependency between cell types (Porteu *et al.*, 1996; Ratajczak *et al.*, 1997; Yan *et al.*, 2013). FLT3 has been demonstrated to suppress erythroid and megakaryocyte development in favour of myeloid-lymphoid differentiation during haematopoiesis by upregulation of PU.1 (Onai *et al.*, 2006; Tsapogas *et al.*, 2014). A substantial reduction in the HSC and mature myeloid cells resulted as a consequence of FLT3 suppression (Mackarehtschian *et al.*, 1995). SCF is a fundamental cytokine with a critical role in HSC proliferation, survival, and differentiation (Broudy, 1997; Hartman *et al.*, 2001). Suppression of SCF production or ablation of the SCF receptor c-kit was

found to induce lethal macrocytic anaemia by depletion of progenitor cells and deficiency of all constituent myeloid and erythroid cell types (Ogawa *et al.*, 1991; Ito *et al.*, 1999).

G-CSF and granulocyte-macrophage CSF (GM-CSF) drive the differentiation and proliferation of myeloid progenitors (Metcalf *et al.*, 1982). GM-CSF is not absolutely required for the formation of derivative cells as determined by tolerated mutations of either GM-CSF or the associated receptor, and indeed, G-CSF is only required for complete granulopoiesis, with mutations of G-CSF resulting in partial neutropenia (Stanley *et al.*, 1994; Nishinakamura *et al.*, 1995).

The incomplete loss of any haematopoietic lineage in response to ablation of a sole cytokine or the associated receptor suggests haematopoiesis retains compensative redundancy enabling toleration of such conditions (Brown, Ceredig, *et al.*, 2018); in addition, this observation presents further evidence for the adoption of a continuum model of haematopoiesis with a greater dynamic capacity of fate (Brown, Tsapogas, *et al.*, 2018). Despite these limitations in understanding, therapeutic administration of recombinant cytokines has proven clinically effective in treating haematopoietic defects such as anaemia, in addition equivalent sequelae of chemotherapy treatment (Gabilove *et al.*, 1988; Lyons *et al.*, 1988).

TF are integral to haematopoiesis and are involved in HSC maintenance, survival, and differentiation. The dysregulation of TF is a known driver of leukaemogenesis, and the understanding of their particular roles has enabled these to be used as informative biomarkers of prognosis and therapeutic approaches targets (Aziz *et al.*, 2017; Gu *et al.*, 2018; Yu *et al.*, 2020).

The principal TF which are involved in the generation of HSC are Runt-related transcription factor 1 (*RUNX1*) and Stem-cell Leukaemia (*SCL*), whilst Growth-factor Independence 1 (*GFII*), and CCAAT enhancer-binding protein alpha (*CEBPA*) enable self-renewal capacities (Thambyrajah *et al.*, 2016). *In vivo*, embryonic null mice of *RUNX1* and *SCL* experience haematopoietic failure and are embryonic lethal; however, *in vitro* adult haematopoietic models have demonstrated no *RUNX1*- or *SCL*-dependency for HSC maintenance, but rather demonstrated issues with lineage-specific differentiation and a myeloproliferative phenotype suggesting further roles for these TF (Ichikawa *et al.*, 2004; Gowney *et al.*, 2005). Myeloid differentiation is coordinated by *PU.1*, *CEBPA*, and interferon-regulatory factor 8 (*IRF8*) (Tanaka *et al.*, 1995; Holtschke *et al.*, 1996; Tenen *et al.*, 1997; Yamanaka *et al.*, 1997; Hock *et al.*, 2003). Together, these promote the expression of receptors for GM-CSF, G-CSF, and macrophage CSF (M-CSF). Granulocyte differentiation is

orchestrated by *GFII*, *CEBPA*, and *CEBPE* with ablation of any these genes found to drive myeloproliferative disorders (Yamanaka *et al.*, 1997; Hock *et al.*, 2003; Thambyrajah *et al.*, 2016). These TF are central to the development of leukaemia through genetic mutations or chromosomal translocations which dysregulate normal HSC maintenance and development (1.2.2).

1.2 Acute Myeloid Leukaemia

1.2.1 Overview

Acute myeloid leukaemia (AML) is a heterogeneous haematological malignancy manifesting with molecular genetic mutations and cytogenetic abnormalities. Rapid clonal expansion of leukaemic cells, initially within the BM, induces a haematopoietic failure in the production of normal haematopoietic cells. A defining characteristic of AML is the infiltration and saturation of the BM niche with immature haematopoietic cells (De Kouchkovsky *et al.*, 2016) which have heightened survival and proliferative capabilities, amongst other advantages, but are functionally compromised because of a block in differentiation (Lowenberg *et al.*, 2016). Overall, five-year survival is approximately 20-25% in AML, with individual patient prognoses refined by age amongst other features (Juliussen *et al.*, 2009). However, disease subtyping and patient contraindications result in a spectrum of treatment options with a broad range of prognostic outcomes (1.2.6).

1.2.2 Aetiology of Acute Myeloid Leukaemia

The aetiology of AML is incompletely characterised, with several potential genetic events generating differing subtypes of AML, most notably with acute promyelocytic leukaemia (APL). Genomic instability is observed in AML, with a normal karyotype observed in only 50% of patients. Recurring mutations or translocations are known to drive leukaemogenesis and influence therapeutic decision making and prognostic outcome, such as FLT3 mutations (John S Welch *et al.*, 2012). The pathogenesis of AML is not yet understood, but methylation of tumour suppressor genes and oncogenes is known to play a substantial role (Larmonie *et al.*, 2018).

Most patients present with *de novo* AML with no predisposing risk factors. It is recognised that, as mutations successively accumulate with age, several cooperating mutations initiate the transition of an HSC to a leukaemic stem cell (LSC) (Ye *et al.*, 2015) with competitive pressures leading to the expansion of a highly proliferative clone. HSC are predicted to suffer 1 ± 0.20 exonic mutations per 7.5-years of life (John S Welch *et al.*, 2012;

T. N. Wong *et al.*, 2015) which increases the probability that initiating mutations will occur with advancing age.

Therapy-related AML (t-AML) accounts for up to 20% of AML cases and typically occurs 1-5 years after treatment with radiotherapy or chemotherapy during the course of treatment for another cancer or related disease (Samra *et al.*, 2020). For example, a specific class of therapeutics known as topoisomerase type-II inhibitors, such as etoposide, are frequently applied in the treatment of acute lymphoblastic leukaemia (ALL); however, up to 15% of patients will later present with t-AML (Schoch *et al.*, 2004). Topoisomerase type-II inhibitors form a complex with DNA and inhibit re-ligation during mitosis, leading to cell death with a inclination to affect more rapidly dividing cancer cells (Pommier *et al.*, 2010). As an unintended sequelae, etoposide can facilitate translocations of the mixed-lineage leukaemia gene (*MLL*) with numerous genes through an unknown mechanism, thereby instigating t-AML with prognosis significantly worse than *de novo* AML (Smith *et al.*, 2003).

In addition to the risks associated with radiotherapy or chemotherapy in driving t-AML, general exposure to ionising radiation, cigarette smoke, and carcinogenic chemicals heightens the risk of genetic mutations triggering leukaemogenesis. Furthermore, certain genetic disorders including Li-Fraumeni syndrome, Down syndrome, and Shwachman–Diamond syndrome substantially increase the risk of AML (Stieglitz *et al.*, 2013). Whilst rare, the recent inclusion of familial myeloid malignancies in the revised World Health Organization (WHO) classification has improved recognition of germline variants associated with AML and driven research efforts to improve identification and management of these at-risk individuals.

The *RUNX1*, *CEBPA*, and *GATA2* genes have been found to be germline mutated (Babushok *et al.*, 2016; Rio-Machin *et al.*, 2020). These germline variants have gained greater appreciation in the last decade as further evidence reveals these variants predispose individuals to AML, demonstrating clinical interest in identifying and characterising these germline anomalies. As AML occurs following the combination of genetic events in the multi-hit (polygenic) model, germline genetic mutations require a secondary hit, though the germline mutation can be characterised into classes with associated risk of disease progression (1.2.3). The identification of germline variants has been challenging owed to limited prospective data (Godley *et al.*, 2017), however, recent genome-wide association studies have identified numerous prospective further germline mutations of interest including *ADA*, *GP6*, *IL17RA*, *PRF1*, *SEC23B*, *DNAH9*, *NAPRT1*, *SH2B3* and *DHX34* (Rio-Machin *et al.*, 2020).

In a case study, a family presented with AML in a son, father, and paternal grandmother with such occurrence indicative of familial predisposition with high penetrance. Subsequently, sequencing identified *DDX41* as the inherited somatic defect predisposing to MDS and AML (Polprasert *et al.*, 2015). Functionally, the role of *DDX41* is unknown, however, roles in RNA splicing have been proposed and the observation of mutual exclusivity with other spliceosomal mutations in AML suggests such a role is founded. *In vitro*, knockdown of *DDX41* has been demonstrated to enhance proliferation and colony formation significantly, demonstrating contributions as a pre-leukaemic contributor to AML pathogenesis (He *et al.*, 2011; Sontakke *et al.*, 2014). Clinically, *DDX41*^{MUT} patients proved to respond positively to treatment with lenalidomide, suggesting a wider study evaluating *DDX41*^{MUT} and lenalidomide could reveal a suitable therapeutic option for patients harbouring this familial or somatic mutation. Such case studies reveal insight into the pathogenesis of AML in addition to revealing more suitable therapeutic interventions; therefore, it is hoped in the coming years greater understanding of familial inherited mutations could provide greater biological understanding of the polygenic model and specific contributions of central genes and mechanisms.

1.2.3 Leukaemogenesis and Clonal Cancer Evolution

In *de novo* cases of AML, the acquisition of genetic and epigenetic mutations within the myeloid progenitor cell population led to the development of the now classical two-hit model of leukaemogenesis. In this model, leukaemogenesis follows a multi-step process in which LSC acquire mutations from two distinct classes, with the presence of both fundamentally required for AML onset (Kelly *et al.*, 2002; Conway O'Brien *et al.*, 2014). The mutations are not leukaemogenic independently but act co-operatively.

The first class relates to genetic aberrations which induce a proliferative and survival advantage to cells. This frequently involves *FLT3*, *KRAS*, *TP53*, *NRAS*, or *c-KIT*, with the resulting consequent perturbed activity of several well characterised pathways (Gu *et al.*, 2018). The second class relates to genetic aberrations which impede differentiation or sustain self-renewal characteristics, exemplified by the translocation events *RUNX1::RUNX1T1* and *PML::RARA*, or mutations of *NPM1* and *CEBPA* (Tonks *et al.*, 2003; Grove *et al.*, 2014). However, further understanding of the biological basis of AML highlighted the overgeneralised nature of the two-step model (S. Jiang *et al.*, 2018). The model was expanded in recent years to incorporate a third class of aberrations which relate to epigenetic regulators such as *DMNT3A*, *TET2*, *WT1*, and *IDH* family members, leading to a three-step hypothesis (Alexandrov *et al.*, 2013; Ley, 2013; Sun *et al.*, 2018). As understanding of leukaemogenesis

develops, it is increasingly likely that the multi-step model will be surpassed by a new model with a greater appreciation of the underlying complexity, including incorporation of extrinsic, stromal cells which harbour mutations which disrupt haematopoiesis and can generate AML (Kode *et al.*, 2014; Galán-Díez *et al.*, 2016).

A particular challenge in producing a new model is the observation that many of these genes are found mutated frequently in the ageing population at low allelic frequencies without any associated disease, supporting the basis of multi-hit initiation of AML (Midic *et al.*, 2020). Clinically, the presence of somatic mutations within genes associated with haematopoiesis at a low allelic frequency is diagnosed as clonal haematopoiesis of indeterminate potential (CHIP), and is found in 10% of those aged between 70-80 years of age and increasing thereafter (Steensma *et al.*, 2015). Critically, the subsequent incidence of haematological malignancies in CHIP patients is 15 times the average rate, resulting in recommendations to screen patients diagnosed with CHIP annually for haematological malignancies (Heuser *et al.*, 2016). These mutations, such as *DMNT3A* and *TET2*, represent pre-leukaemic genetic events which alone are tolerated, but facilitate leukaemogenesis in tandem with further genetic aberrations which act as leukaemic drivers (John S. Welch *et al.*, 2012; Abelson *et al.*, 2018). Leukaemogenic mutations are often members of signalling pathways which are ordinarily expressed in haematopoiesis, with *FLT3*, *RAS*, and *c-KIT* mutated in over half of patients (**Table 1-1**).

Despite shortcomings, the mutational landscape of AML is well characterised as a result of the low mutational burden. Whilst solid tumours often present with a mutational burden of >15 somatic mutations per megabase, somatic mutations in AML are below 1 mutation per megabase (Alexandrov *et al.*, 2013; Ley, 2013). For context, the range in median mutational burden varies from 0.8 mutations per megabase (MDS) to 45 mutations per megabase in skin squamous cell carcinoma, demonstrating the low burden in AML. The mutational profile of each AML patient enables classification, conveys prognostic value, and dictates treatments.

Table 1-1: Frequent Mutations in AML

Table outlining the recurrent cytogenetic and molecular genetic aberrations which are frequently observed in AML. These are subtyped into mutational types based on commonality. Adapted from (Grove *et al.*, 2014; Di Nardo *et al.*, 2016).

Mutation Type	Gene	Frequency
Signal Transduction Genes	<i>FLT3, KRAS, NRAS, KIT, PTPN11, NF1</i>	59%
Epigenetic Regulation	<i>DNMT3A, IDH1, IDH2, TET2</i>	44%
Chromatin Modifiers	<i>MLL-fusions, ASXL1, EZH2</i>	30%
Nucleophosmin	<i>NPM1</i>	27%
Gene Translocations	<i>PML::RARA, MYH11::CBFB, RUNX::RUNX1T1</i>	25%
Transcription Factors	<i>CEBPA, RUNX1, GATA2</i>	22%
Tumour Suppressor Genes	<i>TP53, WT1, PHF6</i>	16%
Spliceosome Genes	<i>SF3B1, SRSF2, U2AF1, ZRSR2</i>	14%
Cohesin Complex	<i>RAD21, STAG1, STAG2, SMC1A, SMC3</i>	13%

1.2.4 The Leukaemic Stem Cell

As a clonal malignancy, AML originates following the accumulation of mutations within a single cell, occurring over an extended period. This initiating cell is known as the LSC, and has remained an area of contentious research for several decades (Fialkow, 1974; Griffin *et al.*, 1986; Lapidot *et al.*, 1994). LSC retain the self-renewal capability of HSC and current research supports a parallel hierarchical organisation of LSC imitating normal haematopoiesis; however, the former leads to the production of poorly differentiated blasts which saturate the BM (Jordan, 2007).

The inherent instability of the cancer genome facilitates the rapid accumulation of genetic aberrations (Suela *et al.*, 2007). An intrinsic selection toward mutations which enhance survival and proliferation will occur over time by means of clonal competition which acts in a linear, branching manner (Grove *et al.*, 2014; Morita *et al.*, 2020). Furthermore, the genetic landscape of AML is also pressured by treatment regimens which can apply an evolutionary pressure towards therapy resistant clones.

LSC were identified through fractionated *ex vivo* transplantation of AML patient material into immunodeficient mice (Bonnet *et al.*, 1997). In this study, patient material was sorted into CD34⁺CD38⁻ and CD34⁺CD38⁺ populations prior to implantation, with only the former leading to onset of disease in the murine model. The CD34⁺CD38⁻ subset was further capable of initiating disease after serial transplantation, demonstrating sustained self-renewal capacity. A difficulty in progressing research relies on the heterogeneity of the LSC population, stimulating research into additional markers of LSC. In recent years, numerous markers differentiating LSC from HSC have been proposed such as CD7 (Wu *et al.*, 2009), CD9 (Liu *et al.*, 2021), CD33 (Krupka *et al.*, 2014), CD44 (Jin *et al.*, 2006), CD47 (Majeti, Chao, *et al.*, 2009), CD96 (Hosen *et al.*, 2007), CD123 (Bras *et al.*, 2019), and CD157 (Krupka *et al.*, 2017), in addition to TF such as HDAC, NF- κ B, HIF-1 α , and β -catenin (Ding *et al.*, 2017). However, these markers remain controversial between studies. For instance, approximately 30% of AML patients present with no detectable CD34 expression, suggesting AML is capable of originating from CD34⁻ haematopoietic progenitors and that the current definition is incomplete (Taussig *et al.*, 2010; Sarry *et al.*, 2011; Ng *et al.*, 2016).

Expanding the understanding of the biology of the LSC is critical to furthering targeted therapy for this population. Although LSC represent a subset of the AML population, their eradication is fundamental to achieving long-term clinical remission. Unfortunately, standard

chemotherapeutic strategies applied clinically to treat AML have limited effect upon the LSC population, perhaps owed to LSC quiescence (Jordan, 2007; Villatoro *et al.*, 2020).

1.2.5 Epidemiology and Clinical Diagnosis of AML

AML is the most prevalent acute leukaemia in adults, accounting for 80% of all cases (Bain *et al.*, 2019), with approximately 3,000 patients diagnosed within the UK annually. AML is an age related disease, with incidence rates rising after 50-years of age onwards, presenting with highest incidence within the 85-89 years old age bracket (Normal, 2008; Shallis *et al.*, 2019). According to the UK Office of National Statistics, the incidence of AML within the UK has increased in the past three decades by approximately 30%. Whilst a proportion of this can be explained by the increasingly aged population of the UK subsequent to the post-World War II 'baby boom', increases in the number of patients presenting with t-AML suggests therapy adverse effects are also contributing a proportion of the rise (McNerney *et al.*, 2017). Occurrence of AML is marginally higher in males than females at 56:44, respectively, and is also more common in Caucasian individuals, as opposed to Hispanics, Africans, and Asians (Kirtane *et al.*, 2017).

Patients with AML will present clinically with a variety of symptoms, including fatigue, paleness, repeated infections, anaemia, bruising, and weight loss; rarer symptoms are a consequence of spleen enlargement (Döhner *et al.*, 2010). The more common symptoms present as a consequence of the accumulation of leukaemic blast cells within the BM, which reduce normal haematopoietic output and function.

A full blood count is performed from peripheral blood which can diagnose anaemia, neutropoenia, and thrombocytopenia, whilst a BM biopsy is able to consider morphological profiles, cytogenetics, and molecular characteristics. A diagnosis of AML is confirmed in the presence of >20% myeloblasts within the peripheral blood; however, presence of lower levels do not exclude AML (Khwaja *et al.*, 2016). Histological analysis of BM cell morphology, in addition to immunophenotypic considerations, is the recognised current standard for diagnosis, with further incorporation of subtype. Expression of MPO, CD13, CD33, CDw65, and CD117 on myeloblasts confirms AML, with further abnormal expression of lymphoid antigens enabling disease stratification (Bain *et al.*, 2019; Basharat *et al.*, 2019). For instance, the B-cell marker CD19 is expressed in up to 35% of AML patients with CD19 expression associated with a positive prognosis and low relapse risk (Poeta *et al.*, 1995; Wang *et al.*, 2021), whilst the T-cell marker CD7 is expressed in up to 30% of patients and is associated with more aggressive disease that proves resistant to standard therapy (Brandt *et al.*, 1997; Gomes-Silva

et al., 2019). AML cell karyotyping is important, as considerations of cytogenetics are also integral for endotyping. Common gene mutations and chromosomal translocations are screened, as these are informative of prognostic and treatment indicators. These include the AML-specific aberrations such as *RUNX1::RUNX1T1* (Swart *et al.*, 2021) and *PML::RARA*; however, these screens are only designed to capture the most frequent genetic aberrations in AML. Reductions in cost have led to calls for adoption of whole exome sequencing, enabling the assessment of the full profile for each patient (Leisch *et al.*, 2019; Duncavage *et al.*, 2021).

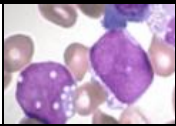
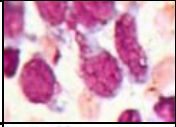

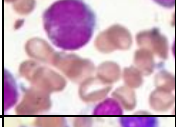
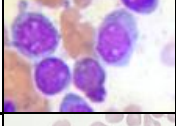


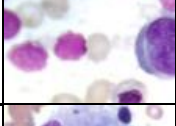

1.2.6 Disease Subtyping and Prognostic Stratification

As AML is derived from a combination of genetic aberrations, its heterogenous nature has challenged classification and prognostic efforts. Historically, patients were diagnosed based on karyotyping and a blast count of 30% or greater for classification with the French-American-British (FAB) system (Bennett *et al.*, 1976). This classified patients AML into eight subtypes ranging from FAB-M0 (undifferentiated) to FAB-M7 (incompletely differentiated megakaryocytic) (**Table 1-2**). Whilst morphological classification was an influential diagnostic platform, half of AML patients present with a normal karyotype and as such the FAB system was limited in its diagnostic and prognostic capability (Grimwade *et al.*, 2001).

In 2008, the WHO succeeded this classification system with an expanded panel of morphologic, cytogenetic, immunophenotypic, genotypic considerations, alongside clinical features, including a reduction of the blast count threshold to 20% (**Table 1-3**) (Falini *et al.*, 2010). In 2017, the European LeukemiaNet (ELN) classification system was developed, which stratified patients into adverse, intermediate, and favourable prognostic groups on the basis of aberrant genetics (**Table 1-4**) (Döhner *et al.*, 2017). In the coming decades, it is likely that the classification system will be further revised as newer technologies uncover previously unappreciated genetic aberrations. For example, deep sequencing has revealed novel chromosomal translocations within normal karyotype AML (Akagi *et al.*, 2009), including *CBFA2T3::GLIS2* (Masetti, Pigazzi, *et al.*, 2013), and *DHH::RHEBL1* (Masetti, Togni, *et al.*, 2013), amongst numerous other fusion genes (Wen *et al.*, 2012). These provide prognostic indication and, hence, represent potential therapeutic targets (Ilyas *et al.*, 2015). In 2021, the ELN system was expanded to include recommendations to measurable residual disease assessment, as the field currently utilises distinct methodologies including qPCR, flow cytometry, and next generation sequencing (NGS) alongside differing sampling sources and timepoints (Heuser *et al.*, 2021). Together, these warrant standardisation to enable comparability and maximise effectiveness.

Table 1-2: French-American-British Classification System for AML

AML subtypes defined per the French-American-British system. Table adapted from (Bennett *et al.*, 1976) and images acquired from (Ladines-Castro *et al.*, 2016).

FAB Subtype	Presentation	Classification
M0		Undifferentiated acute myeloblast leukaemia
M1		Acute myeloblast leukaemia with minimal maturation
M2		Acute myeloblastic leukaemia with maturation
M3		Acute promyelocytic leukaemia
M4		Acute myelomonocytic leukaemia
M4_{EO}		Acute myelomonocytic leukaemia with BM eosinophilia
M5		Acute monocytic leukaemia
M6		Acute erythroid leukaemia
M7		Acute megakaryoblastic leukaemia

FAB – French-American-British Classification System

Table 1-3: The World Health Organisation 2016 AML Classification System

Table describing the AML classification system designed by the World Health Organisation in 2016. Adapted from (Döhner *et al.*, 2017; Hwang, 2020)

Subtype	Description
1	AML with recurrent genetic abnormalities
	AML with t(8;21) (q22;q22.1); <i>RUNX1::RUNX1T1</i>
	AML with inv(16) (p13.1q22) or t(16;16) (p13.1;q22); <i>CBFβ::MYH11</i>
	APL with <i>PML::RARα</i>
	AML with t(9;11) (p21.3;q23.3); <i>MLLT3::KMT2A</i>
	AML with t(6;9) (p23;q34.1); <i>DEK::NUP214</i>
	AML with inv(3) (q21.3q26.2) or t(3;3)(q21.3;q26.2); <i>GATA2, MECOM</i>
	AML (megakaryoblastic) with t(1;22) (p13.3;q13.3); <i>RBM15::MKL1</i>
	Provisional entity: AML with <i>BCR::ABL1</i>
	AML with mutated <i>NPM1</i>
AML with biallelic mutations of <i>CEBPA</i>	
Provisional entity: AML with mutated <i>RUNX1</i>	
2	AML with myelodysplasia related changes
3	Therapy related myeloid neoplasms
4	AML, not otherwise specified (NOS)
	AML with minimal differentiation
	AML without maturation
	AML with maturation
	Acute monoblastic/monocytic leukaemia
	Pure erythroid leukaemia
	Acute megakaryoblastic leukaemia
Acute basophilic leukaemia	
Acute panmyelosis with myelofibrosis	
5	Myeloid sarcoma
6	Myeloid proliferations related to Down syndrome
	Transient abnormal myelopoiesis (TAM)
	Myeloid leukaemia associated with Down Syndrome

Table 1-4: The European LeukemiaNet 2017 AML Prognostic Classifications

Table outlining the prognostic consequence to common genetic aberrations in AML as defined by the ELN 2017 classification. Adapted from (Döhner *et al.*, 2017).

Risk Category	Genetic Abnormality
Favourable	t(8;21) (q22;q22.1); <i>RUNX1::RUNX1T1</i> inv(16) (p13.1q22) or t(16;16)(p13.1;q22); <i>CBFB::MYH11</i> Mutated <i>NPM1</i> without <i>FLT3::ITD</i> or with <i>FLT3::ITD</i> ^{LOW} (allelic ratio < 0.5) Biallelic mutated <i>C/EBPα</i>
Intermediate	Mutated <i>NPM1</i> and <i>FLT3::ITD</i> ^{HIGH} (allelic ratio ≥ 0.5) Wildtype <i>NPM1</i> without <i>FLT3::ITD</i> or with <i>FLT3::ITD</i> ^{LOW} (allelic ratio < 0.5)* t(9;11) (p21.3;q23.3); <i>MLLT3::KMT2A</i> Cytogenetic abnormalities not classified as favourable or adverse
Adverse	t(6;9) (p23;q34.1); <i>DEK::NUP214</i> t(v;11q23.3); <i>KMT2A</i> rearranged t(9;22) (q34.1;q11.2); <i>BCR::ABL1</i> inv(3) (q21.3q26.2) or t(3;3) (q21.3;q26.2); <i>GATA2</i> , <i>MECOM</i> -5 or del(5q); -7; -17/abn(17p) Complex karyotype (≥3 chromosomal abnormalities), monosomal karyotype Wildtype <i>NPM1</i> and <i>FLT3::ITD</i> ^{HIGH} (allelic ratio ≥ 0.5) Mutated <i>RUNX1</i> (if not co::occurring with favourable AML subtypes) Mutated <i>ASXL1</i> (if not co::occurring with favourable AML subtypes) Mutated <i>TP53</i> (associated with AML complex and monosomal karyotype)

For instance, ELN recommends a minimum of five million events to detect LSC which are gated on the basis of CD34⁺CD38⁻ expression, and the presence of an aberrantly expressed marker to enable distinction from HSC (e.g., CD45RA, CD123, CLL-1). Improving the detection methods and sampling timepoints for patients will hopefully improve long term prognostic outcomes.

Age at onset represents the principal dictator of resulting prognosis. Epidemiological studies have determined that five-year survival is approximately 15% for individuals diagnosed in their late 60s, with increasingly poorer survival as age progresses. This is in contrast to the observed 50% five-year survival rate in those under 50 years of age (Juliussen *et al.*, 2009). In part, this could be facilitated by treatment challenges in the elderly, as elevated incidence of co-morbidities contraindicates curative treatment options. This is in addition to the observed poor tolerance of intensive chemotherapy which further restricts treatment options and efficacy (Finn *et al.*, 2017).

1.2.7 Treatment for Acute Myeloid Leukaemia

Until recently, treatment options for AML remained similar for several decades, with improvements generally limited to dose intensification or combinational regimens (Dombret *et al.*, 2016). In recent years, emerging therapeutic options are demonstrating tremendous promise especially with regard to targeted therapies, which are capable of treating specific subtypes of AML (1.2.7.2). After the clinical diagnosis of AML is confirmed, the molecular indicators, in conjunction with individual patients' characteristics, are used to inform how treatment will proceed. Treatment strategies are separated into three regimens of induction chemotherapy, consolidation therapy, and maintenance therapy with each distinct in their therapeutic intention.

1.2.7.1 Standard Therapeutic Approaches

Induction chemotherapy is intended to alleviate the leukaemic burden and achieve complete remission (CR), defined as <5% blast content within the BM, absence of Auer rods and extramedullary leukaemia, and restored normal haematopoiesis as measured by a neutrophil count of >1,000/ μ L, and a platelet count >100,000/ μ L (Döhner *et al.*, 2017). CR without restoration of normal haematopoiesis is recognised as incomplete haematological recovery (CRi) and represents a further treatment challenge (Papaemmanuil *et al.*, 2016). Induction chemotherapy employs a combination of an antimetabolite such as cytarabine (Ara-C; 100-200mg/m²), for 7 days, alongside an anthracycline such as daunorubicin (DNR;

60mg/m²), for the first 3 days of treatment, in a 7+3 continuous infusion, respectively, over 7-days (Tallman *et al.*, 2005).

The mechanism of action for DNR is not fully appreciated, but is believed to act through inhibition of topoisomerase II, which is integral to topological rearrangement of DNA during mitosis (Lehmann *et al.*, 2004). It has also been found that upon cellular accumulation of DNR, the drug is reduced by oxidation-reduction to generate reactive oxygen species such as superoxides, hydroxyl radicals, and hydrogen peroxide which together toxically accumulate to induce cell lethality (Doroshov, 2019). Ara-C is an antimetabolite which inhibits nucleic acid synthesis by acting as a pyrimidine nucleobase analogue. During the S-phase of the cell cycle, the cytarabine metabolite cytarabine triphosphate is incorporated into DNA and exerts cell lethality by obstructing cell cycle progression (Li *et al.*, 2017).

Together, these therapies achieve CR in up to 80% of patients below sixty years old, and in approximately 50% of patients above sixty (Estey, 2009; Schlenk *et al.*, 2018). The discrepancy between cohorts derives from the co-morbidities which contraindicate treatment in the elderly cohort, alongside low tolerance for chemotherapy. As over half of patients are in the elderly cohort, efforts have been made to apply less intensive chemotherapeutic regimens, such as low-dose Ara-C (LDAC), or through the application of novel delivery mechanisms which enable reduced dosages, such as CPX-351, a liposomal delivery platform for dual administration of DNR and Ara-C (Raut, 2015). Alternatively, hypomethylating agents (HMA) can be applied in the elderly, such as Azacitidine, which improves outcome with high tolerance (Dombret *et al.*, 2015; Seymour *et al.*, 2017).

Consolidation therapy is designed to eradicate residual leukaemic cells and eliminate the risk of relapse. Often, it is only suitable for those below sixty years of age in good general health (Watts *et al.*, 2018). Consolidation therapy can take the form of several cycles of high-dose Ara-C (HiDAC) (Schwarer *et al.*, 2016), an allogeneic stem cell transplant (Koreth *et al.*, 2009), or an autologous stem cell transplant (Saraceni *et al.*, 2017). In the elderly cohort, it is possible to perform repeated cycles of LDAC, if tolerated, or a non-myeloablative stem cell transplant can be performed (Pizzola *et al.*, 2019), although these are less successful than the more intensive methods. Consolidation therapy is designed specifically to each patient, by taking into consideration the full molecular profile of the AML, the difficulty in achieving remission, availability of a matching donor for an allogeneic stem cell transplant, or possibility of collecting leukaemia-free BM tissue from the patient for an autologous stem cell transplant.

Most importantly, the overall patient health, age, and wishes will dictate the intensity of consolidation therapy.

Lastly, maintenance therapy is a post-consolidation treatment intended to prolong the period of remission and mitigate relapse. Treatments include continued chemotherapy cycles, HMA, immunotherapy, and targeted inhibitors; however, historically, the benefits of maintenance therapy were negligible or divisive (Sauter *et al.*, 1984; Palva *et al.*, 1991; Löwenberg *et al.*, 1998). The development of novel therapies has, however, demonstrated improvements to clinical outcome, such as with the HMA CC-486 (Wei *et al.*, 2019). The complexity of arising subclones with greater molecular complexity and heightened therapeutic evasion characteristics results in a dilemma for treatment suitability, and it is likely further novel therapies will improve the efficacy of maintenance therapy.

Despite these therapeutic efforts, relapse continues to occur in 50% of patients under sixty and up to 90% of those in the elderly cohort (Thol *et al.*, 2020). Relapsed disease is the most common cause of death in AML (Dombret *et al.*, 2016). Relapse frequently presents with a clonally evolved derivative from the primary AML, which exhibits greater molecular complexity with frequent acquisition of resistance to DNR and Ara-C, amongst other treatments. As a consequence, mortality rates have increased by 63% despite the advances in treating AML (Burnett *et al.*, 2010). Whilst five-year survival rates have improved, these still remain poor, with an expected 40% survival for early (<60 years old) and less than 10% for elderly (>60 years old) documented (Watts *et al.*, 2018). Together, this highlights the need for more targeted therapeutic options which will better treat the young cohort, whilst alleviating concerns of tolerance in elderly patients.

1.2.7.2 Targeted Therapy Approaches

The greater understanding of the biological basis of AML has facilitated the development of targeted therapies with heightened efficacy and reduced sequelae. An early success story in the development of targeted therapy for AML is the treatment of APL. APL is characterised by a reciprocal translocation which results in the expression of the fusion gene *PML::RARA*. Historically, APL used to be considered a poor prognostic indicator in AML, with low overall survival rates. However, treatment with all-trans-retinoic acid (ATRA) and arsenic trioxide (ATO) as a combinational retinoic acid therapy has achieved clinical remission in >90% of patients (Lo-Coco *et al.*, 2013) with long-term survival of over 98% (Sanz *et al.*, 2019). This success highlighted the tremendous promise of targeted therapy.

FLT3 is mutated to a constitutively active form which induces proliferation and suppresses differentiation driving AML (Gary Gilliland *et al.*, 2002). Midostaurin and Sorafenib were first-generation targeted therapies which inhibited the function of *FLT3* with demonstrated clinical benefits (Stone *et al.*, 2017; Liu *et al.*, 2018). However, as Midostaurin was able to inhibit off-target tyrosine kinases, incidence of adverse effects was noted (Short *et al.*, 2018). Similarly, Sorafenib was effective only in the post-transplant context, with no observed improvement to *FLT3* internal tandem duplication (*FLT3-ITD*⁺) patients (Y. Bin Chen *et al.*, 2014). This led to the development of second-generation *FLT3* inhibitors such as Quizartinib (Zarrinkar *et al.*, 2009), Crenolanib (Galanis *et al.*, 2014), and Gilteritinib (Ueno *et al.*, 2019) which had improved efficacy and on-target scores as compared to first-generational equivalents. Unfortunately, the efficacy of these agents is rapidly reduced, as the clonal evolution of AML facilitates the generation of secondary mutations within the *FLT3* tyrosine kinase domain (*FLT3-TKD*) to which these agents are targeted (Daver *et al.*, 2015; M. Wu *et al.*, 2018). Consequently, more recently developed *FLT3* inhibitors, such as Pexidartinib (Smith *et al.*, 2020), Cabozantinib (Fathi *et al.*, 2018), and Ibrutinib (Cortes *et al.*, 2019), are an area of active development with a design to target multiple kinase domains; however, these agents will have to avoid the off-target effects which constrained use of first-generation inhibitors.

The production of resistant clones remains a central concern in the application of targeted therapeutics. Many clinical trials have attempted to combine several therapeutics in order to improve patient outcomes especially within the elderly cohort. When Venetoclax, a BCL-2 inhibitor, was combined with HMA agents Azacitidine or Decitabine, clinical remission rates were improved to 73% and overall survival was extended to 17-months in a treatment regimen that was well tolerated by an elderly cohort (DiNardo *et al.*, 2019). This is in contrast to 8-months with HMA alone. However, clonal evolution toward mutations of *FLT3-ITD*, *FLT3-TKD*, and *TP53* generated resistance to Venetoclax, limiting the success of these therapies (DiNardo *et al.*, 2019). Other targeted therapies are currently in clinical evaluation. Ivosidenib and Enasidenib are isocitrate dehydrogenase 1|2 (*IDH1*, *IDH2*) inhibitors, respectively, and have demonstrated benefit in patients with such mutations (Dhillon, 2018; Dugan *et al.*, 2018). Additionally, Dasatinib acts as a *KIT* inhibitor (Boissel *et al.*, 2015).

As a haematological malignancy, AML is predominantly a disease of the BM. This is of tremendous benefit to the application of antibody-based immunotherapies, which would be able to perfuse the BM readily. The antibody-drug conjugate Gemtuzumab ozogamicin is

formed of an anti-CD33 antibody in combination with the DNA-intercalating agent calicheamicin, and has recently been approved for use (Baron *et al.*, 2018). CD33 is frequently overexpressed in LSC as contrasted to HSC, in which it is functionally unnecessary (Hanekamp *et al.*, 2017). Gemtuzumab ozogamicin was found to significantly improve the survival of young patients with favourable cytogenetics in the Medical Research Council (MRC) AML15 clinical trial when applied in combination with chemotherapy (Burnett *et al.*, 2011). In fact, gemtuzumab ozogamicin has been adopted for treatment of CD33-positive AML at diagnosis or relapse (Williams *et al.*, 2019).

Magrolimab is a monoclonal antibody targeting the macrophage inhibitory immune checkpoint CD47 (Sallman *et al.*, 2020). CD47 interacts with the Signal Regulatory Protein Alpha (SIRP α) receptor on macrophages to inhibit phagocytosis (Logtenberg *et al.*, 2019). In AML, CD47 is significantly overexpressed and correlates with poor patient prognosis (Marple *et al.*, 2021). Magrolimab recently completed a phase 1 clinical trial in combinational application with Azacitidine for administration in patients who were unsuitable intensive chemotherapy. Magrolimab was able to induce clinical remission in 42% of patients with disease-free survival in the majority at 9-month follow up (Sallman *et al.*, 2020). The rate of clinical remission could be improved in further dosage studies, as no patients withdrew due to treatment-related adverse effects, nor was a maximum tolerated dose reached.

A further therapeutic option in development is chimeric antigen receptor T-cell-based therapies (CAR-T). Comparably to gemtuzumab ozogamicin, targeting of CD33 with CAR-T has shown tremendous benefit, though research is limited due to the high costs related to CAR-T treatment. An individual treated with anti-CD33 CAR-T achieved clinical remission in two-weeks; however, the patient relapsed after 8 weeks (Wang *et al.*, 2015). CAR-T therapy is limited by T-cell exhaustion and loss of persistence (Ghorashian *et al.*, 2019; Hsieh *et al.*, 2020).

Since the development of the gene editing technique clustered regularly interspaced short palindromic repeats (CRISPR) CRISPR-associated protein 9 (Cas9) (CRISPR-Cas9), numerous clinical trials have begun aiming to eradicate haematological malignancies by genetic deletion of central mediators; however, little application exists in AML (González-Romero *et al.*, 2019). Targeting of *IL1RAP* with CRISPR-Cas9 was found to significantly impair colony formation capacity *in vitro* in THP-1 cells, with no associated haematopoietic dysfunction in an *in vivo* murine model, though no complete knockout clone was generated (Ho *et al.*, 2021). *IL1RAP* promotes *FLT3*, *c-KIT*, and IL-1 signalling, and is associated with

poor survival in AML (Barreyro *et al.*, 2012; Ho *et al.*, 2016). Vor Biopharma recently received Food and Drug Administration (FDA) approval for clinical use of VOR33, a CRISPR-Cas9 platform enabling allogeneic engineered hematopoietic stem cell transplant which have genetic ablation of CD33. The deletion of this gene enables subsequent high-dose treatment with gemtuzumab ozogamicin without adverse effect on HSC. Similar strategies could be applied to delete therapeutic targets which are redundant in HSC, but critical to LSC. Cancer-specific insertion, deletion, or substitution mutations could be exploited to enable specific targeting with CRISPR-Cas9 without impact on healthy cancers, as has recently been demonstrated *in vitro* in human cell lines, and *in vivo* patient xenograft tumours in mice (Taejoon *et al.*, 2022).

1.3 WNT Signalling

1.3.1 Overview of the WNT Pathways

WNT signalling is an evolutionary conserved signalling pathway with critical roles in normal developmental processes in embryonic and adult cells relating to self-renewal, proliferation, and differentiation. WNT signalling is present in all metazoan species, and even the simplest free-living animal, placozoan, possesses a complete WNT signalling pathway (Srivastava *et al.*, 2008). In humans, WNT signalling is believed to contribute to haematopoiesis (Richter *et al.*, 2017).

The name WNT originated in the 1980s, when the proto-oncogene *Int-1* was discovered and found to be a homolog of *Drosophila wingless*, which controls larval development of drosophila (Rijsewijk *et al.*, 1987); the gene was hence renamed as the portmanteau *Wnt1* (wingless-type integration site family member 1). WNT genes are a family of secreted glycoproteins, of which nineteen are currently recognised within the human genome (Miller, 2002). The interaction between WNT ligands and their associated receptors, in combination with distinct downstream components, was classically suggested to facilitate the promotion of discrete WNT signalling subpathways, leading to downstream WNT target gene regulation; however, an updated integrative model has since then been suggested (Thrasivoulou *et al.*, 2013a).

WNT signalling is divided into two classifications: the canonical WNT signalling pathway, involving the central mediator β -catenin (WNT/ β -catenin); and the non-canonical WNT signalling pathways, independent of β -catenin (**Figure 1-3**) (MacDonald *et al.*, 2009). Classically, the non-canonical pathways comprised the WNT Planar Cell Polarity pathway (WNT/PCP) and the WNT Calcium signalling pathway (WNT/ Ca^{2+}) (Komiya *et al.*, 2008);

however, numerous further non-canonical pathways have been proposed including the WNT receptor tyrosine kinase pathway (WNT/RTK), the WNT receptor-like tyrosine kinase pathway (WNT/RYK), the WNT receptor-like tyrosine kinase orphan receptor pathway 2 (WNT/ROR2), the WNT protein kinase A pathway (WNT/PKA), the WNT protein kinase C

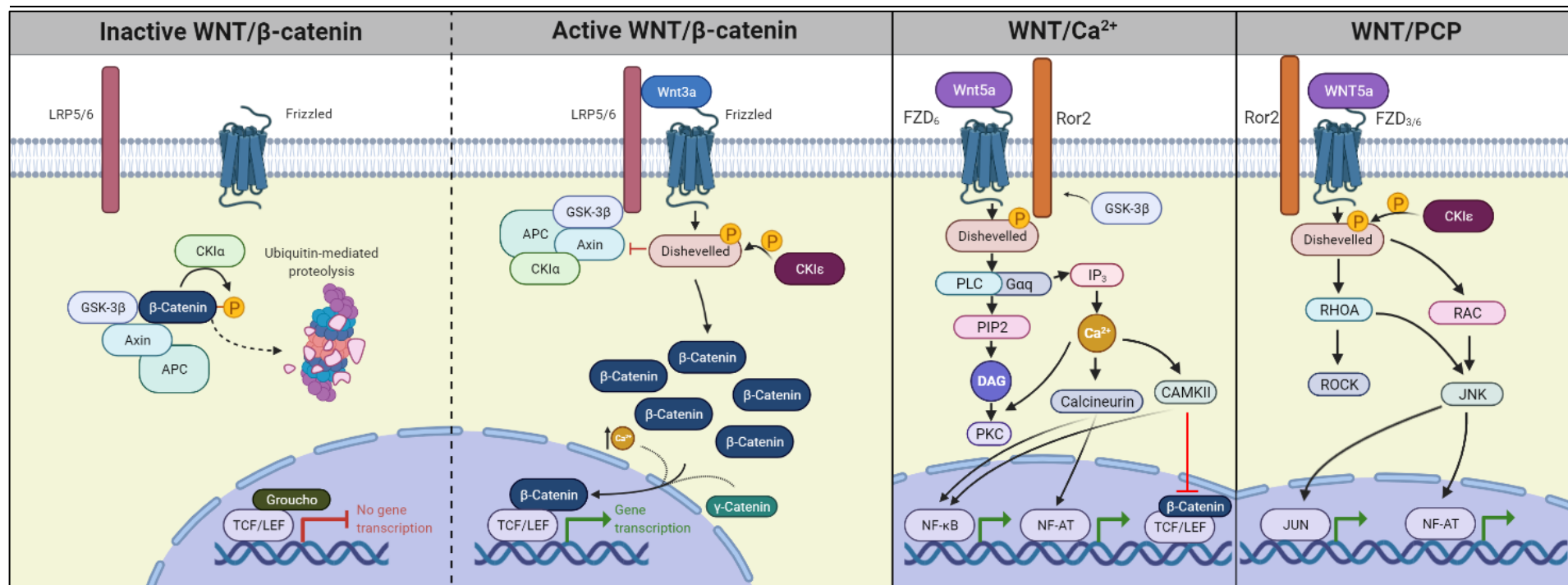


Figure 1-3: The Canonical WNT/ β -catenin Pathway, and the Classical Non-canonical WNT/ Ca^{2+} and WNT/PCP Pathways

Inactive WNT/ β -catenin In the absence of a WNT ligand, Frizzled and LRP5/6 do not associate, and no intracellular signal is generated. β -catenin is rapidly degraded by the destruction complex consisting of CK1 α , GSK3 β , AXIN, and APC, amongst others. The TCF/LEF transcription complex is suppressed by Groucho, amongst other elements, suppressing WNT target gene activation.

Active WNT/ β -catenin In the presence of a WNT ligand, Frizzled and LRP5/6 associate, leading to the disassociation of CK1 ϵ from LRP6 which phosphorylates Dishevelled to an active, LRP6 binding form. This results in inhibition of the β -catenin destruction complex by Dishevelled and re-targeting of GSK3 β to LRP6, resulting in relocalisation toward the membrane. β -catenin accumulates within the cytoplasm and through an incompletely understood process (possibly involving intracellular Ca^{2+} or γ -catenin) translocates to the nucleus. Within the nucleus, β -catenin forms a complex with TCF/LEF which disassociates Groucho and promotes WNT target gene activation.

WNT/ Ca^{2+} - The non-canonical WNT/ Ca^{2+} pathway regulates intracellular calcium and diacylglycerol levels.

WNT/PCP - The non-canonical WNT/PCP pathway controls restructuring of the cytoskeletal elements and has roles in gastrulation.

CK1 ϵ – Casein Kinase Epsilon; **CK1 α** – Casein Kinase Alpha; **GSK3 β** - Glycogen synthase kinase-3 beta; **β -catenin** – Beta catenin; **γ -catenin** – Gamma catenin; **TCF/LEF** – T-cell Factor/Lymphoid Enhancer factor; **APC** – Adenomatous Polyposis Coli; **PLC** – Phospholipase C; **IP $_3$** - Inositol 1,4,5-trisphosphate; **PIP2** - Peroxisome proliferation transcriptional regulator; **DAG** – Diacylglycerol; **Ca^{2+}** - Calcium; **PKC** – Protein Kinase C; **CAMKII** - Calcium/calmodulin-dependent protein kinase II; **NF- κ B** - Nuclear Factor kappa-light-chain-enhancer of activated B cells; **NF-AT** - Nuclear factor of activated T-cells; **RHOA** - Ras Homolog Family Member A; **ROCK** - Rho Associated Coiled-Coil Containing Protein Kinase 1; **RAC** - Ras-related C3 botulinum toxin substrate 1; **JNK** - c-Jun N-terminal kinase; **JUN** - Jun Proto-Oncogene

pathway (WNT/PKC), the WNT microtubule pathway (WNT/MT), the WNT mechanistic target of rapamycin pathway (WNT/MTOR), the WNT signal transducer and activator of transcription 3 pathway (WNT/STAT3), and finally the WNT RAS-associated signalling pathway 1 pathway (WNT/RAP) (Liu *et al.*, 2016). The non-canonical pathways are less well characterised than the canonical counterpart, particularly in the case of the newly proposed non-canonical WNT pathways. This project focused upon the canonical WNT/ β -catenin pathway.

1.3.2 The Catenin Family

Catenins are a family of proteins with varied roles in adherence and signalling, named for their chain-like appearance (Latin, '*catena*'). Four members have been identified in the 1980s: alpha-catenin (α -catenin), beta-catenin (β -catenin), delta-catenin (δ -catenin), and gamma-catenin (γ -catenin) which are encoded by *CTNNA1*, *CTNNB1*, *CTNND1*, and *JUP* (previously *CTNNG1*), respectively (Peyrieras *et al.*, 1985). In relation to WNT/ β -catenin signalling, it has long been suspected that γ -catenin can act compensatively for β -catenin. However, α -catenin cannot act compensatively as it is unable to bind T-cell factor/lymphoid enhancer factor (TCF/LEF) due to the absence of an armadillo region (Knudsen *et al.*, 1995). δ -catenin has been implicated as a regulator of the NF- κ B pathway, with no ability to replace β -catenin in WNT/ β -catenin signalling (Perez-Moreno *et al.*, 2006). However, whilst it has been suggested that δ -catenin can modulate WNT/ β -catenin, no precedent exists in AML and evidence is lacking (Nopparat *et al.*, 2015). Outside the catenin family, β -catenin-like-protein 1 shares homology with β -catenin; however, no evidence exists that it is able to act comparably to β -catenin in WNT/ β -catenin signalling; rather, it is involved in RNA-splicing (Ganesh *et al.*, 2011).

1.3.2.1 β -catenin

β -catenin is produced by the *CTNNB1* gene located at 3p22. In total, 56 transcript variants are recognised, with 43 encoding protein; of these, 24 encode full length β -catenin (781 amino acids). *CTNNB1* variants average 16 exons. As a moonlight protein, β -catenin is a member a family of approximately 100 proteins which are capable of two or more independent functions. However, for the purposes of this study, a focus was placed upon the roles β -catenin, specifically in the WNT/ β -catenin signalling pathway. The alternate roles of β -catenin relate to adhesion regulation, amongst other implicated functions.

Structurally, β -catenin possesses an N-terminal domain which binds - Glycogen synthase kinase-3 beta (GSK3 β) and Casein Kinase (CK1); a central twelve armadillo repeat domains from residues 141-664, each of 40 amino acids, forming a positively charged trench; and a C-terminal domain (Xu *et al.*, 2007). Armadillo repeats 3-10 compose the TCF binding site, with repeat 5-9 proving critical at residue 351-519, approximately. The armadillo region is highly evolutionarily conserved and is integral to regulating β -catenin stability, localisation, and transcriptional activity. The N-terminal region contains a motif responsible for binding beta-transducing repeat-containing protein (β -TrCP), thus mediating β -catenin degradation. In certain cancers, mutations of this region or alternative splicing prevent β -TrCP binding and enable evasion of degradation. The C-terminal region has a strong transactivator motif when associated with DNA, enabling WNT target gene expression. Only the C-terminal segment is recruited for transcriptional regulation, as a C-terminal-truncated form was able to fulfil all known WNT/ β -catenin roles when artificially associated with TCF4/LEF1 (Vleminckx *et al.*, 1999). The central armadillo region is capable of binding several partners, each interacting with a specific site of this region. Certain members bind competitively to β -catenin, whilst others are capable of simultaneous binding, as illustrated in **Figure 1-4**.

The mechanism by which β -catenin translocates into the nucleus is contentious. It is hypothesised that the process requires a chaperone, as nucleoporins prevent unrestricted nuclear entry of proteins ≥ 40 kDa (Sharma *et al.*, 2016), with β -catenin being approximately 92kDa. Further, entry without a chaperone requires a nuclear localisation sequence for importin- α binding, which β -catenin does not possess (Suh *et al.*, 2003). It has been speculated that the N-terminus of β -catenin contributes to nuclear transport activity, suggesting a direct method of regulation; however, as cytoplasmic accumulation of β -catenin can occur without nuclear translocation, it is evident another member is involved (Sharma *et al.*, 2016).

Numerous candidate partners have been proposed. The classical chaperone, LEF1, has long been proposed as the responsible partner (Huber *et al.*, 1996; Simcha *et al.*, 1998). However, it is unlikely LEF1 represents the only chaperone partner, as nuclear entry has been observed independent of LEF1 (Lilien *et al.*, 2005). A multi-modal system is the more likely hypothesis, as it has been established that Rap guanine nucleotide exchange factor 5 (RAPGEF5) and the associated RAP1a/b GTPases regulate nuclear transport in a mechanism comparable to Ran/Importin- β (Griffin *et al.*, 2018).

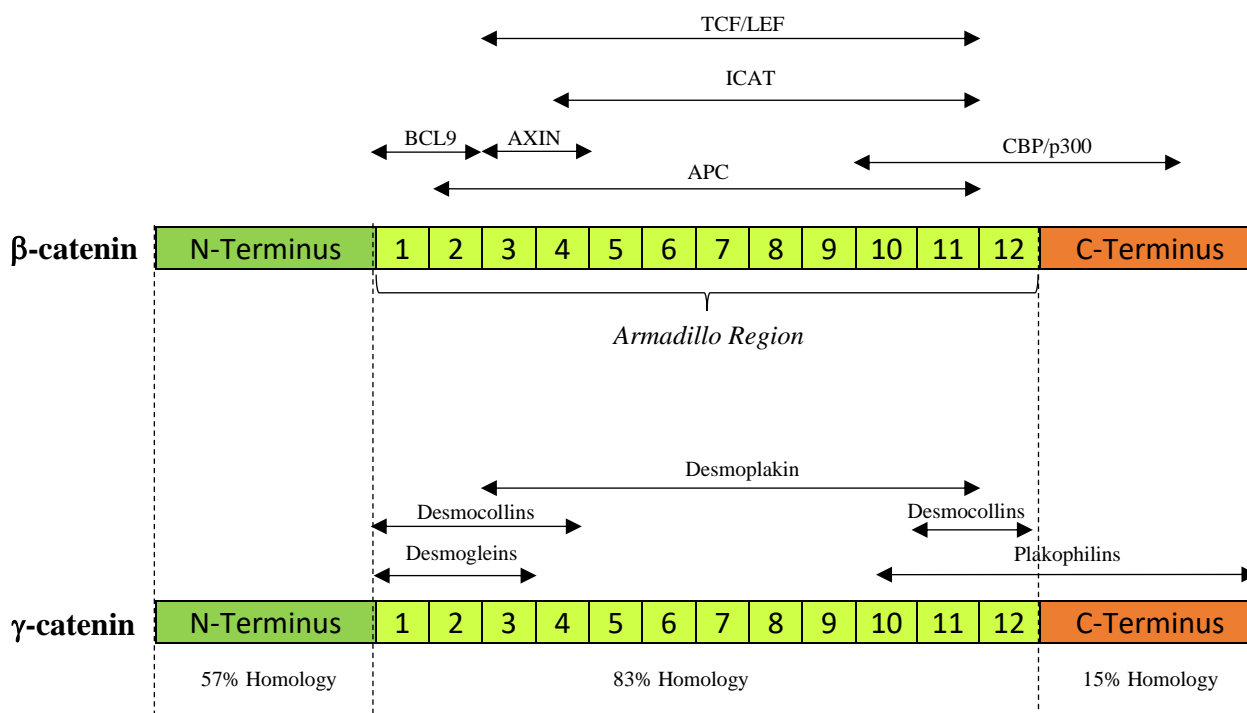


Figure 1-4: The Structure of Beta-catenin and Gamma-catenin

A schematic representation of β -catenin (top) and γ -catenin (bottom) from the N-terminus, through the twelve repeating components which generate the rigidly folded armadillo repeat domain, and finally the C-terminus. Binding sites for interaction partners are indicated, alongside the homology within each sub-region of γ -catenin to β -catenin.

TCF/LEF – T-cell Factor/Lymphoid Enhancer factor; **APC** – Adenomatous Polyposis Col

In AML cell lines, overexpression of LEF1 promoted β -catenin translocation, whereas knockdown of LEF1 inhibited its translocation (Morgan *et al.*, 2019). It has also been proposed that γ -catenin promotes nuclear accumulation of β -catenin in AML cells through an unknown mechanism (Morgan *et al.*, 2013).

1.3.2.2 γ -catenin

γ -catenin is encoded by the *JUP* gene located at chromosome 17q21. In total, 12 transcript variants are recognised, with 10 encoding protein; of these, 3 encode full length γ -catenin (745 amino acids) (Whitlock *et al.*, 2000). *JUP* variants average 13 exons. γ -catenin is a homolog of β -catenin and shares a highly similar structure, including ligand binding capacities (**Figure 1-4**). γ -catenin is a component of adherens junctions and desmosomes, playing an integral role in regulation of cell-cell adhesion in epithelial cells. γ -catenin also harbours a N-terminal β -TrCP binding motif, indicating a shared ancestry and destruction processing system as β -catenin (Sadot *et al.*, 2000). This has enabled speculation that γ -catenin can act compensatively to β -catenin as an inbuilt mechanism of redundancy, an observation well established at adherens junctions, but contentious in WNT/ β -catenin signalling (Wickline, Du, Donna B. Stolz, *et al.*, 2013). However, the C-terminal transactivator motif is absent in γ -catenin, suggesting limited transactivation potential and the proposal that γ -catenin serves to inhibit the WNT/ β -catenin pathway (Aktary *et al.*, 2012). Inhibition of WNT/ β -catenin signalling by γ -catenin has been reported in numerous contexts (Garcia-Gras *et al.*, 2006; Williamson *et al.*, 2006). The binding capabilities of γ -catenin are weak for common binding partners of β -catenin, in particular LEF1, which is poorly recruited by γ -catenin. Whilst overexpression of LEF1 induced nuclear translocation of β -catenin, no effect was observed for γ -catenin (Simcha *et al.*, 1998).

Overexpression studies of β -catenin and γ -catenin have observed significant increases in WNT reporter assays for the former, but not latter member, indicating little involvement of γ -catenin; this was supported by the absence of any detectable γ -catenin-TCF/LEF complexes, though heightened γ -catenin expression levels increased β -catenin levels, leading to an indirect elevation in WNT reporter response (Klymkowsky *et al.*, 1999; Zhurinsky *et al.*, 2000). In other *in vitro* models, γ -catenin-TCF/LEF complexes were detected, and it was found these were capable of inducing very weak WNT/ β -catenin signalling activity independent of β -catenin; however, it was also found that γ -catenin was able to directly bind and inhibit β -

catenin-TCF/LEF complexes, as TCF4 contains independent binding sites for each catenin member, enabling simultaneous association (Miravet *et al.*, 2002). This indicates that γ -catenin can act to suppress excessive WNT/ β -catenin; inversely γ -catenin can activate WNT/ β -catenin signalling when β -catenin levels are low or not localised to the nucleus. Hence, a spatiotemporal influence over WNT regulation is suggested. However, inducible Cre-*lox* knockout murine studies of β -catenin have demonstrated no compensative effect from γ -catenin (Haegel *et al.*, 1995; Teulière *et al.*, 2004). Whilst these results are compelling, Cre-*lox* methods are incapable of complete knockout; however, as with β -catenin, knockout of γ -catenin is embryonically lethal and, as such, these were the best methods available. Curiously, the resulting mechanism of embryonic lethality presentation differs, with β -catenin associated with ectodermal migration failure, whilst γ -catenin results in cardiac structure defects.

In AML patients, γ -catenin is frequently overexpressed and may promote the stabilisation and nuclear translocation of β -catenin (Morgan *et al.*, 2013). Elevated γ -catenin has also been shown to promote the self-renewal capacity of AML cells (Zheng *et al.*, 2004; Qian *et al.*, 2020). It is also possible that elevated γ -catenin levels saturate the potentially shared destruction complex, thus indirectly stabilising β -catenin (Salomon *et al.*, 1997). Conversely, stimulation of WNT/ β -catenin signalling in a β -catenin knockout murine model resulted in increased γ -catenin levels (Berge *et al.*, 2011).

Extrinsic to a role in WNT/ β -catenin signalling, γ -catenin has an established role for interacting with p53 and regulating gene expression (Aktary *et al.*, 2013). This interaction is integral for its capacity to reduce cell growth, migration, and invasion (Alaee *et al.*, 2016). Considering that γ -catenin is frequently downregulated in solid tumours, and that p53 is frequently mutationally inactivated in tumours, indicates a tumour suppressive role for γ -catenin which is perhaps relevant in haematological malignancies.

In haematopoiesis, the involvement and requirement of γ -catenin remains contentious. Numerous studies observed functioning haematopoiesis independent of γ -catenin (Jeannet *et al.*, 2008a; Koch *et al.*, 2008a); however, knockdown of γ -catenin has been reported to inhibit monocyte lineage differentiation of normal human progenitors *in vitro*; the authors showed that this was due to reduction in the expression of the WNT target gene, *PU.1*, a master regulator of myeloid development (Morgan *et al.*, 2013).

Further research into γ -catenin is necessary to reveal precise roles in AML and haematopoiesis both independent of and in contribution to WNT/ β -catenin signalling.

1.3.3 Regulation of the Canonical WNT/ β -catenin Pathway

WNT/ β -catenin signalling is a strictly regulated pathway through the modulation of a series of ligands, receptors, and TF which enable changes to target genes. The central mediator of WNT/ β -catenin signalling, β -catenin, is constitutively degraded in the absence of a WNT ligand agonist, such as WNT3a, leading to the suppression of the pathway (Stamos *et al.*, 2013). Following activation by the binding of a WNT agonist to membrane bound frizzled (FZD), the co-receptor lipoprotein receptor-related protein 5/6 (LRP6) is recruited to form a ternary FZD/WNT/LRP6 complex (Bilić *et al.*, 2007). The FZD/WNT/LRP6 complex subsequently associates with Dishevelled (DVL) and Axis Inhibition Protein (AXIN) to form a WNT activator complex, coined the WNT signalosome (DeBruine *et al.*, 2017). LRP6 becomes phosphorylated by several kinases, enabling binding of GSK3 β , which ultimately re-localises the β -catenin destruction complex to the cytoplasmic membrane. GSK3 β induces self-inhibition in this process, as a conformational change is promoted, switching the molecular target of GSK3 β from β -catenin to LRP6. This also results in the rearrangement of the destruction complex, thus facilitating membrane-localised association with LRP6 in a process that attenuates GSK3 β -induced β -catenin destruction (Woodgett *et al.*, 2017). As a result, β -catenin accumulates in the cytoplasm before localisation to the nucleus through a mechanism which is not fully understood. Nuclear β -catenin associates with the TCF/LEF TF through its central armadillo region, forming a transcription complex that disassociates the inhibition complex and promotes the expression of WNT target genes, such as cyclin D1 (Jamieson *et al.*, 2014).

In an inactive state, levels of β -catenin are limited by a destruction complex consisting of adenomatous polyposis coli (APC), CK1 α , E3 ligase (E3L), β -TrCP, and GSK3 β which associates with an AXIN-1/2 scaffold (MacDonald *et al.*, 2009; Stamos *et al.*, 2013). Mechanistically, CK1 α phosphorylates Serine 45 on β -catenin and GSK3 β phosphorylates it at Serine 33, 37, and Threonine 41; together, these produce a recognition site for β -TrCP which ubiquitinates β -catenin for subsequent proteasomal degradation (Ranes *et al.*, 2021). GSK3 β also phosphorylates AXIN, modifying it to an open conformational state, further associating with LRP6 and β -catenin (Woodgett *et al.*, 2017). In the absence of nuclear β -

catenin, WNT target genes are suppressed by a complex consisting of Groucho, transducin-like enhancer protein 1 (TLE), histone deacetylases (HDAC) and CtBP (Stamos *et al.*, 2013).

In addition to the above regulatory mechanism, inactivation of WNT/ β -catenin is also achieved by competitive binding of WNT mimics to the receptor FZD forming a complex which attenuates WNT ligand activity without inducing intracellular propagation of the pathway. Recognised WNT mimics include WNT inhibitory factor (WIF), Dickkopf-related protein 1 (DKK1), and a family of soluble frizzled-related proteins (sFRP) (Niida *et al.*, 2004; Galli *et al.*, 2006; Poggi *et al.*, 2018). Within the cytoplasm, modulation of Tankyrase is able to regulate the propagation of FZD/WNT signals by stabilising AXIN (Huang *et al.*, 2009). Within the nucleus, the β -catenin interacting protein (ICAT) is able to inhibit association of β -catenin to transcription complex members TCF/LEF and attenuates target gene activation (Tago *et al.*, 2000; Daniels *et al.*, 2002).

Mechanistically, all members of the CK1 family regulate WNT/ β -catenin; however, the exact individual roles are incompletely understood owing to similar kinase specificities, with CK1 members demonstrating negative or positive regulation of WNT/ β -catenin. CK1 α is a member of the β -catenin destruction complex involving AXIN phosphorylation, as previously mentioned, but it is also capable of phosphorylation LRP6 at Serine 1420 and Serine 1430, resulting in the negative regulation of the WNT signalosome by disassociation of CK1 ϵ from the complex, attenuating active WNT/ β -catenin signalling (Swiatek *et al.*, 2004). CK1 ϵ is a positive regulator of WNT/ β -catenin signalling through several distinct but incompletely understood mechanisms. CK1 ϵ is constitutively inactivated by association to LRP6; however, CK1 ϵ is released from LRP6 upon activation via a WNT ligand (del Valle-Perez *et al.*, 2011). CK1 ϵ phosphorylates both LRP6 and DVL independently to significantly enhance binding affinity between the two molecules, resulting in association and formation of the FZD/WNT/LRP6 complex (Wong *et al.*, 2003; Swiatek *et al.*, 2006; del Valle-Perez *et al.*, 2011). It has also been suggested CK1 ϵ associates with β -catenin to increase its stabilisation, thus increasing its association to TCF members (Lee *et al.*, 2001). The regulatory subunit of CK1 ϵ was recently identified as DDX3, which becomes associated upon WNT ligand activation, thereby directly stimulating kinase activity and β -catenin stabilisation (Cruciat *et al.*, 2013). CK δ has been suggested to act comparably to CK1 ϵ , possibly as a mechanism of redundancy (Gu *et al.*, 2013; Cruciat, 2014). Following CK1 ϵ phosphorylation of DVL, CK γ

is able to associate with DVL enabling further phosphorylation of LRP6 at Threonine 1479, a process critical to AXIN recruitment (Zeng *et al.*, 2008).

It is increasingly proposed that WNT ligands are capable of acting in multiple discrete subpathways, and that these are integrated rather than discrete (van Amerongen *et al.*, 2009; Van Amerongen *et al.*, 2012). For instance, WNT/ β -catenin and WNT/ Ca^{2+} are believed to act in consort as elevated intracellular Ca^{2+} is suggested to be necessary for β -catenin translocation into the nucleus (Thrasivoulou *et al.*, 2013a; Ashmore *et al.*, 2019). This suggests the full mechanism by which WNT/ β -catenin is regulated remains to be elucidated.

1.3.4 WNT/ β -catenin in Haematopoiesis

The WNT/ β -catenin pathway has proposed roles in self-renewal and maintenance of HSC, in addition to roles in haematopoiesis, such as lineage fate decisions, differentiation, and proliferation. However, the role of WNT/ β -catenin in haematopoiesis remains contentious, with evidence supporting both the absolute necessity and dispensability of the pathway. WNT/ β -catenin is active in normal human haematopoiesis and is believed to enhance HSC self-renewal and facilitate lineage commitment (Reya *et al.*, 2003; Fleming *et al.*, 2008a; Luis *et al.*, 2011); however, recent studies conflict over the absolute requirement of WNT/ β -catenin in this process (Cobas *et al.*, 2004a; Koch *et al.*, 2008a; Lento *et al.*, 2014).

HSC self-renew to maintain a pool throughout life. Early *in vitro* studies, in which HSC were cultured in conditioned media supplemented with WNT ligands WNT1, WNT5a, and WNT10b, showed a significant expansion of the HSC population, suggesting that WNT signalling provided a survival and proliferative advantage to HSC (Austin *et al.*, 1997). Follow-up studies characterising the expression of WNT ligands in haematopoietic cells and cells present within the niche found that only WNT5a was expressed within the HSC population, and that the stromal support cells further expressed and secreted WNT2b, WNT5a, and WNT10b exclusively (Stoddard, 2009). However, WNT5a in the classical model is a promoter of non-canonical WNT signalling and leads to inhibition of WNT/ β -catenin signalling (Nemeth *et al.*, 2007). Subsequent research examined the WNT/ β -catenin pathway more specifically in HSC maintenance and haematopoiesis.

Early efforts to examine WNT/ β -catenin signalling specifically involved the inhibition of GSK3 β , which attenuates the degradation of β -catenin. Inhibition of GSK3 β with CHIR-911 resulted in enhanced self-renewal of human HSC *in vivo* in immunodeficient mice, and

expanded the HSC population *in vitro* (Trowbridge *et al.*, 2006). This was followed by the discovery that GSK3 β inhibition maintained stemness traits of the HSC population (Holmes *et al.*, 2008). However, GSK3 β also regulates several other signalling pathways such as the TGF β , Hedgehog and Notch pathways (Kockeritz *et al.*, 2012), and hence, a more precise modulation of WNT/ β -catenin was necessary. Culture of HSC supplemented with WNT3a was shown to reduce their self-renewal capacity (Malhotra *et al.*, 2008). However, *in vivo* research established that WNT3a maintained HSC characteristics whilst WNT5a promoted differentiation of HSC, suggesting a complex balance of WNT activity exists to regulate maintenance and differentiation of HSC (Malhotra *et al.*, 2008) making interpretation of the effects of individual WNT ligands difficult.

To overcome such limitations, transgenic mice expressing constitutively active- β -catenin form were developed. In one such study an expansion of the HSC population by 100-fold was observed, with significantly enhanced self-renewal capacity and long-term maintenance (Reya *et al.*, 2003). However, similar research reported that constitutive activation of β -catenin established a significant reduction to self-renewal potential and long-term maintenance (Kirstetter *et al.*, 2006; Scheller *et al.*, 2006). β -catenin has essential roles in embryogenesis, hence targeted inducible gene deletion methods have been applied *in vivo* to examine the absolute requirement of β -catenin. Early *in vivo* gene ablation research established β -catenin as redundant in haematopoiesis (Cobas *et al.*, 2004a), with further studies again finding no requirement for β -catenin nor its close homolog γ -catenin (1.3.2.2) (Jeannet *et al.*, 2008b; Koch *et al.*, 2008b). However, TCF/LEF activity remained detectible, suggesting the Cre-*lox* deletion of β -catenin and γ -catenin was incomplete raising the possibility that sufficient functional protein remained to sustain HSC and associated characteristics (Jeannet *et al.*, 2008b). Subsequent research established that WNT/ β -catenin was essential for LT-HSC self-renewal and maintenance, with a phenotype often only presenting in secondary transplantation experiments (Fleming *et al.*, 2008b; Tiago C. Luis *et al.*, 2009). These findings suggest WNT/ β -catenin is required to maintain long-term self-renewal.

It has been proposed that dose dependent phenotypes could explain the discrepancies between studies, with low WNT/ β -catenin activity enhancing HSC self-renewal, whilst high WNT/ β -catenin activity impairs HSC self-renewal and blocks terminal differentiation (Luis *et al.*, 2012). It was recently suggested that a gradual shift exists from a reliance upon canonical WNT pathway in foetal haematopoiesis to a greater reliance upon the non-canonical WNT

pathway throughout life. This was classified into three divisions: in foetal development, canonical WNT responds to WNT3a and is essential for foetal haematopoiesis; in young adults, haematopoiesis relies upon a balance of canonical and non-canonical WNT signalling activity to maintain HSC self-renewal and quiescence; lastly, in the elderly, HSC become near entirely reliant upon non-canonical WNT and the loss of repopulation potential occurs in parallel with a disproportionate myeloid preference to haematopoiesis, predisposing to AML (Chen *et al.*, 2018). Mechanistically, this is derived from the skewing of canonical WNT ligand WNT3a to the non-canonical WNT5a ligand with increasing age. Mostly notably, it was discovered that non-canonical WNT signalling is suppressed during stress conditions whilst canonical WNT signalling is enhanced, suggesting the latter provides the capacity to tolerate short-term high-stress conditions (Sugimura *et al.*, 2012). Irrespective of the role of WNT/ β -catenin in haematopoiesis, WNT/ β -catenin signalling has been shown to be frequently dysregulated in AML, potentially contributing to leukaemogenesis, drug resistance, and relapse of disease (1.3.5). A further consideration is the activation of subsequent pathways; for instance, it is known WNT/ β -catenin activity directly upregulates Notch signalling, with both critical to HSC self-renewal (Mikesch *et al.*, 2007).

1.3.5 WNT/ β -catenin Activity in Acute Myeloid Leukaemia

WNT/ β -catenin signalling has well characterised roles in the generation and maintenance of several cancers, most notably colorectal (Johnson *et al.*, 2005). Mechanistically, the source of pathway activation can be intrinsic to the cell of interest, which can further be deemed direct, such as a destruction avoidance mutation in β -catenin, or indirect, such as a mutated destruction complex member. Alternatively, the source can be extrinsic to the cell type in question, such as activating mutations of β -catenin in osteoblasts driving AML leukaemogenesis (Kode *et al.*, 2014). Whilst inactivating mutations of APC are frequent in colorectal cancer (CRC), genetic mutations of the WNT/ β -catenin pathway are almost never observed in AML (Johnson *et al.*, 2005; Fujikura *et al.*, 2018). Despite the absence of intrinsic WNT/ β -catenin activating mutations in HSC or LSC, gene expression studies have frequently identified the WNT signalling pathway as a principally dysregulated pathway in AML (Daud *et al.*, 2012). This is most pronounced in gene expression studies of LSC (Majeti, Becker, *et al.*, 2009).

Expression of WNT ligands has been detected in AML patient BM biopsy samples that are not observed in HSC, including WNT1, and critically WNT3a (Simon *et al.*, 2005a;

Kawaguchi-Ihara *et al.*, 2008). In addition, LEF1 (Metzeler *et al.*, 2012), FZD4 (Tickenbrock *et al.*, 2008), and TCF4 (In't Hout *et al.*, 2014) are observed to be upregulated relative to normal HSC, whilst GSK3 β (Abrahamsson *et al.*, 2009), and sFRP family members were suppressed (Guo *et al.*, 2017). Numerous studies have found β -catenin is overexpressed at mRNA and protein levels in 40-60% of patients, though the levels are highly heterogenous, with heightened β -catenin associated with poor clinical outcomes (Ysebaert *et al.*, 2006; Chen *et al.*, 2009). In normal HSC, overexpression of β -catenin has been shown to block multilineage differentiation and expand the immature cell population, mimicking the AML phenotype (Reya *et al.*, 2003; Kirstetter *et al.*, 2006).

Common aberrant mutations in AML have been linked to dysregulation of WNT pathway components. For example, patients with *FLT3-ITD* mutations often present elevated β -catenin levels due to upregulation of FZD4; this results in the elevated expression of WNT target genes and enhanced proliferation in an *in vitro* cell line model (Tickenbrock *et al.*, 2005). *NPM1* mutations were found to facilitate excessive WNT/ β -catenin signalling activity, as confirmed by repression through the expression of the WNT inhibitor DKK1 in zebrafish; this was further confirmed in AML blasts presenting *NPM1* mutations (Barbieri *et al.*, 2016). Dishevelled-axin domain containing 1 (*DIXDC1*) protein was recently identified as overexpressed in AML in both cell lines and patient blasts (Xin *et al.*, 2018). *DIXDC1* was found to elevate β -catenin levels with associated enhanced growth *in vitro* in cell lines (Xin *et al.*, 2018). Phosphatase of regenerating liver-3 (*PRL-3*) has been implicated in LSC for contributing to excessive WNT/ β -catenin signalling as the substrate of *PRL-3*, *LEO1*, can bind and promote the nuclear accumulation of β -catenin (J. Zhou *et al.*, 2017; Chong *et al.*, 2019). *PRL-3* is expressed in 47% of AML samples but absent in HSC (Zhou *et al.*, 2011). Remaining sources of excessive WNT/ β -catenin signalling are found in hypermethylation of inhibitors, with 90% of primary AML samples harbouring at least one hypermethylated WNT inhibitor gene: *sFRP2* (66%), *sFRP5* (54%), *sFRP1* (34%), *WIF1* (32%), *SOX17* (29%), *RUNX3* (27%), *DKK1* (16%) (Griffiths *et al.*, 2010a).

While activating mutations are rare in AML, they have been reported in approximately 40% of osteoblasts, which has been established to generate AML in an *in vivo* mouse model (Raaijmakers *et al.*, 2010; Kode *et al.*, 2014). Further, transplantation of wildtype (WT) HSC into mice harbouring deleterious APC mutations within BM components induced WNT/ β -catenin signalling activity in these cells and facilitated the generation of myelodysplastic syndrome (MDS), which is known to occasionally transform in to AML (Stoddart *et al.*, 2017).

However, it has been proposed that LSC possess intrinsic activation of WNT/ β -catenin, demonstrating independence from niche-derived signals (Lane *et al.*, 2011).

It has been speculated that WNT/ β -catenin activity generates the *RUNX1::RUNX1T1* translocation by transcriptional and spatial translocation of both genes (Ugarte *et al.*, 2015). Further, fusion genes such as *RUNX1::RUNX1T1*, *PML::RARA*, and *PLZF1::RARA* have been demonstrated to upregulate genes involved in promoting WNT/ β -catenin signalling. *LEF1* is overexpressed frequently in AML particularly in *RUNX1::RUNX1T1* patients (Morgan *et al.*, 2019). Ectopic expression of *LEF1* or a constitutively active form of *LEF1* were both able to induce leukaemia *in vivo* (Petropoulos *et al.*, 2008). γ -catenin, a close homolog of β -catenin, is overexpressed in AML and is implicated for acting similarly to β -catenin in addition to promoting β -catenin nuclear localisation (Morgan *et al.*, 2013). The fusion proteins *RUNX1::RUNX1T1*, *PML::RARA*, and *PLZF1::RARA* have further been implicated in driving an overexpression of γ -catenin in primary tissue (Müller-Tidow *et al.*, 2004; Mikesch *et al.*, 2007). In addition, *FLT3* mutations have also been suggested to increase β -catenin nuclear localisation indirectly through γ -catenin, (X. Jiang *et al.*, 2018a). Moreover, studies have demonstrated elevated nuclear localised β -catenin in relapsed AML versus *de novo* diagnosis suggesting a role in relapse (Griffiths *et al.*, 2015). However, a recent study utilising a Cre-*lox* deletion method *in vivo* in an AML mouse model found no consequence to maintenance or self-renewal even after deletion of β -catenin, γ -catenin, and the entire TCF/LEF family of TCF1 (*TCF7*), LEF1 (*LEF1*), TCF3 (*TCF7L1*), and TCF4 (*TCF7L2*) (X. Zhao *et al.*, 2020).

1.3.6 WNT/ β -catenin-derived Resistance to Standard Chemotherapeutic Agents

Active WNT/ β -catenin has been linked to chemoresistance to DNR (Xiao *et al.*, 2020), and Ara-C (L. Chen *et al.*, 2020). Further, γ -catenin overexpression has been associated with poor prognosis, and knockdown of γ -catenin has sensitised AML cell lines to Ara-C (Qian *et al.*, 2020). LRP6 has been targeted with Niclosamide, increasing Ara-C sensitivity *in vitro* and efficacy *in vivo* (Kamga *et al.*, 2020). Therefore, silencing of WNT/ β -catenin has the potential to sensitise cells to chemotherapeutic agents.

P-glycoprotein (PGP), encoded by the WNT/ β -catenin target gene *ABCB1*, is one of several proposed mechanisms by which activated WNT/ β -catenin can induce chemoresistance. PGP is a member of the ATP-binding cassette (ABC) transporter superfamily, specifically the multi-drug resistance (MDR) subfamily, and is an ATP-dependent drug efflux pump with broad

specificity (Steinbichler *et al.*, 2018). PGP is well recognised for its capability to expel a broad range of chemotherapeutic agents from cancer cells. PGP activity has been observed in 58% of AML patients, in which it proved a poor prognostic indicator and was associated with worse overall and event free survival (Singh *et al.*, 2010; Gréen *et al.*, 2012; Shaffer *et al.*, 2012; Corrêa *et al.*, 2014; Boyer *et al.*, 2019). HSC express high *ABCB1* levels and this is also found in LSC (Shaffer *et al.*, 2012; Corrêa *et al.*, 2014). *ABCB1* is a target of β -catenin/TCF4 transcriptional promotion, with the *ABCB1* promoter containing repeating TCF4/LEF1 binding motifs, suggesting a direct modulation of chemoresistance by WNT/ β -catenin (Martin-Orozco *et al.*, 2019). PGP inhibitors (such as Zosuquidar) have been used to improve uptake of DNR (Tang *et al.*, 2008). The exact mechanism of PGP upregulation is disputed, with several WNT-derived mechanisms proposed to induce *ABCB1* expression. For example, *FZD1* has been reported to upregulate *ABCB1* through WNT/ β -catenin, with knockdown of *FZD1* reducing WNT signalling and *ABCB1* levels (Corrêa, Binato, Du Rocher, Morgana T.L. Castelo-Branco, *et al.*, 2012). Interestingly in AML, elevated *FZD1* has been associated with poor remission rates and relapse (Wang *et al.*, 2018).

The S100 family are calcium-binding cytosolic proteins with a wide range of intracellular and extracellular functions. S100A4 is a WNT/ β -catenin target gene that is frequently overexpressed in AML and has been associated with resistance to doxorubicin (Dong *et al.*, 2018; Alanazi *et al.*, 2020). S100A8 and S100A9 are frequently overexpressed in AML and convey resistance to Venetoclax by inhibiting the migration of Ca^{2+} to the mitochondrion to inhibit apoptosis, alongside resistance to doxorubicin and vincristine (Yang *et al.*, 2012a; Karjalainen *et al.*, 2019). S100A8 and S100A9 are upregulated in AML in a dose-dependent manner following treatment with DNR (Stewart *et al.*, 2018), etoposide (Yang *et al.*, 2016), and vincristine (Yang *et al.*, 2012b). Critically, S100A8 and S100A9 are recognised to promote WNT/ β -catenin signalling and are suspected target genes (Duan *et al.*, 2013).

Cell-cell communication is another important consideration as a driver of chemoresistance in AML. WNT/ β -catenin activity is observed in leukaemic, epithelial, mesenchymal, and other cells within normal and diseased BM (Malhotra *et al.*, 2009). It is recognised that extracellular vesicles can transport WNT ligands, such as WNT3a, suggesting another mechanism of cell-cell communication (McBride *et al.*, 2017). A summary of WNT/ β -catenin involvement in AML is shown in **Figure 1-5**.

1.3.7 Therapeutic Targeting of WNT/ β -catenin

As WNT/ β -catenin signalling is implicated in the self-renewal, proliferation, and metastatic dissemination of several cancers, substantial effort has been made to generate targeted therapies aimed at silencing pathway activity to improve patient outcomes. Much of this research is in the context of solid tumours which have a well characterised WNT/ β -catenin component; however, limited studies are ongoing in AML (**Table 1-5**).

Research into targeted therapeutics for WNT/ β -catenin began two decades ago. As the WNT/ β -catenin pathway became increasingly well characterised, a continual progression in the development of agents able to target specific molecules within the pathway has followed (Emami *et al.*, 2004). Whilst WNT/ β -catenin signalling is continuously activated in numerous cancers, the mechanism by which this occurs varies between disease, and even within subtypes of each disease. This complexity has required the development of targeted therapeutics encompassing the WNT ligand:receptor interface, activators of the β -catenin destruction complex, inhibitors of the β -catenin:TCF/LEF transcription complex, and target gene suppression (**Figure 1-6**). Targeting WNT target genes, such as the S100 family calcium-binding protein *S100A4*, via Niclosamide inhibition of WNT/ β -catenin signalling is currently in a phase II clinical trial in CRC after demonstration of efficacy *in vivo*; results are yet to be released (Burock *et al.*, 2018).

Despite substantial efforts, no WNT inhibitors have been approved by the FDA or the Medicines and Healthcare Regulatory Agency (MHRA, UK) (Morris *et al.*, 2021). Poor efficacy has been the predominant reason therapies have been abandoned, however, the safety of targeting WNT/ β -catenin, specifically regarding haematopoiesis and other essential functions within the body which could rely upon WNT/ β -catenin signalling, remains a concern (Y. Zhang *et al.*, 2020a). This highlights the need to fully elucidate the requirement of WNT/ β -catenin to haematopoiesis to determine the viability of targeting the pathway in AML (Kahn, 2014; Pai *et al.*, 2017; Cui *et al.*, 2018).

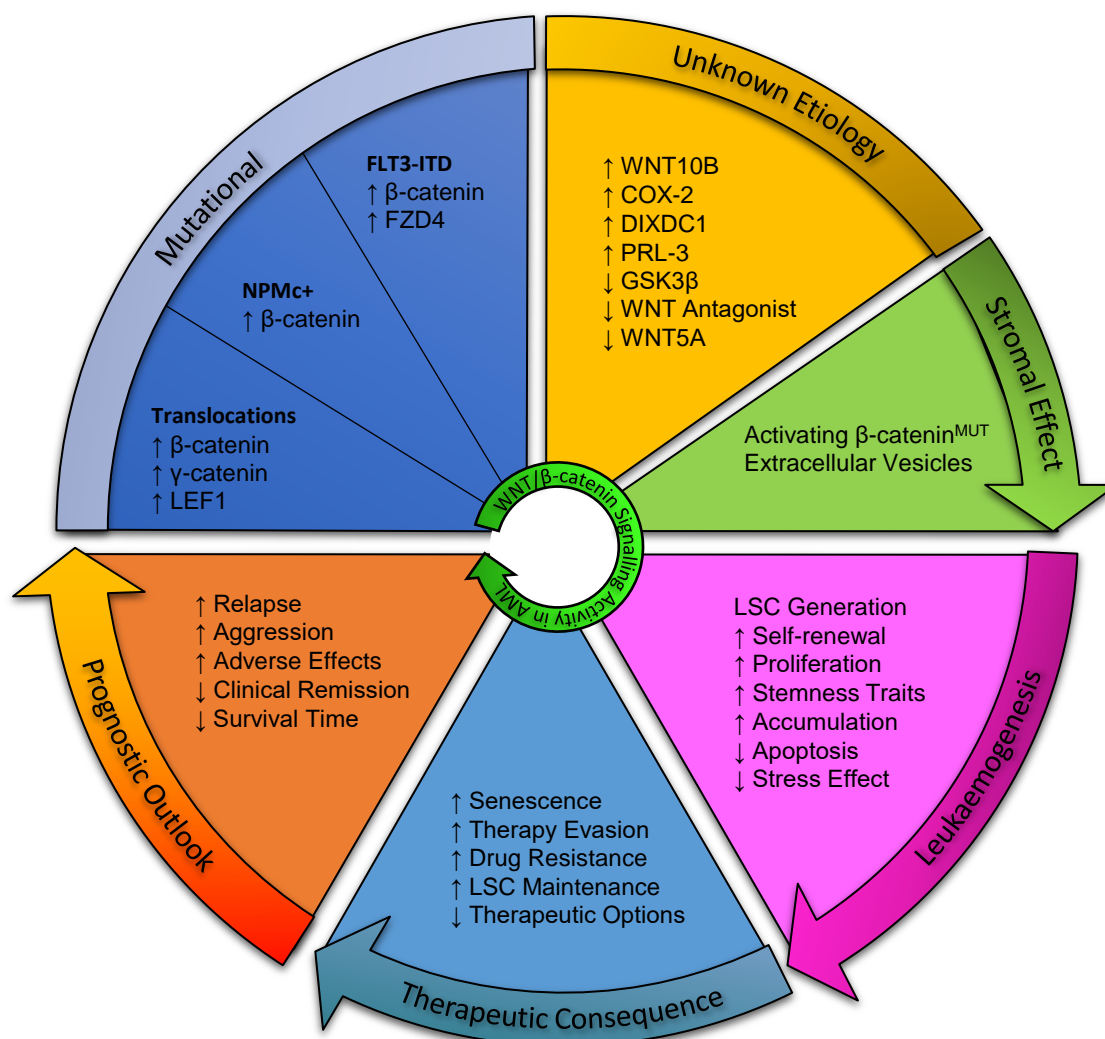


Figure 1-5: Involvement of WNT/β-catenin Signalling in AML

A summary of confirmed and speculated mechanistic events which result in activation of the WNT/β-catenin signalling pathway, and the consequent effect upon leukaemogenesis, therapeutic consequence, and prognostic outlook. Unknown etiology represents altered expression validated by mRNA and protein analyses, but without mechanistic understanding at current. Adapted from (Gruszka *et al.*, 2019).

Table 1-5: Targeted Therapies for WNT/ β -catenin in Preclinical or Clinical Trials

A table detailing the current targeted therapies against the WNT/ β -catenin pathway in preclinical and clinical trials. Adapted from (Jung *et al.*, 2020; Y. Zhang *et al.*, 2020b; Yu *et al.*, 2021).

Therapeutic Target	Therapeutic Name(s)	Clinical Trial ID	Disease(s)	
β -Catenin Degradation Promoters	KYA1797K/ KY1220	Preclinical	BC, CRC	
	BC2059	NCT03459469	DT	
	SM08502	NCT03355066	ST	
	iCRT14	Preclinical	ALL	
β -Catenin:TCF/LEF Association Inhibitors	LF3	Preclinical	CRC	
	iCRT3/5	Preclinical	CRC	
	ZINC02092166	Preclinical	CRC	
	NLS-StAx-h	Preclinical	CRC	
CBP/ β -Catenin Antagonist	PRI-724	NCT01606579	AML	
	GNE-781	Preclinical	AML	
	ICG001	Preclinical	AML	
CK1 α Activator	SSTC3	Preclinical	CRC	
CK1 δ Inhibitor	Umbralisib	NCT04163718	CLL, HL	
DKK1 mAb	DKN-01	NCT03645980	HCC	
DVL Inhibitor	FJ9	Preclinical	OC, LC	
	3289–8625	Preclinical	OC, BC	
FZD-1, 2, 5, 7, 8 mAb	OMP-18R5	NCT01345201	ST	
FZD10 Antagonist	90 γ -OTSA-101	NCT01469975	BC, PC, CRC	
FZD7 Antagonist	Fz7-21	Preclinical	HCC, CRC	
FZD8 Decoy Receptor	OMP-54F28	NCT01608867	ST	
GSK3 β Inhibitor	LY2090314	NCT01214603	AML	
LRP5/6 Inhibitor	Salinomycin	Preclinical	CLL	
Pan-FZD Receptor mAb	OMP-18R5	NCT01973309	ST	
	ETC-159	NCT02521844	CRC	
	WNT974	NCT02649530	CRC	
	RXC004	NCT03447470	ST	
	CGX1321	NCT03507998	CRC	
	IWP-2/IWP-4	Preclinical	AML	
PORCN Inhibitor	CGX-1321	NCT02675946	CRC	
	ROR1 mAb	UC-961	NCT02222688	CLL, SLL, BC
	SAM68 Inhibitor	CWP291	NCT01398462	AML
		XAV939	Preclinical	AML
	Tankyrase Inhibitor	IWR-1	Preclinical	APL
		XAV939	Preclinical	OS, CRC
JW74/ JW55		Preclinical	HC, CRC	
NVP-TNKS656		Preclinical	CRC	
LZZ-02		Preclinical	CRC	
WNT5a Peptide Mimic	Foxy-5	NCT02020291	BC, PC, CRC	

BC – Breast Cancer; **CRC** – Colorectal Cancer; **DT** - Desmoid Tumour; **ST** – Solid Tumours; **ALL** – Acute Lymphoblastic Leukaemia; **AML** – Acute Myeloid Leukaemia; **CLL** – Chronic Lymphoblastic Leukaemia; **HL** – Hodgkin’s Lymphoma; **HCC** - Hepatocellular carcinoma; **OC** – Ovarian Cancer; **LC** – Lung Cancer; **SLL** - Small lymphocytic lymphoma; **PC** – Pancreatic Cancer

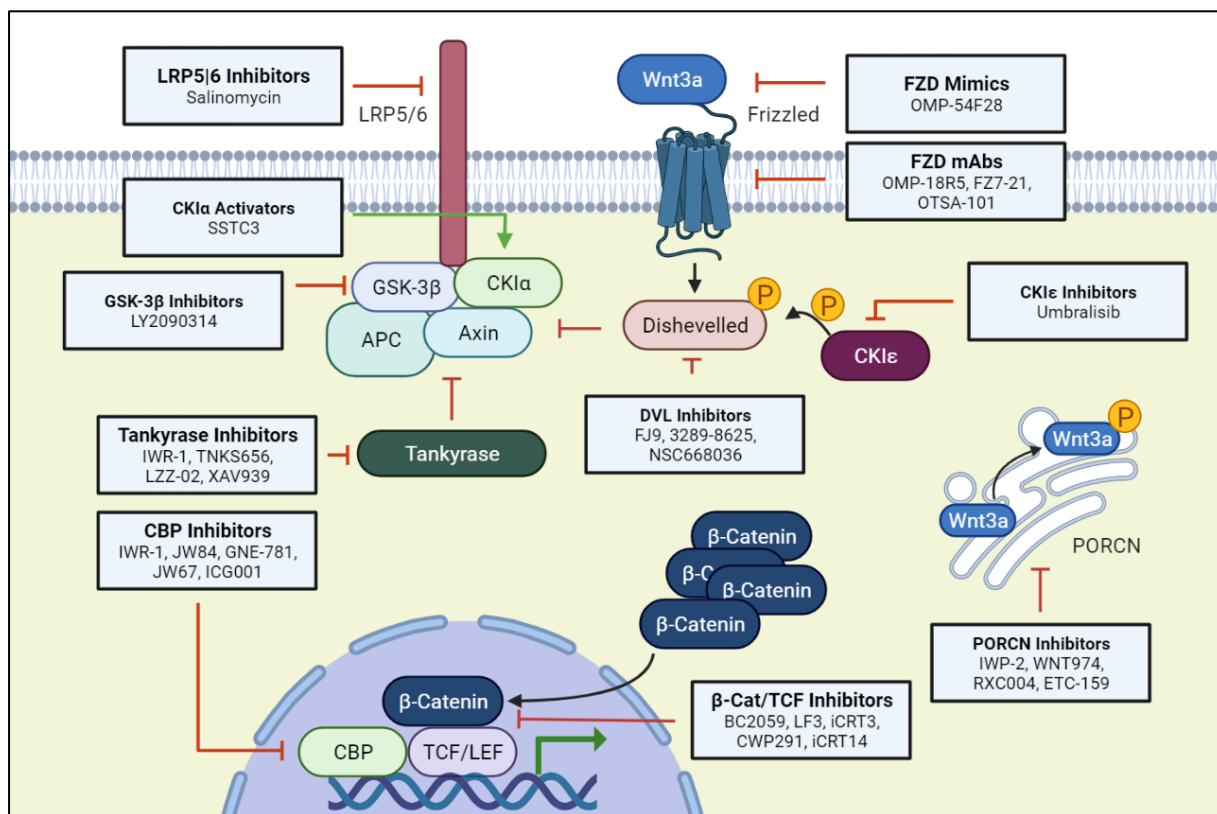


Figure 1-6: Molecular Targets of Therapeutics in WNT/β-catenin Signalling

A demonstration of the multiple molecular targets which targeted therapies are able to inhibit or activate. Many of these targeted therapies are in clinical trials of solid tumours and haematological malignancies (see **Table 1-5**).

CK1ε – Casein Kinase Epsilon; **CK1α** – Casein Kinase Alpha; **GSK3β** - Glycogen synthase kinase-3 beta; **β-catenin** – Beta catenin; **TCF/LEF** – T-cell Factor/Lymphoid Enhancer factor; **APC** – Adenomatous Polyposis Coli; **CBP** - CREB-binding protein; **PORCN** - Porcupine O-Acyltransferase. (PORCN is an endoplasmic reticulum transmembrane protein with roles in the processing of WNT proteins such as WNT3a by performing O-Palmitoylation.)

1.3.7.1 Therapeutic Targeting of WNT/ β -catenin in Colorectal Cancer

In the colon, WNT/ β -catenin is normally active within the lower intestinal crypt which harbours stem cells that maintain the tissue (Novellasademunt *et al.*, 2015). CRC is the archetypal WNT/ β -catenin-derived disease, with 80% of CRC patients harbour inactivating APC mutations, an integral component of the β -catenin destruction complex, enabling excessive β -catenin accumulation and hyperactive WNT/ β -catenin transcriptional activation (Kwong *et al.*, 2009). In the remaining non-APC^{MUT} patients, activating mutations of β -catenin or other WNT members such as TCF4 and LEF1 are found, demonstrating the variable source of WNT/ β -catenin hyperactivity within disease (Morin *et al.*, 1997; Cuilliere-Dartigues *et al.*, 2006). In CRC, abnormal WNT/ β -catenin activation disturbs the normal growth and differentiation of colonic crypt stem cells, generating colorectal cancer stem cells and CRC (Ben-Ze'ev *et al.*, 2016). WNT/ β -catenin signalling mediates chemoradiotherapy resistance, heightens the risk of metastatic dissemination, and enhances relapse potential (M. A. Lee *et al.*, 2014; Páez *et al.*, 2014; Emons *et al.*, 2017) making it an attractive target in this disease.

Therapeutically, repurposing the COX-2 inhibitor Celecoxib, a non-steroidal anti-inflammatory drug (NSAID), reduced relapse risk by 50% in CRC, potentially, at least in part, through the inhibition of WNT/ β -catenin signalling (Arber *et al.*, 2006). However, the precise mechanism is not understood. Monoclonal antibody inhibition of WNT ligand activity has demonstrated upstream attenuation of WNT activity and growth inhibition of CRC cell lines *in vitro* (He *et al.*, 2005). Similar research applying monoclonal antibodies to inhibit FZD receptors also found growth inhibition, self-renewal reduction, and chemosensitisation (Gurney *et al.*, 2012). The β -catenin destruction complex activity has been enhanced with agents such as JW67, JW74 and JW55 (**Table 1-5**), which inhibited growth of CRC cells in a mouse xenograft model (Waalder *et al.*, 2011, 2012). KYA1797K was shown to enhance the binding affinity of β -catenin to the destruction complex, resulting in the suppression of CRC growth (Cha *et al.*, 2016). At the level of pathway activation, DVL has been inhibited with FJ9, aimed at disrupting the association of DVL with FZD, thus attenuating the activation cascade and inducing growth inhibition in *in vitro* cell line models and mouse xenograft models (Fujii *et al.*, 2007). At the level of the TF complex association, numerous compounds have been generated which block the association of β -catenin and TCF4, resulting in growth arrest, apoptosis, improved chemotherapeutic efficacy, and significant reduction of self-renewal of CRC *in vitro* (Gonsalves *et al.*, 2011; Tian *et al.*, 2012; Xie *et al.*, 2012).

1.3.7.2 Therapeutic Targeting of WNT/ β -catenin in Acute Myeloid Leukaemia

Several studies have demonstrated positive outcomes when WNT inhibitors are applied in the context of AML. Both CGP049090 and PFK115-584 (**Table 1-5**), which inhibit the association of β -catenin and LEF1, promoted apoptosis of AML cell lines and primary AML, whilst peripheral blood mononuclear cells were unaffected (Minke *et al.*, 2009). BC2059, an enhancer of β -catenin destruction, has been shown to induce a dose-dependent apoptotic effect in xenograft models with primary AML (Fiskus *et al.*, 2015). The inhibitor of β -catenin-TCF4 association, iCRT3, was also found to inhibit growth of primary AML, though an expansion of the CD34⁺ population was observed, suggesting a more complex outcome than expected (Griffiths *et al.*, 2015).

Four clinical trials of WNT/ β -catenin inhibitors have been reported, with several ongoing. Recently, results were published for the phase I trial of CWP232291 in AML (NCT01398462), a β -catenin degrading molecule which, in a dose-escalation cohort, demonstrated favourable outcomes, with one patient achieving clinical remission (Lee *et al.*, 2020). A phase I study of PRI-724, an AMP-response element binding protein-binding protein (CBP) β -catenin antagonist, was completed in AML in 2016; however, the results were never released (NCT01606579). A clinical trial of OMP-54F28 in ovarian cancer recently demonstrated positive outcomes, although bone toxicity was a concern at optimal dosages (NCT02092363). WNT974 showed single-agent activity with positive outcomes in a Phase I trial with CRC and other solid WNT/ β -catenin-involved cancers (Pancreatic, Melanoma, Breast, Head and Neck Squamous, Cervical, Oesophageal, and Lung) (NCT01351103, (Rodon *et al.*, 2021)).

1.4 CRISPR/Cas9 Genetic Engineering

CRISPR are DNA sequences found within prokaryotic species that are derived from viral DNA fragments (Barrangou *et al.*, 2007). Cas9 is an enzyme which recognizes DNA complementary to the CRISPR sequence, cleaving the foreign DNA strand (Barrangou, 2015). Together, they form a primitive adaptive antiviral defence system known as CRISPR-Cas9 (Redman *et al.*, 2016).

CRISPR-Cas9 has the potential to be employed to enable precise, efficient, and practical genetic editing, thus facilitating the generation of knockout or knock-in mutations of DNA. More recently, CRISPR-Cas9 has been adapted to enable imaging of DNA in live cells, editing of RNA, alongside numerous other developments (Hsu *et al.*, 2014; Zhang *et al.*, 2014; Ishino

et al., 2018). CRISPR-Cas9 relies upon a guide-RNA (gRNA) sequence which defines the target site for DNA binding that must be immediately adjacent to a specific protospacer adjacent motif (PAM) site. The alternate Cas family enzyme Cas12a can be used to recognise different PAM sequence sites, thus overcoming some limitations to DNA targeting. Creation of artificial Cas enzymes have further diversified PAM recognition capacity. Recently, newly developed techniques have enabled targeting of nearly any region of the genome by bypassing the PAM site requirement, though this technique is in its infancy (Christie *et al.*, 2021) (**Figure 1-7**).

Mechanistically, the classical CRISPR-Cas9 knockout method functions following the formation of a ribonucleoprotein complex consisting of gRNA containing a scaffold region which binds to positively charged trenches on Cas9. Complex formation adjusts the Cas9 enzyme into an active DNA-binding conformation, which, following 3'-5' gRNA binding to a sufficiently complementary sequence, cleaves the DNA, leading to a double strand break (DSB) 3-4 nucleotides upstream of the PAM site. DSB are frequently repaired by the efficient non-homologous end joining (NHEJ) mechanism, or by the less efficient, but accurate, homology directed repair (HDR) mechanism. Without a homologous strand as a guide, NHEJ is error-prone, leading to random insertions and deletions (InDel) that lead to reading frame shifts, possibly resulting in nonsense-mediated decay (NMD), a truncated protein, or a full-length non-functional protein. NMD is a conserved surveillance pathway which functions to minimise gene expression errors by removing mRNA transcripts with a premature stop codon. Critically, even if HDR or NHEJ repairs the target site correctly, the site will be recognised and cleaved again by Cas9 leading to an InDel event. However, such frameshift mutations can be tolerated and lead to the production of protein with normal or near normal functional capacity. Therefore, it is critical to generate complete knockout clones which can then be checked for protein expression.

Optimal use of CRISPR-Cas9 relies upon effective selection of a target site and gRNA. Ideally, the gene is targeted at the earliest possible point to maximise the impact of a frameshift mutation and greatly improve the chance of mRNA NMD. The gRNA target must be present in all transcript variants, and the site should not possess a common single nucleotide polymorphism (SNP) which would affect site recognition. It is also possible to delete a large proportion of a gene by utilising two or more gRNA targeting an early and late exon, respectively. The inexpensive nature of CRISPR-Cas9, in combination with the development

of scRNA-seq, has enabled the high-throughput screening of thousands of genes within a disease in a technique known as CRISPR-seq (Dixit *et al.*, 2016).

More recent developments using a deactivated Cas9 (dCas9) was shown to selectively inhibit, or promote, the transcription of target genes in techniques known as CRISPRi-dCas9 and CRISPRa-dCas9, respectively (**Figure 1-7**). At the gene expression level, CRISPRi is able to reduce expression levels by as much as 99%, whilst CRISPRa can increase expression levels by as much as 1000-fold, depending on the recruited transcriptional partners and basal expression levels (Gilbert *et al.*, 2014). To achieve this, the RuvC and HNH nuclease domains of Cas9 are mutationally inactivated to remove the capacity to generate a DSB, whilst retaining the DNA binding capacity. In turn, the gRNA targets the 5' UTR region upstream of the exonic regions of a gene. In place of the DSB activity, transcriptional activators or repressors are recruited to modulate the transcriptional activity of the target gene. Specific design considerations enable multiplexed application of knockout, activation, and repression constructs. This can be achieved by applying orthogonal Cas9 enzymes (Esvelt *et al.*, 2013), truncated gRNA (Dahlman *et al.*, 2015), or engineered gRNA harbouring TF binding sites within hairpin loops, thus enabling specific partner recruitment (Zalatan *et al.*, 2015; Martella *et al.*, 2019; McCarty *et al.*, 2020).

The next generation of CRISPR-Cas9 is at an early stage, and is known as prime editing, which was first described in 2019 (Anzalone *et al.*, 2019). Prime editing functions as a 'search-and-replace' technology using dCas9 and a prime editing gRNA (pegRNA), which contains the site complementary guide in complex with the replacement sequence. Contrary to classical CRISPR-Cas9, no DSB, donor DNA templates, or reliance upon random InDel mutations is necessary; however, the method still requires mismatch repair to incorporate the modified strand into the unedited complementary strand, in order to permanently integrate an edit (Scholefield *et al.*, 2021). Prime editing is believed to suffer minimal off-target effects, whilst reproducibly generating the intended DNA outcome, either an insertion of 44bp, a deletion of 80bp, or a combination of both applications (Nelson *et al.*, 2021). Prime editing is currently within the method development stage and is not widely adopted; nevertheless, the tremendous promise both in the laboratory and clinical setting indicate this technology will eventually supersede classic approaches where appropriate (Matsoukas, 2020).

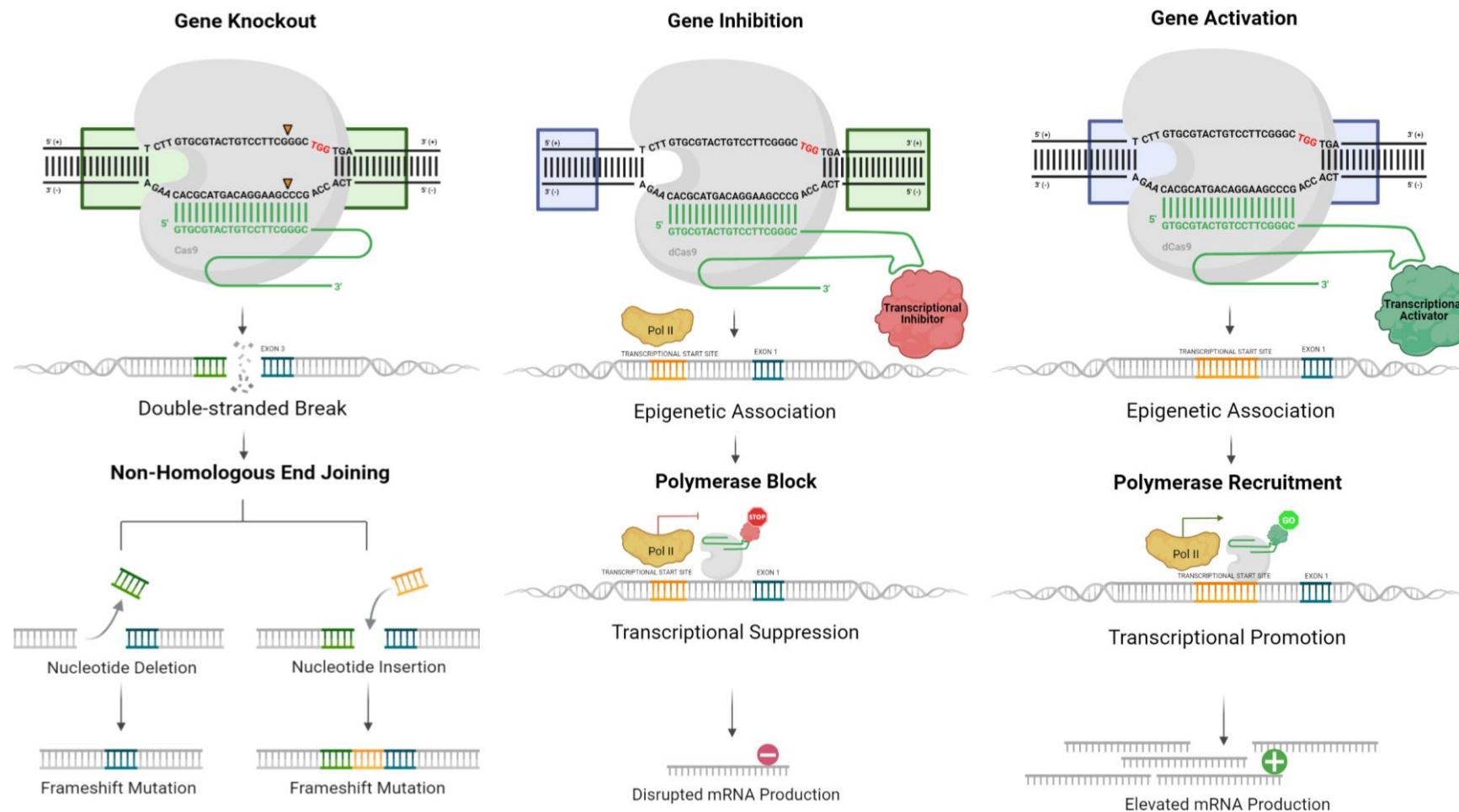


Figure 1-7: Mechanisms of Genetic Knockout, Inhibition, and Activation with CRISPR-Cas9

Gene knockout is facilitated when Cas9 forms a complex with the designed guide RNA (gRNA). The Cas9:gRNA complex binds the Cas9-related PAM recognition site (NGG). A conformational change in Cas9 enables a double strand break to be generated at a specific DNA location (orange arrows). If the damage is repaired by homology directed repair, this will result in correct repair most frequently, however, this will restore the sequence to one which is targeted again. In time, non-homologous end joining will result in an insertion or deletion events resulting in disrupted DNA by frameshift mutation. **Gene inhibition** can be facilitated by engineering the gRNA to contain a binding site to recruit a transcriptional inhibitor and selecting a target site after the gene start site. This enables transcriptional repression by a polymerase block. **Gene activation** can be achieved by engineering the gRNA to contain a binding site to recruit a transcriptional activator and selecting a target site within the genes upstream transcriptional activation site. This enables transcriptional activation by polymerase recruitment resulting in mRNA production. Numerous alternate designs for each respective technique exist.

1.5 Aims and Objectives

The requirement of β -catenin and γ -catenin for WNT/ β -catenin signalling and the necessity of this pathway for normal haematopoiesis and AML maintenance remains a contentious topic within the literature (Cobas *et al.*, 2004a; Serinsöz *et al.*, 2004; Hu *et al.*, 2009; Wang *et al.*, 2010). If β -catenin is critical to AML maintenance, but not haematopoiesis, it would represent an attractive therapeutic target. Previous experiments claiming β -catenin and γ -catenin are dispensable for haematopoiesis and AML have used murine models, which may not appropriately model human cells (1.3.4). For example, the 100-fold HSC expansion documented in murine models upon addition of WNT3a, or expression of constitutively active β -catenin, has not been reproduced in human HSC (Reya *et al.*, 2003; Willert *et al.*, 2003). Another confounding factor is incomplete knockout (Yeung *et al.*, 2010). For instance, human cell line research has relied upon incomplete knockout with small interference RNA (siRNA), leading to discrepancies between findings as differences in remaining β -catenin levels affect phenotype in a dose dependent manner (Jeannet *et al.*, 2008b).

I hypothesise that very low levels of β -catenin are necessary to maintain AML cell survival and proliferation. The levels required would have remained in previous human cell siRNA-based knockdown experiments, and *cre-lox in vivo* research methods. The tools necessary to conclusively determine the role of WNT/ β -catenin signalling in human cells exists in the form of recent advancements in CRISPR-Cas9 technology. By generating complete knockouts, it will be possible to address these discrepancies within the field and evaluate the potential of WNT/ β -catenin signalling as a target for clinical treatment in AML. This aim will be achieved through the following objectives:

Characterise WNT/ β -catenin signalling activity in AML cell lines and the role in normal haematopoiesis.

AML cell lines will first be characterised for WNT/ β -catenin signalling capacity. CRISPR-Cas9 will be utilised to knockout β -catenin and γ -catenin singly and in combination, in order to determine the resulting consequence to AML growth and survival at the bulk level¹. Similarly, CRISPR-Cas9 will be used to study the consequence of knockout in normal haematopoietic cells using CD34⁺ HSPC (**Chapter 3**).

Investigate the role of WNT/ β -catenin signalling activity in AML cell lines and in patient-derived primary AML samples.

Recovery and analysis of complete dual knockout AML cell lines will be performed to examine the consequence to AML features in both WNT/ β -catenin active and inactive cell lines. Specifically, these will be examined for characteristics inherent to WNT/ β -catenin signalling such as proliferation, cell cycle progression, apoptosis, differentiation, drug resistance, and clonogenicity. This will be furthered through the use of several patient-derived primary AML samples which will be studied with CRISPR-Cas9 knockout, in addition to WNT/ β -catenin small molecule inhibitors (**Chapter 4**).

Determine the mechanistic consequence downstream of WNT/ β -catenin signalling at the transcriptomic level and recover clonogenicity *in vitro* in knockout models.

RNA-sequencing of HEL and THP1 AML cell lines treated with WNT3a to generate active WNT/ β -catenin signalling profile will be contrasted with clonal knockout equivalents to allow the assessment of the respective transcriptomic profiles. Integrative analysis will reveal a subset of genes and pathways reciprocally perturbed, thus allowing the identification of candidate genes and pathways for further investigation. The pathways of interest will be investigated *in vitro* to confirm *in silico* findings by recovering expression and assessing clonogenicity and other characteristics (**Chapter 5**).

¹ Here-in, bulk level refers to the CRISPR-Cas9 knockout culture post-selection which contains cells harbouring knockout, incomplete knockout, and cells which have evaded knockout. These are non-clonal in nature.

Chapter 2

Materials and methods

2.1 Cell Culture

2.1.1 Culture of Cell Lines in Suspension

Cell lines were cultured according to individualised culture techniques with media prepared as detailed in **Table 2-1**. Cell lines were verified to be mycoplasma free with the MycoProbe™ detection kit (R&D Systems, CUL001B) and were authenticated with the Eurofins authentication service. All cell culture experiments were undertaken in a Class II biological safety cabinet, with the flow cabinet and equipment decontaminated with 70% ethanol (v/v) before use. Growth media was pre-warmed to 37°C for sub culturing. Cell lines were incubated at 37°C within a humidified atmosphere of 5% CO₂ balance air. Cells were inspected for signs of infection before use. Excess cells were expelled by pipette into a waste bottle containing chlorine at 1250ppm (½ Haz-Tab™) overnight before disposal into an autoclave bin; the strength was doubled to 2500ppm for viral waste.

2.1.2 Culture of Adherent Cell Lines

To isolate adherent cell lines, the spent growth medium was expelled into a waste bottle and 3mL trypsin was pipetted directly to the flask ensuring complete coverage by tilting. After 4 minutes at room temperature (RT), equal volume of growth media (**Table 2-1**) was added to quench trypsin activity and the contents were centrifuged for 10 minutes at 280g. Subsequently, the supernatant was discarded, and the cell pellet was resuspended for counting.

2.1.3 Quantification of Live/Dead Cells

Cell number was estimated using a Neubauer™ haemocytometer and light microscope. 1mL of culture was removed from the culture flask aseptically using a Stripette™, allowing 10µL of cell culture to be pipetted under the cover slip of a prepared haemocytometer. Cell density of culture was determined by counting the number of cells within four quadrant sections, determining the average *per* quadrant, and calculating the total number per mL of culture by multiplying through 1×10^4 .

Table 2-1: The List of Cell Lines Used for Studies

Cell line	Description	FAB	Characteristics	Media	Seeding (cells/mL)	Doubling time	Cytogenetics	Source
HEL	Erythroleukaemia (Relapse)	M6	mutJAK2 (V617F)	RPMI 1640 10% FBS	1 x 10 ⁵	ca. 30hr	Hypotriploid (60-64) -17	ECACC
PLB985	APL (Relapse)	M4	t(5;17)(p11;q11)	RPMI 1640 10% FBS	1 x 10 ⁵	ca. 36hr	Near Diploid (44-50)	ATCC
K562	CML	N/A	t(9;22)(q34;q11) – BCR::ABL1	RPMI 1640 10% FBS	1 x 10 ⁵	ca. 30hr	Hypotriploid (61-68) -3	ECACC
Kasumi-1	AML (Childhood)	M2	t(8;21)(q22;q22) – RUNX1::ETO	RPMI 1640; 20% FBS	3 x 10 ⁵	ca. 76hr	Hypodiploid (45) +3mar	DSMZ
KG1	Erythroleukaemia	M6	-	RPMI 1640 10% FBS	1 x 10 ⁵	ca. 30hr	Hypodiploid (42-47) -17	ATCC
KG1a	<i>Sub-clone of KG1</i>							Donated (Dr Zabkiewicz)
MV-4-11	AML (Childhood)	M5	t(4;11)(q21;q23) – KMT2A::AFF1	IMDM 10% FBS	2 x 10 ⁵	ca. 50hr	Hyperdiploid (46-48)	ATCC
NB4	APL (Relapse)	M3	t(15;17)(q22;q11-12) - PML::RARA	RPMI 1640 10% FBS	1 x 10 ⁵	ca. 36hr	Hypertriploid (56-66) +17	ATCC
NOMO-1	AML (Relapse)	M5	t(9;11)(p22;q23) – KMT2A::MLLT3	RPMI 1640 10% FBS	1 x 10 ⁵	ca. 40hr	Hyperdiploid (46-47)	DSMZ
OCI-AML2	AML	M4	mutDNMT3A (R635W)	αMEM; 20% FBS	1 x 10 ⁵	ca. 30hr	Hyperdiploid (43-49)	DSMZ
OCI-AML5	AML (Relapse)	M4	t(1;19)(p13;p13)	αMEM; 20% FBS; 10 ng/mL GM-CSF	1 x 10 ⁵	ca. 30hr	Hyperdiploid (44-48)	DSMZ
SKNO-1	AML (Relapse)	M2	t(8;21)(q22;q22) – RUNX1::ETO	RPMI 1640; 10 ng/mL GM-CSF	2 x 10 ⁵	ca. 46hr	Near-diploid (42-48)	DSMZ
TF1	Erythroleukaemia	M6	-	RPMI 1640 10% FBS	1 x 10 ⁵	ca. 30hr	Hyperdiploid (52-57) +3	ATCC
THP-1	AML (Childhood)	M5	(9;11)(p21;q23) - KMT2A::MLLT3	RPMI 1640 10% FBS	2 x 10 ⁵	ca. 36hr	Near Tetraploid (88-96) +3	ECACC
U937	Histiocytic Lymphoma	M5	t(10;11)(p12;q14) – MLLT10::PICALM	RPMI 1640 10% FBS	1 x 10 ⁵	ca. 30hr	Hypotriploid (58-69)	ATCC
ME-1	AML (Relapse)	M4	Inv(16)(p13q22) – CBFβ::MYH11	RPMI 1640 10% FBS	2 x 10 ⁵	ca. 46hr	Hyperdiploid (45-48)	ATCC
ML-1	AML (Relapse)	M4	t(6;11) – MLL::AF6	RPMI 1640 10% FBS	2 x 10 ⁵	ca. 50hr	Not specified	ECACC
HEK293T	Embryonic Kidney	N/A	N/A	DMEM 10% FBS	N/A	ca. 30hr	N/A	ATCC
MS-5	Fibroblast, Murine Stromal	N/A	N/A	αMEM 10% FBS	N/A	ca. 40hr	N/A	ATCC
HS-5	Fibroblast, Human Stromal	N/A	N/A	DMEM 10% FBS	N/A	ca. 40hr	N/A	Donated (Dr Zabkiewicz)
L / L- WNT3a	Fibroblast, Murine Stromal	N/A	N/A	DMEM; 0.4 mg/ml G-418	N/A	ca. 40hr	N/A	Donated (Prof. Dale)

RPMI - Roswell Park Memorial Institute-1640 Medium; **αMEM** - Minimum Essential Medium Eagle- Alpha Modification; **IMDM** - Iscove Modified Dulbecco's Medium; **AML** – Acute Myeloid Leukaemia; **CML** – Chronic Myeloid Leukaemia; **APL** – Acute Promyelocytic Leukaemia; **ATCC** – American Type Culture Collection (USA); **DMEM** - Dulbecco's Modified Eagle's Medium; **DSMZ** - German Collection of Microorganisms and Cell Cultures (Germany); **ECACC** - European Collection of Authenticated Cell Cultures (UK); **FBS** – Heat-Inactivated Foetal Bovine Serum (Labtech, East Sussex, UK); **FAB** – French American British Classification

2.1.4 Cryopreservation and Recovery of Cells

Cryopreservation of cells was achieved by centrifuging $5 \times 10^6 - 1 \times 10^8$ of cells for 10 minutes at 280g to form a pellet. These cells were resuspended in 0.5mL of the appropriate medium and transferred into pre-labelled and colour-capped 1.8mL cryopreservation vial. Dropwise addition of 0.5mL of 2x freezing media (50% Roswell Park Memorial Institute-1640 Medium (RPMI), 30% Foetal Bovine Serum (FBS), 20% Dimethyl Sulfoxide (DMSO), *v/v*) was added to the cell suspension giving a final DMSO concentration of 10% (*v/v*). Cryovials were placed into a Corning CoolCell® which was transferred immediately into a -80°C freezer for 24 hours. After this period, cells were transferred to liquid nitrogen for long term storage.

To recover cryopreserved cell lines, vials were recovered from liquid nitrogen and transferred on dry ice. Vials were placed into a 37°C water bath for rapid thawing. Cells were slowly added dropwise to 5mL of appropriate media to limit cell stress, before centrifuging for 10 minutes at 280g. The formed pellet was resuspended in 6mL of the appropriate growth medium (**Table 2-1**) and seeded into a labelled F25 for overnight recovery before transfer to a F75.

2.2 Primary Cell Culture: Haematopoietic Model

2.2.1 Isolation Of Mononuclear Cells from Human Neonatal Cord Blood

Informed consent was obtained to receive donations of human neonatal umbilical cord blood (CB) from healthy full-term pregnant mothers undergoing an elective caesarean at the University Hospital of Wales, Cardiff. Authorisation for the use of CB was obtained in agreement with the Southeast Wales Local Ethics Committee (06/WSE03/6). As an alternative source, fresh CB was also requisitioned from the London NHS BM and Transplant Unit at cost.

Mononuclear cells (MNC) were isolated from heparinised cord blood by density gradient centrifugation using Ficoll-Paque™ (GE Healthcare). CB was initially diluted by addition of equivalent volume Hank's Balanced Salt Solution (HBSS; Gibco) supplemented with 10mg/mL heparin, 25mM HEPES solution (Gibco), and 20µg/mL gentamicin (Gibco). At a ratio of 8:5, diluted CB was carefully layered atop 5mL of Ficoll-Paque™ and centrifuged at 400g for 40-minutes, with a reduced rate of acceleration and deceleration as not to disturb the layer. MNC were recovered from the interphase between the Ficoll-Paque™ and plasma using a Pasteur pipette and transferred to a UC containing CB wash (CBW; RPMI, 5% FBS *v/v*, 10mg/mL heparin, and 20µg/mL gentamicin) and centrifuged at 270g for 10-minutes. MNC were washed repeatedly until a clear supernatant was achieved, indicating no platelet

contamination remained. After recovery, MNC were resuspended in 20mL of CBW, and enumeration was achieved by recovering 10 μ L which was added to 1.5 μ L Zaponin (Beckman-Coulter) to remove red blood cells, and 190 μ L CBW before cell counting (2.1.3). MNC were subsequently cryopreserved at 5x10⁷ cells *per* vial (2.1.4).

2.2.2 Isolation of CD34⁺ HSPC from Mononuclear Cells

CD34⁺ haematopoietic stem and progenitor cells (HSPC) were isolated from MNC using a MiniMACS[®] Indirect CD34 MicroBead Kit (Miltenyi Biotec) per the manufacturer's instructions. In brief, frozen vials of MNC were recovered on dry ice and 1mL of FBS supplemented with 0.2 μ g/mL DNase was added before rapid thawing in a 37°C water bath. Following thaw, vial contents were recovered and an equal volume of a 1x Phosphate Buffer Saline (PBS) solution supplemented with 5 mM magnesium chloride (MgCl₂; Sigma-Aldrich) was added dropwise over three minutes, before two further doubling dilution steps were undertaken.

A gentle centrifugation at 200g for 10-minutes pelleted the MNC, with an additional 10 μ L of DNase (10 μ g/mL) added. Ensuing steps were performed with volumes adjusted *per* 1x10⁸ MNC recovered. MNC were resuspended in 400 μ L of chilled column buffer (MACS buffer; 1x PBS; 1% Bovine Serum Albumin (BSA) *v/v*; 5 mM MgCl₂) and incubated at 4°C for 15-minutes with 100 μ L hapten-conjugated monoclonal CD34 antibody with FcR blocking agent. After the incubation, MNC were washed with 5mL of MACS buffer and centrifuged at 270g for 5-minutes. Washed MNC were resuspended in 400 μ L MACS buffer and incubated with 100 μ L anti-hapten microbeads for 15-minutes at 4°C. After, 5mL of MACS buffer was added and the cell suspension was filtered through a 40 μ m cell strainer before centrifugation at 270g for 5-minutes. During this centrifugation, an MS column was pre-equilibrated with MACS buffer within the magnetic core. The MNC pellet was resuspended in 500 μ L MACS buffer and transferred to the MS column for positive selection. Gravity-driven flow was allowed to complete, and, once column outflow had ceased, the column was washed thrice with 500 μ L of MACS buffer. Subsequently, the MS column was recovered from the magnetic core and the CD34⁺ HSPC were eluted in 1mL of MACS buffer using a syringe. The recovered cells underwent a second immunomagnetic bead selection to maximise purity. After the second isolation, the HSPC were cultured at 2x10⁵ cells/mL in 36S^{HIGH} medium (**Table 2-2**), with this considered day zero for subsequent experiments.

2.2.3 *In Vitro* Culture of CD34⁺ HSPC

HSPC were cultured in 36S^{HIGH} medium (Iscove's Modified Dulbecco's Media (IMDM) containing 20% FBS *v/v*, 1% BSA *v/v*, 45µM β-mercaptoethanol (β-ME; Sigma-Aldrich), 360µg/mL human transferrin (Roche Diagnostics) and 20µg/mL gentamicin) to promote recovery prior to lentiviral transduction on days one and two. Subsequent to lentiviral transduction, HSPC were recovered and maintained in 3S^{LOW}G/GM medium to support HSPC differentiation (**Table 2-2**). Cells were inspected every second or third day, with the 3S^{LOW}G/GM medium replenished to maintain cytokine stimulation. Cells were seeded at increasing densities with differentiation to ensure high recovery for assays.

Cells were cultured at a seeding density of 0.5x10⁵ cells/mL prior to day six, enabling maximum growth potential. At day six until day ten cells were seeded at 2x10⁵, before the density was raised to 3x10⁵ from day ten onwards.

2.3 Primary Cell Culture: Primary AML

2.3.1 *In Vitro* Culture of Primary AML

AML-patient derived cells used within this study were established from BM biopsies collected from individuals enrolled into the National Cancer Research Institute AML15 UK Clinical Trial, obtained following full ethical approval from the AML Clinical Trials Research Tissue Bank in the Haematology Department at Cardiff University. Clinical data was available on some, but not all, patients involved within this study (**Table 2-3**). Primary AML material was frozen as previously described (2.1.4). Primary AML were carefully thawed to maximise recovery by addition of 1mL of complete IMDM prior to thawing in a 37°C water bath, after which point, dropwise addition of 5mL complete IMDM was added to further dilute the DMSO. Cells were centrifuged at 270g for 5-minutes before resuspension at 2x10⁵ cells *per* mL in primary AML growth medium (**Table 2-4**). Cells were maintained at 2x10⁵ cells *per* mL by addition of media every 72 hours.

Table 2-2: Cell Culture Medium Used for Growth and Development of CD34⁺ HSPC

Media	Days	Context	Cytokine	Concentration	Source*
36S ^{HIGH}	0-3	HSPC Recovery	IL-3	50ng/mL	578002
			SCF	50ng/mL	573902
			FLT3	50ng/mL	710802
			IL-6	25ng/mL	570806
			G-CSF	25ng/mL	578602
			GM-CSF	25ng/mL	572902
3S ^{LOW} G/GM	3-17	Extended Culture	IL-3	5ng/mL	578002
			SCF	5ng/mL	573902
			G-CSF	5ng/mL	578602
			GM-CSF	5ng/mL	572902

*Human recombinant cytokines were purchased from BioLegend.

IL-3 – Human Interleukin-3; **SCF** – Human Stem Cell Factor; **FLT3** - Human Fms-Like Tyrosine Kinase-3 Ligand; **IL-6** - Human Interleukin-6; **G-CSF** - Human Granulocyte Colony-Stimulating Factor; **GM-CSF** - Human Granulocyte-Macrophage Colony Stimulating Factor.

Table 2-3: Patient-derived Primary AML Samples

Patient	ID	Gender	Age	FAB	Karyotype	Outcome	Relapse
AML92	-	<i>No clinical data available</i>					
AML148	15-2296	Male	46	M4	46 (X,Y) del(9), q(13q22.3)	Survived	Clinical Remission
AML160	15-2422	Female	26	M4	46 (X,X)	Deceased	Clinical Remission
AML162	15-2465	Male	40	-	46 (X,Y)	Deceased	IND Death
AML164	15-2468	Female	56	M4	46 (X,X) del(7), q(32q36)	Deceased	Clinical Remission
AML165	15-1121	<i>No clinical data available</i>					
AML172	15-2552	Female	52	M1	46 (X,X)	Survived	Censored
AML177	-	<i>No clinical data available</i>					

FAB – French American British Classification; **IND** – Investigative New Drug; **del** – Deletion.

Table 2-4: Patient-derived Primary AML Culture Medium

Media	Cytokine	Concentration	Source*
Primary AML Growth Medium	IL-3	5ng/mL	578002
	SCF	5ng/mL	573902
	FLT3	5ng/mL	710802
	IL-6	5ng/mL	570806
	G-CSF	5ng/mL	578602
	GM-CSF	5ng/mL	572902
	M-CSF	5ng/mL	574802

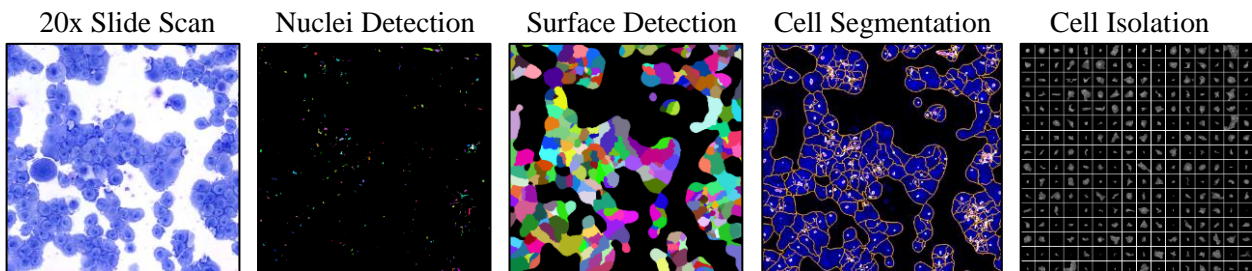
*Human recombinant cytokines were purchased from BioLegend.

IL-3 – Human Interleukin-3; **SCF** – Human Stem Cell Factor; **FLT3** - Human Fms-Like Tyrosine Kinase-3 Ligand; **IL-6** - Human Interleukin-6; **G-CSF** - Human Granulocyte Colony-Stimulating Factor; **GM-CSF** - Human Granulocyte-Macrophage Colony Stimulating Factor; **M-CSF** – Macrophage Colony Stimulating Factor.

2.3.2 Assessment of Cell Morphology

Cell morphology was examined through cytopins. Briefly, 100 μ L of culture medium containing 3×10^5 cells were transferred to an assembled cytopins unit constituting a chamber and glass slide. This unit was loaded into a Cytospin 3 (Fisher Scientific) and centrifuged at 60g for 5-minutes to disperse the cells onto the slide. Slides were airdried for 5-minutes before staining with May–Grünwald–Giemsa stain. Slides were subsequently mounted with DPX and scanned using a Zeiss Axioscan Z1 slide scanner (Carl Zeiss) at 20x magnification.

For cell lines, recovered images were analysed using the EBImage (Pau *et al.*, 2010) package within R, with cells segmented into image moments based upon nuclei detection and subsequent Voronoi tessellation to determine membrane bounds. Individual cells, or moments, were examined for cell radius (size), eccentricity (roundness), and haralick texture features (granularity), alongside stain intensity. For CD34⁺ HSPC models, subtype counts were performed using QuPath (University of Edinburgh). Cells were defined as being in an early, intermediate, or late phase of development based upon their presentation as myeloblasts-promyelocytes, myelocytes-metamyelocytes, and band-segmented cells, respectively. For primary AML samples, a more bespoke visual analysis was necessary as each patient sample would present with different types of AML.



2.4 Limiting Dilution Cloning

In the context of generating complete knockout clones from AML cell lines, bulk knockout cell populations were cloned by limiting dilution. Cells were cultured within log-phase growth to >85% viability with TOPRO (2.11.9), before three accurate counts were taken and averaged. Cells were recovered and diluted to 1000 cells *per* mL in fresh media, before a second dilution into 1 cell *per* 150 μ L in fresh media. 50 μ L of the diluted cells were then plated into 96-well U bottom plates, leading to one cell *per* three wells. Plates were then boxed and allowed to gas in the incubator with the addition of a wet tissue to maintain humidity, thereby minimising evaporation. After 7, days 50 μ L of additional media was added. Depending upon

the cell lines growth, 7 to 10 days later cells were examined under a light microscope and expanded from 96-well plates up through 48-well and 24-well. At the 24-well stage, cells were analysed with the WNT reporter assay (2.9), with only non-responder clones continued for further expansion. Non-responder clones were expanded to 12-well plates, then 6-well plates, before further use in research and cryopreservation. MV4;11 was supplemented with 20% FBS (v/v) for cloning.

Clonal rescue conditions focused upon the addition of factors which could support clonal growth during limiting dilution cloning. These included addition of cytokines, conditioned media (CM) from the scrambled or dual knockout cultures, and CM which had been sourced from cells with activated WNT signalling (2.9). These conditions are described in **Table 2-5**. These conditions were applied for limiting dilution cloning (2.4).

Further co-culture conditions were applied to rescue cells in which a single knockout cell was co-cultured with a supportive population of cells. These conditions included the use of stromal support cells which were expected to better reflect the *in vivo* condition. To this end, plates were prepared with the stroma support cell lines MS-5 (murine) or HS-5 (human) stromal support cells which were mitotically inhibited by treatment with mitomycin C at 10 μ g/mL for 2-hours at 37°C prior to addition of AML cells. Co-culture with parental cells (1:10) was achieved by preparing 96 well plates with 10 parental cells *per* well. These are described in **Table 2-6**. Knockout cells were plated with the standard limiting dilution cloning process (2.4). Recovery was measured by flow cytometry, as scrambled and knockout cells contained the pBARV reporter, which constitutively expressed DsRed (2.9.3). DsRed was used to screen all 96-wells of each plate to isolate those containing a scrambled or knockout clonal population.

Complete knockout clones which were rescued in co-culture conditions would require subsequent isolation. As knockout cells harbour the pBARV reporter, which constitutively expressed DsRed (2.9.3), this was used to pre-screen all 96-wells of each plate to isolate those containing a knockout cell. DsRed⁺ wells were expanded, and after a further 7 days the WNT reporter assay was conducted to isolate only non-responsive clones which would be DsRed⁺Venus⁻ (2.11.5). Candidate clones were fluorescence activated cell sorting (FACS) based on DsRed⁺, after which they were expanded to produce protein lysates (2.10.1) for western blot screening of β -catenin and γ -catenin at protein level (2.10). Clones which were negative for β -catenin and γ -catenin protein were taken forward for DNA examination of InDel knockout (2.12.3).

For CD34⁺ HSPC models, limiting dilution was similarly performed in 96-well U plates at a density of 0.3 cells *per* well and incubated at 37°C with 5% CO₂. After 7 days, each well was scored as individual myeloid colonies (>50 cells) or clusters (>5 cells) by brightfield microscopy. To assess self-renewal efficiency, the colonies were harvested, counted, and re-plated at a density of 1 cell *per* well for a further 7 days of culture. These re-plated cultures were then again scored as before with several colonies retained for potential DNA isolation to validate survival of complete knockout clones.

For primary AML models, limiting dilution was performed in 96-well U plates at a density of 1 cell *per* well and incubated at 37°C with 5% CO₂. After 7 days, each well was scored as having self-renewed if greater than three cells were present by brightfield microscopy. Wells with two to three cells were considered a potential pipetting error, whilst those with one had proved incapable of self-renewal.

Table 2-5: Single Cell Supplemented Media Conditions for Rescue

Describing the supplemented media used for limiting dilution cloning within this study. Conditioned media was prepared immediately before use to minimise concerns of degradation over time.

Rescue Condition	Additive(s)	Preparation
Cytokines	IL3, IL6, SCF, G-CSF, GM-CSF, FL3, M-CSF	5ng/mL in Fresh Media
SCR CM	4x10 ⁵ scrambled cells cultured for 24 hours, media was centrifuged 300g for 5min and 0.45µM filtered	1:1 (v/v) with Fresh Media
SCR CM + CHIR	4x10 ⁵ scrambled cells cultured with 5µM CHIR for 24 hours, media was centrifuged 300g for 5min and 0.45µM filtered	1:1 (v/v) with Fresh Media
dKO CM	4x10 ⁵ dual knockout cells cultured for 24 hours, media was centrifuged 300g for 5min and 0.45µM filtered	1:1 (v/v) with Fresh Media
dKO CM + CHIR	4x10 ⁵ dual knockout cells cultured with 5µM CHIR for 24 hours, media was centrifuged 300g for 5min and 0.45µM filtered	1:1 (v/v) with Fresh Media

CM – Conditioned Media

SCR – Scrambled

dKO – Dual Catenin Knockout

Table 2-6: Co-culture Conditions for Rescue of Dual Knockout AML Responder Lines

Describing the preparation of co-culture conditions used for limiting dilution cloning within this study. MS-5 and HS-5 methods required preparation of plates (96w, 48w, 24w, 12w, 6w) before recovered knockout cells were expanded. Parental co-cultures were considered a single culture and expanded under normal conditions.

Rescue Condition	Preparation
MS-5	96w Flat Bottomed TC plates were prepared with 2x10 ³ MS-5 cells. MS-5 cells were treated with Mitomycin C to stop excessive growth during limiting dilution cloning. After 24-hours, the media within wells was removed and replaced with knockout cell growth media containing 1 cell per 3 wells.
HS-5	96w Flat Bottomed TC plates were prepared with 2x10 ³ HS-5 cells. HS-5 cells are anchorage-dependent for growth and as such required no growth suppressing treatment. After 24-hours, the media within wells was removed and replaced with knockout cell growth media containing 1 cell per 3 wells.
Parental	96w U-Bottomed TC plates was prepared with 10 parental cells in the respective knockout line's growth media in 50µL. 50µL of media containing 1 knockout cell per 3 wells was added thereafter.

2.5 Molecular Biology

Lentiviruses are a sub-member of the *Retroviridae* viral family and are characteristically capable of integrating DNA into non-dividing host cells. Lentiviruses produce DNA via reverse transcriptase which is incorporated by integrase colocalizing viral cDNA with host DNA for insertion. A full list of plasmids used within this study can be found in **Table 2-8**.

2.5.1 Plating and liquid growth of *Escherichia coli* bacteria

Plasmids were designed and purchased from VectorBuilder™ or AddGene™ with the plasmid harboured within Stbl3 *E. coli* bacteria at high-copy number. Using a sterile inoculation loop, a small portion of frozen glycerol bacterial stock was spread upon a prewarmed selective agar plate created from 30mL of Sigma™ LB Agar (L2897) supplemented with 100µg/mL ampicillin with a sterile plastic spreading tool. Plates were returned to the 37°C incubator for an overnight culture. The subsequent morning, plates were removed from the incubator and a single colony was selected into a universal container holding 5mL of prewarmed Sigma™ LB Broth (L3022) for an over-day incubation at 37°C with shaking at 225RPM. 150µL of this culture was transferred to a sterile 1L flask containing 150mL LB broth supplemented with 100µg/mL ampicillin before an overnight incubation at 37°C with shaking at 225RPM.

2.5.2 Isolation of Plasmid DNA

Plasmid was isolated with the QIAGEN® Plasmid Maxi Kit as per the manufacturer's instructions (12163). In brief, bacterial cells were recovered from the incubator and pelleted by centrifugation at 6000g for 15-minutes at 4°C. The supernatant was removed, and cells were resuspended and vortexed in 10mL of Buffer P1. 10mL of Buffer P2 was added and mixed by inverting 5-times for 3-minutes. After this incubation, 10mL of Buffer P3 was added and mixed by inverting 5-times. The lysate was immediately transferred into a QIAfilter cartridge and incubated for 10-minutes, during which time, a HiSpeed Maxi tip was equilibrated with 10mL of Buffer QBT. Following the incubation, the lysate was expelled through the QIAfilter cartridge into the equilibrated HiSpeed Maxi tip. The lysate was cleared by gravity, after which 60mL of Buffer QC was added and allowed to clear by gravity again to wash DNA. DNA was eluted by addition of 15mL of Buffer QF which was collected into a 50mL falcon tube and precipitated through a 5-minute incubation with 10.5mL of room temperature isopropanol, whilst the QIAprecipitator Maxi Module was prepared. The eluate mixture was transferred to the QIAprecipitator and expelled, before a second expulsion using 2mL 70% ethanol (*v/v*), and

a dry expulsion all into waste. A labelled 1.5mL extract vial was prepared, and a final expulsion using 500µL of water was repeated twice to ensure effective DNA recovery. DNA concentration and quality metrics were determined using the Thermo Scientific™ NanoDrop™ spectrophotometer before storage at -20°C.

2.6 Viral Transfection

2.6.1 Transfection of HEK293T Cells

HEK293T, a subline of HEK293, were used to generate assembled virus. HEK293T were cultured in Dulbecco's Modified Eagle Medium (DMEM) supplemented with 10% FBS, 2mM L-glutamine, and 1/2500 Gentamicin to confluency (30×10^6 cells *per* flask). F75 culture flasks were coated with Poly-L-lysine (Sigma) for 30-minutes and rinsed with medium before addition of 15×10^6 HEK293T cells for an overnight culture to ensure adherence. The Lipofectamine 3000 Kit™ (Thermo) was used to enhance lipofection. Two tubes were prepared at a 1:1 ratio. The first universal container was prepared containing 2mL of Opti-MEM I Reduced Serum Medium (Gibco, 31985062), 6.6µg of pMD.2G and 12µg of psPAX2 packaging vectors, 6.3µg of the chosen transfer vector, and 16µL of P3000 reagent. A second tube contained 2025µL OptiMEM and 57µL Lipofectamine 3000. The prepared reagents were mixed and incubated for 15-minutes, during which time the F75 media was reduced to 6mL. The primed lipid-DNA complex mix was added and mixed to the HEK293T culture for a 6-hour incubation at 37°C 5% CO₂, following which the media was replaced to 9mL and incubated overnight. This protocol could be reduced or expanded for alternate flask sizes.

2.6.2 Harvesting of Lentiviral Virions

Generated virions were harvested on each of the two days after lipofection. The supernatant was removed from the HEK293T packaging cells on day two and stored in a universal container at 4°C overnight, whilst the media replenished to 7.5mL. On day three, the supernatant was combined with the previous extraction and centrifuged at 280g for 5-minutes. The virus containing supernatant was aliquoted into 1mL vials which were snap frozen in liquid nitrogen to lyse contaminating HEK293T cells. Virus stocks were stored at -80°C. Virus titre was determined where necessary with the Clontech™ Lenti-X GoStix per manufacturers instruction, or by titration in K562 by green fluorescent protein (GFP) against an established in-house benchmark.

2.7 Lentiviral Transduction

2.7.1 Lentiviral Transduction of Suspension Cell Lines

Cells were transduced in non-tissue culture treated 24-well plates. Lentiviral mediated transduction was enhanced with the assistance of RetroNectin™ (Takara, T202), a recombinant human fibronectin fragment (rFN-CH-296), which facilitates colocalisation of lentivirus with target cells. 24-well plates were pre-coated overnight at 4°C with 300µL of RetroNectin at a concentration of 30µg/mL. Wells were washed with 300µL 1% (v/v) BSA in PBS solution for 30-minutes whilst frozen virus was collected and rapidly thawed in a water bath at 37°C. The BSA was removed and 1mL of virus was added to each well before the plate was centrifuged in a containment box at 2500g for 90-minutes at 20°C for viral coating. During this time, the recipient cells were counted and 1mL of cells were prepared at a density of 5×10^5 cells *per* mL in the appropriate medium. After the centrifugation, the supernatant containing unbound virus was removed and replaced with the diluted cells for an overnight incubation at 37°C.

The following day the plate was recovered, and the supernatant was discarded. Bound cells were resuspended in 1mL of the appropriate medium before transfer to a universal container with 5mL of pre-warmed medium for centrifugation at 280g for 5-minutes. The supernatant was once again discarded, with the pellet resuspended in 2mL and cultured in a 12-well dish at 37°C for expansion. Subsequent divergence in selection occurs with considerations to the inserted plasmid. Cells were selected based upon incorporation of a marker, such as DsRed, or through addition of selective antibiotics such as puromycin or geneticin if the plasmid harboured genes enabling resistance (2.8.2).

2.7.2 Lentiviral Transduction of Adherent Cell Lines

Lentiviral mediated transduction of adherent cell lines was enhanced with the assistance of Polybrene, which facilitates colocalisation of lentivirus with target cells. 5×10^5 cells were cultured in a non-tissue culture treated 24-well plate overnight. The following morning, frozen virus was collected and rapidly thawed in a water bath before 1mL of virus was added to the well, alongside addition of Polybrene at 8µg/mL. After 48 hours, the plate was recovered, and the cells resuspended by pipetting for transfer to a universal container with 5mL of pre-warmed medium for centrifugation at 280g for 5-minutes. The supernatant was once again discarded, with the pellet resuspended in 2mL and cultured in a 12-well dish at 37°C for expansion. Cells were selected based upon incorporation of a marker, such as DsRed, or through addition of selective antibiotics.

2.7.3 Lentiviral Transduction of CD34⁺ HSPC

For lentiviral transduction of CD34⁺ HSPC, plates were prepared equivalent to suspension cell lines (2.1.1). Following centrifugation, the viral supernatant was removed and the CD34⁺ cells that had been previously seeded at 2×10^5 cells/mL were added to the wells. The following day, cells were temporarily transferred to a UC and placed at 37°C in the incubator, during which time the plate was once again prepared with a viral base coat by centrifugation; HSPC were then transferred to the virally re-coated plate for a further 24-hours of transduction.

2.7.4 Lentiviral Transduction of Primary AML

For lentiviral transduction of primary AML cells, plates were prepared equivalent to suspension cell lines (2.1.1). Following centrifugation, the viral supernatant was removed and the primary AML cells that had been previously seeded at 2×10^5 cells *per* mL were added to the wells. For primary AML studies cells were incubated with lentiviral particles for 48-hours before harvesting for further study.

2.8 CRISPR-Cas9

2.8.1 *In Silico* Generation of guide-RNA

For knockout studies, which rely on the generation of InDel, leading to a frameshift mutation, NHEJ of DSB was necessary. The targeting gRNA was designed in chopchopTM (v2) with a 5'-NGG-3' PAM recognition motif. Target gRNA selection was limited to targets present in all alternate transcripts as verified via SpliceMinerTM which did not exhibit SNP as assessed with the UCSCTM genome browser (v. GRCh38/hg38). Selected gRNA showed minimal off-target and self-complementarity effects, as mismatches in the 5' end can be tolerated due to the 5'-3' binding activity of CRISPR-Cas9. GC content should ideally be between 40-80% to stabilize the RNA:DNA duplex whilst reducing off-target hybridization. Self-complementarity refers to the number of self-recognizing areas within the strand predicted (**Figure 2-1**). Predicted cleavage efficiencies were calculated (Doench *et al.*, 2016), with the highest three predicted gRNA tested. Six plasmids were constructed through VectorBuilderTM which contained the designed gRNA sequences, alongside Cas9 in a T2A dual-expression system with Puromycin or Neomycin resistance for selection as described in 2.7.1, and ampicillin resistance for selection during bacterial growth (**Table 2-8**).

For CRISPRa and CRISPRi studies, the Broad Institute CRISPickTM software was used to rank and select an optimal guide-RNA to maximise the on-target activity whilst minimising

off-target concerns. Guide-RNA were comparably validated with SpliceMiner™ and the UCSC genome browser™.

2.8.2 Selection of Transduced Cells

Following lentiviral transduction, cells were selected on the basis of the transduced plasmids incorporated resistance gene, or alternatively by a fluorescent marker. Cells were selected by addition of Puromycin (Sigma) at 1µg/mL, 200–1000µg/mL of Geneticin (G418; Gibco), 5-10µg/ml Blasticidin (Sigma) and 1000µg/mL of Hygromycin B (ThermoFisher) (**Table 2-7**). Selection pressure was applied for 2-14 days with a killing control performed in parallel to verify complete selection.

Table 2-7: The Determined Antibiotic Minimum Lethal Concentrations After Seven Days

Minimum lethal concentrations of Puromycin, Blasticidin, and Geneticin for each cell line as determined. Manufacturers recommend a concentration between 400 to 1000 $\mu\text{g/mL}$ for seven to fourteen days to generate a stable population. A drug sensitivity assay was completed over seven days with a range of concentrations. An untreated population was used as a control reference.

Cell Line	Geneticin: Minimum Lethal Concentration ($\mu\text{g/mL}$)	Blasticidin: Minimum Lethal Concentration ($\mu\text{g/mL}$)	Hygromycin B: Minimum Lethal Concentration ($\mu\text{g/mL}$)	Puromycin: Minimum Lethal Concentration ($\mu\text{g/mL}$)
NOMO1	200	<i>Not tested</i>	<i>Not tested</i>	1
K562	400	5	500	1
HEL	600	8	500	1
KG-1a	600	8	500	1
ML-1	600	<i>Not tested</i>	<i>Not tested</i>	1
MV4;11	600	6	500	1
OCI-AML2	600	<i>Not tested</i>	<i>Not tested</i>	1
SKNO-1	600	<i>Not tested</i>	<i>Not tested</i>	1
PLB985	800	<i>Not tested</i>	<i>Not tested</i>	1
U937	800	10	500	1
OCI-AML5	1000	<i>Not tested</i>	<i>Not tested</i>	1
TF-1	1000	<i>Not tested</i>	<i>Not tested</i>	1
THP-1	1000	10	500	1

Table 2-8: Plasmid Vectors used within this Study

Context	Type	Target	Vector Name	Vector ID	Target sequence	Exon	Marker	Host bacteria	Source	
Lentiviral Generation	Packaging Plasmid	Packaging	pMD2 Addgene_12259	158	<i>N/A</i>	<i>N/A</i>	<i>N/A</i>	<i>Stb13</i>	Addgene	
			pMD2 Addgene_12260	189	<i>N/A</i>	<i>N/A</i>	<i>N/A</i>	<i>DH5α</i>		
WNT Reporter	Reporter (Cell Lines)	Active Reporter	pBARV Reporter	200	<i>N/A</i>	<i>N/A</i>	DsRed	<i>Stb13 E.coli</i>	Prof. Randall Moon	
		Inactive Reporter	pfuBARV Control	202	<i>N/A</i>	<i>N/A</i>	DsRed	<i>Stb13 E.coli</i>	Prof. Randall Moon	
WNT Knockout	CRISPR-KO (Cell Lines)	Scrambled	CRISPR-SCR-1 [AIO]	VB170925-1200uae	GCACTACCAGAGCTAACTCA	<i>N/A</i>	Puro	<i>UltraStable E.coli</i>	VectorBuilder	
			CRISPR-CTNNB1-1 [AIO]	VB181017-1120bsy	ACCCAGCGCCGTACGTCCAT	10	Puro	<i>UltraStable E.coli</i>	VectorBuilder	
			CRISPR-CTNNB1-2 [AIO]	VB181017-1121uss	GTGCGTACTGTCTTCGGGC	9	Puro	<i>UltraStable E.coli</i>	VectorBuilder	
		<i>CTNNB1</i> (Beta)	CRISPR-CTNNB1-3 [AIO]	VB181017-1119nfm	TACCCAGCGCCGTACGTCCA	10	Puro	<i>UltraStable E.coli</i>	VectorBuilder	
			CRISPR-CTNNB1-4 [AIO]	VB190603-1087sew	TATAGCTGATTTGATGGAGT	3	Puro	<i>UltraStable E.coli</i>	VectorBuilder	
			CRISPR-CTNNB1-5 [AIO]	VB190603-1093heq	GATGGAGTTGGACATGGCCA	3	Puro	<i>UltraStable E.coli</i>	VectorBuilder	
			CRISPR-CTNNB1-6 [AIO]	VB190603-1091rjh	TGATTTGATGGAGTTGGACA	3	Puro	<i>UltraStable E.coli</i>	VectorBuilder	
		<i>JUP</i> (Gamma)	CRISPR-JUP-1 [gRNA]	VB181218-1048cve	AGTTACGCATGATCTGCACG	6	Neo	<i>UltraStable E.coli</i>	VectorBuilder	
			CRISPR-JUP-2 [gRNA]	VB181218-1049xfj	CGAGTGGATACCCGAGTCGT	2	Neo	<i>UltraStable E.coli</i>	VectorBuilder	
			CRISPR-JUP-3 [gRNA]	VB181218-1050rfg	TACGACTCGGGTATCCACTC	2	Neo	<i>UltraStable E.coli</i>	VectorBuilder	
			CRISPR-JUP-1-AIO [AIO]	VB200218-1050qmv	AGTTACGCATGATCTGCACG	6	Neo	<i>UltraStable E.coli</i>	VectorBuilder	
		CRISPR-KO (HSPC, P-AML)	Scrambled	CRISPR-SCR-GFP [AIO]	VB210615-1141war	GCACTACCAGAGCTAACTCA	<i>N/A</i>	GFP	<i>UltraStable E.coli</i>	VectorBuilder
			<i>CTNNB1</i> (Beta)	CRISPR-CTNNB1-GFP [AIO]	VB210615-1138aud	GTGCGTACTGTCTTCGGGC	9	GFP	<i>UltraStable E.coli</i>	VectorBuilder
		RAP1 Signalling	CRISPRa	Scrambled	CRISPRa-SCR	VB211013-1065art	GTGTAGTTCGACCATTCGTG	<i>N/A</i>	Neo	<i>UltraStable E.coli</i>
<i>RAPGEF4</i>	CRISPRa-RAPGEF4-MS2			VB211003-1013cfw	CGGACGCCTGGCGACCAGCG	UTR	Neo	<i>UltraStable E.coli</i>	VectorBuilder	
<i>N/A</i>	dCas9-VPR			VB220104-1097pr	<i>N/A</i>	<i>N/A</i>	Hygro	<i>UltraStable E.coli</i>	VectorBuilder	
CRISPRi	Scrambled		CRISPRi-SCR	VB211013-1071ksb	GTGTAGTTCGACCATTCGTG	<i>N/A</i>	Bst	<i>UltraStable E.coli</i>	VectorBuilder	
	<i>SIPA1L1</i>		CRISPRi-SIPA1L1	VB211013-1070qbv	CCCCGGGGACCCTCCAGCCG	UTR	Bst	<i>UltraStable E.coli</i>	VectorBuilder	
	<i>N/A</i>		dCas9-KRAB-MeCP2	VB220104-1129cuu	<i>N/A</i>	<i>N/A</i>	Hygro	<i>UltraStable E.coli</i>	VectorBuilder	
RAP1	RAP1 WT	RAP1-CONTROL	AG#156173	<i>N/A</i>	<i>N/A</i>	Neo	<i>NEB Stable E.coli</i>	AddGene [Friedel]		
	RAP1 E63	RAP1-E63	AG#156174	<i>N/A</i>	<i>N/A</i>	Neo	<i>NEB Stable E.coli</i>	AddGene [Friedel]		

pBARV - β -catenin Activated-Reporter Venus; **pfuBARV** – Found unresponsive β -catenin Activated-Reporter Venus; **SCR** - Scrambled; **KO** – Knockout; **Puro** – Puromycin Resistance; **Neo** – Geneticin Resistance; **Bst** – Blasticidin Resistance; **GFP** – Green Fluorescent Protein; **DsRed** - Discosoma Red; **AIO** – All-in-one CRISPR construct; **gRNA** – Guide-RNA-only construct; **HSPC** – Haematopoietic Stem Progenitor Cell (CD34⁺); **P-AML** – Primary Acute Myeloid Leukaemia; **WT** – Wildtype; **CRISPR-KO** – CRISPR Knockout construct; **CRISPRa** – CRISPR Activator construct; **CRISPRi** – CRISPR Inhibitor construct; **UTR** – Untranslated Promoter Region; **NEB** – New England Biolabs

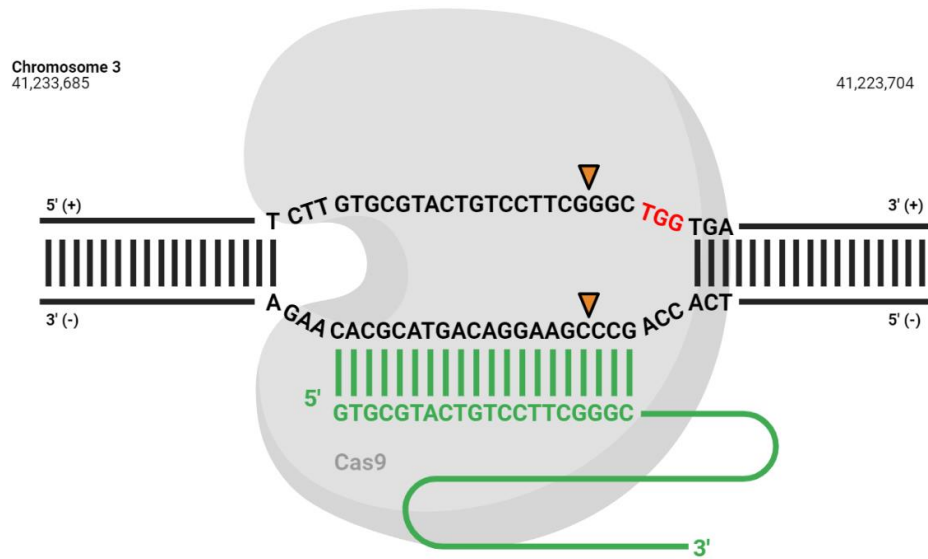


Figure 2-1: The CRISPR-CTNNB1-2 gRNA Target Site

gRNA CRISPR-CTNNB1-2 drawn in green will target the specific complementary sequence in the gene *CTNNB1*. The Cas9:guide-RNA complex will bind the antisense strand (-) of the gene and generate a double-stranded break at location 41,233,685 three nucleotides upstream of the PAM recognition site (red nucleotides), as indicated with two orange triangle markers. Repair of this double strand break by non-homologous end joining will facilitate the generation of a frameshift mutation by producing InDels, or homology-directed repair will return the sequence to the wild-type state. This will lead to Cas9 generating another double-strand break.

2.9 Modulating and Quantifying WNT Signalling

2.9.1 Stabilisation of β -catenin

To assess the WNT response and β -catenin translocation capability of each cell line, stabilisation of β -catenin was necessary. This was primarily achieved by inhibiting the β -catenin destruction complex with CHIR99021 (Tocris, 4423), a GSK3 β inhibitor which competes with ATP to bind the destruction component GSK3 β . Alternatively, recombinant WNT3a (R&D, 5036-WN-010) or WNT3a CM produced from L-WNT3a cells was applied to stimulate WNT signalling through binding of a FZD surface receptor. Mechanistically, these methods stop phosphorylation and degradation of β -catenin by blocking the kinase activity of GSK3 β .

Culture conditions were prepared with 5 μ M CHIR, 1 μ g/mL rWNT3a, or WNT3a CM with culture medium for 24 hours. WNT3a CM was applied at 1:1 to 1:10 (v/v) with normal growth medium, ranges which are widely adopted in the literature (Tickenbrock *et al.*, 2005; Aly *et al.*, 2013; Powell *et al.*, 2017; VanDussen *et al.*, 2019); some studies reduced the levels of CM to 1:4 (Yamane *et al.*, 2001), 1:8 (Hamidouche *et al.*, 2008; Rao *et al.*, 2018), or 1:10 (James *et al.*, 2012), with these variances likely explained by batch effects and different objectives. In order to prepare samples for western blotting, overnight cultures were expanded to a culture of 1x10⁶ cells for total protein levels or 5x10⁶ cells for fractionation (2.10.1, 2.11.5).

2.9.2 Generating WNT3a Conditioned Media

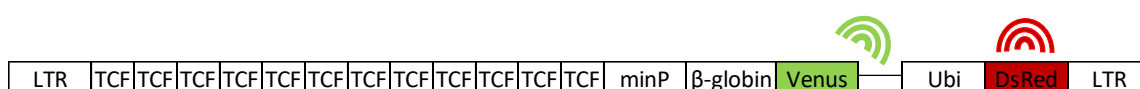
WNT3a is one of several natural agonists which stimulate WNT signalling. WNT3a CM was produced from the L-WNT3A (CRL-2647) cell line, which are L cells that have been transduced to constitutively produce WNT3a. Parental L cells were also prepared as a CM control.

WNT3a L cells and parental L cells were thawed *per* 2.1.4, and the WNT3a line was cultured under 0.4mg *per* mL G418 for a period of 7 days. When confluent, cells were passaged 1:10 into a T175 totalling 30mL of culture medium. After 4 days, the media was harvested and replaced with 20mL of fresh culture medium. The first batch of harvested CM was retained in the fridge at 4°C. At day 7, the second batch of CM was harvested, and the spent flasks were discarded. Both batches were centrifuged at 1200g for 5-minutes to remove any carryover of material, before they were sterile filtered (0.22 μ m).

2.9.3 pBARV and pfuBARV TCF Reporters

To quantify and assess WNT signalling, the β -catenin Activated Reporter Venus (pBARV) lentiviral plasmid was incorporated into cell lines. pBARV encompasses twelve TCF response elements (5'-CCTTTGATC-3') representing a concatemer, which are pair linked to lessen loss of elements to recombination. Upstream of pBARV is a minimal *thymidine kinase* promoter (minP) which controls transcription of Venus, a fluorescent protein derived from *Aequorea victoria* (Ex- λ : 515, Em- λ : 528). Downstream, a Ubiquitin promoter constitutively drives DsRed expression, a second fluorescent protein derived from *Discosoma sp.* (Ex- λ : 558, Em- λ : 583). The construct is flanked by long terminal repeats. An alternate construct with a two-base substitution in the TCF response element acts as a non-responsive control and is known as found-unresponsive pBARV (pfuBARV). A diagram is shown below.

The structure of the pBARV and pfuBARV constructs



2.10 Protein Analysis by Western Blotting

2.10.1 Whole Protein Extraction

For western blotting analysis, 1×10^6 cells were centrifuged at 280g for 10 minutes. Supernatant was discarded, and cell pellets were washed using 10 mL of ice-cold tris-buffered saline (TBS; 50 mM Tris (Sigma) dissolved in dH₂O and adjusted to pH 7.6 with HCl; 150 mM NaCl (Sigma) dissolved in dH₂O). Supernatant was discarded and pellets were snap frozen in liquid nitrogen before protein extraction. When required, frozen cell pellets were thawed on ice in the presence of 1 mg *per* mL DNase for 5 minutes and resuspended in 50 μ L of homogenisation buffer (0.25 M sucrose (Sigma), 10 mM HEPES-KOH pH7.2 (Gibco), 1mM magnesium acetate (Sigma), 0.5 mM EDTA (Sigma), 0.5 mM EGTA (Sigma), 12.6 M β -ME (Sigma), 1 tablet of EDTA free-protease inhibitor (Roche), 1% v/v x100-Triton (Sigma)). Cells were incubated on ice for 30 minutes and subjected to occasional vortexing. Then, the cell suspension was transferred to ice cold Eppendorf tubes and centrifuged for at 16,000g for 5 minutes at 4°C. Supernatant was collected transferred to a new pre-chilled Eppendorf and stored at -80°C until required. Protein concentration was determined by Bradford assay (2.10.3).

2.10.2 Cytosolic and Nuclear Cell Protein Fractionation

An adapted version of the procedure obtained with the BioVision™ fractionation kit (K266-100) was utilised to obtain cytoplasmic and nuclear fractionation protein lysates for western blotting. Briefly, 5×10^6 cells were pelleted and carefully washed with 20mL of TBS, before a second 10-minute centrifugation at 280g. After removing the supernatant, the pellet was resuspended in 0.2mL of cytosol extraction buffer A (CEB-A) containing 1x protease inhibitor cocktail (PIC) and 1mM dithiothreitol (DTT) through vortexing, before incubation for 10-minutes on ice. 11µL of cytosol extraction buffer B (CEB-B) was added and vortexed, before a 1-minute incubation on ice. After, cells were vortexed and centrifuged at 13,000RPM for 8-minutes at 4°C. The resulting supernatant contained the cytoplasmic lysate and was transferred for protein quantification into a fresh labelled 1.5mL Eppendorf. Any residual supernatant was removed which would contaminate the nuclear fraction before 500µL of PBS with 5mM $MgCl^{2+}$ pellet wash was added.

The nuclear pellet was centrifuged maximally at 10,000g for 3-minutes, with the pellet wash subsequently discarded. The pellet was snap frozen in liquid nitrogen and freeze-thawed thrice further in the vapour phase of liquid nitrogen. 2µL of benzonase was added to the pellet and centrifuged briefly to ensure mixing before a 30-minute incubation on ice. The tube was vortexed every 10-minute interval. 100µL of TAEB buffer per 1×10^7 cells, or 50µL per 1×10^7 AML blasts, was added and the tube incubated a second time for 30-minutes on ice, with vortexing every ten minutes. A final centrifugation at 10,000g at 4°C for 10-minutes produces a supernatant containing the nuclear extract, which is transferred to a fresh tube and stored at -80°C until protein quantification (2.10.3).

2.10.3 Determining Protein Concentration by Bradford Assay

The Bradford's reagent protein assay was used to determine the concentration of protein in whole and fractionated cell lysates (2.10.10). Protein standards were generated to act as a standard range within which protein levels could be interpolated to determine extract concentrations. These standards were prepared from diluted BSA in lysis buffer (100, 70, 40, 10, 0µg *per* mL). Bradford reagent (Merck, B6916) was diluted 1:1 (v/v) with dH₂O and allowed to reach room temperature. Samples were diluted 1:100 in dH₂O, before transfer of duplicate 10µL aliquots to a 96-well plate, in addition to the protein standards. 190µL of diluted Bradford's reagent was mixed with each duplicated sample and absorbance was measured at 590nm on a Chameleon spectrophotometer (Noki Technologies) after a 10-minute incubation.

The BSA standards were used to generate a standard curve, allowing protein levels to be determined, as below.

$$\text{Concentration (ug/mL)} = \frac{A^{595} - y^{int}}{s}$$

A^{595} = Sample absorbance at 595nm

y^{int} = Y-axis intersection

s = Slope of the linear regression

2.10.4 Polyacrylamide Gel Electrophoresis and Electroblothing

The Invitrogen™ NuPAGE® XCell SureLock™ Mini-Cell and XCell II™ blot module (Thermo, EI0002) was used to perform western blotting with proteins separated by size migration through sodium dodecyl sulphate polyacrylamide gel electrophoresis (SDS-PAGE). Protein extracts were prepared to a standard concentration of 500µg/mL (10µg of protein per well of 12-well) by addition of sterile H₂O, NuPAGE™ 10x reducing agent (NP0004), and NuPAGE™ 4x lithium dodecyl sulphate (LDS) sample buffer (NP0008) before an incubation in a water bath at 70°C for 10-minutes to denature proteins. Pre-cast 12-well NuPAGE™ 12% Bis-Tris (NP0342BOX; 20µL maximum) or 17-well NuPAGE™ 12% Bis-Tris (NP0349BOX; 10µL maximum) protein gels were washed, inserted into the XCell blotting module, and filled with 200mL of 1x NuPAGE™ MOPS SDS Running Buffer (NP0001) with 500µL NuPAGE™ Antioxidant (NP0005) prior to sample loading. Flanking wells were loaded with Invitrogen™ MagicMark™ XP Western protein standard ladder (LC5602) in order to estimate the molecular weight (MW) of detected protein bands. The external chamber was filled with 600mL of 1x Running Buffer (NP0001) before gel electrophoresis was electroporated at 200 volts for 50-minutes. Prior to the run completing, blotting pads and Invitrolon™ filter paper was soaked in 1x NuPAGE™ Transfer Buffer (NP00061) with 10% methanol and 1% NuPAGE™ Antioxidant (v/v) whilst 0.45µm Invitrolon™ Polyvinylidene Fluoride membranes were soaked for 10-minutes in methanol. Upon conclusion of the run, the gel was carefully removed and placed into the constructed transfer sandwich of layered pre-soaked filter pads and filter paper, with the gel contacting the PVDF membrane and orientated toward the anode. The transfer sandwich was pressed to ensure trapped air bubbles were expelled before insertion into the XCell blotting module. The inner module was filled with transfer buffer whilst the external area was filled with 600mL of dH₂O before the transfer was conducted at 30 volts for 60-minutes.

After the transfer, the membrane was extracted from the transfer sandwich and washed with for 5-minutes on a plate shaker with 20mL ultrapure H₂O to remove residual gel fragments. To assess successful transfer of protein, and as a visible inspection of equal loading and fractionation of lysates, membranes were incubated with 20mL of Ponceau S solution (Merck, P7170) and agitated for 60-seconds. Membranes were cut at this point, if necessary, before washing twice with 20mL of ultrapure H₂O to remove the Ponceau S solution. The membrane was then incubated at RT for 30-minutes in 10mL of 2.5% Marvel Milk blocking solution in Tris-Buffered-Saline-Tween (TBS-T). Blocked membranes were rinsed with 10mL of TBS-T and then washed for 15-minutes with 20mL of TBS-T, before three further washes for 5-minutes. Washed membranes were incubated with diluted primary antibody in 1% Marvel Milk solution in TBS-Tween for 24-hours at 4°C (**Table 2-9**).

2.10.5 Protein Detection Methods

2.10.5.1 Chemiluminescent detection of protein

On the day following electroblotting, probed membranes were washed with TBS-T as before and were subsequently incubated for 60-minutes in secondary GE Healthcare® Horseradish Peroxidase conjugated anti-mouse or anti-rabbit antibody solution which was prepared in 10mL of TBS-T at 1:5000 (**Table 2-9**). Membranes were then washed in TBS-T as before for 15-minutes and thrice for 5-minutes, during which time the GE Healthcare™ ECL™ Prime western blotting detection agent (12994780) was prepared by combining equal volumes of solutions A and B in the dark at RT. After washing, the membrane was placed upon a layer of acetate and the prepared enhanced chemiluminescent prime detection agent was added dropwise to the membrane for a 5-minute incubation in the dark. Excess detection agent was then removed with blotting paper, and a second layer of acetate was added to seal the membrane for transfer to the Fujifilm® LAS3000 digital imaging unit. Exposures ranged from 10-seconds to 30-minutes.

To assess successful fractionation of lysates and verify equal loading, GAPDH and Histone H1 were probed for cytosolic and nuclear fractions, respectively. GAPDH was probed immediately following chemiluminescent detection, see 2.10.5.2, as it was detected using fluorescent methods.

2.10.5.2 *Fluorescent detection of protein*

As a cytoplasmic loading control, GAPDH protein levels were investigated by incubating membranes with mouse anti-human DyLight® 680 mAb (Invitrogen) at 1:10000 for 60-minutes at RT before a further TBS-T wash. Membranes were transferred for fluorescent detection at 700nm on the LI-COR® Odyssey® Fc imaging system with an exposure time of 30-seconds. For the nuclear control, the same process was repeated using a mouse anti-human Histone H1 (SCBT) at 1:2000 (**Table 2-9**).

2.10.6 Densitometric Quantification of Protein

Digital images were stored in the Tagged Image File Format lossless format (.TIFF) for analysis with the Fiji edition of ImageJ2 (v. 2.0.0.71 acquired Dec 2018). Background levels and noise effects were corrected for by measuring the area immediately surrounding each individual band, before protein bands were quantitated by conversion to a histogram and measured by area surrounding peak intensity. The resulting area was normalized to a common control, which was present across western blots to allow for cross-blot normalization of protein levels. By measuring protein loading of cytosolic and nuclear fractions with GAPDH and Histone H1 bands, respectively, protein measurements were corrected for unequal sample loading.

Table 2-9: Western Blot Antibodies used within Study

Antibody Target	mW	Cat.N ^o	Species	Conjugate	Conditions	Detection Method	Dilution	Source
Primary antibodies								
Beta-catenin	92kDa	610153	Mouse	N/A	4°C - 24Hr	Chemiluminescent	1:5000	BD Biosciences
Gamma-catenin	83kDa	75550	Rabbit	N/A	4°C - 24Hr		1:2500	Cell Signalling
LEF1	25-58kDa	2230	Rabbit	N/A	4°C - 24Hr		1:2000	Cell Signalling
RAPGEF4	116kDa	19103-1-AP	Rabbit	N/A	4°C - 24Hr		1:1000	Proteintech
SIPA1L1	220kDa	25086-1-AP	Rabbit	N/A	4°C - 24Hr		1:2500	Proteintech
Secondary Antibodies								
Anti-mouse	N/A	NA931	Donkey	HRP	RT - 1Hr	Chemiluminescent	1:5000	GE Healthcare
Anti-rabbit	N/A	NA934	Donkey	HRP	RT - 1Hr		1:5000	GE Healthcare
Loading Controls								
GAPDH DyLight® 680	37kDa	15738-D680	Mouse	DyLight680	RT - 1Hr	Fluorescent	1:10000	Fisher Scientific
Histone H1 AF @ 790	22kDa	8030-AF790	Mouse	AF790	RT - 1Hr		1:2000	Santa Cruz

mW – Molecular Weight; kDa – Kilodalton; HRP – Horseradish peroxidase; AF790 – AlexaFluor790.

2.11 Flow Cytometry

Flow cytometry is a technique enabling the analysis of cells on a single cell level based upon individual cells size, granularity, and expression of up to fifty select markers either bound upon on the membrane or intracellularly depending on the capabilities of the chosen cytometer. The sample is propelled through a flow cell containing laminar flowing sheath fluid in which single cells are separated linearly by hydrodynamic focusing into a stream. Cells pass through a series of lasers individually, which vary depending upon the cytometer, allowing capture of measurements. Measurements can include fluorescent-conjugated antibodies, fluorescent chemicals, and integrated fluorescent elements.

Locally, a BD Accuri™ C6 Plus was available which can detect up to four fluorescent colours. It was equipped with a red and blue laser alongside four fluorescence detectors. Two light scatter detectors for forward scatter (FSC) and side scatter (SSC) measure size and granularity respectively, enabling six total parameters to be explored (**Table 2-10**). For more complex studies, the Cardiff University Central Biotechnology Service (CU-CBS) provided access to two tri-laser BD FACSCanto™ II cytometers and one hepta-laser BD LSRFortessa™ which can detect ten and twenty parameters, respectively. In addition, the CBS provided access to a BD FACSAria™ III cell sorter which can measure 20 parameters simultaneously to isolate a cell population of choice.

Flow data was stored in the FCS 3.0 format and analysis was undertaken in the De Novo Software™ FCS Express™ software (v6.0) or the statistical software language R (v4).

2.11.1 Estimation of CD34⁺ HSPC Cell Proportion

In parallel with the isolation of MNC from umbilical CB, examination for CD34, a marker of HSPC, was performed to enable the percentage of HSPC to be determined. In brief, 100µL of undiluted blood was recovered and stained with 10µL of CD34-phycoerythrin (PE) and 5µL of CD45-allophycocyanin (APC^F). A control stain with 10µL of IgG1-PE and 5µL of CD45-APC^F was performed (**Table 2-11**). Samples were incubated at 4°C for 30-minutes, after which time, 5mL of FACS™ Lysis Buffer (BD) was added to each tube and a further RT incubation for 10-minutes was performed. The cells were recovered and washed in 5mL 1x PBS and centrifuged at 200g for 5-minutes to form a pellet, with the supernatant discarded and the cells resuspended in residual supernatant. Samples were then transferred to miniflow tubes and acquired on the Accuri flow cytometer, with CD34⁺ percentage determined with the gating strategy demonstrated in **Figure 2-2**.

Table 2-10: Technical Specifications of the Accuri C6 Plus

Classifier	Characteristic	Detection Example
Laser excitation	488nm	N/A
	640nm	N/A
Emission Detection	533/30nm (FL1)	FITC, GFP, AF488
	585/40nm (FL2)	PE, PI
	670nm LP (FL3)	PerCP-Cy5.5, DsRed
	675/25nm(FL4)	APC ^F , TO-PRO-3
Flow rate	10-100 μ L/min	N/A

FITC - Fluorescein isothiocyanate; **GFP** - Green fluorescent protein; **AF488** - Alexa Fluor 488; **PE** - Phycoerythrin; **PI** - Propidium iodide; **PerCP-Cy5.5** - Peridinin chlorophyll protein–Cyanine5.5; **DsRed** – Discosoma Red; **APC^F** - Allophycocyanin; **TO-PRO-3** - TO-PRO®-3 iodide

Table 2-11: Flow Cytometry Antibodies used for Cord Blood HSPC Estimation

Antibody	Fluorescent-marker	Clone	Dilution	Source	Cat. N°
IgG1	PE	MOPC-21	1/10	BioLegend	400112
CD34	PE	581	1/10	BioLegend	343506
CD45	APC ^F	HI30	1/20	BioLegend	304012

APC^F - Allophycocyanin; PE - Phycoerythrin

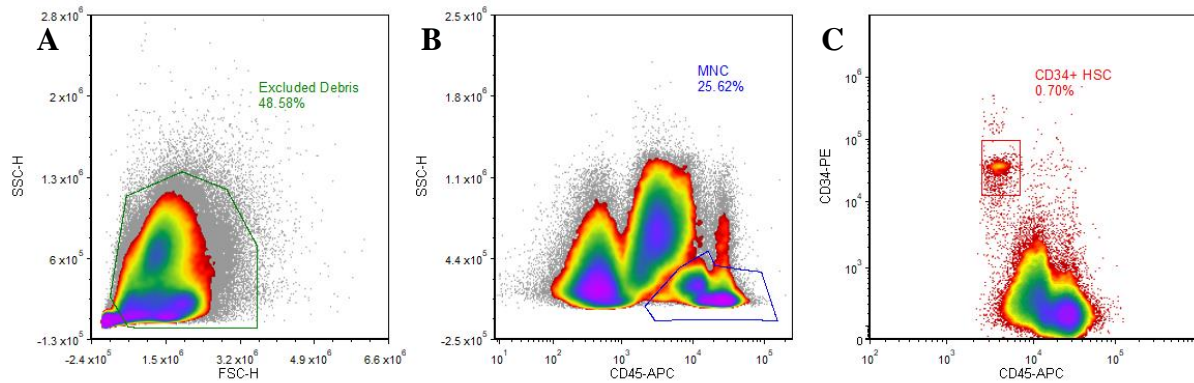


Figure 2-2: Gating Strategy used to Estimate CD34⁺ HSPC Percentage by Flow Cytometry

Representative bivariate density plots showing the gating strategy applied to estimate CD34⁺ HSPC from a human cord blood donation. **(A)** A debris exclusion gating based on FSC and SSC. **(B)** Within the non-debris gating, mononuclear cells were identified on the basis of CD45⁺ and low side scatter profile. **(C)** Within the mononuclear cell gating, the percentage of CD34⁺ cells were estimated based upon background autofluorescence determined with the isotype control IgG1-PE.

FSC – Forward scatter; **SSC** – Side scatter; **APC^F** - Allophycocyanin; **PE** - Phycoerythrin; **MNC** – Mononuclear Cells; **HSPC** – Haematopoietic Stem Progenitor Cells.

2.11.2 Fluorescence Activated Cell Sorting of Transduced CD34⁺ HSPC

Following lentiviral transduction, transduced HSPC were sorted using a BD FACSAria™ III within the CU-CBS facilities at Cardiff University. Transduced HSPC were counted and centrifuged at 270g for 10-minutes to form a pellet, with the supernatant discarded. HSPC were resuspended in 1×10^6 cells/mL in 1x PBS containing 1% BSA (v/v) and 5ng/mL IL-3. Resuspended cells were filtered through a 40µM cell strainer into labelled 15mL falcon tubes. Transduced HSPC were sorted on the basis of GFP positivity with a mock (non-infected) population used to design the gating strategy (**Figure 2-3**). Cells were sorted at RT at low flow rate with the 100µm nozzle. Cells were sorted into a 15mL falcon tube containing 8mL of IMDM media supplemented with 10% FBS (v/v) and 20mg/mL gentamicin. After returning to tissue culture, sorted populations were transferred to UC and centrifuged at 270g for 10-minutes with the supernatant discarded. Cells were resuspended in 1mL 3S^{LOW}G/GM and counted by flow cytometry. Density was then adjusted to 0.5×10^5 /mL.

2.11.3 Sorting Populations for pBARV and pfuBARV Construct Incorporation

Cell lines transduced with pBARV and pfuBARV lentivirus were cultured to a total of 8×10^6 cells, with a continuation culture maintained. The cells were pelleted and resuspended in 500µL of PBS + 1% BSA (v/v). Cells were passed through a 40µm strainer into a BD FACS tube to remove aggregate bodies. Receiver tubes were prepared containing 5mL of the appropriate growth medium. The BD FACSAria™ III was maintained at RT, and the maximal nozzle of 100µm was fitted to reduce cell compression stress. Parental cells were used to exclude debris and doublets before a threshold gate was devised for DsRed positivity which avoided inclusion of autofluorescent events. Sorted cells were transferred to a universal container and centrifuged at 280g for 5-minutes at RT before resuspending at 5×10^5 cells per mL for culture based upon the sorted event count.

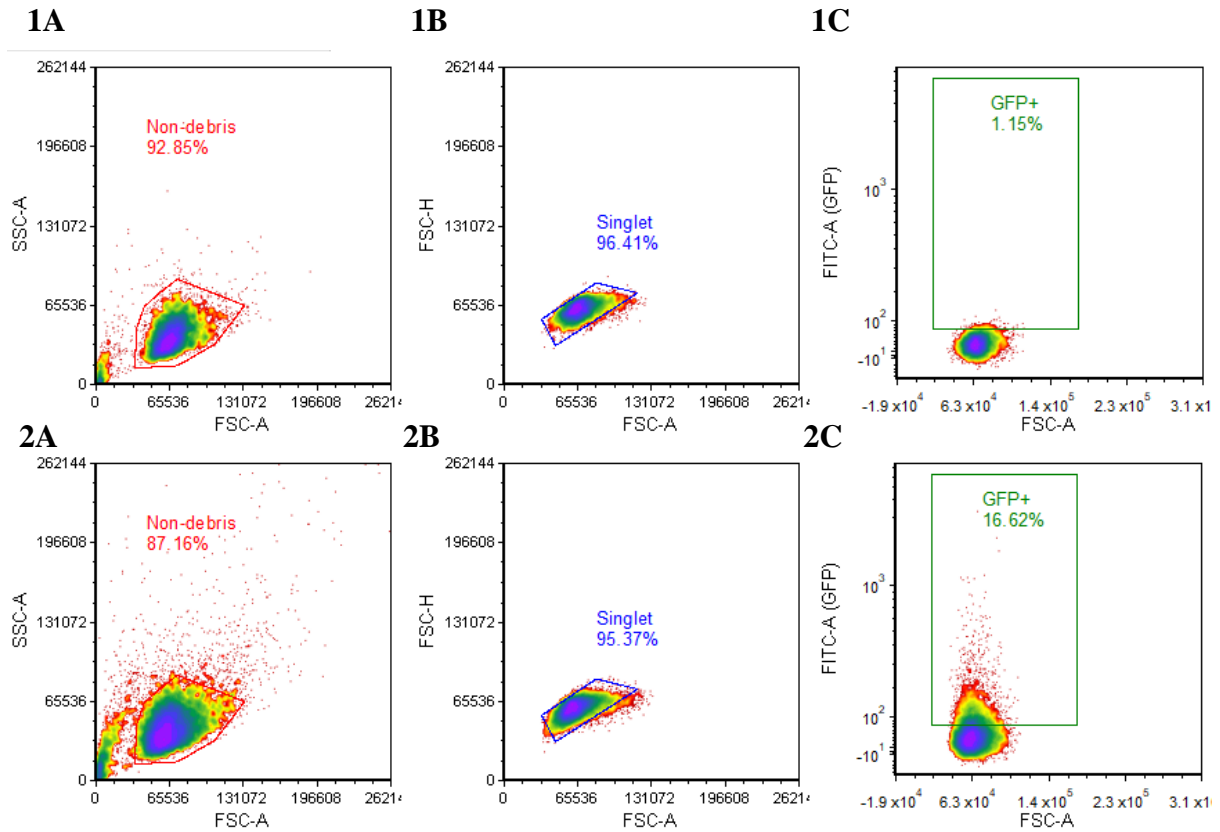


Figure 2-3: Flow Cytometry Gating Strategy applied to Sort Transduced CD34⁺ HSPC

Representative bivariate density plots demonstrating transduced CD34⁺ HSPC cultures as revealed by GFP positivity versus Mock on a BD FACSAria™ III. **(1)** Mock **(2)** Scrambled Lentivirus **(A)** A debris exclusion gating based on FSC and SSC. **(B)** Within the non-debris gating, singlet cells were identified. **(C)** Within the two prior gates, the percentage of GFP⁺ cells within a bulk culture were established based upon the background autofluorescence which was established using a mock culture which was otherwise treated comparably with the exception of lentiviral coating.

2.11.4 Immunophenotyping of Transduced CD34⁺ HSPC

Immunophenotyping was performed to assess myeloid cell differentiation over the time course of 13 days. CD13-APC^F and CD36-biotin were utilised for lineage discrimination, with the latter requiring a secondary streptavidin PerCP-Cy5.5. Cells were further stained independently with IgG1, CD11b, CD14, CD15, and CD34 conjugated to PE (**Table 2-12**). In brief, 3×10^5 cells were washed by addition of staining buffer (SB; 1x PBS supplemented with 0.02% (v/v) sodium azide and 1% (v/v) BSA)) and centrifugation at 270g for 5-minutes. The pellet was resuspended in 75 μ L SB. 96V-bottom plates were prepared with additions of antibodies before addition of 15 μ L cell suspension. Plates were centrifuged at 15-seconds to associate the contents, before a brief vortex prior to incubation at 4°C for 30-minutes. After the incubation, the reaction was quenched by addition of 150 μ L of SB and the resuspended contents were transferred to miniflow tubes. Samples were centrifuged at 270g for 5-minutes, with the pellet resuspended in SB containing PerCP-Cy5.5 Streptavidin secondary antibody and were incubated again at 4°C for 30-minutes. Finally, stained cells were washed by addition of 150 μ L SB and centrifugation at 270g for 5-minutes before the pellet was resuspended in 100 μ L of SB. Prepared samples were acquired on the Accuri C6 Plus and the gating strategy was applied as in **Figure 2-4**.

Table 2-12: Flow Cytometry Antibody Panel used for CD34+ HSPC Immunophenotyping

Antibody Target	Fluorescent-marker	Clone	Dilution	Source	Cat. N°
IgG1	PE	MOPC-21	5ng/μL	BioLegend	400112
CD11b	PE	ICRF44	5ng/μL	BioLegend	301306
CD13	APC ^F	WM15	5ng/μL	BioLegend	301706
CD14	PE	HCD14	5ng/μL	BioLegend	325606
CD15	PE	W6D3	5ng/μL	BioLegend	323006
CD34	PE	581	5ng/μL	BioLegend	343506
CD36	Biotin	SMO	1ng/μL	Ancell Corporation	185-030
PerCP-Cy5.5 Streptavidin	PerCP-Cy5.5	-	1ng/μL	BD Biosciences	551419

PE – Phycoerythrin; **APC^F** - Allophycocyanin; **PerCP-Cy5.5** – Peridinin chlorophyll protein–Cyanine5.5

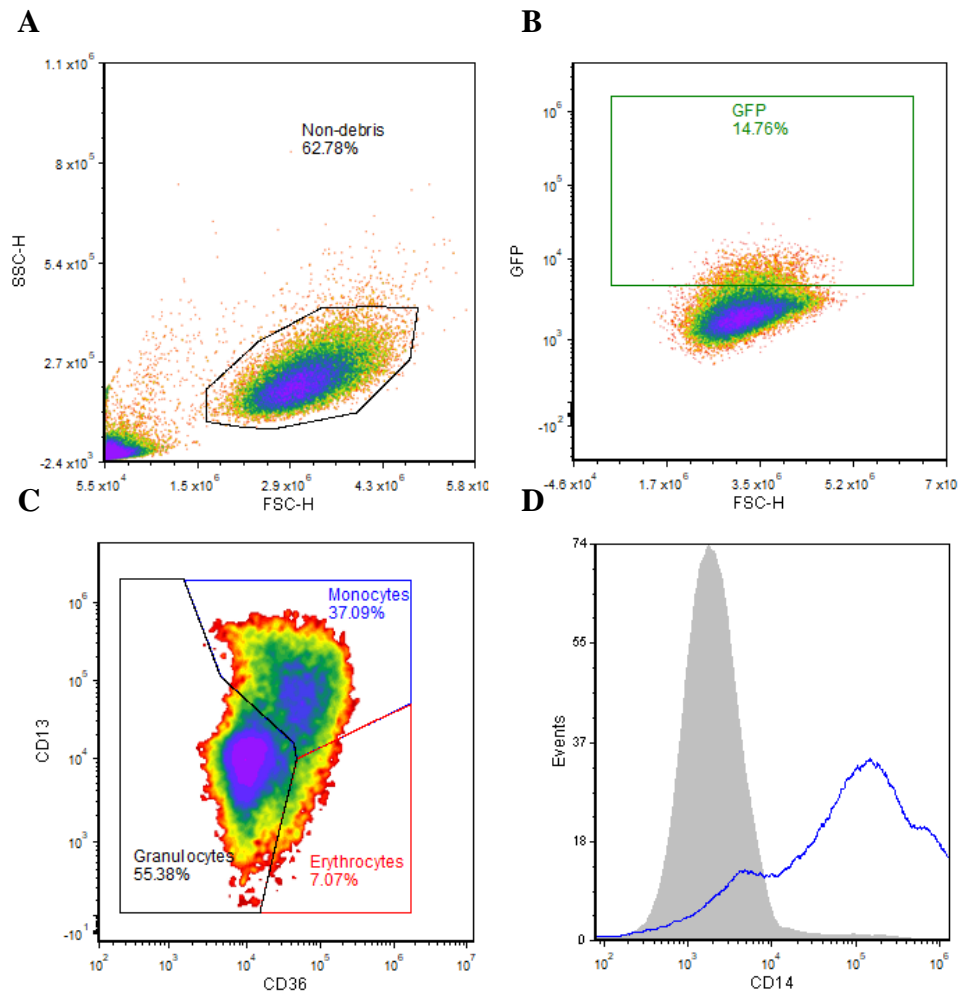


Figure 2-4: Immunophenotyping Gating Strategy for Lineage Determination

Representative bivariate plots and a histogram detailing the gating strategy applied for immunophenotyping HSPC at day 13. (A) Cells were excluded from debris on the basis of removal of events below $<5 \times 10^5$. (B) Cells were subset to those transduced and expressing GFP. (C) Expression of the lineage discrimination markers CD13 and CD36 were applied to resolve the monocytic, granulocytic, and erythroid progenitor populations within the bulk culture. (D) Within the monocytic and granulocytic populations the expression of established maturation markers (CD14 - blue) were applied to examine maturation against an isotype control (Isotype - grey).

2.11.5 Measuring the pBARV Response

WNT/ β -catenin signalling levels were assessed by the percentage of responder cells and shift in mean fluorescent intensity (MFI) based upon the emission from Venus. Venus is measured with the 533/30nm channel (Venus ex. 515, em. 528). Doublets and debris are first removed from the cell population before cells are identified. By contrasting the different conditions within an experiment, histogram subtraction can be applied which will show the difference in positivity and show any shifts in MFI. This measurement represents the pBARV response, further controlled against pfuBARV which represents a background noise reading for the β -catenin/TCF-axis controlled pBARV reporter.

2.11.6 Monitoring Cell Viability

For experiments assessing cell viability, the monomeric cyanine stain TOPRO (T3605) was used to bind dsDNA which would only be accessible in non-viable cells undergoing apoptosis or autophagy. TOPRO was added at a concentration of 50nM and incubated at RT for 30-minutes before analysis. TOPRO has excitation and emission wavelengths of 642nm and 661nm, respectively. The FL-3 channel (670nm LP) was used for analysis.

2.11.7 Proliferation and Viability Assay

As cell number can be determined by counting with a flow cytometer, proliferation can be determined by counting cells on a time course. TOPRO can be used as a dead cell indicator as detected with the FL-3 (670nm LP) channel. Cells were prepared in a 12-well tissue culture plate at their minimal recommended subcultural concentration, typically between 1×10^5 and 2×10^5 cells *per* mL. Each day, 50 μ L was recovered and TOPRO was added at 50nM, before 10 μ L was acquired on an Accuri C6 Plus. Cells were expanded as populations approached the upper bound of the log-phase growth by moving to an appropriate plate or flask. A time course of 5 or greater days was followed.

2.11.8 DNA Content Assay

Propidium iodide (PI) is a DNA binding dye which provides a measure proportional to the amount of DNA within cells. Cells within G2 phase of mitosis have twice the DNA content than cells in G1, therefore, they will uptake proportionally twice the dye and fluorescence with a greater MFI. By utilising this, cell cycle condition was measured. Cells were required to be fixed to enable DNA accessibility by addition of ethanol. 2×10^5 cells were recovered and centrifuged at 280g for 10 minutes to pellet cells. Cells were then resuspended in 300 μ L PBS

and placed on ice for 5 minutes, before addition of 700 μ L of 100% ethanol before returning the samples to ice for a further 30 minutes, after which they were transferred to -20°C overnight. Later, cells were retrieved and pelleted by addition of 10mL PBS and centrifugation at 280g for 10 minutes. During this spin, a dye mix was prepared in PBS containing PI at 40 μ g/ml and RNase at 0.1mg/ml. After centrifugation, the supernatant was carefully aspirated, cells were resuspended in 75 μ L PBS, and transferred to a miniflow tube. 25 μ L staining solution was added, and cells were covered with a plate sealer before transfer to a 37 °c water bath for 30 minutes. Subsequently, cells were analysed on an Accuri C6 Plus. Cells were gated as per **Figure 2-5**.

2.11.9 Annexin V Assay

Population-based cell viability was determined with Annexin V and 7-AAD. Annexin V detects apoptotic cells by binding to phosphatidylserine, an apoptotic marker present on the outer region of the plasma membrane as apoptosis occurs. 1×10^5 cells were recovered and washed in PBS by centrifugation at 280g for 5 minutes. This was repeated in 1x Binding Buffer. Cells were resuspended in 1x Binding Buffer at 1×10^6 cells *per* mL and 5 μ L of Annexin-APC^F was added for a 15-minute incubation at RT. Subsequently, cells were washed in 1mL of 1x Binding Buffer, then resuspended in 200 μ L of 1x Binding Buffer. 5 μ L of 7-AAD was added before immediate acquisition on an Accuri C6 Plus for analysis (**Figure 2-6**).

2.11.10 Migration Assay

The motility capacity of cells to migrate toward a chemoattractant was assayed using the Transwell® cell migration system which constitutes an upper and lower chamber separated by a membrane. A negative control for migration was used by preparing a well with only chemotaxis medium (serum-free IMDM containing 1% *v/v* BSA) to account for free movement and validate membrane integrity. Chemotaxis medium or filtered CM was pre-warmed and a 24-well Transwell plate was prepared by addition of 600 μ L the lower chamber and 100 μ L to the upper chamber, respectively; this was placed in the incubator whilst cells were prepared. 1×10^5 cells were washed and resuspended in 590 μ L of chemotaxis medium, with 100 μ L of this suspension used to replace the chemotaxis media in the upper chamber. 5 μ L of SDF1 α (Peprotech, 300-28A-10) at 12 μ g/mL was added to relevant lower wells.

Plates were incubated at 37°C and 5% CO₂ for 4 hours, after which time 50 μ L of the cell suspension in the upper chamber was harvested and transferred to miniflow tubes. The full contents of the lower chamber were harvested and centrifuged at 280g for 5minutes, before

resuspending in 100µL for transfer to a miniflow tube. 10µL of the upper and lower chamber was acquired on an BD Accuri™ C6 Plus and the counts recovered were converted into percentage migration through division of the number of cells having migrated to the lower chamber respective to those in the upper chamber.

2.11.11 Immunophenotyping Assay

To study for perturbed differentiation of AML cell lines as a result of gene knockout, a panel of cell surface members which are well characterised as markers of certain lineages were studied (**Table 2-13**). Cell lines were examined for presence of markers which are documented to be present, alongside markers of differentiation which would not be present normally. To determine marker expression, 1×10^5 cells were harvested *per* antibody of interest, and these were washed by centrifugation at 280g for 5-minutes, before resuspending in cold SB to 1×10^5 cells *per* mL. Antibodies were added to wells to an appropriate final dilution, with 15µL of the cell suspension added subsequently. The plate was centrifuged at 280g for 3-minutes to bring together well contents, before a 30-minute incubation at 4°C. After the incubation, 150µL of SB was added to each well to quench reactions, and these contents were transferred to miniflow tubes. Samples were centrifuged at 280g for 5-minutes, with the supernatant discarded. Cells were then resuspended in 100µL of SB and analysed on a BD Accuri™ C6 Plus. Isotype control antibodies were used in order to determine appropriate marker placement. FSC and SSC were used as approximate indicators of cell size and surface granularity, respectively.

Table 2-13: Cell Line Immunophenotyping Marker Antibody Panel

Antibody	Marker	Clone	Dilution	Supplier	
				Company	Cat. N°
PerCP-Cy5.5 IgG1	N/A	MOPC-21	1/20	BioLegend	400150
APC ^F IgG1		MOPC-21	1/20	BioLegend	400120
CD3 PerCP-Cy5.5	T-cell	SK7	1/20	BD Biosci	641397
CD4 PerCP-Cy5.5	Monocytic	SK3	1/20	BD Biosci	332772
CD13 APC ^F	Myeloid	WM15	1/20	BioLegend	301706
CD14 APC ^F	Monocytic	HCD14	1/20	BioLegend	325608
CD15 PerCP	Granulocyte	W6D3	1/20	BioLegend	323018
CD19 APC ^F	Progenitor	HIB19	1/20	BioLegend	302212
CD33 APC ^F	Myeloid	P67.6	1/20	BioLegend	366606
CD34 APC ^F	Myeloblasts	581	1/20	BioLegend	343510
CD235a PerCP-Cy5.5	Erythroid	HI264	1/20	BioLegend	349109

APC^F - Allophycocyanin; PerCP-Cy5.5 – Peridinin chlorophyll protein–Cyanine5.5

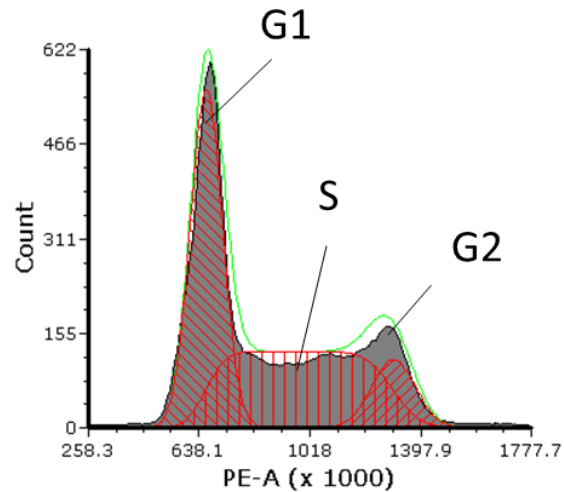


Figure 2-5: Cell Cycle Strategy

DNA-content analysis elucidates the cell cycle condition of a population of cells. To achieve this propidium iodide was used which is an intercalative agent capable of binding DNA. Detection of PI with a flow cytometer (FL-2) was used, with the subsequent fluorescence profile used to predict cell cycle staging. A multi-cycle model was fit to the data with FCS Express, allowing the determination of per-phase population proportion.

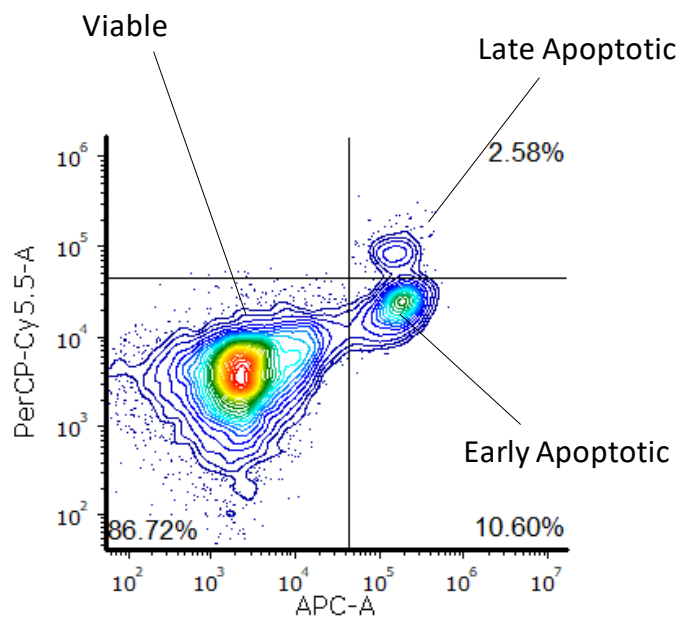


Figure 2-6: Apoptosis Gating Strategy

Analysis of apoptosis can be achieved with annexin-V to determine the early stages of apoptosis, whilst late apoptotic cells can be delineated with agents including 7-ADD, TOPRO, and propidium iodide. Phosphatidylserine (PS) in healthy cells was expressed exclusively within the intracellular leaflet of the plasma membrane, however, during early apoptosis, membrane condition is affected and translocates to the external leaflet. This enables Annexin-V to bind PS. In our study, Annexin-V is bound to the fluorochrome APC^F which was detected on a flow cytometer with FL-4. Late apoptotic cells was detected through DNA binding agents which bind DNA after the nuclear membrane disassociates and DNA fragmentation occurs. In this study, 7-Aminoactinomycin D (7-AAD) was used which was detected with FL-3.

2.11.12 Drug Sensitivity Assay

To perform the drug sensitivity assay, serial dilutions of DNR (Cayman, 14159) and Ara-C (Merck, C1768) were prepared in order to generate working dilutions. 1.6×10^6 cells were harvested and washed with a 280g for 5-minute centrifugation, before being resuspended in 8mL of appropriate fresh growth medium. 0.4mL of suspended cells were plated into each well of a 48-well dish and 4 μ L additions of prepared DNR or Ara-C were added. Final concentrations used were 50nM, 100nM, 200nM, 400nM, 800nM for Ara-C, and 3nM, 12nM, 25nM, and 50nM for DNR. A control well with a vehicle control was used. Treated cells were incubated at 37°C and 5% CO₂ for 48 hours. After 48 hours, a harvest mix was prepared constituting 10xHEPES with 2xTOPRO in RPMI complete medium. Cells were resuspended and 225 μ L was added to miniflow tubes containing 25 μ L of the HEPES/TOPRO harvest mix. 10 μ L of each miniflow tube was acquired on the BD Accuri™ C6 Plus. Cell counts were computed into growth inhibition polynomial regressions, which were used to determine the point at which 50% growth inhibition was obtained (GI50) using the GRmetrics package as described (Hafner *et al.*, 2016).

2.11.13 Stress-induction Assays

2.11.13.1 Serum-depletion Assay

Foetal-bovine serum provides cells with growth factors that are essential to cell maintenance and growth, alongside amino acids, sugars, lipids, and hormones. Cell lines often require between 10% and 20% FBS (v/v). To achieve this, serum-free medium for the respective cell line was prepared, alongside a serial dilution of 2x FBS media providing final concentrations of 10%, 5%, 2.5%, 1.25%, 0.5%, 0.25%, and 0.125% (v/v). 250 μ L of 2xFBS media was plated into each well of a 48-well plate, alongside a serum-free culture as a control; this was allowed to pre-warm in the incubator at 37°C and 5% CO₂. 1×10^6 cells were harvested and pelleted through centrifugation at 280g for 5-minutes. The cells were then washed with 10mL of serum-free medium to reduce FBS carryover, before resuspending in 2.5mL of serum-free medium (<0.01% FBS carryover). 250 μ L was transferred to each of the pre-prepared wells within the plate. Cells were incubated at 37°C and 5% CO₂ for 72 hours. After 72 hours, miniflow tubes were prepared containing TOPRO (50nM) and 100 μ L of culture was harvested after resuspending. 10 μ L of each miniflow tube was acquired on the BD Accuri™ C6 Plus. Cell counts were computed into growth inhibition polynomial regressions, which were used

to determine the point at which 50% growth inhibition was obtained (GI50) using the GRmetrics package as described (Hafner *et al.*, 2016).

2.11.13.2 *Low-density Assay*

As clonal issues presented, low-density assays were designed which were well below the recommended culture densities in efforts the stress of culture under such conditions which could reveal susceptibilities. Cells were serially diluted to prepare culture densities of 1×10^5 , 5×10^4 , 1×10^4 , 5×10^3 , 1×10^3 , and 1×10^2 cells in 1mL and were plated into a 24-well TC plate for incubation at 37°C and 5% CO₂ for 72 hours. After 72 hours, miniflow tubes were prepared containing TOPRO (50nM) and 100µL of culture was harvested after resuspending. 10µL of each miniflow tube was acquired on the BD Accuri™ C6 Plus. Cell counts were computed into growth inhibition polynomial regressions, which were used to determine the point at which 50% growth inhibition was obtained (GI50) using the GRmetrics package as described (Hafner *et al.*, 2016).

2.12 Genomics

2.12.1 Cleavage Detection by Polymerase Chain Reaction

To determine the InDel mutation rate, the Invitrogen™ GeneArt® Genomic Cleavage Detection Kit (A24372) was used. Primers were designed to amplify the DSB gRNA target site, and this locus was amplified by PCR. The PCR product was denatured and reannealed enabling mismatches to form as strands with differing InDel mutations or no InDel combine. Mismatches were cleaved by an endonuclease enzyme, which generates shortened products that were detected via electrophoresis and quantified by densitometry.

2.12.1.1 *Determining InDel Hit Rate*

Genomic DNA was amplified prior to detection, requiring primers be designed for the target loci. Primers were designed with a $T_m > 55^\circ\text{C}$ and a length of 22bp with 45-60% GC content, these are detailed in **Table 2-14**. To do this, 2×10^6 cells were centrifuged at 200g for 5-minutes at 4°C to harvest cells. 50µL of cell lysis buffer and 2µL protein degrader were mixed in a microcentrifuge tube, before 50µL of this mix was added to each pellet for resuspension. The resuspended pellet was transferred to a PCR tube and run in a GeneAmp® PCR 9700 to lyse cells and extract DNA with the following parameters: 68°C for 15-minutes, 95°C for 10-minutes, and held at 4°C. The samples were recovered and vortexed, with 2µL of sample was transferred to a fresh PCR tube containing 1µL of 10µM forward/reverse primer mix, 25µL of

AmpliAq Gold® 360 Master Mix, and 22µL of dH₂O for PCR amplification. DNA was amplified in the PCR machine with the following parameters: enzyme activation at 95°C for 10-minutes once, cycling through a 95°C denaturing step for 30-seconds, an annealing step at 55°C for 30-seconds, and an extension stage at 72°C for 30-seconds 40-times over. A final extension was completed by a 7-minute 72°C incubation, before finally holding at 4°C. 3µL of PCR product was combined with 1µL of 10x detection reaction buffer and brought to a volume of 9µL of dH₂O. A re-annealing reaction enabled heteroduplexes to form and was undertaken in the Techne® Prime™ thermal cycler with the following parameters: 95°C for 5-minutes, temperature stepped at -2°C per second from 95°C to 85°C, before a second stepping at -0.1°C per second from 85°C to 25°C, before a final hold at 4°C. Samples were immediately advanced to enzyme digestion to produce cleaved products. 1µL of Detection Enzyme was added to each sample and incubated for 37°C for 1-hour, vortexed, and centrifuged for detection by microfluidic electrophoresis on a Bioanalyzer 2100 (2.12.2).

Table 2-14: Primer Design for Cleavage Detection

To detect cleavage events, primers were designed to immediately flank the double-strand break target site. These primers were designed to have no predicted off-target effects, and to possess a predicted melting temperature of approximately 60 degrees Celsius. The cleavage site was centred relative to the flanking primer location, ensuring ease of detection as cleaved products would be approximately half the size of wild-type, unaffected sequences. Product size was maintained below 250bp to ensure ample PCR product production for accurate prediction of cleavage, alongside ease of running on a DNA gel or with the Agilent Technologies™ Bioanalyzer 2100™.

Target	ID	Left primer coordinates	Left primer (5-3')	TM	Right primer coordinates	Right primer (5'-3')	TM	Product size
<i>CTNNB1</i>	#1	chr3:41234119	TTCTTCCTTCTGTTTTTCAGGC	60	chr3:41234335	TCCTTTGGATTTATGCATTCCT	60	238
<i>CTNNB1</i>	#2	chr3:41233552	GACTCTTGTTTCAGCTTCTGGG	60	chr3:41233736	TCAGATGACGAAGAGCACAGA	60	206
<i>CTNNB1</i>	#3	chr3:41234119	TTCTTCCTTCTGTTTTTCAGGC	60	chr3:41234335	TCCTTTGGATTTATGCATTCCT	60	238
<i>JUP</i>	#1	chr17:41765064	TCCCTCTTTACCCATAGCTG	60	chr17:41764915	ATACTCACCAGCCTCCACAATG	61	171
<i>JUP</i>	#2	chr17:41771870	CTTCCTGACTTCCTCCTTTGTG	60	chr17:41771680	TGGTTTTCTTGAGCGTGTACTG	60	212
<i>JUP</i>	#3	chr17:41771870	CTTCCTGACTTCCTCCTTTGTG	60	chr17:41771680	TGGTTTTCTTGAGCGTGTACTG	60	212

TM – Melting temperature.

2.12.2 Quantifying DNA by Capillary Electrophoresis

To quantify the cleavage products, samples were analysed by microfluidic electrophoresis with the Agilent Technologies™ Bioanalyzer 2100™. The Agilent DNA 1000 Chip™ was used. A gel-dye mix was equilibrated to room temperature for 30-minutes before a DNA chip was prepared on the priming station. 9µL of gel-dye mix was loaded, and the mix plunged for 60-seconds to disperse throughout the chip. 9µL of gel-dye mix was loaded into two further preparatory wells. 5µL of flanking marker was loaded into each sample well and the 1µL of DNA ladder was loaded into the ladder channel. 1µL of prepared sample was loaded into each of the 12 available wells. The chip was primed by vortexing in an adapter for 1-minute at 2400RPM. The chip was then immediately transferred to the Bioanalyzer 2100.

2.12.3 DNA Sequencing

To validate knockouts sequencing of the DNA at regions immediately flanking the CRISPR-Cas9 target site was necessary. To achieve this, DNA was extracted from an expanded clone before PCR amplification of the target site, and subsequent sequencing.

2.12.3.1 *Extracting DNA*

In total, a minimum of 150ng of DNA was necessary for each PCR reaction, therefore, to obtain 2µg of DNA, only 2×10^5 cells were required for extraction (0.01ng/cell). High quality DNA was extracted with a Qiagen DNeasy Blood & Tissue Kit which in principle relies upon cell lysis with proteinase K and DNA isolation using a filter membrane containing a chaotropic salt rich buffer. Extracts were verified for purity with a Nanodrop A_{260}/A_{280} ratio of 1.7 to 1.9.

Cells were first centrifuged at 280g x 5 minutes and resuspended in a mixture of 200µL PBS, 200µL Buffer AL, and 20µL Proteinase K before vortexing and incubation at 56°C for 10 minutes. After this, 200µL 100% Ethanol was added and samples were vortexed to homogenise the solution. The solution was transferred to a prepared DNeasy Mini spin column and centrifuged at 6000g for 1 minute, before the flow-through was discarded. The spin column was then transferred to a fresh collection tube and 500µL Buffer AW1 was added before a second centrifugation at 6000g for 1 minute, allowing the flow-through to be discarded a second time. 500µL of Buffer AW2 was then pipetted onto the membrane before a centrifugation at 20,000g for 3 minutes with the flow-through discarded. Subsequently, the column was transferred to a final collection tube and 200µL of Buffer AE was added before a 1-minute incubation, after which, the column was centrifuged at 6000g for 1 minute to elute

DNA. The elute was then transferred and centrifuged again to maximise the DNA extraction. With the extraction complete, DNA was quantified, and purity checked using a Nanodrop.

2.12.3.2 PCR Amplification for Sequencing

PCR is a technique for DNA amplification. Taq DNA Polymerase is a thermostable enzyme derived from *Thermus aquaticus*; it is capable of functionally withstanding repeat heating to 95°C in order to amplify DNA fragments. An initial DNA denaturation step denatures the DNA to ensure efficient utilisation of the primary templates. Following this, a cycle repeats between denaturation, primer annealing, and extension. The denaturation step occurs at 95°C to separate strands. Primer annealing then occurs at 55°C, which is below the melting temperature of the primers. Finally, extension at 72°C occurs. These three stages repeat 30-40 times to amplify the DNA region of interest. A final extension cycle occurs at 72°C for 10 minutes to ensure complete reaction products. In this case, two primers are used for each gene of interest, enabling a 200bp region of each allele to be sequenced for the presence of InDel events.

A reagents mastermix was prepared without the primer and template (**Table 2-15**). The mastermix was then transferred to PCR tubes depending upon the reaction volume before primers and template DNA were added. Contents were gently mixed by vortexing, before amplification occurred (**Table 2-16**). Extracts were verified by DNA gel.

2.12.3.3 PCR Product Verification

The PCR amplification stage generates substantial quantities of the same length of DNA. To verify that no off-target amplification has occurred, a small quantity of the PCR product was run by electrophoresis on an agarose gel. As DNA is negative and all strands should be of the same length, they form a single uniform band. 0.8% agarose was prepared in 1 x Tris base, boric acid, and EDTA (TBE) and melted using a microwave. 25mL was transferred to a universal container, and 1µL of Peq Green, a fluorescent DNA-binding dye, was added to the liquid gel. Rapidly, the mixture was transferred to a pre-assembled gel electrophoresis box and allowed to set over 30 minutes. With the gel set, 1 x TBE was poured over the gel until sufficiently covered, and the well comb was then removed. Samples were prepared by addition of a loading dye and were added to designated wells for a run at 120V for 45minutes. A UV box illuminated bands.

2.12.3.4 PCR Product Purification

PCR purification was necessary to remove contaminant enzymes, nucleotides, primers, and buffer components which would interfere with downstream DNA sequencing. The Qiagen QIAquick PCR Purification kit (28104) was used which purifies with up to 95% efficiency. Buffer PE was first prepared by adding 100% ethanol. To purify PCR products, 5 volumes of Buffer PB was added to each volume of PCR product and mixed. The sample was then transferred to a prepared QIAquick column and centrifuged for 1 minute at 18000g with the flow-through discarded. 750µL of Buffer PE was then added to the QIAquick column to wash the sample, allowing centrifugation for 1 minute as before with the flow-through once again discarded. The QIAquick column was then transferred to a fresh 1.5mL collection tube and centrifuged with 30µL PCR grade water for 1 minute as before. The resulting purified product was then verified on the Nanodrop and stored at -20°C for DNA-sequencing.

Table 2-15: Mastermix Composition for PCR

Component	25µL Reaction	50µL Reaction	Final Concentration
10X Gold DNA Polymerase Buffer	2.5µL	5µL	1X
10mM dNTP Mix (each)	1.25µL	2.5µL	500µM
10uM Primer (each)	2µL	4µL	0.8µM
AmpliTaq Gold DNA Polymerase	0.125µL	0.25µL	1.25U/50uL
25mM MgCl ₂	1.5µL	3µL	1.5mM
Template DNA	<i>Variable</i>	<i>Variable</i>	200ng
Nuclease-free Water	To 25µL	To 50µL	N/A

DNA – Deoxyribonucleic Acid; dNTP - Deoxynucleotide triphosphate; MgCl₂ – Magnesium Chloride.

Table 2-16: PCR Cycle Conditions

PCR was completed with a GeneAmp® PCR 9700 on conditions as stated. These conditions are adapted from Thermofisher' recommended guidelines, with the denaturation, annealing, extension, and terminal extension durations extended to ensure complete cycling success. A cycle count of thirty-five was found to produce sufficient downstream PCR product for DNA-sequencing.

PCR Stage	Temperature	Duration	Cycles
Initial Denaturation	95°C	10 Minute	1
Denaturation	95°C	1 Minute	35
Annealing	55°C	1 Minute	
Extension	72°C	1 Minute	
Terminal Extension	72°C	10 Minutes	1
Hold	4°C	∞	N/A

2.12.3.5 Sample DNA-Sequencing

To reveal the presence and exact nature of an InDel event, DNA-Sequencing of the flanking region was completed. To achieve this, purified PCR product was shipped to Eurofins with sequencing primers. This involved mixing 15 μ L of purified PCR product at 10ng/ μ L with 2 μ L of sequencing primer at 10uM. This mix was then transferred to a Mix2Seq Eurofins sample tube and shipped to Eurofins (Eurofins Genomics, Germany) for DNA-Sequencing.

2.12.3.6 Resolving DNA InDels by Digital Deconvolution

Genetic mutations facilitated by erroneous NHEJ are likely to differ between alleles which, in cases of aneuploid cell lines such as THP-1, will generate up to three different DNA sequences. Sanger sequencing of a combined population will lead to a mixed spectrogram. Classically, this is solved by cloning the mixture of alleles into a bacterial vector and sequencing numerous colonies to elucidate the individual alleles. This method is laborious and expensive, especially with the high throughput screening required for this project. To overcome this, Dehairs, J. *et al.* developed a digital deconvolution method to resolve up to three alleles that have been concurrently sequenced against a reference sequence. To achieve this, DNA sequences are aligned, trimmed, and scored allowing determination of each allele sequence. With this, the presence of InDels in each allele can be confirmed, and the individual alleles mutations can be determined, alongside the resulting presence of possible early stop codons. These were independently validated with the Synthego™ Inference of CRISPR edits (ICE) tool which functions comparably and was released in October 2019.

2.13 Transcriptomics

2.13.1 Total RNA Extraction

Total RNA was extracted from cell lines with the RNeasy® Plus Mini Kit (Qiagen, 74034) per the manufacturer's instruction. Briefly, 1x10⁶ cells were harvested and plated with rWNT3a (R&D Systems, 5036-WN-010) to stimulate canonical WNT signalling activity, or with a vehicle control (1xPBS), in a 12-well plate. After 24 hours these cells were resuspended and harvested for centrifugation at 280g for 5minutes. Cells were resuspended in 350 μ L RLT Plus containing β -ME (10 μ L/mL) to lyse cells. The resuspended cells were then passed through a QIAshredder spin column (Qiagen, 79656) by centrifuging at 10,000g for 2minutes to fully homogenise the cell lysate. DNA was subsequently removed by passing the homogenised lysate through a gDNA Eliminator spin column at 8000g for 30seconds. 350 μ L of 70% ethanol (v/v) was added to the flow-through and vortexed, before the sample was

transferred into a RNeasy spin column. The sample was centrifuged at 8000g for 15seconds, with the flow-through discarded and the upper chamber replenished with 700 μ L of Buffer RW1. After an 8000g centrifugation for 30seconds, the flow-through was discarded and 500 μ L Buffer RPE containing ethanol was added to the RNeasy spin column before a further centrifugation at 8000g for 30seconds. This was repeated a second time to reduce ethanol carryover, but with an extended two-minute centrifugation. A final dry centrifugation into a fresh tube was performed to ensure no carryover. Finally, 40 μ L of RNase-free water was added directly to the spin column membrane and this was centrifuged at 8000g for 1 minute to elute the RNA. RNA concentration and purity were determined by assessment on a Nanodrop™ and through capillary electrophoresis with an Agilent 2100 Bioanalyzer, which scored RNA quality as an RNA integrity number (RIN) based upon the ratio of the area under the 18S and 28S rRNA peaks to the total area under the graph.

2.13.2 Generation of Data

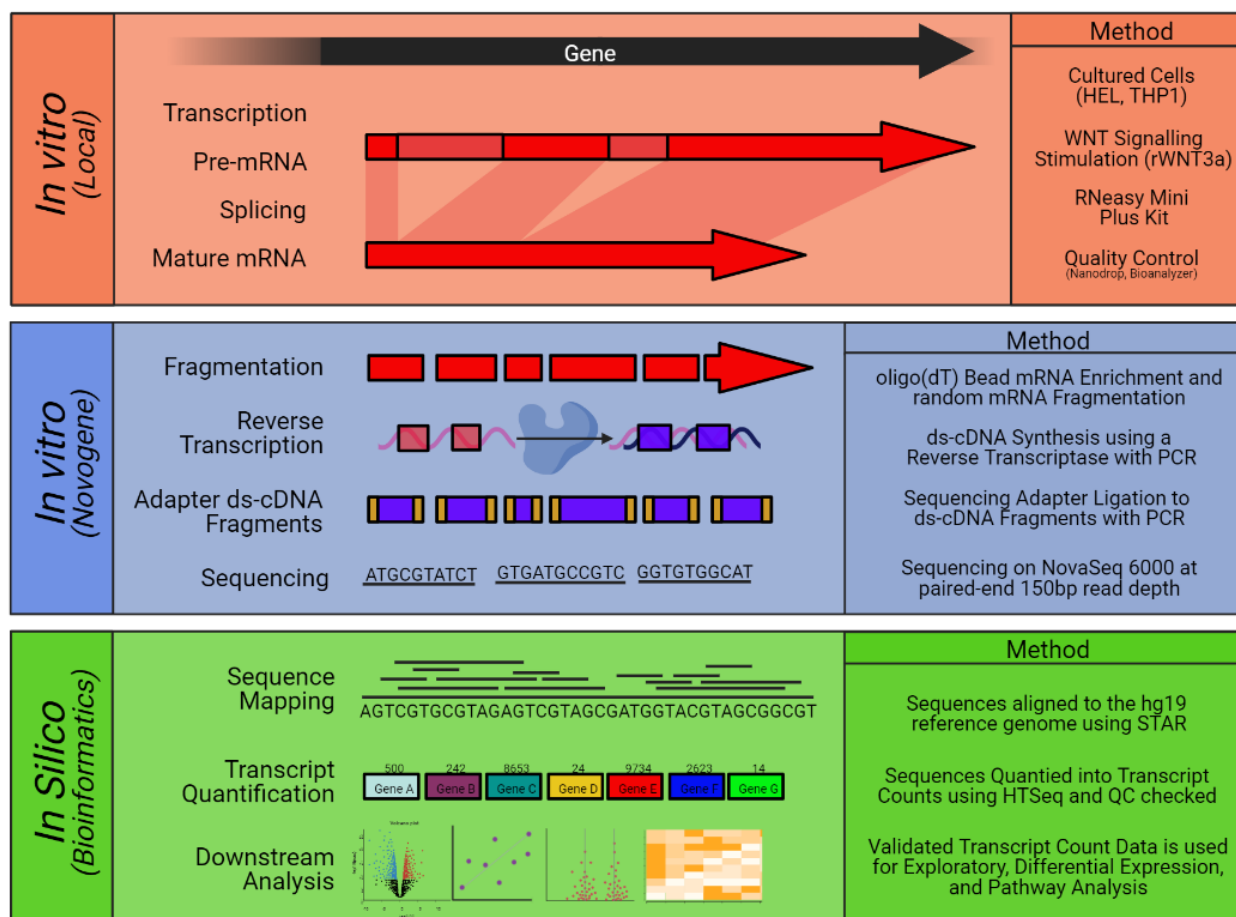
Sixteen total RNA samples (**Table 2-17**) were shipped to the NGS specialist Novogene (Cambridge, UK). Novogene verified the RNA was of acceptable quality before proceeding with a Nanodrop to test RNA purity (OD^{260}/OD^{280}), an Agarose Gel Electrophoresis to test RNA degradation and potential contamination, and finally with an Agilent 2100 Bioanalyzer to check RNA integrity before library preparation, adaptor addition, and sequencing. Library preparation includes mRNA enrichment to remove tRNA, mRNA fragmentation, double-strand cDNA synthesis, sequencing adapter addition, before PCR amplification of cDNA products (**Figure 2-7**). The cDNA library was scored to assess the quality and concentration of the library preparation using a Qubit 2.0 fluorometer (Life Technologies) and insert size was verified on an Agilent 2100 Bioanalyzer. An Illumina NovaSeq 6000 was used to sequence the cDNA library with a paired end read depth of 150bp, totalling 20 million reads per sample. Raw sequencing data was transformed to sequence reads by base calling, producing FASTQ files in both directions. Base call error rates were assessed for quality control (QC), with a quality score per base limited to those over 80% confidence. Sequence reads were assessed with FASTQC (v0.11.9) to assess per base sequence quality, content, GC content, no call content, length distributions, sequence duplication, and overrepresentation. Trimming of adapter sequences was performed where necessary with trimmomatic (v0.4).

Table 2-17: Samples Preparation for RNA-Seq

Summary of the clones and their respective treatment contexts for RNA preparation toward RNA-sequencing.

Cell Line	Clone	Context	rWnt3a
THP1	SCR C1	Control	
		Control Stimulated	+
	SCR C2	Control	
		Control Stimulated	+
	dKO C29	Dual Knockout	
		Dual Knockout Stimulated	+
dKO C47	Dual Knockout		
	Dual Knockout Stimulated	+	
HEL	SCR C1	Control	
		Control Stimulated	+
	SCR C2	Control	
		Control Stimulated	+
	dKO C17	Dual Knockout	
		Dual Knockout Stimulated	+
dKO C17	Dual Knockout		
	Dual Knockout Stimulated	+	

SCR - Scrambled; dKO – Dual Knockout.

**Figure 2-7: RNA-Sequencing Overview**

RNA-sequencing for the purposes of this study is segregated into the in vitro preparation of samples with or without WNT stimulation with WNT3a (2.9.1), and then subsequent RNA isolation (2.13.1). Isolated RNA was shipped to Novogene for library preparation and sequencing as a service before alignment and quantification of counts (2.13).

Sequence reads were then mapped to the hg19 reference genome using STAR (v2.5) with default parameters, resulting in a SAM file. The SAM alignment file was converted to a BAM format file using Samtools (v1.12). Mapping quality of these BAM files was assessed using MultiQC (v1.10.1) which quantified alignment scores, adapter sequence trimming, and feature counts. Aligned sequence reads were quantified using HTSeq (v0.6.1), producing a comma separated value file of transcript counts. As transcript abundance is proportional to gene length, transcript abundance was normalised for gene length.

2.13.3 RNA-Sequencing Bioinformatic Analysis

2.13.3.1 Exploratory Analysis

All high-level analyses of RNA-Seq data were performed with R. Samples were normalised with the DESeq2 package which performs normalisation for each transcript to account library size and RNA composition bias. Samples were inspected through use of correlation matrices and hierarchical clustering which were drawn between experimental replicates to determine reproducibility. A principal component analysis (PCA) was performed, which is a linear dimensional reduction technique for visualising variance between samples from high-dimensional data, which separates samples based upon components (eigenvectors) distanced from mean (eigenvalues). The primary and secondary components were used, and a scree plot was performed to demonstrate that a significant degree of the variance was explained by these components alone.

2.13.3.2 Differential Expression

Differential gene expression was performed with DESeq2 which fits a negative binomial linear model for each gene and performs a Wald test for significance testing, which incorporated a multi-level design to account for the pairwise nature of samples and cell lines where appropriate. DESeq2 enables detection of outliers based upon Cooks' distance of fold change between replicates, allowing removal of these transcripts to lessen the impact of multiple test correction. P-values were corrected with the Benjamini-Hochberg multiple test correction method. Resulting p-values which were below the minimum floating point number limitation were adjusted to the machine minimum ($5e-324$). Transcripts with an adjusted p-value < 0.05 and a fold change ± 1.5 were considered significantly differentially expressed transcripts (DET). Differential expression was visualised using volcano plots, and the unadjusted p-value distribution was assessed to examine test validity. Heatmaps were drawn for accepted DET to demonstrate the homogeneity of expression between classifiers.

2.13.3.3 WNT Signalling Annotation

As the broad range of target genes of WNT/ β -catenin signalling is capable of being activated or repressed by active signalling or knockout conditions, it was necessary to construct a list of known or suspected WNT-target genes for ease of identification. A comprehensive meta-list was constructed by merging the WNT-target gene related pathways, a public database of identified target genes (in CRC) (Herbst *et al.*, 2014), and the list of WNT targets from the online WNT homepage². In total, 617 genes were considered WNT-target genes or closely related.

2.13.3.4 Pathway Analysis

Pathway analyses were performed to translate the gene-level findings to consequences upon established pathways, thereby enhancing the biological interpretability. The current consensus recommends the parallel study of transcriptomic data using numerous curated *priori* databases to maximise interpretability as database choice can influence results of enrichment (Mubeen *et al.*, 2019). Whilst it is has recently become possible to integrate different databases in order to generate a meta-pathway database using PathMe (Domingo-Fernández *et al.*, 2019b), this often limits statistical power due to the higher number of comparisons performed and expanded gene-set size and was thus not applied (Mubeen *et al.*, 2019). Further, pathways may not have a comparable equivalent between databases as is often the case; for example, whilst one database considers pathways at a higher level, such as WNT signalling activity as a whole component, other databases divide the pathway into constituent subsets. Analyses were performed using the curated *priori* databases Exploratory Kyoto Encyclopaedia of Genes and Genomes (KEGG) (Ogata *et al.*, 1999), Gene Ontology (GO) (Carbon *et al.*, 2019), REACTOME (REAC) (Croft *et al.*, 2014), WikiPathways (WP) (Kutmon *et al.*, 2016), Hallmark Molecular Signatures (MSIG) (Liberzon *et al.*, 2015), and Biocarta (BC) (Nishimura, 2001).

As an extension to applying multiple databases to improve interpretation, distinct statistical techniques were applied to comprehensively examine the transcriptomic data. These include classical techniques and more modern methods. These included classic overrepresentation analysis (ORA), Gene Set Enrichment Analysis (GSEA), and Gene Set Variance Analysis (GSVA), before the application of more recently developed techniques

² https://web.stanford.edu/group/nusselab/cgi-bin/wnt/target_genes

which further consider the topology of pathways; these include Pathway Topology Analysis (PTA) and Mechanistic Pathway Analysis (MPA). DET as previously described were used where necessary, with some techniques applying the entire transcriptome.

ORA performs a hypergeometric probability test to examine the enrichment of pathways based upon the list of genes found differentially expressed irrespective of the direction of change (Boyle *et al.*, 2004). ORA was performed with the gProfiler2 package (Raudvere *et al.*, 2019). ORA does not provide directional interpretation, nor does it account for the interaction between genes, rather, ORA provides a means to identify the top candidate pathways for further detailed inspection.

GSEA examines all genes. Classically, genes are ranked by fold-change, however, due to the small sample size within this experiment, a ranking method incorporating p-value and fold-change was applied, which has been demonstrated to perform more robustly (Xiao *et al.*, 2014). A series of random walks are performed through this ranked list which attempts to find gene-sets which are enriched disproportionately within the ranking which is computed into a pathway score. GSEA was performed with the Clusterprofiler (Yu *et al.*, 2012) package. GSEA can provide an approximate directional measure of pathway activity based upon term rank trending, however, closer inspection is required as negative regulation of pathway inhibitions would activate the pathway, acting inversely to the pathway enrichment. Further, GSEA is limited in regard to the identification of pathways which are centrally controlled rather than linear and consecutively regulated, as these pathways often exhibit both inhibition and activation around a central mediator. In summary, GSEA has poor sensitivity for pathways which behave in a ‘see-saw’ like manner of regulation.

GSVA overcomes the requirement to define groupings when the study in question contains heterogeneous data sets, which is applicable here due to the use of patient data and two cell lines with two stimulation states. GSVA utilises the entire transcriptome and does not rely upon fold changes from a defined contrast (Hänzelmann *et al.*, 2013). Rather, GSVA fits a model and ranks genes based upon normalised count data to respective pathways in order to generate a *per* pathway score on a *per* sample basis. With pathways scored *per* sample, variations are revealed irrespective of groupings. In this way, GSVA can offer greater statistical power over GSEA when groups contain heterogeneous samples.

The priorly mentioned classical techniques are widely used and are useful to identify pathways of interest, however, they are incapable of considering the topology of pathways, and further, cannot accurately capture whether a pathway is considered activated or repressed.

Modern techniques enable the study of sub-pathways and are capable of considering whether a pathway, or elements of a pathway, are activated. Study of sub-pathways are a particular interest for this study, as the canonical WNT signalling pathway is often not considered independently from the wider non-canonical WNT calcium and Planar Cell Polarity Pathway such as in the KEGG database which could conceal findings.

Pathway topology analysis applies the found differentially expressed genes for analysis and was performed with the PathfindR (Ulgen *et al.*, 2019) and Signalling Pathway Impact Analysis (SPIA) packages (Tarca *et al.*, 2009). PathfindR considers the interaction between gene members within a pathway to identify pathways which are perturbed; however, as many pathway databases do not define interactions as activators or repressors, PathfindR cannot establish whether a pathway is activated or repressed. An alternative to PathfindR is SPIA, which is able to consider the nature of gene interactions and therefore compute a prediction as to whether a pathway is activated or repressed. This is currently possible with select databases which include information on gene-level interactions, limiting the technique to the KEGG and REAC databases. The current KEGG (v99, 01/07/21) and REAC (v77, 09/06/21) databases were downloaded in full and converted into a gene network using the Graphite package (Sales *et al.*, 2012). A final analysis technique known as MPA was applied which extends PTA. MPA was performed with MinePath (Koumakis *et al.*, 2016). These techniques are distinct from the PTA methods as they utilise the entire transcriptome, similarly to GSEA and GSVA, in order to examine consistent fluctuations.

To study TF activity, the package Corto (Mercatelli *et al.*, 2020) was used to perform TF and co-TF master regulator analysis (MRA). Factor annotations were acquired from the human TF database (v1.01) (Lambert *et al.*, 2018). Enrichment of target genes for each centroid factor was performed using an integrative model of spearman's correlation and data processing inequality as described (Reverter *et al.*, 2008). Together, this enabled co-expression and co-regulation networks to be constructed, revealing significant factors between conditions. MRA is able to identify significantly perturbed factors which are unaltered at the mRNA level which limits identification by differential analysis; this is often owed to factors which are regulated post-translationally, such as *CTNNB1*, from which mRNA levels are unable to convey the biological state. MRA is biased by aneuploidy and sample impurities, however, aneuploidy is rare in AML, and low quality samples have been removed (2.13.4) (Schubert *et al.*, 2020).

A caveat to each advancing technique is a greater reliance upon the established *priori*, and as such, better statistical techniques may not reveal novel insights if the underlying

database information is insufficient. Pathways can act differently between cell types, diseases, and in different conditions. To overcome the reliance upon a *priori*, co-expression analyses were performed which do not rely upon established *priori*; this was performed with the Differential Gene Correlation Analysis (DGCA) (McKenzie *et al.*, 2016) package to identify differential correlation of co-expressed genes, and extended with the CEMiTool (Russo *et al.*, 2018) package which identifies co-expressed modules.

A summation of the techniques applied can be found in **Table 2-18** and represented in **Figure 2-8**.

2.13.4 Publicly Available Data

2.13.4.1 Bloodspot

The bulk population data relating to *CTNNB1*, *JUP*, *TCF7L2*, and *LEF1* mRNA expression in human HSPC and constituent cell types was mined from the Bloodspot repository (Bagger *et al.*, 2019). Expression was determined by microarray (GSE42519). If multiple probe sets related to an individual gene the resulting values were averaged.

2.13.4.2 Cancer Dependency Map

The Cancer Dependency Map (DEPMAP) is a collaborative project between the Wellcome Sanger Institute and the Broad Institute and represents a public repository of pooled CRISPR-Seq data performed in human cancer cell lines (Tsherniak *et al.*, 2017). AML and CRC cell line dependency data was mined to examine gene necessity in AML based upon determined fitness scores. In brief, CRISPR-Seq enables high-throughput examination of gene necessity in disease by performing a highly multiplexed (pooled) gRNA knockout. After application of CRISPR, pooled populations are scRNA-seq and DNA barcoding of gRNA enables deconvolution of the remaining gRNA within the pooled population. The gRNA which are absent are deemed to be essential, however, as this is performed in a non-clonal setting, the resulting essentiality score is derived from a population of complete, incomplete, and escape gene inactivation events.

Table 2-18: The Statistical Pathway Analysis Methods Applied

Statistical Method	Package	Database	Runtime	Input	Output	Considerations	
						Benefits	Drawbacks
Over-representation Analysis	gProfiler2	All	Seconds	List of differentially expressed genes, no associated statistic	Per-pathway hypergeometric scores	<ul style="list-style-type: none"> • Simple • Identifies most impacted pathway • Computationally inexpensive 	<ul style="list-style-type: none"> • Arbitrary threshold required • No associated statistics • Sample size independent
Gene Set Enrichment Analysis	Cluster profiler	All	<30 Minutes	List of pre-ranked genes with summary statistics	Per-pathway enrichment scores	<ul style="list-style-type: none"> • Includes all genes • Measures general coordination • Widely adopted methodology 	<ul style="list-style-type: none"> • Computationally expensive • Relies upon a defined contrast • Limited in low sample size
Gene Set Variance Analysis	GSVA	All	<30 Minutes	Normalised count expression matrix	Per-pathway per-sample enrichment scores	<ul style="list-style-type: none"> • Does not require defined groups • Enhanced sensitivity in heterogeneous sets 	<ul style="list-style-type: none"> • Requires >10 samples minimum • Computationally expensive • Inexact measure of directionality
Pathway Topology Analysis	PathfindR	KEGG Reactome GO, BC	Hours	List of differentially expressed genes, with associated statistic	Per-pathway hypergeometric scores	<ul style="list-style-type: none"> • Incorporates gene interaction • Examines numerous databases 	<ul style="list-style-type: none"> • Computationally expensive • Arbitrary threshold required • Cannot determine directionality
	SPIA	KEGG Reactome	Hours++	List of differentially expressed genes, with associated statistic	Per-pathway activation scores	<ul style="list-style-type: none"> • Incorporates gene interactions • Capable of predicting pathway activation or repression 	<ul style="list-style-type: none"> • Computationally expensive • Arbitrary threshold required • Limited compatible datasets
Mechanistic Pathway Analysis	MinePath	KEGG	Hours+++	Normalised count expression matrix	Per-pathway per-group enrichment scores	<ul style="list-style-type: none"> • Incorporates gene interactions • Examines the entire transcriptome • Predicts pathway status 	<ul style="list-style-type: none"> • Computationally expensive • Limited compatible dataset • Requires defined groupings
Differential Co-expression Correlation	DGCA	N/A	Hours+++	Normalised count expression matrix	Co-expression scores	<ul style="list-style-type: none"> • Identifies co-regulated genes • Provides novel insight 	<ul style="list-style-type: none"> • Computationally expensive • Requires >20 samples ideally • Frequent false findings
Module Co-expression	CemiTools		Hours+++	Normalised count expression matrix	Module co-expression scores	<ul style="list-style-type: none"> • Capture co-regulated module • Provides novel pathway insight • Examines entire transcriptome 	<ul style="list-style-type: none"> • Computationally expensive • Requires >20 samples ideally • Limited biological interpretability
Transcription Factor Regulator Analysis	Corto	Human TF Database	Hours+++	Variance stabilised normalised count matrix	Per-factor Enrichment Scores	<ul style="list-style-type: none"> • Utilises entire transcriptome • Identifies targets regulated by post-translational mechanisms 	<ul style="list-style-type: none"> • Computationally expensive • Biased by ploidy, contaminants • Inexact measure of directionality

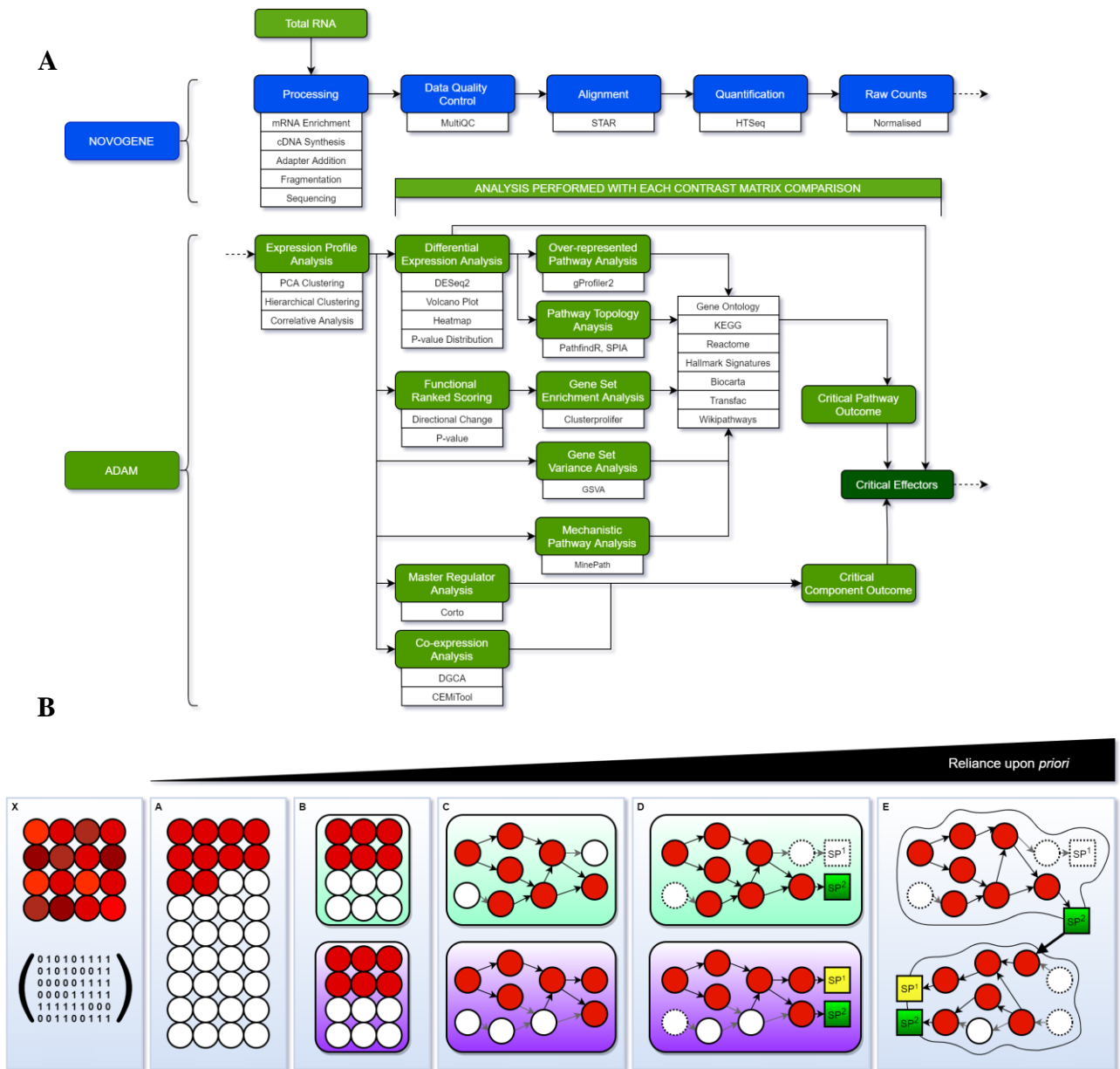


Figure 2-8: A Flowchart of the RNA-Sequencing Analysis Plan

(A) The plan for RNA-sequencing involved multiple facets in order to determine critical gene expression and pathway perturbation. This included study of differentially expressed genes, pathway analyses, co-expression analyses, and meta-pathway considerations. (B) Recently developed pathway analysis techniques are able to prove more informative as to the exact biological consequences, though this requires greater reliance upon the *priori* databases. X represents a co-expression study, with no reliance upon the *priori*. A is a gene enrichment analysis in which all genes are considered. B is a gene set enrichment analysis, where pre-defined lists of genes are examined for involvement in a specified pathway. C is a topology pathway analysis, which incorporates weighting of gene members contributions to the pathway. A recently developed extension of topology analysis is mechanistic analysis, D, which sub-divides pathways based upon specific downstream roles. Cross-pathway interactions can be revealed through network enrichment analysis.

2.13.4.3 *The Cancer Cell Line Encyclopaedia*

The Cancer Cell Line Encyclopaedia (CCLE) is a public repository provided by the Broad Institute which avails proteomic, RNA-seq, mutation, fusion, methylation, splicing, miRNA, chromatin profiling, and a select subset of proteomic data in the context of human cancer cell lines. This data was mined to enable contrast of characterised AML cell lines (Barretina *et al.*, 2012; Ghandi *et al.*, 2019; Nusinow *et al.*, 2020).

2.13.4.4 *The Cancer Genome Atlas*

The public cancer genome atlas (TCGA) database provides RNA data as non-integer RNA-Seq by Expectation-Maximization (RSEM) normalised values based on a dated pre-processing pipeline rather than raw counts. RSEM normalised values are unsuitable for use with DESeq2 and it has further been established that this method of normalisation can conceal results (Rahman *et al.*, 2015). Alternate databases were screened, but unfortunately most are only available as Fragments Per Kilobase of transcript per Million mapped reads (FPKM) or Reads Per Kilobase of transcript, per Million mapped reads (RPKM) normalised data; whilst these normalisation techniques were initially designed to facilitate cross-sample comparisons (Mortazavi *et al.*, 2008), and are hence widely adopted, recent studies have demonstrated this is highly misinformative and unsuitable for differential studies (Wagner *et al.*, 2012; S. Zhao *et al.*, 2020). Raw counts were acquired from GSE62944 which is a public repository of TCGA data that has been pre-processed with a more modern Rsubread pipeline, and the data is provided as raw counts. Raw counts were processed comparably to the raw counts from the generated data as previously mentioned (2.13). Use of a consistent, modern pipeline is critical to accurate results as it was recently revealed that 12% of all genes (2068 total) differ in abundance estimates by greater than 4-fold between pipelines despite the use of the *same* samples and *same* RNA-seq reads; this represents a major challenge in the field of bioinformatics currently (Arora *et al.*, 2020). Indeed, many of these genes are known to be involved in leukaemia and other diseases, hence, results could differ on the basis of alternate processing rather than the underlying biological state (Arora *et al.*, 2020). One source of this variability is found from alternate mapping, particularly of multi-mapped reads (Wu *et al.*, 2013), which is caused by the use of different reference genomes during alignment, as these vary in gene exon and length considerably (Frankish *et al.*, 2019). This was found in 52% of the inconsistent genes (Arora *et al.*, 2020).

In addition, as these samples are prepared from whole BM, some degree of cellular contamination was anticipated. This was examined by analysing the transcriptomic profile of each sample with the XCell 489-gene signature which scores RNA profiles based on contributions from 64 independent cell types (Aran *et al.*, 2017). This revealed seven core clusters of predicted cell types, with a notable cluster of patient samples containing high T-cell characteristics. These samples were considered contaminated by T-cells and were removed (**Figure 2-9**). This left 109 patient RNA profiles for analysis.

2.13.4.5 Survival and Disease-Free Analysis

Survival analysis was performed with the survival (Lin *et al.*, 2002) and survminer (Kassambara *et al.*, 2017) packages. RNA-seq data from the TCGA AML NEJM 2013 study (Ley, 2013) was acquired, filtered, and pre-processed (2.13.2). Patients were annotated based upon individual gene expression levels as either above and below median expression levels, or by upper and lower quartiles, with both representing widely adopted methods to study prognostic influence of genes. It would be expected a gene found significant by the prior method would be significant in the later, however, gene expression distributions can conceal results which necessitated the latter approach. Kaplan-Meier curves were constructed to examine the prognostic relationship between specific gene expression levels and overall survival, and disease-free survival. The package Regparallel was used to study hundreds of genes in high-throughput (Blighe K, 2021).

2.14 Statistical Analyses

Statistical analyses were performed in R version 4.0³. Statistical methods included Student's t-test and ANOVA with Tukey's honestly significant difference post-hoc test. Graphs represent the mean expression observed between repeats. Error bars represent one standard deviation. Significance symbols: ****= < 0.0001 ; *** = 0.0001 to 0.001 ; ** = 0.001 to 0.01 ; * = 0.01 to 0.05 ; not significant (NS) = >0.05 .

³ Obtained from <https://www.r-project.org/>

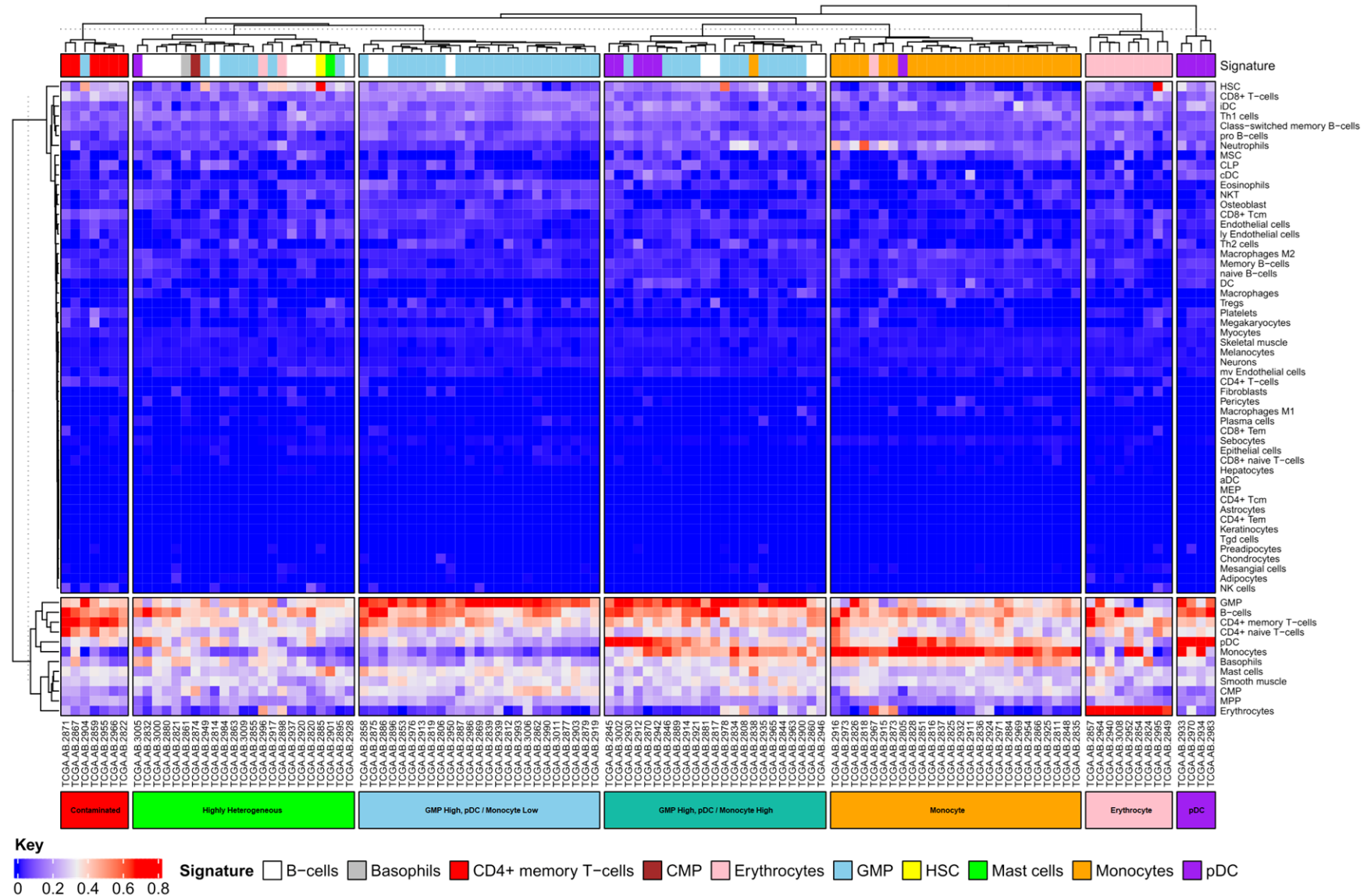


Figure 2-9: XCell Cell Type Contributions to Total RNA Profile Identifies T-Cell Contaminated Samples

Profiling of the total RNA profile with the XCell gene signature enabled contributions of each cell type to the overall RNA expression profile. Samples were clustered without supervision into seven distinct subsets: Contaminated, pDC, Erythrocytes, Monocytes, GMP High with Monocyte High, GMP High with Monocyte Low, and Highly Heterogeneous.

Chapter 3

Characterising WNT/beta-catenin signalling and gamma-catenin in AML and haematopoiesis

3.1 Introduction

WNT/ β -catenin signalling is an integral pathway for normal developmental processes and has been implicated in human haematopoiesis and AML maintenance (Richter *et al.*, 2017). Up to 70% of AML patients have increased WNT/ β -catenin signalling (Simon *et al.*, 2005b). Previous studies have used incomplete RNA silencing methods or animal models which led to conflicting results (1.3.5); some have concluded that substantial knockdown did not affect haematopoiesis or AML maintenance, even with a 95% reduction in protein levels of β -catenin (Cobas *et al.*, 2004b; Koch *et al.*, 2008a). To conclusively determine the individual role of β -catenin, alongside its close homolog γ -catenin, these will be independently and simultaneously deleted genetically with CRISPR-Cas9 in AML cell lines, enabling consequent assessment to AML characteristics and maintenance. Firstly, and prior to the application of CRISPR-Cas9, this study will characterise the WNT/ β -catenin signalling activity within AML cell lines, to continue with an appropriate panel of WNT/ β -catenin signalling activity capable cell lines.

Further to the AML context, as several authors have documented that loss of β -catenin is detrimental to, or possibly incompatible with, HSC differentiation and self-renewal (Zhao *et al.*, 2007; Fleming *et al.*, 2008a; T. C. Luis *et al.*, 2009), it will be vital to examine the consequence of β -catenin and γ -catenin knockout in the context of haematopoiesis and HSPC self-renewal. If β -catenin is required for normal haematopoiesis, efforts to target WNT/ β -catenin signalling clinically with targeted therapeutics would be unsuitable.

3.2 Aims

I hypothesise that a subset of AML patients relies on WNT/ β -catenin signalling for maintenance, based upon analysis of AML patients and AML cell lines.

To test this, CRISPR-Cas9 will be used to generate complete deletion of β -catenin and γ -catenin, thereby facilitating the production of a clonal line without functional β -catenin and γ -catenin, with minimal off-target effects. This will provide a conclusive answer regarding the role of these catenin members, and further elucidate the exact role of WNT/ β -catenin signalling in AML.

Objective 1: Characterise central WNT/ β -catenin signalling members contribution to survival, disease subtypes, and haematopoiesis.

Initially, I will make use of available transcriptomic and clinical characteristic patient data to determine whether WNT/ β -catenin signalling members are associated with patient survival or are associated with specific genetic aberrations, as has been suggested in the literature. Finally, central WNT/ β -catenin signalling members will be examined in the context of haematopoiesis for expression changes throughout lineage development, providing an indication of WNT/ β -catenin signalling activity in HSPC and derivatives.

Objective 2: Characterise basal and stimulated WNT/ β -catenin signalling activity capacity in AML cell lines.

Prior to investigating the consequence of knockout, AML cell lines will require characterisation, both at basal levels and within an activated state. The stimulation method will require optimisation to ensure the activation is not dosage limited and will be achieved through inhibition of GSK3 β . Cell lines will be classified as responders or non-responders based on a combination of a fluorescent WNT reporter and western blots of nuclear and cytosolic subcellular fractions to determine β -catenin nuclear translocation.

Objective 3: Use CRISPR-Cas9 to characterise a bulk single knockout of β -catenin or γ -catenin independently, and in a dual knockout setting in AML cell lines.

Following characterisation of AML cell lines for WNT/ β -catenin signalling activity, single and dual knockout of β -catenin and/or γ -catenin will be generated at a bulk level⁴ using CRISPR-Cas9. This will enable initial assessment of necessity for each of these genes for AML maintenance, and the impact on WNT/ β -catenin signalling activity for each knockout condition.

Objective 4: Characterise WNT/ β -catenin signalling activity in normal haematopoietic development, through CRISPR-Cas9 knockout.

In order to therapeutically target WNT/ β -catenin signalling in the clinical setting, consideration of the implications to normal haematopoiesis and HSPC self-renewal is necessary. To this end, HSPC will be recovered from umbilical cord blood for culture *in vitro* under conditions

⁴ Bulk level refers to the non-clonal nature of the CRISPR-Cas9 knockout which contains complete biallelic knockout, incomplete knockout (monoallelic wildtype), and CRISPR-Cas9 evading cells.

Characterising WNT/beta-catenin signalling and gamma-catenin in AML and haematopoiesis supporting myeloid development. CRISPR-Cas9 will be applied to knockout β -catenin and/or γ -catenin to determine whether WNT/ β -catenin signalling is integral to myeloid development.

3.3 Results

3.3.1 Examination of WNT/ β -catenin Gene Expression in Haematopoiesis and AML

3.3.1.1 *CTNNB1* and *JUP* are Variably Expressed in Haematopoiesis and AML subtypes

WNT/ β -catenin signalling is implicated in essential roles, such as proliferation, differentiation, and self-renewal (1.3); however, the expression patterns of β -catenin, γ -catenin, and several WNT-associated genes have not been explored to determine whether a pattern of expression implies a role in development. To examine the transcriptomic levels of *CTNNB1* and *JUP*, publicly available transcriptomic data was analysed in both the haematopoietic and AML context.

Expression of *CTNNB1* was not significantly differentially regulated during normal haematopoiesis (**Figure 3-1A**). Differences between molecular profiles in AML was statistically significant after correction when subtypes were contrasted with normal karyotype AML, harbouring no molecular abnormalities, as suggested in the literature (1.2.6). AML t(8;21) patients were found to express significantly greater levels of *CTNNB1*, a finding supported by a proposed WNT/ β -catenin-induced model of t(8;21) (1.3.5). Inversely, *CTNNB1* was reduced in numerous karyotypes compared to normal karyotype, and in MDS which frequently transforms into AML (Rio-Machin *et al.*, 2020). However, the narrow range of *CTNNB1* expression suggests that while these differences may be statistically significant, they may not be biologically consequential, especially given that β -catenin levels are further controlled post-translationally.

Expression of *JUP*, on the other hand, was shown to decrease during haematopoiesis, between HSC and differentiated cells, with the exception of monocytes which present transcriptomic levels comparable to HSC (**Figure 3-1B**). These data could indicate a role in maintaining stemness, however, little literature evidence supports this. In AML, a greater range of expression presented when compared with *CTNNB1*, with *JUP* levels elevated as compared to normal karyotype. As with *CTNNB1*, t(8;21) demonstrated significantly higher levels of *JUP* again suggesting a potential involvement of WNT/ β -catenin signalling with this translocation. In contrast, MDS demonstrated significantly less *JUP* expression. These findings were later

Characterising WNT/beta-catenin signalling and gamma-catenin in AML and haematopoiesis
confirmed in a scRNA-seq dataset which was recently released (S1. ; **Figure S-6-1, Figure S-6-2**) (Triana *et al.*, 2021).

In the TCGA patient cohort, the expression pattern of *CTNNB1* demonstrated a gaussian distribution with no notable separation of a low and high expression group (**Figure S-6-3**). All patients were found to express *CTNNB1* at appreciable levels, though the established post-translational regulation of β -catenin limits interpretation of mRNA expression as an indicator of protein presence. Contrastingly, *JUP* expression was low in most TCGA patients, though a noted population exists with high expression of *JUP* whom also express high *CTNNB1* levels. As only ten patients form the elevated *JUP* group, the observation of elevated *CTNNB1* levels in such a limited number of patients is insufficient to conclude a connection.

3.3.2 *CTNNB1* and *JUP* Expression do not Significantly Impact Clinical Outcome in AML

To study the relationship between WNT/ β -catenin signalling activity and patient outcome, the TCGA dataset was examined. Expression patterns of specific genes have been demonstrated to convey prognostic indications, such as *CXCR4* and *CD47* (Majeti, Chao, *et al.*, 2009; Du *et al.*, 2019). If WNT/ β -catenin target genes are involved in disease severity or drug resistance, an association with poor survival would be expected. Patients were stratified into high or low mRNA expression from mean expression for the central members of the WNT/ β -catenin signalling pathway respectively (*CTNNB1*, *LRP6*, *GSK3B*, *TCF7L2*, *LEF1*) and γ -catenin (*JUP*), to best capture a potential WNT/ β -catenin signalling profile.

CTNNB1 was significantly associated with an elevated BM blast percentage which is an established poor prognostic indicator for remission (DiNardo *et al.*, 2016) (**Figure 3-2A|B**). Conversely, high levels of *JUP* expression were associated with a significant decrease in BM blast percentage suggesting an association with improved prognosis (DiNardo *et al.*, 2016).

To examine whether expression of WNT/ β -catenin member impacted overall survival and disease-free survival, Kaplan-Meier survival curves were generated for the aforementioned mRNA targets. No statistical significance was found (**Figure 3-3A|B**). Together, these data suggest central members of the WNT/ β -catenin at the mRNA level are not intrinsically linked to patient survival.

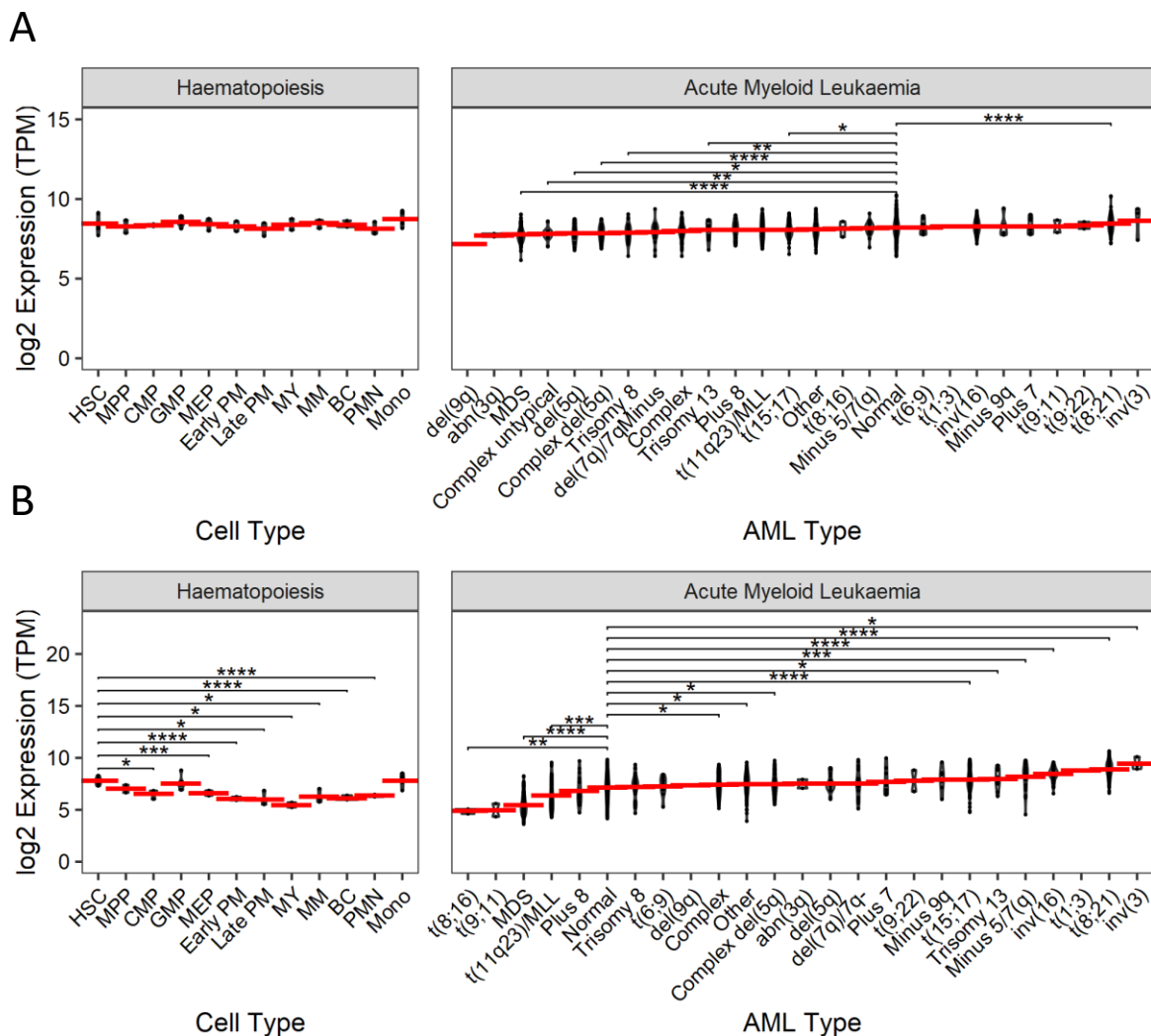


Figure 3-1: Expression of *CTNNB1* and *JUP* in Haematopoiesis and AML Subtypes

Normalised microarray mRNA expression data for **A**) *CTNNB1* (β -catenin) and **B**) *JUP* (γ -catenin) in normal human haematopoiesis and AML.

Human normal haematopoiesis data are from GSE42519. Human AML data are from: GSE13159, GSE15434, GSE61804, GSE14468 and TCGA. If applicable, multiple probes matching an individual gene were averaged. Data indicates mean \pm 1SD. Significant differences were analysed by one-way ANOVA with Tukey's multiple test correction; * denotes $p < 0.05$; ** denotes $p < 0.01$; *** denotes $p < 0.001$; **** denotes $p < 0.0001$. Red line indicates mean within each group.

HSC - Hematopoietic stem cell; **MPP** - Multipotential progenitors; **CMP** - Common myeloid progenitor cell; **GMP** - Granulocyte monocyte progenitors; **MEP** - Megakaryocyte-erythroid progenitor cell; **Early PM** - Early Promyelocyte; **Late PM** - Late Promyelocyte; **BC** - Band cell; **MM** - Metamyelocytes; **MY** - Myelocyte; **Mono** - Monocytes; **PMN** - Polymorphonuclear cells; **Normal** - AML with Normal karyotype; **Complex** - AML with Complex karyotype; **inv(16)** - AML with inv(16); **t(15;17)** - AML with t(15;17); **t(8;21)** - AML with t(8;21); **t(11q23)/MLL** - AML with t(11q23)/MLL; **MDS** - MDS; **Trisomy 8** - AML with Trisomy 8; **del(5q)** - AML with del(5q); **del(7q)/7q-** - AML with del(7q)/7q-; **t(9;11)** - AML with t(9;11); **Other** - AML with Other abnormalities; **Plus 7** - AML with +7; **Complex del(5q)** - AML with Complex del(5q); **Complex untypical** - AML with Complex untypical karyotype; **inv(3)** - AML with inv(3); **Trisomy 11** - AML with trisomy 11; **Trisomy 13** - AML with trisomy 13; **t(6;9)** - AML with t(6;9); **t(8;16)** - AML with t(8;16); **del(9q)** - AML with del(9q); **t(1;3)** - AML with t(1;3); **-5/7(q)** - AML with -5/7(q); **-9q** - AML with -9q; **Plus 8** - AML with +8; **t(9;22)** - AML with t(9;22); **abn(3q)** - AML with abn(3q)

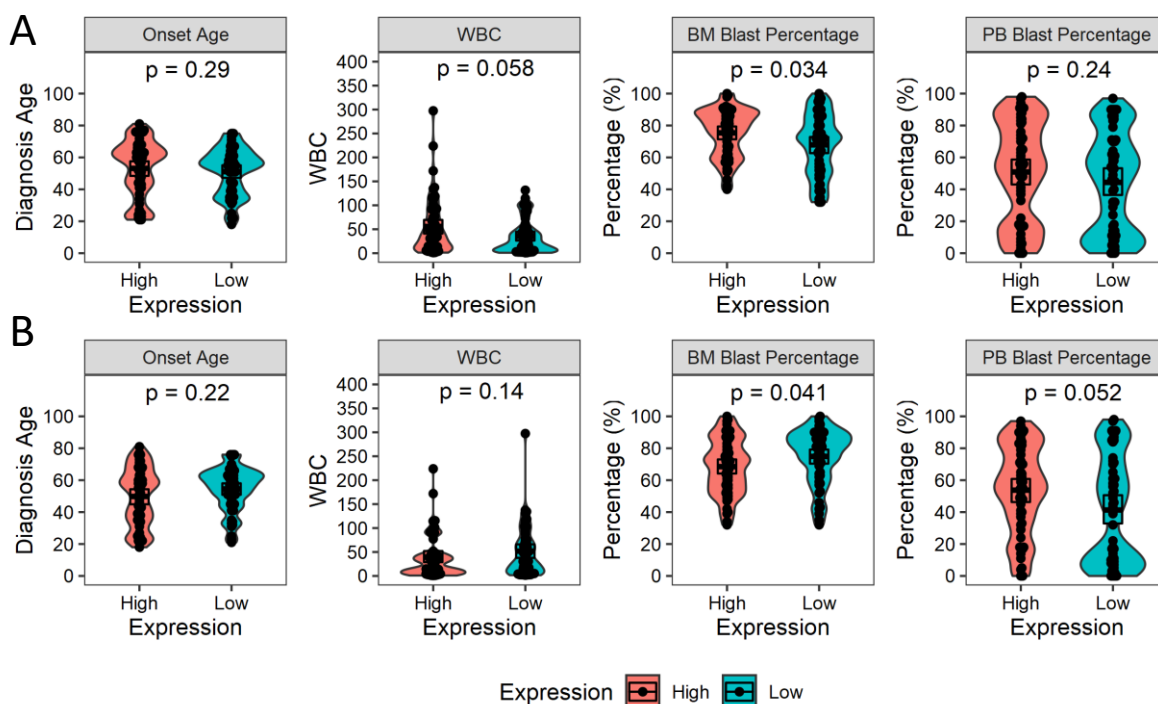


Figure 3-2: *CTNNB1* and *JUP* Expression are Indicative of Clinical Characteristics

A) Violin plots showing the relationship between clinical characteristics and *CTNNB1* (β -catenin) high (n=55) and low (n=55) classifications in AML patients based upon distance from mean expression in mRNA expression data. **B)** Relationship between clinical characteristics and *JUP* (γ -catenin) high (n=55) and low (n=55) classifications in AML patients based upon mRNA expression data. Multiple test correction was performed as a collective set.

Expression and clinical data sourced from TCGA (Ley, 2013). Statistical differences between high and low expression classifications in AML patients were analysed using a Mann-Whitney test.

WBC – White blood cell; **BM** – BM; **PB** – Peripheral blood.

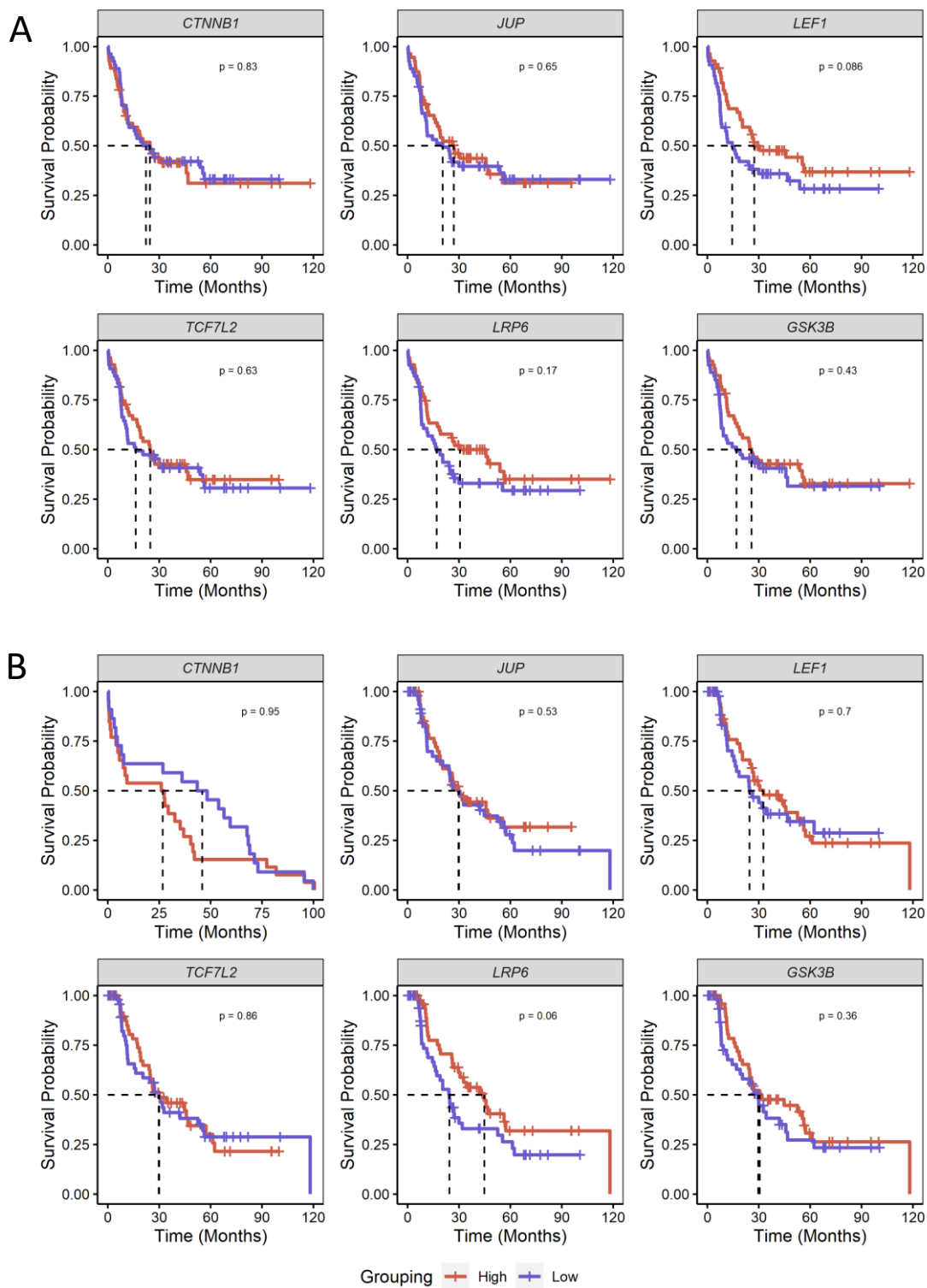


Figure 3-3: Overall Survival Analysis of Central WNT/β-catenin Members

(A) Normalised mRNA expression data was applied to study OS of patients based upon selected WNT/β-catenin members, with each stratified by median expression into high (n=55) and low (n=55) cohorts. (B) Normalised mRNA expression data was applied to study disease free survival of patients based upon selected WNT/β-catenin members, with each stratified by median expression into high (n=55) and low (n=55) cohorts. Untreated patients, t(15;17) AML patients, and non-AML contaminated samples were excluded from this analysis. Statistical analysis was performed using the log-rank test between high and low expression groups. Multiple test correction was not performed. Data obtained from TCGA (Ley, 2013).

3.3.3 Characterising WNT/ β -catenin Activity in AML

3.3.3.1 *Lentiviral Insertion of WNT Reporter Constructs into AML cell lines*

To study the WNT/ β -catenin signalling activity of AML cell lines, the pBARV and pfuBARV WNT reporter constructs were incorporated into cell lines by lentiviral transduction, corresponding to response read and background read, respectively (2.9.3). Cells were sorted based on DsRed⁺ expression, driven by the pBARV and pfuBARV constructs (**Figure 3-4**). Successful integration was achieved in K562, HEL, THP1, KG1, KG1a, TF1, SKNO1, NOMO1, PLB985, MV4;11, ML1, OCI-AML2, OCI-AML5, Kasumi-1, and U937. At basal state without antagonism of the pathway, no cell line presented detectable basal WNT reporter activity compared to control pfuBARV, though low-level signalling below the limits of detection cannot be ruled out by this comparison.

3.3.3.2 *Optimisation of GSK3 β Inhibitor Treatment*

To enable assessment of WNT/ β -catenin signalling capacity, cells were treated with GSK3 β inhibitors. Moreover, to validate reporter data, western blotting of β -catenin protein in the cytosolic and nuclear compartments was also carried out.

The GSK3 β inhibitor, 6-Bromoindirubin-3'-oxime (BIO; C₁₆H₁₀BrN₃O₂), previously used within the group has the disadvantage of being fluorescent in FL1 and FL2 channels (**Table 2-10**) which are used for reporter analysis. To circumvent this, validation of the more recently developed GSK3 β inhibitor, 6-[[2-[[4-(2,4-dichlorophenyl)-5-(5-methyl-1H-imidazol-2-yl)-2-pyrimidinyl]amino]ethyl]amino]-3-pyridinecarbonitrile, known as CHIR99021, (hereafter referred to as CHIR; C₂₂H₁₈Cl₂N₈) was performed. To optimise inhibitor concentration, an overnight incubation of K562 pBARV and pfuBARV cells with CHIR at a range between 0.25 μ M to 25 μ M was performed. Despite being a CML model, the K562 cell line was selected for this optimisation experiment because of its strong response to WNT agonists. A concentration of 5 μ M was shown to induce the greatest response, at approximately 90% positive *versus* vehicle control (**Figure 3-5**). Higher concentrations presented lower positivity, possibly because the viability of the cells was impacted, which became evident for both inhibitors when the time of exposure was extended beyond 24 hours (**Figure 3-6**). These results indicate that the use of either agent would not be suitable for incubation times of more than 24 hours.

3.3.4 WNT/ β -catenin Signalling Response is Heterogeneous in AML Cell Lines

Treatment with the GSK3 β inhibitors CHIR and BIO was able to induce a consistent WNT reporter readout in HEK293T⁵, K562, HEL, THP1, KG1a, TF1, SKNO1, NOMO1, and PLB985 cell lines (**Figure 3-7**), whilst MV4;11, ML1, OCI-AML2, OCI-AML5, and U937 never displayed any detectable WNT response. The response to each inhibitor was consistent. A detectable response over the vehicle treated DMSO threshold enabled the classification as a *responder* cell line, whilst absence of a WNT response despite treatment with either GSK3 β inhibitor classified them as a *non-responder* line.

⁵ HEK293T was assessed as a potential control WNT responder line with established tolerance of β -catenin knockout based on published data (Guan *et al.*, 2018). K562 subsequently fulfilled this role and HEK293T was not applied further.

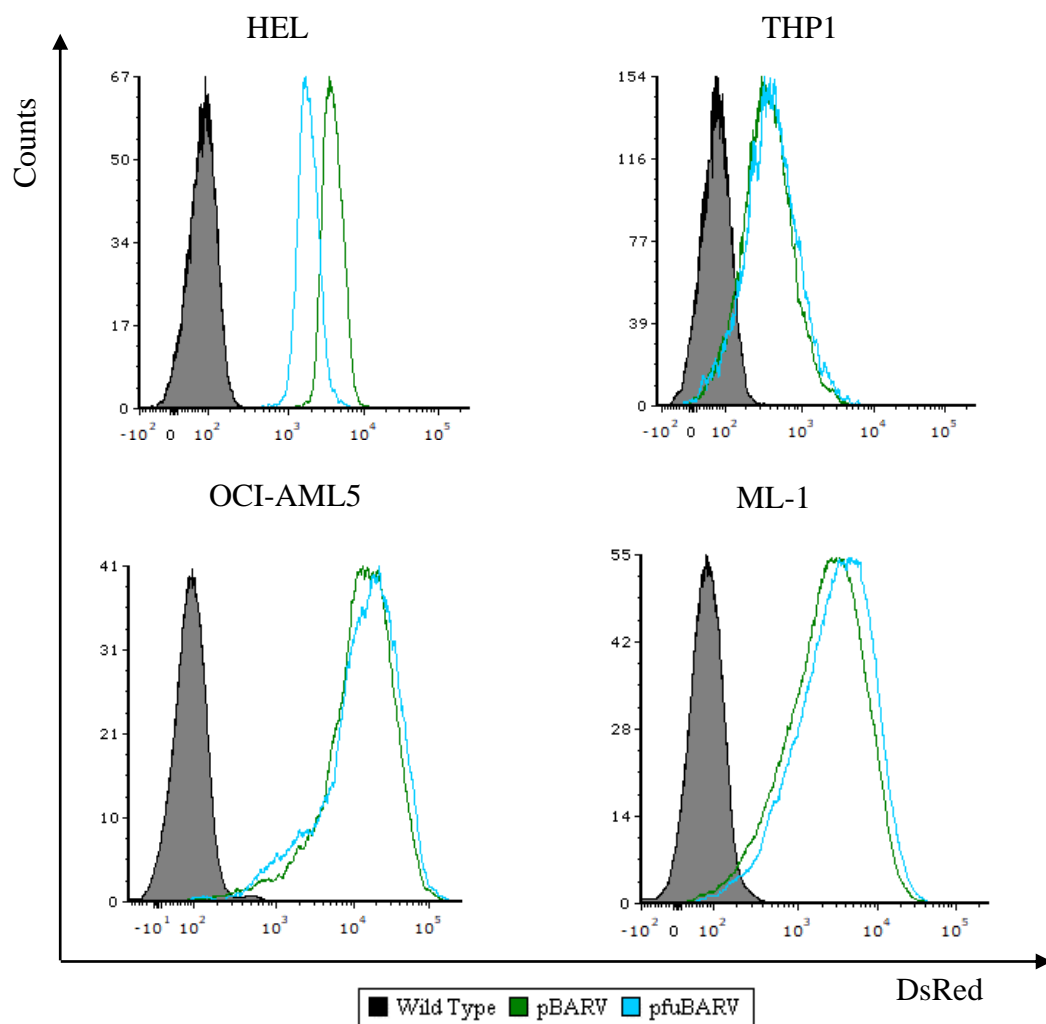


Figure 3-4: Expression of pBARV and pfuBARV in AML cell lines

Representative histograms demonstrating expression of pBARV and pfuBARV constructs (2.9.3) following FACS based upon the DsRed fluorescence which was constitutively expressed by the constructs (2.11.3).

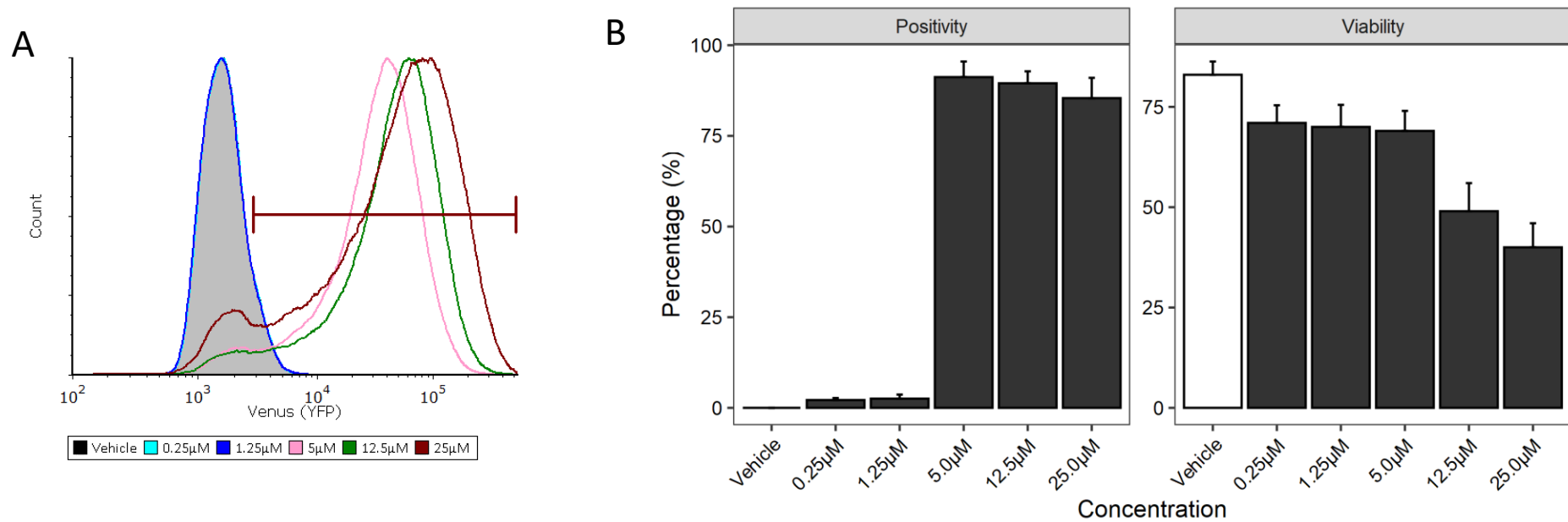


Figure 3-5: CHIR Induces WNT/β-catenin Signalling in K562 pBARV

A) Representative histograms for the WNT reporter readout (2.11.5) following treatment with CHIR for 24-hours compared to vehicle control. **B**) Bar charts demonstrating the percentage positivity of the WNT reporter (Venus YFP) and cell viability of K562 pBARV and pfuBARV lines following CHIR incubation at indicated concentrations for 24 hours compared to vehicle control (0.1% DMSO, v/v). (n=3; data indicates mean +1SD).

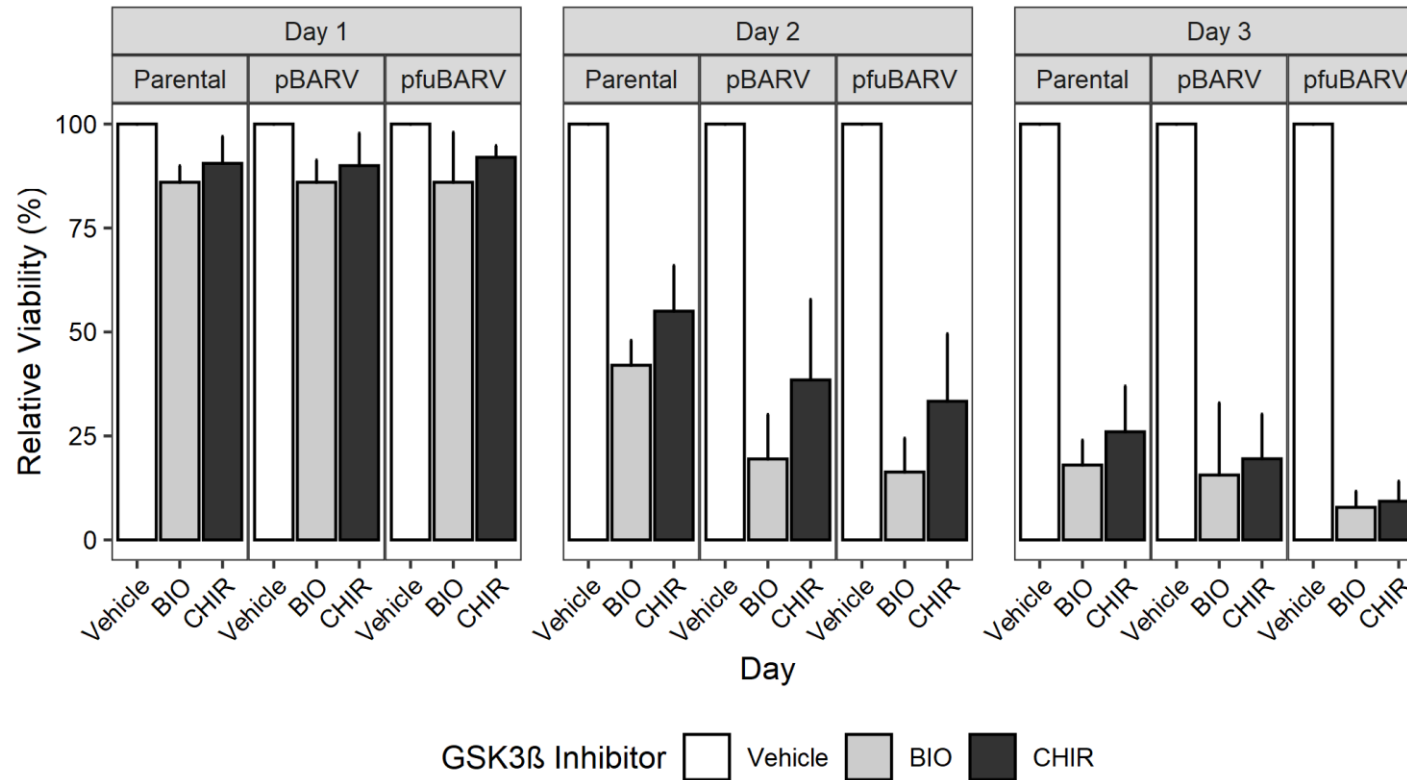


Figure 3-6: Relative Viability Changes over 72-hours with CHIR and BIO GSK3β Treatment

A bar chart demonstrating the percentage cell viability determined using TOPRO (2.11.6) following BIO, and CHIR treatment (2.9.1) of K562 parental, pBARV, and pfuBARV cells at 2.5μM and 5μM respectively over 24-hour, 48-hour, 72-hour timepoints normalized to vehicle control (0.1% DMSO, v/v). (n=3; data indicates mean +1SD).

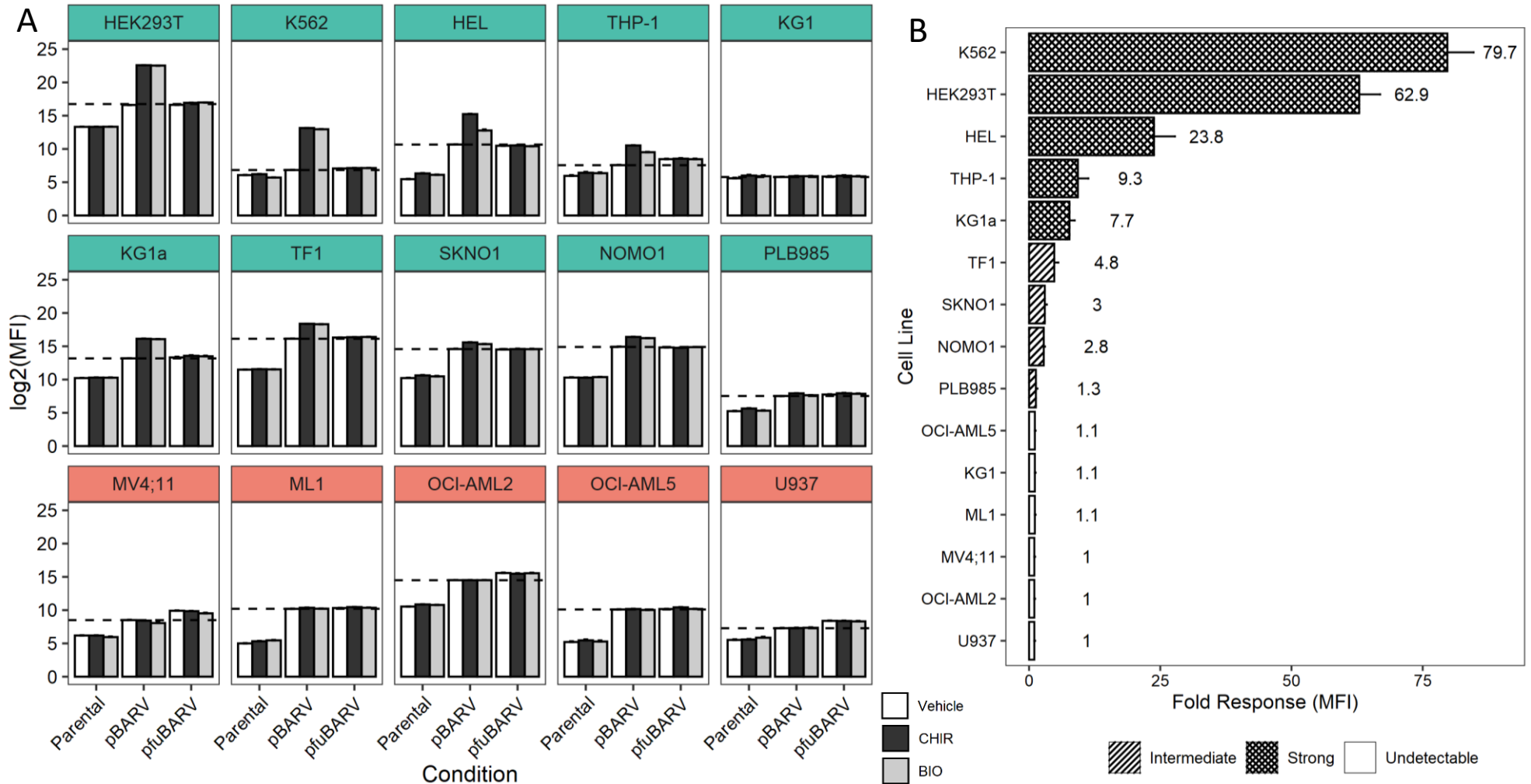


Figure 3-7: AML Cell Line WNT Reporter Assessment Following Treatment with GSK3β Inhibitors

A) Bar charts representing the response to GSK3β inhibitors as established with the WNT reporter, pBARV (2.11.5). White bars represent DMSO vehicle control (0.1% v/v), black represents CHIR (5.0μM) and grey represents BIO (2.5μM) (2.9.1). The horizontal dashed line represents the pBARV unstimulated levels within each respective cell line (n=5; data indicates mean ±1SD; note, error bars are often too small for visibility on panel A). **B)** Bar chart representing fold-induction in cell lines categorised based on fold response with >5-fold induction deemed strong, <5 fold & >1-fold considered intermediate, and <1.1 fold considered undetectable(n=5; data indicates mean +1SD).

3.3.5 Validating β -catenin Translocation in AML Cell Lines by Western Blot

As nuclear accumulation of β -catenin is critical to WNT/ β -catenin signalling, and to validate the flow cytometry findings, cells from each line were fractionated into cytoplasmic and nuclear components, with and without CHIR treatment. Basal levels of β -catenin were extremely low, below the levels required for reliable quantification (**Figure 3-8**). Following CHIR treatment, all lines accumulated β -catenin in the cytoplasm; however, only HEL, THP1, KG1a, KG1, TF1, NOMO1, NB4, PLB985, and SKNO1 translocated β -catenin into the nucleus upon stimulation and were thus confirmed as *responders*. The *non-responders* U937, OCI-AML2, OCI-AML5, MV4;11, and ML1 all showed cytoplasmic accumulation of β -catenin without nuclear translocation. These data agree with the WNT reporter assay, with the exception of KG1 due to WNT reporter silencing (3.3.4). A summary is provided in **Table 3-1**.

3.3.6 Validating γ -catenin Expression in AML Cell Lines by Western Blot

γ -catenin has potential direct and indirect roles in WNT/ β -catenin signalling. As with β -catenin, fractionated western blots under basal and CHIR-treated conditions were examined. However, the antibody used for γ -catenin demonstrated significant vertical streaking which hindered quantification efforts (data not shown). Despite this, it was possible to determine that GSK3 β inhibition did not affect the levels of γ -catenin, nor was γ -catenin translocated in response to GSK3 β inhibition. Together, these results demonstrate that γ -catenin levels are regulated independently from the β -catenin destruction complex.

With this established, a second screen was applied to examine γ -catenin expression in a series of AML cell lines by total unstimulated expression. γ -catenin levels were shown to be low in AML when compared to the CML line K562 (**Figure 3-9**). The absence of γ -catenin in three responder lines (TF1, NB4, PLB985) suggests γ -catenin is not an essential feature of responder AML cells. Both t(8;21) lines, Kasumi-1 and SKNO1, were found to express high levels of γ -catenin, supporting the earlier transcriptomic observations in AML patient data (3.3.1.1). However, when public CCLE RNA-seq data was analysed to assess the conformity between mRNA expression levels and protein presence, no correlation was found (**Figure 3-9D**). This indicates that transcriptomic levels of *JUP* are not broadly indicative of γ -catenin expression levels. Though, as the CCLE data was not prepared internally, culture conditions and other confounding factors may affect direct comparison between these data sets. A full summary is provided in **Table 3-1**.

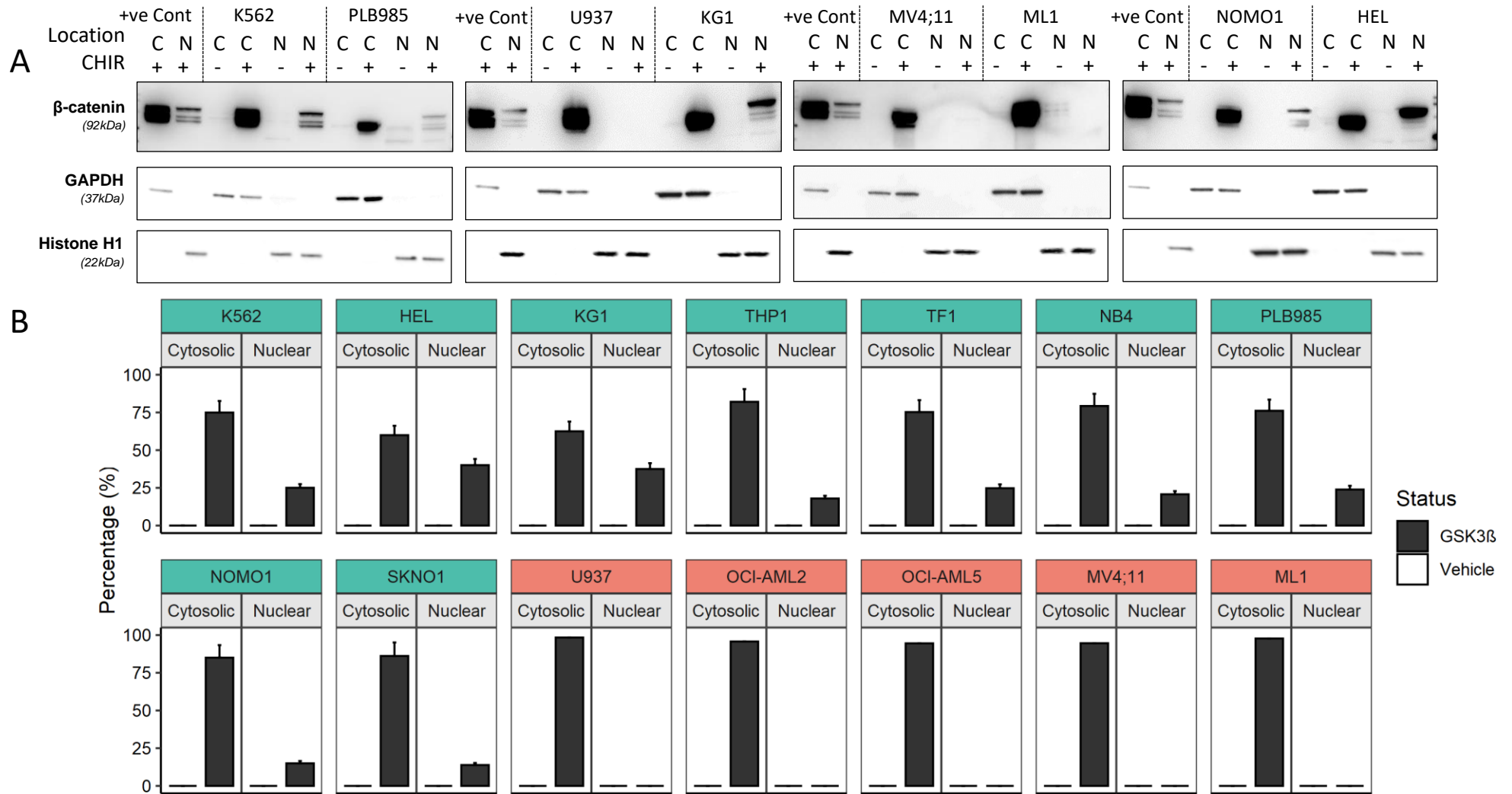


Figure 3-8: β -catenin Expression in AML Cell Lines

A) Representative western blot analysis showing sub-cellular localisation of β -catenin (2.10.2) following a 24-hour treatment with vehicle control (0.1% DMSO *v/v*) or GSK3 β inhibition with 5 μ M CHIR in select cell lines (2.9.1). Treated K562 were used as a positive control (+ve Cont), GAPDH was used as a cytoplasmic loading control, Histone H1 was used as a nuclear loading control (2.10.5). **B**) Summary bar chart showing β -catenin normalised expression relative to the positive control and refactored to relative percentages based on cytoplasmic or nuclear location. Facets are coloured by translocation status: green indicates nuclear translocation, red none (n=2; data indicates mean +1SD). C – Cytoplasmic; N – Nuclear.

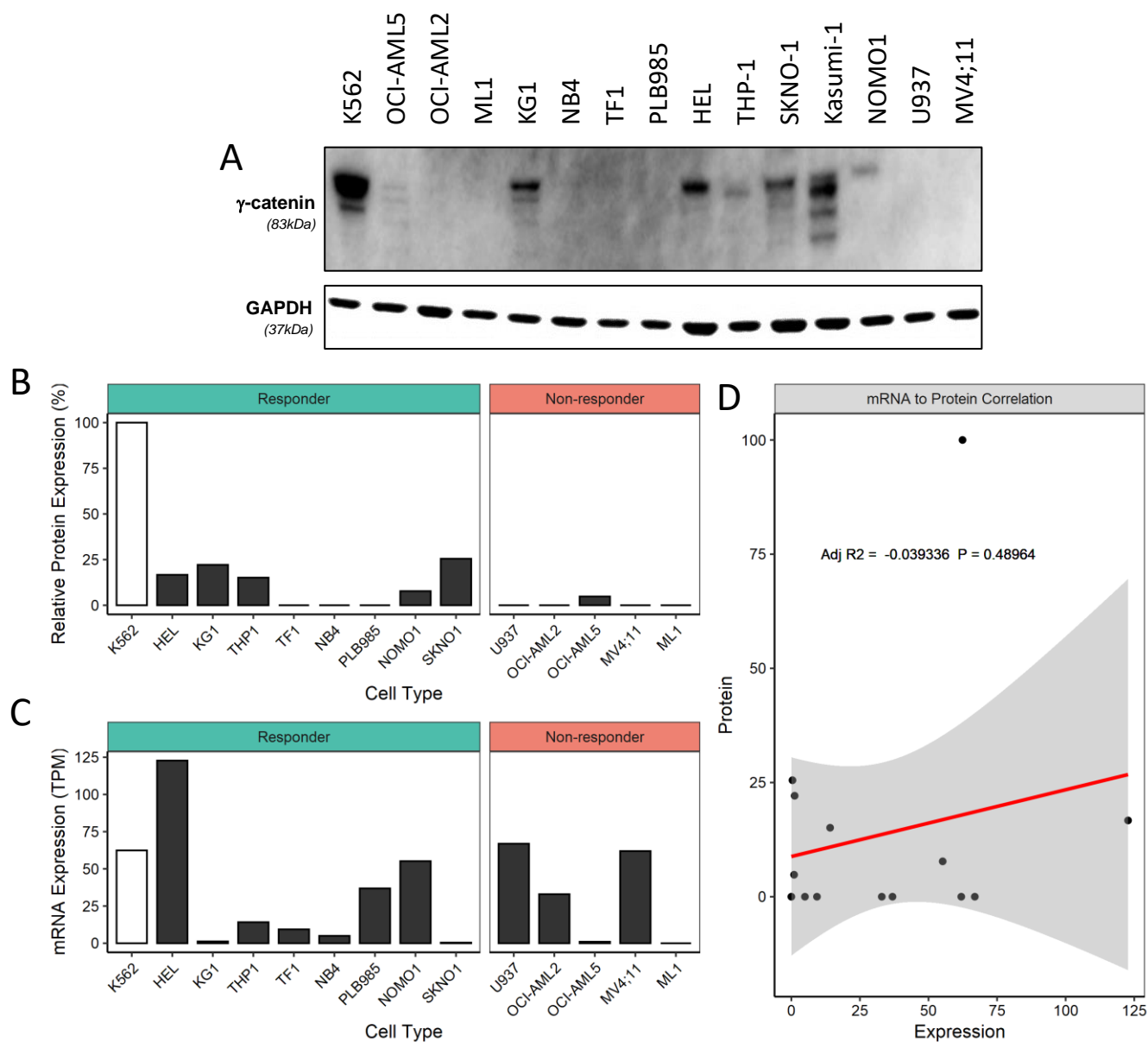


Figure 3-9: γ -catenin Expression in AML Cell Lines

A) Western blot analysis showing basal expression levels of γ -catenin (2.10). The K562 cell line was used as a positive control, GAPDH was used as a loading control (2.10.5). **B)** Bar chart showing normalised protein expression values relative to K562 protein expression levels (n=1). **C)** Bar chart showing normalised mRNA expression values acquired from the CCLE database (Barretina *et al.*, 2012). **D)** Linear regression analysis between protein expression levels and mRNA expression levels.

Table 3-1: Summary Table of β -catenin and γ -catenin Expression

Summary table representing the basal state detection of β -catenin, γ -catenin, and associated WNT reporter activity, alongside the GSK3 β inhibitor treatment state.

Line	Basal State					GSK3b Inhibitor				
	β -catenin		γ -catenin		Reporter Activity	β -catenin		γ -catenin		Reporter Induction
	Cytosolic Expression	Nuclear Expression	Cytosolic Expression	Nuclear Expression		Cytosolic Expression	Nuclear Expression	Cytosolic Expression	Nuclear Expression	
K562	-/+	-	+++	+	-	+++	++	+++	+	+++
HEL	-/+	-	+++	+	-	+++	++	+++	+	+++
THP1	-/+	-	+	+	-	+++	+	+	+	++
KG1	-/+	-	++	+	-	+++	++	++	+	++
KG1a	-/+	-	++	+	-	+++	++	++	+	++
TF1	-/+	-	-	-	-	+++	+	-	-	+
NOMO1	-/+	-	+	-	-	+++	+	+	-	+
SKNO1	-/+	-	+	-	-	+++	+	-	-	+
NB4	-	-	-	-	-	+++	+	-	-	+
PLB985	-/+	-	-	-	-	+++	+	-	-	+
OCI-AML2	-/+	-	-	-	-	+++	-	-	-	-
OCI-AML5	-/+	-	+	-	-	+++	-	+	-	-
ML1	-	-	-	-	-	+++	-	-	-	-
MV4;11	-/+	-	-	-	-	+++	-	-	-	-
U937	-/+	-	-	-	-	+++	-	-	-	-

- No detection

-/+ Non-quantifiable presence

+ Low detection

++ Moderate detection

+++ High detection

3.4 CRISPR-Cas9 Knockout Method Development

3.4.1 Evaluation of *CTNNB1* CRISPR-Cas9 gRNA in K562

The gRNA were designed to target all known transcript variants of *CTNNB1* to avoid sites with SNP and were of minimal off-target risk (2.8). To evaluate each gRNA for *CTNNB1*, the K562 pBARV line was transduced with all six gRNA in parallel. The *CTNNB1* CRISPR-Cas9 vectors were all-in-one designs harbouring the gRNA and Cas9. Following transduction and selection with the appropriate antibiotic (2.8.2), K562 pBARV cells were subsequently assessed for WNT reporter activity over fifteen days. A statistically significant reduction in WNT reported activity was apparent by day three after transduction with each of the *CTNNB1* targeting guides (**Figure 3-10A**). The reduction in WNT reporter activity following *CTNNB1* deletion was stable over the course of two weeks, indicating rapid and stable deletion (**Figure 3-10B**). Construct guide 517 was optimal with levels reduced by approximately 75%.

3.4.2 Genetic Cleavage Assay Verifies DNA-level Presence of InDels

A genetic cleavage assay was used to validate the *CTNNB1* knockout and the efficacy of *JUP* gRNA (where the WNT reporter could not be used). DNA was examined from the *CTNNB1* knockout 517 population on day 3, day 6, and day 15 to verify the proportion of knockout within the population was stable, whilst the three *JUP* constructs were examined on day 15. For *CTNNB1* construct 517, the cleavage efficiency was 45% at day 3, which plateaued at 60% on day 6 (**Figure 3-11**). *JUP* constructs 519, 521, and 523 showed cleavage efficiencies of 75%, 77%, and 60%, respectively, by day 15. Cleavage efficiency above 50% is indicative of a non-critical gene in a diploid cell.

3.4.2.1 Protein Levels of β -catenin and γ -catenin following knockout with CRISPR-Cas9

To further validate the knockout at protein level, western blot analysis was performed. K562 pBARV transduced with each respective combination of *CTNNB1* and *JUP* knockout was tested. β -catenin levels were shown to be significantly reduced regardless of gRNA. The most effective construct was 517, as found previously, which reduced β -catenin levels to $39\% \pm 12$, as compared to scrambled levels (**Figure 3-12A**). Regarding γ -catenin, protein levels were reduced to $25\% \pm 2$, $47\% \pm 4$, and $39\% \pm 15$ for gRNA 519, 521, and 523, respectively (**Figure 3-12B**). Protein assessment was performed on days six and fifteen following transduction. These data showed that the knockout is sustained within the mixed population. These results indicate that knockout of both β -catenin and γ -catenin is tolerated in K562 cells, and is best achieved with constructs 517 and 519, respectively.

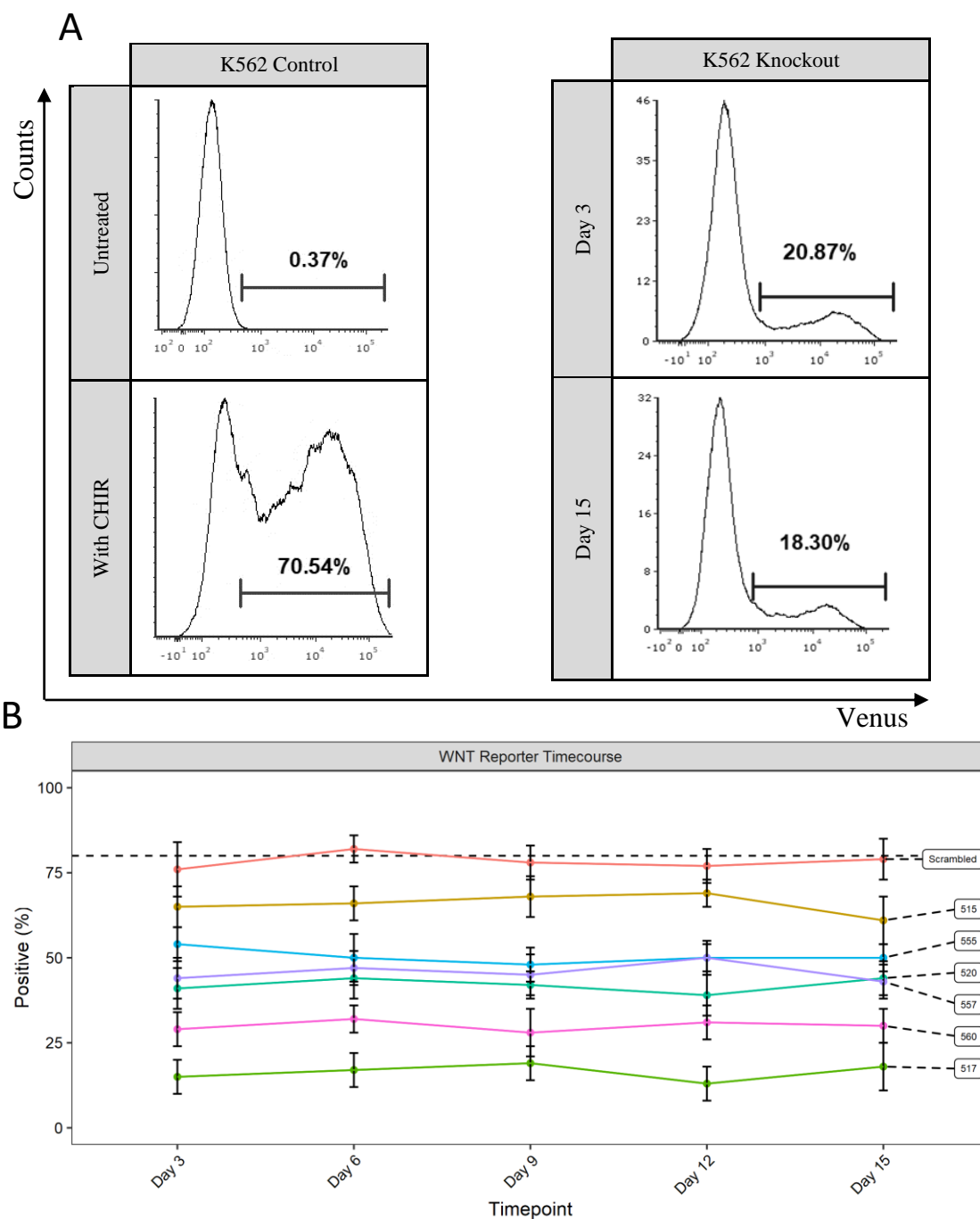


Figure 3-10: CRISPR-Cas9 Knockout Rapidly and Stably Reduces WNT Reporter Activity

A) Representative histograms of WNT reporter activity following CHIR treatment (5 μ M) for 24-hours in K562 scrambled control lines, alongside construct 517 CRISPR-Cas9 knockout lines on day three and day fifteen (2.11.5, 2.9.1). **B)** Line charts representing the response to CHIR treatment (5 μ M) for 24-hours, as established using the WNT reporter at the indicated time points. DMSO vehicle concentrations were maintained at 0.1% v/v. The horizontal dashed line represents the wildtype pBARV stimulated levels (n=3; data indicates mean \pm 1SD).

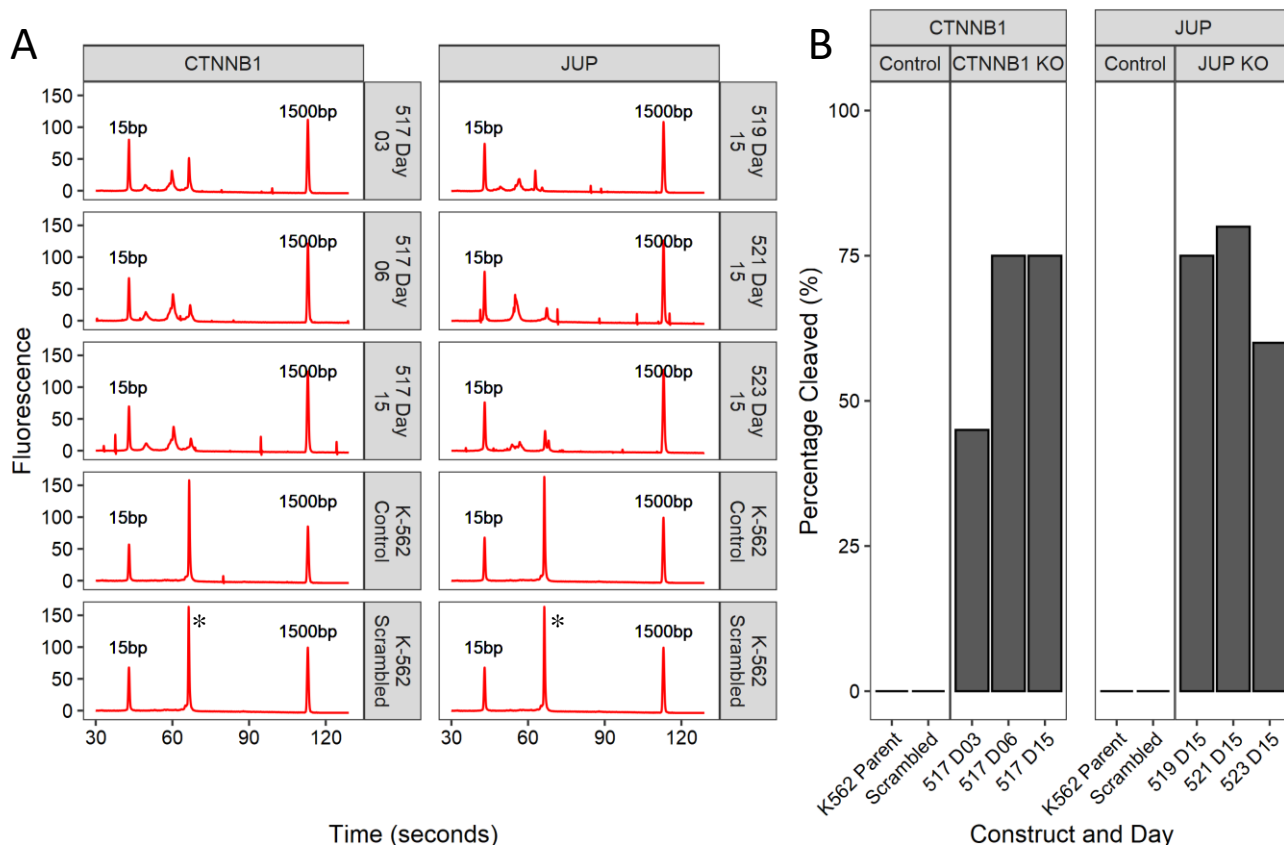


Figure 3-11: Genetic Cleavage Assay Reveals InDel Rate and Stability

A) A genetic cleavage assay was conducted using a T7 endonuclease to measure the proportion of target sites exhibiting an InDel mutation, which are cleaved due to mismatch (2.12.2). DNA was detected with a Bioanalyzer 2100 through a fluorescent DNA dye in fluorescent units relative to quantity, appearing as peaks. Elution time is relative to DNA length. Samples were flanked with a 15bp and 1500bp DNA ladder. Summed peak area was divided by peak wildtype area to determine cleavage efficiency as a percentage. As construct 517 (517-Puro) had been established as the best gRNA for targeting CTNNB1 (β -catenin), the cleavage assay was conducted as a time course upon DNA extracted at day three, six, and fifteen. For gRNA targeting JUP (γ -catenin) guides 519-Neo, 521-Neo, and 523-Neo were considered at day fifteen to determine which produced the greatest extent of InDel generation. (n=1)

* - Full length wildtype gene (*CTNNB1* and *JUP*) detected in control and scrambled samples. Smaller fragments were identified in knockout conditions of varying length as a consequence of CRISPR-Cas9 cleavage, as shown to the left of the control peak. Control peaks were of comparable size in the *CTNNB1* and *JUP* samples as the target site was flanked by PCR primers producing a comparable template length.

B) Bar charts representing the quantified InDel proportion as measured by proportion cleaved. By contrasting the full-length DNA against cleaved products, a cleavage score was obtained.

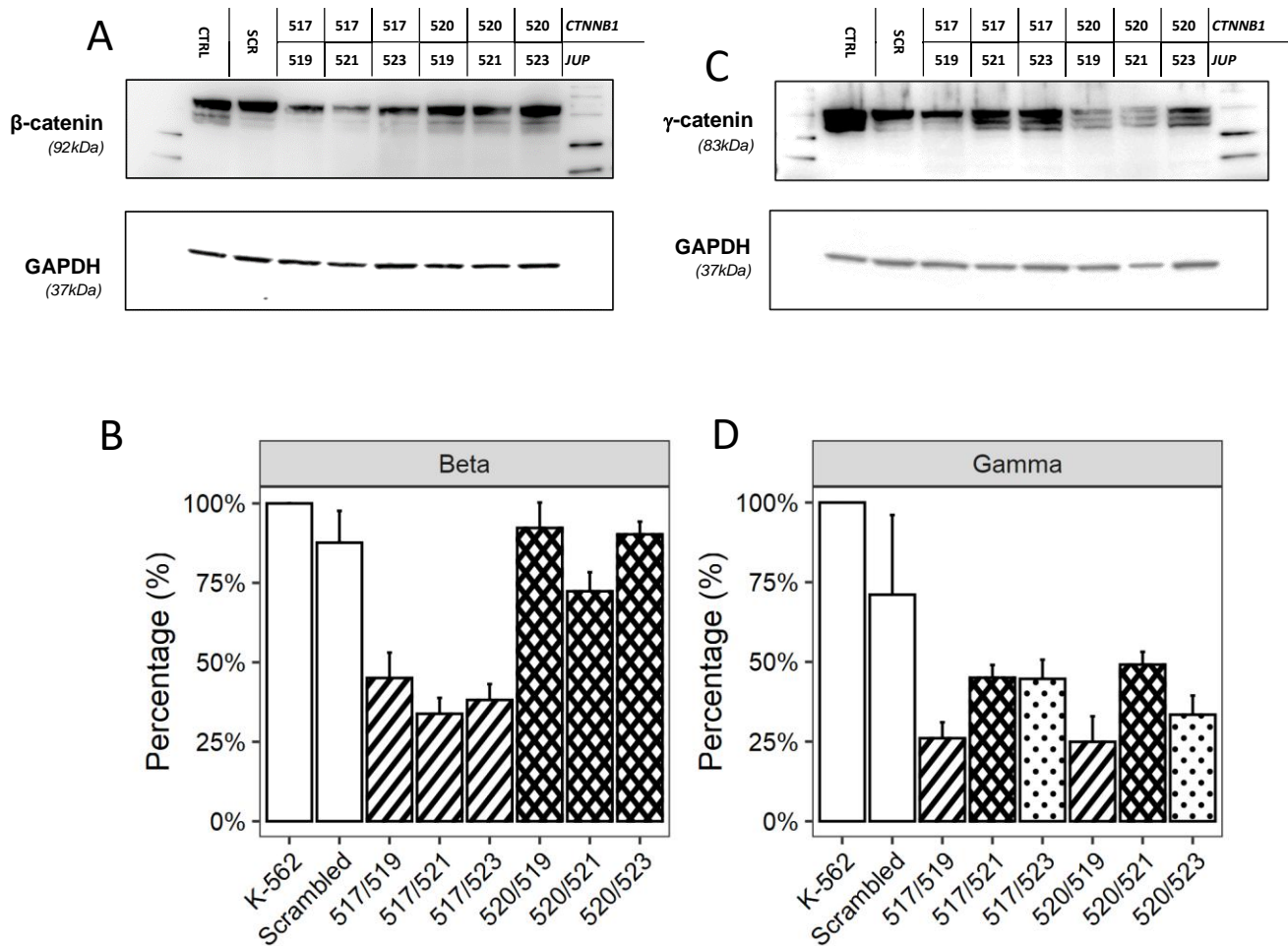


Figure 3-12: Protein Analysis of β -catenin and γ -catenin Following Knockout

Western blots demonstrating protein-level reductions in (A) β -catenin and (C) γ -catenin (2.10). K562 pBARV cells were transduced with scrambled control (Scrambled-Puro; 463), β -catenin target gRNA (517-Puro, 520-Puro), and γ -catenin target gRNA (519-Neo, 521-Neo, 523-Neo) lentivirus. Non-transduced cells were removed by addition of puromycin (2.8.2). Whole lysates were prepared 24 hours following the addition of 5 μ M CHIR to cultures of K562 WT, scrambled, and bulk knockout cells (2.9.1). GAPDH was used as a loading control (2.10.5). Ladders flank the samples. (C) β -catenin and (D) γ -catenin protein expression was normalised to loading control. (n=2; data indicates mean +1SD).

3.5 Selection of AML Cell Lines for Knockout

3.5.1 Establishment of AML Cell Lines for Knockout Studies

With cell lines characterised as *responders* and *non-responders* based upon their capability to translocate stabilised β -catenin (3.3.3), in addition to the selection of an optimal gRNA for *CTNNB1* and *JUP* (3.4), it was necessary to determine the most appropriate panel of cell lines for subsequent knockout research. Some lines were excluded based upon general characteristics: KG1 was replaced with the subline KG1a, which did not exhibit the problematic rapid silencing of reporter constructs. Similarly, PLB985 was also discarded due to gradual reporter silencing issues. The slow doubling time of ML1 cells (3-7 days) would prolong cloning times, so it was not considered for knockout. The AML cell lines HEL, THP1, KG1a, TF1, NOMO1, OCI-AML2, OCI-AML5, U937, and MV4;11 were selected to cover the broad range of subtypes within AML to limit confounding factors (**Table 2-1**).

For knockout studies, HEL, THP1, KG1a, TF1, and NOMO1 were selected as the *responder* group, whilst the *non-responder* group consisted of OCI-AML2, OCI-AML5, U937, and MV4;11. In place of the generated pBARV lines previously used, pre-existing clonal pBARV WNT reporter lines were used in the case of HEL, THP1, U937, and MV4;11; these were kindly provided by Prof. Richard Darley. The previously mentioned remaining cell lines were non-clonal. Using a clonal WNT reporter cell line to generate knockout clones reduced concerns regarding selection variation, such as ploidy variants within a cell line population, as the WNT reporter line represents a singular ploidy status. This is notable for lines with additional copies of the targeted genes. K562, a responder CML cell line, was included as a non-AML control which has no ploidy variations. Representative WNT reporter responses of the clonal and non-clonal lines selected for the panel are shown in **Figure 3-13**, with clonal pBARV lines demonstrating a near complete response.

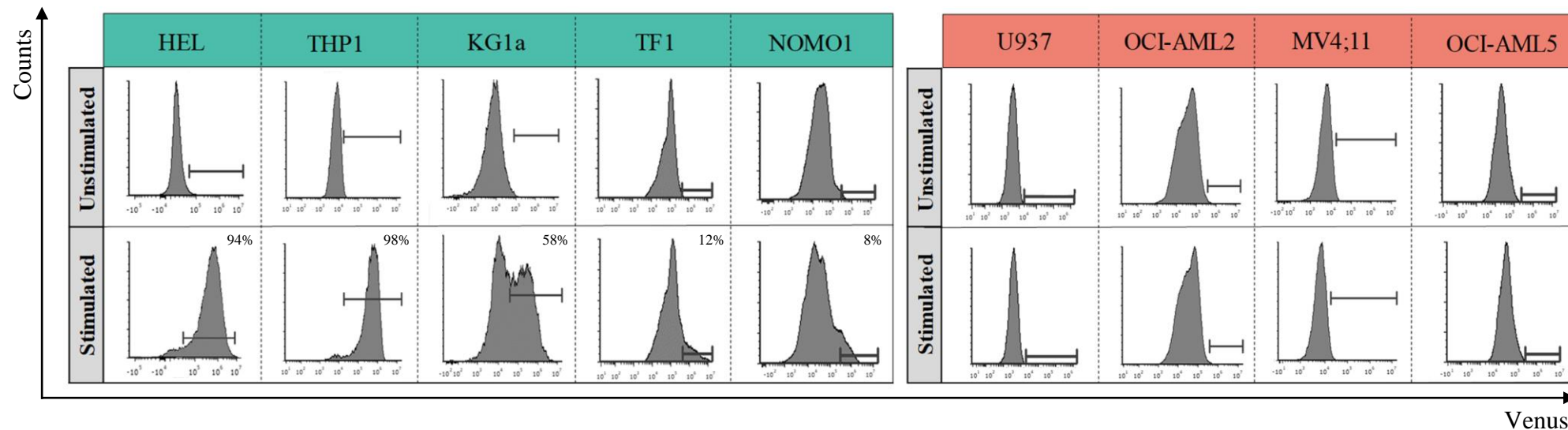


Figure 3-13: WNT Signalling Activity Delineates AML Cell Lines in Knockout Panel

Representative histograms showing WNT reporter activity (Venus fluorescence) of pBARV WNT reporter transduced AML cell lines demonstrating responder cell lines (**green**) and non-responder lines (**red**) (2.11.5). Cells were cultured with 5 μ M CHIR for 24-hours prior to recovery (2.9). A vehicle control (0.1% DMSO, v/v) was used for each line to define a threshold of positivity (n=3).

3.6 Single β -catenin Knockout in AML

As two genes were considered as part of this study, it was necessary to generate individual knockouts for β -catenin and γ -catenin to determine conclusive roles of each member prior to attempting to both genes simultaneously. β -catenin knockouts were established in all cell lines, γ -catenin knockouts are discussed in 3.7.

3.6.1 WNT Signalling was Significantly Reduced in Responder Lines with Knockout

WNT/ β -catenin signalling was examined with the pBARV flow reporter following the generation of a bulk stable population (2.9.3). No change to the *non-responder* group was noted, as expected (data not shown). *Responder* lines, on the other hand, displayed significantly reduced response. The clonal pBARV cell lines HEL, and THP1 were reduced by 85%, and 75%, respectively (**Figure 3-14**). Non-clonal *responder* lines KG1a, TF1, and NOMO1 were reduced by 82%, 86%, and 99%, respectively. These results show that β -catenin knockout reduces WNT/ β -catenin signalling activity. That residual activity remains indicates either a proportion of the population has evaded CRISPR-Cas9 knockout, or there is redundancy of β -catenin function (e.g., γ -catenin). This was the predicted outcome based on the typical known knockout capacity of CRISPR-Cas9, with the single-guide method applied here-in expected to achieve 10-60% knockout at an average of 34% efficiency (Dang *et al.*, 2015; Farboud *et al.*, 2015). Alternatively, γ -catenin could be providing a limited residual compensatory effect.

3.6.2 β -catenin Protein Levels are Substantially Reduced by CRISPR-Cas9 KO

By total protein assessment through western blot, bulk knockout of β -catenin level varied between cell lines, ranging from 20 to 75% reduction in protein readout (**Figure 3-15**). Knockout was most substantial in HEL, THP1, KG1a, TF1, and U937. OCI-AML2 and MV4;11 presented very little reduction in β -catenin levels. Levels of γ -catenin were unaffected by β -catenin knockout, demonstrating no co-regulation mechanism and the specificity of the gRNA.

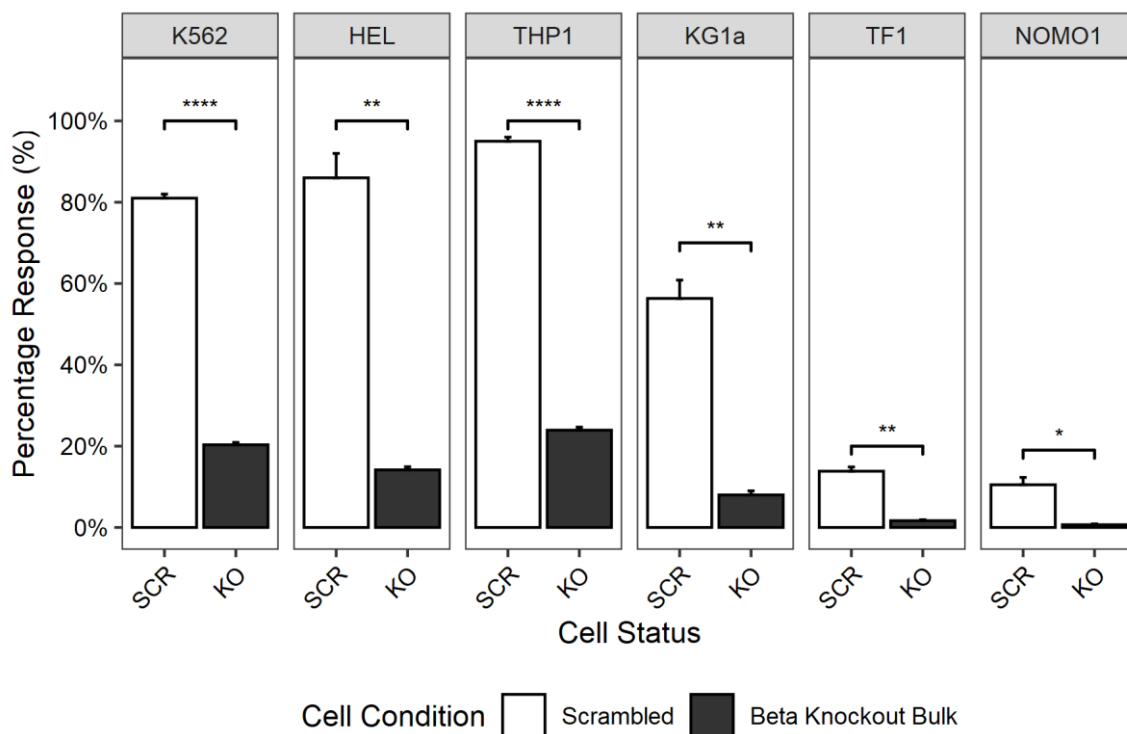


Figure 3-14: β -catenin Knockout Significantly Reduces WNT Reporter Activity

Percentage positive WNT reporter activity (Venus fluorescence, 2.11.5) of AML responder cell lines transduced with control (Scrambled-Puro; 463), and knockout (KO) β -catenin target gRNA (517-Puro) lentivirus. Transduced cells were selected for using puromycin (2.8.2). Cells were cultured in the presence of 5 μ M CHIR for 24 hours or a vehicle control (0.1% DMSO, v/v) (2.9.1). WNT reporter levels were assessed by flow cytometry. An unstimulated vehicle control was used to define a threshold of positivity. (n=3; data indicates mean \pm 1SD; t-test. < 0.0001 = ****, 0.0001 to 0.001 = ***, 0.001 to 0.01 = **, 0.01 to 0.05 = *.)

SCR - Scrambled; KO - *CTNNB1* Partial Knockout

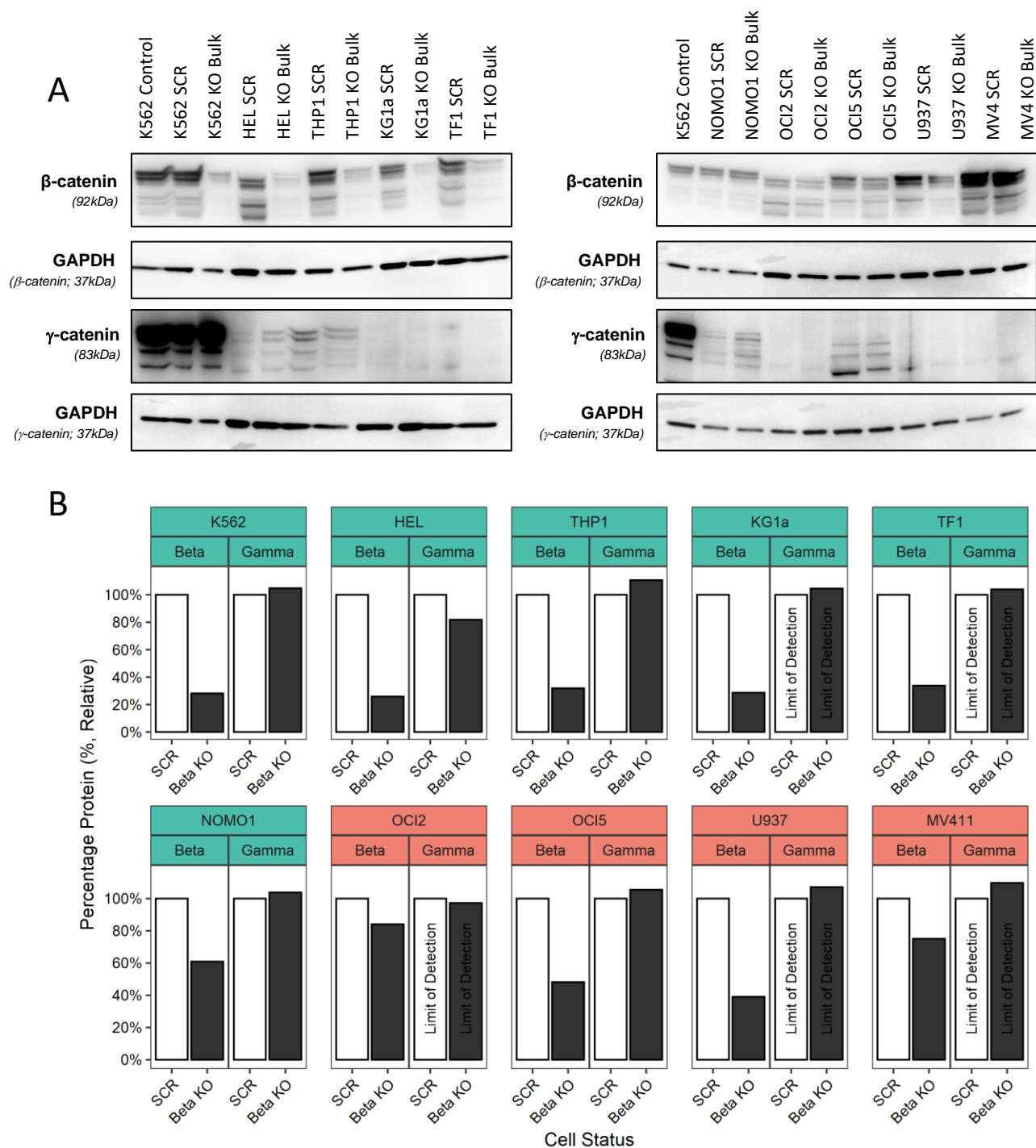


Figure 3-15: Establishing Levels of β -catenin Knockout in Single *CTNNB1* Knockout Cells

A) Western blots showing protein expression for β -catenin and γ -catenin in AML cell lines following transduction with a CRISPR-Cas9 construct targeting *CTNNB1*, or a scrambled control (2.10, 2.8). Whole lysates were prepared 24 hours after addition of $5\mu\text{M}$ CHIR to cultures of scrambled and bulk knockout cells (2.9.1). Protein loading was controlled by analysis of GAPDH, which allowed quantification for (B) β -catenin and γ -catenin (2.10.6, n=1). Bars labelled with limit of detection represent expression levels which required extended exposure to an extent at which background banding was present, indicating potential concerns of reliable quantification.

SCR - Scrambled; KO - *CTNNB1* Partial Knockout.

3.6.3 β -catenin Knockout Does Not Perturb General Characteristics

Examination of the bulk β -catenin knockout population was undertaken to determine if reductions in β -catenin levels resulted in a perturbed phenotype. Proliferation and viability were unaffected between bulk scrambled and β -catenin knockout conditions, suggesting knockout was tolerated (**Figure 3-16A|B**). In addition, an apoptosis assay was performed, again showing no impact of reduced β -catenin levels. (**Figure 3-16C**). DNA content was examined to determine whether any arrest or other perturbation of the cell cycle was present, but again was unaffected by reduced β -catenin levels (**Figure 3-16D**). While these findings do not indicate a role for β -catenin in AML maintenance, these results were based upon incomplete knockout cultures. It is possible that $CTNNB1^{+/-}$ and genetically unaffected cells are able to provide the necessary factors to sustain $CTNNB1^{-/-}$ cells. To address this, it is necessary to clone these cultures to obtain a complete knockout line. Further, these lines did not rule out the possible redundancy of β -catenin in respect of γ -catenin, which was detected in most of the lines.

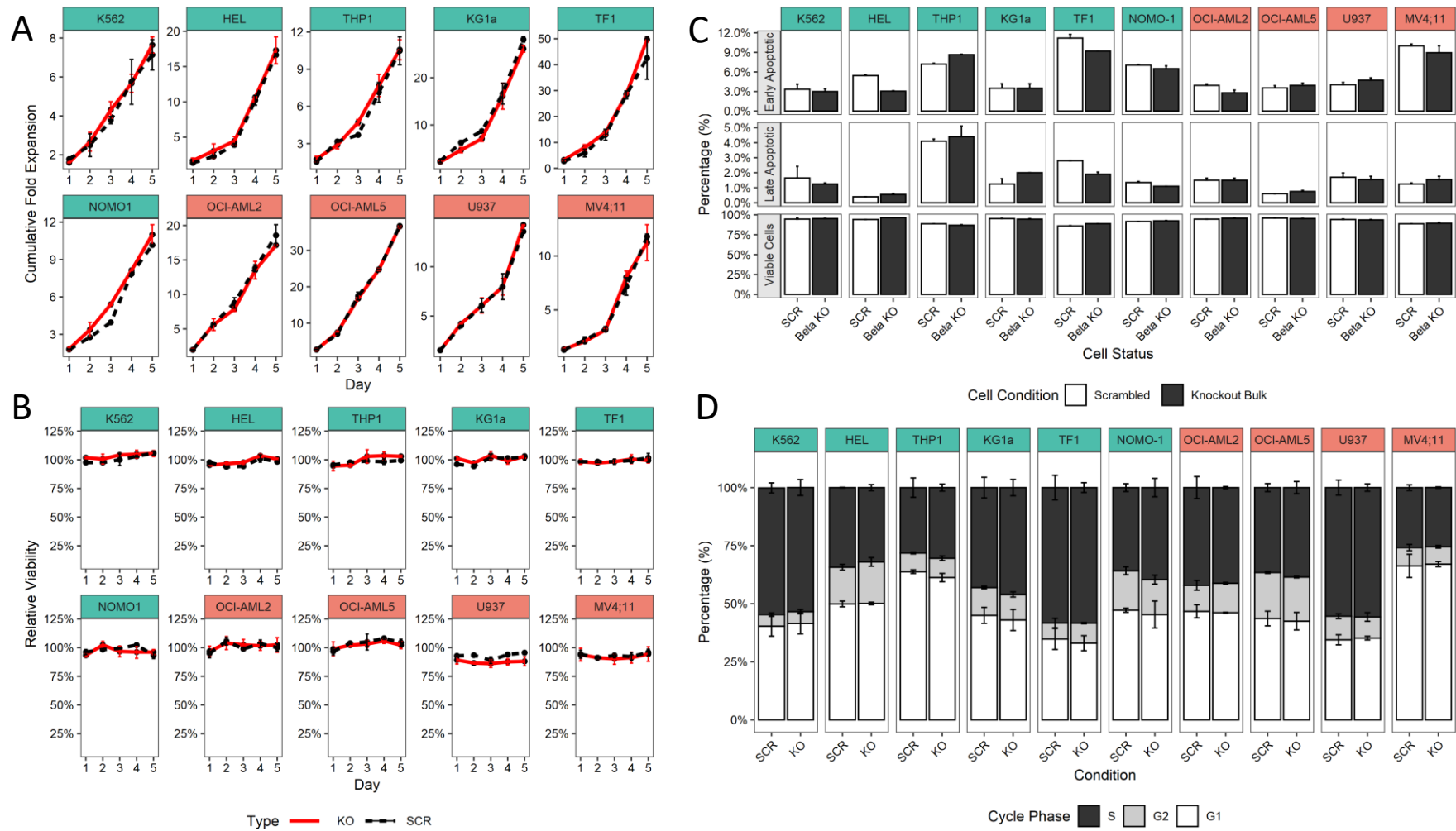


Figure 3-16: Partial Knockout of *CTNNB1* Does Not Perturb General Characteristics of AML in a Bulk Population Setting

A) Proliferation assays were conducted on each line by seeding cells at log-phase growth ($1 \times 10^5 - 2.5 \times 10^5$) and monitored over 5 days (2.11.7). Dashed black line represents scrambled control, solid red line indicates knockout. **B)** Simultaneously, population viability was recorded each day with TOPRO DNA staining (2.11.6). **C)** An apoptosis assay was conducted by staining with Annexin-V and 7-ADD to reveal early and late-stage apoptotic proportions respectively (2.11.9). **D)** DNA content was used to examine cell cycle phase conditions with a propidium iodide-based DNA-content assay (2.11.8). Responders (**green**) or non-responders (**red**). (n=3; data indicates mean \pm 1SD). SCR - Scrambled; KO - *CTNNB1* Partial Knockout

3.6.4 Clonogenicity is Significantly Reduced for Responder Lines with β -catenin Knockout

To determine definitively whether β -catenin is integral to AML maintenance, it was necessary to generate a complete knockout clone. This required limiting dilution cloning, which results in a single-cell *per well* for culture (2.4).

A significant reduction in clonal efficiency was noted between AML bulk scrambled control and β -catenin knockout conditions for the *responder* AML cell lines, whilst *non-responder* cell lines had no observed difference in clonogenicity (**Figure 3-17**). K562 did not present clonal deficiencies, suggesting clonal growth of CML is independent of β -catenin, despite responding to CHIR. The responder lines, HEL, THP1, KG1a, TF1, and NOMO1 generated 97%, 68%, 39%, 48% and 34% fewer clones, respectively. The reduction in WNT reporter activity and protein reductions are closely proportional to the reduction in cloning efficiency. Together these data suggest that knockout is incompatible with cloning, and by extension, that WNT/ β -catenin signalling is required for clonal growth.

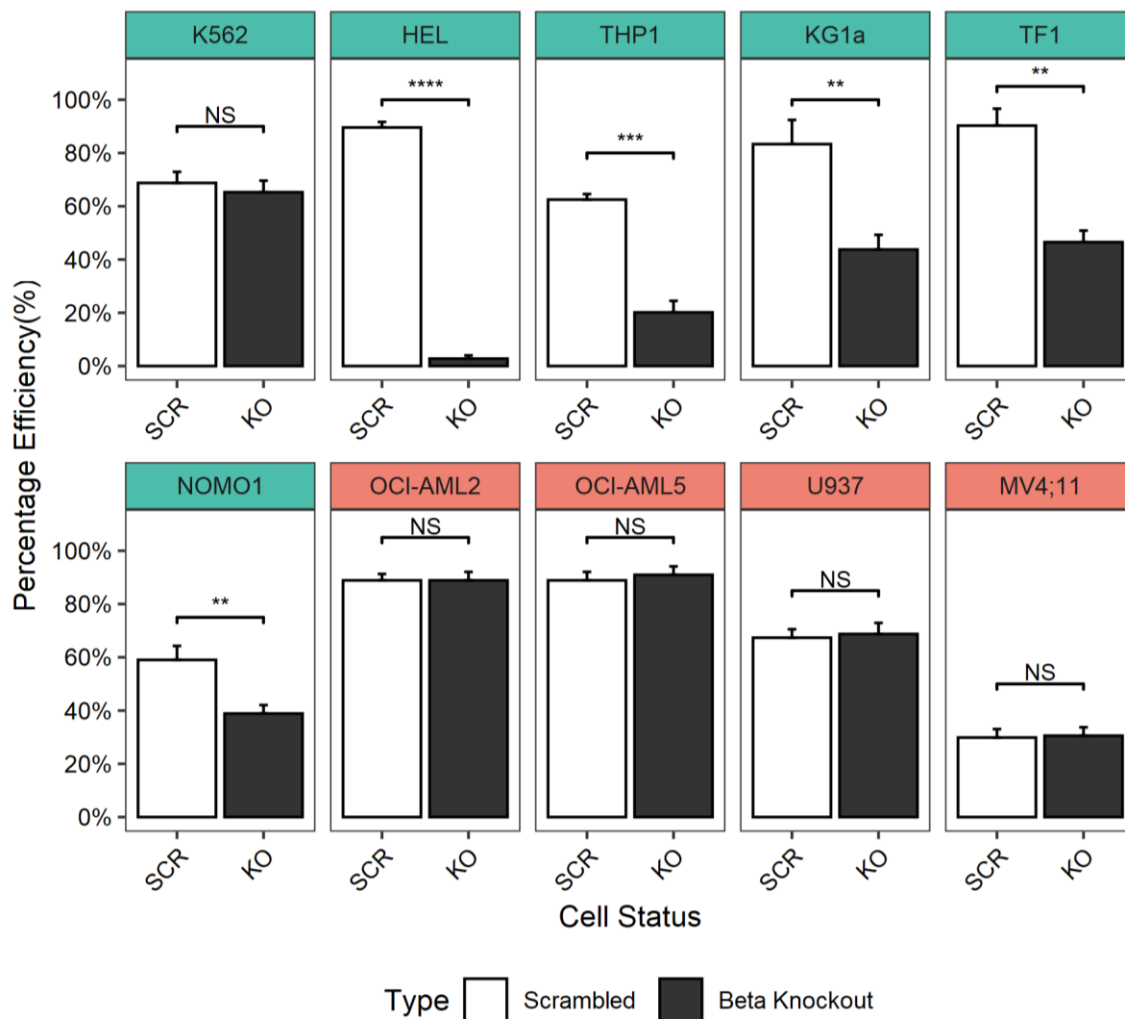


Figure 3-17: Clonogenicity is Significantly Reduced in β -catenin Knockout Responder Lines

Limiting dilution cloning was performed to examine clonal efficiency (2.4). AML cell lines were transduced with scrambled control and β -catenin target gRNA lentivirus (2.8). Non-transduced cells were removed by addition of selective agents puromycin and G418 (2.8.2). After 3 passages cells underwent clonal expansion and were examined 7-14 days later. Responder AML cell lines (**green**); non-responder lines (**red**). K562, a CML cell line, was used as a non-AML control. (n=3; data indicates mean +1SD; t-test. < 0.0001 = ****, 0.0001 to 0.001 = ***, 0.001 to 0.01 = **, 0.01 to 0.05 = *, \geq 0.05 = Not significant)

SCR - Scrambled; KO - *CTNNB1* Partial Knockout

3.7 Single γ -catenin Knockout in AML

3.7.1 WNT Signalling was Unaffected by γ -catenin Knockout in Responder Lines

To examine the contribution γ -catenin provides to WNT/ β -catenin signalling, WNT reporter assay was performed following generation of a stable bulk population. *Responder* lines displayed no alteration to response (**Figure 3-18**). These preliminary data do not support a role for γ -catenin in the WNT/ β -catenin signalling pathway.

3.7.2 γ -catenin Protein Levels are Substantially Reduced by CRISPR-Cas9 KO

Similarly to the *CTNNB1* guide, level of knockout was assessed at the protein level by performing western blot analysis between cell lines (2.10). As expected, bulk knockout of γ -catenin level varied between cell lines, with some showing no reduction, such as NOMO1, whilst TF1 displayed 90% knockout (**Figure 3-19**). A challenge of studying γ -catenin knockout by western blot analysis was the difficulty in detecting γ -catenin expression in certain cell lines. This was particularly troublesome in KG1a, OCI-AML2, and MV4;11, which presented very faint bands even after an extended exposure.

Interestingly, β -catenin levels were reduced by γ -catenin knockout, even within cell lines with very low levels of γ -catenin expression. This suggests a shared destruction mechanism or other method of overlap in catenin turnover.

3.7.3 Clonogenicity and Proliferation are Unaffected by γ -catenin Knockout

As knockout of β -catenin was shown to significantly reduce clonogenicity, an equivalent limiting dilution assay was performed for γ -catenin knockout lines. No alteration to clonal efficiency was observed between AML bulk scrambled control and γ -catenin knockout conditions for any AML cell line or the K562 control line, suggesting γ -catenin is not integral to this process (**Figure 3-20**). Similarly, growth trends were monitored and found to be unchanged from the wildtype condition (data not shown).

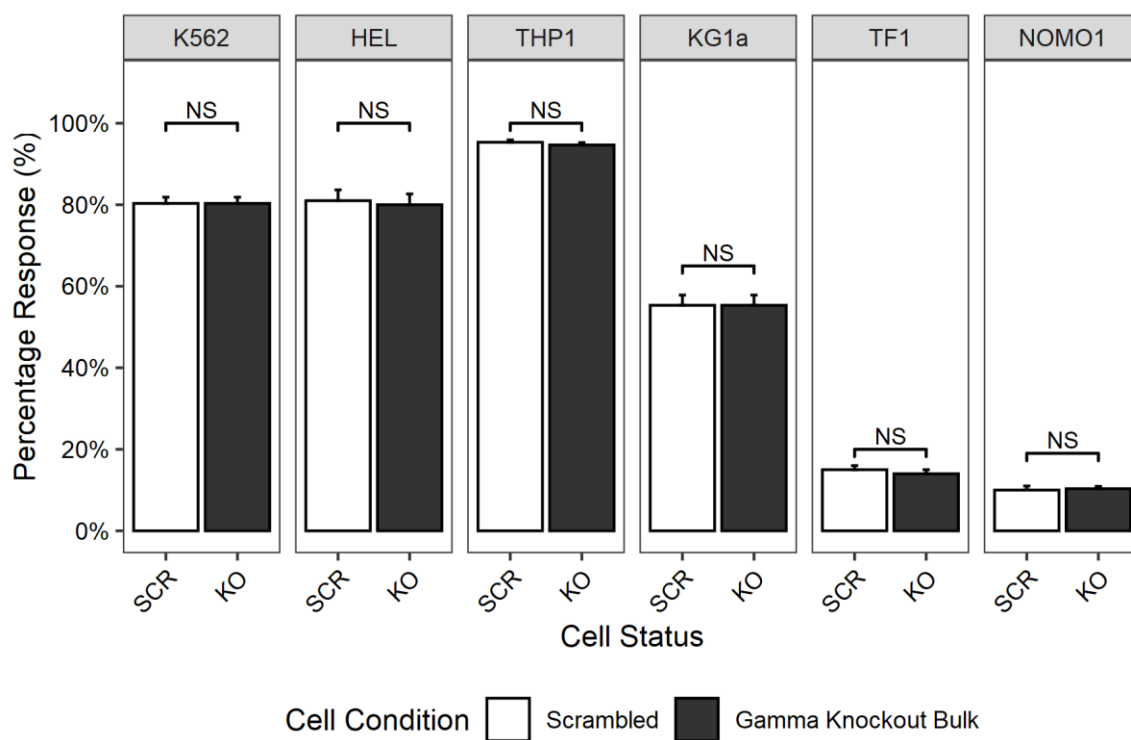


Figure 3-18: γ -catenin Knockout Does Not Influence WNT/ β -catenin Signalling

The WNT reporter assay was performed to assess WNT/ β -catenin signalling activity, indicated as a percentage positive relative to a vehicle control (2.11.5). Cells were treated with 5 μ M CHIR for 24-hours prior to assessment by flow cytometry (2.9.1). An unstimulated vehicle control was used to define a threshold of positivity (0.1% DMSO, v/v). (n=3; data indicates mean +1SD; t-test; NS = Not Significant (p > 0.05)).

SCR - Scrambled; KO - *JUP* Partial Knockout

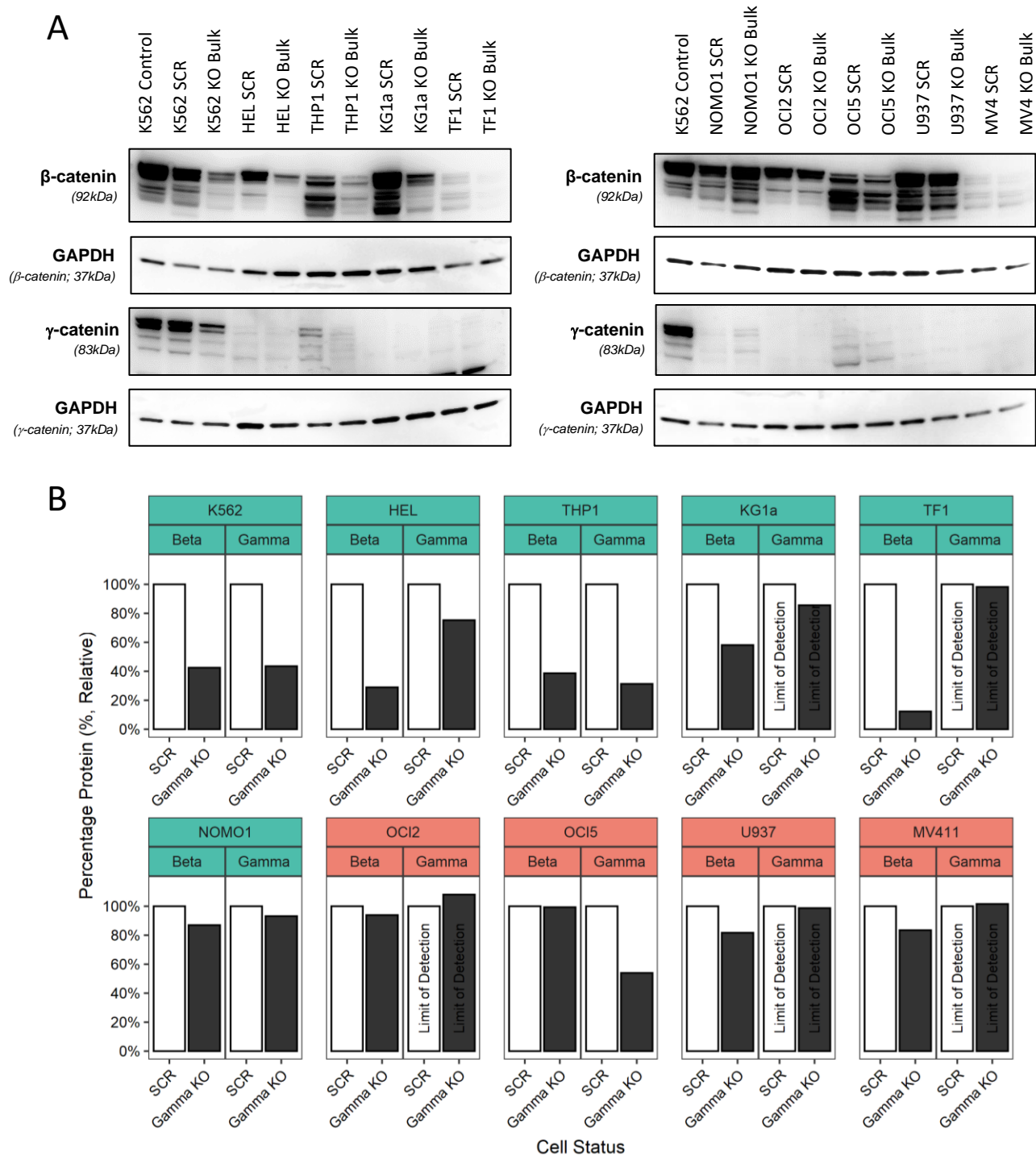


Figure 3-19: γ -catenin Knockout in Single *JUP* Target Cell Lines

A) Western blots demonstrating protein-level states for β -catenin and γ -catenin in AML cell lines following transduction with a CRISPR-Cas9 construct targeting *JUP*, or a scrambled control (2.10). Whole lysates were prepared 24 hours after addition of 5 μ M CHIR to cultures of 1x10⁶ scrambled and bulk knockout cells (2.9.1). Protein loading was controlled by analysis of GAPDH, which allowed quantification for β -catenin and γ -catenin (2.10.6, n=1). Bars labelled with limit of detection represent expression levels which required extended exposure to an extent at which background banding was present, indicating potential concerns of reliable quantification.

SCR - Scrambled; **KO** - *JUP* Partial Knockout

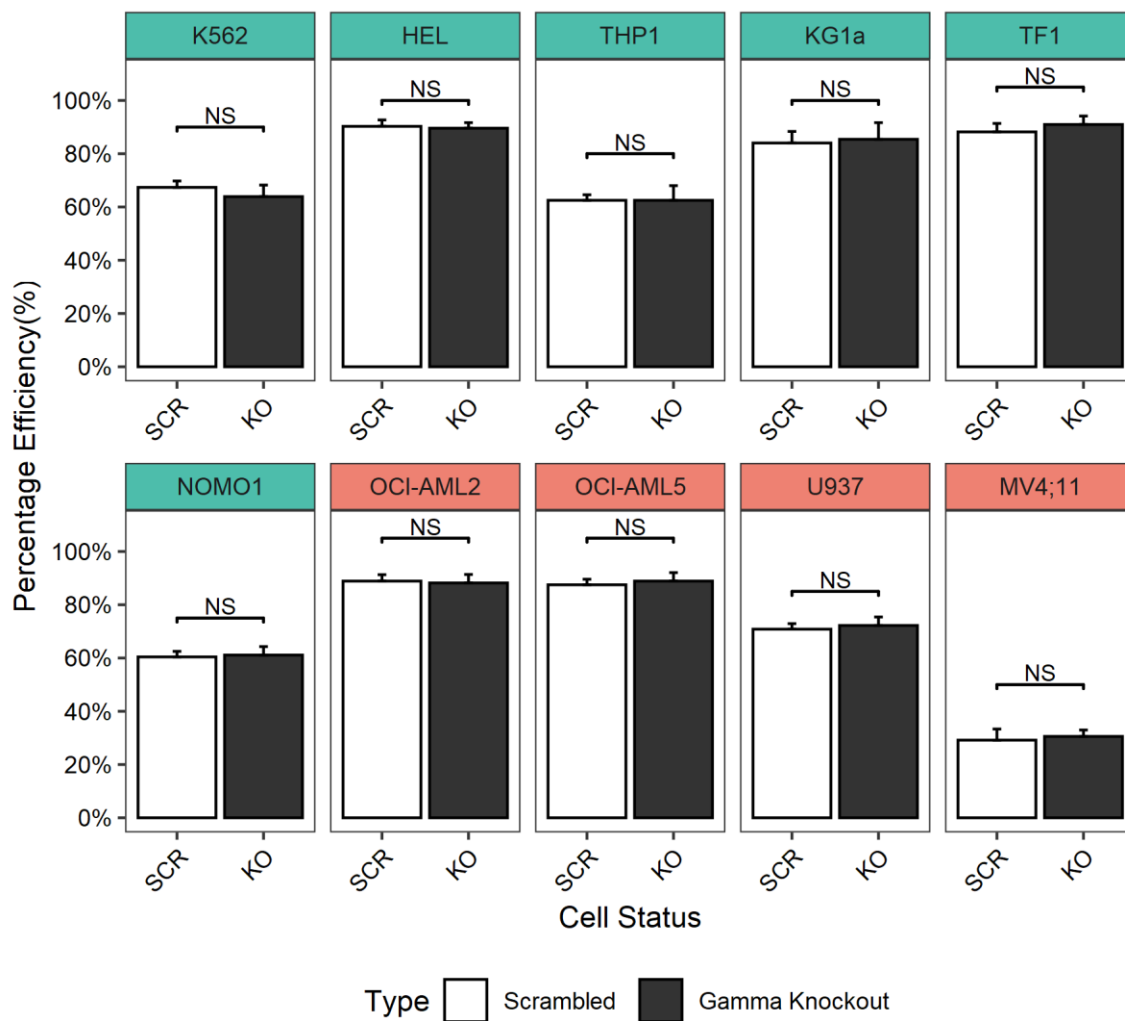


Figure 3-20: Clonogenicity is Unaffected by γ -catenin Knockout

Limiting dilution cloning was performed to examine clonal efficiency (2.4). AML cell lines were transduced with scrambled control and gamma catenin target gRNA lentivirus (2.8). Non-transduced cells were removed by addition of selective agent (2.8.2). After 3 passages cells underwent clonal expansion and were examined 7-14 days later. Responder AML cell lines (**green**) and non-responder lines (**red**). K562, a CML cell line, was used as a control. (n=3; data indicates mean +1SD; t-test. < 0.0001 = ****, 0.0001 to 0.001 = ***, 0.001 to 0.01 = **, 0.01 to 0.05 = *, ≥ 0.05 = Not significant).

SCR - Scrambled; KO - *JUP* Partial Knockout

3.8 Dual β -catenin and γ -catenin Knockout in AML Cell Lines

3.8.1 Generation of Dual Knockout Cell Lines

As previous data indicated β -catenin was linked to clonogenicity (1.3.5), and γ -catenin was perhaps capable of compensating for β -catenin, it was necessary to examine the consequence of simultaneous dual knockout in the bulk setting. As before, cells were transduced with lentiviral scrambled gRNA as a control, whilst both targeting gRNA were utilised in parallel (2.8).

3.8.2 WNT Reporter Activity was Reduced Significantly by Dual KO in Responder Lines

To determine whether dual knockout further reduced WNT/ β -catenin signalling activity, a WNT reporter assay was performed immediately following transduction. *Responder* lines with dual knockout displayed significantly reduced response, regardless of cell line, in agreement with previous studies on single β -catenin knockdown. The clonal pBARV cell lines K562, HEL, and THP1 were reduced by 75%, 85%, and 50%, respectively (**Figure 3-21**). Non-clonal *responder* lines KG1a, TF1, and NOMO1 were reduced by 55%, 86%, and 99%, respectively.

3.8.3 β -catenin and γ -catenin were Reduced by CRISPR-Cas9 Mediated Knockout

To confirm that CRISPR-Cas9 was able to simultaneously induce reductions in β -catenin and γ -catenin levels, protein expression were assessed by western blotting. Dual gRNA targeting was capable of substantially reducing β -catenin and γ -catenin levels simultaneously to levels beyond, or comparable to, previous knockdown studies (1.3.5). However, it is conceded that γ -catenin knockout also reduced β -catenin expression, limiting interpretation. These data indicate a significant proportion of the bulk population in HEL, THP1, U937, and MV4;11 had complete knockout of both genes; however, as had been expected, there was a high degree of variance between cell lines due to target site accessibility, DNA damage response variations, and copy number variations due to ploidy differences. (**Figure 3-22**).

3.8.4 Combined Knockout of β -catenin and γ -catenin Does Not affect Growth and Viability of the Bulk Population

No changes were observed to proliferation, viability, apoptosis, or DNA content for any cell line (**Figure 3-23**). These data suggest that no compensative redundancy mechanism exists between γ -catenin for β -catenin, though a true complete knockout clone would be required to validate this suggestion.

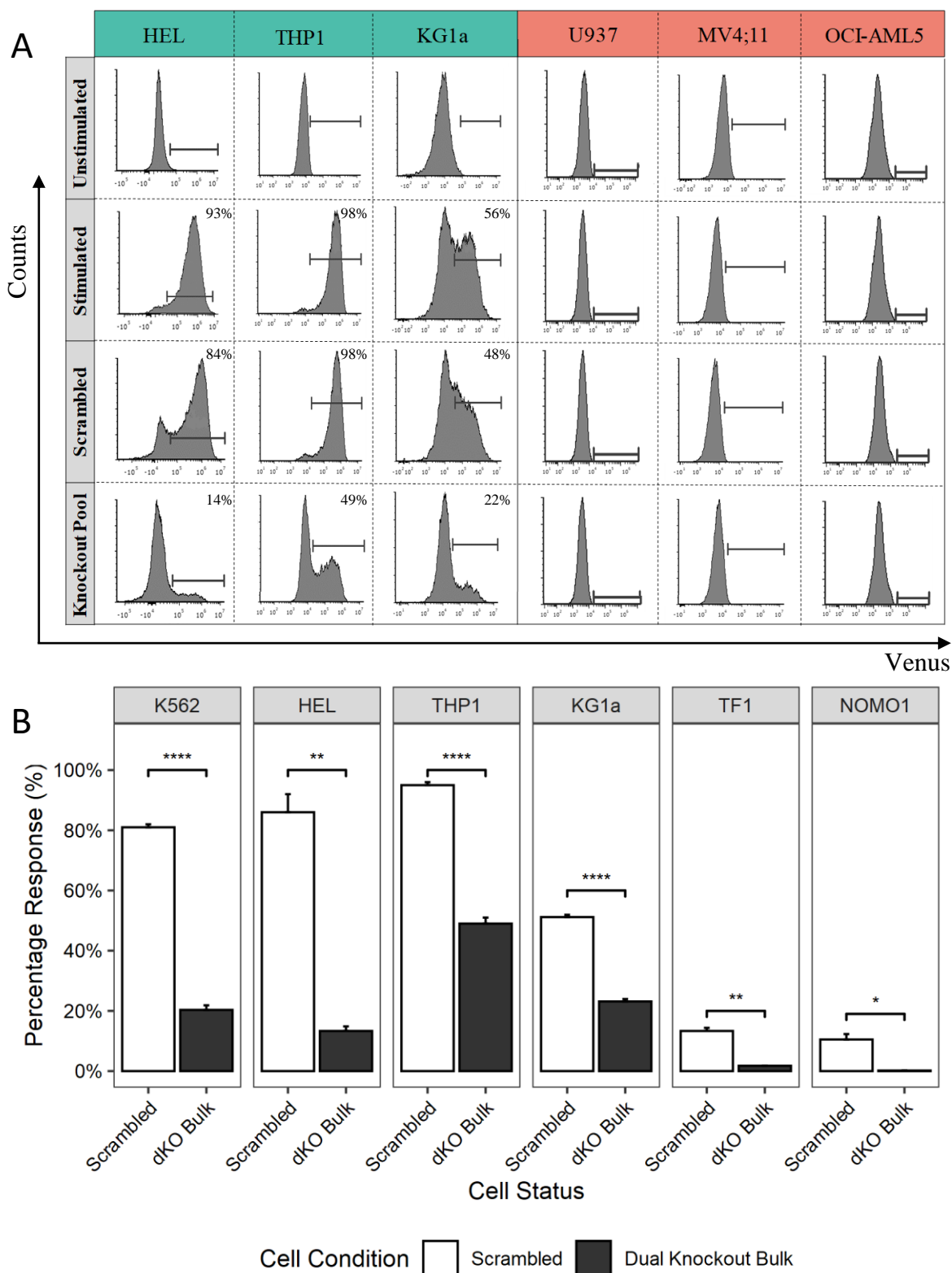


Figure 3-21: Dual-catenin Knockout Significantly Reduces WNT Reporter Activity

A) Representative histograms showing the reduction in WNT reporter activity with dual knockout. **B)** Percentage positive WNT reporter activity (Venus fluorescence) of AML cell lines transduced with control (Scrambled-Puro; 463), or KO β -catenin target gRNA (517-Puro) and γ -catenin target gRNA (519-Neo) lentivirus (2.8, 2.11.5). Non-transduced cells were removed by addition of puromycin and G418 (2.8.2). Cells were treated with 5 μ M CHIR for 24-hours or a vehicle control (0.1% DMSO, v/v) (2.9.1). (n=3; data indicates mean +1SD; t-test. < 0.0001 = ****, 0.0001 to 0.001 = ***, 0.001 to 0.01 = **, 0.01 to 0.05 = *.)

SCR - Scrambled; dKO - Dual Partial Knockout

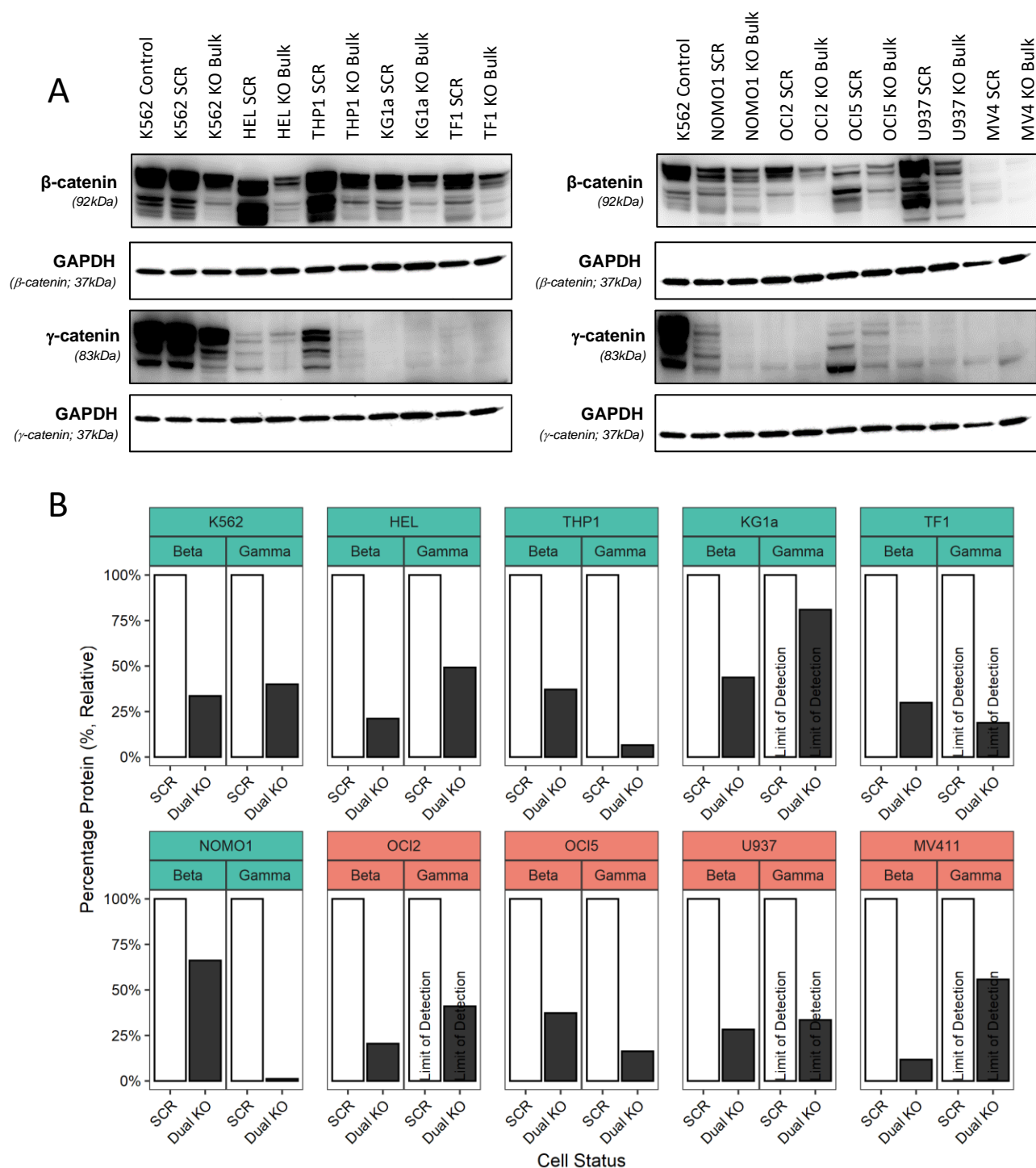


Figure 3-22: Levels of β -catenin and γ -catenin Knockout in Dual gRNA Target Model

A) Western blots demonstrating protein-level states for β -catenin and γ -catenin in AML cell lines following transduction with a CRISPR-Cas9 construct targeting *CTNNB1* and *JUP*, or a scrambled control (2.8, 2.10). Whole lysates were prepared 24 hours after treatment with $5\mu\text{M}$ CHIR to cultures of scrambled and bulk knockout cells (2.9.1). **B)** Protein loading was controlled by analysis of GAPDH, which allowed quantification for β -catenin and γ -catenin (2.10.6, n=1). Bars labelled with limit of detection represent expression levels which required extended exposure to an extent at which background banding was present, indicating potential concerns of reliable quantification.

SCR - Scrambled; dKO - Dual Partial Knockout

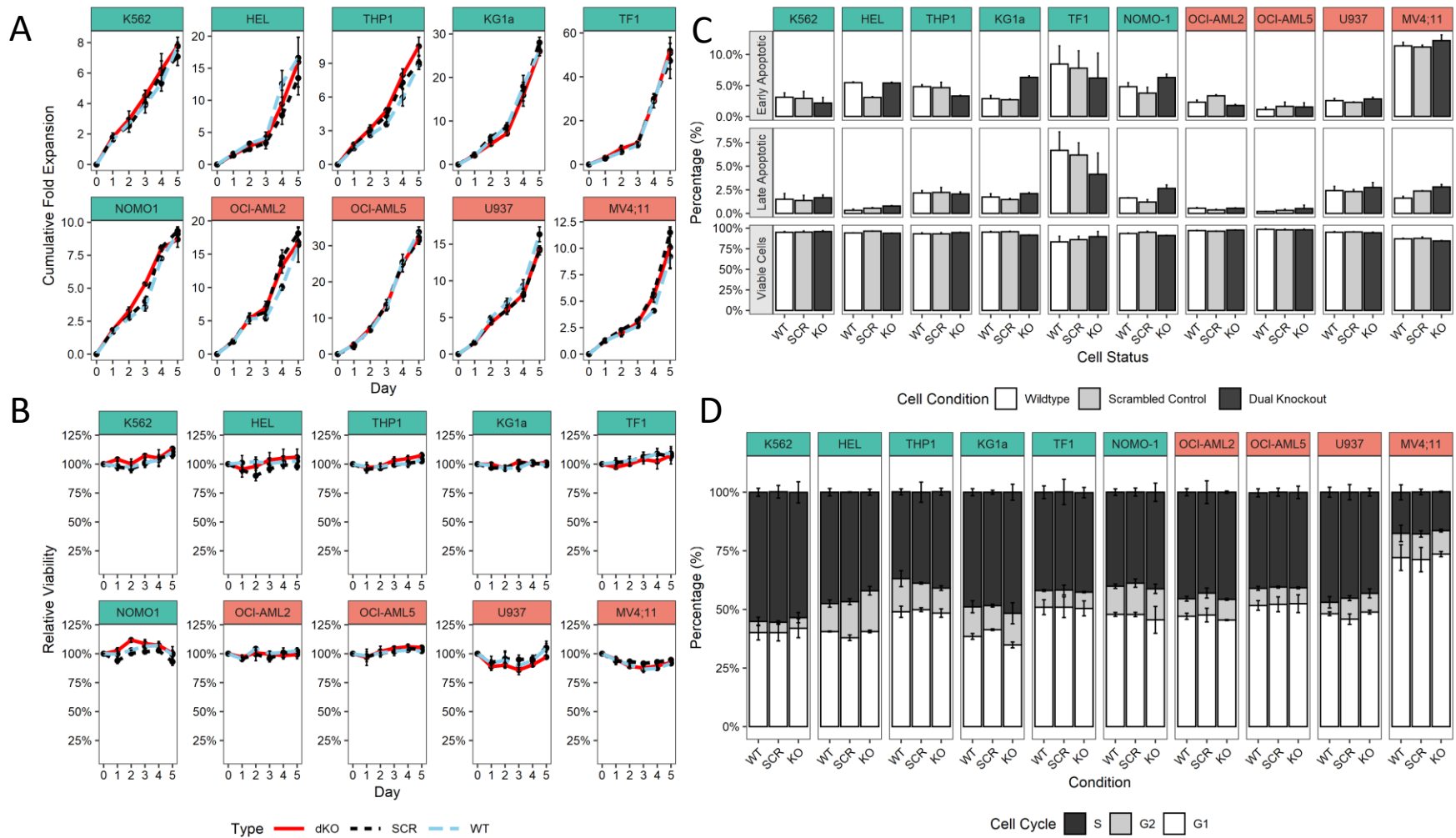


Figure 3-23: Dual Knockout Has No Influence on Proliferation, Apoptosis, and Cell Cycle

A) Proliferation assays were conducted on each line by seeding cells at the lowest bound for log-phase growth and the population was monitored over 5 subsequent days (2.11.7). **B)** Simultaneously, population viability was recorded each day with TOPRO DNA staining (2.11.6). **C)** An apoptotic assay was conducted by isolating 1×10^5 cells from each cell line condition. Populations were stained with Annexin-V and 7-ADD to reveal early and late-stage apoptotic proportions respectively (2.11.9). **D)** DNA content was used to examine cell cycle phase conditions with a propidium iodide-based DNA-content assay (2.11.8). Responders (green) or non-responders (red). (n=3; data indicates mean \pm 1SD). **WT** – Wildtype; **SCR** - Scrambled; **KO** - *CTNNB1* and *JUP* knockout

3.9 Knockout Clones from Responder Lines are Lost During Clonal Expansion

In order to conclusively determine whether knockout of β -catenin and γ -catenin affects AML maintenance, cloning was performed to recover a complete dual knockout clone. This was achieved with limiting dilution cloning (2.4). Efforts to expand clones of β -catenin knockout bulk cultures was achieved in *non-responder* lines without issue, with the same true for γ -catenin knockouts irrespective of responder status. As clonal efficiency was significantly reduced upon knockout of β -catenin, it is suggested that this was incompatible with clonal expansion of the *responder* AML cell lines (3.6.4).

The WNT reporter assay was performed for *responder* AML knockout clones in order to pre-screen incomplete knockout clones, which would retain a WNT responsive profile. A caveat of the WNT reporter construct was the tendency for the activity to become silenced over time. A small proportion of the cells within the bulk cultures of the clonal pBARV lines were not responsive; therefore, false negatives would be expected to the region of 5-20% depending upon the line considered. Following pre-screening, the ratio of responsive clones to non-responsive clones from knockout lines was considered. Knockout clones observed a disproportionate recovery of responder clones. This was particularly observed in the HEL cell line, in which 15% of the bulk knockout population was non-responsive, whilst the few clones recovered were all responsive (**Figure 3-24**). This indicates non-compatibility with cloning for knockouts of β -catenin and a selective pressure for β -catenin⁺ clones.

A total of eight non-responsive THP1 dual knockout clones were identified in the pre-screening process and were expanded to extract DNA. DNA-seq was performed flanking the *CTNNB1* (β -catenin) InDel target site (2.12.3). The spectrogram data for all clones displayed convoluted base calls, as expected, indicating an allele had suffered an InDel CRISPR-Cas9 induced mutation (**Figure 3-25**). However, when the spectrogram was digitally deconvoluted, all clones were revealed to retained at least one functional copy of *CTNNB1* which was confirmed by reverse sequencing. This suggests these non-responsive clones are derived from the small proportion of clonal THP1 pBARV cells which have suffered silencing of the reporter. To validate the DNA-sequencing, stimulated lysates from each non-responder THP1 bulk dual knockout clone were examined. As expected, each clone still showed detectable β -catenin levels, though highly variable, with different presentations than the scrambled control (**Figure 3-25**). These data demonstrate that limiting dilution cloning of β -catenin knockout cells is incompatible with complete knockout *responder* cell lines and a supportive condition would be required. This will be covered in **Chapter 4**.

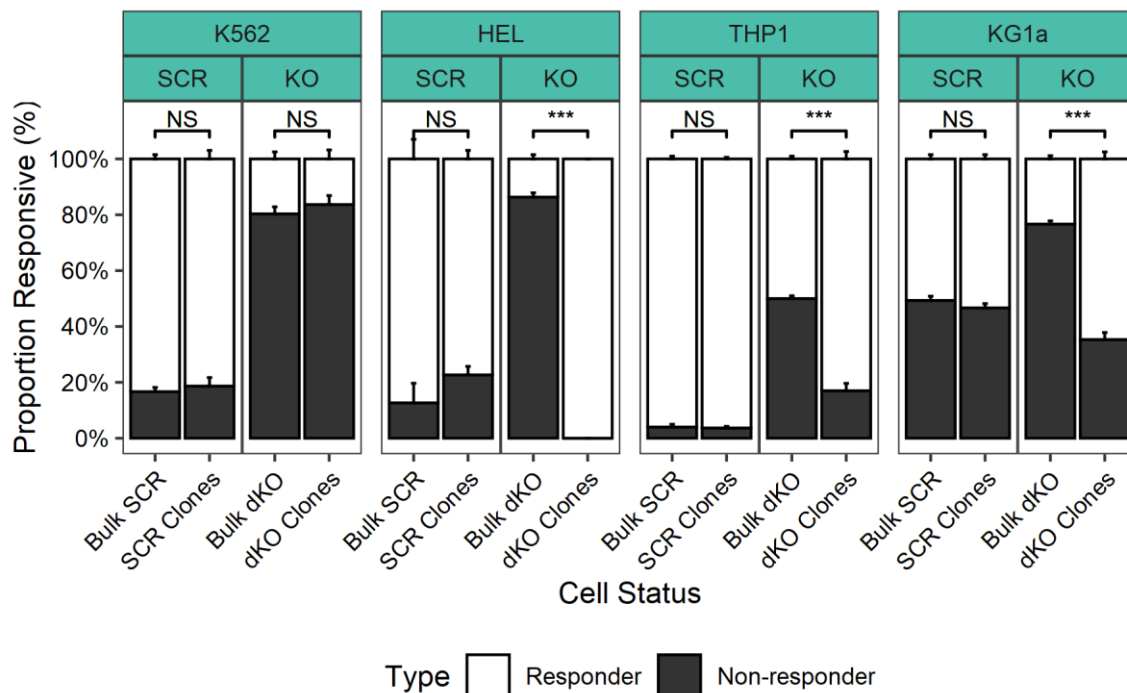


Figure 3-24: Loss of Knockout Clones During Limiting Dilution Cloning

Percentage positive WNT reporter activity (Venus fluorescence) of responder AML cell lines transduced with control or dual β -catenin target gRNA (517-Puro) and γ -catenin target gRNA (519-Neo) lentivirus (2.8, 2.11.5). Cells were treated with 5 μ M CHIR for 24-hours (2.9.1). An unstimulated vehicle control was used to define a threshold of positivity (0.1% DMSO, v/v). Contrasts were drawn between the proportion responsive per the WNT reporter in the bulk population to the proportion of responsive clones after limiting dilution cloning. (n=3; data indicates mean +1SD; t-test. < 0.0001 = ****, 0.0001 to 0.001 = ***, 0.001 to 0.01 = **, 0.01 to 0.05 = *). Unintended selection for responders in the knockout condition suggests knockout responders are lost during cloning.

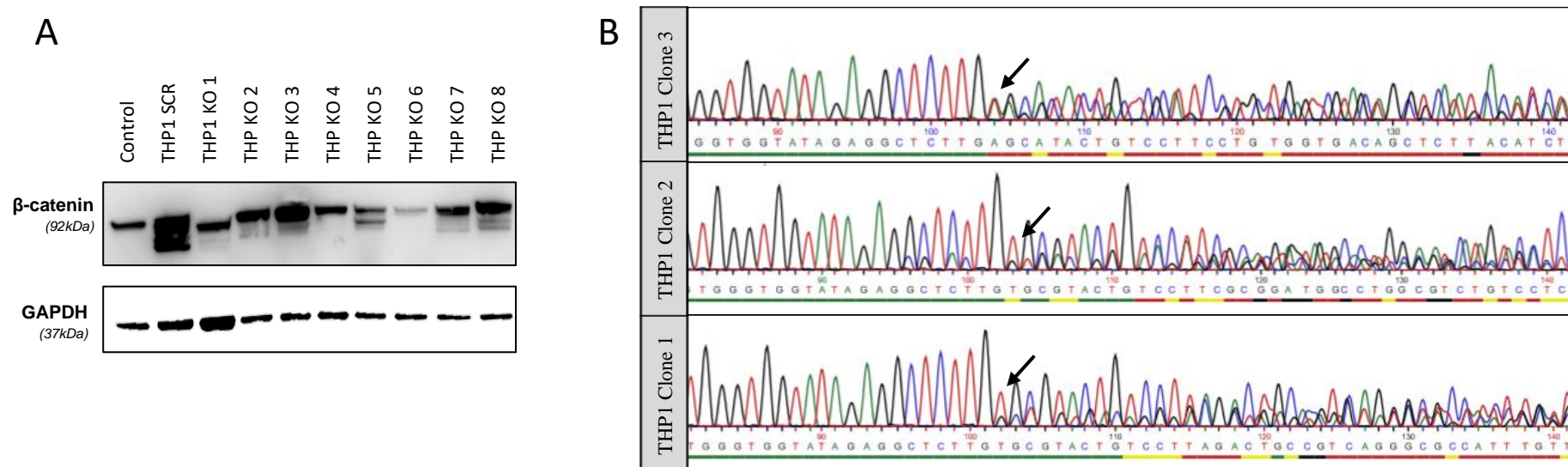


Figure 3-25: THP1 Clones Retained a Functional *CTNNB1* Allele and Protein Expression

A) Western blots demonstrating β -catenin in non-responsive THP1 knockout clones following transduction with a CRISPR-Cas9 construct targeting *CTNNB1* and *JUP*, or a scrambled control (2.8, 2.10). Whole lysates were prepared 24 hours after addition of 5 μ M CHIR to cultures of scrambled and bulk knockout cells (2.9.1). **B)** CRISPR-Cas9-induced mutations were examined by isolating cells from each clonal THP-1 dual knockout culture for DNA-sequencing (2.12.3). Black arrows indicate the InDel mutagenesis site, after which point coherence between spectrogram sequence trace is lost (2.12.3.6). All clones retained at least one functional copy of *CTNNB1*, confirmed by reverse sequencing.

3.10 β -catenin KO in HSPC is Inconsequential for Differentiation and Self-renewal

3.10.1 Generation of *CTNNB1* Knockout in CD34⁺ HSPC

As β -catenin represents an interesting therapeutic target for AML, it was necessary to determine the requirement of this gene for normal haematopoiesis. To address dependency, *CTNNB1* knockout in an *in vitro* model of myeloid development was undertaken. HSPC from normal human umbilical CB were recovered (2.2.1). First, β -catenin was examined by western blot over a time course to determine expression levels during myeloid development (**Figure 3-26**). This demonstrated loss of β -catenin expression by day six, an observation shared for γ -catenin. As the previously applied CRISPR-Cas9 constructs require puromycin selection for 72-hours to achieve a pure population, thus limiting study of the early multipotent stages of haematopoiesis, the original CRISPR-Cas9 construct was substituted with a new plasmid harbouring the same gRNA targeting *CTNNB1*, but with the addition of a GFP selectable marker, to allow for immediate FACS recovery of a GFP⁺ pure population. The new construct was tested in THP1 parental cells with transduction efficiency was above 90% (**Figure 3-27A**). Knockout within the population was approximately 75% (data not shown). When HSPC were transduced with the same batch of lentivirus, transduction efficiency ranged between 10-15% with a lower intensity of fluorescence (**Figure 3-27B**). Within the GFP⁺ FACS population of HSPC, β -catenin expression was reduced by 75% when examined by western blot on day 14 following treatment with 5 μ M CHIR (**Figure 3-28A|B**).

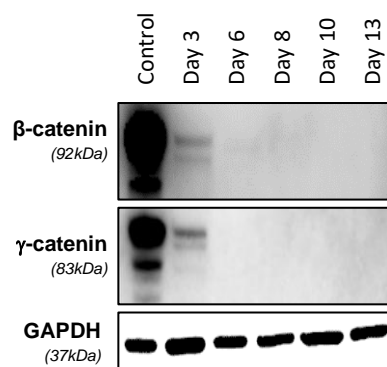


Figure 3-26: β -catenin and γ -catenin Expression Reduces During Haematopoiesis

Western blot analysis showing β -catenin and γ -catenin expression in HSPC over 13 days in culture in IMDM supplemented with IL-3 SCF, G- and GM-CSF ($3S^{LOW}G/GM$) (2.2, 2.10). HSPC and differentiated subsets at later timepoints were recovered on day three, day six, day eight, day ten, and day thirteen for protein lysates. K562 treated with $5\mu M$ CHIR for 24-hours was used as a positive control (2.9.1). GAPDH was used as a loading control (n=1).

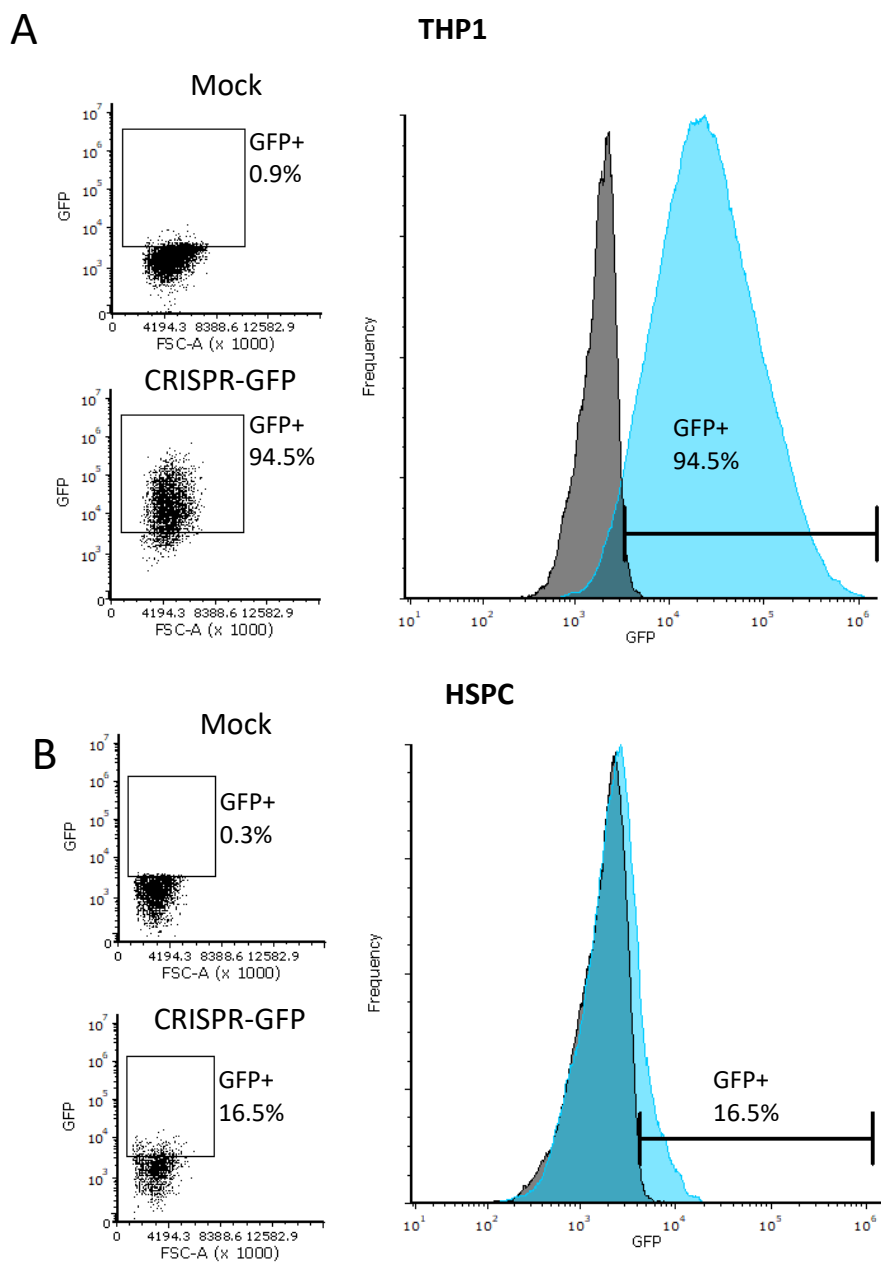


Figure 3-27: Infection Efficiency of CRISPR-Cas9-gRNA-GFP

A) Representative scatter plot and histogram demonstrating the infection efficiency of the CRISPR-Cas9-gRNA-GFP in THP1 parental cell line (2.7.1, 2.11). Top left represents mock, bottom left with lentivirus. Histogram on the right demonstrates the high transduction rate and range of fluorescence characteristics (n=3). **B)** Representative scatter plot and histogram demonstrating the infection efficiency of the CRISPR-Cas9-gRNA-GFP in CD34⁺ HSPC (2.7.3, 2.11). Top left represents mock, bottom left with lentivirus. Histogram on the right demonstrates the low transduction rate and dim fluorescence characteristics observed in HSPC (n=3).

3.10.2 β -catenin Knockout in HSPC Does Not Impact Proliferation or Lineage Development

This study examined the impact of reduced β -catenin expression on cell proliferation and differentiation of human HSPC. Cells were isolated from umbilical CB, transduced with scrambled control and β -catenin knockout CRISPR-Cas9 constructs, sorted for GFP expression, and then cultured in growth conditions such to drive myeloid lineage development (2.2.3). Knockout of β -catenin had no impact on the proliferation or frequency of monocytic, granulocytic and erythroid lineages (**Figure 3-28C**), nor was the expression of developmental markers on these population significantly affected. Together, these data demonstrate that β -catenin knockout has no consequence upon myeloid lineage development and proliferation.

3.10.3 β -catenin Knockout has no Impact on Colony Formation, Apoptosis, and Cell Cycle

As β -catenin had been determined to be involved in cloning efficiency in *responder* AML cell lines (3.6.4), an assessment of colony formation and colony replating (a measure of self-renewal potential) was performed to determine whether similar consequence were observed in HSPC. No impact on colony formation or colony replating was observed (**Figure 3-29**). Neither was there any perturbation of apoptosis or cell cycle distribution or morphology. These data indicate β -catenin is not required for myeloid development of human cells *in vitro*. However, its impact on growth, differentiation and repopulation capacity in a xenograft model would be necessary to fully establish whether β -catenin is redundant for human haematopoiesis.

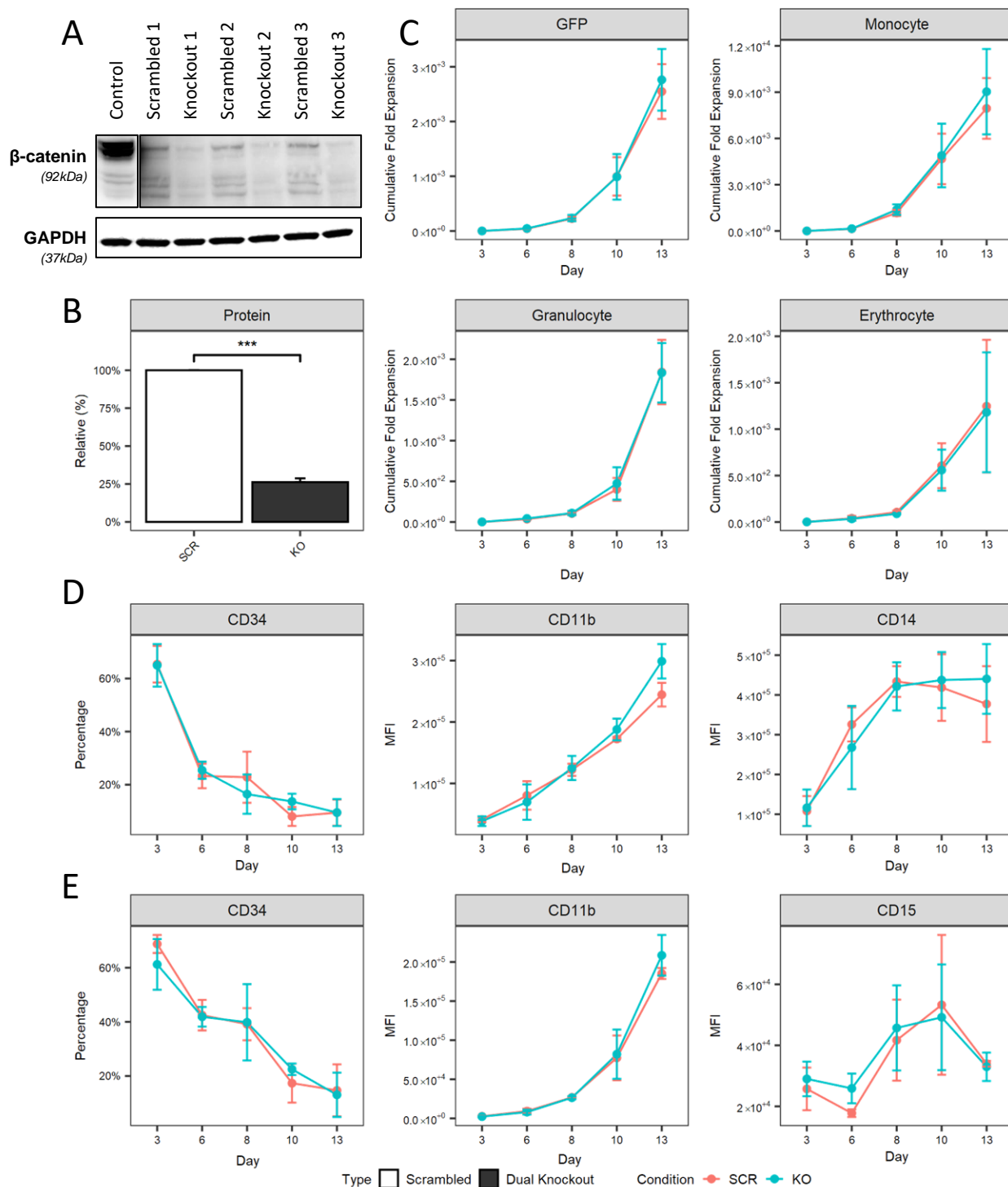


Figure 3-28: β -catenin Knockout Does Not Perturb Lineage Development and Proliferation During Haematopoiesis

A) Western blot analysis showing β -catenin protein expression in myeloid cells transduced with a control scrambled or *CTNNB1*-targeted CRISPR-Cas9-gRNA construct (2.8, 2.10). Lysates were prepared on day 14 of culture following a 24-hour treatment with 5 μ M CHIR (2.9.1). CHIR treated K562 was used as a positive control. GAPDH was used as a loading control. **B**) Bar chart showing densitometry analysis following quantification, normalisation to GAPDH, and relative abundance to scrambled control. **C**) Cumulative fold-expansion of myeloid subsets transduced with scrambled control and knockout cells gated for GFP positive cells in culture medium containing IL-3, SCF, G- and GM-CSF; monocytic cells (CD13⁺ CD36⁺) granulocytic cells (CD13⁺ CD36⁺), and erythroid cells (CD13⁻ CD36⁺). **D**) CD34 expression in monocytic cells over time with associated Mean Fluorescent Intensity (MFI) expression of CD11b and CD14 expression. **E**) CD34 expression in granulocytic cells over time with associated MFI expression of CD11b and CD15 expression (2.11.4). Significant difference between scrambled control and knockout cultures were analysed by t-test with multiple test correction using Benjamini-Hochberg where timepoints were applied (n=3; data indicates mean \pm 1SD).

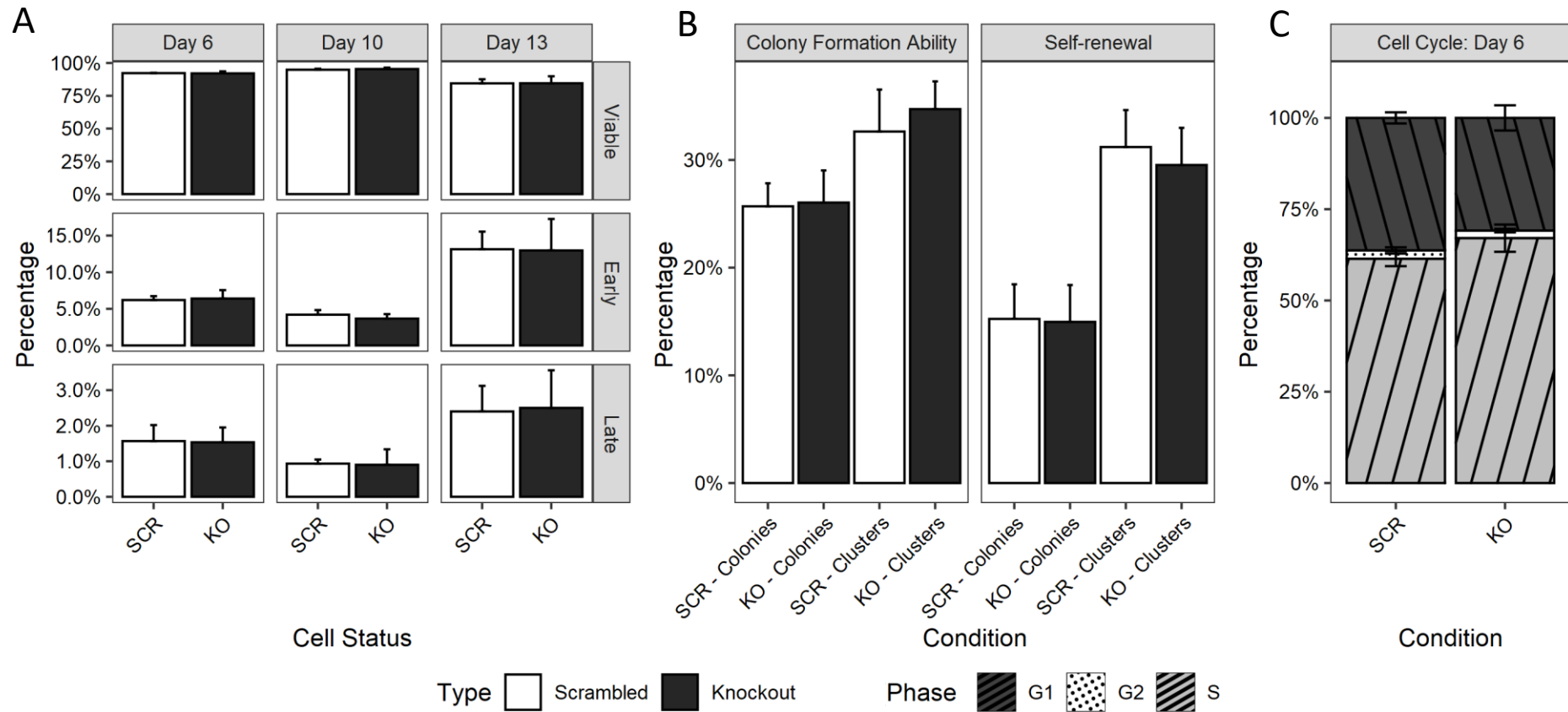


Figure 3-29: β -catenin Knockout Does Not Impact Normal Cell Cycle, Apoptosis, or Self-renewal

A) Summary data showing the effect of β -catenin knockout on apoptosis in HSPC on day six, ten, and thirteen days of culture (2.2). Early apoptotic cells are characterized by Annexin V⁺ / 7-AAD⁻ whilst apoptotic cells are characterised as Annexin V⁺ / 7-AAD⁺ (2.11.9). **B**) Colony forming efficiency of scrambled and β -catenin knockout cultures following limiting dilution assay. After seven days of growth in culture supplemented with IL-3, SCF, G- and GM-CSF colonies (>50 cells) and clusters (<50 cells) were quantified. Self-renewal potential was assessed by recovering colonies after one week and performing a single replating of recovered scrambled and β -catenin knockout cultures in the same conditions as previously stated. These were assessed after a further seven days (2.4). **C**) Stacked bar plot showing cell cycle distribution of CD34⁺ HSPC scrambled and knockout on day six of culture (2.11.8). (n=3; data indicates mean \pm 1SD).

3.11 Discussion

WNT/ β -catenin signalling within the haematopoietic process has been demonstrated to be active in HSPC, but inactivate in early progenitor and differentiated constituent cells, as observed herein, with the latter incapable of self-renewal (1.1.2). Dysregulation of WNT/ β -catenin signalling has been linked with AML initiation and progression (Lane *et al.*, 2011) and has been shown to be essential to LSC survival and self-renewal (Hu *et al.*, 2009; Wang *et al.*, 2010; Dietrich *et al.*, 2014). In fact, LSC and HSC share numerous biological properties, including their self-renewal capacity. The transformation of an HSC into an LSC results from the loss of self-renewal regulation and studies have documented that committed progenitors can regain self-renewal potential by acquiring certain mutations, and form a comparable LSC with partial differentiation capacity (Cozzio *et al.*, 2003; Huntly *et al.*, 2004; Krivtsov *et al.*, 2006; Somerville *et al.*, 2006a). Overexpression of β -catenin is an independent adverse prognostic factor in AML (Ysebaert *et al.*, 2006) and is a frequent observation in patient samples when compared with matched CD34⁺ HSPC (Gandillet *et al.*, 2011a). Critically, β -catenin expression has been documented to be significantly higher in relapsed patients as compared to matched newly diagnosed samples, suggesting a direct mechanism in self-renewal and resurgence of disease (X. Jiang *et al.*, 2018b). This has led to speculations that WNT/ β -catenin is centrally involved in AML onset, progression, and maintenance. However, research has been inconclusive, necessitating further, conclusive work.

Firstly, this study examined the mRNA expression of the central WNT/ β -catenin signalling regulators, alongside *JUP*, both in human haematopoiesis and AML patients. Whilst the expression levels of mRNA are not conclusive indicators of protein levels due to post-translational regulation, they are broadly indicative for most mRNA (Pearson's correlation=0.51), as determined through cross-examination of recently released RNA-seq and mass spectrometry data (Nusinow *et al.*, 2020). However, the correlation between protein β -catenin and mRNA *CTNNB1* was unreliable due to the poor correlation between mRNA and protein (Pearson's 0.27)⁶. As expected, *CTNNB1* mRNA levels remained unchanged throughout haematopoiesis, whilst *JUP* mRNA was found to decrease throughout this process; whilst the former is likely an mRNA:protein discrepancy because of post-translational regulation, the reduction in *JUP* is indicative of a potential contribution to HSC characteristics (3.3.1). These findings were replicated with scRNA-seq data of normal haematopoiesis, which

⁶ Other WNT/ β -catenin signalling genes or target genes had reasonable correlation to protein level (Pearson's – TCF4 - 0.57; GSK3 β - 0.41; LRP6 - 0.54; CCND2 - 0.81; LEF1 - 0.68)

supported these observations (S1.). In AML, as compared to normal karyotype AML or HSC, no biologically meaningful alteration to *CTNNB1* expression levels were observed relative to healthy control. To examine the relationship between mRNA expression and overall or disease-free survival in AML patients, Kaplan-Meier estimates were performed for selected WNT-related genes by stratifying patients according to high and low expression cohorts, though no significance was obtained, suggesting that neither WNT/ β -catenin signalling nor *JUP* convey prognostic indication.

Overall, the public mRNA data supported the observation that the expression of *CTNNB1* is predominantly an HSC feature, which was consistent in *JUP*; however, efforts to align the expression of these genes, alongside other WNT-related genes, with patient characteristics, was unable to capture a consistent consequence to patient survival. The discrepancy could be explained by potential mRNA:protein discrepancies, as β -catenin, which is regulated post-translationally rather than at the transcript level, would be most misrepresented by mRNA-based studies. Further, high levels of β -catenin expression at protein level has been demonstrated to be an unfavourable prognostic indicator in patients at the protein level in which disease severity, treatment resistance, and relapse risk is high (X. Jiang *et al.*, 2018b).

The requirement of β -catenin and the potential participation of γ -catenin in WNT/ β -catenin signalling, alongside the necessity of WNT/ β -catenin signalling for AML maintenance, remains a contentious topic within the literature (Cobas *et al.*, 2004b; Serinsöz *et al.*, 2004; Hu *et al.*, 2009; Wang *et al.*, 2010; Gandillet *et al.*, 2011b). Previous studies claiming β -catenin and γ -catenin are dispensable for haematopoiesis and AML maintenance have mainly relied on murine models, which may not appropriately represent the human condition (Yeung *et al.*, 2010). Studies utilising murine models inherently deviate from the human context; for instance, addition of WNT3a or overexpression of β -catenin resulted in a 100-fold HSPC expansion in this model; yet no comparable effect is documented in human HSPC (Reya *et al.*, 2003; Willert *et al.*, 2003). Alternatively, human research has relied upon incomplete knockdown experiments (Jeannet *et al.*, 2008b; Gandillet *et al.*, 2011a). To overcome this, and conclusively determine the role of β -catenin and γ -catenin in AML, this study applied CRISPR-Cas9; however, this firstly required the characterisation of both catenin members in AML cell lines.

A broad panel of AML cell lines was assessed in this study for WNT/ β -catenin signalling activity by examination of β -catenin expression through western blots, along with a flow cytometry-based WNT reporter. It was not possible to determine basal activation by flow

cytometry; however, basal levels of nuclear β -catenin, a proxy measure of activation, were detected by western blot, though the extended exposure necessary to document this precluded quantification as very low levels were present. Treatment with CHIR stabilised β -catenin, enabling assessment by the WNT reporter and reliable detection by western blot (3.3.3). This further enabled the classification of AML cells into *responder* or *non-responder*, based on nuclear β -catenin translocation ability and WNT reporter activity, a feature not often considered in the literature, which could explain discrepancies between studies (Gandillet *et al.*, 2011a). Of the AML lines considered, 8/13 were shown to be nuclear translocators of β -catenin with associated WNT reporter activity (**Table 3-1**), which is consistent with the heterogeneity documented in patients, 60-65% of which are suggested to exhibit active WNT/ β -catenin signalling (Simon *et al.*, 2005b; Mikesch *et al.*, 2007). CHIR did not stabilise γ -catenin, indicating the mechanism of regulation by GSK3 β is not shared, although reductions in β -catenin with sole γ -catenin knockout suggests some shared processing through alternate mechanism. γ -catenin was detectable in 7/14 cell lines compared to 80% in patients (Morgan *et al.*, 2013).

The extremely low basal levels of β -catenin in AML cell lines are supported by public data, corroborated by recently released data from the CCLE. The Mass Spectrometry Proteome dataset (Nusinow *et al.*, 2020) found levels were within the bottom 10% of all cancer cell lines considered, and were hence below background after normalisation. However, despite the use of a highly sensitive mass spectrometer, proteomic techniques remain incapable of detecting low-abundance proteins without targeting (De Graaf *et al.*, 2011; Gillet *et al.*, 2012; Schmidlin *et al.*, 2016). The CCLE Reverse Phase Protein Array (RPPA) dataset (Ghandi *et al.*, 2019), on the other hand, is more sensitive than mass spectrometry-based approaches. The RPPA dataset found very low β -catenin expression within all AML cell lines. In fact, expression of β -catenin in AML is lower than all other diseases considered, with the exception of non-Hodgkin lymphoma. These observations are in contrast to the CCLE RNA-seq dataset (Barretina *et al.*, 2012), in which *CTNNB1* was found to be abundantly expressed at the mRNA level within all AML cell lines, regardless of classification (considered in S2.). However, as mentioned above, *CTNNB1* is well recognised for its poor correlation between mRNA and protein levels, due to post-translational regulation. These data suggest low expression of β -catenin exists in AML cell lines; a finding also observed in the literature (Morgan *et al.*, 2019). As CHIR was not found to stabilise γ -catenin, this suggests γ -catenin may be expressed when WNT/ β -catenin activity is excessive in an attempt to suppress β -catenin transcriptional activity through

competitive binding of γ -catenin to TCF4, as documented in the literature (Zhurinsky *et al.*, 2000; Miravet *et al.*, 2002; Wickline, Du, Donna B Stolz, *et al.*, 2013). Collectively, the flow-based WNT reporter results agreed with western blotting analysis, which showed an accumulation of β -catenin in the nucleus. However, the KG1 cell line is an exception, though the absence of detectable DsRed expression suggests that promotor silencing had occurred in this engineered line. Indeed, the KG1 subline, KG1a, was responsive in the flow-based reporter assay without WNT reporter silencing issues. The presence of AML cell lines without detectable nuclear β -catenin and γ -catenin indicates that these lines have no requirement of WNT/ β -catenin signalling for maintenance, though the limited sensitivity of western blotting cannot conclusively establish this.

With the AML cell lines classified based upon translocation capability, the public CCLE RNA-seq dataset was applied to contrast the two groups and determine whether a WNT-active profile could be established, and whether the prior observation of γ -catenin expression correlating with responder status via western blot was also seen at the transcriptomic level (discussed in S2.). Notably, *CTNNB1* was abundantly expressed in both *responder* and *non-responder* lines. When specific genes were examined in the *responder* cell lines with respect to *non-responder* cell lines, a significant increase in *JUP*, *LEF1*, *TCF7L2*, *LRP6*, *PTK7*, *FZD6*, *WNT3*, and *WNT5a* expression was documented, alongside the repression of *DACT3* and *DKK4*. *DACT3*, encoding Dishevelled Binding Antagonist of Beta Catenin 3, is an established epigenetic repressor of WNT/ β -catenin signalling with important roles in CRC progression (Jiang *et al.*, 2008). *DKK4*, encoding Dickkopf WNT Signalling Pathway Inhibitor 4 inhibits β -catenin accumulation and self-renewal characteristics in CRC and hepatocellular carcinoma (HCC) (Fatima *et al.*, 2012). Contrarily, *WNT3*, a close homolog of *WNT3a*, is recognised as the driver of WNT/ β -catenin signalling in *APC^{MUT}* CRC (Voloshanenko *et al.*, 2013). *WNT5a* is classically regarded as a prototypical non-canonical WNT ligand; however, *WNT5a* is overexpressed in CRC, and has been demonstrated to drive WNT/ β -catenin signalling via *FZD7*, suggesting context specific roles (Li *et al.*, 2018; Astudillo, 2021). *FZD6* is a recognised WNT ligand receptor for WNT/ β -catenin signalling, though it is classically considered a non-canonical receptor, and was found significantly overexpressed in the *responder* lines, an observation also documented in CRC (Kim *et al.*, 2015). *LRP6*, encoding LDL Receptor Related Protein 6, is the central WNT/ β -catenin co-receptor and has similarly been shown to be frequently overexpressed in CRC and other cancers, in which it is critical to the excessive WNT ligand response observed in cancer associated fibroblasts (Astudillo, 2021; F. Wu *et al.*,

2021; Jeong *et al.*, 2021), and was recently demonstrated to be the only co-receptor required for WNT/ β -catenin signalling through CRISPR-Cas9 knockout in CRC (Chen *et al.*, 2021). *PTK7*, encoding Protein Tyrosine Kinase 7, was classically considered a non-canonical WNT pathway receptor, which repressed canonical WNT signalling (Peradziryi *et al.*, 2011; Hayes *et al.*, 2013); however, recent evidence has demonstrated *PTK7* increases the WNT/ β -catenin signalling response to WNT3a, and this amplification is reliant upon the co-receptor LRP6 (Puppo *et al.*, 2011). *PTK7* is overexpressed in CRC and conveys a poor prognostic indication (Tian *et al.*, 2016), and was proposed to act as a mechanistic switch by upregulating LRP6 to alternate between canonical and non-canonical WNT signalling (Bin-Nun *et al.*, 2014). A recent study has also reported *PTK7* can bind β -catenin directly to enhance WNT/ β -catenin target gene expression, with small molecule inhibitors blocking the association of these two members capable of reducing WNT/ β -catenin activity and proliferation in CRC (Ganier *et al.*, 2021). The overexpression of *LEF1* supports recent research suggesting *LEF1* is a mediator of β -catenin translocation (Morgan *et al.*, 2019), whilst the overexpression of *JUP* supports further investigation of γ -catenin for contributory or redundancy roles, or suppressive roles. Taken together, these results indicate that WNT/ β -catenin signalling is active at low levels within *responder* cells with increased levels of core WNT signalling members that could facilitate a primed state from which further extrinsic activation would enable a substantially stronger response.

To conclusively determine whether β -catenin and γ -catenin are involved in AML (e.g., for maintenance or drug resistance) CRISPR-Cas9 was applied to AML cell lines. To achieve this, selection of gRNA was first required; however, this remains an area of intense development and optimisation within the field (Wilson *et al.*, 2018; Liu *et al.*, 2020; G. Zhang *et al.*, 2021). Whilst application of early generation gRNA would achieve <5% knockout efficiencies, thus requiring the assessment of hundreds of clones (Friedland *et al.*, 2013; Waaijers *et al.*, 2013; Kim *et al.*, 2014), this has been optimised to 10-60% in a single-guide approach, with an average of 34% efficiency (Dang *et al.*, 2015; Farboud *et al.*, 2015). Whilst multi-guide approaches have become commonplace in recent years, enabling average editing efficiencies >75% (Joberty *et al.*, 2020), a single-guide approach was applied due to the need to target two different genes, which limited the expected knockout efficiency.

In K562, a CML cell line, CRISPR-Cas9 was able to successfully generate InDel events within three days of transduction, as deduced by detectable reductions in the flow-based reporter assay, and through genetic cleavage assessment (3.4). The knockout achieved was

greater than 50%, indicating haplosufficiency, and the readout by both the western blot and WNT reporter assay measures was consistent over three weeks, indicating no proliferative alterations as a consequence of knockout. If both copies of a gene are being actively transcribed to produce minimal protein levels required for survival, hemizyosity will be incompatible with survival, as cells are unable to produce sufficient protein and are deemed haploinsufficient (Delaney *et al.*, 2017; Song *et al.*, 2017). MDS, which can be a precursor to AML, is associated with 5q- or 7q- hemizyosity, leading to gene dosage leukaemia (Ebert, 2009, 2011; J. C. Wong *et al.*, 2015; Sperling *et al.*, 2017). Cells are haplosufficient if survival occurs with reduced protein, or through increased production of protein when hemizygous. Cells without a transcriptionally active second allele are inherently haplosufficient. Having selected an optimal guide for each gene, these were applied in AML cell lines singly and in combination.

In AML cell lines, CRISPR-Cas9 reduced β -catenin levels by 20-80%, whilst γ -catenin was reduced by 20-90% (3.6, 3.7, 3.8). The discrepancy between cell lines can be explained by differences in DNA accessibility due to condensed regions, inherent variations in DNA error repair pathways, which are often perturbed in cancer cells, or as a result of copy number variations due to aneuploidy. Indeed, the random nature of InDel incorporation, with an average of 81% of InDels causing a frameshift mutation (Chakrabarti *et al.*, 2019), also complicates frameshift mutation generation. Curiously, β -catenin levels were reduced by γ -catenin knockout, even within cell lines with very low levels of γ -catenin expression. It is not likely that the gRNA targeting *JUP* is targeting *CTNNB1* despite the shared homology, as the specific target sequence differs enough to preclude an unintended pan-catenin effect. Rather, these results suggest that γ -catenin either directly stabilises accumulated β -catenin or, alternatively, elevated proteasomal clearance of β -catenin is a result of increased availability of the destruction complex as an indirect consequence of reduced γ -catenin levels, as suggested in the literature (Morgan *et al.*, 2013). The former is perhaps more likely, as CHIR inhibition did not stabilise γ -catenin levels, suggesting the destruction complex does not act comparably upon γ -catenin as β -catenin.

Through examination of proliferation, viability, apoptosis, and DNA content within the bulk knockout culture condition, no effect of β -catenin or γ -catenin knockout was documented, even in the combined knockout cultures (3.6, 3.7, 3.8). A significant feature, however, was the reduction in clonogenicity of *responder* AML cell lines with β -catenin knockout at a bulk level (3.9). The proportion of knockout was approximately comparable to the reduction in β -catenin at the protein level which, alongside the recovery of only clones with incomplete knockout,

indicated that β -catenin knockout was incompatible with clonal expansion. Inhibition of WNT/ β -catenin signalling has been reported to reduce clonogenicity in the literature *in vitro* (Wang *et al.*, 2010; Gandillet *et al.*, 2011a; Pepe *et al.*, 2022), supporting these observations. No alteration to clonal efficiency was observed with bulk γ -catenin knockout conditions for any AML cell line, suggesting γ -catenin is not required for this process.

The consequence of β -catenin knockdown in the literature is an area of active debate. Several studies in cell lines, primary tissue, and murine MLL leukaemic models found no alteration to phenotype with β -catenin knockdown, even when reduced by >95% (Kim *et al.*, 2002; Cobas *et al.*, 2004b; Yeung *et al.*, 2010). Conversely, drug inhibition and knockdown studies of β -catenin in cell lines or primary samples have been documented to induce G1 cell cycle arrest, heighten apoptosis, and lead to reduced proliferation and viability, even with only 50% reduction in protein levels of β -catenin (Siapati *et al.*, 2008; Gandillet *et al.*, 2011a; Saenz *et al.*, 2019).

Here, I found no observable anti-proliferative, apoptosis inducing, or cell cycle perturbation; however, there is concordance with studies which have documented alterations to clonogenicity. Gandillet *et al.* reported reductions in cloning efficiency through an short hairpin RNA (shRNA) knockdown study in HL60 cells, a *responder* cell line, with little other effect, in concordance with the observations within this study (Gandillet *et al.*, 2011a). However, Siapati *et al.* applied shRNA to knockdown β -catenin levels by 40% in U937 cells, a *non-responder* line, and noted minor reductions in proliferation, without change to TCF4 or LEF1 levels, suggesting an off-target effect (Siapati *et al.*, 2008). An explanation for the discrepancies observed in β -catenin knockdown response has been proposed to be due to variant reductions in the remaining protein levels between studies. However, numerous studies have obtained a high degree of knockdown without observing any resulting anti-proliferative, apoptosis inducing, or cell cycle perturbing effect in murine models, cell lines, and primary tissue indicating the observed effects are more likely off-target effects. Studies have demonstrated that CRISPR-Cas9 has negligible off-target activity, whilst RNA inhibition methods have frequent off-target effects, something underappreciated in the literature (Smith *et al.*, 2017; Subramanian *et al.*, 2017). Further to this, the use of unsuitable models, either through study of WNT/ β -catenin signalling in *non-responder* cell lines, *non-responder* primary samples, or murine models, has further complicated interpretation.

DEPMAP, a repository of loss-of-function data, determined CRISPR as the gold standard for studies over misinformative RNA inhibition data, and has developed future builds with CRISPR technology exclusively (Subramanian *et al.*, 2017). The finding of non-dependency observed in this study is in-line with this public data (S3.). CRISPR-Seq was recently developed and has enabled mass screening of gene dependency. As CRISPR-Seq represents a marrying of scRNA-seq and CRISPR-Cas9 genetic manipulation, it was simultaneously published by distinct groups. The recently published DEPMAP database of pooled single-cell CRISPR-Seq data in cancer cell lines from the Achilles, Sanger and GeCKO projects (Dempster *et al.*, 2019) were examined to determine the predicted necessity of β -catenin and γ -catenin for AML maintenance, with no resulting consequence observed (**Figure S-6-6**). As a benchmark reference, CRC, which is well recognised for being a WNT/ β -catenin signalling driven cancer (Morin *et al.*, 1997; Emons *et al.*, 2017), was demonstrated to have dependency upon β -catenin, with a small proportion of the cell lines also showing dependency for γ -catenin. However, it was observed that β -catenin and γ -catenin are unnecessary for AML maintenance in any cell line, which is supported by smaller scale, independent CRISPR-Seq screens, as mentioned above (Wang *et al.*, 2014; Tzelepis *et al.*, 2016; Meyers *et al.*, 2017; T. Wang *et al.*, 2017; Behan *et al.*, 2019; Chen *et al.*, 2019; Nechiporuk *et al.*, 2019; Sharon *et al.*, 2019; X. Wu *et al.*, 2020). Ultimately, however, it is not possible to definitively conclude that knockout is incompatible with clonogenicity without attempting to clone these cells to generate either a validated knockout clone, or through the inability to recover such a clone. Even in the case of substantial knockout, it is possible that residual WT cells are capable of producing factors necessary to sustain the population in paracrine fashion. Reductions in clonogenicity with knockout of β -catenin are indicative of an inability to survive clonal stresses and this would necessitate the use of a different approach, or a supportive environment. Recent developments in CRISPR-Cas9 technology have enabled the study of knockout lethal genes through conditional expression systems known as knockout-rescue CRISPR (B. Wang *et al.*, 2019). These allow for complete deletion of endogenous alleles by rescuing cells with a conditionally controlled copy of the gene. The provided gene contains synonymous mutations of the DNA sequence within the gRNA target site such that it enables evasion of CRISPR-Cas9 mediated knockout, whilst producing the same resulting amino acid sequence. The system relies upon a tetracycline-regulated inducible gene promoter system. Unfortunately, the system is not capable of completely terminating transcription and mRNA levels remain detectable to the region of 2-5% after tetracycline treatment (B. Wang *et al.*, 2019). For this reason alone,

the system is unsuitable for use within this research. Instead, it was necessary to examine supportive conditions, as described in **Chapter 4**.

As knockout of β -catenin, but not γ -catenin, was shown to influence clonogenicity in AML cell lines, I determined whether β -catenin was integral in an *in vitro* myeloid development and HSPC self-renewal by colony replating. Firstly, assessment of expression through an *in vitro* model of myeloid development was performed, which revealed detection of β -catenin solely at day three, at which point most of the population consists of undifferentiated HSPC. After this, with differentiation into the several lineages, there was no detectable expression (3.10). These findings are consistent with the literature. CRISPR-Cas9 knockout in CD34⁺ HSPC and subsequent sorting of the GFP⁺ population enabled the analysis of proliferation, lineage development, apoptosis, cell cycle, colony formation ability, and, critically, self-renewal capacity by colony replating. As expected, no impact was found as a consequence of β -catenin knockout, which is consistent with the consensus reached in the literature (X. Zhao *et al.*, 2020; Pepe *et al.*, 2022). These data indicate that β -catenin is not required for the myeloid development of human cells *in vitro*, though it is acknowledged that these data were generated as an incomplete knockout model. However, generation of a complete knockout clone is not possible with these methods. To better assess the impact on growth, differentiation, and repopulation capacity, a xenograft model would be necessary to fully establish whether β -catenin is redundant for human haematopoiesis. This would also benefit from the application of a tandem multi-gRNA CRISPR-Cas9 platform, although size limitations would make the generation of an all-in-one vector difficult and multiple vectors would likely be required.

Collectively, these results demonstrate that β -catenin could be a valid therapeutic target as no evidence was found that indicates β -catenin is required for HSPC function. Recent *cre-lox* knockout *in vivo* murine models support this finding (X. Zhao *et al.*, 2020), alongside *in vitro* models (Pepe *et al.*, 2022), although further investigation into a complete knockout clone would be required to fully appreciate the effect on AML cells, as explored in **Chapter 4**.

Chapter 4

Functional Consequences of Catenin Knockout

4.1 Introduction

4.1.1 Canonical WNT/ β -catenin Signalling in AML

WNT/ β -catenin signalling is an integral pathway for normal developmental processes and has been implicated in human haematopoiesis, leukaemogenesis, and AML maintenance (Richter *et al.*, 2017). WNT/ β -catenin signalling in AML is documented to be perturbed at all stages of signal transduction: from receptors, ligands, transducers, catenin stabilisation, to nuclear translocation (Cate *et al.*, 2009; Kim *et al.*, 2011; Ghosh *et al.*, 2019; Gruszka *et al.*, 2019). In fact, 50-70% of AML patients have elevated WNT signalling (Simon *et al.*, 2005a). Evidence has suggested adult human HSC do not show absolute dependency on WNT signalling for self-renewal or differentiation, rendering the pathway an attractive target (Wang *et al.*, 2010; X. Zhao *et al.*, 2020; Pepe *et al.*, 2022). Consistent with these findings, previous research has demonstrated WNT/ β -catenin signalling was dispensable in an *in vitro* model of haematopoiesis and self-renewal (3.10), whilst also delimiting AML cell lines into *responder* and *non-responder* groups (3.3.4), with the former demonstrating potential dependency on WNT/ β -catenin signalling for clonogenicity (3.6.4).

Existing *in vivo* studies have either relied on incomplete gene inactivation methods, represent a rare subset of AML, or are less pertinent to the human condition due to the murine setting, resulting in conflicting results (Günschmann *et al.*, 2014; Song *et al.*, 2018). *In vivo* murine studies have concluded that substantial knockdown or knockout of β -catenin does not affect haematopoiesis or AML maintenance, even in cases with 95% reduction of total β -catenin protein (Cobas *et al.*, 2004a; Koch *et al.*, 2008a; X. Zhao *et al.*, 2020; Pepe *et al.*, 2022). However, others have documented apoptosis in a dose dependent behaviour (Lento *et al.*, 2014). Several *in vivo* murine studies document that loss of β -catenin is detrimental for, or possibly incompatible with, LSC self-renewal (Wang *et al.*, 2010; Yeung *et al.*, 2010; Lane *et al.*, 2011; Fiskus *et al.*, 2015; S. Ma *et al.*, 2015). Recently, a murine *in vivo* study showed LSC self-renewal, AML onset, and AML maintenance despite β -catenin, γ -catenin, and TCF/LEF family depletion (X. Zhao *et al.*, 2020).

Current *in vitro* studies have applied incomplete RNA silencing methods or pharmacological inhibitors and present conflicting results. Promising research on BC2059, a small molecule anthraquinone oxime-analog, promoted β -catenin degradation and induced anti-proliferative and apoptotic-inducing effects in AML cell lines and primary AML samples (Fiskus *et al.*, 2015). Targeting of β -catenin with PRI-724, an inhibitor of β -catenin and CBP

interaction, had a mild anti-proliferative and pro-apoptotic effect on some AML cell lines, with no effect observed in several lines; however, primary AML samples were highly sensitive to PRI-724 with significant apoptosis and growth inhibition observed (X. Jiang *et al.*, 2018b). Critically, no impact was observed for normal BM CD34⁺ cells. Treatment of primary AML samples *in vitro* with iCRT3, a small molecule inhibitor of β -catenin and TCF family interaction, significantly reduced proliferation, however, a significant expansion of the CD34⁺ pool was also observed (Griffiths *et al.*, 2015). Application of RNA silencing methods have also revealed discrepant results. In an shRNA knockdown experiment, HL60 was found to incur anti-proliferative and pro-apoptotic effects, whilst also reducing leukaemogenic potential assessed by *in vivo* implantation; yet, in primary AML samples, no effect was observed (Gandillet *et al.*, 2011b). Exploring WNT/ β -catenin signalling and γ -catenin in a broad range of human AML cell line models and patient-derived primary AML models will prove more informative in this regard.

Concerns of incomplete protein removal or functional inhibition limits interpretation; therefore, to conclusively determine role of β -catenin, alongside the close homolog γ -catenin, both genes need to be deleted. No published or pre-print publications have accomplished this to date. This study will achieve this by using CRISPR-Cas9 to derive complete knockout clones, i.e. deletion in all alleles, which is the subject of this chapter.

4.1.2 Deductions from Chapter 3

WNT/ β -catenin signalling activity is reliant upon subcellular translocation of cytosolically accumulated β -catenin into the nucleus. Previously, all AML cell lines were documented to accumulate β -catenin in the cytoplasm when treated with the GSK3 β inhibitor CHIR, but only two-thirds of cell lines presented detectable nuclear β -catenin following treatment. Cell lines which were capable of nuclear β -catenin translocation were termed *responders*, whilst cell lines which could not translocate β -catenin were termed *non-responders* (3.3.3). A panel of *responders* and *non-responders*' cells were selected to undergo β -catenin (*CTNNB1*) and γ -catenin (*JUP*) knockout through the use of CRISPR-Cas9 (3.5). The final responder panel comprised HEL, THP1, KG1a, TF1, and NOMO1 cells, alongside the non-responders OCI-AML2, OCI-AML5, U937, and MV4;11. Limiting dilution was applied to generate a complete knockout clone; however, attempts to clone the *responder* cell lines failed, whilst *non-responders* cloned without issue, suggesting a WNT-dependency for clonal growth in responder lines only (3.6). Further efforts were therefore necessary to generate a complete

knockout clone to determine whether WNT/ β -catenin signalling is critical to AML maintenance.

In addition to roles in AML maintenance, recent publications have linked chemoresistance to active WNT/ β -catenin signalling in the case of DNR (Xiao *et al.*, 2020), Ara-C (L. Chen *et al.*, 2020), and other chemotherapeutic agents (Wang *et al.*, 2018; Perry *et al.*, 2020). In addition, high expression of γ -catenin is associated with poor patient prognosis, with knockdown of γ -catenin demonstrated to sensitise AML cell lines to Ara-C (Qian *et al.*, 2020). LRP6, previously established to be overexpressed in *responder* AML cell lines (S2.), has been targeted with Niclosamide, which increased drug sensitivity *in vitro* and synergistically enhanced Ara-C efficacy *in vivo* (Kamga *et al.*, 2020). Silencing of WNT/ β -catenin signalling could therefore sensitise cells to chemotherapeutic agents, thus representing an attractive synergistic agent particularly for multi-drug resistant AML cells which frequently presents at relapse.

4.2 Aims

The aim of this chapter is to generate complete knockout cell lines for subsequent analysis. This will reveal whether WNT/ β -catenin signalling represents a viable target in AML. This will be achieved through the following objectives:

Objective 1: Rescue of clonal growth for dual β - and γ -catenin knockout *responder* AML cell lines through development of a supportive condition.

Generation of a complete knockout clone will require the application of a supportive system to rescue *responder* AML cell lines during the limiting dilution cloning process. A series of single-cell and co-culture conditions will be applied to further provide insight into the mechanism by which cells are incapable of clonal growth.

Objective 2: Investigate the consequence to AML characteristics as a result of complete knockout of β -catenin, γ -catenin, and combined knockout of β -catenin and γ -catenin in clonal *responder* and *non-responder* cell lines.

Complete knockout clones will be assessed with a panel of assays designed to evaluate the consequences upon proliferation, cell cycle, apoptosis, morphology, and differentiation.

Objective 3: Determine whether the catenin knockout conditions derived above affect the sensitivity of AML cell lines to standard chemotherapeutic agents.

Complete knockout clones will be assessed with the standard chemotherapeutics DNR and Ara-C applied in the clinical setting to evaluate whether knockout sensitises cells to therapy.

Objective 4: Validate the findings in patient-derived primary AML samples with CRISPR-Cas9 knockout of β -catenin and alternatively with β -catenin-targeting small molecule inhibitors.

To better represent the clinical condition, patient-derived primary AML samples will be characterised for WNT/ β -catenin signalling activity. β -catenin⁺ and β -catenin⁻ (equivalent to *responder* and *non-responder*) primary AML samples then be subjected to CRISPR-Cas9 knockout and small molecule inhibitors, to determine their dependency on β -catenin signalling.

4.3 Results

4.3.1 Generating Complete Knockout Clones

4.3.1.1 Supportive Media Did Not Improve Clonal Recovery for Responder AML Cells

As determined in the previous results chapter, bulk β -catenin knockout was found to significantly reduce clonogenicity in *responder* AML cell lines only (3.6.4). Furthermore, it was only possible to recover incomplete β -catenin knockout cells by limiting dilution (3.9). Therefore, it was hypothesised that a supportive condition could rescue these cells. Several strategies were employed to rescue the growth of knockout clones from the *responder* AML cell lines, HEL and THP1, which included cytokines, conditioned media from parental cultures, with and without WNT stimulation (2.4). No improvement to clonal efficiency was noted above background recovery of incomplete knockout cells, suggesting single-cell conditions are incompatible with clonal growth, regardless of supportive media conditions (**Figure 4-1**).

4.3.1.2 Co-culture Conditions Rescue Knockout Responder AML Clonal Growth

Within the *in vivo* context, stromal components provide cells with cytokine WNT factors, which are reported to be short-range and labile (Tamai *et al.*, 2004; Boutros *et al.*, 2016; Farin *et al.*, 2016; Seth *et al.*, 2016). Stromal components would also provide cell-cell adhesion properties. In the prior supportive media context (4.3.1.1), short-range, labile WNT factors could be depleted before rescue occurs, and no cell-cell contact was afforded in initial clonal monoculture. To determine whether a stromal microenvironment could rescue clonal growth of β -catenin knockout cells (HEL and THP1), these were bulk co-cultured with MS-5 murine stromal cells (2.4). However, when knockout clones were co-cultured with these cells, there clonal efficiency was actually impaired (**Figure 4-2**). A human-derived stromal line, HS-5, on the other hand, was able to recover knockout cells, demonstrating successful rescue of complete β -catenin knockout clones. Alternatively, high efficiency rescue of clonal growth was achieved through co-culture with matched parental cells to levels comparable to scrambled controls (**Figure 4-2**). This indicates that while β -catenin knockout is incompatible with growth in the single-cell condition, knockout clones can be rescued by co-culture.

It was necessary to determine whether the rescue of the clonal growth of knockout cells through parental co-culture or with HS-5 was due to provided factors which are perhaps a result of active WNT/ β -catenin signalling or, alternatively, if this was due to cell-cell contact. To examine this, scrambled and dual knockout HEL and THP1 cells were co-cultured with clonal U937 scrambled and dual knockout cells, which have no WNT/ β -catenin signalling activity regardless of knockout status (4.3.3). U937 cells were selected over MV4;11, as HEL, THP1, and U937 share the same culture medium, circumventing concerns of medium-based growth problems. After a period of 10 days, wells were combined and analysed for DsRed fluorescence, as U937 and HEL expressed distinct DsRed intensities, thus enabling a clear separating of cell populations (**Figure 4-3A**). U937 cells were able to successfully rescue HEL knockout cells at levels comparable to previous successful rescue attempts, indicating the rescue was due to cell-to-cell contact rather than the presence of a WNT-derived factor (**Figure 4-3B**)

4.3.2 Generation and Isolation of Putative Knockout Clones

While co-culture conditions were successful in increasing clonal recovery, it was necessary to validate a complete dual knockout clone for further study. As previously mentioned, *non-responder* clones did not require co-culture, as no reduction in clonal efficiency was noted, as was also the case for all γ -catenin knockout lines (3.7.3).

For the generation of β -catenin and dual knockout clones in *responder* AML cell lines, co-culture conditions with matched parental cells were required. As an initial screen to identify complete β -catenin knockout clones from the *responder* AML lines HEL and THP1, WNT reporter-negative clones grown within a supportive co-culture with parental matched cells were identified (**Figure 4-4**). Scrambled clones were generated in the same manner for control purposes. Scrambled and knockout clones expressed DsRed constitutively (through the WNT pBARV reporter construct) enabling these cells to be differentiated from supporting parental cells by FACS (**Figure 4-5**). A total of 288 co-culture wells were screened for scrambled and an equal number of dual knockout clones within each cell line and condition, with every third culture expected to contain a knockout clone, resulting in a hypothetical maximum of 96 possible putative knockout clones. This was limited by the clonogenicity characteristics of each cell line. A maximum of ten reporter-negative clones underwent FACS *per* line with matched scrambled clones. The putative knockout clones were subsequently able to proliferate without the support of parental cells. Next, these clones were screened for β -catenin and γ -catenin

expression using western blot (**Figure 4-6**). These data showed successful isolation of β -catenin and dual knockout clones in responder AML cell lines. For THP1, 5/9 clones demonstrated no β -catenin, 7/9 demonstrated no γ -catenin, and 4/9 presented with loss of both catenins. In HEL, 2/3 clones demonstrated no β -catenin, 2/3 demonstrated no γ -catenin, and only 1/3 presented with absence of both catenins of three total clones.

For the generation of single γ -catenin knockout, single β -catenin knockout in *non-responder* AML lines, and dual knockouts in K562, co-culture conditions with matched parental cells were not required and clones were recovered by limiting dilution. The WNT reporter pre-screen was not possible in *non-responder* lines as these have no WNT response. Rather, the putative knockout clones were screened for β -catenin and γ -catenin expression using western blot (**Figure 4-7**). These data showed successful isolation of β -catenin, γ -catenin, and dual knockout clones. In K562, 5/12 clones had β -catenin knockout, 6/12 had γ -catenin knockout, and 2/12 had knockout of both catenins. In U937, 7/15 had β -catenin knockout, whilst γ -catenin was not reliably detectable above diffuse banding. In MV4;11, 11/14 had β -catenin knockout, whilst γ -catenin was similarly not reliably detectable above diffuse banding.

4.3.3 Sequence Validation of Complete Knockout AML Responder Clones

For the clones which showed absence of either/both catenins by western blot, a final validation was carried out at the DNA-level by examining the DNA sequence flanking the gRNA target site. DNA was isolated from every clone, before PCR amplification of the gRNA target sites, and subsequent high-read DNA-seq was performed. This revealed successful generation and isolation of β -catenin (**Table 4-1**) and γ -catenin (**Table 4-2**) knockout clones. With the exception of cases in which γ -catenin could not be reliably detected (U937, MV4;11), all lines with absent protein demonstrated complete allelic knockout.

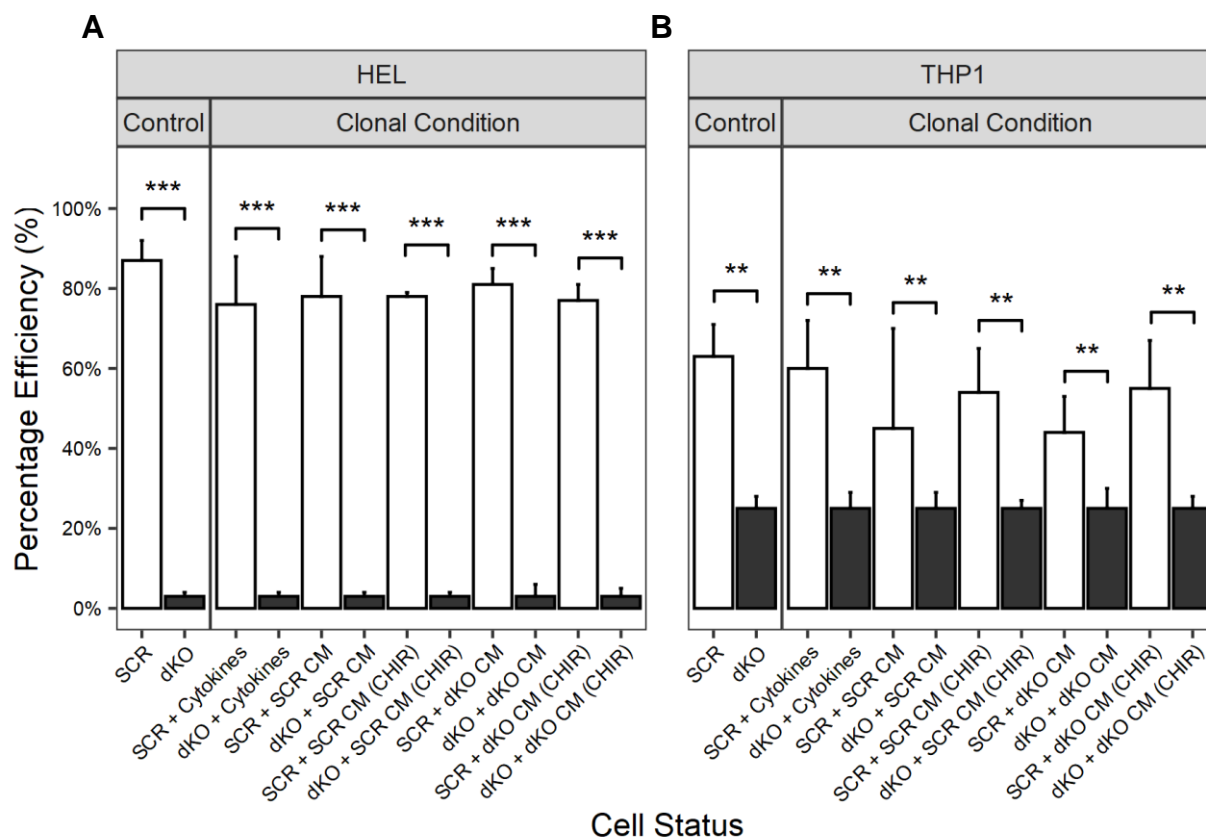


Figure 4-1: Soluble Rescue Conditions Do Not Rescue Clonal Growth of Dual Knockout Responder AML Cells

Bulk dual knockout responder AML cell lines HEL and THP1 were cultured with several supportive conditions in order to recover a complete knockout cell line from a bulk knockout culture. Samples were cultured alone, with cytokine supplementation, with conditioned media, and with conditioned media prepared after CHIR stimulation. These conditions are detailed in 2.4. (n=3; data indicates mean +1SD; t-test; *** = <0.001; **=<0.01).

SCR – Scrambled transduced cells

dKO – Dual knockout transduced cells

Cytokines - IL3, IL6, SCF, G-CSF, GM-CSF, FL3, M-CSF at 5ng/mL in fresh media

SCR CM - Scrambled cells cultured for 24 hours, media was centrifuged 300g for 5min and 0.45μM filtered then used at 1:1 (v/v) with fresh media

SCR CM + CHIR - Scrambled cells cultured with 5μM CHIR for 24 hours, media was centrifuged 300g for 5min and 0.45μM filtered then used at 1:1 (v/v) with fresh media

dKO CM - Dual knockout cells cultured for 24 hours, media was centrifuged 300g for 5min and 0.45μM filtered then used at 1:1 (v/v) with fresh media

dKO CM + CHIR - Dual knockout cells cultured with 5μM CHIR for 24 hours, media was centrifuged 300g for 5min and 0.45μM filtered then used at 1:1 (v/v) with fresh media

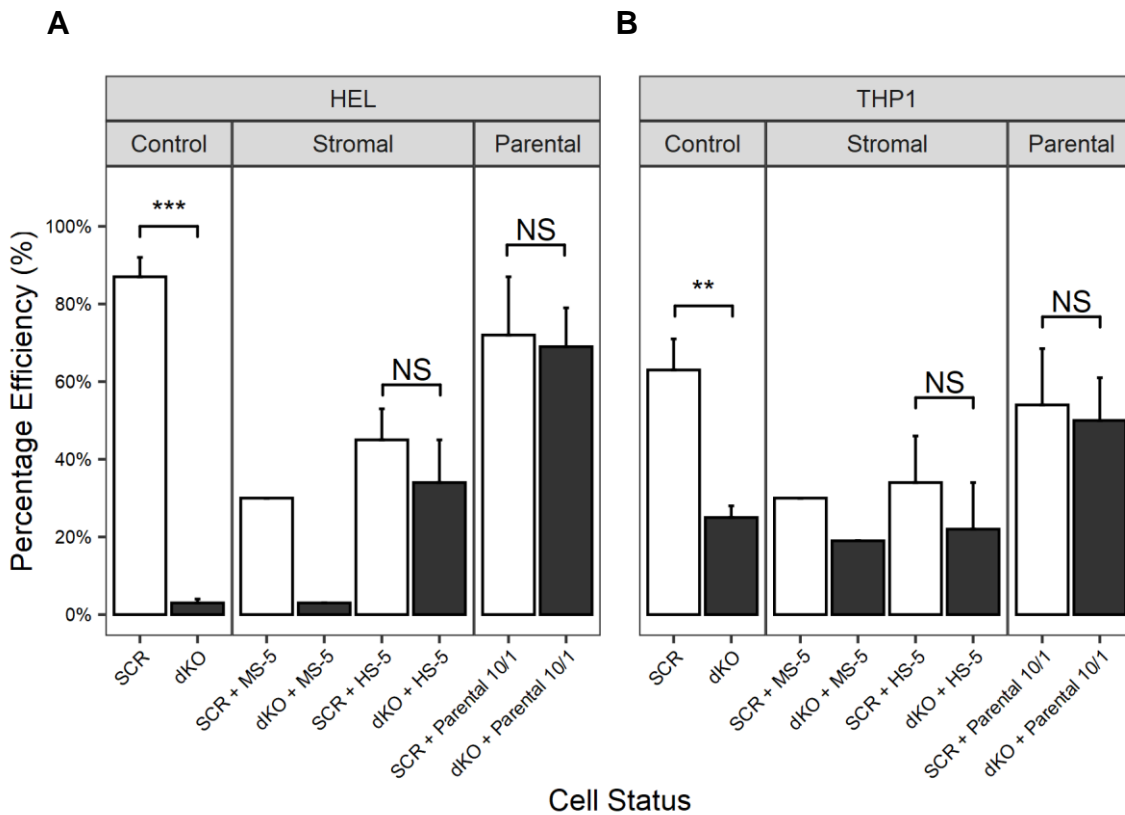


Figure 4-2: Parental Co-culture Improves Clonal Growth of Dual Knockout Responder AML Cells

Bulk dual knockout responder AML cell lines HEL and THP1 were cultured with several supportive conditions in order to recover a complete knockout cell line from a bulk knockout culture. These are described in 2.4. Clones were cultured with (A) supplemented media, or (B) co-culture conditions, in which a stromal or parental support was applied. (n=3 for control, n=1 for MS-5 co-culture, n=3 for HS-5 and parental co-culture; data indicates mean +1SD; t-test; *** = <0.001; **=<0.01; NS = not significant).

SCR – Scrambled transduced cells
dKO – Dual knockout transduced cells
HS-5 – Human stromal (5) cells
MS-5 – Mouse stromal (5) cells

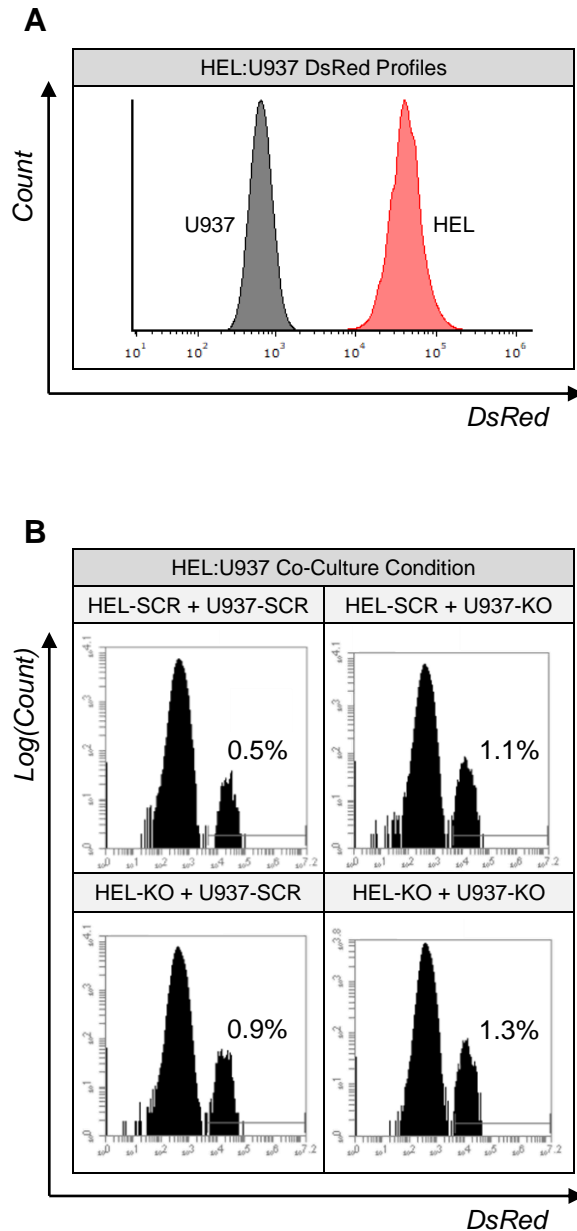


Figure 4-3: Co-culture with Dual Knockout U937 cells Rescues Clonal Growth of Dual Knockout Responder HEL Cells

(A) Representative fluorescence histograms demonstrating distinct DsRed expression derived from the WNT pBARV reporter for clonal pBARV HEL and U937, enabling separation based on spectral profiles (2.9.3). (B) Representative fluorescence histograms demonstrating rescue of dual knockout clones after limiting dilution co-culture at 10:1 ratio of U937 to HEL (2.4). Cultures were examined after 10-days with the WNT reporter (2.11.5). The marker was determined in U937 monoculture to elucidate the HEL DsRed expression profile (n=2).

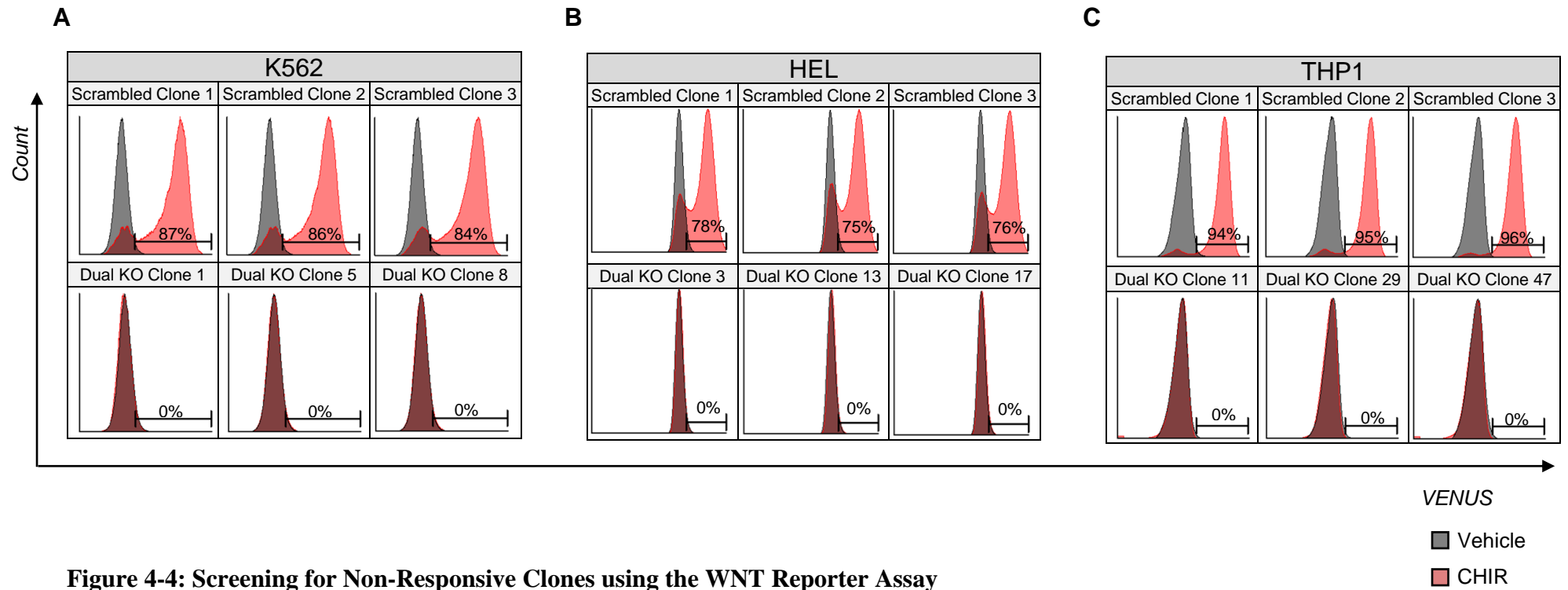


Figure 4-4: Screening for Non-Responsive Clones using the WNT Reporter Assay

Representative histograms generated with the WNT pBARV reporter (2.9.3). The reporter was used as a screen for β -catenin knockout in clones generated by limiting dilution cloning supported with parental co-culture (1:10; 2.4). Expanded colonies were treated with 5 μ M CHIR and screened after 24 hours incubation or a vehicle control (0.1% DMSO, v/v). (2.9.1). Clones were differentiated from the parental supporting cells by presence of DsRed, determined by a parental monoculture (2.9.3). Complete knockout clones were deemed incapable of generating a WNT reporter response in (A) K562 (B) HEL and (C) THP1; top panels represent clones isolated from scrambled knockout controls, whilst the bottom panel shows negative clones from the dual knockout bulk cultures. (n=3).

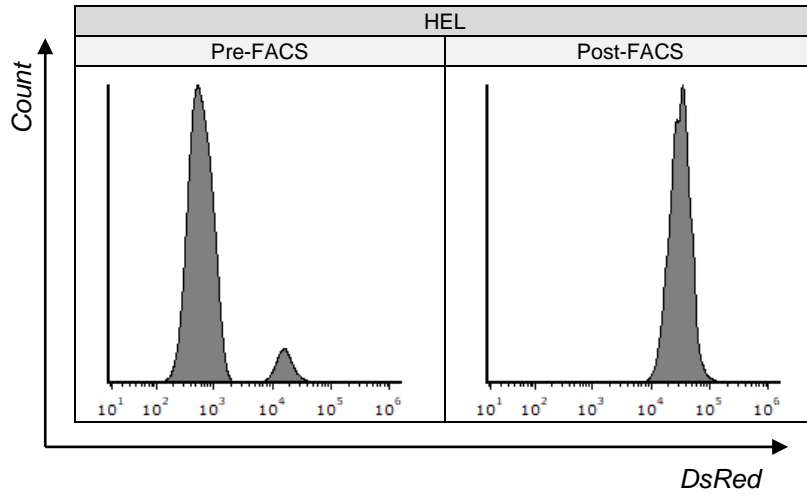


Figure 4-5: Representative Histograms Illustrating Purification of Putative Knockout Clones by FACS

Representative histograms demonstrating the DsRed profile pre-FACS and post-FACS putative knockout isolation process (2.9.3, 2.11.3). Left pre-FACS histogram demonstrates the mixed spectra profile from parental and DsRed⁺ knockout clones, whilst the right histogram demonstrates the pure putative knockout population post-sort.

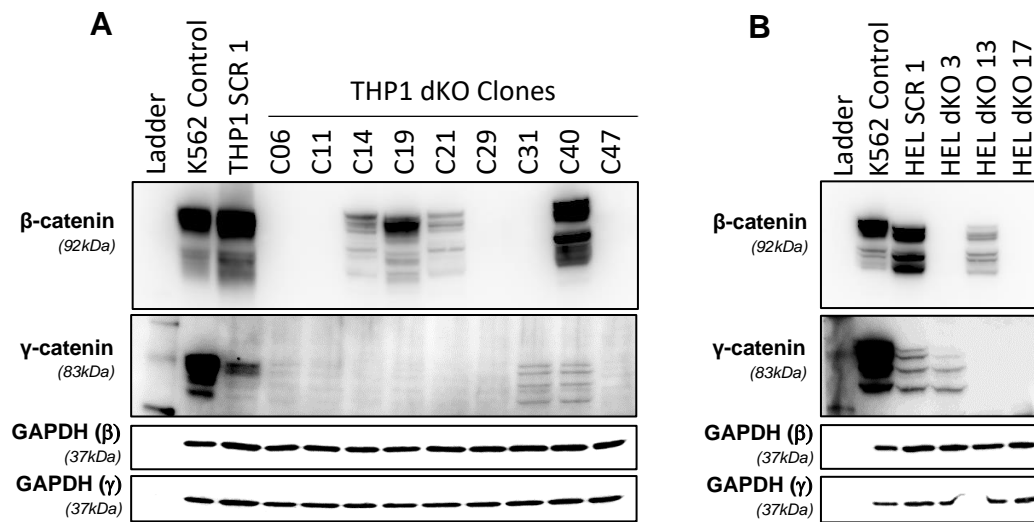


Figure 4-6: Absence of β -catenin and γ -catenin in Recovered Putative Dual Knockout Clones Generated by Parental Co-culture

Western blot of putative β -catenin and γ -catenin knockout clones in THP1 (A) and HEL (B). Clones were generated by parental co-culture (2.4). Putative knockout clones were recovered by FACS (2.11). Samples were treated with $5\mu\text{M}$ CHIR for 24-hours before lysates were prepared (2.10.1). K562 wildtype and a matched scrambled clone generated in the same method were treated with $5\mu\text{M}$ CHIR for 24-hours before lysates were extracted and acted as positive controls. Protein loading was confirmed by assessment of GAPDH (2.10.5). Western blots were performed in parallel due to the close proximity of each catenin.

SCR – Scrambled; **dKO** – Dual Knockout; **C** - Clone

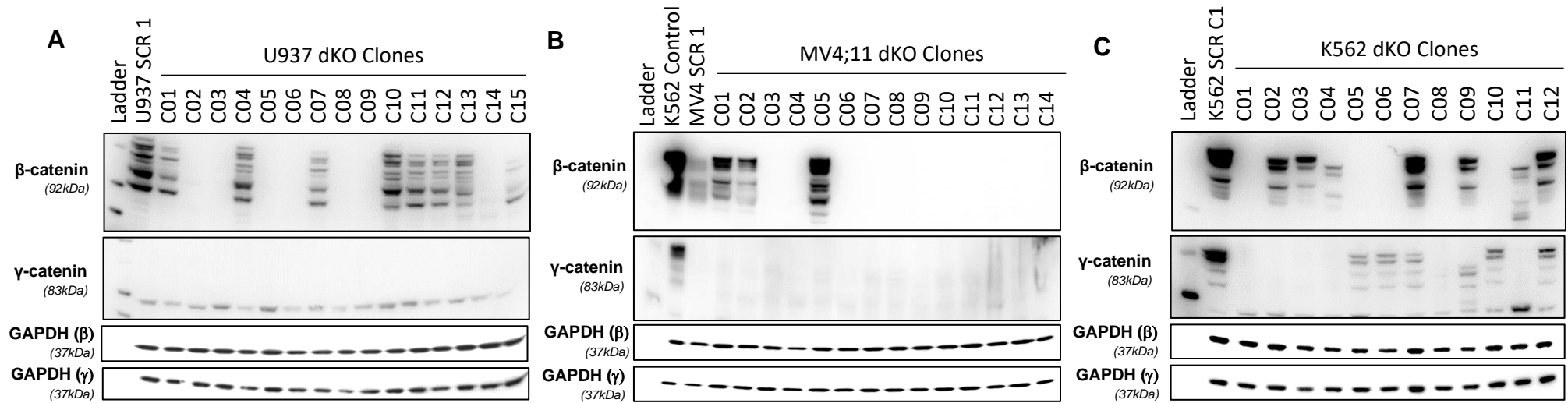


Figure 4-7: Absence of β -catenin and γ -catenin in Putative Dual Knockout Clones

Western blot of putative β -catenin and γ -catenin knockout clones in U937 (A), MV4;11 (B), and K562 (C). Clones were generated by limiting dilution without support (2.4). Samples were treated with 5 μ M CHIR for 24-hours before lysates were prepared (2.9). K562 wildtype and a matched scrambled clone were treated with 5 μ M CHIR for 24-hours before lysates were extracted and acted as positive controls. Protein loading was confirmed by assessment of GAPDH (2.10.5). Western blots were performed in parallel due to the close proximity of each catenin.

SCR – Scrambled; dKO – Dual Knockout; C - Clone

Table 4-1: *CTNNB1* DNA-Sequencing Reveals InDel Events

DNA-deconvolution was applied to validate an InDel event had occurred, and that knockout had been established; the resulting sequence was deconvoluted with high prediction accuracy (2.12.3.6). The sequences are displayed following multiple sequence alignment. The clones used here were negative for WNT pBARV reporter activity, if applicable (**Figure 4-4**), and were selected for negative expression of either catenin based upon western blot (**Figure 4-6**). DNA was isolated from these clones (2.12.3.1) before the gRNA target region was amplified by PCR (2.12.3.2) for subsequent DNA-sequencing (2.12.3.5). Red vertical line represents the expected InDel cut site, three base pairs downstream of the PAM recognition site. The dashed fields are deleted base pairs, or in the case of wildtype, represent an insertion event as a consequence of an InDel event.

Cell Line	Allele	Sequence	Status
WT	WT	GGTGGTATAGAGGCCTCTTGTGCGTACTGTCC TTC - - - - - G - - GGC TGG TGACAGGGAAGACATCACTGAG	WT
K562 C1	1	GGTGGTATAGAGGCCTCTTGTGCGTACTGTCC TTC - - - - - G - - GGC TGG TGACAGGGAAGACATCACTGAG	Biallelic Knockout
	2	GGTGGTATAGAGGCCTCTTGTGCGTACTGTCC TTC - - - - - G - - GGC TGG TGACAGGGAAGACATCACTGAG	
K562 C8	1	GGTGGTATAGAGGCCTCTTGTGCGTACTGTCC TTC - - - - - G - - GGC TGG TGACAGGGAAGACATCACTGAG	Biallelic Knockout
	2	GGTGGTATAGAGGCCTCTTGTGCGTACTGTCC TTC - - - - - G - - GGC TGG TGACAGGGAAGACATCACTGAG	
HEL C3	1	GGTGGTATAGAGGCCTCTTGTGCGTACTGTCC TTC GGC ACTGGGTACGGCGCTGGGTATCCTGATG - - - - - GGC TGG TGACAGGGAAGACATCACTGAG	Biallelic Knockout
	2	GGTGGTATAGAGGCCTCTTGTGCGTACTGTCC TTC GGC ACTGGGTACGGCGCTGGGTATCCTGATG - - - - - GGC TGG TGACAGGGAAGACATCACTGAG	
HEL C13	1	GGTGGTATAGAGGCCTCTTGTGCGTACTGTCC TTC - - - - - G - - GGC TGG TGACAGGGAAGACATCACTGAG	Wildtype
	2	GGTGGTATAGAGGCCTCTTGTGCGTACTGTCC TTC - - - - - G - - GGC TGG TGACAGGGAAGACATCACTGAG	
HEL C17	1	GGTGGTATAGAGGCCTCTTGTGCGTACTGTCC TTC - - - - - G - - GGC TGG TGACAGGGAAGACATCACTGAG	Biallelic Knockout
	2	GGTGGTATAGAGGCCTCTTGTGCGTACTGTCC TTC - - - - - GGA GGC TGG TGACAGGGAAGACATCACTGAG	
THP C11	1	GGTGGTATAGAGGCCTCTTGTGCGTACTGTCC TTC - - - - - GGC TGG TGACAGGGAAGACATCACTGAG	Triallelic Knockout
	2	GGTGGTATAGAGGCCTCTTGTGCGTACTGTCC TTC - - - - - CCGTGCG - - - - - GGC TGG TGACAGGGAAGACATCACTGAG	
	3	GGTGGTATAGAGGCCTCTTGTGCGTACTGTCC TTC - - - - - CCGTGCG - - - - - GGC TGG TGACAGGGAAGACATCACTGAG	
THP C29	1	GGTGGTATAGAGGCCTCTTGTGCGTACTGTCC TTC - - - - - GGC TGG TGACAGGGAAGACATCACTGAG	Triallelic Knockout
	2	GGTGGTATAGAGGCCTCTTGTGCGTACTGTCC TTC - - - - - GGC TGG TGACAGGGAAGACATCACTGAG	
	3	GGTGGTATAGAGGCCTCTTGTGCGTACTGTCC TTC - - - - - GGC TGG TGACAGGGAAGACATCACTGAG	
THP C47	1	GGTGGTATAGAGGCCTCTTGTGCGTACTGTCC TTC - - - - - GGC TGG TGACAGGGAAGACATCACTGAG	Triallelic Knockout
	2	GGTGGTATAGAGGCCTCTTGTGCGTACTGTCC TTC - - - - - GGC TGG TGACAGGGAAGACATCACTGAG	
	3	GGTGGTATAGAGGCCTCTTGTGCGTACTGTCC TTC - - - - - GGC TGG TGACAGGGAAGACATCACTGAG	
U937 C3	1	GGTGGTATAGAGGCCTCTTGTGCGTACTGTCC TTC - - - - - G - - GGC TGG TGACAGGGAAGACATCACTGAG	Biallelic Knockout
	2	GGTGGTATAGAGGCCTCTTGTGCGTACTGTCC TTC - - - - - G - - GGC TGG TGACAGGGAAGACATCACTGAG	
U937 C5	1	GGTGGTATAGAGGCCTCTTGTGCGTACTGTCC TTC - - - - - G - - GGC TGG TGACAGGGAAGACATCACTGAG	Biallelic Knockout
	2	GGTGGTATAGAGGCCTCTTGTGCGTACTGTCC TTC - - - - - G - - GGC TGG TGACAGGGAAGACATCACTGAG	
U937 C6	1	GGTGGTATAGAGGCCTCTTGTGCGTACTGTCC TTC - - - - - G - - GGC TGG TGACAGGGAAGACATCACTGAG	Biallelic Knockout
	2	GGTGGTATAGAGGCCTCTTGTGCGTACTGTCC TTC - - - - - G - - GGC TGG TGACAGGGAAGACATCACTGAG	
MV4;11 C3	1	GGTGGTATAGAGGCCTCTTGTGCGTACTGTCC TTC - - - - - G - - GGC TGG TGACAGGGAAGACATCACTGAG	Biallelic Knockout
	2	GGTGGTATAGAGGCCTCTTGTGCGTACTGTCC TTC - - - - - G - - GGC TGG TGACAGGGAAGACATCACTGAG	
MV4;11 C7	1	GGTGGTATAGAGGCCTCTTGTGCGTACTGTCC TTC - - - - - G - - GGC TGG TGACAGGGAAGACATCACTGAG	Biallelic Knockout
	2	GGTGGTATAGAGGCCTCTTGTGCGTACTGTCC TTC - - - - - G - - GGC TGG TGACAGGGAAGACATCACTGAG	
MV4;11 C9	1	GGTGGTATAGAGGCCTCTTGTGCGTACTGTCC TTC - - - - - G - - GGC TGG TGACAGGGAAGACATCACTGAG	Biallelic Knockout
	2	GGTGGTATAGAGGCCTCTTGTGCGTACTGTCC TTC - - - - - G - - GGC TGG TGACAGGGAAGACATCACTGAG	

Table 4-3: Summary Table of Generated Knockout Clones

Knockout clones generated within this study, and associated allele status. Red indicates knockout, green indicates wildtype, whilst grey represents not present within cell line, or a replicated deletion has occurred masking detection by Sanger sequencing (2.12.3).

Cell Line	WNT Type	Result	Clone ID	β Allele			γ Allele			Status		
				1	2	3	1	2	3	β	γ	
K562 (CML)	Responder	Dual	B1C01	Red	Red	Grey	Red	Red	Grey	Knockout	Knockout	
			B1C08	Red	Red	Grey	Red	Red	Grey	Knockout	Knockout	
		β	B1C05	Red	Red	Grey	Green	Green	Grey	Knockout	Wildtype	
			B1C06	Red	Red	Grey	Green	Green	Grey	Knockout	Wildtype	
			B1C10	Red	Red	Grey	Green	Green	Grey	Knockout	Wildtype	
		γ	B1C11	Green	Green	Grey	Red	Red	Grey	Wildtype	Knockout	
			B1C02	Green	Green	Grey	Red	Red	Grey	Wildtype	Knockout	
			B1C03	Green	Green	Grey	Red	Red	Grey	Wildtype	Knockout	
		THP1	Dual	B5C11	Red	Red	Red	Red	Red	Grey	Knockout	Wildtype
				B5C29	Red	Red	Red	Red	Red	Grey	Knockout	Knockout
				B5C47	Red	Red	Red	Red	Red	Grey	Knockout	Knockout
β	B5C31		Red	Red	Red	Green	Green	Grey	Knockout	Wildtype		
γ	B1C04		Green	Green	Green	Red	Red	Grey	Wildtype	Knockout		
	B1C08		Green	Green	Green	Red	Red	Grey	Wildtype	Knockout		
	B1C10	Green	Green	Green	Red	Red	Grey	Wildtype	Knockout			
HEL	Dual	B5C17	Red	Red	Red	Red	Red	Grey	Knockout	Knockout		
	β	B5C03	Red	Red	Red	Green	Green	Grey	Knockout	Wildtype		
	γ	B5C13	Green	Green	Green	Red	Red	Grey	Wildtype	Knockout		
U937	Dual	B1C03	Red	Red	Red	Red	Red	Grey	Knockout	Knockout		
		B1C05	Red	Red	Red	Red	Red	Grey	Knockout	Knockout		
	β	B1C06	Red	Red	Red	Green	Green	Grey	Knockout	Wildtype		
		B1C08	Red	Red	Red	Green	Green	Grey	Knockout	Wildtype		
		B1C09	Red	Red	Red	Green	Green	Grey	Knockout	Wildtype		
	γ	B1C04	Green	Green	Green	Red	Red	Grey	Wildtype	Knockout		
		B1C07	Green	Green	Green	Red	Red	Grey	Wildtype	Knockout		
		B1C12	Green	Green	Green	Red	Red	Grey	Wildtype	Knockout		
	MV4;11	Dual	B1C03	Red	Red	Red	Red	Red	Grey	Knockout	Knockout	
B1C07			Red	Red	Red	Red	Red	Grey	Knockout	Knockout		
B1C09			Red	Red	Red	Red	Red	Grey	Knockout	Knockout		
β		B1C08	Red	Red	Red	Green	Green	Grey	Knockout	Wildtype		
		B1C10	Red	Red	Red	Green	Green	Grey	Knockout	Wildtype		
		B1C12	Red	Red	Red	Green	Green	Grey	Knockout	Wildtype		
γ		B1C01	Green	Green	Green	Red	Red	Grey	Wildtype	Knockout		
		B1C02	Green	Green	Green	Red	Red	Grey	Wildtype	Knockout		
		B1C05	Green	Green	Green	Red	Red	Grey	Wildtype	Knockout		

Status refers to complete knockout; clone is considered wildtype if even a singular wildtype allele is detected.

Green – Wildtype

Red – Knockout Allele

Grey – Not present in Cell Line

4.3.4 Characterisation of Complete Dual Knockout Clones

4.3.4.1 *Dual Knockout has no Impact on General Characteristics*

Use of incomplete knockout methods *in vitro* and *in vivo* to study β -catenin and γ -catenin have yielded conflicting results (4.1.1). Studies have documented induction of cell differentiation, slowed growth, perturbed cell cycling, and increased apoptosis, yet others have observed no effect (Gandillet *et al.*, 2011a; Fiskus *et al.*, 2015; X. Jiang *et al.*, 2018b; Saenz *et al.*, 2019). To investigate this in the context of complete dual knockout clones, a series of assays to examine cell characteristics was performed. These included growth and viability, cell cycle, apoptosis, morphology, and changes to cell surface marker expression. In order to control for clonal variation, three scrambled controls and three dual knockout clones were examined in each assay. In brief, no difference in any of the above cell characteristics was observed between scrambled controls and dual knockouts for the *responder* AML cell lines, HEL (**Figure 4-8**), and THP1 (**Figure 4-9**), or in the *non-responder* AML lines, U937 (**Figure 4-10**), and MV4;11 (**Figure 4-11**). These data indicate that β -catenin and γ -catenin have no role in the maintenance of AML *responder* or *non-responder* lines in complete clonal dual catenin knockout conditions.

4.3.4.2 *γ -catenin Cannot Compensate for β -catenin Knockout in Responder AML Lines*

WNT reporter activity was assessed in β -catenin knockout clones, as well as in dual knockout clones to determine their respective roles in WNT signalling. WNT reporter activity was ablated in β -catenin knockout clones, solely or in combination with γ -catenin knockout (**Figure 4-12**), suggesting absolute requirement of β -catenin for WNT signalling activity and that γ -catenin was unable to compensate for β -catenin absence under these conditions.

4.3.4.3 *Knockout Responder AML Retain Dependence on β -catenin for Clonogenicity*

In order to determine whether these clones remained incapable of single-cell expansion, it was necessary to re-examine clonogenicity through limiting dilution cloning. Dependency on β -catenin for clonal growth was found to be retained in the *responder* AML cell line clones, with no dependency noted for *non-responder* AML lines (**Figure 4-13**). No dependency was found for γ -catenin in any context. Concurrent complete knockout clones of both β -catenin and γ -catenin were used for further experiments, as γ -catenin could compensate for β -catenin deletion, in different, unconsidered contexts.

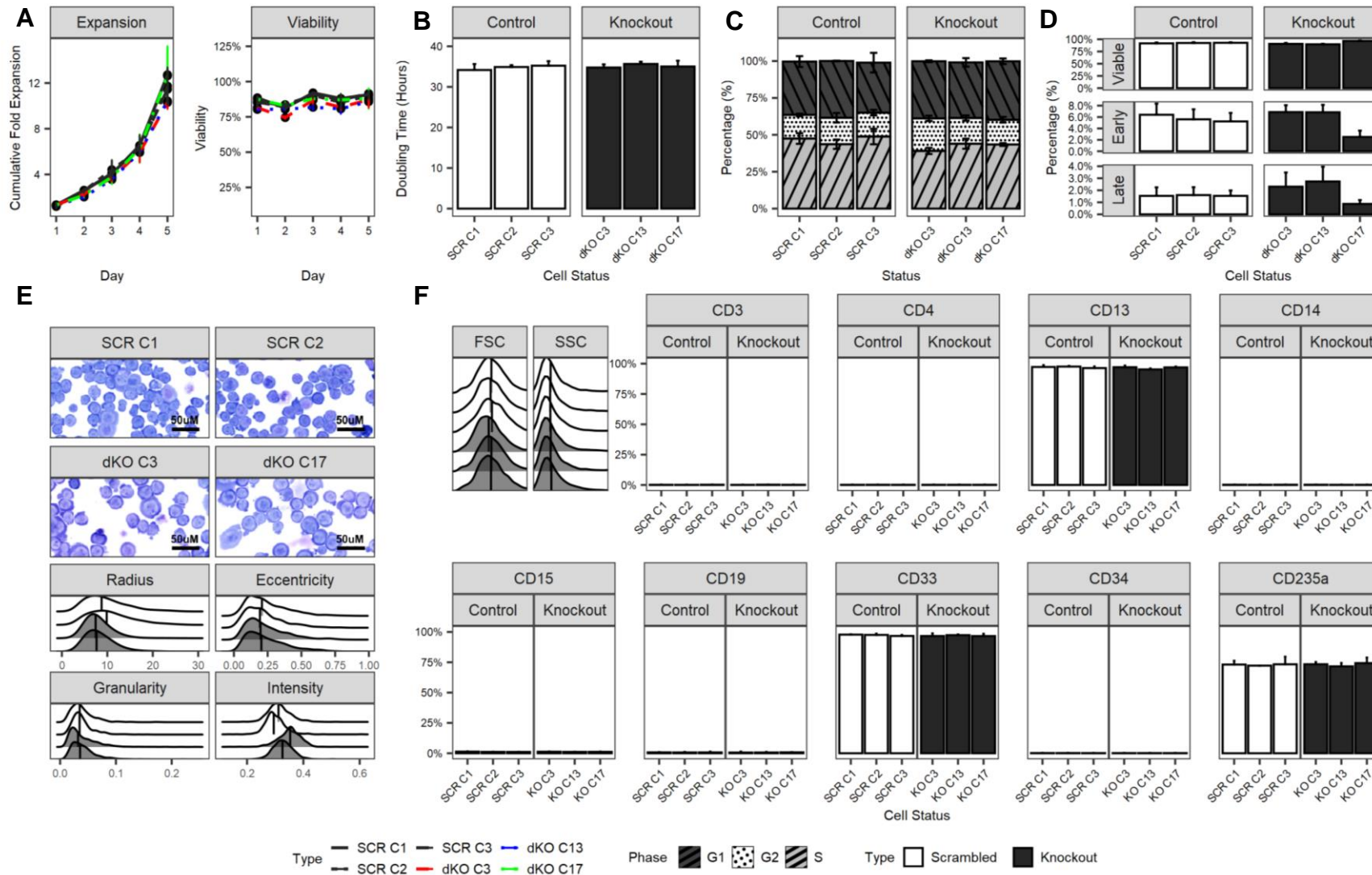


Figure 4-8: Dual Knockout Has No Impact on Cell Characteristics of HEL

Cell characteristics were examined in complete knockout HEL clones and were found to be unchanged by (A-B) growth, viability, and doubling time (2.11.7), (C) cell cycle distribution (2.11.8), (D) apoptosis (2.11.9), (E) morphological assessment by cytopins (2.3.2, radius in μM), and (F) through immunophenotypic analysis of known surface markers and indicators of differentiation (2.11.11). Scrambled clones were applied as a control. (n=3 for growth and viability, cell cycle, apoptosis, and immunophenotyping; n=1 for cytopins; data indicates mean \pm 1SD).

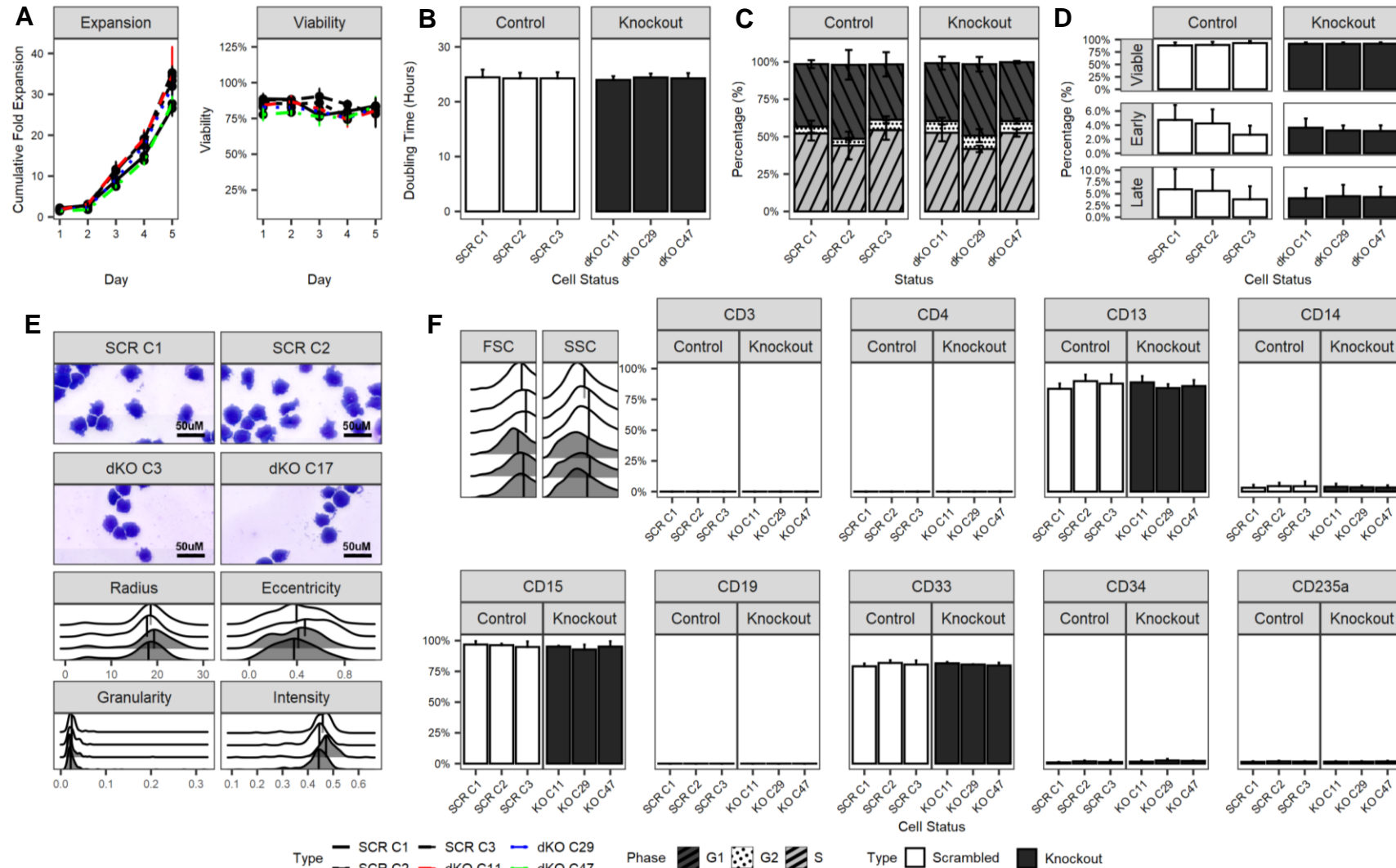


Figure 4-9: Dual Knockout Has No Impact on Cell Characteristics of THP1

Cell characteristics were examined in complete dual knockout THP1 clones and were found to be unchanged by (A-B) growth, viability, and doubling time (2.11.7), (C) cell cycle distribution (2.11.8), (D) apoptosis (2.11.9), (E) morphological assessment by cytopins (2.3.2, radius in μM), and (F) through immunophenotypic analysis of known surface markers and indicators of differentiation (2.11.11). Scrambled clones were applied as a control. (n=3 for growth and viability, cell cycle, apoptosis, and immunophenotyping; n=1 for cytopins; data indicates mean \pm 1SD).

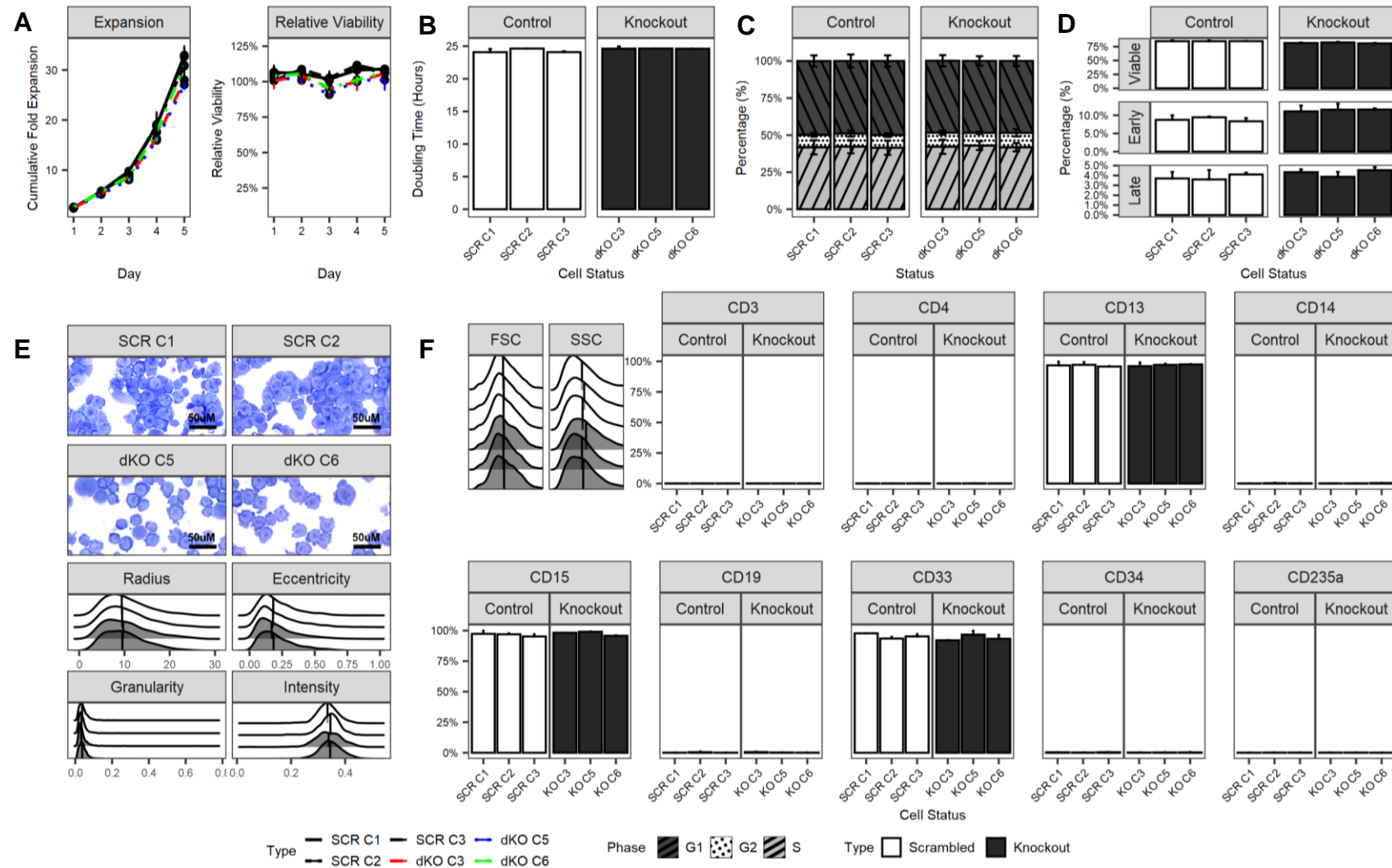


Figure 4-10: Dual Knockout Has No Impact on Cell Characteristics of U937

Cell characteristics were examined in complete dual knockout U937 clones and were found to be unchanged by (A-B) growth, viability, and doubling time (2.11.7), (C) cell cycle distribution (2.11.8), (D) apoptosis (2.11.9), (E) morphological assessment by cytopins (2.3.2, radius in μM), and (F) through immunophenotypic analysis of known surface markers and indicators of differentiation (2.11.11). Scrambled clones were applied as a control. (n=3 for growth and viability, cell cycle, apoptosis, and immunophenotyping; n=1 for cytopins; data indicates mean \pm 1SD).

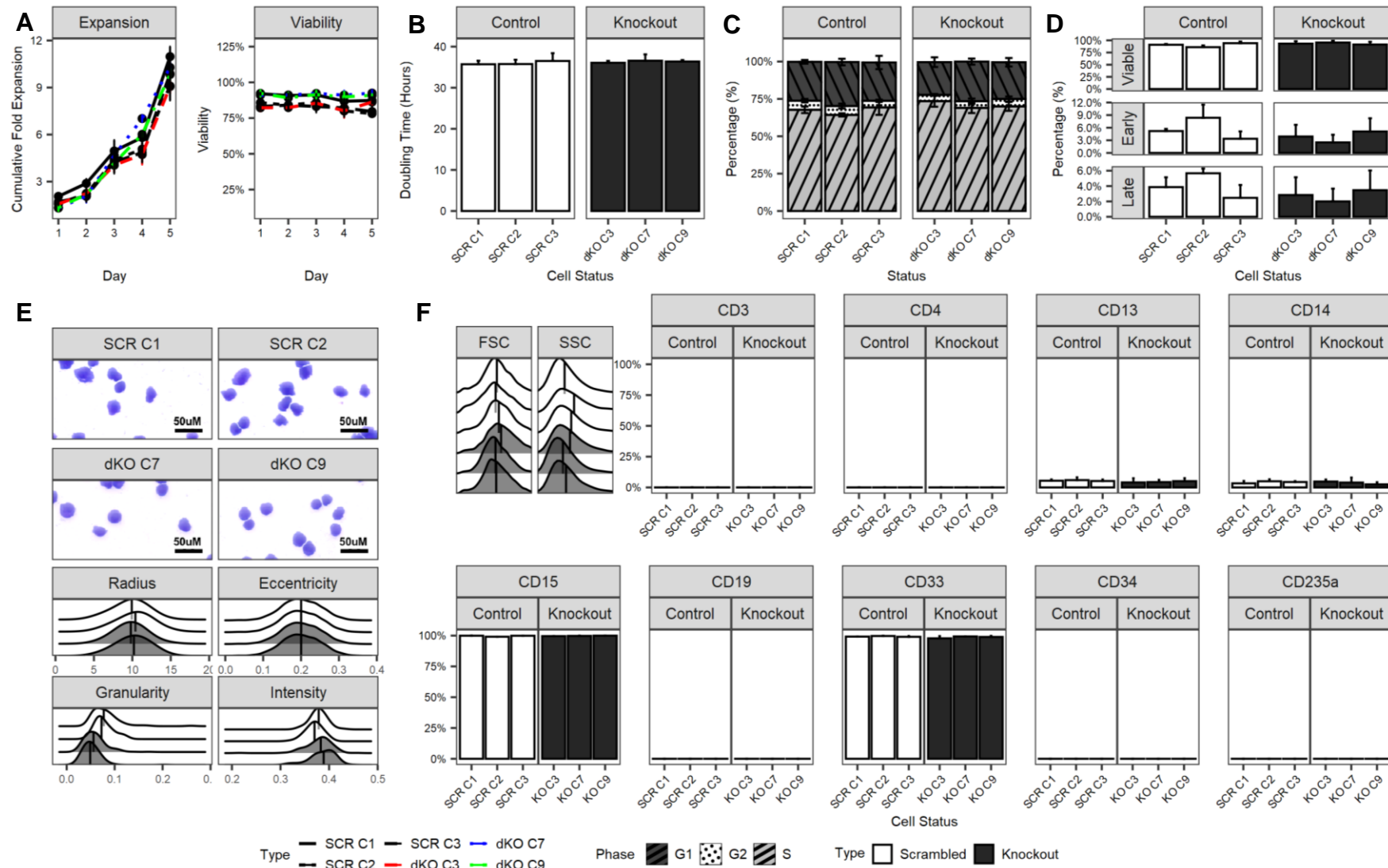


Figure 4-11: Dual Knockout Has No Impact on Cell Characteristics of MV4;11

Cell characteristics were examined in complete dual knockout MV4;11 clones and were found to be unchanged by (A-B) growth, viability, and doubling time (2.11.7), (C) cell cycle distribution (2.11.8), (D) apoptosis (2.11.9), (E) morphological assessment by cytopins (2.3.2, radius in µM), and (F) through immunophenotypic analysis of known surface markers and indicators of differentiation (2.11.11). Scrambled clones were applied as a control. (n=3 for growth and viability, cell cycle, apoptosis, and immunophenotyping; n=1 for cytopins; data indicates mean ±1SD).

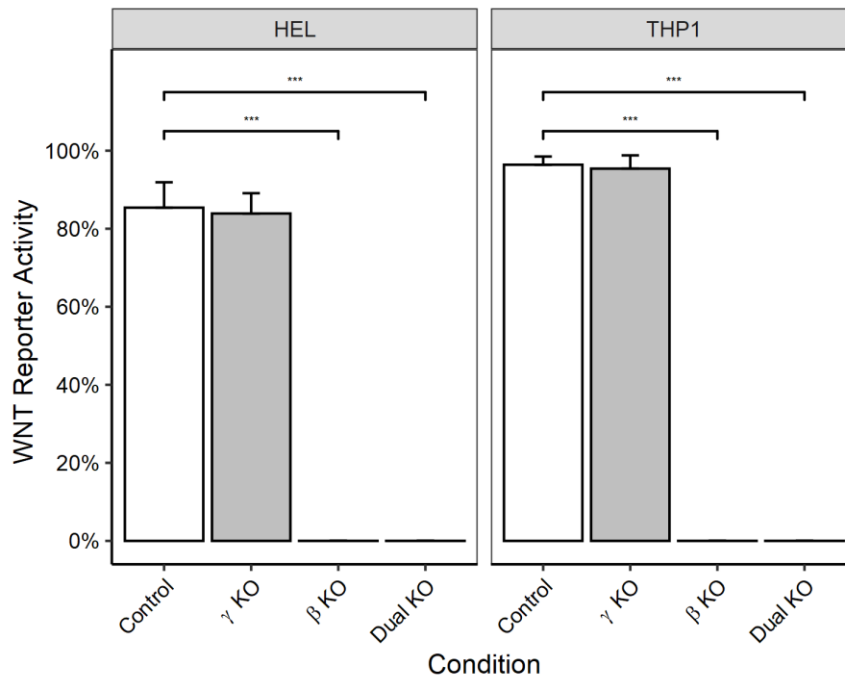


Figure 4-12: WNT Reporter Activity is β -catenin Dependent in Responder AML Cells

Established complete knockout clones of γ -catenin, β -catenin, or dual knockout were examined for WNT reporter activity with the flow-based WNT reporter relative to vehicle treatment (2.9.3). Samples were treated with $5\mu\text{M}$ CHIR for 24-hours before analysis, or a vehicle control (0.1% DMSO, v/v). (2.9.1). A scrambled clone was applied as a control. ($n=3$, data indicates mean \pm 1SD; $***<0.001$; ANOVA with post-hoc Tukey).

Control – Scrambled Control 1 (Matched Cell Line)

γ -catenin Knockout – HEL: B5C13; THP1: B1C04

β -catenin Knockout – HEL: B5C03; THP1: B5C31

Dual-catenin Knockout – HEL: B5C17; THP1: B5C47

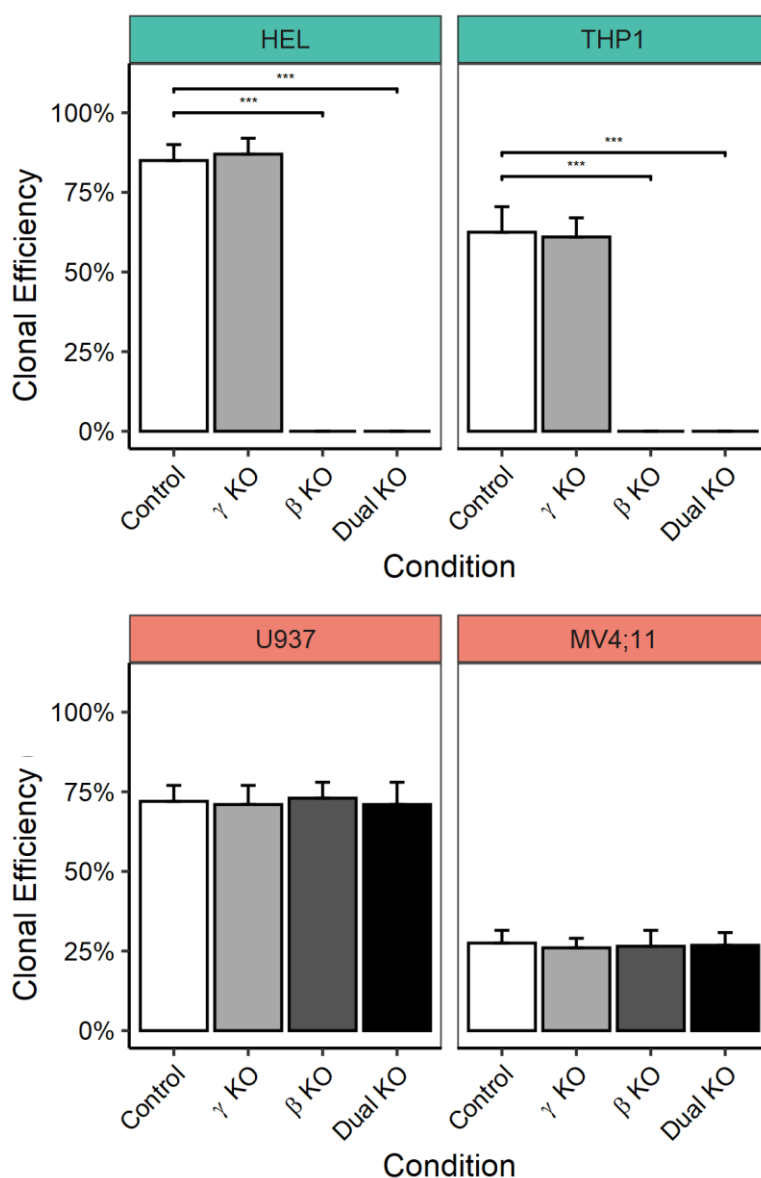


Figure 4-13: Responder AML Cell Lines Retain Dependence on β -catenin for Clonal Growth

Validated complete knockout clones of γ -catenin, β -catenin, or dual knockouts were examined for clonal growth with a limiting dilution assay, with colonies scored after fourteen days of culture (2.4). Green facets represent responder cell lines (HEL, THP1), whilst red facets are non-responder cell lines (U937, MV4;11). A cell line matching scrambled clone was applied as a control. (n=3, data indicates mean +1SD; ***<0.001; ANOVA with post-hoc Tukey)

Control – Scrambled Control 1 (Matched Cell Line)

γ -catenin Knockout – HEL: B5C13; THP1: B1C04; U937: B1C04; MV4;11: B1C01

β -catenin Knockout – HEL: B5C03; THP1: B5C31; U937: B1C06; MV4;11: B1C08

Dual-catenin Knockout – HEL: B5C17; THP1: B5C47; U937: B1C05; MV4;11: B1C07

4.3.4.4 *Dual Knockout Does Not Sensitise Cells to Standard Chemotherapeutics*

WNT-derived mechanisms of chemoresistance indicate WNT signalling would represent an attractive target to synergistically enhance the efficacy of existing chemotherapeutic agents (4.1.2). To investigate whether silencing of WNT/ β -catenin signalling sensitises cells to standard chemotherapeutic agents, a drug sensitivity assay was undertaken using DNR and Ara-C. To examine potential sensitisation, scrambled and dual knockout clones were treated with increasing concentrations of these agents and the resulting impact upon growth and viability was examined (2.11.12).

No significant difference was observed with dual knockout as compared to scrambled clones in HEL (**Figure 4-14A-B**), THP1 (**Figure 4-14C-D**), U937 (**Figure 4-15A-B**), and MV4;11 (**Figure 4-15C-D**). THP1, U937, and MV4;11 remained consistently sensitive to DNR, whilst HEL remained insensitive as expected (Quillet-Mary *et al.*, 1996). In addition, no WNT/ β -catenin reporter activity was noted in response to either chemotherapy regardless of dosage in scrambled clones (data not shown), indicating chemotherapy treatment did not induce WNT/ β -catenin signalling activity as suggested in the literature (Martin-Orozco *et al.*, 2019). These data indicate WNT/ β -catenin signalling, and γ -catenin do not convey demonstratable chemoresistance in this context.

4.3.4.5 *Dual Knockout Does Not Impair Survival Through Serum-Depletion*

Growth under single-cell conditions was expected to impose stresses that are not present in a clonal mass culture. Hence, the phenotype of dual knockout cells may be explained by a reduced capacity to survive stress conditions. To model this, the effect of serum-depletion on *responder* and *non-responder* AML cell lines with dual knockout or a scrambled control was determined (2.11.13.1). Reductions in growth were observed for all cell lines which correlated with serum concentration. After contrasting scrambled clones with dual knockout clones within each respective line, differences were not significant. This was true for the *responder* cell lines HEL (**Figure 4-16A**), and THP1 (**Figure 4-16B**), and for the *non-responder* cell lines U937 (**Figure 4-16C**), and MV4;11 (**Figure 4-16D**). No WNT activity was seen in scrambled control cells through the examination of the WNT reporter, suggesting WNT/ β -catenin signalling is not activated or required for stress tolerance at the low serum concentrations considered (data not shown).

4.3.4.6 *Low-Density Does Not Delimit Stress Response*

As β -catenin knockout *responder* lines are incapable of growth under single-cell conditions, this suggested growth could be affected by the culture density as reduced densities incur stress. Scrambled and dual knockout clones were cultured at densities far below recommendations. To achieve this, an extreme low-density growth assay was undertaken (2.11.13.2).

All cell lines demonstrated reduced growth rates as culture density was reduced. When contrasting dual knockout clones with scrambled clones within each cell line, no significant differences were observed (**Figure 4-17**). Again, no WNT activity was noted in scrambled control cells through examination of the WNT reporter, suggesting WNT/ β -catenin signalling is not activated or required for stress tolerance at the densities considered (data not shown).

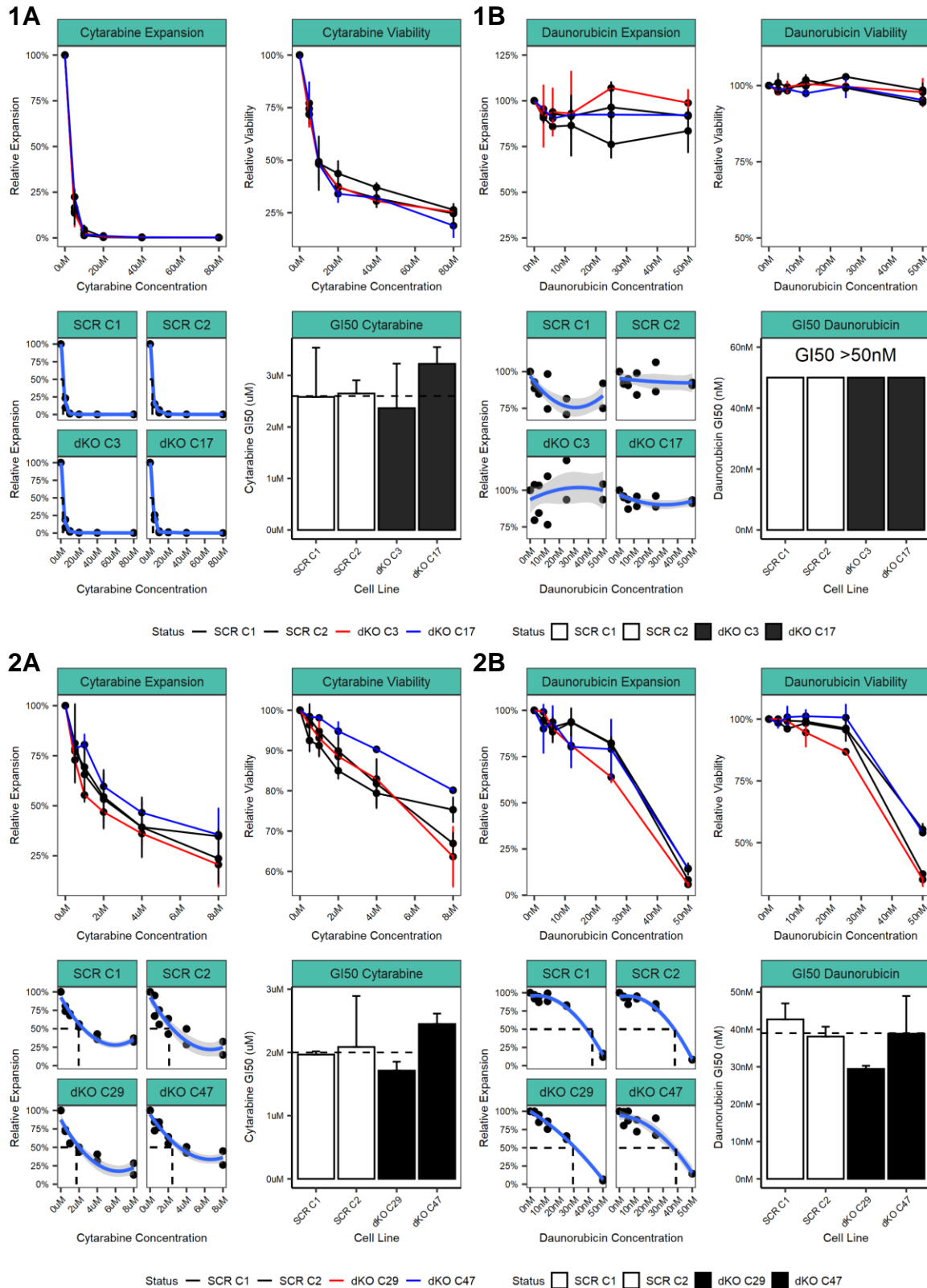


Figure 4-14: Responder Knockout Cells are Not Sensitised to Chemotherapeutics

Standard chemotherapeutic agents daunorubicin and cytarabine were applied to examine potential sensitivity in the dual knockout context for responder AML lines (2.11.12). HEL (1) was assessed for sensitivity to cytarabine (A), and daunorubicin (B); THP (2) was similarly contrasted. Within each quadrant from the upper left, these plots represent the growth after 48-hours, viability, loess regression fit for each line, and bar plots of the calculated 50% growth inhibition (GI50). The growth and viability were relative to the vehicle condition. Scrambled clones were used as a control. (n=3; data indicates mean ±1SD).

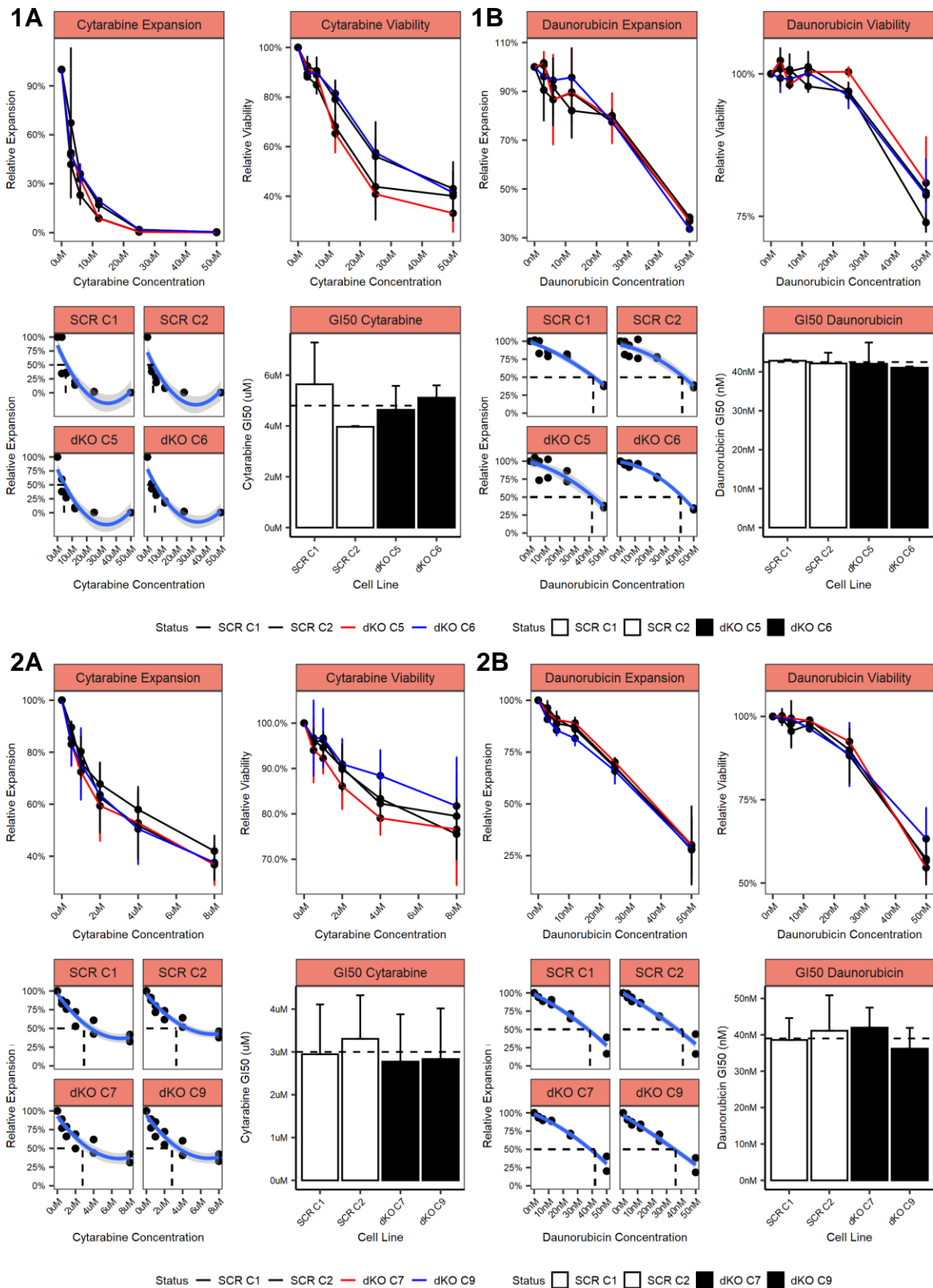


Figure 4-15: Non-responder Knockout Cells are Not Sensitised to Chemotherapeutics

Standard chemotherapeutic agents daunorubicin and cytarabine were applied to examine potential sensitivity in the dual knockout context for responder AML lines (2.11.12). U937 (1) was assessed for sensitivity to cytarabine (A), and daunorubicin (B); MV4;11 (2) was similarly contrasted. Within each quadrant from the upper left, these plots represent the growth after 48-hours, viability, loess regression fit for each line, and bar plots of the calculated 50% growth inhibition (GI50). The growth and viability were relative to the vehicle condition. Scrambled clones were used as a control. (n=3; data indicates mean ±1SD).

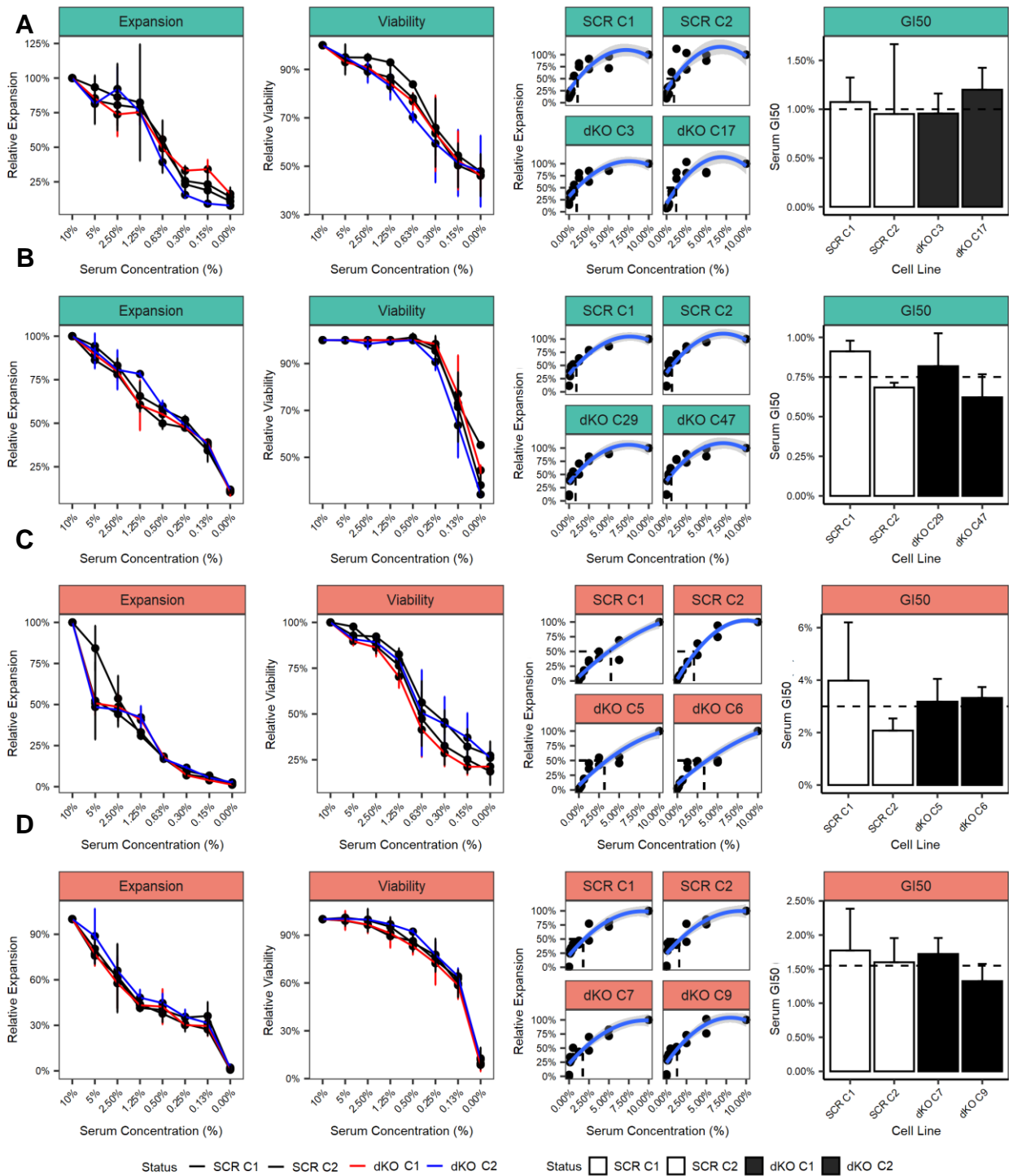


Figure 4-16: Dual Knockout Has No Effect on Response to Serum-depletion Conditions

Demonstrating the effect of serum-depletion on growth and viability for responder AML cell lines (A) HEL and (B) THP1 (coloured green), and for non-responder cell lines (C) U937 and (D) MV4;11 (coloured red) based on a serum-depletion assay (2.11.13.1). From left to right in each line: line plots showing growth and viability relative to 10% FBS, loess regression plots, and finally calculated GI50 scores (n=2; data indicates mean \pm 1SD). Colouring labels represent the following knockout clones, respectively:

HEL dKO = B5C03; B5C17.

THP1 dKO = B5C29; B5C47.

U937 dKO = B1C05; B1C06.

MV4;11 dKO = B1C07; B1C09.

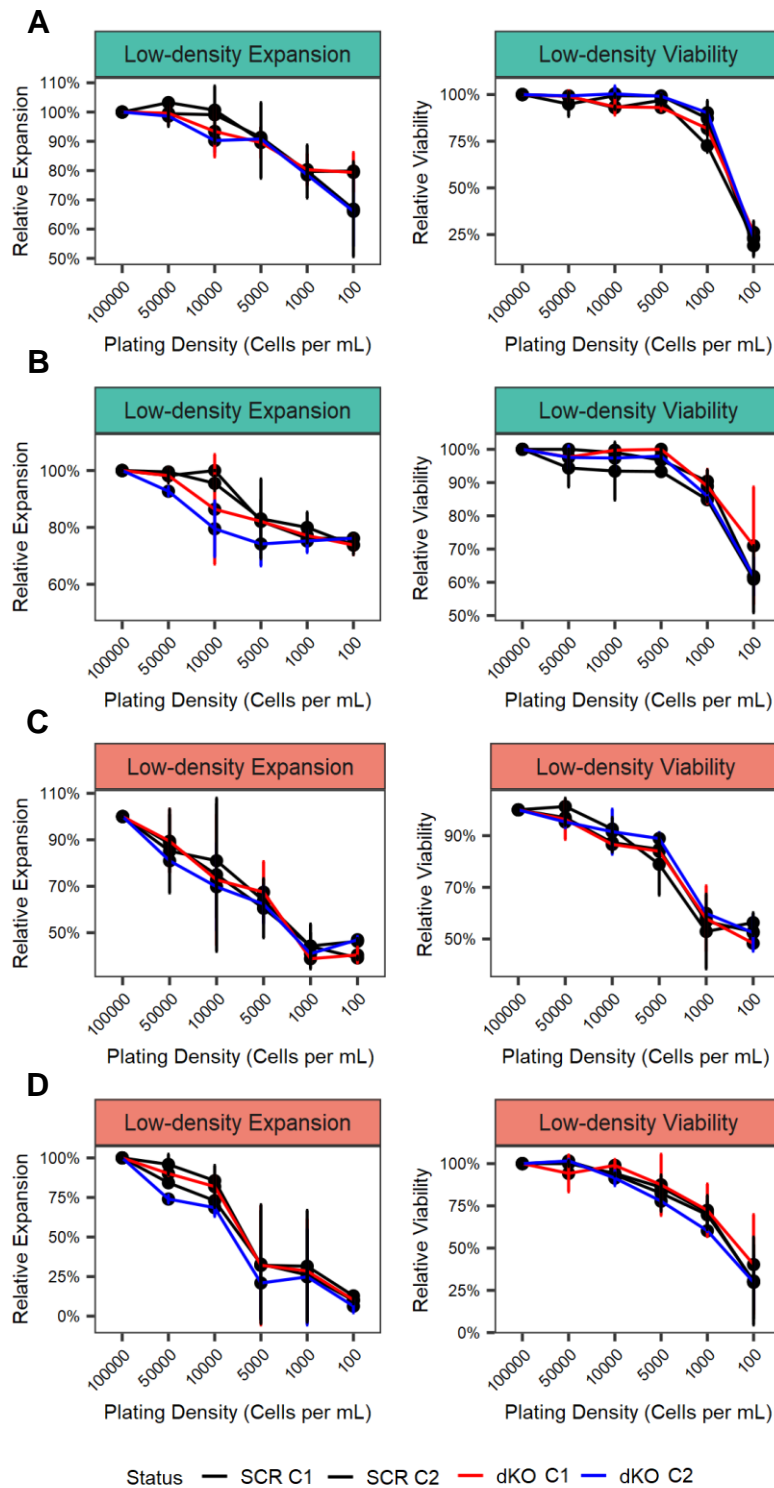


Figure 4-17: Dual Knockout Has No Effect on Growth at Low-density

Demonstrating the effect of low-density growth on growth and viability for responder AML cell lines (A) HEL and (B) THP1 (coloured green), and for non-responder cell lines (C) U937 and (D) MV4;11 (coloured red)(0). From left to right in each line: line plots showing growth and viability relative to 1×10^5 /mL plating density ($n=2$; data indicates mean \pm 1SD). Colouring labels represent the following knockout clones, respectively:

HEL dKO = B5C03; B5C17.

THP1 dKO = B5C29; B5C47.

U937 dKO = B1C05; B1C06.

MV4;11 dKO = B1C07; B1C09.

4.3.5 Characterising WNT/ β -catenin Activity in Primary AML Cultures

It is well recognised that to better represent the clinical condition from which cell lines can deviate, analysis in the context of patient-derived primary AML blasts is essential, where possible. Eight primary AML blast samples were obtained and cryopreserved for later use. Before proceeding, it was necessary to determine the activity levels of WNT/ β -catenin signalling, in order to characterise each primary sample as β -catenin⁺ (akin to *responder*) and β -catenin⁻ (akin to *non-responder*). However, the limited cell number and limited growth potential precluded the generation of WNT reporter clonal lines and fractionated western blots. Instead, it was necessary to rely upon β -catenin and LEF1 protein expression to classify these samples. Based on this analysis, putative WNT-active primary samples were determined as AML162, AML165, and AML172, whilst absence of β -catenin and low LEF1 levels enabled AML92, AML148, and AML160 to be deemed WNT-inactive (**Figure 4-18**). The two final samples, AML164 and AML177, were inconclusive due to non-specific banding and low protein content, respectively. No primary samples presented detectable γ -catenin, which was unexpected based on observations in the literature. Research comparing primary AML samples to HSPC found heterogeneous γ -catenin expression in AML, with 18% of AML samples demonstrating overexpression of whilst 20% did not express γ -catenin (Morgan *et al.*, 2013).

4.3.5.1 Generating CRISPR-Cas9 Knockout in Primary AML Samples

As β -catenin was readily detectible in primary samples, replicating CRISPR-Cas9 knockout of β -catenin as in AML cell lines was performed to provide further conclusion to the necessity of this protein for AML maintenance. γ -catenin was not considered for knockout as no prior result indicated a contributory or augmentative role to WNT/ β -catenin signalling (4.3.4.2, 4.3.4.3), nor was γ -catenin found to be expressed with these primary samples (4.3.5).

For this purpose, the CRISPR-Cas9 all-in-one lentiviral vector encoding a gRNA targeting β -catenin and incorporating GFP to facilitate identification of transduced cells was applied for lentiviral transduction (3.10). An equivalent scrambled control vector was also used. Transduction efficiency was low, as expected, with the levels suitable for subsequent analyses without need for sorting, but unsuitable for subsequent FACS due to the limited expected recovery (**Figure 4-19**). GFP intensity was low, with no delimitation of the negative and positive populations, suggesting it was possible the transduction rate was potentially higher than recorded for dimly fluorescent transduced cells.

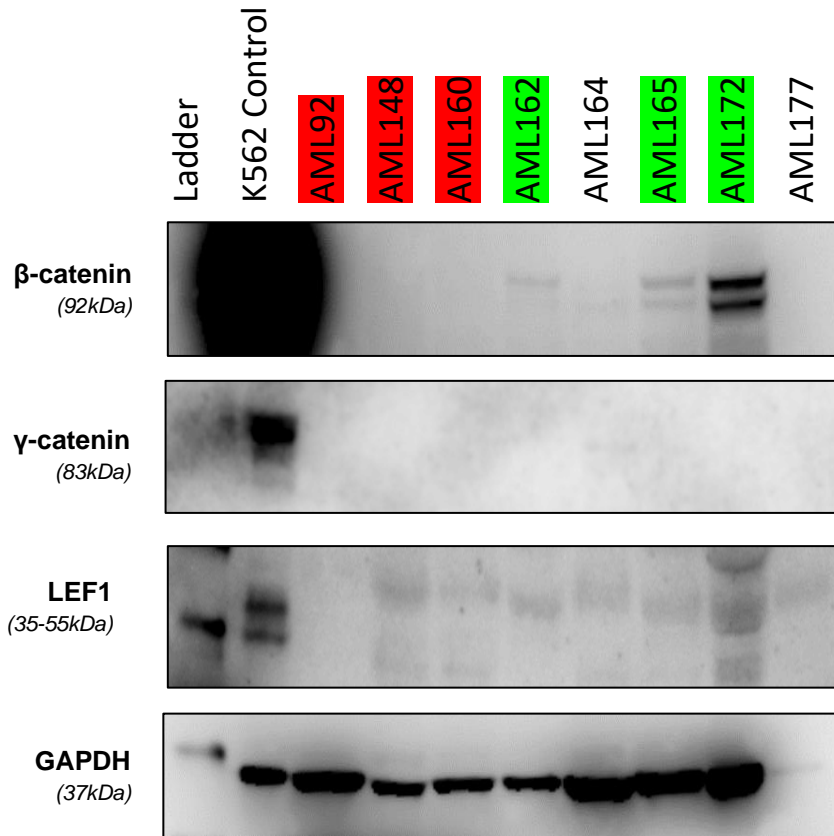


Figure 4-18: Analysis of Primary AML Cultures for WNT/ β -catenin Mediators

Western blot screening of β -catenin, γ -catenin and LEF1 presence in primary AML cultures (2.10). Lysates were kindly provided by Dr Rachael Nicholson and were untreated. K562 was used as a positive control and treated with $5\mu\text{M}$ CHIR for 24-hours before lysates were prepared (2.9.1). GAPDH was used as a loading control (2.10.6). Samples highlighted green indicate those deemed WNT active, whilst those highlighted red are WNT inactive. Those without highlighting are inconclusive owed to either limited protein for assessment (AML177 – see faint GAPDH) or indefinite banding (see potential faint band in AML164 for β -catenin which is at the limit of detection) (n=1).

4.3.5.2 *β-catenin Knockout in Primary AML Does Not Affect AML Maintenance*

Following lentiviral transduction, if the loss of β -catenin was incompatible with normal growth or survival, it would lead to a reduction in the frequency of GFP⁺ cells in the knockout population compared to the scrambled control. To examine this, the proportion of the population documented to be GFP⁺ was examined by flow cytometry relative to a mock over the course of ten days (2.11.7).

No reduction in GFP positivity was noted between knockout and scrambled controls irrespective of WNT-status (**Figure 4-20**). In fact, GFP expression levels increased by approximately 10-15% over the first three days and stabilised thereafter. However, it must be conceded that the GFP⁺ knockout population, which is not a pure, sorted population, will further comprise a combination of complete knockout, incomplete knockout, and unaffected cells which have evaded any InDel event. However, it was anticipated that sufficient complete knockout would occur as to generate a detectable, but not definitive, phenotype.

In order to validate the knockout of β -catenin within the bulk population, cultures were recovered at the end of the proliferation assay for protein analysis by western blot of β -catenin levels. The levels of β -catenin within the knockout population were reduced by 10-60% (**Figure 4-21**). Bulk knockout was proportional to the GFP⁺ transduction rate, with the exception of AML160 which presented with a ~50% reduction in β -catenin, despite only ~5-15% GFP⁺. At the same time, the levels of γ -catenin were considered to determine whether any stabilisation occurred following reductions in β -catenin. As had been observed in AML cell lines (4.3.2), γ -catenin remained undetectable despite reasonable reductions in β -catenin expression levels. Biological repeats would be required to verify these findings.

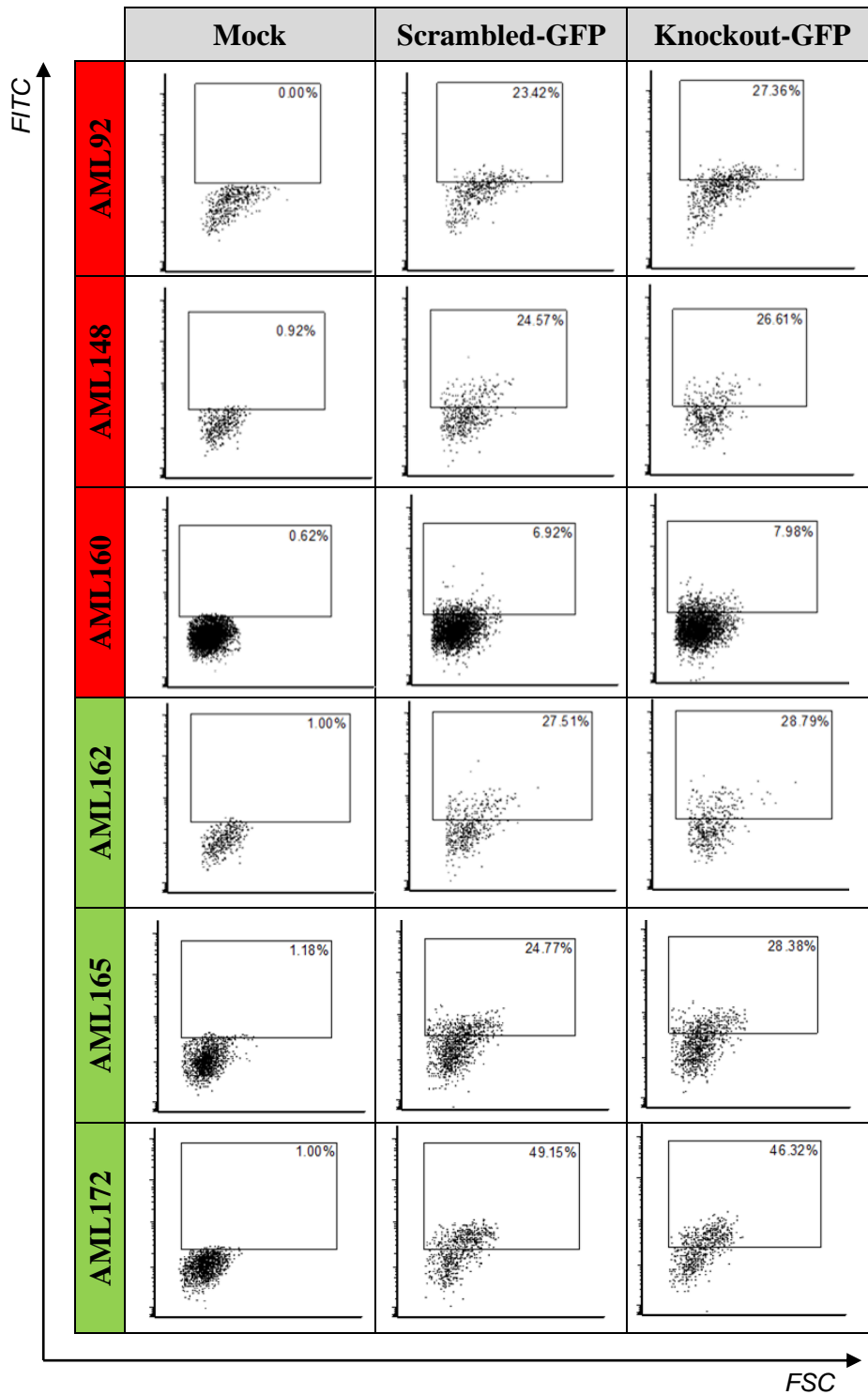


Figure 4-19: Frequency of Lentiviral CRISPR-Cas9 Transduction in Primary AML Cultures

Dot plots demonstrating the transduction efficiency in primary AML samples immediately following a second round of lentiviral transduction, as determined by flow cytometry (2.11). Gates were set against a culture which had been transduced with mock virus (without inclusion of the vector during lentiviral generation) and otherwise processed comparably (2.7). Red facets represent WNT-inactive samples, whilst green facets represent WNT-active samples (n=1).

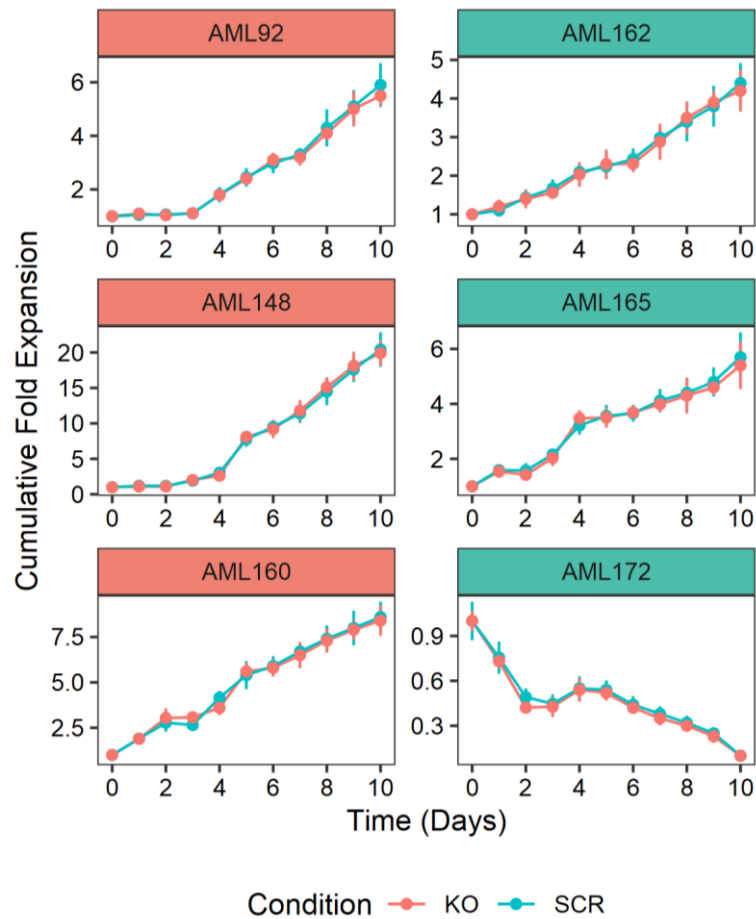


Figure 4-20: Growth of CRISPR-Cas9 Transduced Primary AML Cultures is Unaffected by β -catenin Knockout

Line charts demonstrating growth of primary AML samples *in vitro* in a cytokine enriched medium for ten days following lentiviral transduction with CRISPR-Cas9-gRNA-GFP constructs containing scrambled or *CTNNB1* targeting guide sequences. Growth was examined each day in duplicate by flow cytometry. TOPRO staining was applied to assess viable cells only, which was further gated for GFP+ fluorescence against a reference mock (2.11.6). Red facets represent WNT-inactive samples, whilst green facets represent WNT-active samples (technical n=2, biological n=1; data indicates mean \pm 1SD).

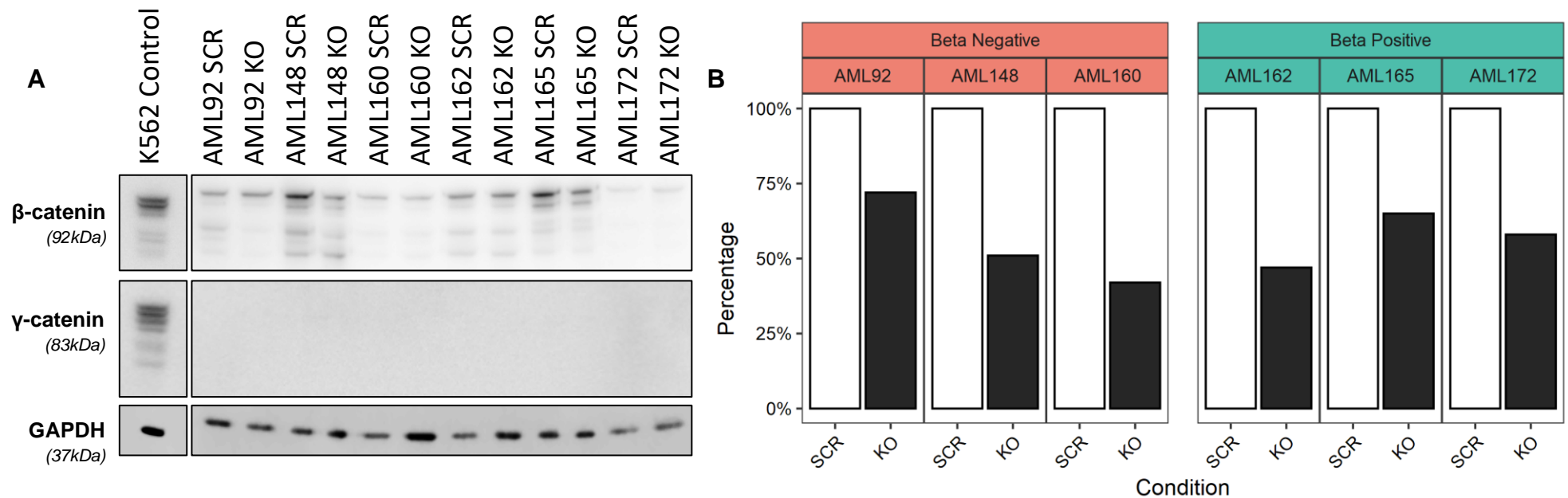


Figure 4-21: Quantification of β-catenin Knockout in Primary AML Samples by Western Blot

A) Western blot analysis of β-catenin and γ-catenin following lentiviral transduction of CRISPR-Cas9-gRNA-GFP scrambled control or *CTNNB1* targeting constructs in primary AML samples (2.8, 2.10). K562 control samples were treated with 5μM CHIR for 24-hours before lysates were prepared (2.9.1). Primary AML samples were prepared on day ten of study with 5μM CHIR for 24-hours, following which lysates were prepared. AML172 was immediately prepared due to the inability to expand this material. GAPDH was applied as a loading control. **B**) Bar plots demonstrating the quantified β-catenin expression following normalisation to GAPDH. Samples highlighted green indicate those deemed WNT active, whilst those highlighted red are WNT inactive (n=1).

4.3.5.3 *β-catenin Knockout in Primary AML Reduces Clonal Growth Capacity*

Next, I examined whether the reduction in clonal efficiency observed in *responder* AML cell lines was recapitulated in primary AML cells (4.3.4.3). The proportion of knockout was approximately consistent with the GFP⁺ hit rate for AML92, AML148, AML162, AML165, and AML172, suggesting these lines were suitable for assessment of clonal dependence.

To this end, following lentiviral transduction, limiting dilution cloning was performed and assessed after 14-days (2.4). WNT-inactive samples had comparable clonal capacity despite β-catenin knockout; however, WNT-active samples were found to suffer significant reductions in clonal efficiency following β-catenin knockout at a bulk level (**Figure 4-22**). Whilst insufficient sample size exists to perform a regression analysis, the approximate reduction in β-catenin determined by western blotting approximately corresponds to the reduction in clonogenicity (**Table 4-4**). Discrepancies with AML160 between GFP⁺ and β-catenin reductions by western blot complicate interpretation, however, remaining lines were sufficient to indicate non-dependency in β-catenin⁻ primary AML. Biological repeats would be required to verify these findings.

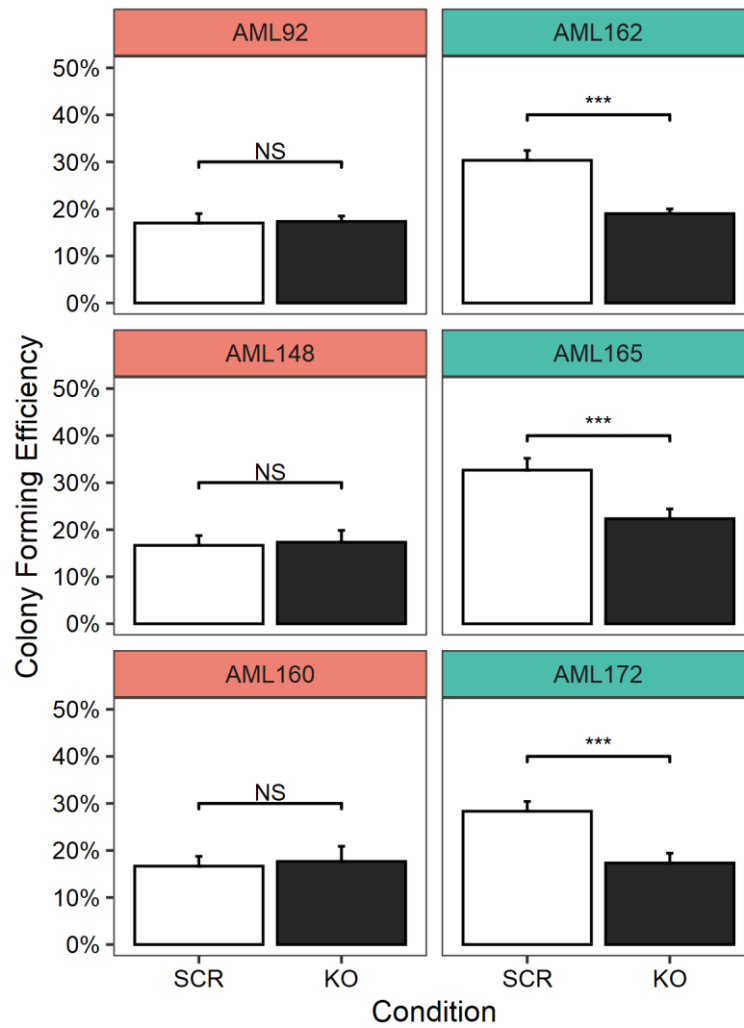


Figure 4-22: Knockout of β -catenin Reduces Colony Forming Efficiency of WNT Active Primary AML Cultures

Scrambled and *CTNBI* CRISPR-Cas9 transduced primary AML lines were examined for clonal growth with the limiting dilution assay on days one, two, and three following lentiviral transduction and scored ten days after plating at 1 cell per well (2.4). A t-test was performed to examine the statistical difference between scrambled and knockout clonogenicity (n=3, data indicates mean +1SD; NS=Not significant, ***<0.001).

Table 4-4: Summary Data for CRISPR-Cas9 Transduced Primary AML samples

Table demonstrating the approximate relationship between transduction rate, as scored by GFP⁺ (2.11) in comparison to a mock, β -catenin reduction, as scored by western blot (2.10), and clonal efficiency reduction, as scored by limiting dilution assay (2.4).

Primary AML	Class	Maximal GFP ⁺	β -catenin Reduction	Clonal Efficiency Reduction
AML92	β -catenin ⁻	~30%	~25%	0%
AML148		~35%	~50%	0%
AML160		~15%	~50%	0%
AML162	β -catenin ⁺	~35%	~50%	~40%
AML165		~35%	~30%	~30%
AML172		~50%	~45%	~37%

4.3.5.4 Targeted WNT/ β -catenin Inhibitors Reduce AML Cell Line Clonogenicity

Whilst CRISPR-Cas9 is beginning to reach clinical application (1.2.7.2), targeting of WNT/ β -catenin signalling could be more easily achieved using available small molecule inhibitors. iCRT3, iCRT14, and LF3 are small molecule inhibitors which specifically block the TCF binding site of β -catenin, resulting in the inability to recruit TCF4 and generate the β -catenin-TCF4:LEF1 transcription complex. The reported IC₅₀ of iCRT3, iCRT14, and LF3 are 8nM, 40nM, and 2 μ M respectively (Gonsalves *et al.*, 2011; Fang *et al.*, 2016).

Before applying these small molecule inhibitors to primary AML cultures, it was necessary to screen an optimal compound concentration for use. This was achieved with the clonal WNT reporter AML cell lines, by performing both proliferation and clonogenicity assays, alongside WNT reporter assessment (2.11.5). The expected outcome of inhibitor treatment (based on the phenotype of the β -catenin knockout cells) is that WNT reporter readouts would be reduced in a dose-dependent manner, proliferation would be unaffected, and clonogenicity would be reduced. However, while WNT reporter levels were reduced with low concentrations of treatment (5nM), levels did not decrease in a dose-dependent manner and were only modestly reduced before non-specific lethality was observed when applied simultaneously with CHIR treatment in HEL and THP1 (**Figure 4-23A**). Several potential mechanisms explain this observation. Whilst it is possible that the inhibitors were metabolised, or expelled through efflux pumps, elevated doses would be expected to eventually overcome this effect. Rather, it is likely that CHIR treatment, which induces stabilisation of β -catenin to levels substantially greater than *in vivo* activity, enables the competitive inhibitors to be overwhelmed. Therefore, the inhibitors are unable to reduce WNT/ β -catenin signalling completely under such a strong stimulus.

A maximum dosage of 5 μ M was selected which represented the highest concentration before lethality. The inhibitors were applied in a proliferation and clonogenicity assay to examine whether comparable findings to the β -catenin knockout setting were demonstrated. As expected, no impact on proliferation or viability was noted *versus* vehicle control, (**Figure 4-23B|C**) whilst clonogenicity was significantly reduced following treatment at 5 μ M in *responder* AML cell lines (**Figure 4-23D**). Clonogenicity was reduced most significantly by iCRT3 (c50% reduction), less so by iCRT14 (c40% reduction), and only modestly by LF3 (c30% reduction) in both HEL and THP1 cells. U937 and MV4;11 were unaffected, as expected based upon knockout data. Notably, clones were still recovered, suggesting WNT/ β -

catenin activity remains despite the presence of inhibitors. As the pBARV lines are clonal, it would not be expected that variations within the cell line enabled a proportion of the population to possess an advantage or evasive mechanism; rather, this suggests that low levels of WNT/ β -catenin signalling activity remain, perhaps as β -catenin stabilisation varies between individual cells.

4.3.5.5 Targeted WNT/ β -catenin Inhibitors Do Not Affect Primary AML Maintenance

Having optimised the targeted inhibitors (4.3.5.4), primary AML samples were thawed and cultured immediately with 5 μ M of iCRT3, iCRT14, and LF3 inhibitors. As was observed in the CRISPR-Cas9 context, application of small molecule inhibitors did not impact proliferation or viability of the cells (**Figure 4-24**). These results support the CRISPR-Cas9 knockout findings and are consistent with the conclusion that β -catenin is not required for AML maintenance in bulk culture conditions. Biological repeats would be required to verify these findings.

4.3.5.6 Targeted WNT/ β -catenin Inhibitors Reduces AML Clonogenicity

To examine whether inhibition of β -catenin:TCF binding impacts AML clonogenicity as was observed with CRISPR-Cas9 knockout (4.3.4.3), limiting dilution cloning was performed in the presence of 5 μ M of iCRT3, iCRT14, and LF3. As had been previously demonstrated (4.3.4.3), application of targeted small molecule inhibitors resulted in a significant reduction in clonogenicity for β -catenin⁺ primary AML samples, whilst no effect was observed in β -catenin⁻ primary AML samples. (**Figure 4-25**). In β -catenin⁺ primary AML samples, iCRT3 reduced clonogenicity by c85%, iCRT14 by 75%, and LF3 by c70%. Collectively, these data demonstrate that WNT/ β -catenin signalling is essential for clonogenicity in AML cell lines and patient-derived primary samples. Therefore, targeting of β -catenin using existing small molecule inhibitors has the potential to significantly decrease cell clonogenicity in AML as a therapeutic approach to improve patient outcome and relapse risk.

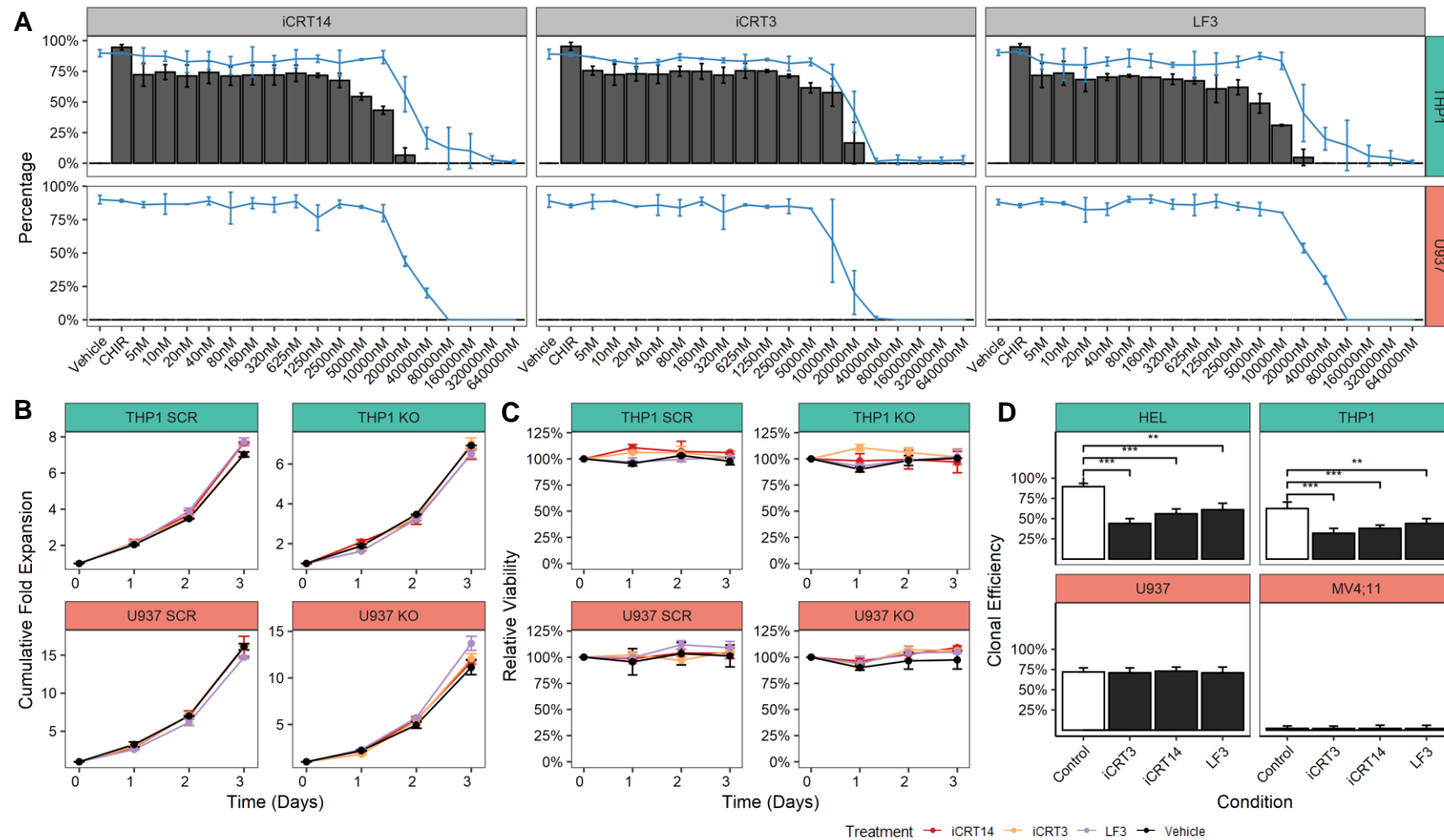


Figure 4-23: Optimising WNT/ β -catenin Inhibitors in AML Cell Lines

A) Drug sensitivity screen of the β -catenin:TCF inhibitors iCRT3, iCRT14, and LF3 scored by WNT reporter readout after 24-hours following simultaneous addition of 5 μ M CHIR, as indicated by the grey bars (2.11.5). Cell viability was examined with TOPRO and is represented by the blue line (2.11.6) (n=3). B) Examination of growth following treatment with WNT inhibitors (5 μ M) or a vehicle control (0.1% v/v DMSO) C) Examination of viability by TOPRO staining as assessed by flow cytometry following treatment (5 μ M) or vehicle. D) Assessment of clonogenicity following treatment (5 μ M) after ten days of culture (n=3, data indicates mean \pm 1SD; ANOVA with Tukey's; *= <0.05 ; **= <0.01 ; ***= <0.001). Green facets represent responder AML cell lines, whilst red facets represent non-responder cell lines.

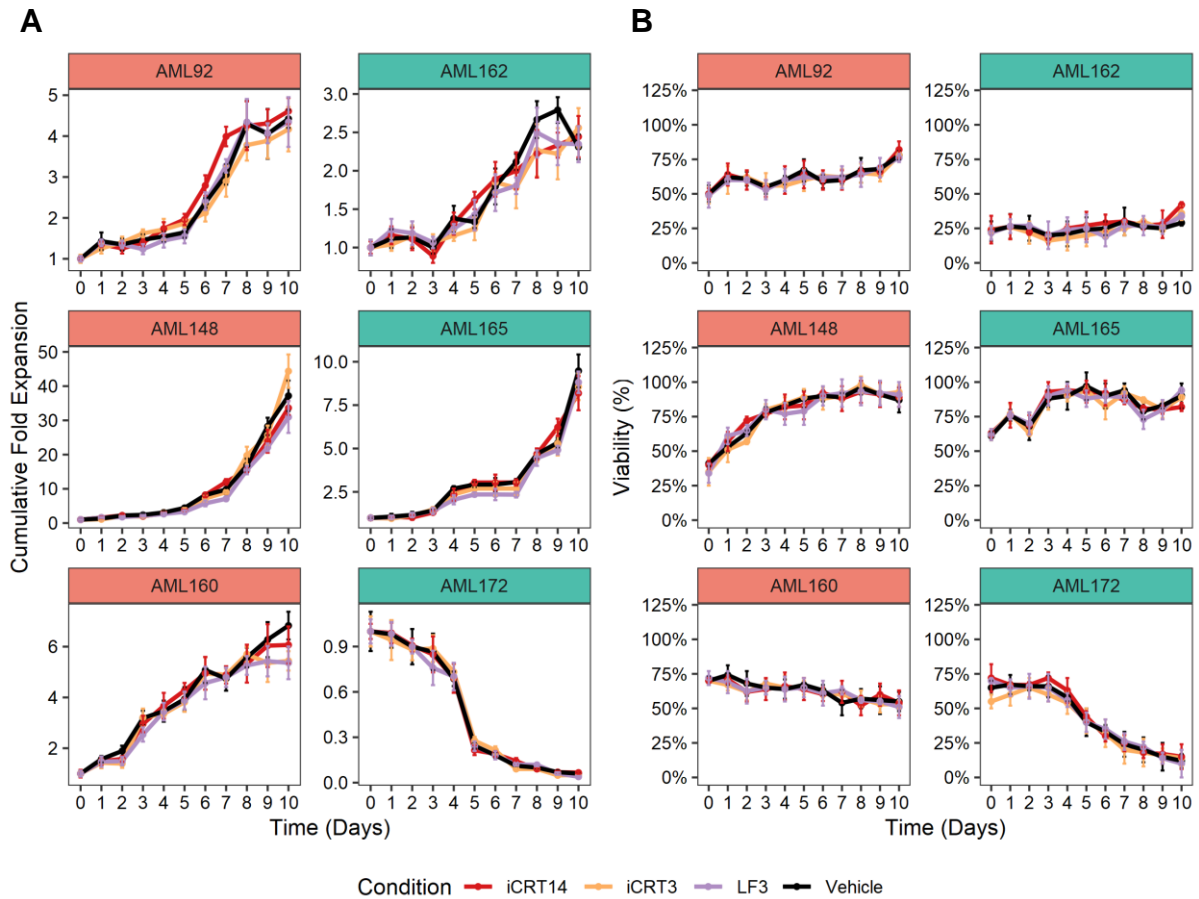


Figure 4-24: β -catenin Inhibitors are Inconsequential to Proliferation and Viability in Primary AML

A) Line charts demonstrating growth of primary AML samples *in vitro* in a cytokine enriched medium for ten days following treatment with 5 μ M WNT inhibitor or a DMSO vehicle control (0.1% *v/v*). Growth was examined each day by flow cytometric counting (2.11.7). **B)** Line charts demonstrating viability of primary AML samples *in vitro* as determined by flow cytometry with TOPRO staining (2.11.6) (technical n=2, biological n=1; data indicates mean \pm 1SD).

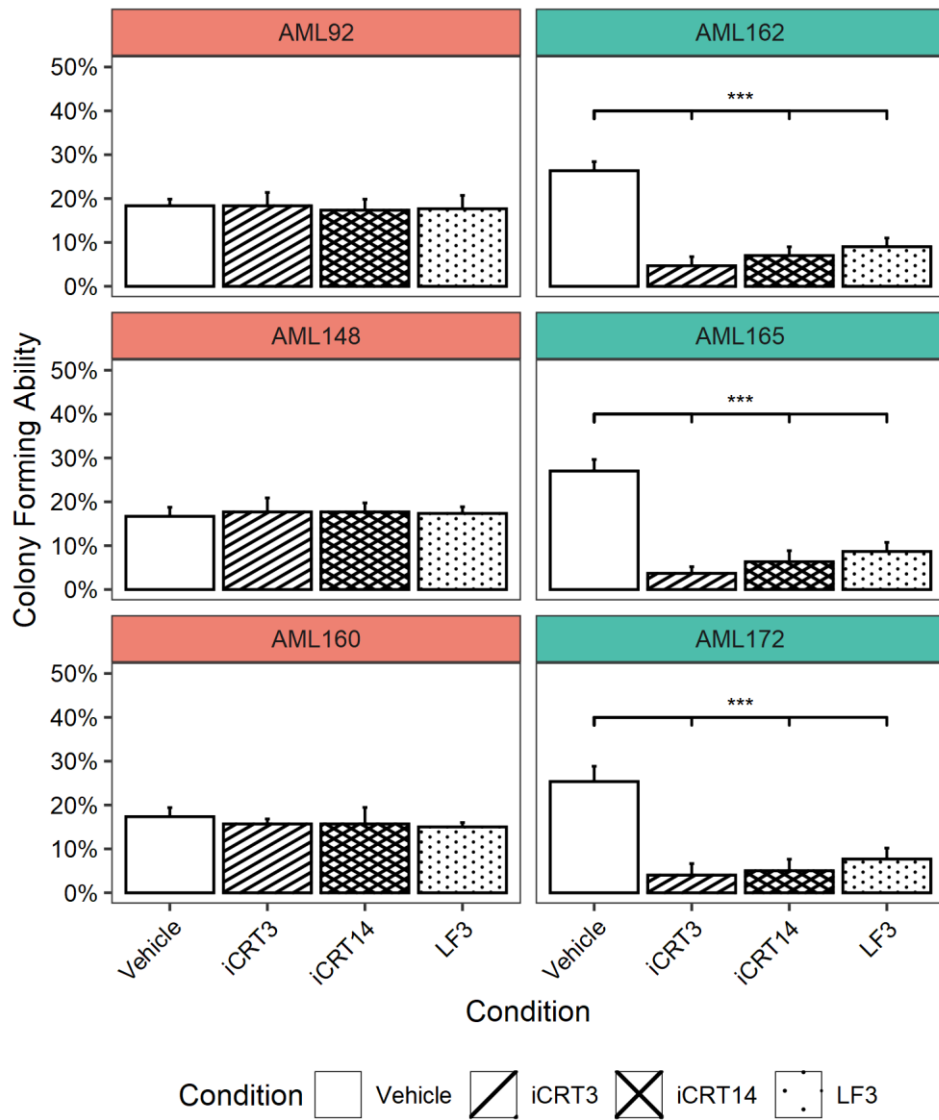


Figure 4-25: WNT/ β -catenin Inhibitors Reduce the Clonogenicity of Primary AML

Primary AML samples were incubated with 5 μ M of the indicated WNT inhibitors or vehicle control (0.1% DMSO *v/v*) and plated at a density of one cell per well to assess colony forming efficiency (2.4). After fourteen days, colonies were scored by light microscopy. Red facets represent β -catenin⁻ samples, whilst green facets represent β -catenin⁺ samples (4.3.5) (n=3, data indicates mean +1SD; ANOVA with post-hoc Tukey was performed; ***<0.001; ANOVA with post-hoc Tukey)

4.4 Discussion

In the previous chapter, β -catenin, but not γ -catenin, was associated with a significant reduction in clonogenicity, impacting the generation of complete knockout clones (3.6, 3.7). As clonogenicity is a central feature of leukaemia, which often relapses due to self-renewal characteristics of LSC, establishing the conditions necessary to rescue a complete dual knockout clone was critical to further investigation. To explore this, several experiments were designed to recover clones through supplemented and assistive conditions, through the addition of cytokines and CM, or supportive co-culture, respectively.

Cytokine network deregulation is often observed in AML patients, and has previously been shown to convey prognostic value (Sanchez-Correa *et al.*, 2013; Binder *et al.*, 2018). Further, Yeung *et al.* reported diminished cytokine independence in a murine model of AML, when β -catenin was knocked down by >80% (Yeung *et al.*, 2010). This study determined that cytokine supplementation of fresh media with IL-3, IL-6, SCF, GM-CSF, TPO, G-CSF, FLT3, and M-CSF did not improve cloning efficiency, suggesting cytokine dependence is not the mechanism by which clones are lost (4.3.1.1). It is possible that other cytokines, which were not considered, could represent the critical factor; for instance, studies of AML patient samples have found TNF- α , IL-1 β , IL-4, IL-5, IL-8, and IL-12p70 were elevated and associated with disease severity (Sanchez-Correa *et al.*, 2013; Binder *et al.*, 2018). Additionally, experiments with CM similarly failed to rescue clones, both with and without stimulation with CHIR. These findings indicate that complete knockout clones require contact interaction for survival. Alternatively, within the *in vivo* context, stromal components provide cells with WNT factors which are reported to be short-range and labile (Tamai *et al.*, 2004; Boutros *et al.*, 2016; Farin *et al.*, 2016; Seth *et al.*, 2016). It is possible that a factor provided by WT or incomplete knockout cells was able to support the knockout cells during co-culture, but that these are rapidly depleted or inactivated, and as such they cannot sustain knockout clones during cloning when provided in CM.

To address both contact deficiencies and to provide continuous cytokine stimulation, murine marrow stromal (MS-5) cells were co-cultured with knockout clones. MS-5 cells have known ability to amplify HSC survival and to improve colony forming capacities (Lee *et al.*, 2015). As the human BM stroma consists of numerous cell types and an extracellular matrix, comprising a microenvironment niche which modulates quiescence, self-renewal, and lineage commitment, closely replicating these conditions *in vitro* could assist in recovering knockout clones. However, when cultured with MS-5 cells, a reduction was noted to scrambled clonal

efficiency (4.3.1.2). Biologically, this could be due to incompatibilities between murine and human cells. Human-derived stromal HS-5 cells provided similar characteristics to the microenvironment niche and are reported to generate and excrete WNT ligands in exosomes which enhance clonogenicity (Gross *et al.*, 2012; Johnson *et al.*, 2014). HS-5 were found to be compatible with AML cell lines in co-culture and increased clonal recovery. However, a difficulty with HS-5 co-culture was the observation of cobblestone formation of the AML cells. As HS-5 were treated with mitomycin-C to prevent their growth, this was not caused by outgrowth of fibroblasts, but rather ‘burrowing’ of AML cell lines beneath the monolayer. This complicated rescue of cells for replating, as demonstrated by the reduction compared to monoculture scrambled cloning.

Co-culture with parental cells was next examined, which circumvented issues with recovery. Parental co-culture was found to completely recover knockout clones, as determined by DsRed positivity, with concomitant absence of a flow-based reporter readout after CHIR treatment. These newly generated *responder* knockout clones were recovered by FACS (4.3.2). Putative knockout clones were assessed by western blotting, thus enabling the detection of clones which had absence of both β -catenin and γ -catenin and exclusion of false-negatives arising from silencing of the flow-based reporter in some clones. Candidate clones were subsequently assessed by targeted DNA-seq flanking the InDel site, revealing the exact nature of the InDel present and establishing true complete knockout clones. Whilst aneuploidy is observed in only 20% of AML patients, it is a more common feature of AML cell lines as a result of their greater genetic instability (Simonetti *et al.*, 2019). It was further anticipated that additional copies of chromosome three (*CTNNB1*) and chromosome seventeen (*JUP*), alongside potential double minutes, would result in the observation of differing numbering of Sanger tracks between cell lines for each respective allele (2.12.3.6). Whilst MV4;11 has a diploid karyotype, U937, THP1, and HEL are aneuploid and are expected to possess three copies of chromosome three. However, the presence of greater than two alleles was only observed for THP1 with *CTNNB1*.

It is not possible to confidently conclude a specific karyotype of a cell line due to the continuing evolution of cell line genomes over time *in vitro* giving rise to differences between tissue bank collections; in fact, ancestry analyses have revealed branching points between suppliers based on the accumulation of *in vitro* variances (Mackinnon *et al.*, 2013; MacKinnon *et al.*, 2020). For instance, U937 was first described in 1976 (Sundstrom, 1976), but its karyotyping from different laboratories in 1988 revealed divergent profiles (Shipley *et al.*,

1988), which has further branched in the years since (Matteucci *et al.*, 2002). This is most extreme for the THP1 cell line, which was established in 1980 with a near-diploid karyotype (Tsuchiya *et al.*, 1980), but branched into THP-1-R and THP-1-Cs5; THP-1-R was characterised as near-tetraploid (Hyodoh, 1987), whilst THP-1-R was characterised as hypotriploid in 2000 (Odero *et al.*, 2000). Both forms of THP1 are sold and often published without regard of the subtype, with ATCC selling the hypotriploid variant (Adati *et al.*, 2009), whilst the DSMZ supplies the near-tetraploid variant (Hultmark *et al.*, 2021). HEL and U937 were recently fully characterised and displayed similar variances (Mackinnon *et al.*, 2013; MacKinnon *et al.*, 2020). Alternatively, the discrepancy between expected allele number can be explained by the presence of identical InDel. Single-nucleotide InDel are the most frequently observed consequence of CRISPR-Cas9-induced DSB, and account for approximately 70% of resulting effects (Chakrabarti *et al.*, 2019). Nonetheless, this study was able to establish complete dual knockout clones for further study.

The necessity of β -catenin and γ -catenin in AML maintenance remains a contentious topic within the literature. Views are polarised between β -catenin proving dispensable for AML maintenance, whilst others report β -catenin is integral to maintaining AML. Here, the generation of complete dual knockout clones added further evidence that both catenin members, and more broadly WNT/ β -catenin signalling, are dispensable for AML maintenance. Individually, γ -catenin knockout did not reduce the flow-based reporter activity levels (4.3.4.2), nor was γ -catenin able to act compensatively to β -catenin during limiting dilution cloning (4.3.4.3). That β -catenin and γ -catenin are not required at the bulk culture level in AML cell lines agrees with studies which obtained a high degree of knockdown, without observing any resulting phenotype. These findings also suggest that changes in phenotype arising from RNA or β -catenin binding inhibition in cell lines that have no documented capacity to translocate β -catenin are likely due to off-target effects. Gandillet *et al.* reported that shRNA-mediated knockdown of β -catenin in the responder cell line HL60 reduced expression levels by 70%, and resulted in minor reductions to proliferation rate and elevated cell apoptosis, though no changes were observed in cell cycle (Gandillet *et al.*, 2011a). Siapati *et al.* reported β -catenin knockdown at the protein level by 40% in U937, a line deemed a non-responder in this study, resulting in reduced proliferation, cell cycle arrest in G1, and increased apoptosis, yet no change to TCF4 or LEF1 expression (Siapati *et al.*, 2008). Evidently, based upon the findings here that U937 is a non-responder, it would be unexpected the latter would have consequence, whilst the minor impacts noted in the former suggest a mild off-target effect. Fortunately,

CRISPR-Cas9 has negligible off-target activity in comparison with alternate methods, which have frequent off-target effects often exceeding on-target effects (Smith *et al.*, 2017; Subramanian *et al.*, 2017). *In vivo* findings have been speculated to be due to the generation of truncated dominant negative β -catenin protein as a result of Cre-Lox methods, which possess unintended adverse effects, leading to consequent effects to proliferation, apoptosis, and cell cycle which have been misinterpreted as dependency (X. Zhao *et al.*, 2020).

Here, study of dual knockout of β -catenin and γ -catenin in AML cell lines investigated proliferation, apoptosis, cell cycle condition, basic morphological features, and a panel of immunophenotypic markers both expected to be expressed, and indicators of differentiation. No resulting perturbation was documented because of dual catenin knockout (4.3.4.1) in any of the parameters mentioned. These findings support prior studies in which knockdown of β -catenin had no consequence in AML (Kim *et al.*, 2002; Cobas *et al.*, 2004a; Gandillet *et al.*, 2011b; X. Zhao *et al.*, 2020).

In addition to speculated contributions to AML maintenance, WNT/ β -catenin signalling, and γ -catenin, have independently been proposed as driving chemoresistance in AML (Wang *et al.*, 2018; Zhao *et al.*, 2018; Perry *et al.*, 2020). It has been shown that β -catenin and γ -catenin can independently promote mechanisms resulting in resistance to Ara-C or DNR, amongst other agents, through chemotherapeutic induction of a WNT/ β -catenin signalling response (Martin-Orozco *et al.*, 2019), necessitating investigation. Here, no sensitisation of AML cell lines to DNR or Ara-C in the context of dual knockout, regardless of classification, was documented, nor was a WNT/ β -catenin signalling response induced (4.3.4.4). These findings suggest that the heightened expression of the WNT target gene *ABCB1*, encoding PGP, in *responder* AML cell lines (S2.), and established in the literature for facilitating chemoresistance of numerous cancers (Lim *et al.*, 2008; Corrêa, Binato, Du Rocher, Morgana T.L. Castelo-Branco, *et al.*, 2012; Riganti *et al.*, 2013; Staal *et al.*, 2016), was not impacting drug resistance in the context of these cell line models, with the caveat that expression of PGP was not validated at the protein level within this study. PGP was not explored further as recent research has demonstrated poor results in clinical trials (Cripe *et al.*, 2010) with no direct link between PGP activity and DNR drug resistance established in AML patients (Boyer *et al.*, 2019). As PGP activity remains a validated indicator of prognostic outcome, and it has been found that the *ABCB1* gene is expressed in close correlation with *BAALC*, *CD34*, *CD200*, and *CD7*, PGP activity is perhaps a passenger characteristic for high-risk AML (Boyer *et al.*, 2019).

Further evidence in the literature supports WNT/ β -catenin signalling activity as secondary to chemoresistance mechanisms. Ubiquitin-specific protease 7 (USP7) is a member of the deubiquitinating enzyme family and is highly expressed in relapsed AML (Cartel *et al.*, 2021). USP7 is reported to participate in the regulation of apoptosis and senescence through modulation of the p53 pathway (An *et al.*, 2017). USP7 can further promote WNT/ β -catenin signalling activity by deubiquitinating β -catenin (Novellademunt *et al.*, 2017), and its inhibition was found to sensitise primary cells and AML cell lines (HEL, HL-60) to Ara-C, thus inhibiting WNT/ β -catenin signalling, and reducing colony-forming potential (Cartel *et al.*, 2021). Overexpression of USP7 would provide LSC with chemoresistance properties, whilst simultaneously upregulating WNT/ β -catenin signalling promoting survival and self-renewal ability. A further example of concurrent chemoresistance and WNT promotion is CD44, which is overexpressed in LSC and is established as a poor prognostic indicator in AML (Legras *et al.*, 1998; Jin *et al.*, 2006). CD44 is documented to upregulate the expression of cell cycle inhibitors, anti-apoptotic proteins, ABC transporters, alongside simultaneous promotion of WNT/ β -catenin signalling through LRP6 activation (Schmitt *et al.*, 2015). It has been suggested that LSC require interaction with a niche to maintain stem cell properties in an *in vivo* study which documented that CD44 inhibition eradicates LSC (Jin *et al.*, 2006). The secondary promotion of WNT/ β -catenin signalling was not considered, but it is possible that CD44 inhibition also reduced WNT/ β -catenin signalling activity, contributing to LSC eradication. Curiously, anti-CD44 experiments were found to induce differentiation in AML cell lines which were found to be responders in this study (THP1, KG1a, and HL60) (Gadhoum *et al.*, 2016). A separate study found HS-5 stromal co-culture rescued AML cell lines from anti-CD44 induced differentiation; again, the involved cell lines were established as responders in this study (THP1, HL60, NB4). These findings could be due to loss of WNT/ β -catenin signalling augmented by CD44, which was rescued through stromal co-culture (Chen *et al.*, 2015).

Whilst it is disappointing that AML cell lines demonstrated no dependency on β -catenin or γ -catenin for maintenance, tolerance of stress conditions, or as a mechanism of chemoresistance, a limitation of these *in vitro* findings surrounds the concern that β -catenin, and hence WNT/ β -catenin signalling activity, is very low in expression in AML cell lines, which is supported in the literature (Morgan *et al.*, 2019), and in public proteomic databases (Ghandi *et al.*, 2019; Nusinow *et al.*, 2020). This suggests that AML cell lines are perhaps not representative of the patient context in this respect. To this end, primary AML samples were

investigated for β -catenin expression, response to CRISPR-Cas9-induced β -catenin knockout, and response to small molecule inhibitors. Primary AML samples were found to express β -catenin at heterogeneous levels, thus enabling the classification of a panel of samples as β -catenin⁺ and β -catenin⁻, suggesting that *responder* and *non-responder* phenotypes may also exist in patients (4.3.5). Subsequent knockout of β -catenin with CRISPR-Cas9 did not affect AML maintenance (4.3.5.2), nor when treated with three small molecule inhibitors of β -catenin:TCF interaction. A recent *in vivo* murine study has shown that knockout of β -catenin was unnecessary for AML onset, maintenance, and LSC self-renewal (X. Zhao *et al.*, 2020). The authors additionally examined the downstream TCF/LEF family of transcription factors (TCF1, TCF3, TCF4, and LEF1), and found simultaneous knockout of these members was redundant in AML. However, this research used the potentially incomplete *Cre-lox* knockout methodology, and was only capable of representing the murine MLL AML model, which accounts for a mere 5-10% of human AML (Basecke *et al.*, 2006).

A consistent effect within the *responder* AML cell line population was the absolute, continual inability for complete β -catenin knockout *responder* AML cells to clonally grow, which represents an advancement of previous reports that shRNA knockdown in cell lines lead to reductions in cloning efficiency (Gandillet *et al.*, 2011b). The knockout was replicated at bulk level in primary AML samples with CRISPR-Cas9 which demonstrated a significant reduction in clonal growth capacity was documented only in β -catenin⁺ primary AML lines (4.3.5.3), supporting the AML cell line findings. These findings were reproduced with three small molecule inhibitors of β -catenin:TCF interaction, demonstrating clinical translatability, which is consistent with recently published findings (Pepe *et al.*, 2022) (4.3.5.6). Collectively, these findings conclusively expose β -catenin as indispensable for a subset of AML patients with regard to clonogenicity. Similarly, the application of targeted small molecule inhibitors of the WNT/ β -catenin pathway has significantly reduced the self-renewal capacity of cancer stem cells in CRC, HCC, lung cancer, breast cancer, and bowel cancer (Fang *et al.*, 2016; Hwang *et al.*, 2016; Kim *et al.*, 2016; Löcken *et al.*, 2018; Cheng *et al.*, 2019). The results within this study suggest comparable benefit could exist for AML with particular regard to disease relapse; however, further research in an *ex vivo* or *in vivo* method would be required to substantiate this, which is unfortunately beyond the scope of this research.

Together, these results disagree with a recent publication, which is the only other published study to apply CRISPR-Cas9 to target *CTNNB1* in AML cell lines (Saenz *et al.*, 2019). The

central focus of the Saenz publication covered drug-mediated β -catenin inhibition with BC2059, but also included use of CRISPR-Cas9. Saenz *et al.* established a dose-dependent anti-leukaemic effect of BC2059, furthered by CRISPR-Cas9 knockout, which showed that after five passages (approximately fifteen days), the HEL bulk knockout culture completely began to collapse over the subsequent twelve days in a viability assay. No explanation was offered for the delay in lethality, nor why the entire population collapsed in an incomplete knockout model. If β -catenin knockout is incompatible with survival, these cells would not have survived the approximately fifteen days of culture necessary to progress through selection prior to the viability assessment over five subsequent passages considering the half-life of β -catenin is <1 hour (Aberle *et al.*, 1997; Stamos *et al.*, 2013). Consequently, bulk knockout cultures will never completely collapse as a proportion of the population will invariably possess unaffected or one functional allele. This proportion, which is perhaps around half of the culture in the authors conditions, would have expanded and repopulated the culture before the initial five passages were completed, and certainly during the two-week viability assay. Methodologically, Saenz *et al.* nucleofected HEL cells with three anti-*CTNNB1* gRNA and Cas9 before a three-day puromycin selection. Critically, complete knockout cell lines were not generated but rather the bulk knockout condition was examined. Saenz *et al.* reported incomplete knockout HEL cultures had ‘depleted’ β -catenin protein, despite detectable protein levels by immunofluorescence microscopy. Moreover, Saenz *et al.* did not quantify the remaining β -catenin protein levels nor examine the DNA, but through densitometric assessment of the provided representative confocal images, I determined β -catenin had been reduced by c40% when compared to scrambled control levels. Considering three gRNA had been applied, the level of knockout achieved is poor and, fundamentally, knockout and an incompletely ‘depleted’ state are not comparable.

Mechanistically, CRISPR-Cas9 mediated knockout will never achieve complete knockout of a gene within all target cells due to numerous escape mechanisms which enable the continued expression of WT, or near WT, functional protein. Escape methods include component silencing, silent mutations, synonymous mutations, in-frame InDel, translation reinitiation, biological plasticity (exon skipping), alongside other considerations (Mianné *et al.*, 2017; García-Tuñón *et al.*, 2019; Smits *et al.*, 2019). Therefore, it is a certainty that a proportion of the cells which incorporate the selection marker will not experience loss of functional protein. A consensus has been reached that the non-clonal application of CRISPR-Cas9 to generate InDel should be assessed by Sanger spectrogram analysis to determine

knockout rate, rather than potentially misrepresentative techniques such as western blot, immunofluorescence microscopy, or qPCR (Bloh *et al.*, 2021; Conant *et al.*, 2022). Saenz *et al.* did not disclose critical information which would allow their application of CRISPR-Cas9 to be assessed. For example, the gRNA target sequences or even target exon(s) were not disclosed, which would inform whether alternative splice variants could circumvent knockout. Further, they disclose that each *CTNNB1* gRNA plasmid independently harboured Cas9 and puromycin resistance, and as such, this does not represent a true multi-guide approach, and the resulting selection would recover even single gRNA incorporating cells; this explains the poor knockout achieved. A true multi-guide approach typically incorporates tandem gRNA separated by a T2A self-cleaving peptide, or alternate promoter sites, ensuring each cell has equivalent components, which target immediately adjacent sites to enhance InDel generation. The authors do not state whether they controlled for the fact three plasmids were utilised in the *CTNNB1* knockout nucleofection method *versus* one in the scrambled population. Excessive plasmid input in electroporation can be cytotoxic even with very small increases to loading, which could explain these findings (Lesueur *et al.*, 2016; Chicaybam *et al.*, 2017; Batista Napotnik *et al.*, 2021). However, it is more likely that these findings are an artefact as only a technical replicate was performed, further, such observations should never occur with CRISPR-Cas9 methodology unless a particular protein has an extended half-life enabling latency before a phenotype emerges as existing protein is depleted, at which point loss of knockout cells will occur and haplosufficient or CRISPR-Cas9 escape cells will repopulate the culture. The turnover of β -catenin within a cell has been established to be within 24 hours, negating any concern of residual, supportive β -catenin enabling survival of cells following selection (Mo *et al.*, 2009).

The discrepancies between the finding that β -catenin knockout was incompatible with clonal growth represent an *in vitro* finding which is perhaps not replicated in the *in vivo* condition, as recently observed (X. Zhao *et al.*, 2020). Cells within the microenvironment would assist clonal growth, which was the case even with dual knockout *non-responder* U937 cells, demonstrating the rescue effect is not WNT-mediated. However, this would rely upon LSC migration to a supportive microenvironment niche, which could explain discrepancies between *in vivo* studies (Jin *et al.*, 2006; Lane *et al.*, 2011; Ruan *et al.*, 2020). Further, LSC self-renewal is assessed through the injection of between 10^3 and 10^4 cells *in vivo*, rather than a single LSC alone, and hence the chance of an LSC reaching a sustaining microenvironment is perhaps high, and LSC may sustain one another despite knockout. However, a representative

number of LSC is impossible to determine at current, as the definition of an LSC is in dispute and as such the population size of the pool is inconclusive due to the different approaches applied to estimate the LSC pool in patients (Marchand *et al.*, 2021). The *in vitro* to *in vivo* discrepancy was recently reproduced in a publication studying the novel WNT inhibitor WNT974 (porcupine inhibitor), which resulted in a significant reduction in clonogenicity *in vitro* (75-90%) that was not reproducible in an *in vivo* murine model (Pepe *et al.*, 2022). No other effect was observed in cell lines *in vitro*, nor was an effect on overall survival or engraftment after re-transplantation noted, despite application of WNT974 at doses in excess of human tolerance, enabling the authors to conclude WNT inhibition was not limited by poor pharmacokinetics or pharmacodynamics; rather, alternate pathways were sustaining cells or, as the study here-in suggests, WNT/ β -catenin signalling is not required unless cells are spatiotemporally isolated. Nonetheless, the findings of elevated WNT/ β -catenin signalling activity at relapse suggests a contributory effect even if the pathway is not completely essential, perhaps through activation of a secondary pathway.

In conclusion, the mechanism through which β -catenin knockout was incompatible with clonal growth remains elusive despite substantial efforts to provide supplementary cytokines, examine differentiation status, or stress effects, and as such, a transcriptomic analysis by RNA-seq is necessary in order to best capture the full consequence of knockout. Identification of the precise mechanism by which cells are sustained by WNT/ β -catenin signalling could further explain the *in vitro* to *in vivo* discrepancy, thereby revealing potential new and more effective therapeutic targets. This will be explored in **Chapter 5**.

Chapter 5

A WNT/beta-catenin/RAP1 signalling axis in AML

5.1 Introduction

In previous chapters, knockout of β -catenin, the central mediator of WNT/ β -catenin signalling, was shown to be incompatible with clonal growth, but did not perturb the AML phenotype within the bulk culture in terms of proliferation, cell cycle, apoptosis, and differentiation (4.3.4). Considering that *in vitro* methodologies to study a single cell or even a low number of cells are limited and challenging, the study progressed to examine the impact of dual catenin knockout on the transcriptome of these cells to understand the mechanism by which clonogenicity process is affected. Transcriptomic analysis represents an unsupervised method to examine the entire transcript expression profile of the cells, enabling the assessment of genes and pathways which might not necessarily be considered related to WNT/ β -catenin signalling based on current biological understanding. Whilst the methodology underlying RNA-seq has become highly standardised in recent years, bioinformatic analyses have improved to better incorporate and interpret biological features (Rahman *et al.*, 2015; J. Ma *et al.*, 2019; Liao *et al.*, 2019). Classical methods, such as ORA and GSEA, can reveal pathways of interest; however, they do not consider the constituent member interactions and, therefore, cannot determine true directionality (Koumakis *et al.*, 2016; Yang *et al.*, 2019). Next-generation pathway techniques, such as SPIA and MinePath, are capable of considering mechanistic interactions between proteins, referred to as network topology, which allows more precise mapping of differentially expressed genes to reveal a pathway activation state, resulting in substantially more information regarding the underlying biology involved (Koumakis *et al.*, 2016; Domingo-Fernández *et al.*, 2019b; Yang *et al.*, 2019; Geistlinger *et al.*, 2021).

5.2 Aims

This study hypothesises that dual β -catenin and γ -catenin knockout silences WNT/ β -catenin signalling activity and perturbs the activity of specific genes and related pathways. In turn, these changes are responsible for the loss of clonogenicity observed in previous chapters (4.3.4.3). The main aim of this chapter is to examine the mechanistic basis for this observation using transcriptomic profiling of scrambled cells treated with rWNT3a, anticipated to activate WNT/ β -catenin signalling, as compared to dual β -catenin and γ -catenin knockout cultures which are incapable of WNT/ β -catenin signalling activation.

Objective 1: Conduct RNA-seq in β -catenin and γ -catenin knockout in AML cell lines.

Total RNA will be extracted from HEL and THP1 dual β -catenin and γ -catenin knockout or scrambled control clones, along with cells treated with the WNT ligand rWNT3a (or vehicle), to examine the impact on WNT/ β -catenin signalling. Following sequence quality assessment, mRNA samples will be shipped to Novogene for library preparation and RNA-seq.

Objective 2: Determine the genes and pathways activated by rWNT3a treatment and perturbed as a result of dual knockout.

Differentially expressed genes and the entire transcriptomic dataset will be used to perform pathway analysis techniques (ORA, GSEA, GSVA, SPIA, Minepath) against independent pathway databases to fully dissect the transcriptomic consequences of rWNT3a stimulation and β/γ -catenin knockout in AML. This analysis will range from the classical widely applied techniques to next-generational methods. These results will be contrasted with the CCLE data, and finally public patient TCGA data, enabling identification of clinical relevancy by comparing gene expression profiles with clinical survival outcomes.

Objective 3: Investigate pathways of interest perturbed by dual-catenin knockout and verify roles in clonogenicity disruption *in vitro*

Speculatively identified genes and pathways identified in dual β -catenin and γ -catenin knockout cells will be examined *in vitro* to confirm *in silico* findings. Modulation of the respective genes and pathways through incorporation of constitutively active forms, or by gene expression regulator technologies such as CRISPRa-dCas9 and CRISPRi-dCas9 will determine the specific contributions of specific genes and whole pathways to clonogenicity in AML. By extension, these *in vitro* experiments should reveal precise downstream partners of WNT/ β -catenin signalling with critical roles in AML.

5.3 Results

5.3.1 Preparation of samples for RNA-Sequencing

To identify the changes associated with dual β -catenin and γ -catenin knockout at the transcriptomic level in *responder* AML cell lines, it was necessary to examine the transcriptomic profile of WNT-active and knockout cell lines. To achieve this, cells were cultured with rWNT3a, rather than CHIR, as rWNT3a is a natural ligand for WNT signalling activation, whilst CHIR is a potent GSK3 α/β inhibitor with established non-relevant off-target effects, as described in the literature (Naujok *et al.*, 2014; Laco *et al.*, 2018; Merenda *et al.*, 2020; Miao *et al.*, 2020). The full experimental design has been represented in **Figure 5-1**.

Biological replicate dual CRISPR-Cas9 β -catenin and γ -catenin knockout clones were selected for RNA-seq, with the exception of HEL, in which only one dual β -catenin and γ -catenin knockout clone was derived, alongside scrambled control clones. In THP1, scrambled clones 1 and 2, alongside dual knockout clones 29 and 47 were used; in HEL, scrambled clones 1 and 2, and dual knockout clone 17 was applied (**Table 4-3**). These were cultured with and without rWNT3a (1 μ g/mL) for 24-hours, thus enabling an immediate assessment of WNT/ β -catenin signalling response by the flow-based reporter assay, followed by RNA extraction. THP1 scrambled cultures showed a response to rWNT3a ligand (**Figure 5-2**) whilst HEL, however, did not respond to rWNT3a treatment when measured with the WNT reporter, possibly due to the absence of receptor for this ligand in the clonal pBARV parental line. RNA was isolated and assessed for quality by spectrophotometry (Nanodrop method) and by electrophoresis (Agilent 2100 Bioanalyzer method), revealing recovery of abundant, pure RNA. Total RNA samples were sent to Novogene, where they were also examined for RNA QC (**Table 5-1**), prior to library preparation, mRNA enrichment, cDNA synthesis, adapter ligation, fragment PCR, and RNA-seq.

5.3.1.1 Pre-processing of Raw RNA-Sequencing Data

RNA-seq relies upon accurate sequence read alignment to a reference genome, with the sequencing in this experiment performed in a paired format, thus increasing the accuracy of resulting sequence calls (Liao *et al.*, 2019). Novogene performed the pre-processing of RNA-seq data, including library preparation, in which sequencing adapters were ligated to each 150bp sequence, followed by trimming with Trimmomatic (v0.39), prior to alignment. During

this process, filtering to remove poor quality reads was also performed. The pre-processed data was aligned to the GRCh38.p13 genome using Spliced Transcripts Alignment to a Reference (STAR, v2.5), and aligned reads were converted to counts with HTSeq (v0.6.1). At this stage, the count data was returned from Novogene. This study analysed the alignment and quantification, which were deemed to be acceptable, using MultiQC (v1.10.1). The error rate was consistently low and minimal filtering was necessary (**Table 5-2**); moreover, STAR alignment successfully mapped most of the sequences to unique regions (**Table 5-3**). These results demonstrate a successful RNA-seq run has been performed by Novogene. Resulting counts demonstrated a comparable distribution between samples, with only a small proportion of the overall transcriptome in active expression. The low abundance genes were filtered out before differential expression analyses was performed, thus ensuring maximal statistical power to capture the significantly DET. Accordingly, the data was successfully prepared for downstream analysis. Reads were filtered with the standard cut-off of less than ten total reads across all samples. This removed 40,531 transcripts, leaving 18,204 for subsequent analysis (**Figure 5-3**). The filtered data was then normalised, and log transformed. As these samples were sequenced on the same flow cell, minimal normalisation was necessary, as indicated by the boxplot of library sizes shown in **Figure 5-4**.

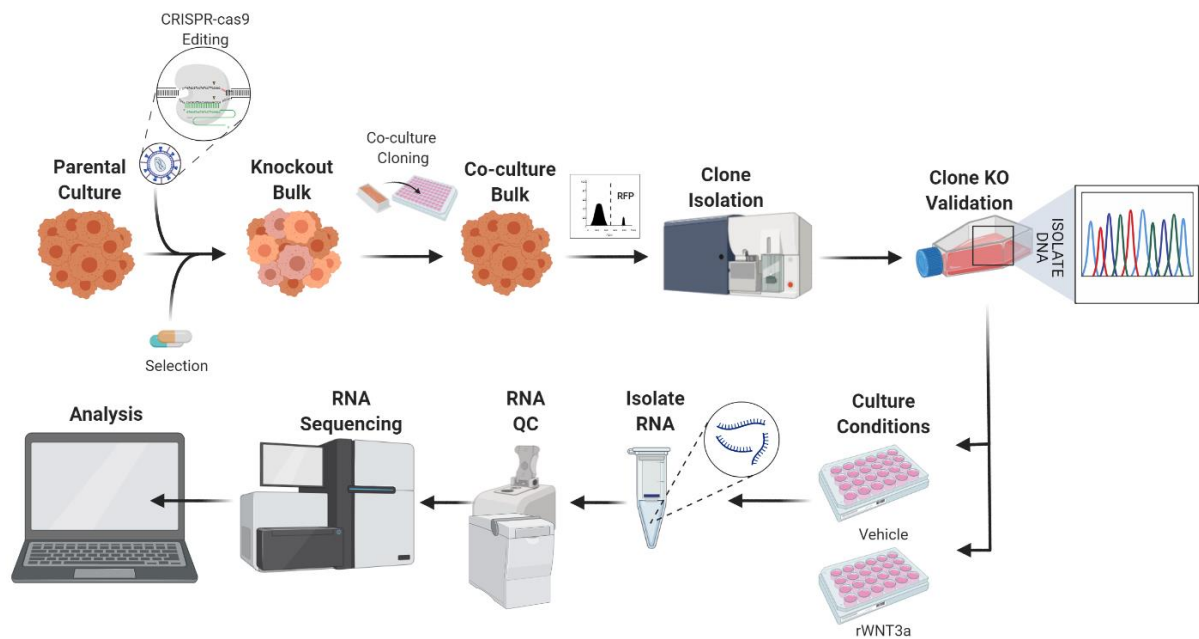


Figure 5-1: RNA-Sequencing Experimental Design

Schematic of the experimental design, ranging from the laboratory generation of complete knockout clones with CRISPR-Cas9, to the resulting preparation and validation of clones before subsequent preparation for sequencing.

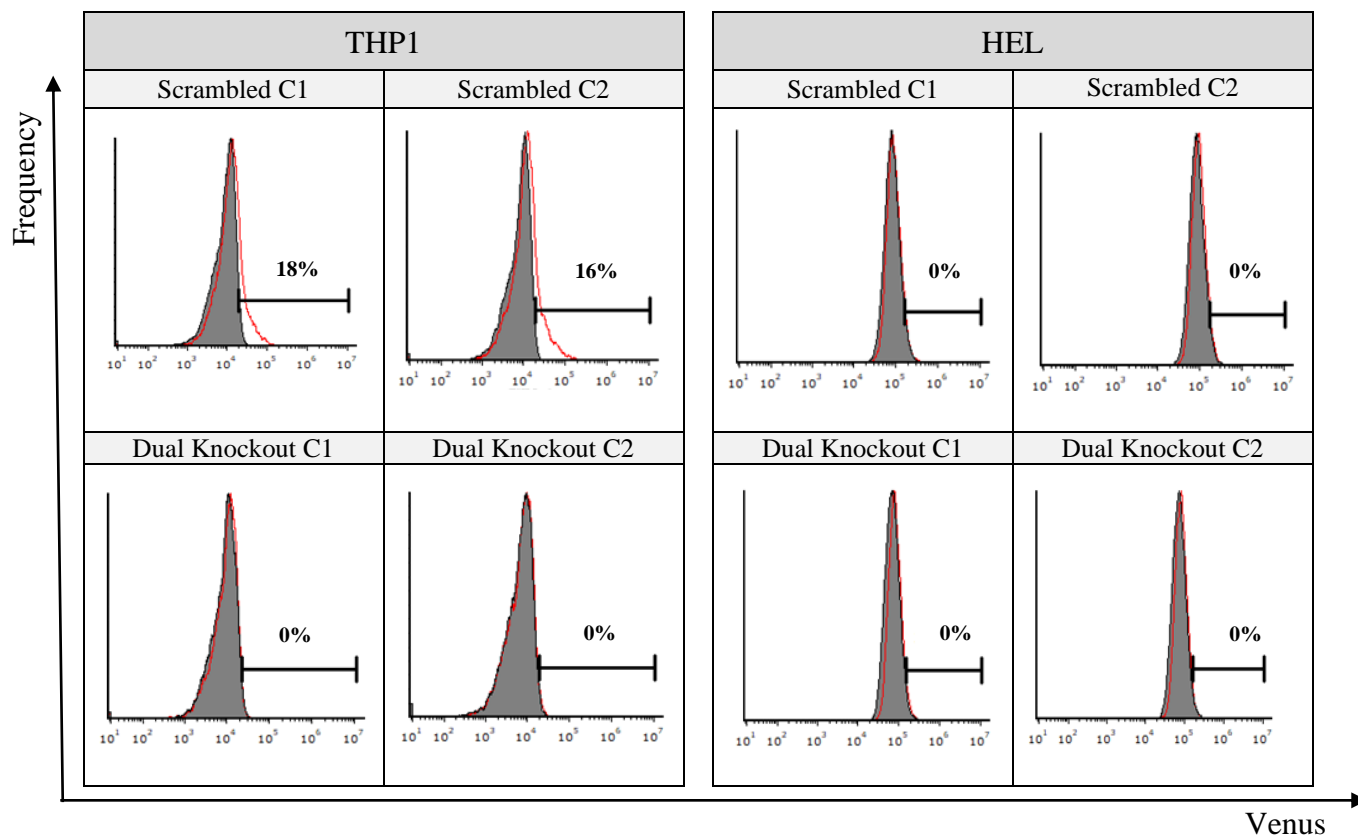


Figure 5-2: rWNT3a Stimulates WNT Signalling in THP1

Flow cytometric histograms of scrambled and knockout clones from THP1 and HEL treated with 1µg/mL rWNT3a or PBS vehicle control (0.1% v/v) for 24-hours, prior to WNT reporter assessment (2.9.1, 2.11). Filled grey represents vehicle control, red line indicates rWNT3a treated cells. Marker bar was set to 1% of control cell Venus fluorescence (n=1).

Table 5-1: Quantification and Quality Control of Total RNA Isolate Samples

Summary information for the total RNA samples extracted and assessed for quantity and quality, both locally and by Novogene. Internally, samples were assessed with a Nanodrop for concentration and purity (A260/280, A260/230) before a more in-depth validation using an Agilent 2100 Bioanalyzer, which calculates an RNA integrity number (RIN) score (0-10).

Identifier	Sample	Result	Performed Locally				Novogene		
			NanoDrop		Agilent 2100		Agilent 2100		
			RNA ng/ μ L	A260/280	A260/230	RNA ng/ μ L	RIN	RNA ng/ μ L	RIN
T_SCR1_U	THP SCR1	Pass	189.90	2.10	2.00	190	10.00	203	9.7
T_SCR2_U	THP SCR2	Pass	169.00	2.10	2.04	179	10.00	171	9.8
T_KO1_U	THP dKO 1	Pass	86.20	2.09	1.63	72	10.00	93	10
T_KO2_U	THP dKO 2	Pass	151.30	2.10	2.03	169	10.00	158	9.8
H_SCR1_U	HEL SCR 1	Pass	147.10	2.09	1.94	169	10.00	153	9.8
H_SCR2_U	HEL SCR 2	Pass	156.30	2.09	1.92	180	10.00	158	9.8
H_KO1_U	HEL dKO 1	Pass	45.70	2.05	1.61	61	10.00	50	10
H_KO2_U	HEL dKO 2	Pass	45.50	2.07	1.58	61	10.00	51	10
T_SCR1_T	THP SCR1 +	Pass	134.80	2.09	2.13	173	10.00	137	9.7
T_SCR2_T	THP SCR2 +	Pass	97.90	2.08	2.08	128	10.00	108	9.7
T_KO1_T	THP dKO 1 +	Pass	51.90	2.10	1.99	75	10.00	58	9.9
T_KO2_T	THP dKO 2 +	Pass	69.80	2.07	2.05	97	10.00	72	9.9
H_SCR1_T	HEL SCR 1 +	Pass	150.60	2.10	1.81	149	10.00	156	9.8
H_SCR2_T	HEL SCR 2 +	Pass	122.90	2.09	1.97	127	10.00	128	9.8
H_KO1_T	HEL dKO 1 +	Pass	190.90	2.09	1.99	194	10.00	190	9.7
H_KO2_T	HEL dKO 2 +	Pass	190.80	2.10	1.99	187	10.00	196	10.00

Vehicle is equal volume of PBS.

H_SCR_U = HEL Scrambled Untreated (Vehicle)

H_SCR_T = HEL Scrambled rWNT3a Treated

H_KO_U = HEL Dual Knockout Untreated (Vehicle)

H_KO_T = HEL Dual Knockout rWNT3a Treated

T_SCR_T = THP1 Scrambled rWNT3a Treated

T_KO_U = THP1 Dual Knockout Untreated (Vehicle)

T_KO_T = THP1 Dual Knockout rWNT3a Treated

T_SCR_U = THP1 Scrambled Untreated (Vehicle)

Table 5-2: Pre-filtering of Poor-Quality Sequence Reads

Summary statistics of the pre-alignment filtering of low-quality reads, which were removed from further RNA-sequencing analysis. Error rate represents the percentage of reads not above the quality control threshold.

Sample	Raw reads	Clean reads	Raw bases	Clean bases	Error rate (%)	Q20 (%)	Q30 (%)	GC content (%)
T_SCR1_U	22388335	21568470	6.7G	6.5G	0.03	97.76	93.77	50.86
T_SCR1_T	24566228	23480324	7.4G	7.0G	0.02	98.15	94.76	50.2
T_SCR2_U	22688701	21963405	6.8G	6.6G	0.03	97.97	94.22	50.39
T_SCR2_T	21923755	21311546	6.6G	6.4G	0.03	97.87	93.95	50.08
H_KO1_U	22700019	22083762	6.8G	6.6G	0.03	97.73	93.64	49.73
H_KO1_T	22206013	21572172	6.7G	6.5G	0.03	98.00	94.19	49.00
T_KO2_U	23016712	22318003	6.9G	6.7G	0.02	98.03	94.28	49.01
T_KO2_T	23781545	22891610	7.1G	6.9G	0.02	98.00	94.26	49.25
H_SCR1_U	22460736	21616669	6.7G	6.5G	0.02	98.04	94.13	48.83
H_SCR1_T	19762105	18547319	5.9G	5.6G	0.02	98.15	94.57	47.11
H_SCR2_U	23574238	22165364	7.1G	6.6G	0.03	97.92	94.03	47.24
H_SCR2_T	23077045	22062484	6.9G	6.6G	0.02	98.06	94.43	50.69
T_KO1_U	22885441	21851935	6.9G	6.6G	0.03	97.90	94.21	50.66
T_KO1_T	21733743	20899371	6.5G	6.3G	0.02	98.02	94.33	51.02
H_KO2_U	21951936	21117420	6.6G	6.3G	0.02	97.98	94.25	50.28
H_KO2_T	22290979	21575897	6.7G	6.5G	0.02	98.16	94.68	50.32

H_SCR_U = HEL Scrambled Untreated (Vehicle)
H_SCR_T = HEL Scrambled rWNT3a Treated
H_KO_U = HEL Dual Knockout Untreated (Vehicle)
H_KO_T = HEL Dual Knockout rWNT3a Treated
T_SCR_U = THP1 Scrambled Untreated (Vehicle)
T_SCR_T = THP1 Scrambled rWNT3a Treated
T_KO_U = THP1 Dual Knockout Untreated (Vehicle)
T_KO_T = THP1 Dual Knockout rWNT3a Treated

Table 5-3: STAR Alignment Results to the GRCh38.p13 Genome

Summary alignment data representing the proportion of samples uniquely mapped after STAR alignment. Reads not uniquely mapped were excluded from further study, as these are invalid. Samples were aligned to the GRCh38.p13 Genome.

Sample name	Total Mapped	Uniquely Mapped	Multiple Mapped
T_SCR1_U	41696304 (96.66%)	40621934 (94.17%)	1074370 (2.49%)
T_SCR1_T	45531208 (96.96%)	44374092 (94.49%)	1157116 (2.46%)
T_SCR2_U	42681152 (97.16%)	41623210 (94.76%)	1057942 (2.41%)
T_SCR2_T	41426946 (97.19%)	40376274 (94.73%)	1050672 (2.47%)
H_KO1_U	42761210 (96.82%)	41405242 (93.75%)	1355968 (3.07%)
H_KO1_T	41917948 (97.16%)	40561250 (94.01%)	1356698 (3.14%)
T_KO2_U	43440912 (97.32%)	42392466 (94.97%)	1048446 (2.35%)
T_KO2_T	44428448 (97.04%)	43238362 (94.44%)	1190086 (2.6%)
H_SCR1_U	42080454 (97.33%)	40765880 (94.29%)	1314574 (3.04%)
H_SCR1_T	35895436 (96.77%)	34828112 (93.89%)	1067324 (2.88%)
H_SCR2_U	42923404 (96.83%)	41597054 (93.83%)	1326350 (2.99%)
H_SCR2_T	42804774 (97.01%)	41334760 (93.68%)	1470014 (3.33%)
T_KO1_U	42273520 (96.73%)	40987558 (93.78%)	1285962 (2.94%)
T_KO1_T	40541018 (96.99%)	39510662 (94.53%)	1030356 (2.47%)
H_KO2_U	40968592 (97.00%)	39613782 (93.79%)	1354810 (3.21%)
H_KO2_T	41944872 (97.2%)	40398642 (93.62%)	1546230 (3.58%)

H_SCR_U = HEL Scrambled Untreated (Vehicle)
H_SCR_T = HEL Scrambled rWNT3a Treated
H_KO_U = HEL Dual Knockout Untreated (Vehicle)
H_KO_T = HEL Dual Knockout rWNT3a Treated
T_SCR_U = THP1 Scrambled Untreated (Vehicle)
T_SCR_T = THP1 Scrambled rWNT3a Treated
T_KO_U = THP1 Dual Knockout Untreated (Vehicle)
T_KO_T = THP1 Dual Knockout rWNT3a Treated

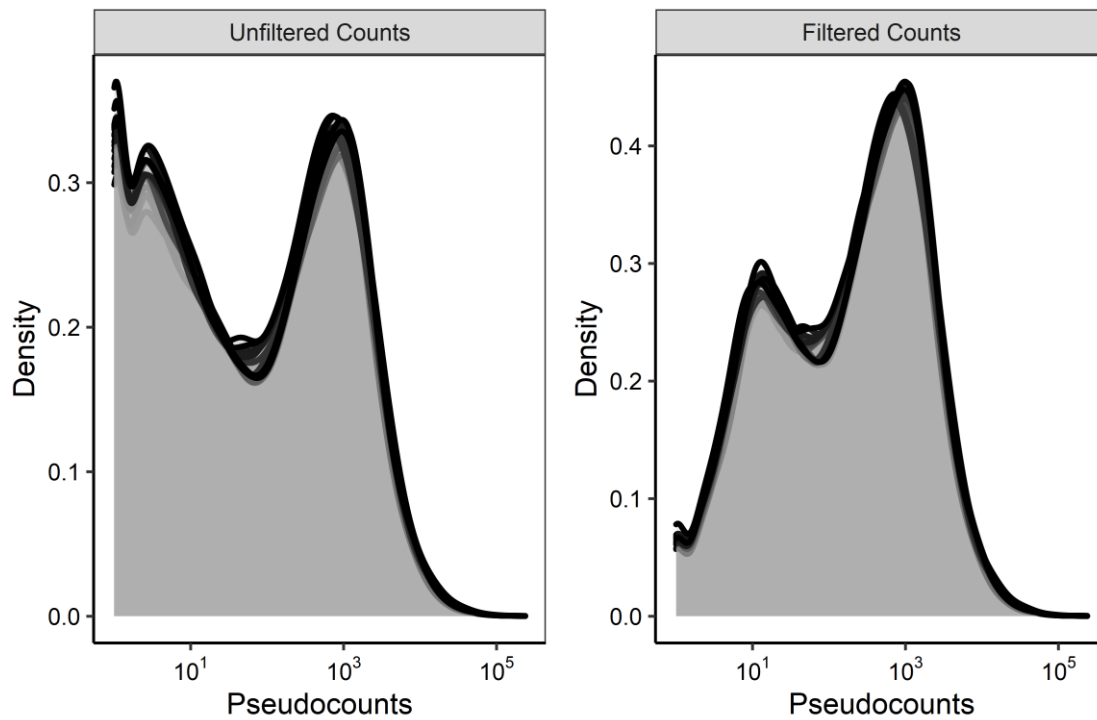


Figure 5-3: Pre-filtering of Low Abundance Genes

Representation of the filtering of low counts, representing transcripts not expressed within these sample types (<10 counts in whole dataset). Low counts were automatically removed with DESeq2 in order to maximise statistical power. Left panel demonstrates a density histogram of the transcriptome for each sample represented as individual lines, whilst the right panel shows the filtered dataset with low reads removed.

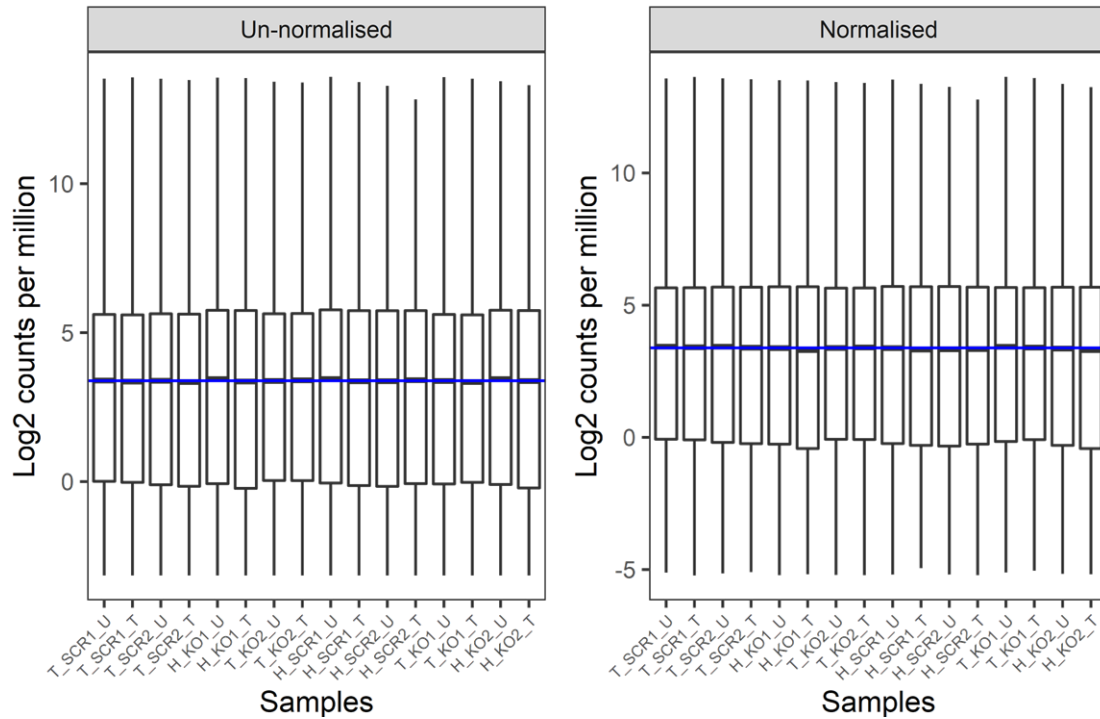


Figure 5-4: Normalisation of Filtered RNA-Seq Counts

Boxplot demonstration of sample library size prior (left) and following normalisation (right). X-axis represents samples. Blue line indicates the mean library size amongst samples, whilst the black bar represents mean within each sample.

- H_SCR_U = HEL Scrambled Untreated (Vehicle)
- H_SCR_T = HEL Scrambled rWNT3a Treated
- H_KO_U = HEL Dual Knockout Untreated (Vehicle)
- H_KO_T = HEL Dual Knockout rWNT3a Treated
- T_SCR_U = THP1 Scrambled Untreated (Vehicle)
- T_SCR_T = THP1 Scrambled rWNT3a Treated
- T_KO_U = THP1 Dual Knockout Untreated (Vehicle)
- T_KO_T = THP1 Dual Knockout rWNT3a Treated

5.3.1.2 *Sample Distancing and PCA Demonstrates Cell Line Variance*

Correlation within biological replicates is critical to confer statistical power in downstream analyses. An indicator of sample similarity was determined using a correlation coefficient matrix, which compared samples based upon Pearson's correlation. Samples showed a high degree of dissimilarity between cell lines, which is secondary to similarities between the conditions of scrambled clones and knockout clones within each cell line, suggesting that the biological variance between cell lines is greater than the variance incurred due to dual knockout, as would be expected (**Figure 5-5**).

To examine the differences in gene expression profiles between samples, a PCA was performed. In a PCA analysis, the high-dimensional RNA-seq data is dimensionally reduced into a set of linear principal components (eigenvectors), each of which are orthogonal to each other. The value of each component (eigenvalue) is based upon a set of genes with a significant degree of variance. As expected, cell lines clustered together and the separation of knockout and scrambled cultures was secondary to this effect, supporting the outcome that cell line biological variance is greater than condition variance (**Figure 5-6**).

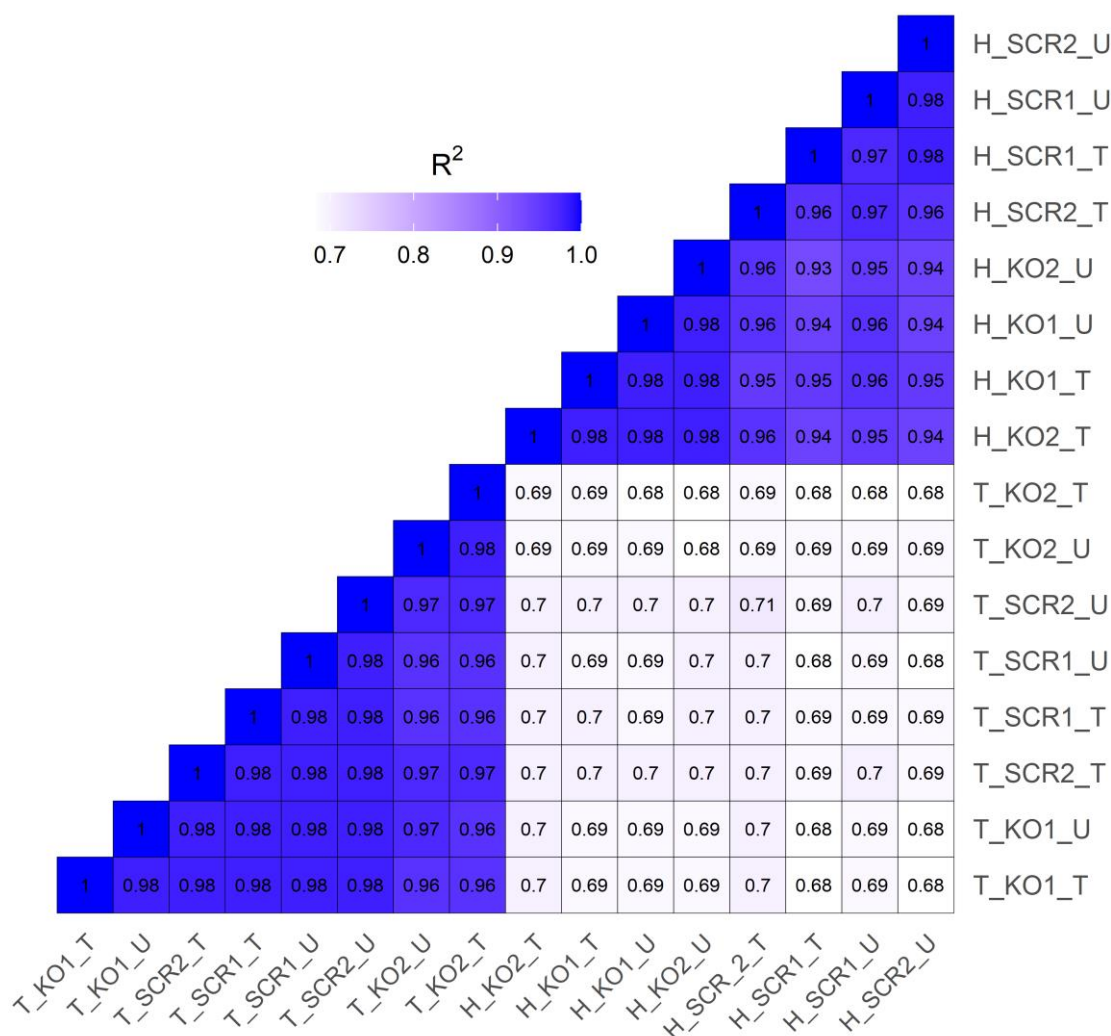


Figure 5-5: Pearson Correlation Matrix Demonstrating the Similarity Between Cell Lines

Heatmap demonstrating the transcriptomic similarity between samples as computed through a Pearson’s correlation score based upon the entire transcriptome. Samples were coloured by their coefficient values, as indicated. Samples self-segregate into THP1 and HEL blocs without supervision as the greatest measure of variance exists between cell line type.

- H_SCR_U = HEL Scrambled Untreated (Vehicle)
- H_SCR_T = HEL Scrambled rWNT3a Treated
- H_KO_U = HEL Dual Knockout Untreated (Vehicle)
- H_KO_T = HEL Dual Knockout rWNT3a Treated
- T_SCR_U = THP1 Scrambled Untreated (Vehicle)
- T_SCR_T = THP1 Scrambled rWNT3a Treated
- T_KO_U = THP1 Dual Knockout Untreated (Vehicle)
- T_KO_T = THP1 Dual Knockout rWNT3a Treated

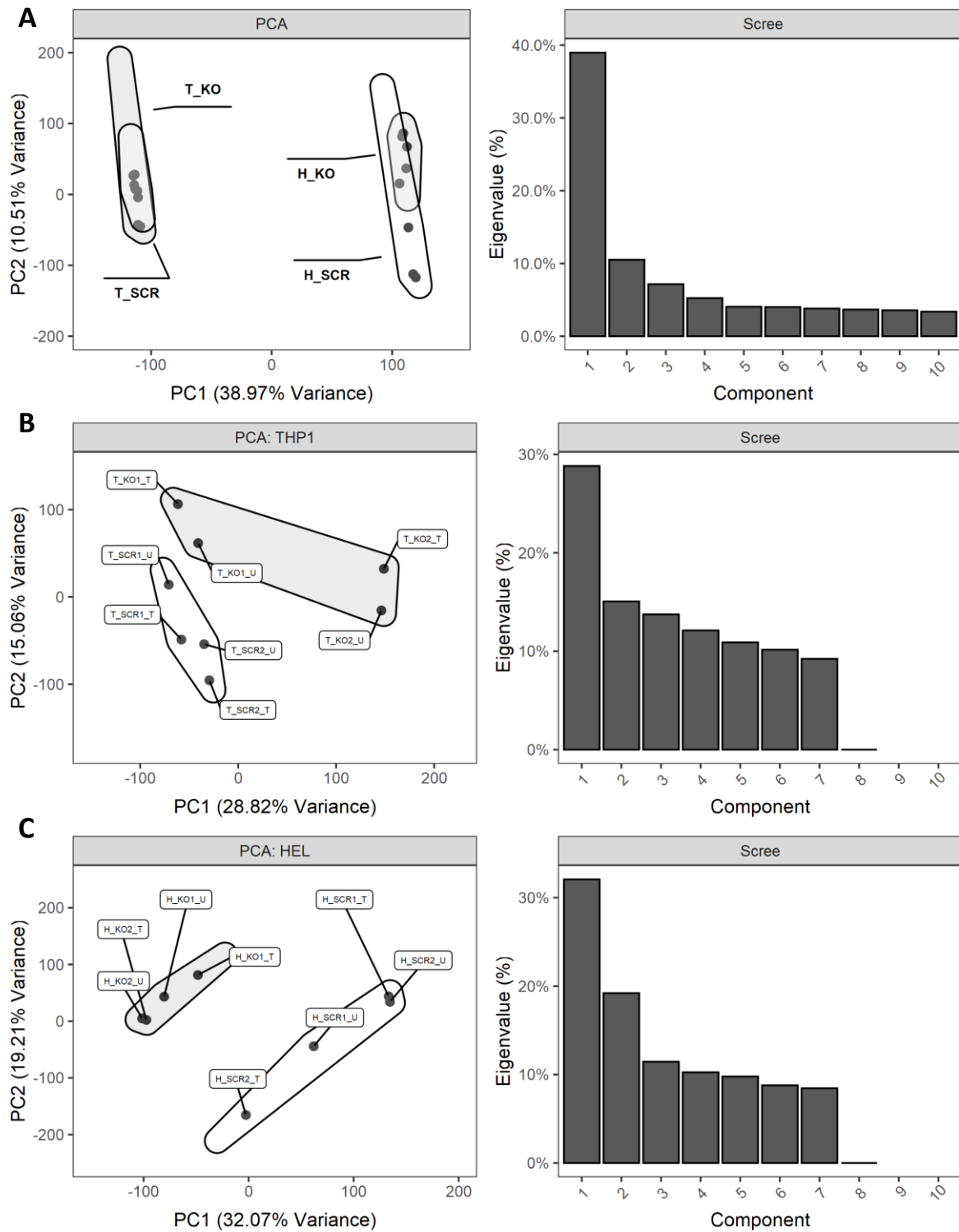


Figure 5-6: PCA Biplots Showing the Separation of Scrambled and Knockout Clones

PCA and associated scree plots demonstrate the separation of expression profiles for samples. Samples were displayed upon the first two principal components, which explained a significant proportion of the variation (2.13.3.1). **A**) Samples segregation based upon cell line type. **B**) THP1 sample segregation based upon catenin status. **C**) HEL sample segregation based upon catenin status.

5.3.1.3 *CTNNB1 and JUP are successfully ablated at the mRNA level*

CRISPR-Cas9 causes changes at the DNA level through a frame-shift mutation with the intention to induce nonsense mediated decay (NMD) of mRNA and stop protein production. Analysis of mRNA levels was informative as to whether nonsense mediated decay was occurring, or a truncated non-functional form of β -catenin and γ -catenin was being actively expressed. As RNA-seq examines fragments with no regard to the reading frame, it was anticipated that levels would remain detectable despite knockout. *CTNNB1* and *JUP* mRNA levels were found to be significantly reduced to borderline undetectable levels (**Figure 5-7**), suggesting that NMD of mRNA was occurring within these samples. In addition, these observations establish that a truncated form of the protein is not being produced, which might otherwise allow some normal function or, alternatively, a dominant negative effect.

5.3.1.4 *WNT/ β -catenin Signalling Pathway and WNT Targets are Unchanged as a Whole*

To explore WNT/ β -catenin signalling pathway alterations, the impact on members of the WNT/ β -catenin pathway (GO term GO:0060070) and potential WNT target genes were compared between conditions (**Table 5-4**). No statistically significant alterations to these two respective collections of genes were identified (**Figure 5-8**), which could be interpreted to indicate that the pathway and targets remained unchanged. However, such a broad contrast between all gene members was perhaps limiting the resulting interpretation as the GO WNT/ β -catenin pathway and the potential WNT target gene list is context dependent and are possibly not totally relevant in myeloid tissues, limiting statistical outcome.

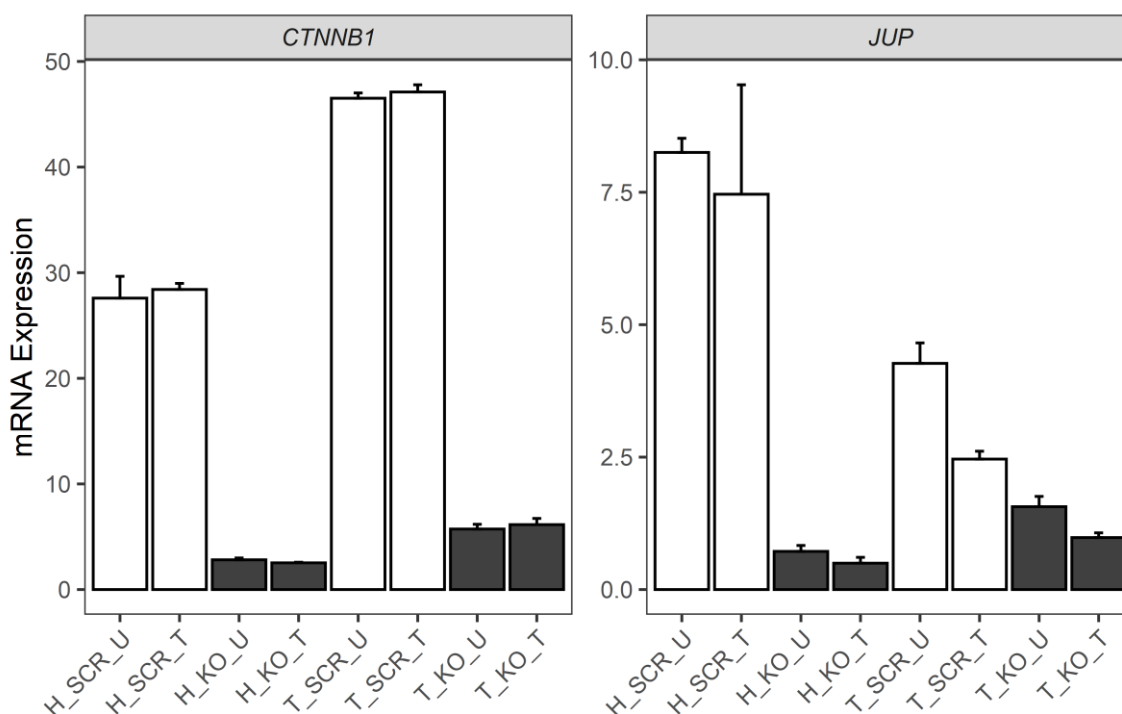


Figure 5-7: *CTNNB1* and *JUP* are Ablated at the mRNA Level

Summary chart showing *CTNNB1* (β -catenin) and *JUP* (γ -catenin) mRNA expression, as measured in normalised counts. Scrambled control clones are coloured white, whilst dual knockout clones are coloured dark grey. Data represents mean +1SD (n=2).

H_SCR_U = HEL Scrambled Untreated (Vehicle)
H_SCR_T = HEL Scrambled rWNT3a Treated
H_KO_U = HEL Dual Knockout Untreated (Vehicle)
H_KO_T = HEL Dual Knockout rWNT3a Treated
T_SCR_U = THP1 Scrambled Untreated (Vehicle)
T_SCR_T = THP1 Scrambled rWNT3a Treated
T_KO_U = THP1 Dual Knockout Untreated (Vehicle)
T_KO_T = THP1 Dual Knockout rWNT3a Treated

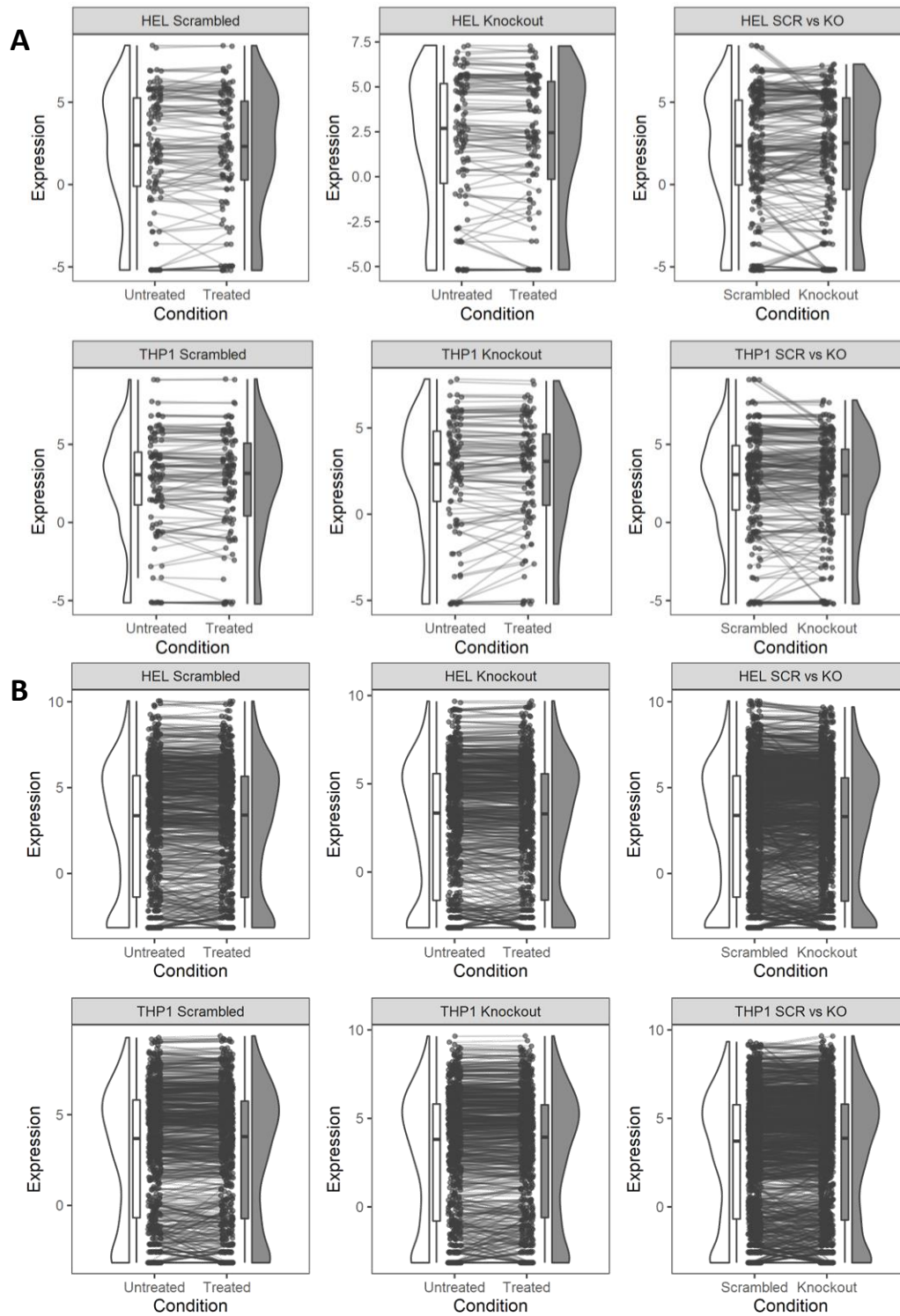


Figure 5-8: WNT/ β -catenin Signalling is Not Perturbed as a Whole Pathway

A) Raincloud plots investigating the change in mRNA expression (TPM) between untreated vehicle control samples and rWNT3a treated samples based upon the WNT signalling pathway GO Term. Total gene expression is represented in a violin plot alongside the connected points. (n=2) **B)** Raincloud plots investigating the change in mRNA expression (TPM) between untreated vehicle control samples and rWNT3a treated samples based on WNT-target genes. Total sample expression is represented in a violin plot alongside the connected points. (n=2).

5.3.2 Differential Expression Analysis Reveals WNT-Active and Knockout Profile

To determine the transcripts that are differentially expressed by normal WNT/ β -catenin signalling activity, regarding dual knockout cultures, it was necessary to compare the obtained transcriptomic profiles between rWNT3a treated scrambled THP1 cells and dual catenin knockout cells. To do this, two independent sets of analyses were performed (**Table 5-4**). The first one relied on the identification of differentially expressed transcripts in rWNT3a *versus* vehicle in scrambled clones, to determine normal WNT/ β -catenin activity profile. Subsequently, this study analysed knockout *versus* scrambled cultures, thus determining the altered expression profile as a result of β -catenin knockout. However, due to the inability to detect a WNT response in rWNT3a treated HEL, comparisons were made on a *per line* basis prior to overall comparing. The full list of cell line comparisons performed is shown in **Table 5-4**.

To determine the transcripts in THP1 cells activated in response to rWNT3a, scrambled samples treated with rWNT3a were compared to equivalent vehicle controls. The p-value distribution demonstrates the desired anti-conservative distribution, indicative of a proper test (Breheny *et al.*, 2018), though some mild bimodal skewing presents, likely caused by low sample size (**Figure 5-9A**). A total of 96 transcripts were found to be differentially expressed after correction, of which 38 were overexpressed and 58 were repressed in treated samples, as compared to the control vehicle alone (**Figure 5-10A, Table 5-5**). As expected, given the lack of reporter response (**Figure 5-2**), comparable tests failed to reproduce these findings in HEL cells (data not shown).

Comparison between untreated knockout and scrambled samples was performed within THP1 cells, in which the p-value distribution displayed an ideal anti-conservative distribution, thus demonstrating the additional statistical power gained from a larger sample size (**Figure 5-9B**). A total of 224 differentially expressed transcripts were found after correction, of which 134 were overexpressed and 90 were repressed (**Figure 5-10B, Table 5-6**) in knockout samples, as compared to control. These data demonstrate that knockout of β -catenin and γ -catenin had broad transcriptional impact at basal and treated levels.

A critical endpoint of this analysis was to identify the transcripts perturbed by knockout agnostic to a specific cell line, as loss of clonogenicity was a common feature. This was achieved by performing a comparison between scrambled and knockout cells, with the cell line

set as a co-variable, thus maximising the statistical power of the analysis. Both the volcano plot and the p-value distribution indicate a successful test (**Figure 5-11**), furthered by hierarchical distancing based upon DET in a heatmap, demonstrating clear separation between samples (**Figure 5-12**). A total of 688 DET were found after correction, of which 330 were overexpressed and 358 were repressed (**Table 5-7**). As a substantial degree of variance was linked to the cell line rather than the knockout status or treatment, an alternative approach to determine the similarity in expression patterns was performed, by comparing knockout and scrambled in each cell line, respectively. This method found 21 commonly directionally perturbed DET in both analyses (**Figure 5-13**).

Together, these results show that rWNT3a activates WNT/ β -catenin signalling at the transcriptional level in scrambled controls, based upon WNT-target gene expression changes, and that this activation is dependent upon β -catenin. Numerous genes found upregulated or repressed are not recognised WNT/ β -catenin target genes, potentially representing false positives, genes regulated by pathways perturbed by WNT/ β -catenin or are actually true target genes which have not been previously recognised, as much of the published research has been performed in epithelial tissues, not AML. Dual catenin knockout was shown to perturb transcriptional activity both at basal levels and activated WNT/ β -catenin levels, demonstrating transcriptional consequence. Further examination of these perturbed genes through current and novel pathway analysis techniques will enable contextual insight into the consequence of active WNT/ β -catenin signalling and knockout states, performed in 5.3.3. A reciprocal promotion of a pathway lost in the knockout state would represent a promising target of interest, warranting closer examination of the genes perturbed.

Table 5-4: Comparisons Applied For RNA-Sequencing

Summary of the comparisons applied in the study, alongside the associated design grouping and sizes applied, with intent for each comparison. Lines were examined independently before being combined to fully realise the transcriptomic changes. Public data was acquired from the TCGA.

Source	Comparison	Cell Type	Group 1	Group 2	n	Design Notes	Intent
Generated Data	1	THP1	THP1 Scrambled Treated	THP1 Scrambled Untreated	2 v 2	Paired	Find WNT activated transcripts
	2		THP1 Knockout Treated	THP1 Knockout Untreated	2 v 2	Paired	Demonstrate WNT silencing
	3	THP1, HEL	Knockout	Scrambled	4 v 4	Paired, Grouped	Find commonly perturbed transcripts
Public Data	4	Patient Data	High LEF (Top 3 rd)	Low LEF (Bottom 3 rd)	High: 36 Low: 37	N/A	Investigate if WNT-active effects are comparable within the patient data
	5		Deceased	Survived	Dead: 67 Alive: 42	N/A	Investigate the impact upon overall survival

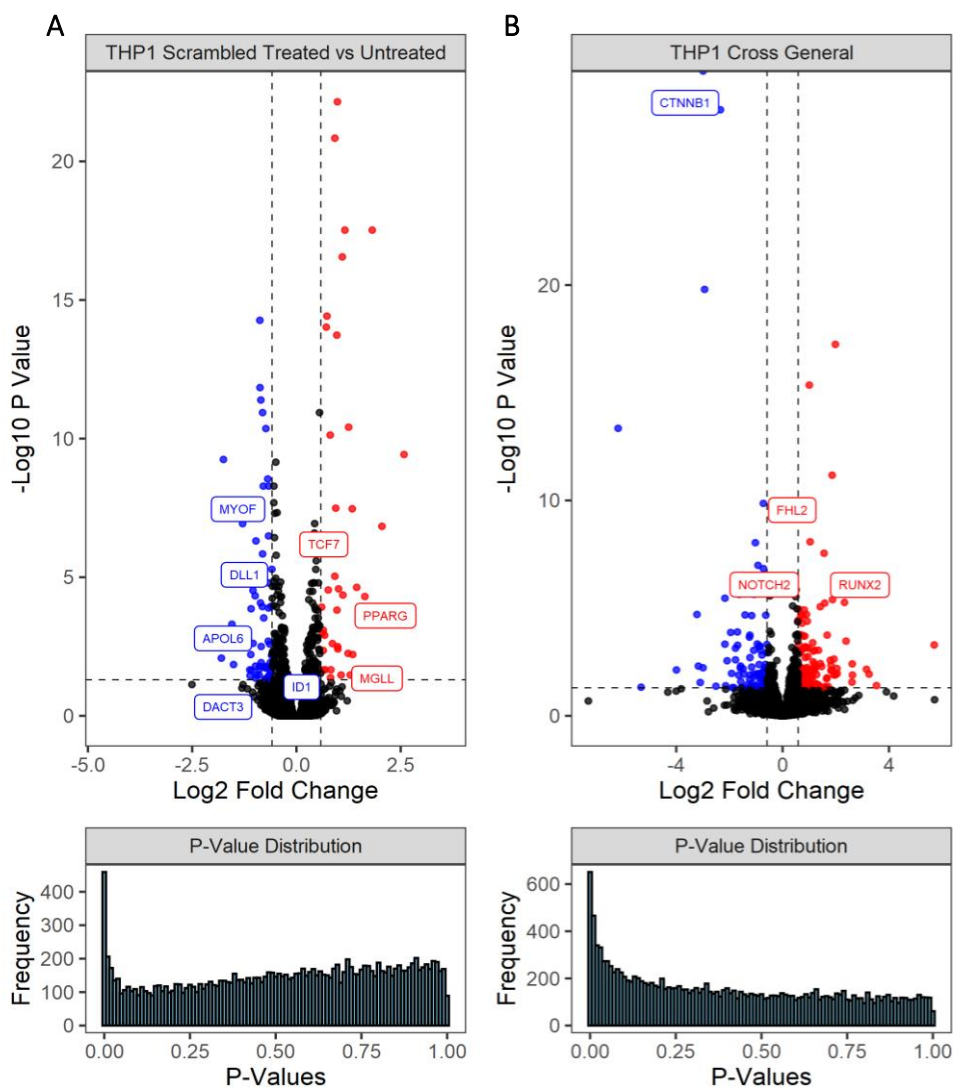


Figure 5-9: Volcano Plots and p-value Distribution Histograms for THP1 Comparisons

Volcano plots demonstrating the transcripts identified as differentially expressed based on p -value < 0.05 (Benjamini-Hochberg corrected), represented by the horizontal line, and absolute fold change of 1.5-fold, as represented by the two vertical lines (positive and negative expression change). Associated uncorrected p -value distributions are shown below each comparison, which enable a general indication of statistical soundness for each contrast. Genes which are significantly overexpressed are coloured red, whilst repressed are coloured blue; non-significant genes are coloured black. Annotated genes are those identified as members of the WNT/ β -catenin pathway or speculated members.

A) THP1 scrambled rWNT3a treated *versus* THP1 scrambled vehicle control

B) THP1 scrambled *versus* THP1 knockout i.e., *general cross-examination*

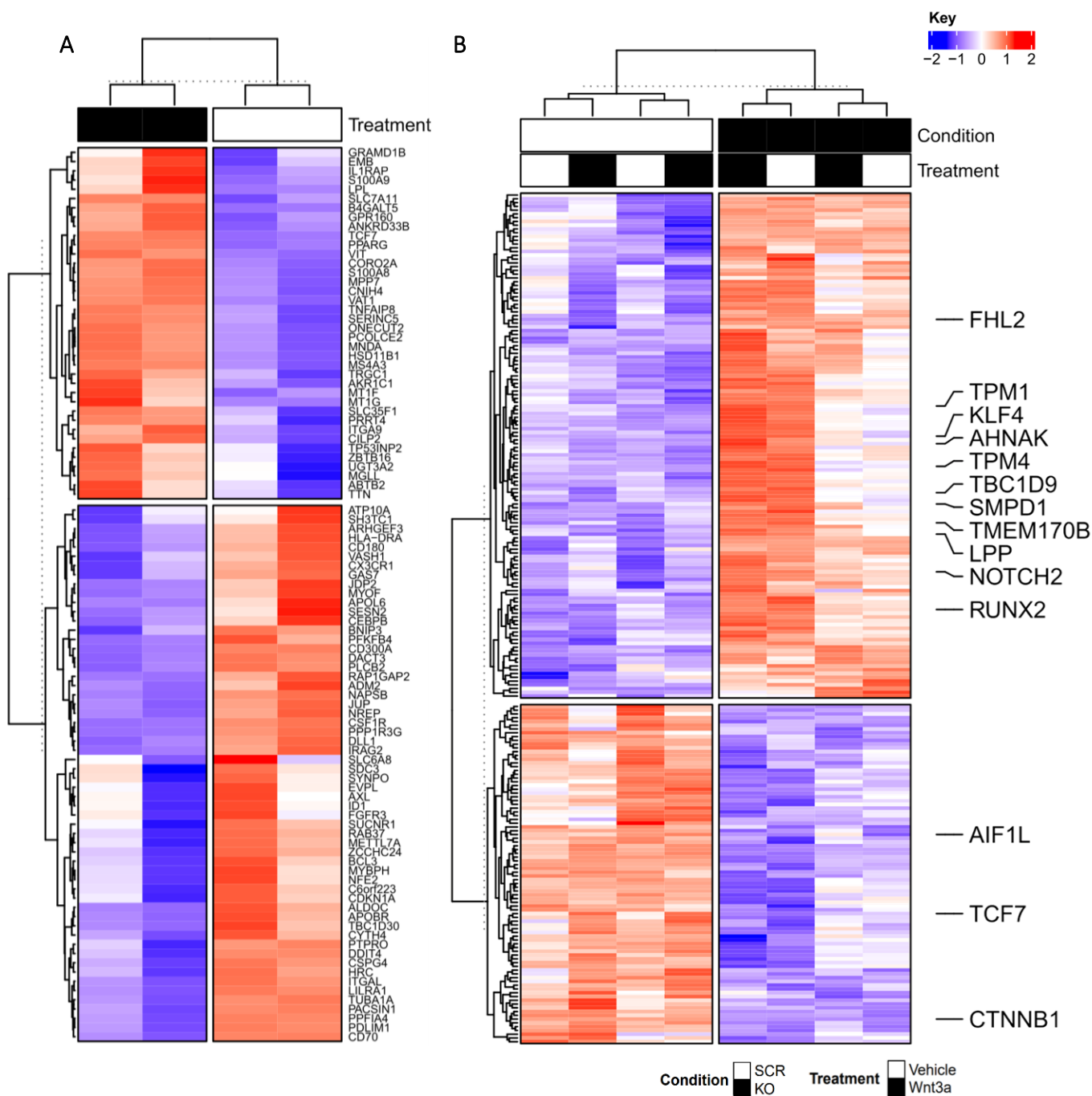


Figure 5-10: Heatmap of Differentially Expressed Transcripts in THP1

Heatmap of the identified differentially expressed transcripts. **A)** THP1 scrambled rWNT3a treated *versus* THP1 scrambled vehicle control. **B)** THP1 scrambled *versus* THP1 knockout. Columns represent samples whilst rows are genes. Samples were z-score scaled around expression mean, with red indicating high expression levels and blue low. Samples segregate without supervision into two groups with k-means clustering. In A, all HGNC gene symbols are shown. In B, only WNT-related genes are annotated (A, n=2), (B, n=4).

Table 5-5: Top Differentially Expressed Transcripts in THP1 Scrambled Treated with rWNT3a

ENSG	HGNC	Log2FC	PAdjusted	Description
ENSG00000163710	PCOLCE2	2.58	3.75e-10	Procollagen c-endopeptidase enhancer 2
ENSG00000150054	MPP7	2.05	1.46e-07	Membrane palmitoylated protein 7
ENSG00000205221	VIT	1.82	3.01e-18	Vitrin
ENSG00000164300	SERINC5	1.34	3.40e-08	Serine incorporator 5
ENSG00000151012	SLC7A11	1.25	3.86e-11	Solute carrier family 7 member 11
ENSG00000117594	HSD11B1	1.16	3.01e-18	Hydroxysteroid 11-beta dehydrogenase 1
ENSG00000145779	TNFAIP8	1.10	2.79e-17	Tnf alpha induced protein 8
ENSG00000108828	VAT1	0.98	7.08e-23	Vesicle amine transport 1
ENSG00000149516	MS4A3	0.97	1.85e-14	Membrane spanning 4-domains a3
ENSG00000164236	ANKRD33B	0.94	3.23e-08	Ankyrin repeat domain 33b
ENSG00000170571	EMB	0.92	1.46e-21	Embigin
ENSG00000163220	S100A9	0.84	4.67e-07	S100 calcium binding protein a9
ENSG00000163563	MNDA	0.81	7.46e-11	Myeloid cell nuclear differentiation antigen
ENSG00000173890	GPR160	0.73	3.82e-15	G protein-coupled receptor 160
ENSG00000158470	B4GALT5	0.72	9.52e-15	Beta-1,4-galactosyltransferase 5
ENSG00000173546	CSPG4	-1.75	5.66e-10	Chondroitin sulfate proteoglycan 4
ENSG00000167851	CD300A	-1.75	1.73e-08	Cd300a molecule
ENSG00000114268	PFKFB4	-1.29	1.17e-07	6-phosphofructo-2-kinase/fructose-2,6-biphosphatase 4
ENSG00000131401	NAPSB	-1.28	3.23e-08	Napsin b aspartic peptidase, pseudogene
ENSG00000168329	CX3CR1	-1.01	3.91e-08	C-x3-c motif chemokine receptor 1
ENSG00000138119	MYOF	-0.97	4.90e-07	Myoferlin
ENSG00000100055	CYTH4	-0.88	5.41e-15	Cytohesin 4
ENSG00000182578	CSF1R	-0.87	1.45e-12	Colony stimulating factor 1 receptor
ENSG00000133055	MYBPH	-0.85	4.05e-12	Myosin binding protein h
ENSG00000107438	PDLIM1	-0.81	1.15e-11	Pdz and lim domain 1
ENSG00000007237	GAS7	-0.79	5.18e-09	Growth arrest specific 7
ENSG00000124762	CDKN1A	-0.73	4.34e-11	Cyclin dependent kinase inhibitor 1a
ENSG00000134986	NREP	-0.69	2.86e-09	Neuronal regeneration related protein
ENSG00000167552	TUBA1A	-0.67	3.25e-07	Tubulin alpha 1a
ENSG00000204287	HLA-DRA	-0.66	5.18e-09	Major histocompatibility complex, class ii, dr alpha

Summary data of the top fifteen overexpressed and repressed transcripts, as ranked first by adjusted p-value and secondly by fold change (\log_2). Fold changes are coloured green to signify overexpression and red to signify repression. Transcripts identified between THP1 scrambled treated and untreated. Increasing shades of green indicate degree of overexpression, whilst increasing shades of red represent repression (n=2).

Table 5-6: Top Differentially Expressed Transcripts between THP1 knockout and scrambled

ENSG	HGNC	Log2FC	PAdjusted	Description	ENSG	HGNC	Log2FC	PAdjusted	Description
ENSG00000225107		5.70	5.12e-04	Novel transcript	ENSG00000148798	INA	-6.18	4.48e-14	Internex neuronal intermediate filament protein alpha
ENSG00000249437	NAIP	2.62	3.88e-03	Nlr family apoptosis inhibitory protein	ENSG00000168661	ZNF30	-3.99	7.42e-03	Zinc finger protein 30
ENSG00000250138		2.39	3.39e-04	Pom121 membrane glycoprotein-like 1 (pom1211) pseudogene	ENSG00000160161	CILP2	-3.65	3.10e-29	Cartilage intermediate layer protein 2
ENSG00000162849	KIF26B	2.33	5.43e-06	Kinesin family member 26b	ENSG00000130822	PNCK	-3.22	1.97e-05	Pregnancy up-regulated nonubiquitous cam kinase
ENSG00000143546	S100A8	1.98	5.67e-18	S100 calcium binding protein a8	ENSG00000274080		-3.17	4.90e-03	Novel transcript
ENSG00000174672	BRSK2	1.93	2.30e-03	Br serine/threonine kinase 2	ENSG00000170365	SMAD1	-2.99	5.90e-03	Smad family member 1
ENSG00000171049	FPR2	1.88	4.02e-06	Formyl peptide receptor 2	ENSG00000168036	CTNNB1	-2.99	0.00e+00	Catenin beta 1
ENSG00000163220	S100A9	1.86	6.74e-12	S100 calcium binding protein a9	ENSG00000126353	CCR7	-2.93	1.59e-20	C-c motif chemokine receptor 7
ENSG00000109158	GABRA4	1.82	4.47e-03	Gamma-aminobutyric acid type a receptor subunit alpha4	ENSG00000182168	UNC5C	-2.34	7.27e-29	Unc-5 netrin receptor c
ENSG00000169508	GPR183	1.79	2.64e-03	G protein-coupled receptor 183	ENSG00000168077	SCARA3	-2.17	4.71e-04	Scavenger receptor class a member 3
ENSG00000144619	CNTN4	1.68	1.79e-04	Contactin 4	ENSG00000178772	CPN2	-2.17	3.46e-06	Carboxypeptidase n subunit 2
ENSG00000183023	SLC8A1	1.58	8.5e-06	Solute carrier family 8 member a1	ENSG00000009950	MLXIPL	-2.09	2.78e-03	Mlx interacting protein like
ENSG00000124813	RUNX2	1.56	2.83e-08	Runx family transcription factor 2	ENSG00000139269	INHBE	-1.95	1.35e-04	Inhibin subunit beta e
ENSG00000179104	TMTC2	1.47	5.13e-03	Transmembrane o-mannosyltransferase targeting cadherins 2	ENSG00000272636	DOC2B	-1.92	1.07e-02	Double c2 domain beta
ENSG00000136826	KLF4	1.42	3.74e-03	Kruppel like factor 4	ENSG00000273108		-1.77	7.26e-04	Novel transcript, antisense to sh3pxd2a
ENSG00000137642	SORL1	1.42	8.58e-06	Soritin related receptor 1	ENSG00000184868	FAM171A1	-1.77	2.50e-03	Family with sequence similarity 171 member a1
ENSG00000103313	MEFV	1.35	9.02e-04	Mefv innate immunity regulator, pyrin	ENSG00000188338	SLC38A3	-1.70	1.28e-04	Solute carrier family 38 member 3
ENSG00000154096	THY1	1.25	5.50e-03	Thy-1 cell surface antigen	ENSG00000260139	CSPG4P13	-1.69	5.28e-04	Chondroitin sulfate proteoglycan 4 pseudogene 13
ENSG00000100292	HMOX1	1.22	9.05e-04	Heme oxygenase 1	ENSG00000163792	TCF23	-1.63	2.29e-06	Transcription factor 23
ENSG00000134955	SLC37A2	1.19	3.88e-03	Solute carrier family 37 member 2	ENSG00000115884	SDC1	-1.59	6.05e-03	Syndecan 1
ENSG00000091409	ITGA6	1.15	9.91e-04	Integrin subunit alpha 6	ENSG00000184985	SORCS2	-1.58	4.90e-03	Soritin related vps10 domain containing receptor 2
ENSG00000088827	SLGLE1	1.15	3.11e-03	Sialic acid binding ig like lectin 1	ENSG00000228709	LINC02575	-1.48	6.61e-03	Long intergenic non-protein coding rna 2575
ENSG00000187791	FAM205C	1.13	4.05e-04	Family with sequence similarity 205 member c	ENSG00000173801	JUP	-1.41	2.07e-05	Junction plakoglobin
ENSG00000115641	FHL2	1.03	8.32e-09	Four and a half lim domains 2	ENSG00000107954	NEURL1	-1.25	2.22e-04	Neutralized e3 ubiquitin protein ligase 1
ENSG00000117114	ADGRL2	1.00	4.41e-16	Adhesion g protein-coupled receptor l2	ENSG00000081059	TCF7	-1.23	1.79e-04	Transcription factor 7
ENSG00000135218	CD36	0.97	7.26e-04	Cd36 molecule	ENSG00000130540	SULT4A1	-1.23	1.98e-03	Sulfotransferase family 4a member 1
ENSG00000273151		0.95	1.79e-03	Novel transcript, antisense to get4	ENSG00000144485	HES6	-1.16	2.22e-05	Hes family bhlh transcription factor 6
ENSG00000137177	KIF13A	0.93	4.06e-05	Kinesin family member 13a	ENSG00000277631	PGM5P3-AS1	-1.16	5.45e-03	Pgm5p3 antisense rna 1
ENSG00000160229	ZNF66	0.92	5.70e-03	Zinc finger protein 66	ENSG00000187017	ESPN	-1.09	9.11e-04	Espin
ENSG00000105639	JAK3	0.90	6.66e-04	Janus kinase 3	ENSG00000140835	CHST4	-1.07	2.29e-06	Carbohydrate sulfotransferase 4
ENSG00000125730	C3	0.90	1.97e-05	Complement c3	ENSG00000123689	G0S2	-1.02	9.19e-09	G0/g1 switch 2
ENSG00000100234	TIMP3	0.89	6.75e-04	Timp metalloproteinase inhibitor 3	ENSG00000141622	RNF165	-0.95	4.60e-04	Ring finger protein 165
ENSG00000120594	PLXDC2	0.85	6.14e-04	Plexin domain containing 2	ENSG00000187678	SPRY4	-0.94	1.08e-02	Sprouty rtk signaling antagonist 4
ENSG00000154146	NRGN	0.85	1.96e-03	Neurogranin	ENSG00000175832	ETV4	-0.92	1.03e-07	Ets variant transcription factor 4
ENSG00000136048	DRAM1	0.83	1.98e-04	Dna damage regulated autophagy modulator 1	ENSG00000168243	GNG4	-0.88	4.15e-03	G protein subunit gamma 4
ENSG00000101335	MYL9	0.81	1.21e-05	Myosin light chain 9	ENSG00000167291	TBC1D16	-0.87	5.60e-04	Tbc1 domain family member 16
ENSG00000127124	HIVEP3	0.77	7.56e-04	Hivep zinc finger 3	ENSG00000128567	PODXL	-0.87	5.78e-04	Podocalyxin like
ENSG00000120708	TGFBI	0.77	2.07e-05	Transforming growth factor beta induced	ENSG00000170577	SIX2	-0.86	6.06e-04	Six homeobox 2
ENSG00000143452	HORMAD1	0.77	1.96e-04	Horma domain containing 1	ENSG00000115468	EFHD1	-0.84	1.09e-02	Ef-hand domain family member d1
ENSG00000198223	CSF2RA	0.74	8.24e-04	Colony stimulating factor 2 receptor subunit alpha	ENSG00000138162	TACC2	-0.83	9.02e-04	Transforming acidic coiled-coil containing protein 2
ENSG00000186472	PCLO	0.73	5.02e-05	Piccolo presynaptic cytomatrix protein	ENSG00000112972	HMGCS1	-0.77	1.51e-03	3-hydroxy-3-methylglutaryl-coa synthase 1
ENSG00000166340	TPP1	0.69	1.73e-04	Tripeptidyl peptidase 1	ENSG00000166165	CKB	-0.72	1.37e-10	Creatine kinase b
ENSG00000134250	NOTCH2	0.69	2.42e-05	Notch receptor 2	ENSG00000145247	OCLAD2	-0.72	8.46e-03	Ocia domain containing 2
ENSG00000138061	CYP11B1	0.68	1.08e-03	Cytochrome p450 family 1 subfamily b member 1	ENSG00000076554	TPD52	-0.72	1.47e-07	Tumor protein d52
ENSG00000154265	ABCA5	0.63	1.14e-05	Atp binding cassette subfamily a member 5	ENSG00000100344	PNPLA3	-0.70	7.83e-03	Patatin like phospholipase domain containing 3
ENSG00000145012	LPP	0.61	4.90e-03	Lim domain containing preferred translocation partner in lipoma	ENSG00000177238	TRIM72	-0.67	5.84e-03	Tripartite motif containing 72
ENSG00000118058	KMT2A	0.61	5.04e-04	Lysine methyltransferase 2a	ENSG00000154917	RAB6B	-0.65	4.11e-03	Rab6b, member ras oncogene family
ENSG00000270629	NBPF14	0.60	4.47e-03	Nbpf member 14	ENSG00000159164	SV2A	-0.63	2.13e-05	Synaptic vesicle glycoprotein 2a
ENSG00000180318	ALX1	0.60	9.61e-04	Alx homeobox 1	ENSG00000171914	TLN2	-0.60	1.17e-03	Talin 2
ENSG00000160695	VPS11	0.60	3.56e-05	Vps11 core subunit of corvet and hops complexes	ENSG00000043591	ADRB1	-0.59	4.90e-04	Adrenoceptor beta 1

Summary data of the top fifty overexpressed and repressed transcripts, as ranked first by adjusted p-value and secondly by fold change (log2). Fold changes are coloured green to signify overexpression and red to signify repression. Novel transcripts are unnamed and are represented by the ensemble ID until further annotation in the future. P-values of 0 are below the machine minimum (5e-324). (n=4).

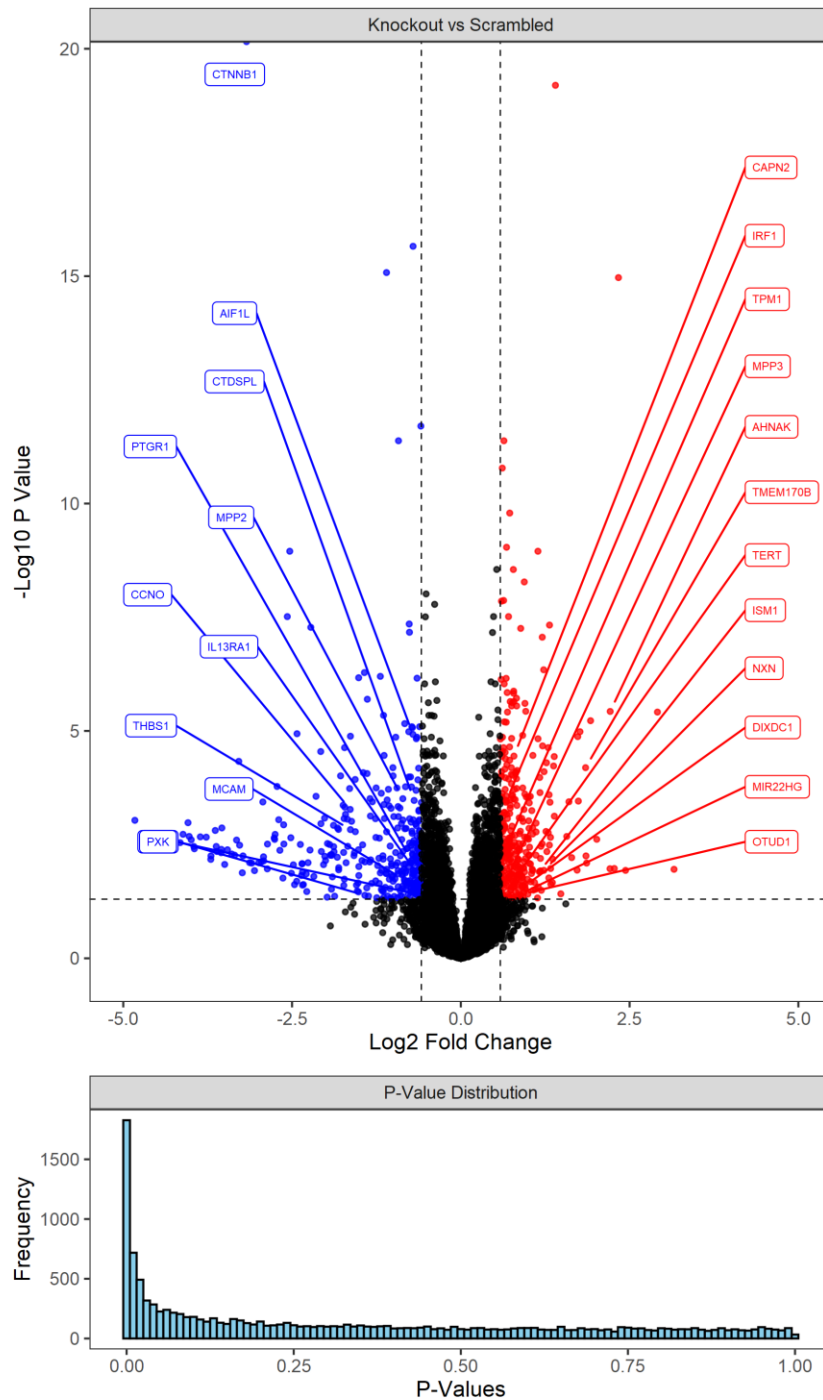


Figure 5-11: Volcano Plot for Scrambled *versus* Knockout

Volcano plot demonstrating the transcripts identified as differentially expressed based on p-value < 0.05 (Benjamini-Hochberg corrected), represented by the horizontal line, and absolute fold change of 1.5-fold, as represented by the two vertical lines (positive and negative expression change). A comparison was drawn between all scrambled samples and all knockout samples, with the cell line and treatment status set as covariates. Associated uncorrected p-value distributions are shown below each comparison, which enable a general indication of statistical soundness for each comparison. Genes which are significantly overexpressed are coloured red, whilst those which are repressed are coloured blue; non-significant genes are coloured black. Labelled points are known WNT-related genes. The adjusted p-value for *CTNNB1* was below the machine minimum ($5e-324$) and was maximised within the plot bounds to best display the remaining data.

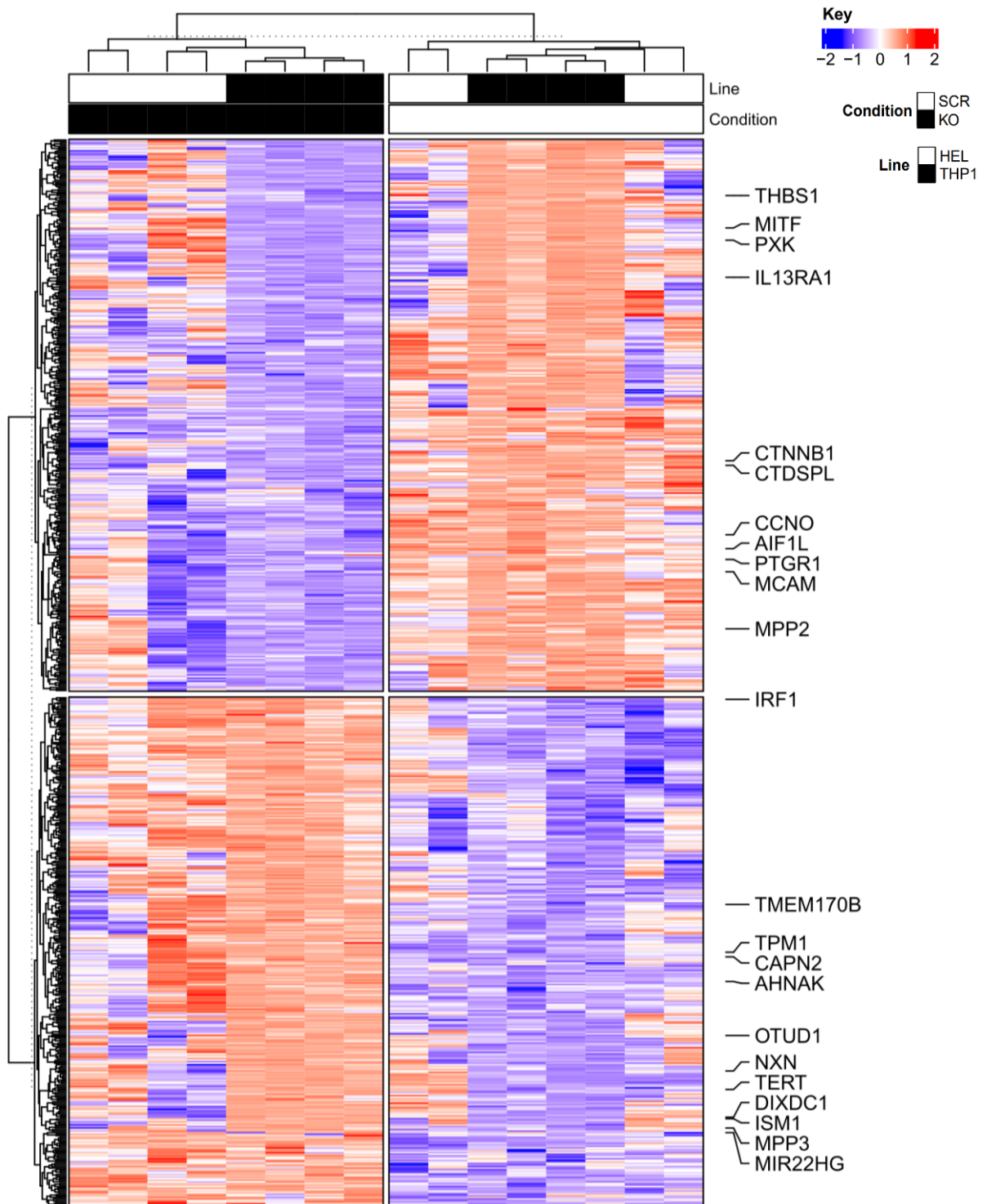


Figure 5-12: Heatmap of Differential Transcripts between Scrambled and Knockout

Heatmap of the identified differentially expressed transcripts. Columns represent samples whilst rows are genes. Samples were z-score scaled around expression mean, with red indicating high expression levels and blue low. Samples segregate without supervision into two groups with k-means clustering. WNT-related genes are annotated accordingly due to the number of transcripts identified (n=8). A comparison was drawn between all scrambled samples and all knockout samples, with the cell line and treatment status set as covariates.

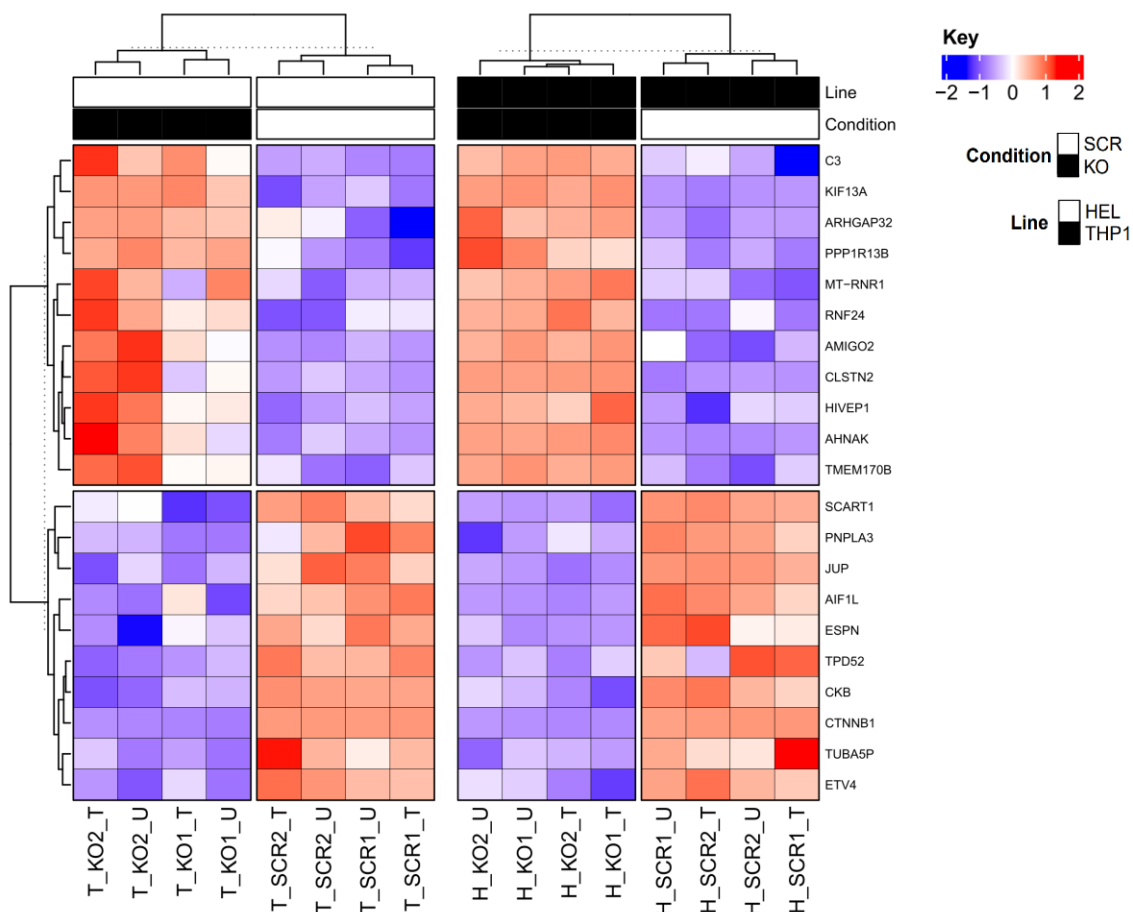


Figure 5-13: Transcripts Changed in Both HEL and THP1 Cell Lines Arising from Dual Knockout of β -catenin and γ -catenin

Heatmap of the identified differentially expressed transcripts. Columns represent samples whilst rows are genes. Samples were z-score scaled around expression mean, with red indicating high expression levels and blue low. Samples segregate without supervision into two groups with k-means clustering (n=8).

Table 5-7: Top Differentially Expressed Transcripts Between Knockout and Scrambled

ENSG	HGNC	Log2FC	PAdjusted	Description	ENSG	HGNC	Log2FC	PAdjusted	Description
ENSG00000158258	CLSTN2	2.91	3.85e-06	Calsyntenin 2	ENSG00000182240	BACE2	-3.29	4.66e-05	Beta-secretase 2
ENSG00000229855		2.33	1.08e-15	Novel transcript	ENSG00000168036	CTNNB1	-3.17	0.00e+00	Catenin beta 1
ENSG00000124942	AHNAK	2.21	3.72e-06	Ahna nucleoprotein	ENSG00000166073	GPR176	-2.72	1.66e-04	G protein-coupled receptor 176
ENSG00000102524	TNFSF13B	1.92	5.96e-06	Tnf superfamily member 13b	ENSG00000214279	SCART1	-2.57	3.06e-08	Scavenger receptor family member expressed on t cells 1
ENSG00000005844	ITGAL	1.76	1.04e-05	Integrin subunit alpha I	ENSG00000173801	JUP	-2.53	1.12e-09	Junction plakoglobin
ENSG00000205592	MUC19	1.73	1.33e-05	Mucin 19, oligomeric	ENSG00000009694	TENM1	-2.43	1.15e-05	Teneurin transmembrane protein 1
ENSG00000137177	KIF13A	1.40	6.36e-20	Kinesin family member 13a	ENSG00000126353	CCR7	-2.22	5.27e-08	C-c motif chemokine receptor 7
ENSG00000125730	C3	1.31	4.71e-08	Complement c3	ENSG00000107281	NPDC1	-2.08	2.84e-05	Neural proliferation, differentiation and control 1
ENSG00000129116	PALLD	1.29	2.33e-05	Palladin, cytoskeletal associated protein	ENSG00000115194	SLC30A3	-1.78	9.73e-05	Solute carrier family 30 member 3
ENSG00000165810	BTNL9	1.23	4.53e-07	Butyrophilin like 9	ENSG00000139269	INHBE	-1.72	2.33e-05	Inhibin subunit beta e
ENSG00000139289	PHLDA1	1.21	2.13e-05	Pleckstrin homology like domain family a member 1	ENSG00000187984	ANKRD19P	-1.65	1.85e-04	Ankyrin repeat domain 19, pseudogene
ENSG00000187239	FNBP1	1.21	8.69e-08	Formin binding protein 1	ENSG00000206052	DOCK6	-1.64	1.31e-05	Docking protein 6
ENSG00000157404	KIT	1.14	1.49e-05	Kit proto-oncogene, receptor tyrosine kinase	ENSG00000142512	SIGLEC10	-1.56	1.17e-04	Sialic acid binding ig like lectin 10
ENSG00000183134	PTGDR2	1.14	1.12e-09	Prostaglandin d2 receptor 2	ENSG00000108188	HIVEP2	-1.51	6.77e-07	Hivep zinc finger 2
ENSG00000134909	ARHGAP32	0.96	3.70e-06	Rho gtpase activating protein 32	ENSG00000100344	PNPLA3	-1.45	8.27e-05	Patatin like phospholipase domain containing 3
ENSG00000139211	AMIGO2	0.95	2.48e-06	Adhesion molecule with ig like domain 2	ENSG00000196517	SLC6A9	-1.43	5.23e-07	Solute carrier family 6 member 9
ENSG00000137965	IFI44	0.94	5.29e-09	Interferon induced protein 44	ENSG00000113083	LOX	-1.39	8.65e-05	Lysyl oxidase
ENSG00000135604	STX11	0.92	1.25e-05	Syntaxin 11	ENSG00000137225	CAPN11	-1.38	2.01e-06	Calpain 11
ENSG00000171777	RASGRP4	0.89	5.57e-08	Ras guanyl releasing protein 4	ENSG00000176834	VSIG10	-1.25	1.79e-04	V-set and immunoglobulin domain containing 10
ENSG00000125814	NAPB	0.83	2.82e-06	Nsf attachment protein beta	ENSG00000188549	CCDC9B	-1.19	6.31e-07	Coiled-coil domain containing 9b
ENSG00000095951	HIVEP1	0.82	1.91e-06	Hivep zinc finger 1	ENSG00000183853	KIRREL1	-1.18	2.35e-04	Kirre like nephrin family adhesion molecule 1
ENSG00000211459	MT-RNR1	0.79	2.26e-06	Mitochondrially encoded 12s rna	ENSG00000170293	CMTM8	-1.14	4.55e-06	Cklf like marvel transmembrane domain containing 8
ENSG00000127415	IDUA	0.78	1.33e-06	Alpha-l-iduronidase	ENSG00000070087	PFN2	-1.14	3.46e-05	Profilin 2
ENSG00000125772	GPCPD1	0.78	1.48e-06	Glycerophosphocholine phosphodiesterase 1	ENSG00000114529	C3orf52	-1.10	8.34e-16	Chromosome 3 open reading frame 52
ENSG00000124588	NQO2	0.78	2.82e-09	N-ribosyldihydro nicotinamide:quinone reductase 2	ENSG00000136295	TTYH3	-1.07	1.92e-04	Tweety family member 3
ENSG00000101236	RNF24	0.76	2.40e-06	Ring finger protein 24	ENSG00000237506	RPSAP15	-1.01	6.43e-05	Ribosomal protein sa pseudogene 15
ENSG00000088808	PPP1R13B	0.75	2.82e-06	Protein phosphatase 1 regulatory subunit 13b	ENSG00000065320	NTN1	-1.00	9.73e-05	Netrin 1
ENSG00000130775	THEMIS2	0.75	1.46e-05	Thymocyte selection associated family member 2	ENSG00000146416	AIG1	-0.96	1.37e-05	Androgen induced 1
ENSG00000080803	JARID2	0.73	2.26e-06	Jumonji and at-rich interaction domain containing 2	ENSG00000124613	ZNF391	-0.95	1.79e-04	Zinc finger protein 391
ENSG00000186951	PPARA	0.72	1.62e-10	Peroxisome proliferator activated receptor alpha	ENSG00000175832	ETV4	-0.92	4.17e-12	Ets variant transcription factor 4
ENSG00000154930	ACSS1	0.72	2.25e-05	Acyl-coa synthetase short chain family member 1	ENSG00000187017	ESPN	-0.83	6.91e-06	Espin
ENSG00000112137	PHACTR1	0.71	3.06e-08	Phosphatase and actin regulator 1	ENSG00000196814	MVB12B	-0.82	1.69e-04	Multivesicular body subunit 12b
ENSG00000101224	CDC25B	0.69	3.85e-06	Cell division cycle 25b	ENSG00000145391	SETD7	-0.77	1.03e-04	Set domain containing 7, histone lysine methyltransferase
ENSG00000137193	PIM1	0.69	1.43e-06	Pim-1 proto-oncogene, serine/threonine kinase	ENSG00000226435	ANKRD18DP	-0.77	1.04e-05	Ankyrin repeat domain 18d, pseudogene
ENSG00000088812	ATRN	0.68	9.15e-10	Attractin	ENSG00000134247	PTGFRN	-0.76	4.45e-08	Prostaglandin f2 receptor inhibitor
ENSG00000124151	NCOA3	0.67	6.44e-06	Nuclear receptor coactivator 3	ENSG00000160932	LY6E	-0.76	6.77e-08	Lymphocyte antigen 6 family member e
ENSG00000101290	CDS2	0.67	6.99e-07	Cdp-diacylglycerol synthase 2	ENSG00000089876	DHX32	-0.74	1.03e-04	Deah-box helicase 32 (putative)
ENSG00000125779	PANK2	0.66	2.96e-05	Pantothenate kinase 2	ENSG00000152952	PLOD2	-0.73	1.70e-04	Procollagen-lysine,2-oxoglutarate 5-dioxygenase 2
ENSG00000088970	KIZ	0.65	6.31e-06	Kizuna centrosomal protein	ENSG00000204899	MZT1	-0.73	8.08e-06	Mitotic spindle organizing protein 1
ENSG00000260997		0.64	9.22e-07	Novel transcript, overlapping myo1g	ENSG00000092621	PHGDH	-0.72	8.48e-06	Phosphoglycerate dehydrogenase
ENSG00000109756	RAPGEF2	0.64	4.17e-12	Rap guanine nucleotide exchange factor 2	ENSG00000126878	AIF1L	-0.71	1.19e-05	Allograft inflammatory factor 1 like
ENSG00000101265	RASSF2	0.63	1.35e-08	Ras association domain family member 2	ENSG00000166165	CKB	-0.71	2.20e-16	Creatine kinase b
ENSG00000197555	SIPAL1L	0.63	2.33e-05	Signal induced proliferation associated 1 like 1	ENSG00000082781	ITGB5	-0.66	2.02e-04	Integrin subunit beta 5
ENSG00000178115	GOLGABQ	0.62	2.80e-05	Golgin a8 family member q	ENSG00000109881	CCDC34	-0.66	1.49e-05	Coiled-coil domain containing 34
ENSG00000197043	ANXA6	0.62	1.37e-05	Annexin a6	ENSG00000076554	TPD52	-0.65	6.93e-07	Tumor protein d52
ENSG00000173821	RNF213	0.61	1.66e-11	Ring finger protein 213	ENSG00000083635	NUFIP1	-0.65	1.38e-05	Nuclear fmr1 interacting protein 1
ENSG00000120451	SNX19	0.60	1.40e-08	Sorting nexin 19	ENSG00000115109	EPB41L5	-0.64	1.19e-04	Erythrocyte membrane protein band 4.1 like 5
ENSG00000136286	MYO1G	0.60	2.96e-05	Myosin ig	ENSG00000177614	PGBD5	-0.63	6.60e-05	Piggybac transposable element derived 5
ENSG00000185880	TRIM69	0.60	7.35e-07	Tripartite motif containing 69	ENSG00000099256	PRTFDC1	-0.61	8.08e-06	Phosphoribosyl transferase domain containing 1
ENSG00000180229	HERC2P3	0.59	1.51e-05	Hect domain and rld 2 pseudogene 3	ENSG00000165152	PGAP4	-0.59	1.98e-12	Post-gpi attachment to proteins galnac transferase 4

Summary data of the top fifty overexpressed and repressed transcripts, as ranked first by adjusted p-value and secondly by fold change (log2). Fold changes are coloured green to signify overexpression and red to signify repression. Novel transcripts are unnamed and are represented by the ensemble ID until further annotation in the future. P-values of 0 are below the machine minimum (5e-324). (n=4).

5.3.3 Mechanistic Pathway Analysis Suggests RAP1 is a Target of WNT/ β -catenin Signalling

5.3.3.1 Impact of *rWNT3a* Activation on Signalling Pathways

To provide better biological context to the perturbed genes, pathway analysis was performed. Two distinct classical subtypes of pathway analysis were performed to examine the transcriptomic findings: ORA and GSEA. These were considered in a range of pathway databases to maximise the potential findings, as different databases vary in the genes considered within each respective pathway (2.13.3.4). Additionally, as each database is considered separately and are of different size, cross-comparison of databases is not appropriate; however, commonality in identified pathways provides greater evidence that a particular pathway is perturbed. A limitation of this approach is the variation in gene members defined within each database for pathways. For instance, *WISP1* and *RUNX1T1* are members of the WNT/ β -catenin signalling pathway in the WP database but both genes are not included in the KEGG and REAC database definition of the WNT signalling pathway. This is well recognised within the field and efforts to overcome this have been suggested, such as combining different databases into a singular priori, though these incur further limitations, such as reduced statistical power (Domingo-Fernández *et al.*, 2019b; Mubeen *et al.*, 2019).

ORA revealed few pathways, largely owed to the low number of differentially expressed genes identified after multiple test correction in the THP1 *rWNT3a* treated *versus* vehicle comparison (5.3.2), corresponding to the input for this analysis. However, terms related to immune and inflammatory activation were indicated by the GO (**Figure 5-14**). Ferroptosis, a type of programmed cell death, was identified in both the KEGG and WP database, suggesting a potential stress effect. The RAP1 signalling pathway was identified within the KEGG dataset. TF analysis further revealed several related factors of interest, such as WT1, SP1, and MIZ-1.

GSEA also identified the RAP1 signalling pathway, amongst others, in the KEGG database (**Figure 5-15**). This analysis further identified significant positive enrichment of the MYC Targets terms V1 and V2, confirming WNT/ β -catenin activation. Negative enrichment of inflammatory response, hypoxia, apoptosis, and interferon α/γ response was found, suggesting WNT/ β -catenin regulates processes associated with stress conditions. In summary,

rWNT3a induction was associated with enrichment for MYC targets, PD-1, RAP1, and p53 signalling pathways.

5.3.3.2 Knockout of WNT/ β -catenin Signalling Perturbs RAP1 Signalling

To examine the impact of dual β -catenin and γ -catenin knockout, an equivalent pathway analysis was performed in the context of scrambled *versus* knockout within both cell lines.

ORA revealed RAP1 signalling to be the only enriched signalling pathway within the KEGG dataset, as was observed in the rWNT3a-induced comparison (5.3.3.1). Remaining pathways from other databases largely related to infection, injury, and other indicators of acute inflammation, suggesting a state of cell stress (**Figure 5-16A**).

As expected, GSEA identified WNT signalling as significantly negatively enriched in the BC, MSIG, REAC, and WP databases. This was particularly of interest within the WP database, which identified repression of the WNT/ β -catenin signalling pathway in leukaemia. MSIG further demonstrated negative enrichment of the MYC targets V1 and V2, which were previously shown to be activated (**Figure 5-16B**). The GO database results indicate modulation of Ca^{2+} levels, as the WNT/ Ca^{2+} was negatively enriched, alongside positive enrichment of Calmodulin activity, GTPase regulator activity, and modulation of the ERK1 and ERK2 cascade - all indicators of altered RAP1 signalling activity (**Figure 5-17**).

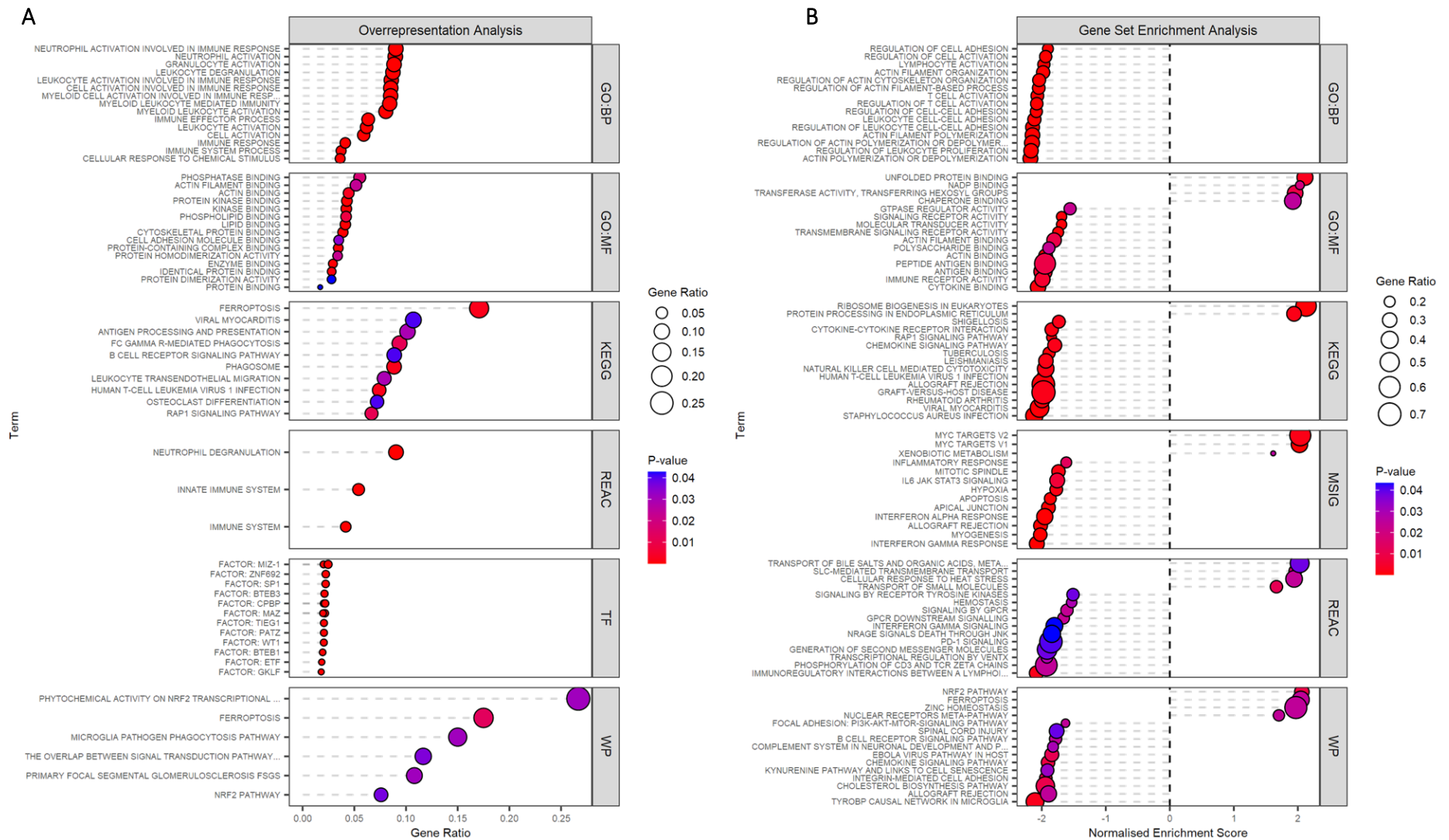


Figure 5-14: Pathway Analysis for THP1 Scrambled with rWNT3a Treatment

The top fifteen pathways by p-value from the overrepresentation analysis (2.13.3.4) are separated by database and ordered by gene ratio (identified genes to total gene set size). **B**) The top fifteen by p-value from the gene set enrichment analysis are separated by database and ordered by their respective Enrichment Scores. Points are coloured and scaled by their p-value and gene ratio, respectively. **GO** – Gene Ontology; **KEGG** – Kyoto Encyclopaedia of Genes & Genomes; **REAC** – Reactome; **TF** – Transfac; **WP** – Wikipathways; **MSIG** – Hallmark Molecular Signatures.

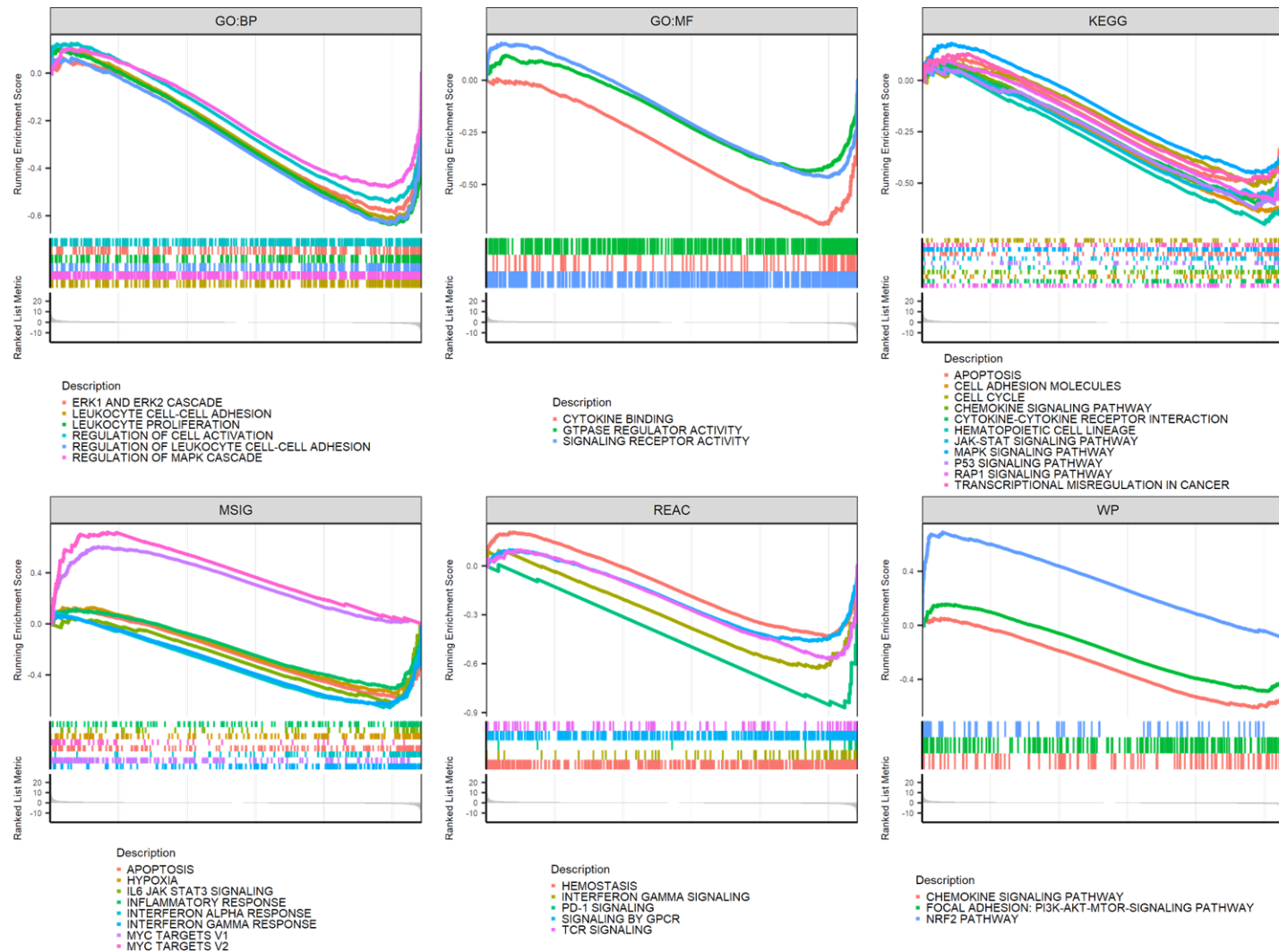
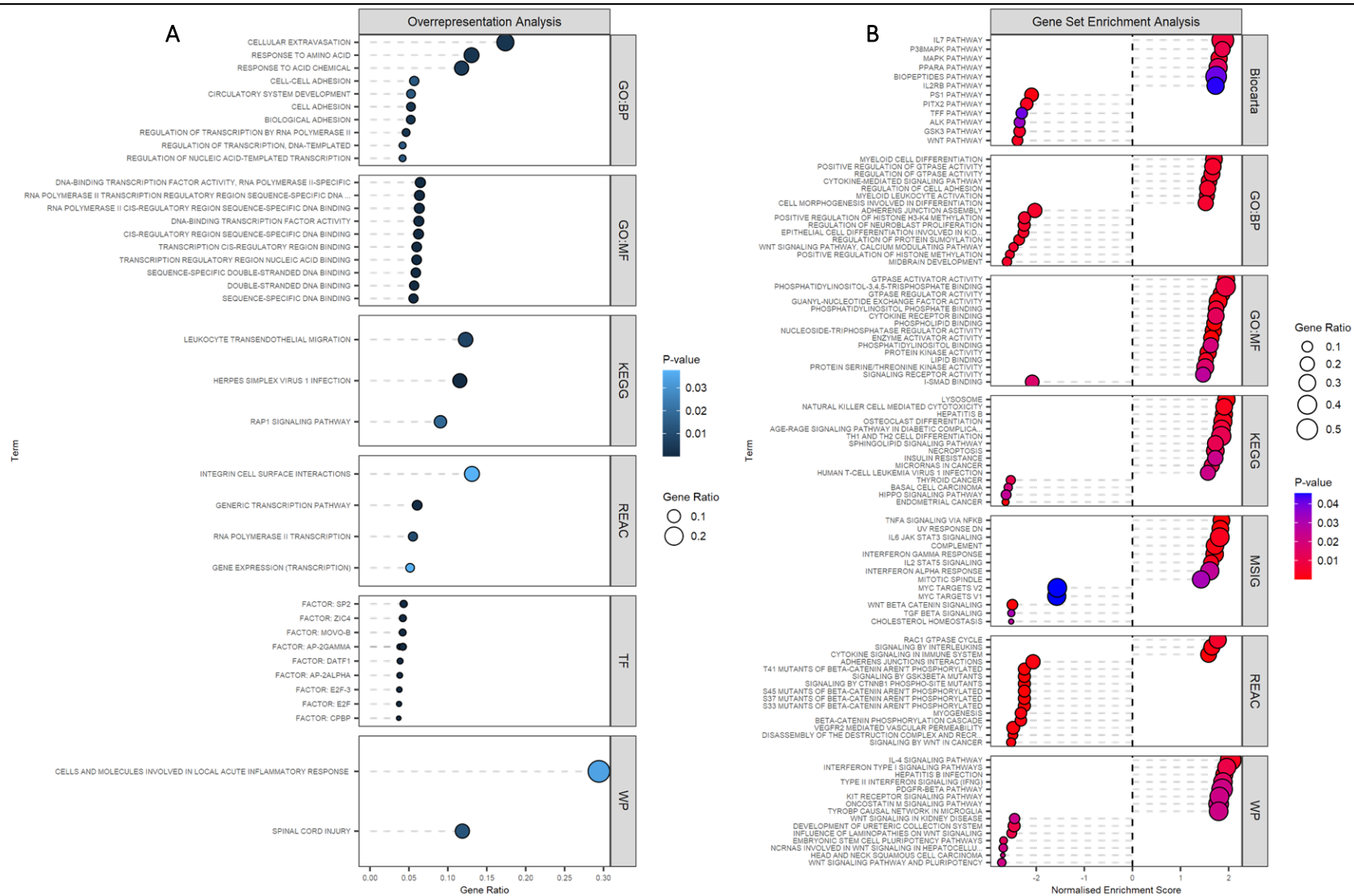


Figure 5-15: GSEA Barcode Plot for Significant Terms with rWNT3a Treatment

GSEA barcode plots demonstrating the transcriptional enrichment of genes identified within specific pathways, between databases (2.13.3.4). Each database represents several independent pathways, as demonstrated by the different colours in both the line and barcode, which is described below each plot. Each pathway shown had a p-value <0.05.



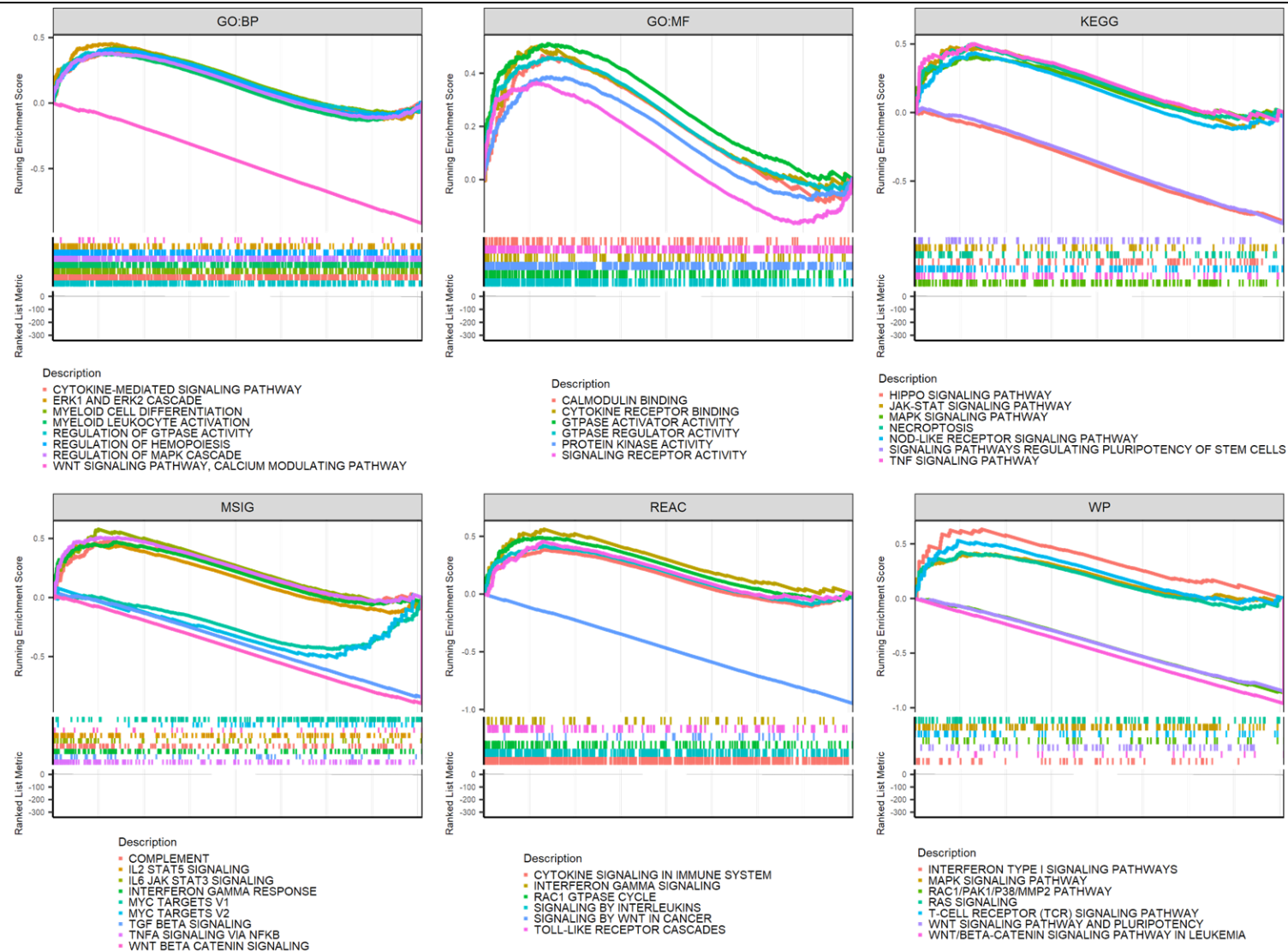


Figure 5-17: GSEA Barcode Plot for Significant Terms with Knockout

GSEA barcode plots demonstrating the transcriptional enrichment of genes identified within specific pathways, between databases (2.13.3.4). Each database represents several independent pathways, as demonstrated by the different colours in both the line and barcode, which is described below each plot. Each pathway shown had a p-value <0.05 and a q-value <0.25.

5.3.3.3 Pathway Impact Analysis Provides Evidence for WNT/RAP Signalling

Even though the previous classical methods (ORA and GSEA) are able to provide an indication of pathways which are perturbed, these are incapable of accurately indicating the resulting status of a perturbed pathway (Koumakis *et al.*, 2016; Domingo-Fernández *et al.*, 2019a). Even when GSEA suggests a directional enrichment, this cannot be reliably interpreted as a pathway being activated or repressed. To overcome this limitation, SPIA was performed (2.13.3.4). This technique incorporates data on the protein level interactions and nature of each respective interaction to incorporate mechanistic study of pathway topology, thus facilitating the calculation of predicted pathway state.

SPIA identified RAP1 signalling as the top signalling pathway by corrected p-value in both comparisons, firstly between rWNT3a treated THP1 scrambled *versus* untreated THP1 scrambled, referred to as WNT-active, and later in the comparison between knockout and scrambled samples, referred to as knockout. Critically, RAP1 signalling was predicted to be active in the first comparison, and inactive in the latter (**Figure 5-18A|B**). This switch in signalling could prove critical to the observed phenotype. WNT signalling was not found to be significantly enriched with SPIA in the WNT-active context, but it was determined to be inhibited in the knockout condition. This inconsistency is owed to limitations in sub-pathway analysis with the KEGG database, as the WNT pathway includes the both the canonical and non-canonical pathways.

The identification of a WNT-RAP1 switch between states suggests that RAP1 signalling is involved in the loss of clonogenicity observed in this study (4.3.4.3). However, the examination of WNT/ β -catenin signalling in the patient context is necessary to provide a greater insight into whether such a finding is comparable in these conditions. To this end, the TCGA dataset, which contains patient RNA-seq data, was analysed (5.3.4, 5.3.5).

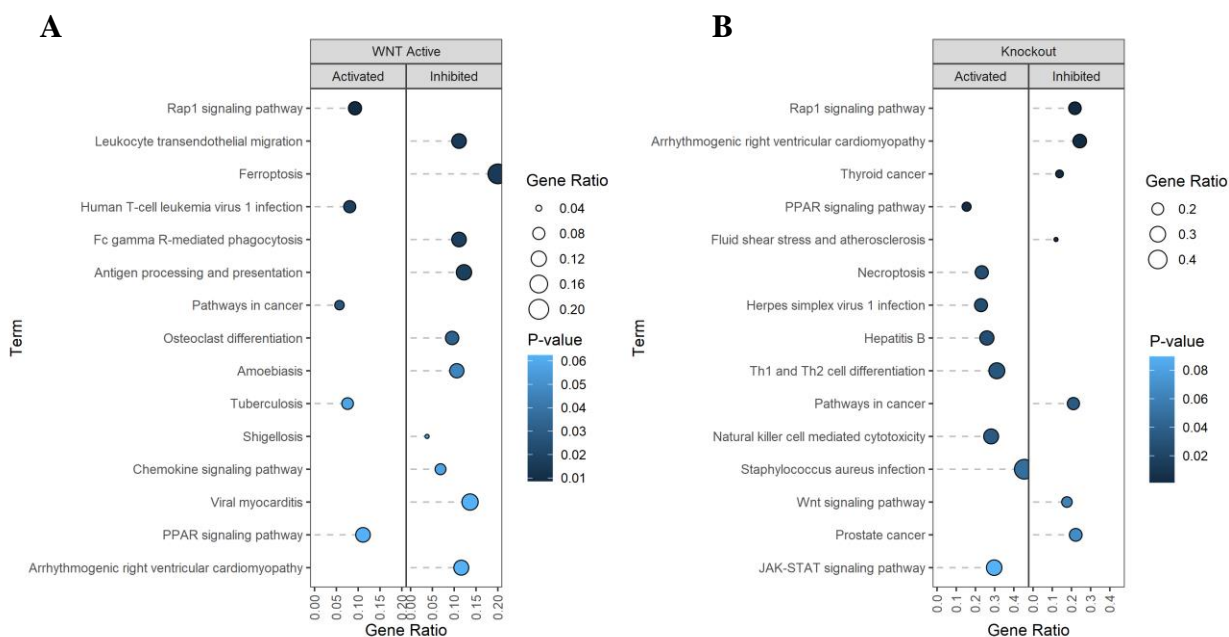


Figure 5-18: SPIA of rWNT3a Treated and Knockout Comparisons

A) The top fifteen KEGG pathways identified via SPIA (2.13.3.4) from the differentially expressed genes identified in the rWNT3a treated *versus* vehicle control test in THP1. Points are coloured and ordered by corrected p-value and scaled by gene ratio. **B)** The top fifteen KEGG pathways identified via SPIA from the differentially expressed genes identified in the knockout *versus* scrambled test in both cell lines, with the points coloured and ordered by corrected p-value and scaled by gene ratio.

5.3.4 Differential Expression based on LEF1 in Patient Data

To investigate whether a comparable analysis of WNT/ β -catenin active *versus* WNT/ β -catenin inactive state could be performed in a patient context, raw count data from the TCGA patient database was acquired. Patient data were pre-screened to remove those with APL, those who had not received treatment, and those with transcriptomic profiles presenting T-cell contamination; all were uninformative to further study (2.13.4.4).

To distinguish patients with active WNT/ β -catenin signalling against those which are inactive, *LEF1* expression was applied as a proxy indicator. Whilst not a definitive indicator, *LEF1* has been documented to be involved in nuclear translocation of β -catenin and is rapidly degraded in lines and patients without WNT/ β -catenin activity (Morgan *et al.*, 2019). *LEF1* was confirmed as overexpressed in the cell line context at the transcriptomic level, indicating this approach is warranted (S2.).

LEF1 expression levels were heterogeneous between patient samples, with a small subset of patients presenting with extreme high expression (data not shown). These perhaps represent samples which have a remaining measure of T-cell contamination, as T-cells express elevated levels of *LEF1* constitutively. Subsequently, patients were stratified according to high and low *LEF1* expression by z-score from mean and compared for differentiation expression (S7.).

ORA was performed on the differentially expressed genes identified by comparing the patients with *LEF1*^{HIGH} and *LEF1*^{LOW} expression, which revealed the enrichment of a broad range of pathways. Notably, calcium channel activity and generation of secondary messenger molecules were within the top pathways, suggesting Ca^{2+} -derived modulation is occurring; interestingly, RAP1 signalling was not detected (**Figure 5-19A**). Ca^{2+} signalling is being increasingly recognised as a central event in HSC maintenance and LSC self-renewal (Lewuillon *et al.*, 2022). The remaining profile largely consisted of immune modulation and PD-1 signalling, consistent with prior findings in the WNT-active expression profile (5.3.3.1).

Alternatively, GSEA was able to identify significant enrichment of the general WNT signalling activity in the GO, KEGG, MSIG, and WP databases (**Figure 5-19B**), alongside the focused WNT/ β -catenin pathway, suggesting *LEF1* is a reasonable indicator of WNT activity. However, MSIG identified MYC targets V1 and V2 as negatively enriched, opposing the enrichment of WNT signalling, perhaps suggesting transcriptional activation was repressed by unknown mechanisms despite active WNT/ β -catenin signalling.

As the patient expression profiles were highly heterogenous, application of a more recently developed pathway analysis technique known as GSVA was performed, to examine the perturbed pathways without the need to pre-classify patients. GSVA identified numerous differentially enriched pathways which, when represented in a heatmap, separated patient samples broadly into high and low *LEF1* groups through unsupervised clustering (**Figure 5-20**). Within the REAC database, GSVA identified positive enrichment of ‘*CTNNB1:TCF/LEF* binding to target gene promoters’, which would suggest WNT/ β -catenin signalling activity; however, as in the GSEA analysis, positive enrichment of the ‘Repression of WNT target genes’ was found, suggesting repression of WNT target genes. The potential source of this inhibition could be via *RUNX3*, which was found to be significantly upregulated in the *LEF1*^{HIGH} patients as the REAC pathway ‘*RUNX3* regulates WNT signalling’. *RUNX3* negatively regulates WNT/ β -catenin signalling by binding to and inhibiting the transcription complex (Ito *et al.*, 2008; Ju *et al.*, 2014; Sweeney *et al.*, 2020). Together, these observations suggest WNT/ β -catenin is possibly active in *LEF1*^{HIGH}-AML patients, but downstream target genes are potentially not modulated due to a *RUNX3*-derived block.

As SPIA relies upon an arbitrary list of differentially expressed genes to compute activity, the modern application of mechanistic pathway analysis, MinePath, was applied. MinePath examines both pathway activation and target gene levels to compute a more accurate pathway state. Minepath did not identify WNT signalling suggesting, instead, suppression of target gene promotion (**Table 5-8**). In conclusion, these pathway analyses indicate *LEF1* is a reasonable, but not exact, proxy to indicate WNT-activity, but that a profile of WNT/ β -catenin repression also exists.

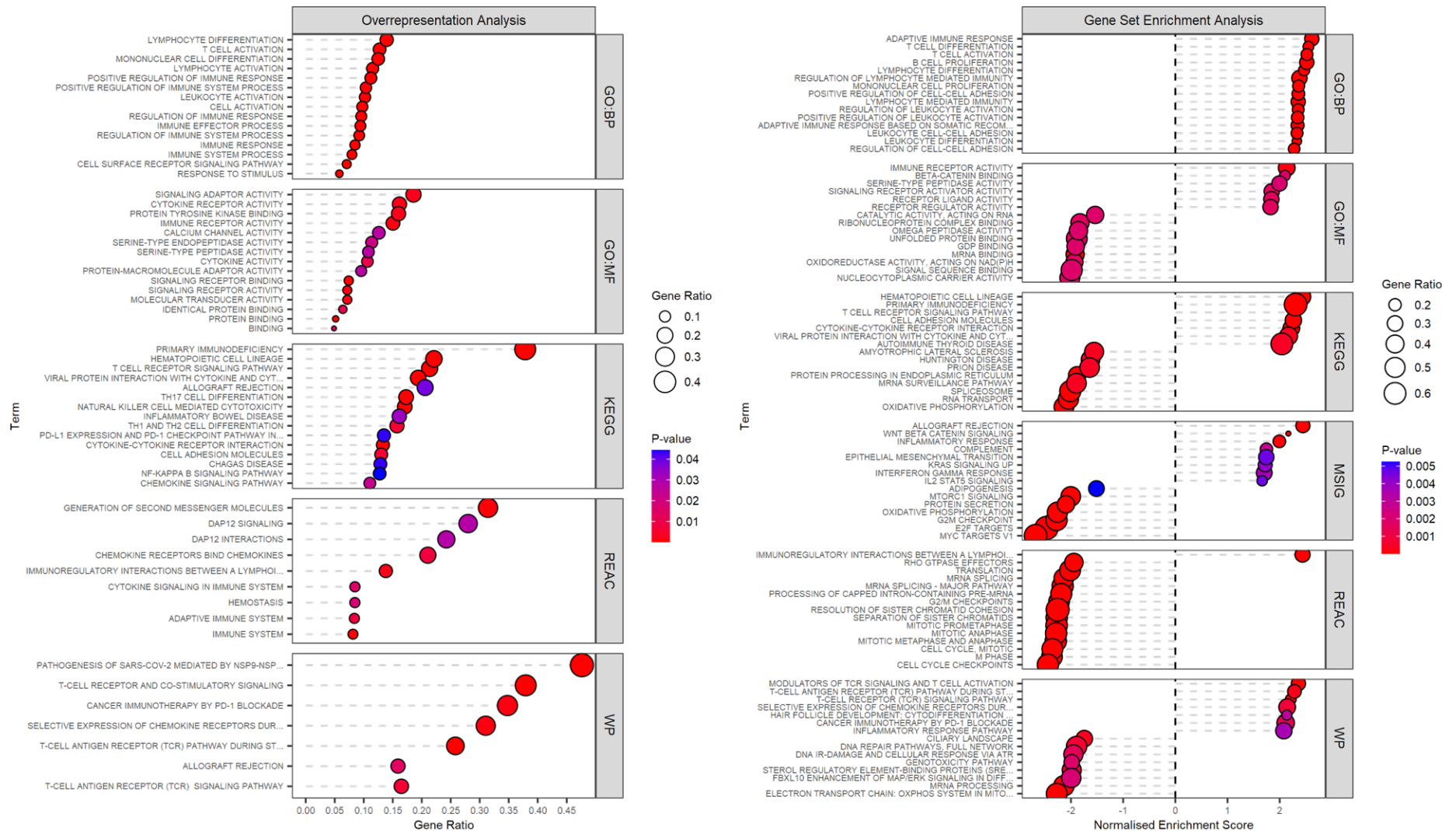


Figure 5-19: Pathway Analysis Results for *LEF1*^{HIGH} versus *LEF1*^{LOW} Contrast

The top fifteen pathways by p-value from the overrepresentation analysis (2.13.3.4) are separated by database and ordered by gene ratio. **B)** The top fifteen by p-value from the gene set enrichment analysis are separated by database and ordered by Enrichment Score. Points are coloured and scaled by their p-value and gene ratio, respectively. **GO** – Gene Ontology; **KEGG** – Kyoto Encyclopaedia of Genes & Genomes; **REAC** – Reactome; **TF** – Transfac; **WP** – Wikipathways; **MSIG** – Hallmark Molecular Signatures.

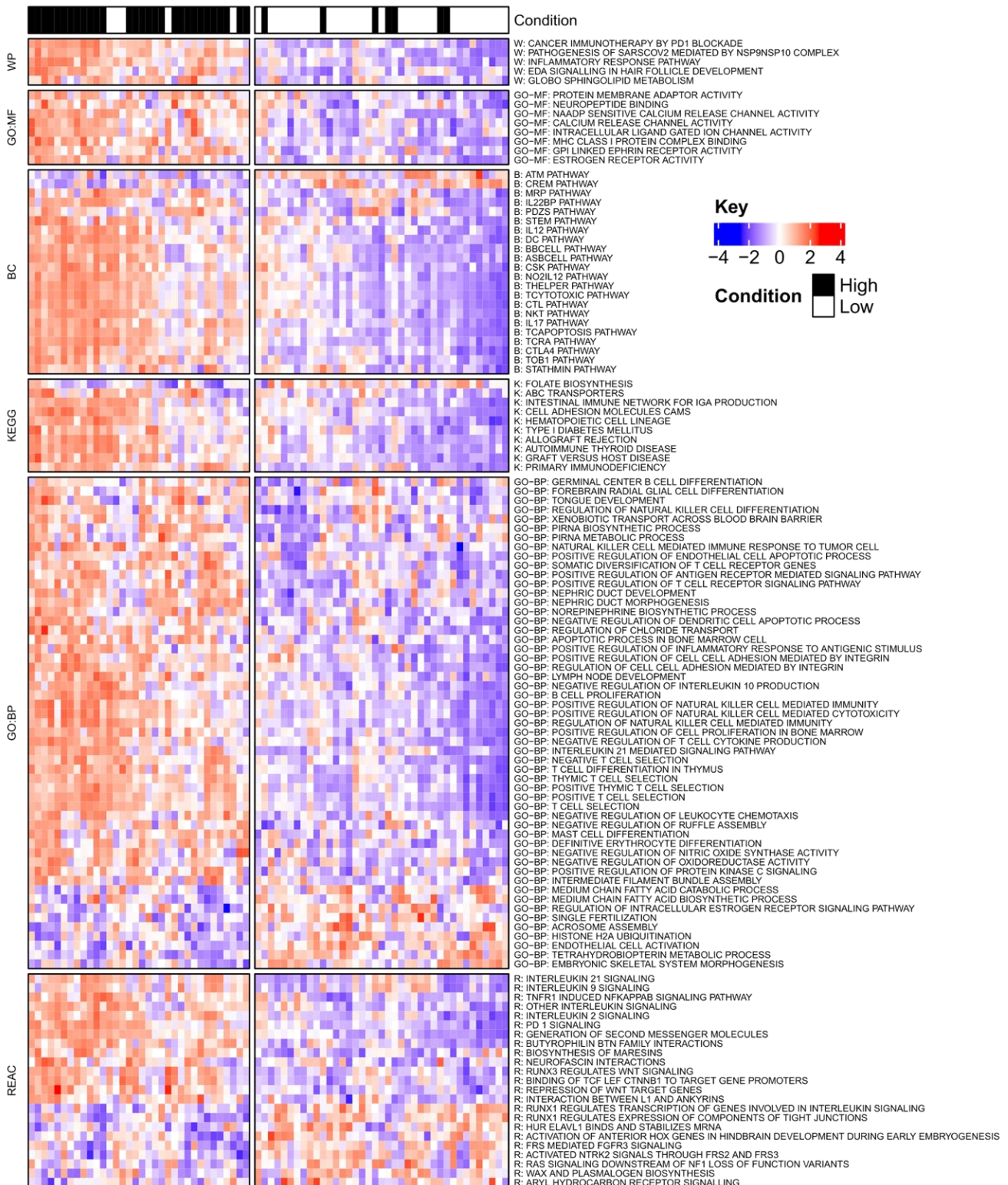


Figure 5-20: GSVA Heatmap of Perturbed Terms Between LEF1 Expression Levels

Heatmap of the identified perturbed pathways by GSVA (2.13.3.4). Columns represent samples whilst rows are pathways. Samples were z-score scaled around expression mean, with red indicating high expression levels and blue low. Samples segregate without supervision into two groups with k-means clustering, with few samples' mis-classified.

Table 5-8: Top Pathways Identified by Minepath Based on *LEF1* Expression Levels

Pathway	Genes	Subpaths	Active In High LEF1	Active In Low LEF1	P-value
<i>Ras signaling pathway</i>	235	1068	22	20	4.186750e-10
<i>Rap1 signaling pathway</i>	213	1503	7	7	2.974390e-04
<i>Sphingolipid signaling pathway</i>	118	150	15	0	6.249320e-04
<i>Fc gamma R-mediated phagocytosis</i>	93	182	18	0	9.431440e-04
<i>Pentose phosphate pathway</i>	26	290	9	0	2.442713e-03
<i>Vitamin B6 metabolism</i>	5	12	4	0	4.757826e-03
<i>Platelet activation</i>	126	266	20	0	6.699552e-03
<i>Phospholipase D signaling pathway</i>	142	212	8	3	6.798327e-03
<i>Glycerolipid metabolism</i>	52	145	0	11	1.110000e-02
<i>Apoptosis</i>	90	121	5	3	1.850000e-02
<i>Selenocompound metabolism</i>	12	27	4	0	1.890000e-02
<i>Notch signaling pathway</i>	49	44	6	0	2.230000e-02
<i>p53 signaling pathway</i>	65	303	2	7	2.490000e-02
<i>Sphingolipid metabolism</i>	40	361	14	0	3.110000e-02
<i>Chemokine signaling pathway</i>	198	230	14	0	3.700000e-02
<i>Prolactin signaling pathway</i>	71	140	7	0	4.010000e-02
<i>Pyrimidine metabolism</i>	99	606	0	8	4.080000e-02
<i>Axon guidance</i>	133	160	9	0	4.180000e-02
<i>Regulation of actin cytoskeleton</i>	219	265	7	0	6.450000e-02

Summary of the differentially perturbed pathways as identified by MinePath (2.13.3.4). Terms were ranked and coloured by corrected p-value.

Pathway – Name of the pathway identified

Genes – Number of genes identified

Subpaths – Number of subpaths computed and assessed

Active in Low/High LEF1 – Number of pathway components which were differentially activated or repressed in each respective group.

5.3.5 Patient Analysis – Survival Delimitation

Whilst *LEF1* expression was used as an indicator of active WNT/ β -catenin signalling in patients, the profile was not conclusive, with significant enrichment of terms and processes related to suppression of WNT target genes. If WNT/ β -catenin signalling indeed has a direct consequence upon disease severity and relapse, it would be expected that WNT/ β -catenin would manifest with a direct consequence upon patient survival. Accordingly, patients were separated according to five-year overall survival irrespective of *LEF1* expression levels. Patients censored prior to achieving five-year survival were not included. In the literature, β -catenin expression has been associated with shortened relapse-free survival and overall survival (Ysebaert *et al.*, 2006) and is frequently found at higher expression levels upon relapse, suggesting a selective pressure toward β -catenin accumulation (X. Jiang *et al.*, 2018a).

GSEA indicated that patients who did not survive five years post-diagnosis were associated with a pattern of significant positive pathway enrichment. The WNT/ β -catenin signalling pathway alongside the MYC targets V1 and V2 were identified as positively enriched, as were the PD-1 and p53 pathways (**Figure 5-22**), consistent with WNT target gene activation in the cell line data (5.3.2). *RUNX3* was identified, but levels were reduced, providing further evidence of WNT activation in this group. Critically, the RAP1 signalling pathway was identified as enriched within the KEGG database, further confirmed by the enrichment of downstream terms, such as the ERK1 and ERK2 cascade in the GO database, previously identified in the literature (Stork, 2003; Gyan *et al.*, 2005; Stork *et al.*, 2005; Yougen Wu *et al.*, 2015; Y. L. Zhang *et al.*, 2017; Keyes *et al.*, 2020).

By applying the MinePath package to account for mechanistic topology, the RAP1 and WNT signalling pathway were both found to be significantly differentially enriched (**Table 5-9**). This was particularly evident for RAP1 signalling, which was identified as the top pathway by p-value, number of activated genes, and number of activated sub-paths. This analysis shows that these patients have a WNT-active form of AML and, further, that WNT signalling conveys poor prognostic indication. Collectively, these data also suggest WNT/ β -catenin interacts to modulate RAP1 signalling activity either through β -catenin alone, or directly through WNT/ β -catenin signalling activity.

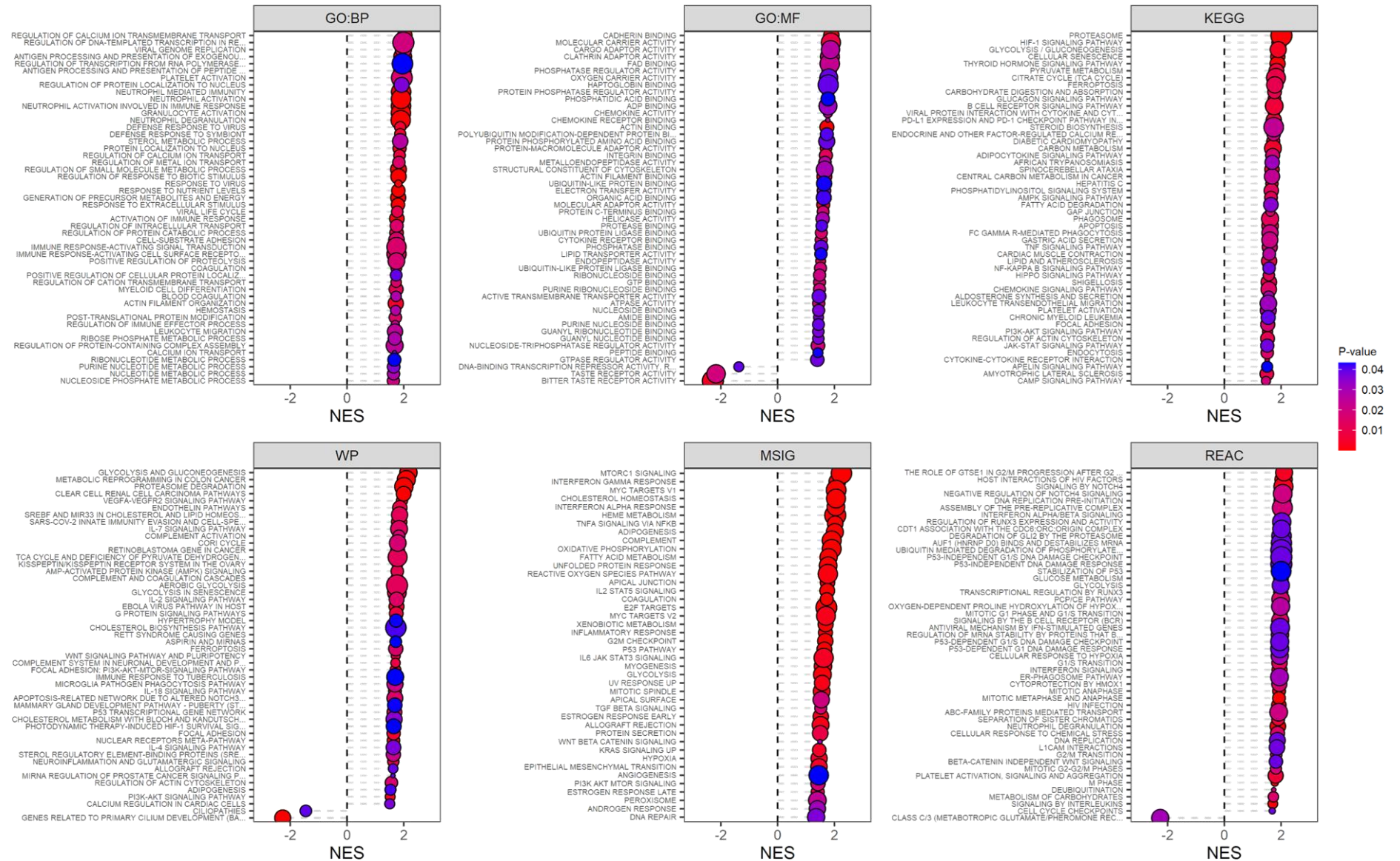


Figure 5-21: Gene-set Enrichment Analysis Results for 5-year Survival Contrast

The top fifty pathways by p-value from the gene set enrichment analysis (2.13.3.4) as separated by database and ordered by enrichment scores. Points are coloured and scaled by their p-value and gene ratio, respectively. **GO** – Gene Ontology; **KEGG** – Kyoto Encyclopaedia of Genes & Genomes; **REAC** – Reactome; **TF** – Transfac; **WP** – Wikipathways; **MSIG** –Molecular Signatures.

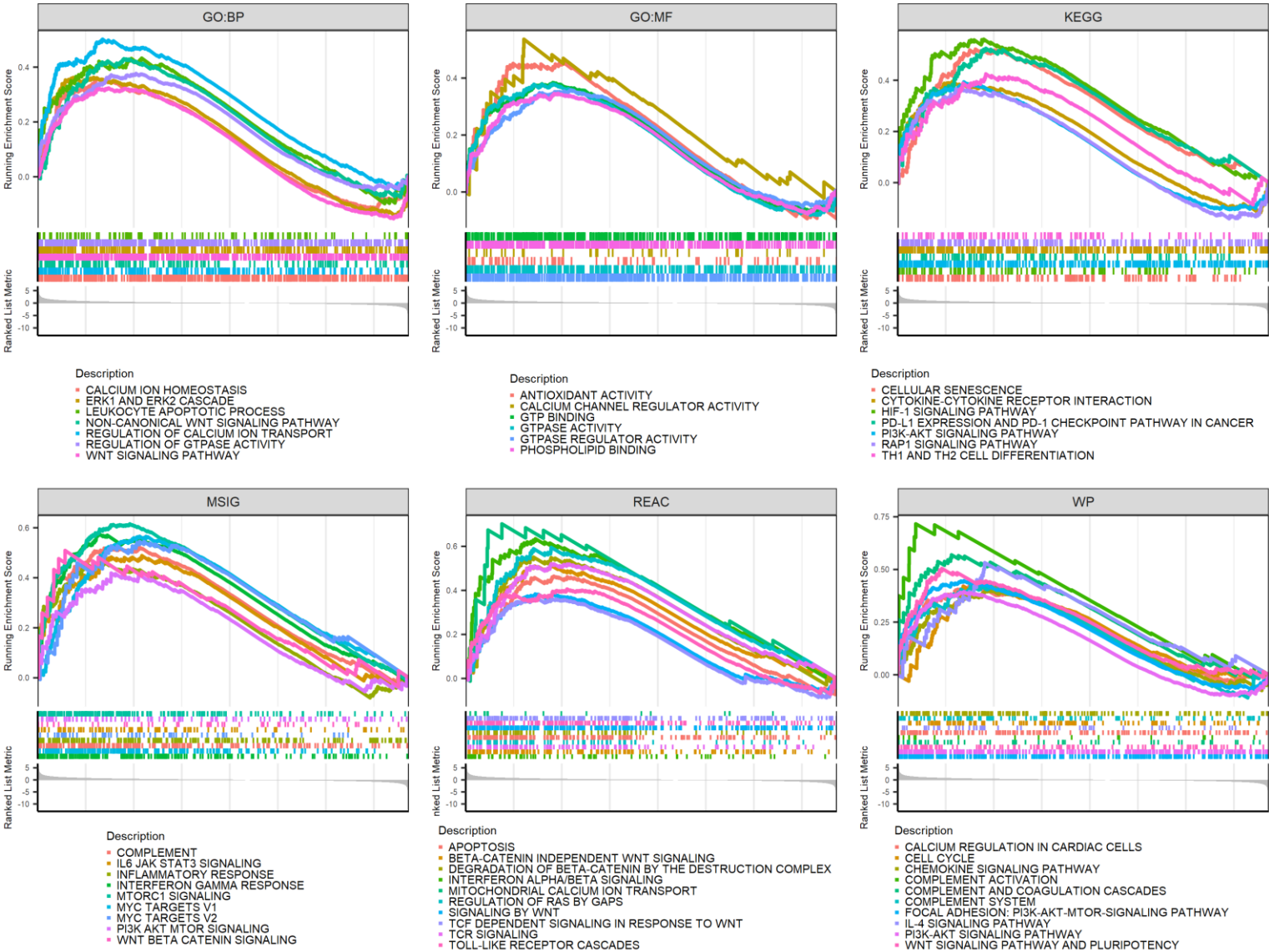


Figure 5-22: GSEA Barcode Plots for Top Enriched Terms Relating to 5-year Survival

GSEA barcode plots demonstrating the transcriptional enrichment of genes identified within specific pathways, between databases (2.13.3.4). Each database represents several independent pathways, as demonstrated by the different colours in both the line and barcode, which is described below each plot. Each pathway shown had a p-value <0.05 and a q-value <0.25.

Table 5-9: Top Pathways Identified by Minepath Relating to 5-year Survival

Pathway	Genes	Subpaths	Active In Deceased	Active In Living	P-value
<i>Rap1 signaling pathway</i>	213	1503	40	1	5.151100e-10
<i>Glycerophospholipid metabolism</i>	84	553	0	25	3.086950e-05
<i>Pantothenate and CoA biosynthesis</i>	17	49	11	0	8.623080e-05
<i>Retinol metabolism</i>	61	343	0	7	1.986708e-03
<i>Thyroid hormone synthesis</i>	73	19	5	1	2.361829e-03
<i>Glycerolipid metabolism</i>	52	145	0	12	2.700070e-03
<i>Sphingolipid signaling pathway</i>	118	150	7	1	4.782967e-03
<i>Fructose and mannose metabolism</i>	28	103	0	6	5.871785e-03
<i>TGF-beta signaling pathway</i>	83	94	2	0	5.871785e-03
<i>Circadian entrainment</i>	93	189	4	1	1.880000e-02
<i>Regulation of actin cytoskeleton</i>	218	265	9	3	1.900000e-02
<i>Wnt signaling pathway</i>	143	306	4	1	2.130000e-02
<i>Drug metabolism - other enzymes</i>	43	58	5	0	2.440000e-02
<i>Pathways in cancer</i>	403	258	3	7	5.710000e-02

Summary of the differentially perturbed pathways as identified by MinePath. Terms were ranked by corrected p-value.

Pathway – Name of the pathway identified

Genes – Number of genes identified

Subpaths – Number of subpaths computed and assessed

Active in Low/High LEF1 – Number of pathway components which were differentially activated or repressed in each respective group.

5.3.6 Perturbed Genes Convey Prognostic Value

Genes dysregulated by active WNT/ β -catenin signalling could convey prognostic consequence. To determine the prognostic value of perturbed genes found from the rWNT3a-treated scrambled comparison and the knockout contrast, the TCGA database was further applied, as each RNA-seq sample is annotated with clinical information on survival, amongst other factors.

Of the 96 genes identified by comparing THP1 scrambled clones with rWNT3a treatment or vehicle control (**Table 5-5**), 31 were found to convey survival value in the TCGA study (**Figure 5-23A**). Kaplan-Meier curves based upon above and below median gene expression, or upper and lower quartile, were able to establish *MMP7*, *GRAMD1B*, *BNIP3*, *AKR1C1*, *SLC7ALL*, *VIT*, *MT1G* and *MGLL* as genes altered by rWNT3a treatment, as compared to vehicle treatment alone, thus conveying a negative prognosis (**Figure 5-23B**).

Within the knockout *versus* scrambled contrast, 110 genes perturbed by knockout were found to convey an indication of survival outcome ($p < 0.1$), with 57 of these showing a significant correlation ($p < 0.05$) (**Table 5-10**). Genes found altered directionally such as to convey positive patient prognoses were discovered in the knockout gene list, and included: *TNFSF13B*, *DHX32*, *ZNF100*, *ZNF345*, *ZNF133*, *ZNF708*, *ERG*, *TSPN2*, *UBE2C*, *COL2A1*, *SLC2A13*, *RNF130*, *SLC46A1*, *CCDC125*, *SEMA4A*, *ARK1C1*, *STXBP5*, *HRH2*, *PIGZ*, *KBTBD8*, *PDE3B*, *PLEKHA6*, *APOBEC3B*, *TRIB2*, *PHGDH*, *PALM*, *PMP22*, *DIXDC1*, *GSTP1*, *KIT*, *CD109*, and *CD7*. Together these observations suggest that knockout of β -catenin and γ -catenin shifted the transcriptomic profile to one indicative of survival, thus indicating that the profile is disadvantageous to AML (**Figure 5-24**).

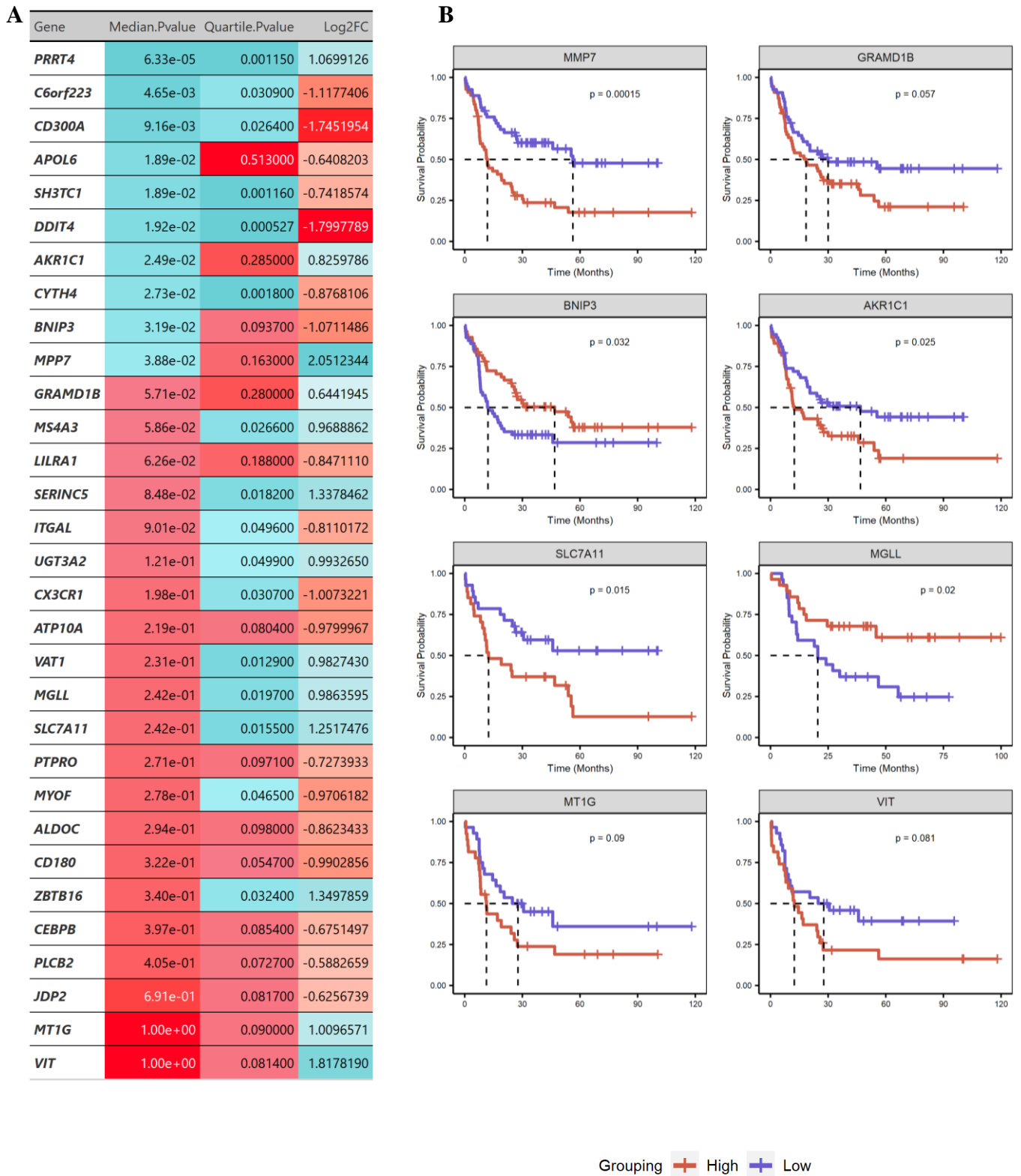


Figure 5-23: Genes Perturbed by WNT-activation Convey Prognostic Value

A) Table of genes which are significantly perturbed (adj.p<0.05, fold change >1.5) by rWNT3a treatment in THP1 scrambled. Genes were contrasted based on median and upper to lower quartile groupings. Significant p-values (log rank) are coloured green, whilst insignificant are coloured red. Fold changes (log₂) are shown relative to the treated THP1 scrambled samples. **B**) Kaplan–Meier survival curves based upon above (red) and below (blue) median mRNA expression, or upper versus lower quartile.

Table 5-10: Significantly Perturbed Genes with Knockout Convey Prognostic Influence

Gene	Median.Pvalue	Quartile.Pvalue	Log2FC
<i>SOCS1</i>	0.000791	0.000269	0.9553993
<i>PLXNC1</i>	0.001640	0.001290	0.7416780
<i>SLC4A7</i>	0.003490	0.041400	-0.5920083
<i>KBTBDB8</i>	0.003710	0.013600	-0.6075388
<i>ZNF133</i>	0.004770	0.191000	0.6523854
<i>PDE3B</i>	0.008860	0.000780	0.7538425
<i>PHACTR1</i>	0.009520	0.186000	0.7068036
<i>ITM2A</i>	0.011800	0.139000	-0.6145087
<i>RNF130</i>	0.011800	0.152000	0.6566952
<i>SEMA4A</i>	0.013000	0.130000	-1.7332391
<i>EPHB6</i>	0.013400	0.142000	-2.0181978
<i>CCDC125</i>	0.014700	0.329000	-0.8590015
<i>TNFSF13B</i>	0.015200	0.168000	1.9216943
<i>AFF2</i>	0.016000	0.000998	-1.5331829
<i>APOBEC3B</i>	0.016500	0.037900	0.5994087
<i>HRH2</i>	0.017200	0.699000	-1.8690281
<i>ZNF790</i>	0.024400	0.103000	-2.9541084
<i>AKR1C1</i>	0.024900	0.285000	-0.7770050
<i>PALLD</i>	0.028400	0.347000	1.2948189

Gene	Median.Pvalue	Quartile.Pvalue	Log2FC
<i>SLC9A3</i>	0.0299	0.197000	-0.8289943
<i>PIGZ</i>	0.0302	0.264000	0.6597471
<i>TSPAN2</i>	0.0302	0.395000	0.8607569
<i>ZNF100</i>	0.0316	0.022600	-1.9751486
<i>COL2A1</i>	0.0340	0.063400	-1.9020558
<i>SLC46A1</i>	0.0349	0.037400	-0.9286532
<i>UBE2C</i>	0.0350	0.078000	-0.6663770
<i>SLC2A13</i>	0.0384	0.165000	1.0317608
<i>STXBPS</i>	0.0387	0.005120	0.8129118
<i>DHX32</i>	0.0395	0.020400	-0.7447795
<i>ZNF254</i>	0.0411	0.052300	-0.9654766
<i>PLEKHA6</i>	0.0425	0.231000	-1.1385756
<i>ZNF345</i>	0.0435	0.079100	-2.6349840
<i>NDUFA4L2</i>	0.0439	0.315000	-1.7184318
<i>ERG</i>	0.0446	0.690000	1.0916599
<i>ZNF708</i>	0.0447	0.102000	-1.5107854
<i>AGPAT3</i>	0.0483	0.043300	0.7512691
<i>CCND2</i>	0.0511	0.014400	-1.0830832
<i>MS4A3</i>	0.0586	0.026600	-0.6484630

Gene	Median.Pvalue	Quartile.Pvalue	Log2FC
<i>AIFM2</i>	0.0599	0.047200	1.8635098
<i>PALM</i>	0.0699	0.027100	0.8111230
<i>CD109</i>	0.0887	0.007260	-1.0170532
<i>ITGAL</i>	0.0901	0.049600	1.7646828
<i>EZR</i>	0.1120	0.024500	0.6040427
<i>CD7</i>	0.1180	0.037100	-2.0034847
<i>FSTL1</i>	0.1480	0.044100	-2.7652421
<i>KIT</i>	0.1820	0.005590	1.1430581
<i>SPIN3</i>	0.1820	0.005520	-1.5764264
<i>OXNAD1</i>	0.1970	0.040300	-0.5856219
<i>GSTP1</i>	0.2140	0.046100	-0.9242342
<i>SLC7A11</i>	0.2420	0.015500	-0.6125117
<i>TRIB2</i>	0.3070	0.022300	1.1864009
<i>PHGDH</i>	0.3080	0.031000	-0.7171179
<i>AHNAK</i>	0.3290	0.022500	2.2124242
<i>PMP22</i>	0.3290	0.023200	0.6327313
<i>PTGFRN</i>	0.7720	0.035300	-0.7643374
<i>CTXN1</i>	0.8510	0.016300	-0.7157120
<i>DIXDC1</i>	0.9060	0.048500	0.9140807

Table of genes which are significantly perturbed by knockout when contrasted with scrambled. Genes were contrasted based on median and upper to lower quartile groupings on survival. Significant p-values (log rank) are coloured green, whilst insignificant are coloured red. Fold changes (log2) are shown relative to the knockout condition.

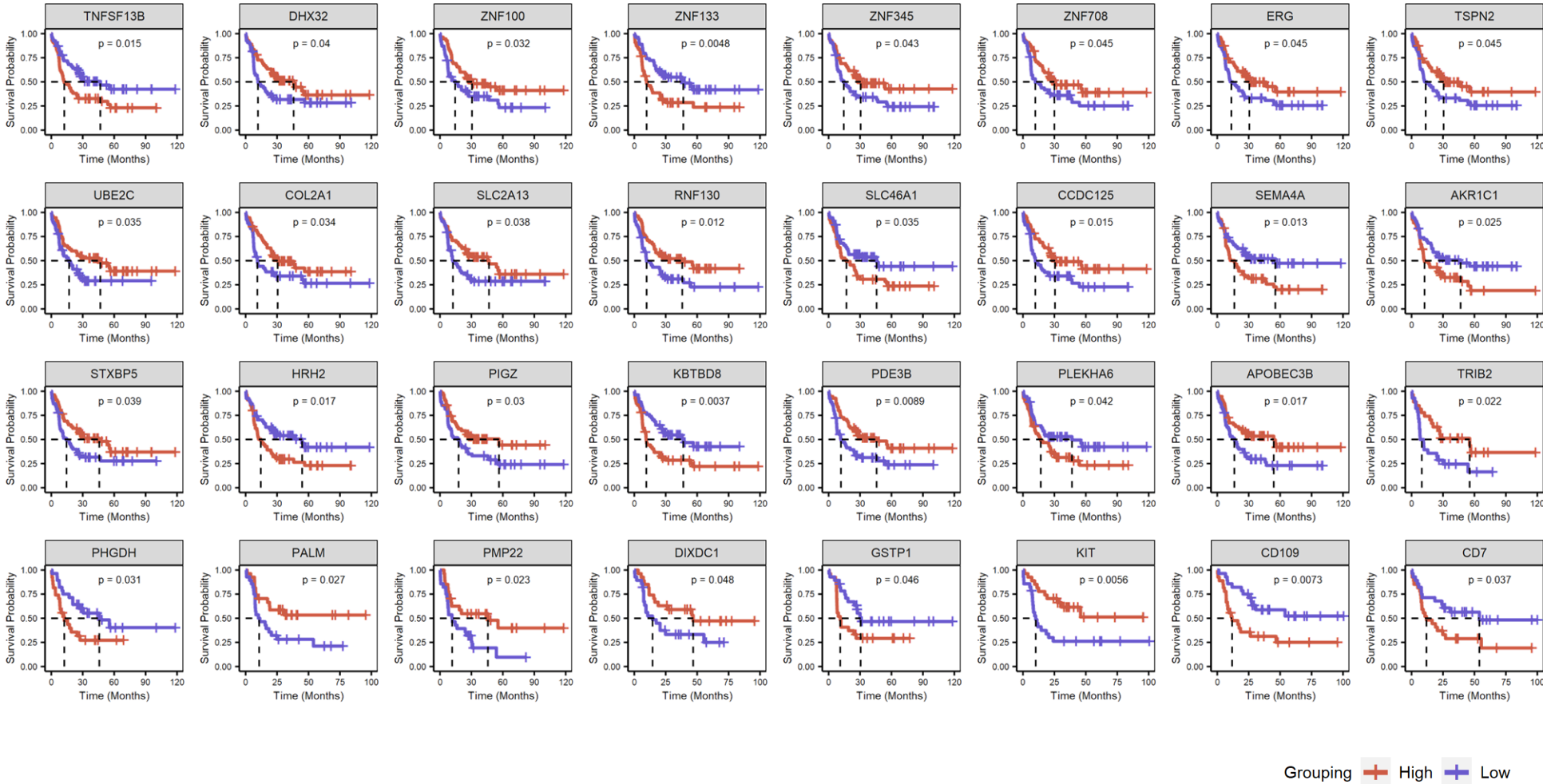


Figure 5-24: Genes Perturbed by Knockout Convey Prognostic Consequence

Kaplan–Meier survival curves based upon above (red) and below (blue) median, or higher and lower, mRNA expression for which alterations by knockout would be adjusted such to improve patient prognoses. Patient samples were separated as indicated previously by either above and below median expression, or upper and lower quartile ranges. P-values below 0.05 were considered significant by either measure.

5.3.7 RAP1 Signalling Affects AML Growth and Modulates Clonogenicity

As RAP1 signalling has been suggested to be modulated by WNT/ β -catenin signalling in AML cell lines through rWNT3a treatment and with dual knockout *in silico* (5.3.3), alongside comparable findings in public cell line data (S2.), and public patient data (5.3.5), it was necessary to examine the impact of hyperactive RAP1 signalling activity in AML maintenance *in vitro*. To achieve this, a lentiviral plasmid containing a modified constitutively active form of the RAP1 signalling central mediator Ras-related protein Rap-1A (RAP1A) was used. This constitutive activation was achieved by mutation of Glutamine 63 to Glutamic acid, and is referred to as RAP1^{E63}; this was applied alongside a WT control RAP1A (RAP1^{WT}). These were a gift from Dr. Roland Friedel. The plasmids were inserted into bulk scrambled control and bulk non-clonal β -catenin knockout lines generated in HEL, THP1, U937, and MV4;11 (3.6) and selected with geneticin over 14-days (2.8.2).

An assessment of growth and viability (2.11.7) following selection revealed that constitutive activation of RAP1 in *responder* AML cell lines induced a growth suppressive effect, yet induced a pro-proliferative effect in *non-responder* AML cell lines (**Figure 5-25**). This was observed in both scrambled and knockout conditions, suggesting the effect is not mediated by β -catenin directly. As no consequence was observed in terms of viability, these were not a result of cell loss. These results indicate that RAP1 has an impact in AML cell line growth *in vitro*; however, the activity levels of RAP1 are perhaps not indicative of the *in vivo* condition, and are likely substantially higher than in normal tissue, limiting interpretation.

When a limiting dilution assay was performed to examine the ability to clonally expand *responder* cell lines, it was apparent that RAP1^{E63} was able to restore clonogenicity to levels comparable with the scrambled equivalent and, further, enhance the clonogenicity of *non-responder* AML cell lines as compared to RAP1^{WT} (**Figure 5-26**). These findings demonstrate that RAP1 signalling modulates clonogenicity and that this effect is downstream of WNT/ β -catenin signalling. Unfortunately, as the levels of RAP1 recorded by western blot are uninformative for determining the activation status of RAP1, a prohibitively expensive protein pulldown would be required to validate the expression levels of active RAP1-GTP. Instead, direct modulation of RAP1 signalling promoters and inhibitors believed to interact with WNT/ β -catenin signalling would provide mechanistic insight into the roles in restoring clonogenicity.

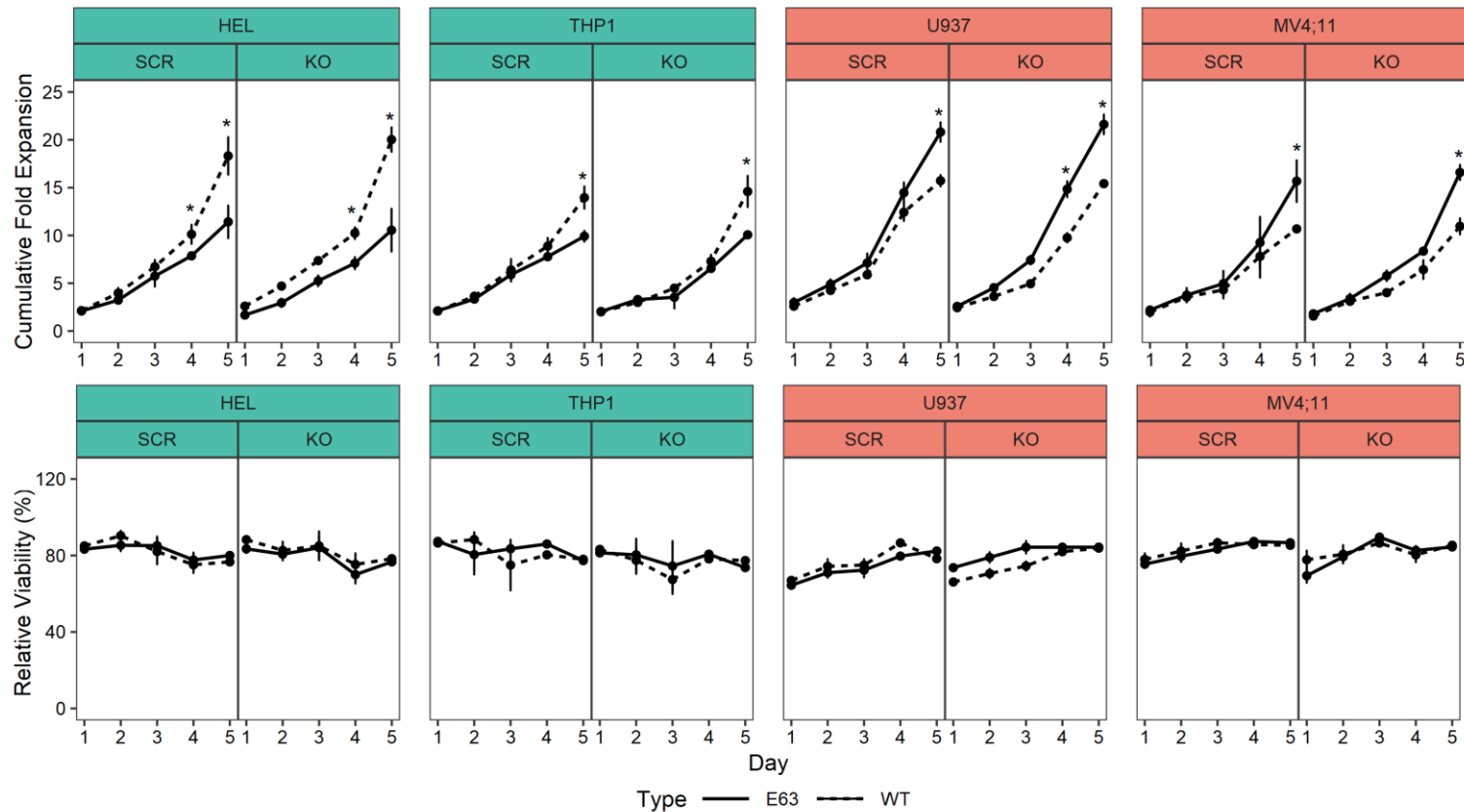


Figure 5-25: Constitutive RAP1 Signalling Activity Affects AML Expansion Variably

Scrambled and *CTNNB1* CRISPR-Cas9 transduced bulk AML lines were transduced with RAP1^{WT} or RAP1^{E63} and examined through a growth assay (2.11.7) and TOPRO3 viability assay (2.11.6) following lentiviral incorporation (2.7.1) and selection with G418 over 14-days (2.8.2). Green facets represent responder AML cell lines, whilst red facets represent non-responder AML cell lines. A paired t-test was performed to examine differences to growth (n=3; p<0.05 = *; data indicates mean ±1SD).

SCR = Scrambled Clone
KO = β -catenin Knockout
E63 = RAP1 Constitutive Expression Form
WT = RAP1 Wildtype Form

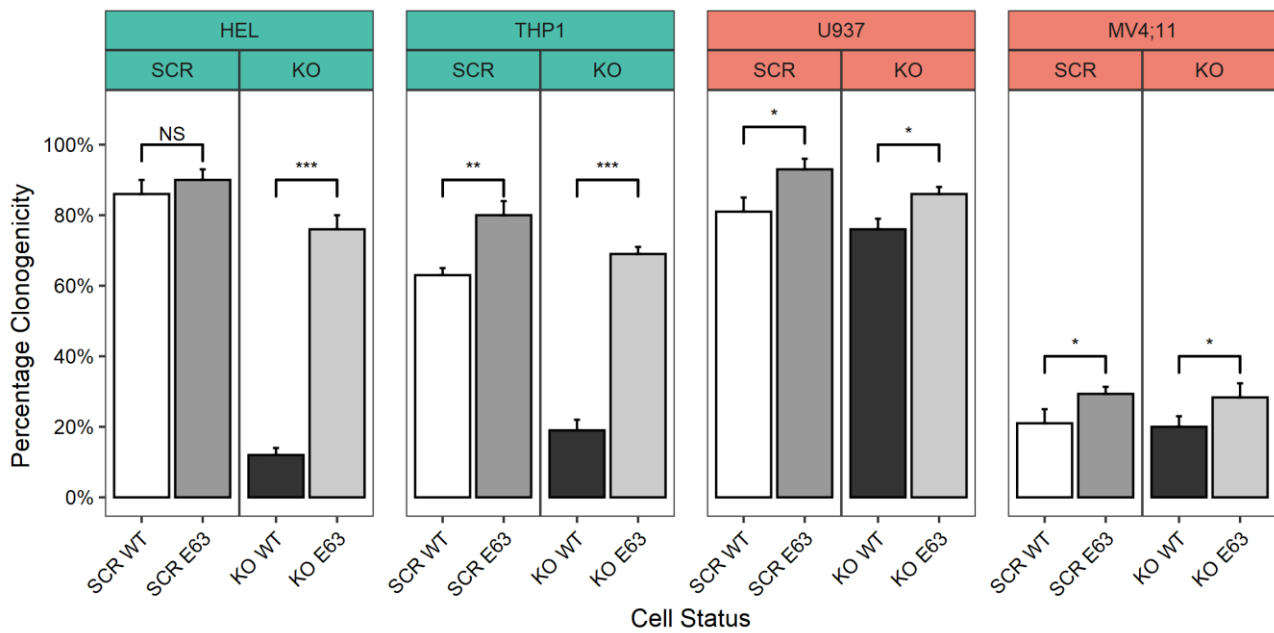


Figure 5-26: RAP1^{E63} Restores Responder AML Clonogenicity

Scrambled and *CTNNB1* CRISPR-Cas9 transduced bulk AML lines were further transduced with RAP1^{WT} or RAP1^{E63} and examined for clonal growth with the limiting dilution assay (2.4) following G418 selection (2.8.2). A t-test was performed to examine the statistical difference between RAP1^{WT} or RAP1^{E63} clonogenicity (n=3; data indicates mean +1SD; NS=Not significant, ***<0.001, **<0.01, *<0.05).

SCR = Scrambled Clone

KO = β -catenin Knockout

E63 = RAP1 Constitutive Expression Form

WT = RAP1 Wildtype Form

5.3.8 *RAPGEF4* and *SIPA1LI* Regulate Clonogenicity in AML

The activation of RAP1 signalling was suggested to be sourced from *RAPGEF4* in the study here-in, in which *RAPGEF4* was overexpressed by rWNT3a and repressed by dual knockout, further, comparable findings in the CCLE and TCGA databases added further credence to a WNT/ β -catenin/*RAPGEF4* axis. In contrast, *SIPA1LI* was identified as repressing RAP1 signalling in PTA and MTA analyses. To determine whether RAP1 signalling activity and the resulting rescue of clonogenicity is directly derived from *RAPGEF4*, a potential WNT/ β -catenin target gene (Schmidt *et al.*, 2013; Rouillard *et al.*, 2016), or indirectly, by inactivation of *SIPA1LI* via CKI ϵ (Tsai *et al.*, 2007), modulation of both targets was performed. To do this, CRISPRa-dCas9 was applied to overexpress *RAPGEF4*, and CRISPRi-dCas9 was applied to inhibit *SIPA1LI* (2.8).

These were inserted into bulk scrambled control and bulk β -catenin knockout lines generated in HEL, THP1, U937, and MV4;11 (3.6) and selected over 14-days (2.8.2). Once a stable population was established, growth and viability assays were performed to examine general AML characteristics, alongside a limiting dilution assay to measure clonogenicity. No change to growth or viability was observed (data not shown). However, overexpression of *RAPGEF4* was able to significantly improve clonogenicity in *responder* AML β -catenin bulk knockout populations, comparable to scrambled, and an improvement to clonogenicity was further observed in the scrambled CRISPR-Cas9 condition (**Figure 5-26**). Additionally, inhibition of *SIPA1LI* was able to improve clonogenicity by a minor, but statistically significant, proportion. These data support the previous findings using RAP1^{E63}, and further indicate that both a direct and indirect mechanism of WNT/RAP crosstalk exists, with *RAPGEF4* directly influencing clonogenicity in AML cell lines.

Unfortunately, efforts to validate the overexpression and repression of *RAPGEF4* and *SIPA1LI* by western blot failed as no bands were detected, even in controls, suggesting issues with the antibodies (data not shown). However, these data support further investigation of RAP1 signalling in the context of AML, particularly with regard to clonogenicity.

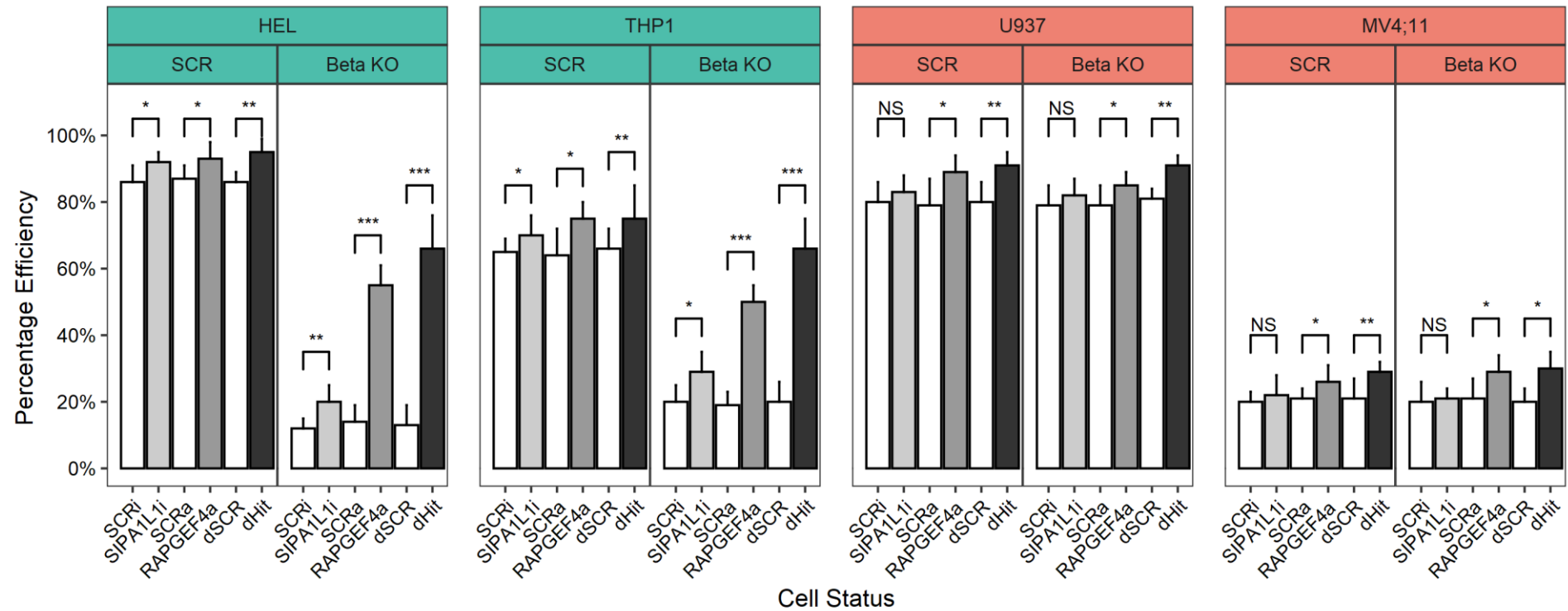


Figure 5-27: *RAPGEF4* and *SIPA1L1* Restore and Enhance Clonogenicity in AML

Scrambled and *CTNNB1* CRISPR-Cas9 transduced bulk AML lines were further transduced with scrambled guide controls (CRISPRa-dCas9 SCR, CRISPRi-dCas9), targeting guides (CRISPRa-dCas9 *RAPGEF4*, CRISPRi-dCas9 *SIPA1L1*) or both simultaneously (dual SCR, dual Hit). Cultures were examined for clonal growth with the limiting dilution assay (2.4) following selection (2.8.2). A t-test was performed to examine the statistical difference between *RAP1*^{WT} or *RAP1*^{E63} clonogenicity (n=3, data indicates mean +1SD; ANOVA with post-Tukey's; NS=Not significant, ***<0.001, **<0.01, *<0.05).

SCRi = Scrambled gRNA CRISPRi-dCas9

SIPA1L1i = *SIPA1L1* gRNA CRISPRi-dCas9

SCRa = Scrambled gRNA CRISPRa-dCas9

RAPGEF4a = *RAPGEF4* gRNA CRISPRa-dCas9

dSCR = Scrambled gRNA CRISPRi-dCas9 and Scrambled gRNA CRISPRa-dCas9

dHit = *SIPA1L1* gRNA CRISPRi-dCas9 and *RAPGEF4* gRNA CRISPRa-dCas9

5.4 Discussion

Previous chapters have established that β -catenin is integral to clonal expansion of WNT-responsive AML cell lines (4.3.4.3), whilst also revealing that knockout of β -catenin and γ -catenin had no consequence upon proliferative rate, cell cycling, apoptosis, specific surface marker expression, and general morphology (4.3.4). This outcome limited the ability to study these mechanistic changes, as few traditionally applied assays are capable of studying a lone single cell. Therefore, this chapter sought to determine the implications of knockout by transcriptomic analysis.

To examine the transcriptome of active WNT/ β -catenin signalling in comparison with dual β -catenin and γ -catenin knockout, clonal scrambled and dual knockout lines were employed, either treated with the natural WNT ligand, rWNT3a, or vehicle control. WNT-activation with rWNT3a treatment was able to activate WNT/ β -catenin signalling activity, as measured by WNT reporter in THP1 but, unexpectedly, not in HEL cells (5.3.1)⁷. Nevertheless, total RNA was isolated from these samples and validated to be of high quality to be suitable for RNA-seq. Novogene successfully performed the library preparation, adapter trimming, sequencing, alignment, and quantification, which this study confirmed to have been of a high standard. Raw counts provided by Novogene were pre-processed to remove low abundance genes, examined with a series of exploratory techniques, and normalised to trimmed mean of M values (TMM) for differential and pathway analysis. TMM normalisation represents the current gold standard which corrects for sequencing depth, RNA composition, and gene length which classical normalisation techniques such as counts per million, transcripts per million, and RPKM cannot achieve and are thus unsuitable for differential expression and pathway analysis (Dillies *et al.*, 2013; Conesa *et al.*, 2016; Zhao *et al.*, 2021).

Exploratory analysis was performed through the application of hierarchical clustering and PCA, which revealed that variances were sourced primarily from the cell lines, as expected; then secondly distancing based upon the CRISPR-status; before finally separating on treatment type, i.e., scrambled clones and knockout clones varied more than the treatment status (5.3.1.2). This was expected as the biological variation between cell lines is greater than a targeted gene

⁷ The clonal pBARV line that the scrambled and knockout clones were generated from was also found to not respond to rWNT3a or WNT3a conditioned media from L Wnt-3A cells (CRL-2647) suggesting alternate WNT ligand activation in this line (data not shown).

deletion, further expected to have greater consequence than application of a single ligand for a specific pathway. Examination of *CTNNB1* and *JUP* revealed that mRNA levels were ablated by CRISPR-Cas9 in the knockout samples. When applying CRISPR-Cas9 techniques, it is possible that frameshift mutations lead to a malformed, non-functional protein despite mRNA analysis revealing unchanged levels as RNA-seq is frame agnostic; however, the ablation of *CTNNB1* and *JUP* mRNA expression with knockout indicates the InDel in each case has triggered mRNA NMD ceasing protein production, or only small fragments remain which would not prove functional. Following rWNT3a treatment, *CTNNB1* remained unchanged in scrambled clones, and *JUP* was reduced (5.3.1.3). The absence of change to *CTNNB1* was expected, as changes to *CTNNB1* in response to WNT ligands is not a common observation, owing to its post-translational regulation (Jothimani *et al.*, 2020). The reduction in *JUP* was not expected and suggests repression by rWNT3a.

5.4.1 Identifying a WNT/ β -catenin/RAP1 Signalling Axis in AML

As knockout of β -catenin had demonstrated loss of clonogenicity, this study initially focussed on identifying genes upregulated by rWNT3a treatment, and inversely suppressed by dual catenin knockout. These dysregulated genes would likely represent the critical element lost, ablating clonogenicity. These dysregulated genes were used for SPIA, which revealed an upregulation of RAP1 signalling by rWNT3a and suppression of RAP1 signalling in the knockout condition (5.3.3). RAP1 signalling activation was previously demonstrated in *responder* AML cell lines (S2.), and subsequently, in patients deceased five years after diagnosis (5.3.5).

Several studies in the literature supports the concept of crosstalk between the WNT/ β -catenin and RAP1 signalling pathways (Habas *et al.*, 2007; Tsai *et al.*, 2007; Goto *et al.*, 2010; Griffin *et al.*, 2018). Evidence here-in at the gene expression level and through *in vitro* analyses further supports crosstalk of the two respective pathways and enables speculation of a central role in AML relapse and overall survival. A summary of the WNT and RAP1 signalling pathways is shown in **Figure 5-28**. Even though research on RAP1 signalling in the context of AML is very limited, the scarce existing literature supports both the involvement of RAP1 signalling in AML, as well as the potential interaction with WNT/ β -catenin signalling (Ishida *et al.*, 2003; Gyan *et al.*, 2005; Qiu *et al.*, 2012).

A WNT/beta-catenin/RAP1 signalling axis in AML

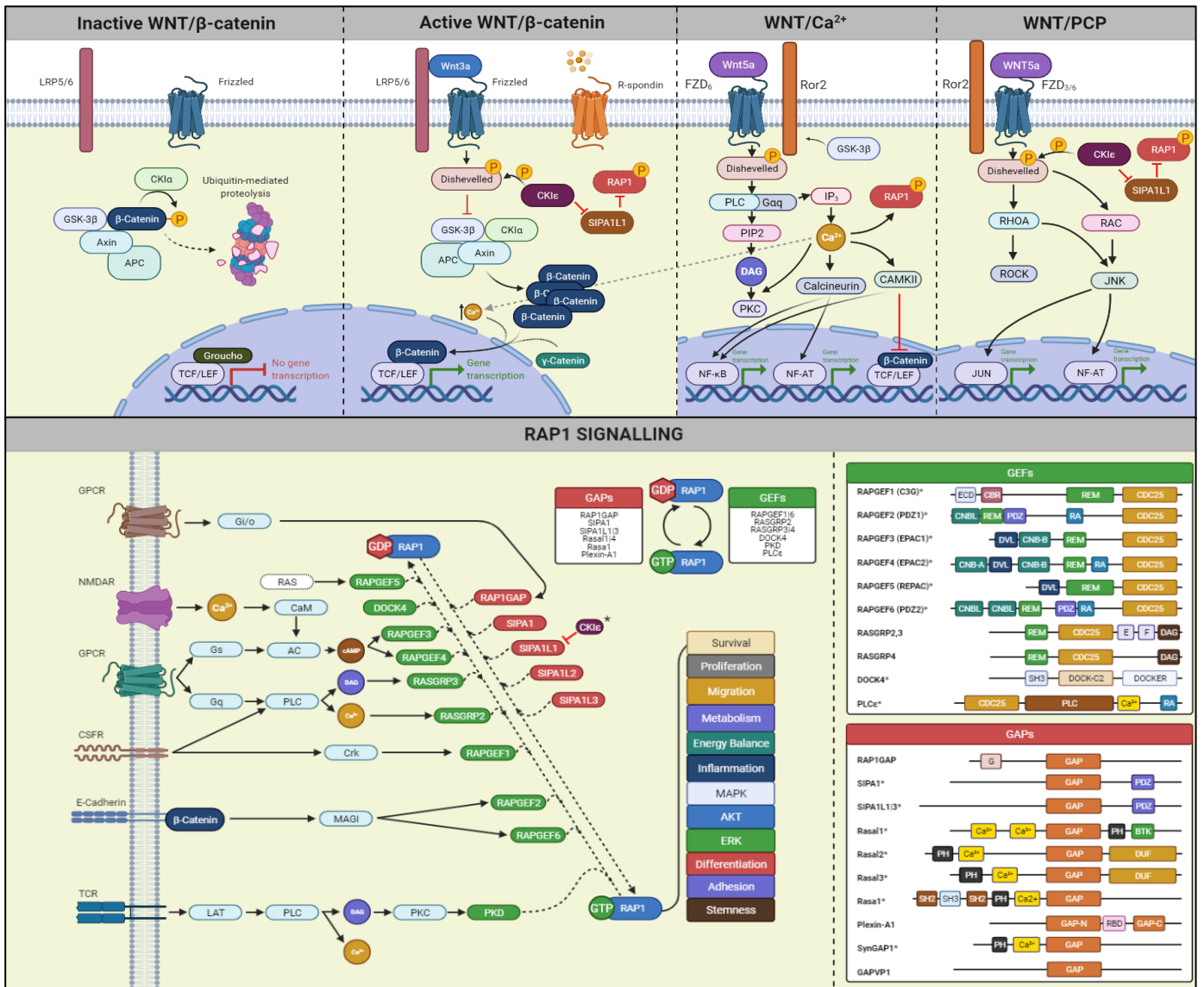


Figure 5-28: Summary of the WNT and RAP1 Signalling Pathways

The three major WNT signalling pathways are shown: WNT/ β -catenin (inactive and active), WNT/ Ca^{2+} , and WNT/PCP.

The RAP1 signalling pathway is controlled by the phosphorylation state of the central mediator RAP1, which in turn is controlled by the activity of RAPGEF (green) and RAPGAP (red). Further interactions between β -catenin and numerous members are known or expected, as indicated by an asterisk.

Whilst β -catenin and WNT/ β -catenin signalling have been implicated for interactions with other critical pathways which are often perturbed in cancer, including RAS/RAP-ERK (Goto *et al.*, 2010; Jeong *et al.*, 2018), Hedgehog (Pelullo *et al.*, 2019), Notch (Tian *et al.*, 2015; L. Ma *et al.*, 2019), TGF- β (Guo *et al.*, 2009; Luo, 2017), Hippo (Attisano *et al.*, 2013), MAPK (Horst *et al.*, 2012; Cheruku *et al.*, 2015), and EGFR signalling (Hu *et al.*, 2010), these were not perturbed here-in. Only a select few pathways were identified as altered, including PI3K-AKT-mTOR (Zeng *et al.*, 2018; Prossomariti *et al.*, 2020), PD-1 signalling (Martin-Orozco *et al.*, 2019; Perry *et al.*, 2020; H. Zhang *et al.*, 2021), p53 signalling (Peng *et al.*, 2014; An *et al.*, 2017), and cell cycle signalling (Jamieson *et al.*, 2014), but these were not reciprocally altered in the knockout state, suggesting they are not absolutely required effects for clonogenicity. When the profile was studied in detail, a clear pattern emerged in support of a WNT/ β -catenin/RAP axis.

Genes found to be positively upregulated in rWNT3a treated THP1, *responder* AML cell lines, and in patients deceased by five years included *RAPGEF4*, a suspected WNT/ β -catenin target gene (Schmidt *et al.*, 2013; Rouillard *et al.*, 2016). *RAPGEF4* serves to promote the RAP1 signalling pathway by acting as a guanine exchange factors (GEF) for RAP1. Numerous upstream regulators of GEF, which activate RAP1, were repressed in the knockout state; these included *F2R*, *P2RY1*, *PDGFD*, *GRIN1*, and *MAG11*. Together, these facilitate reduced expression of *RAPGEF4* and *RASGRP3* (Martemyanov *et al.*, 2012). Further, GTPase-activating protein (GAP), which inactivate RAP1, were found overexpressed; these include *RAP1GAP*, *RAP1GAP2*, *SIPAIL1*, *SIPAIL2*, and whilst only trending towards significance, remaining members *SIPAI* and *SIPAIL3* were also upregulated (Steele *et al.*, 2012). Together, modulation as indicated provides tremendous repressive pressure upon RAP1 signalling activity upon dual catenin knockout.

With RAP1 identified as pathway of interest, a literature search was applied to support further *in vitro* findings. RAP1, belonging to the RAS-associated family of cytosolic proteins, is a small GTPase integral for signal transduction, by acting as a cellular switch (Boriack-Sjodin *et al.*, 1998). RAP1 is activated to a GTP-bound form by guanine nucleotide exchange factors or inactivated to a GDP-bound form by GTPase activating proteins, and regulation of these two factors enables control over numerous cellular processes, such as B-RAF/MEK/ERK activation (Vetter *et al.*, 2001). GEF family members include DOCK4, 3G3,

EPAC1|2, and PDZ-GEF1 whilst GAP family members include RAP1-GAP, SPA1, and the SPA1L1|3 members (Minato, 2013). The balance between these factors dictates overall RAP1 signalling activity (Bos, 2005; Retta *et al.*, 2006).

Recently, RAP1 activity has been identified as a promotor of stemness in long-term adult haematopoiesis and myeloproliferative disorders (Imai *et al.*, 2019). Further, ectopic RAP1 signalling driven by inhibition of GTPases was demonstrated to drive leukaemogenesis and promote HSC proliferation and maintenance (Ishida *et al.*, 2003; Minato, 2013; Imai *et al.*, 2019). In an *in vivo* murine model and *in vitro*, RAP1 signalling was required for leukemogenicity of LSC (Ishida *et al.*, 2003). Furthermore, repression of RAP1 signalling blocked leukaemogenesis, whilst RAP1 active cells rapidly induced aggressive leukaemia (Ishida *et al.*, 2003). The authors reported that cells were only able to propagate on stromal cell lines, immediately dying in the absence of a support cell, but they were also shown to grow underneath stromal support cells like cobblestones. Moreover, no haematopoietic factors were able to rescue these cells (Ishida *et al.*, 2003). Accordingly, these observations have been previously documented within this study in cell lines (4.3.1), suggesting tight regulation of RAP1 signalling is required to promote stemness, and repression of RAP1 removes the clonogenicity of AML cells. RAP1 signalling is an effector of Ca²⁺ signalling and can control cytoplasmic Ca²⁺ levels to reduce stresses, thereby acting as a negative feedback loop to control RAP1 signal maxima (Kosuru *et al.*, 2020). EPAC proteins are able to respond to and regulate the influx of extracellular Ca²⁺, as well as modulate glucose homeostasis (Almahariq *et al.*, 2014; Kaneko *et al.*, 2016). Calcium flux and glucose metabolism are further important factors which are often found perturbed in AML (W.-L. Chen *et al.*, 2014; Monaco *et al.*, 2015).

The necessary question relates to the mechanism by which WNT/ β -catenin and RAP1 signalling intersect, and whether the relationship is direct or indirectly mediated by another participant. No fully defined relationship between these two signalling pathways has been discovered; however, it is likely that the answer is complex and represents both direct and indirect interplay. RAP1 has been recognised to stabilise β -catenin and enhance its transcription in several cancers, with the proposal that RAP1, which shuttles freely between the cytoplasm and nucleus, is perhaps translocating β -catenin into the nucleus (Glading *et al.*, 2010; Goto *et al.*, 2010). Similarly, *RAPGEF5* is proposed to mediate the nuclear

translocation of β -catenin (Griffin *et al.*, 2018). Further, numerous members of the RAP1 signalling pathway contain PDZ binding elements, which β -catenin can hypothetically bind to, such as *SIPAI*, *SIPA1L1*, *SIPA1L2*, and *SIPA1L3* (Stone, 2011; Shah *et al.*, 2016). *DOCK4*, an activator of RAP1, has been described as a member of the WNT/ β -catenin pathway which stabilises β -catenin via a PDZ element, and was suggested to be phosphorylated by GSK3 β to stimulate GEF activity, thereby promoting RAP1 (Yajnik *et al.*, 2003; Upadhyay *et al.*, 2008). These observations suggest direct and indirect interaction between WNT/ β -catenin and RAP1, which has been suggested in the literature as the WNT/RAP pathway (Habas *et al.*, 2007). A hypothetical interplay between WNT/ β -catenin and RAP1 signalling is demonstrated in **Figure 5-29**.

Numerous CK1 family members are involved in the WNT/ β -catenin pathway and have associated roles in the modulation of the RAP1 signalling pathway. Recent research has suggested that CK1 ϵ and CK1 δ , which are integral components of the WNT/ β -catenin initiation cascade and are activated by WNT3a (Valle-Pérez *et al.*, 2011; Cruciat, 2014; Vinyoles *et al.*, 2017), have a secondary function in the degradation process of *SIPA1L1*, thus enabling CK1 ϵ/δ -mediated activation of RAP1 signalling (Tsai *et al.*, 2007; Knippschild *et al.*, 2014). Inversely, in the absence of a WNT ligand, CK1 α phosphorylates β -catenin for degradation and is further established to induce CK1 α -mediated RAPGEF2 degradation, inhibiting RAP1 signalling (Magliozzi *et al.*, 2013; S. Jiang *et al.*, 2018). Together, these CK1 family members are able to positively regulate RAP1 signalling in the presence of a WNT ligand agonist.

The relationship between WNT and RAP1 signalling is complicated as a result of unique β -catenin interactions. For instance, CK1 α -mediated RAPGEF2 degradation in a WNT inactive state would suggest repression upon β -catenin knockout; however, *RAPGEF2* was shown to be upregulated (5.3.2) in this context. This is likely explained by the negative regulatory relationship between MAGI3 and β -catenin (Q. Ma *et al.*, 2015). Through a PDZ region, MAGI3 binds β -catenin, negatively regulating it (Dobrosotskaya *et al.*, 2000), with the inverse also established. In addition, RAPGEF2 has been demonstrated to directly form a complex with β -catenin via a PDZ element, which is enhanced in low intracellular Ca²⁺ conditions (Kawajiri *et al.*, 2000; Bos, 2005; Asuri *et al.*, 2008). As MAGI3 controls RAPGEF2 levels, this explains how β -catenin knockout increases RAPGEF2.

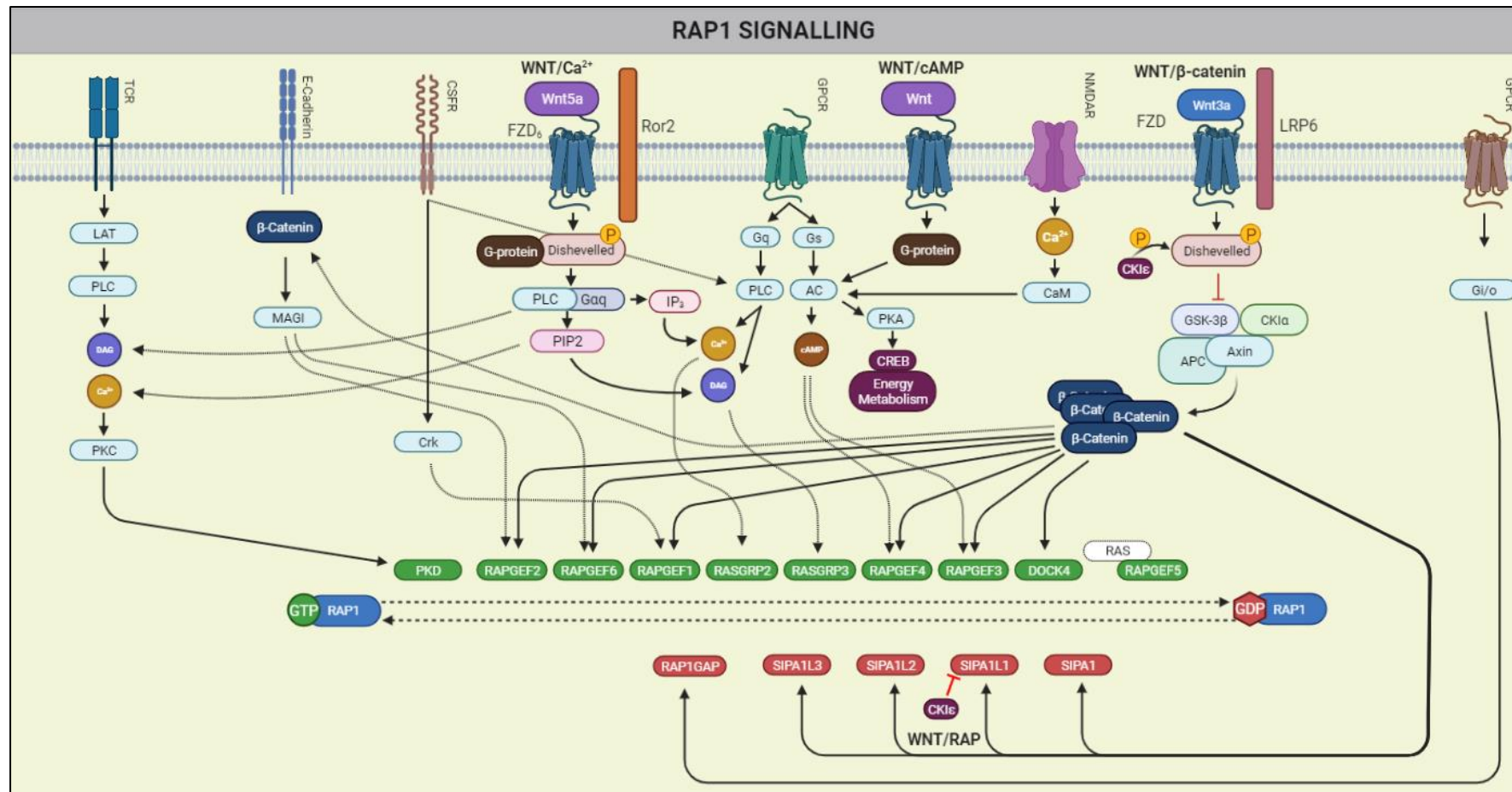


Figure 5-29: Hypothetical Crosstalk Between WNT/ β -catenin and RAP1 Signalling Pathways

Whilst speculative, β -catenin is reportedly or potentially capable of interacting with most members of the RAPGEF (green) and RAPGAP (red) families. Following activation WNT/ β -catenin activation results in an accumulation of β -catenin which is able to interact with RAP1 signalling directly and indirectly via PDZ elements and MAGI, respectively. The WNT/ Ca^{2+} pathway will inherently alter RAP1 signalling, as RAPGEF and RAPGAP contain Ca^{2+} and DAG responsive elements. The WNT/PCP pathway promotes CKIe which is able to repress SIPA1L1, promoting RAP1. All WNT pathways involve Dishevelled (DVL), which is potentially capable to simultaneously promote RAPGEF with DVL sites (EPAC, REPAC).

DVL, another integral component of the WNT/ β -catenin initiation cascade, has been shown to enable the crosstalk between the WNT/ β -catenin, WNT/ Ca^{2+} and the RAP1 pathway, by promoting Ca^{2+} influx, PKC upregulation, and CAMKII activation (Sheldahl *et al.*, 2003; Sharma *et al.*, 2018). Of note, PKC β , found upregulated with β -catenin knockout, alongside PKC ϵ , which was trending toward significant upregulation with knockout, suggest an alternate means of RAP1 activation that is incapable of complete restoration. However, the function of PKC β and PKC ϵ are dependent upon Ca^{2+} and diacylglycerol, or diacylglycerol alone, respectively (Luna-Ulloa *et al.*, 2011). The downstream target of RAP1 signalling, PKC ι , has been demonstrated to be a critical component of cell-survival signal transduction pathways and was shown to be repressed with β -catenin knockout, further suggesting RAP1 inactivation with knockout (Newton, 2010).

As WNT/ Ca^{2+} has been demonstrated to facilitate nuclear translocation of β -catenin, this suggests Ca^{2+} flux represents a critical mediator in the early stages of WNT/ β -catenin initiation (Thrasivoulou *et al.*, 2013b). Indeed, WNT3a, alongside numerous other WNT ligands, have been established to increase intracellular Ca^{2+} levels within minutes (Avila *et al.*, 2010; Thrasivoulou *et al.*, 2013a; Ashmore *et al.*, 2019). Together, this demonstrates a brief, but substantial, period of Ca^{2+} influx, which would serve to activate the RAP1 pathway directly. This would further suggest a complex interplay between the previously divided WNT sub-pathways and RAP1.

Together, these observations demonstrate further evidence for the WNT/RAP1 signalling axis. WNT/ β -catenin and RAP1 share the common phenotype of absolute necessity in embryonic haematopoiesis, but prove disposable for adult haematopoiesis (Satyanarayana *et al.*, 2010); further, inactivation of both pathways attenuates leukemogenicity, whilst hyperactivation drives leukaemogenesis. This relationship suggests these pathways act in consort, perhaps further augmented by non-canonical WNT pathways. Further investigation was necessary to unveil the relationship between the two pathways, and their respective impact on AML.

5.4.2 Validating the WNT/RAP Signalling Axis Modulates Clonogenicity

The transcript expression profiles indicated WNT/ β -catenin promoted RAP1 signalling, whilst dual catenin knockout repressed the pathway. Regulatory GEF and GAP were

perturbed in directional agreement with these findings, both in the generated data here-in, in the CCLE *responder versus non-responder* data, in the *LEF1^{HIGH} versus LEF1^{LOW}* comparison, and the five-year deceased *versus* alive patient data. Furthermore, the ability to demonstrate both WNT and RAP1 signalling activation in patients with poor survival adds further credence to a mechanism of crosstalk with prognostic implications. Firstly, it was necessary to explain how RAP1 signalling has perhaps been missed in prior research.

Primarily, the absence of RAP1 signalling in prior AML research relates to novelty: efforts to classify AML cell lines into *responders* and *non-responders* of WNT/ β -catenin signalling is often not performed in the literature even when research focuses upon WNT/ β -catenin. Secondly, most pathway analyses are performed against the GO alone, or the KEGG database; GO does not contain a RAP1 signalling pathway annotation, whilst the KEGG database does not provide annotation on the RAP1 signalling pathway in the most recent freely available release⁸. Here, the latest releases of both databases alongside several others were applied for analysis, maximising output. Further, the re-processing of raw data, in addition to the application of more modern pathway techniques, provided greater insight. This is particularly valuable for the analysis of patient data, which demonstrates a far higher degree of variability, both sourced from biological and technical variances. Lastly, greater understanding of the distinct and dual roles of RAP proteins in recent years has allowed for better understanding of the regulatory consequences of gene perturbations, particularly in relation to β -catenin. Together, these considerations could explain why RAP1 signalling was previously overlooked. Data from the rWNT3a and dual knockout profiles indicated that *RAPGEF4* (EPAC2) and *SIPA1L1* (SIPA1L1) were the principal activator and repressor of RAP1 signalling, respectively, with the former a speculative direct WNT target gene (Schmidt *et al.*, 2013), and the latter modulated indirectly by CK1 ϵ of the WNT/ β -catenin pathway (Tsai *et al.*, 2007).

As RAP1 signalling is controlled by GEF and GAP proteins, which modulate RAP1 to an active RAP1-GTP or inactive RAP1-GDP form, respectively, it was necessary to bypass this modulation and incorporate a constitutively active form of RAP1 to demonstrate clonogenicity was restored. RAP1^{E63}, a constitutively active form of RAP1, was able to restore the clonogenicity of *responder* AML cell lines to clonal efficiencies comparable to controls, whilst

⁸ RAP1 signalling added in v. 68 (30/10/2013); final free KEGG database release v60 (01/06/2011)

a mild but appreciable increase in clonogenicity within *non-responder* lines was noted (5.3.7). A pull-down assay to recover RAP1-GTP would be required to assess the active form RAP1 protein levels in the AML cell lines, as total RAP1 levels are uninformative for the activation status; unfortunately, this was cost prohibitive to conduct. Instead, direct modulation of GAP and GEF was undertaken to demonstrate directly involved members controlled clonogenicity.

As transcriptomic analyses on the generated rWNT3a and knockout data, alongside the cell line and patient data, supported *RAPGEF4* and *SIPA1L1* as the driver modulators, it was necessary to examine both. CRISPR-Cas9 activation and inhibition was applied to enable study of both, respectively. The consequence on clonogenicity was scored by limiting dilution cloning, which enabled elucidation of *RAPGEF4* as the central member enabling activation of RAP1 signalling and restoring clonogenicity, whilst *SIPA1L1* inhibition was able to only mildly improve clonogenicity (5.3.8). These data indicate that the knockout condition lacks sufficient alternate GEF activity even with inhibition of the GAP *SIPA1L1* and hence was unable to restore RAP1 signalling activity. Rather, *RAPGEF4* is likely directly upregulated as a WNT/ β -catenin target gene, which enables subsequent activation of RAP1 signalling to an extent sufficient to overcome GAP activity. Unfortunately, quantification of the activation and inhibition could not be validated by western blot as antibodies for both were unsuccessful with no bands detected at the expected size despite appropriate antibody concentration and use of ultra-sensitive ECL (data not shown). Whilst this was expected for *SIPA1L1*, for which no validated antibodies are available and only one supplier could be found, *RAPGEF4* was expected to be detected based upon recent published data using the same antibody under comparable methods (Kusnadi *et al.*, 2020).

The results generated support the existence of a WNT/ β -catenin/RAP pathway, and that this pathway directly contributes to the clonogenicity of AML. Such a finding is supported by the literature, in which RAP1 activity has been documented to be required for HSC and LSC maintenance and self-renewal (Imai *et al.*, 2019), as well as being a driver of leukaemogenesis (Ishida *et al.*, 2003; Minato, 2013; Imai *et al.*, 2019). Indeed, many of the findings here-in are concordant with those of Minato *et al.*, though the authors research did not consider WNT/ β -catenin signalling, nor was the source of excessive RAP1 signalling activity examined. The observation that RAP1 signalling is required for leukemogenicity of LSC (Ishida *et al.*, 2003;

Imai *et al.*, 2019), and high pathway activation in patient deceased by five years suggests a central involvement of RAP1 signalling in AML biology.

The complete pathway interaction between WNT/ β -catenin signalling and RAP1 signalling is difficult to resolve with current findings, with the literature supporting the interaction of WNT and RAP1 bidirectionally, complicating interpretations. WNT/ β -catenin is documented to be able to activate RAP1 (Habas *et al.*, 2007; Tsai *et al.*, 2007) but, equally, RAP1 is able to activate or augment WNT/ β -catenin (Goto *et al.*, 2010; Griffin *et al.*, 2018). This relationship between pathways is difficult to interpret due to the limited research specifically on the WNT/RAP axis (Habas *et al.*, 2007; Tsai *et al.*, 2007). Research in HCC has revealed that both inhibition and activation of β -catenin is able to induce repression and activation of RAP1, respectively, suggesting a direct β -catenin-derived interaction (Mo *et al.*, 2018). Research in embryonic stem cells found that RAP1 was required for clonogenicity (Li *et al.*, 2010), supporting a role as described here-in, whilst in HNSCC, RAP1 has been demonstrated to promote the nuclear localisation of β -catenin (Goto *et al.*, 2010), suggesting a co-operative function or positive feedback effect. However, inhibition of RAP1 was not reported to alter β -catenin-regulated gene expression during gastrulation in mice, suggesting interaction is directed from WNT to RAP1, and any roles in augmentation of the WNT pathway or in the translocation of β -catenin to the nucleus are compensated for by other means (Tsai *et al.*, 2007). Regardless of whether WNT and RAP1 are capable of mutual activation, EPAC1|2 are well recognised for roles in driving chemoresistance in AML, and have been shown to be frequently overexpressed in patients (Kusnadi *et al.*, 2020). RAP1 GAP family members are often repressed in AML patients, such as RAP1GAP, with restored activity of RAP1GAP inducing differentiation and apoptosis in cell lines *in vitro* (Qiu *et al.*, 2012).

Whilst RAP1 signalling is often found as a top perturbed pathway in recent AML studies, little or no investigation follows (Huang *et al.*, 2017; Lv *et al.*, 2018; S. Wu *et al.*, 2019; L. Zhu *et al.*, 2020; S. Chen *et al.*, 2020; He *et al.*, 2021; zhang *et al.*, 2021; Hong *et al.*, 2021; Lu *et al.*, 2021; Rodríguez González *et al.*, 2021; Almajali *et al.*, 2022; Ling *et al.*, 2022). In fact, RAP1 signalling was recently identified as the top pathway altered following treatment in AML, with WNT signalling also identified, regardless of the treatment applied clinically (J. Wu *et al.*, 2021). Small molecule inhibitors of EPAC2 are available, such as ESI-05, which have been demonstrated to reduce AML cell line viability *in vitro* (Kusnadi *et al.*, 2020). GGTI

298, a CAAZ peptidomimetic geranylgeranyl transferase I inhibitor which inhibits the processing of geranylgeranylated RAP1A was found to induce dose-dependent growth inhibition and reduced colony forming ability in AML cell lines and primary AML cells (Morgan *et al.*, 2003). Loss of RAP1GAP, a suppressor of RAP1 signalling, is reduced in AML compared to non-malignant blood diseases and upregulation has demonstrated induction of differentiation, apoptosis, and migratory effects (Qiu *et al.*, 2012). RAP1 signalling has been documented to have pleiotropic effects and care is required to study RAP1 signalling in a cancer-specific manner, which unfortunately limits interpretation as scarce research is available in AML (Looi *et al.*, 2020). CRC, an archetypical WNT/ β -catenin cancer, represents the closest approximate relative, and similarly RAP1 signalling activation is associated with poorer prognosis and correlates negatively with MMP9 (Gao *et al.*, 2018), a known WNT/ β -catenin target gene (M. A. Lee *et al.*, 2014). Repression of RAP1 signalling has been documented to induce apoptosis, suppress cell cycle progression, inhibit proliferation, reduce tumour progression, and reduce clonogenicity in CRC, HCC, and other WNT-associated cancers (Li *et al.*, 2021). Together, these data indicate RAP1 signalling requires further investigation and represents an overlooked aspect of AML with promising treatment implications.

Further expression profile alterations were explored, revealing interesting insights into transcripts upregulated and repressed in response to rWNT3a treatment and dual catenin knockout. These represent speculative findings, as these were not validated at the protein level; these are discussed in S4. , S5. , S6. .

Chapter 6

Discussion, conclusion, and future work

6.1 Background

AML is a heterogeneous haematological malignancy characterised by the clonal expansion of leukaemic cells with heightened survival and proliferative capabilities (Lowenberg *et al.*, 2016), saturating the BM niche with immature haematopoietic cells (De Kouchkovsky *et al.*, 2016). AML originates from LSC (Fialkow, 1974; Griffin *et al.*, 1986; Lapidot *et al.*, 1994), which retain the self-renewal capability of HSC (Jordan, 2007). Five-year survival in AML is approximately 25-30% (Noone *et al.*, 2018), though broad differences between molecular abnormalities and age are observed, as previously stated (1.2.5). Critically, incidence and mortality rates have increased in recent years, particularly in males with a 35% increase to incidence and a 12% increase to mortality globally (Ahmed *et al.*, 2022), demonstrating a pressing therapeutic need.

Treatment options for AML had stagnated in recent decades, with improvements generally limited to dose intensification or combinational regimens (Dombret *et al.*, 2016). Targeted therapies have revolutionised treatment in specific subtypes; the treatment of APL with retinoic acid therapy has transformed this disease subtype into the most treatable form of AML, with CR rates of greater than 95% (Lo-Coco *et al.*, 2013; Sanz *et al.*, 2019). However, retinoic acid therapy cannot eliminate the leukaemic clone which requires further chemotherapy or a differentiation agent such as ATO, enabling long-term remission in over 90% of patients (Degos *et al.*, 2001; Kantarjian *et al.*, 2021). The combination of ATRA and ATO \pm anthracycline has reduced relapse from ~50% to <10% in adult patients with APL since its introduction two decades ago (Sanz *et al.*, 2019). In non-APL AML, therapies achieve CR in up to 80% of patients below sixty years old, and in approximately 50% of patients above sixty (Estey, 2009; Schlenk *et al.*, 2018); unfortunately, relapse occurs in 50% of patients under sixty and up to 90% of those in the elderly cohort (Thol *et al.*, 2020), making it the most frequent cause of death in AML (Dombret *et al.*, 2016). Relapse often presents with a clonally evolved derivative from primary AML, frequently exhibiting greater molecular complexity with the acquisition of resistance to therapeutics (Ho *et al.*, 2016; Hanekamp *et al.*, 2017), and elevated WNT/ β -catenin signalling (Valencia *et al.*, 2009; Griffiths *et al.*, 2010a; Gruszka *et al.*, 2019). Therefore, targeted therapeutics may enable better therapeutic outcomes, requiring identification and validation of WNT/ β -catenin axis in AML.

The WNT/ β -catenin pathway has proposed roles in self-renewal and maintenance of HSC (Reya *et al.*, 2003; Fleming *et al.*, 2008a; Luis *et al.*, 2011), in addition to roles in haematopoiesis; however, the role and necessity of WNT/ β -catenin remains contentious in these processes. Genetic mutations of the WNT/ β -catenin pathway are not found in AML (Johnson *et al.*, 2005; Griffiths *et al.*, 2010b; Gunes *et al.*, 2020); rather, WNT/ β -catenin signalling is a commonly dysregulated pathway via other mechanisms in AML which is notably pronounced in LSC (Majeti, Becker, *et al.*, 2009; Perry *et al.*, 2020). Mechanistically, several central WNT/ β -catenin-related proteins have been shown to be altered in AML, including elevated expression of WNT3a (Simon *et al.*, 2005a; Kawaguchi-Ihara *et al.*, 2008), LEF1 (Metzeler *et al.*, 2012), and TCF4 (In't Hout *et al.*, 2014), alongside repression of GSK3 β (Abrahamsson *et al.*, 2009), and sFRP family members (Guo *et al.*, 2017) that promote pathway activation. In fact, 90% of AML harbour at least one hypermethylated WNT/ β -catenin signalling inhibitor gene. These include *sFRP2* (66%), *sFRP5* (54%), *sFRP1* (34%), *WIF1* (32%), *SOX17* (29%), *RUNX3* (27%) or *DKK1* (16%) (Griffiths *et al.*, 2010a). β -catenin is overexpressed at the mRNA and protein levels in 40-60% of patients with associated poor clinical outcomes (Ysebaert *et al.*, 2006; Chen *et al.*, 2009). Moreover, WNT/ β -catenin has been linked to chemoresistance to DNR (Xiao *et al.*, 2020), and Ara-C (L. Chen *et al.*, 2020). Further, γ -catenin overexpression has been associated with poor prognosis, and knockdown of γ -catenin has sensitised AML cell lines to Ara-C (Qian *et al.*, 2020). Therefore, silencing of WNT/ β -catenin by CRISPR-Cas9 knockout, alongside the close homolog γ -catenin, has the potential to sensitise leukaemic cells to chemotherapeutics and eradicate LSC, which has formed the central focus of this study.

6.2 WNT/ β -catenin Signalling Activity is Heterogenous in AML and Reveals an Expression Profile of Stemness and Chemoresistance Traits

As previous research into WNT/ β -catenin signalling in AML has resulted in both demonstration of dependency (Wang *et al.*, 2010; Fiskus *et al.*, 2015; S. Ma *et al.*, 2015) and dispensability (Cobas *et al.*, 2004b; Gandillet *et al.*, 2011b) for AML maintenance, it was necessary to first characterise a panel of AML cell lines and primary AML samples to examine WNT/ β -catenin necessity and address prior inconsistent findings. This was explored by western blots of cytosolic and nuclear fractions together with a flow-based WNT reporter in **Chapter 3** (AML cell lines) and in **Chapter 4** (Primary AML), which revealed that AML cell

lines have variable capacity to translocate β -catenin into the nucleus and presented with variable γ -catenin expression levels. In this study, β -catenin ‘activity’ was used to characterise lines as *responders* or *non-responders* based on β -catenin nuclear translocation capacity. These classifications potentially explain inconsistent prior research, as inappropriate cell lines have been applied as models; furthermore, prior research in *non-responder* lines suggests off-target effects are responsible for observations of dependency (1.3.5).

Cross-comparison of RNA expression data here-in between *responder* and *non-responder* AML revealed an expression profile in *responders* consistent with stemness, proliferative effects, and mechanisms of potential chemoresistance (S2.). Further, elevated *JUP* (γ -catenin) expression levels were documented, though protein detection by western blot only partly supported this observation. A significant increase in *LEF1*, *TCF7L2*, *LRP6*, *PTK7*, *FZD6*, *WNT3*, and *WNT5a* expression was documented in *responder* AML, alongside the repression of *DACT3* and *DKK4*, demonstrating an expression profile biased to active WNT/ β -catenin signalling. Notable WNT/ β -catenin target genes, such as *ABCBI* were found significantly overexpressed with established roles in driving chemoresistance (Patel *et al.*, 2013).

6.3 β -catenin and γ -catenin are Dispensable for AML Maintenance and Chemoresistance, but β -catenin is Absolutely Required for Clonogenicity in Responder AML cell lines

The necessity of WNT/ β -catenin signalling and potential compensative role of γ -catenin in AML has remained inconclusive, with some authors supporting the absolute necessity of β -catenin for AML maintenance (Saenz *et al.*, 2019), whilst others demonstrate expendable roles for both catenin and TCF family members in maintenance and clonogenicity (X. Zhao *et al.*, 2020; Pepe *et al.*, 2022). To address this in the current study, CRISPR-Cas9 was applied to delete both genes independently and simultaneously in a panel of *responder* and *non-responder* AML cell lines (**Chapter 3**, **Chapter 4**). CRISPR-Cas9 was validated to generate efficient knockout within 72 hours, and the knockout efficiency remained stable over a 3-week period of passaging. Within a panel of AML cell lines, knockout of β -catenin and γ -catenin had no effect upon proliferation, apoptosis, cell cycle, or migration under bulk culture conditions, despite significant reductions in β -catenin and γ -catenin individually or in combination (3.8); however, only β -catenin knockout had an impact upon WNT/ β -catenin

signalling activity (3.6). β -catenin knockout was found to incur a significant reduction in clonogenicity, and indeed, no complete knockout clones could be recovered through cloning, necessitating the use of supportive conditions. No consequence of γ -catenin knockout on clonogenicity was documented.

Once complete knockout clones were obtained, using co-culture with supportive fibroblasts or AML cells (4.3.2), this study again found no effect upon proliferation, apoptosis, cell cycle, differentiation status, chemoresistance, or stress tolerance, despite absence of both catenin members and silencing of WNT/ β -catenin signalling activity (4.3.4). Single knockout of β -catenin alone showed that this was absolutely required for WNT/ β -catenin signalling activity, with no redundancy function of γ -catenin (4.3.4.2). Correspondingly, γ -catenin knockout had no consequence on WNT/ β -catenin signalling activity, despite reductions in total β -catenin protein levels. These findings agree with evidence studied in other contexts, such as gastrulation (Haegel *et al.*, 1995) and HCC (Wickline, Du, Donna B. Stolz, *et al.*, 2013), in which γ -catenin cannot act in place of β -catenin for WNT/ β -catenin signalling and instead suppresses WNT/ β -catenin signalling. It is acknowledged that γ -catenin can compensate for β -catenin in non-WNT roles (Wickline *et al.*, 2011); however, these are not of interest to the study here-in. As before, complete β -catenin knockout was found to be incompatible with clonal growth, whilst no consequence of γ -catenin knockout on clonogenicity was observed.

Examination of the role β -catenin and γ -catenin provide for AML maintenance and clonogenicity was furthered by examination of primary AML material, which similarly presented no growth defects in a bulk culture following either CRISPR-Cas9-induced knockout of β -catenin or by small molecule inhibition of the β -catenin:LEF1:TCF4 transcriptional complex (4.3). γ -catenin was not detectable in these samples, even with knockout of β -catenin, confirming no compensative effect or contribution. As with the *responder* cell lines, however, β -catenin expressing primary AML lines did show significantly reduced clonal growth following β -catenin knockout and following treatment with small molecule inhibitors of WNT/ β -catenin signalling. Conversely, primary AML lines not expressing β -catenin lines showed no phenotype following β -catenin knockout under any culture conditions. These data suggest WNT/ β -catenin signalling is an appropriate target for AML eradication in a subset of patients with a WNT-dependent profile; however, a secondary population of patients exists

with no observable WNT/ β -catenin signalling profile, nor requirement on WNT/ β -catenin for clonal growth. This suggests a proportion of patients, perhaps 40-60%, would benefit from WNT/ β -catenin inhibition if these findings translate to relapse *in vivo*.

6.4 WNT/ β -catenin is Dispensable for Myeloid Lineage Development in Normal Haematopoiesis and for HSC Self-Renewal

As the precise role and necessity of β -catenin and γ -catenin in the literature is inconclusive in regard to normal haematopoiesis, it was necessary to examine these in a comparable CRISPR-Cas9-induced knockout model (4.3.4). In normal haematopoiesis, *JUP* mRNA levels decreased throughout myeloid differentiation, with highest expression found in HSC, suggesting a role in HSC proliferation and maintenance. *CTNNB1* levels were high and remained high despite differentiation status, though post-translational regulation limits interpretation of mRNA expression data. Examination of protein expression in a human primary HSPC model confirmed β -catenin and γ -catenin are present until day three, after which point protein levels are undetectable. As γ -catenin had been determined to have no compensative role, and no data indicated necessity in AML, only β -catenin was considered for knockout studies in HSPC. These studies showed that bulk knockout of β -catenin was inconsequential to myeloid colony formation and in a simplified *in vitro* model of self-renewal potential. Similarly to the observations in AML cell lines, β -catenin knockout had no consequences regarding growth, cell cycle, apoptosis, or differentiation status. These results indicate that, in agreement with much of the recent literature (Cobas *et al.*, 2004a; Jeannet *et al.*, 2008b; Koch *et al.*, 2008b; X. Zhao *et al.*, 2020), WNT/ β -catenin signalling is not required for myeloid development. These findings support the therapeutic suitability of targeting β -catenin, though further *in vivo* studies would be required to validate this. It is conceded that, as in the CRISPR-Cas9 primary AML data, these data are generated in the context of a bulk, non-clonal CRISPR-Cas9 knockout population state rather than a complete clonal knockout state. However, findings in the AML cell line and primary AML context demonstrate the ability to detect consequence of knockout under these conditions.

6.5 Dual catenin Knockout Perturbs the AML Transcriptome and RAP1 Signalling

To further study the consequences of dual catenin knockout, RNA-seq was performed to examine the normal WNT-active and the knockout condition profile, as examined in **Chapter 5**. This was achieved by application of rWNT3a, or vehicle, for active and basal WNT status,

respectively. Examination of the transcriptome revealed numerous upregulated and repressed genes as a consequence of rWNT3a treatment or knockout related to loss of stemness, evasion of apoptosis, and chemosensitivity. Whilst the findings related to stemness support a possible role in clonal growth, elevated expression of genes suppressing apoptosis in the knockout state suggests a potential role in promoting AML survival in the absence of WNT/ β -catenin.

To better capture a biologically interpretable effect, pathway analysis was performed (5.3.3), which indicated that rWNT3a activated the RAP1 signalling pathway, supporting previous reports of a WNT/RAP1 signalling axis (Habas *et al.*, 2007; Tsai *et al.*, 2007; Goto *et al.*, 2010; Griffin *et al.*, 2018), whilst the knockout state demonstrated repression of the RAP1 signalling pathway. Together, these observations suggest that WNT/ β -catenin signalling promotes RAP1 activity, and that this is an effect mediated by β -catenin via upregulation of the GEF RAPGEF4. As a WNT/ β -catenin signalling profile had been determined within the *responder* AML cell lines based upon public CCLE RNA-seq data when compared with the *non-responder* group, it was also noted that RAP1 signalling was the only other signalling pathway overrepresented within the *responder* AML group. To this end, this study investigated whether WNT/ β -catenin and RAP1 signalling was perturbed in the patient context. By comparing patients with high and low *LEF1* mRNA expression, which was previously determined to be an approximate indicator of WNT/ β -catenin activity and is supported in the literature (Morgan *et al.*, 2019), or based upon five year survival, a WNT/ β -catenin/RAP profile in high *LEF1* expression patients and patients deceased after five years was revealed. Cell line and patient data indicated that *RAPGEF4* (EPAC2) and *SIPA1L1* (SIPA1L1) were the activator and repressor of RAP1 signalling, respectively, with the former a possible direct WNT target gene (Schmidt *et al.*, 2013), and the latter suppressed by CKI ϵ of the WNT/ β -catenin pathway (Tsai *et al.*, 2007). Speculative evidence of pathway crosstalk has been documented within the literature (Habas *et al.*, 2007; Tsai *et al.*, 2007; Goto *et al.*, 2010), and scarce evidence on RAP1 has suggested roles in leukaemogenesis and an absolute requirement for clonogenicity *in vivo* and *in vitro* (Ishida *et al.*, 2003; Qiu *et al.*, 2012; Imai *et al.*, 2019).

6.6 Restoration of RAP1 Signalling Activity in β -catenin Knockout AML Restores Responder Clonogenicity and Enhances Non-responder AML Clonogenicity

Expression of a constitutively active form of RAP1, RAP1^{E63}, was able to restore the clonogenicity of *responder* AML cell lines to clonal efficiencies comparable to controls (5.3.7).

As transcriptomic analyses of rWNT3a and knockout data, alongside the cell line and patient data, supported the RAP1 activating GEF *RAPGEF4* was a WNT/ β -catenin target gene and the RAP1 inhibiting GAP *SIPA1L1* was inhibited by CKI ϵ of the WNT/ β -catenin pathway in the presence of a WNT agonist, it was necessary to examine both. In principle, CRISPR-Cas9 activation of *RAPGEF4* and inhibition of *SIPA1L1* would restore the expression profile to a state comparable to the WNT/ β -catenin active state and was expected to restore clonogenicity. Activation of *RAPGEF4* restored a significant proportion of the clonogenicity compared to scrambled knockout control, suggesting *RAPGEF4* promoted RAP1 enabling clonal growth. Further, *SIPA1L1* inhibition was able to only mildly improve clonogenicity. These data indicate that the knockout condition is incapable of sufficient RAP1 signalling activity to facilitate clonogenicity. *RAPGEF4* is a likely WNT/ β -catenin target gene, upregulated directly by β -catenin, which enables subsequent activation of RAP1 signalling. Unfortunately, quantification of the activation of *RAPGEF4* and inhibition of *SIPA1L1* could not be validated by western blot as antibodies for both were unsuccessful.

In conclusion, this study has demonstrated that it is possible to stratify cell lines and primary AML samples based upon WNT/ β -catenin signalling activity. Secondly, WNT/ β -catenin signalling activity is absolutely required for the clonal growth of AML cells with WNT/ β -catenin signalling activity, which further indicates clonal growth is also supported by alternate mechanisms in AML. β -catenin is indispensable for WNT/ β -catenin signalling activity, as expected, and γ -catenin is unable to act compensatively for this purpose. Co-culture with fibroblasts and dual knockout AML cell lines was able to restore clonogenicity, indicating that the effect is only apparent at the single cell level *in vitro*.

This study has also shown evidence for a WNT/ β -catenin/RAP1 signalling axis as a central mechanism of contributing to clonal growth in AML. The RAP1 signalling pathway has been largely overlooked despite appearing amongst the top identified perturbed pathways in numerous differing bioinformatics studies of AML (Huang *et al.*, 2017; Lv *et al.*, 2018; S. Wu *et al.*, 2019; L. Zhu *et al.*, 2020; S. Chen *et al.*, 2020; He *et al.*, 2021; zhang *et al.*, 2021; Hong *et al.*, 2021; Lu *et al.*, 2021; Rodríguez González *et al.*, 2021; Almajali *et al.*, 2022; Ling *et al.*, 2022), especially as recent bioinformatics research performed on patient data indicates it is the most perturbed pathway following treatment regardless of the therapeutic agent applied, suggesting a direct, central role in AML biology (J. Wu *et al.*, 2021). The limited existing

research on RAP1 or its regulators supports a putative role in AML. As targeted EPAC2 inhibitors are in development, and have shown promise *in vitro* in AML cell lines (Kusnadi *et al.*, 2020), further investigation of RAP1 signalling could provide new treatment possibilities.

6.7 Future Directions and Limitations

Based on these findings, investigation of the role RAP1 signalling in haematopoiesis, HSC self-renewal, and AML is a promising starting point for further research. High sensitivity ChIP-seq assays of β -catenin could be performed to validate potential binding partners within the RAP1 signalling axis, as reported for several members (Upadhyay *et al.*, 2008; Griffin *et al.*, 2018). Alternatively, a recently developed technique for examining binding partners of β -catenin at substantially reduced cost which is currently in pre-print could provide an improved method to decipher β -catenin interaction partners in numerous conditions (Zambanini *et al.*, 2022). Similarly, it is conceded that only a single timepoint was considered to examine the effect of rWNT3a treatment in AML lines for RNA-seq, with a recently released pre-print demonstrating temporal transcriptional effects ranging from hours to days, potentially necessitating an assessment of the effect of rWNT3a over further timepoints (Pagella *et al.*, 2022). A small-scale preconfigured qPCR panel could be applied to research rWNT3a response in AML cell lines at a wide range of timepoints at low cost.

Furthermore, as RAP1 signalling is modulated by several GEF, numerous potential alternate mechanisms of RAP1 activation could be derived from mechanisms other than WNT/ β -catenin signalling, with potential relevance for the *non-responder* AML enabling broader therapeutic application. An assessment of the impact of RAP1 signalling inhibition on *non-responder* AML clonogenicity could reveal whether the pathway is commonly involved in clonogenicity, independent of WNT/ β -catenin signalling. RAP1 signalling could be explored broadly with the RAP1A inhibitor GGTI-298 (Chan *et al.*, 2011), or with the specific EPAC2 inhibitors ESI-05 (Kirton *et al.*, 2018), ESI-09 (Zhu *et al.*, 2015), and HJC-0350 (Ramos *et al.*, 2018). However, a recent review has suggested potential off-target effects of these compounds, and as such, a CRISPR-Cas9-based approach may be better suited for in-depth investigation (Ahmed *et al.*, 2019).

Regarding WNT/ β -catenin, it would be beneficial to conduct *in vivo* murine studies to determine whether the *in vitro* finding of inability to clonally expand alone was reproducible in the more supportive environment of the BM. Recent research applying a WNT inhibitor

demonstrated near complete *in vitro* inhibition of clonogenicity, whilst *in vivo* no effect was demonstrated (Pepe *et al.*, 2022). As an alternative to *in vivo* experiments, complex co-culture experiments could be used to investigate the impact of the microenvironment. Simplified mono- and co-culture methods as applied here-in are recognised for the inability to reflect the true heterogeneity, mechanical effects, and cell-cell interactions present *in vivo*. To this end, novel 3D-based culture methods are beginning to be developed which incorporate multiple cell types and scaffold structures to better represent the *in vivo* BM condition and state (Bray *et al.*, 2017; Cucchi *et al.*, 2020; Syama *et al.*, 2021). Unfortunately, the expense of these platforms and difficulty of subsequent analyses limits widespread application at current, but this remains a direction the field will progress into to better represent the condition and to enable more informative outcomes to be realised. This is particularly important for AML in the context of WNT/ β -catenin signalling, as genetic alterations in WNT/ β -catenin signalling components are not principle drivers of AML (Papaemmanuil *et al.*, 2016; Tyner *et al.*, 2018), rather, evidence classically suggests WNT activity is secondary to translocation products, oncogenic mutations (*FLT3*, *NPM1*, *DNMT3A*), and methylation changes which result in heightened expression of β -catenin and γ -catenin (Müller-Tidow *et al.*, 2004; Zheng *et al.*, 2004; Tickenbrock *et al.*, 2005; Kajiguchi *et al.*, 2007; Hou *et al.*, 2011; Lane *et al.*, 2011; Barbieri *et al.*, 2016; Meyer *et al.*, 2016; Gruszka *et al.*, 2019).

However, research has suggested that the surrounding stromal cells within the microenvironment are able to secrete alternate WNT ligands and factors contributing to WNT/ β -catenin activation, which the monoculture cell line model cannot mimic. For instance, cancer-associated fibroblasts and tumour-associated macrophages secrete WNT3a, WNT5a, as well as other components, such as biglycan, which can act as a pericellular WNT ligand reservoir, whilst also enhancing LRP6-ligand binding capacity (Berendsen *et al.*, 2011; Zhao *et al.*, 2013; Wang *et al.*, 2016). While WNT-related mutations are rare in intrinsic cell types in AML, they have been reported in approximately 40% of osteoblasts, which has been established to generate AML in an *in vivo* mouse model (Raaijmakers *et al.*, 2010; Kode *et al.*, 2014). Activation of Notch and WNT/ β -catenin signalling pathways, which have close crosstalk, has been demonstrated as essential for the maintenance of HSC (Bigas *et al.*, 2010). Myelopoiesis is associated with low levels of Notch as much as WNT/ β -catenin signalling (De Obaldia *et al.*, 2013). Indeed, the close crosstalk between the two pathways has resulted in the

so-called 'WNTCH' pathway (Song *et al.*, 2015; Takam Kamga, Cassaro, *et al.*, 2016; Azadniv *et al.*, 2020). Stromal WNT/ β -catenin signalling induces expression of JAG1, DLL1, DLL4, and other Notch ligands which subsequently activate Notch signalling, supporting self-renewal in a cell-cell contact-dependent manner (Kadekar *et al.*, 2015). Fibroblasts demonstrate active WNT/ β -catenin and subsequently Notch to support LSC by providing them with proliferative, chemoresistive, and self-renewal capacities (Takam Kamga, Bassi, *et al.*, 2016). WNT/Notch inhibition is able to sensitise LSC, nullifying the protective effect of stromal cells (Kamga *et al.*, 2020). Whilst not identified during pathway analysis, modulation of Notch ligands by rWNT3a and the knockout condition was noted and could be worth further investigation.

In addition to the cell types and models not considered, numerous promising genes which were upregulated by rWNT3a and repressed in knockout, such as *IL1RAP*, were not investigated further and would be worth further examination. Interleukin 1 Receptor Accessory Protein (IL1RAP) is long recognised as highly expressed on LSC, but absent or minimally expressed on normal HSPC, with roles in LSC self-renewal suggested (Barreyro *et al.*, 2012). Targeting of IL1RAP has demonstrated LSC eradication, whilst normal HSC were spared (Askmyr *et al.*, 2013a; Ågerstam *et al.*, 2016). Recently, IL1RAP was shown to play a potential critical role in AML onset and LSC clonogenicity in a fibroblast co-culture model (De Boer *et al.*, 2021), which was furthered by a CRISPR-Cas9-derived knockout model of IL1RAP which demonstrated impaired clonogenicity in an *in vitro* THP1 fibroblast co-culture model, and a reduction of engraftment in an *in vivo* murine model (Ho *et al.*, 2021). The source of excessive IL1RAP is speculative, but evidence here-in would indicate WNT/ β -catenin or RAS1 signalling involvement.

CRISPR-Cas9 has long demonstrated potential as a clinical therapy (Tufail, 2022), and one particular clinical trial recently approved by the FDA (NCT05066165) is of particular interest to the works here-in. The trial has commenced treating AML patients with NTLA-5001, an *ex vivo* CRISPR/Cas9 genome editing candidate which targets WT1. WT1 is recognised to drive LSC self-renewal (Zhou *et al.*, 2020), and has been shown to promote β -catenin stability, nuclear translocation, and WNT target expression (Li *et al.*, 2014; N. Wang *et al.*, 2017; Tan *et al.*, 2018; F. Wu *et al.*, 2021; Wagstaff *et al.*, 2022). The results of this trial could further elucidate a WT1:WNT/ β -catenin axis, and potentially, RAS1 signalling

involvement. Within this thesis, WT1 was predicted as perturbed by rWNT3a treatment and dual catenin knockout in TF analyses of the transcriptomic profiles.

To conclude, this thesis has provided a potential mechanism through which WNT/ β -catenin signalling drives RAP1 signalling, thereby providing clonogenicity in AML. This was demonstrated *in vitro* in complete dual-catenin CRISPR-Cas9 knockout AML cell line model, eliminating doubts of residual protein expression sustaining maintenance which previous studies with shRNA inhibition, compounds suppression, and recent incomplete CRISPR-Cas9 knockout models were limited by. *In silico* analyses of AML cell line and patient data revealed further indication of RAP1 signalling involvement in disease relapse and overall patient survival, demonstrating a potential clinical benefit to further research. Additional investigation of RAP1 signalling in AML would be necessary to consolidate these findings and could present an exciting advancement of the treatment avenues in AML.

Appendix

S1. Examining β -catenin and γ -catenin in Human Haematopoiesis

As β -catenin represents an interesting target for AML, it was necessary to determine the expression levels and necessity of β -catenin to normal haematopoiesis and HSC self-renewal. If β -catenin is dispensable to these processes, targeting it in AML could prove an effective strategy.

As mounting evidence indicates haematopoiesis exists in a continuum model, efforts to apply recently released public scRNA-seq data to study *CTNNB1* and *JUP* expression within the human context was applied. A significant benefit to scRNA-seq is the absence of need to pre-sort populations to defined subsets which biases an analysis. Instead, scRNA-seq is able to capture significantly greater granularity, enabling examination of haematopoiesis in a method more representative of the continuum context.

A recently published dataset was examined, generated from healthy human BM samples (Triana *et al.*, 2021). The dataset was prepared as indicated in the publication, with clusters identified based upon well recognised expression patterns; for instance, *CD34* expression was applied as a reference for HSC and early multipotent haematopoietic cells. The continuum of haematopoiesis was immediately apparent, with a spectrum of cells bridging classically distinct cell types (**Figure S-6-1A|C**). Feature profiling of *CTNNB1* demonstrated poor correlation with *CD34* expression, with levels expressed by most cell types at heterogeneous levels. When *JUP* was considered, greater correlation with *CD34* expression was found, with a notable absence in terminally differentiated cell types. Statistical analysis between clustered populations in the context of the HSC reference revealed statistically significant upregulation of *CTNNB1* in neutrophils and eosinophils, whilst downregulation was found for erythroid progenitors and erythroblasts. When *JUP* was considered, HSC were found to have significantly higher expression levels against nearly all differentiated cell subtypes (**Figure S-6-2A|B**).

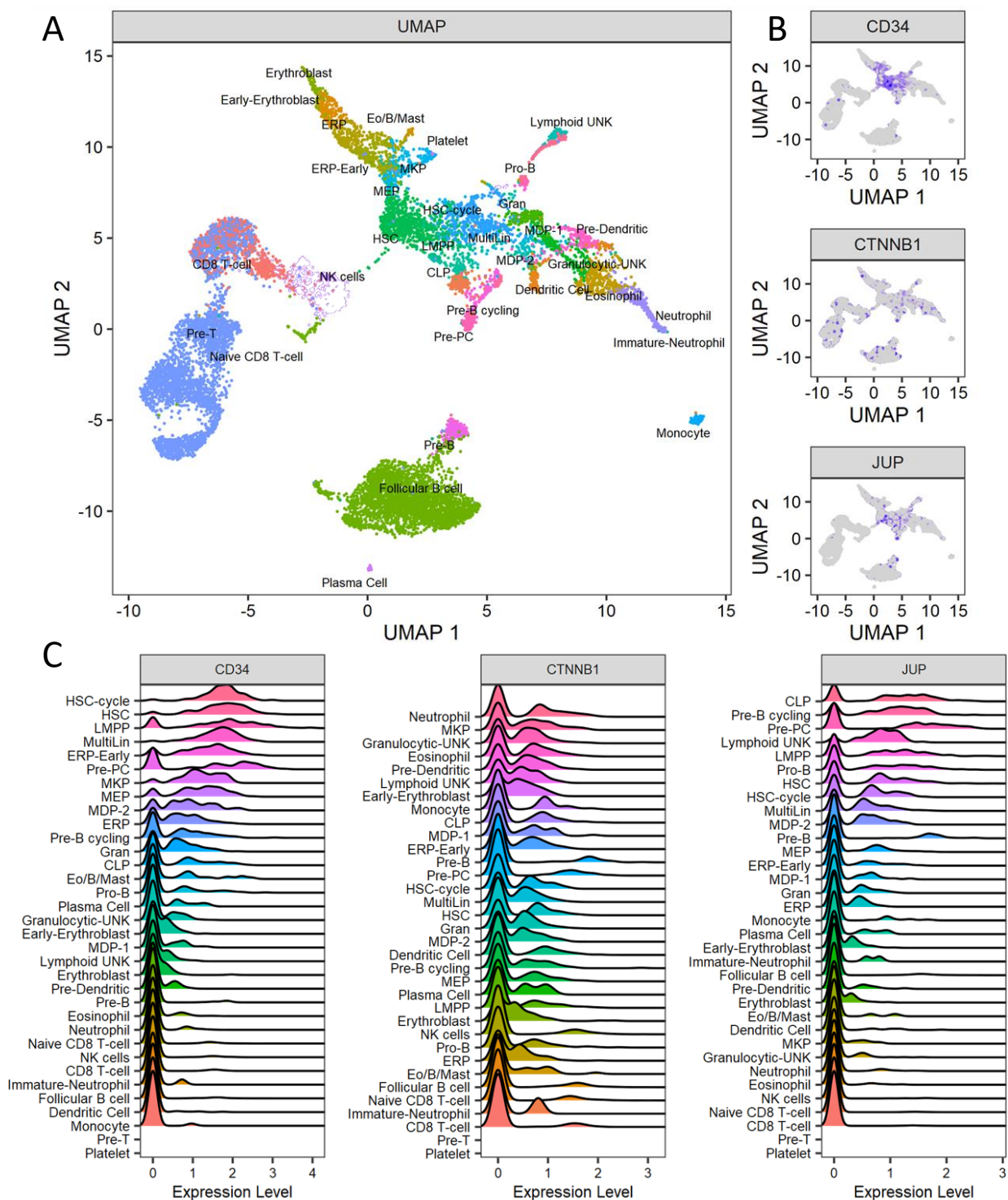


Figure S-6-1: *CTNNB1* Poorly Indicative for HSC in the Continuum of Haematopoiesis

A) Uniform Manifold Approximation and Projection (UMAP) display of single-cell transcriptomics data (n = 70,017 single cells). Clusters are labelled and colour-coded by unsupervised clustering. **B)** Uniform Manifold Approximation and Projection (UMAP) display of single-cell transcriptomics data (n = 70,017 single cells). Cells are coloured blue based on high expression of the indicated transcript. **C)** Expression ridge plots demonstrating the heterogeneous transcript expression within cell types. **HSC** – Haematopoietic stem cell; **LMPP** - Lymphoid-primed multipotent progenitor; **ERP** - Erythrocyte progenitor; **MultiLin** – Multipotent (MPP); **MKP** - Megakaryocyte progenitors; **MEP** - Megakaryocyte–erythroid progenitor cell; **MDP** - Monocyte-dendritic cell progenitors; **CLP** - Common lymphoid progenitor; **UNK** – Unknown (incomplete definition).

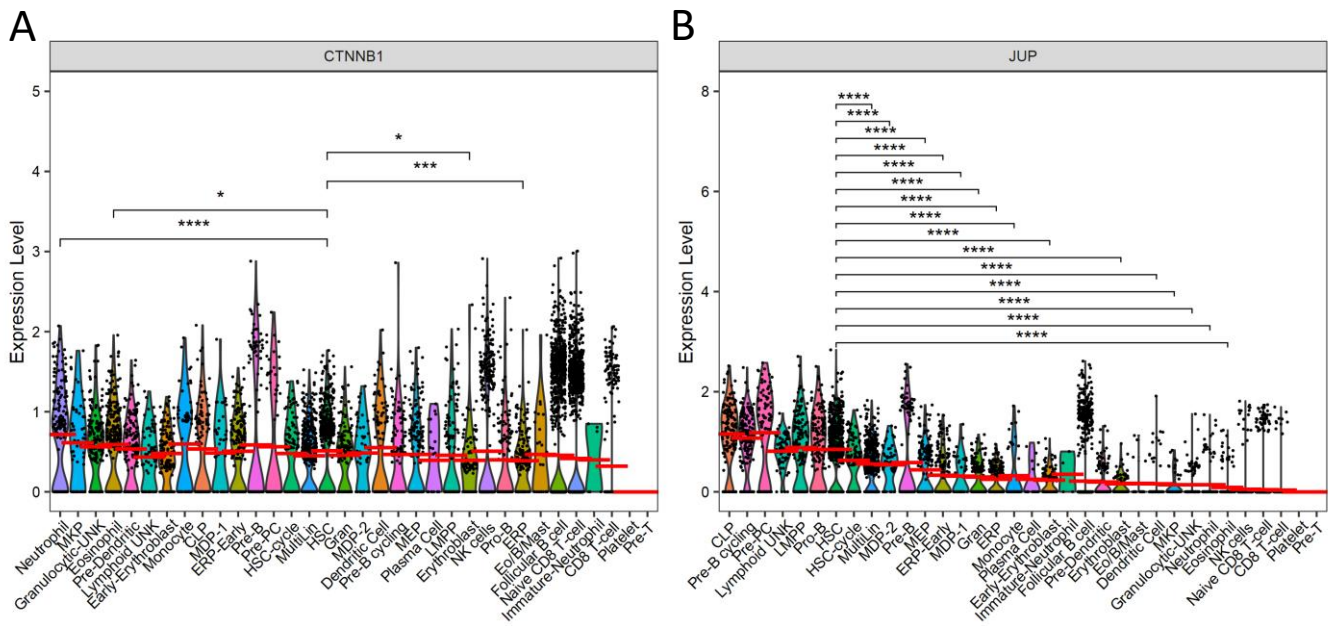


Figure S-6-2: β -catenin and γ -catenin Expression Reduces During Haematopoiesis

A) Violin plot demonstrating single-cell transcriptomics data for *CTNNB1*. **B)** Violin plot demonstrating single-cell transcriptomics data for *JUP*. Cell types were ordered by expression, with the red bar indicating mean expression within each group. Groups were contrasted against the HSC reference with a t-test; p-values were corrected for multiple tests with Benjamini-Hochberg correction. Data from 70,017 single cells.

HSC – Haematopoietic stem cell; **LMPP** - Lymphoid-primed multipotent progenitor; **ERP** - Erythrocyte progenitor; **MultiLin** – Multipotent (MPP); **MKP** - Megakaryocyte progenitors; **MEP** - Megakaryocyte–erythroid progenitor cell; **MDP** - Monocyte-dendritic cell progenitors; **CLP** - Common lymphoid progenitor; **UNK** – Unknown (incomplete definition).

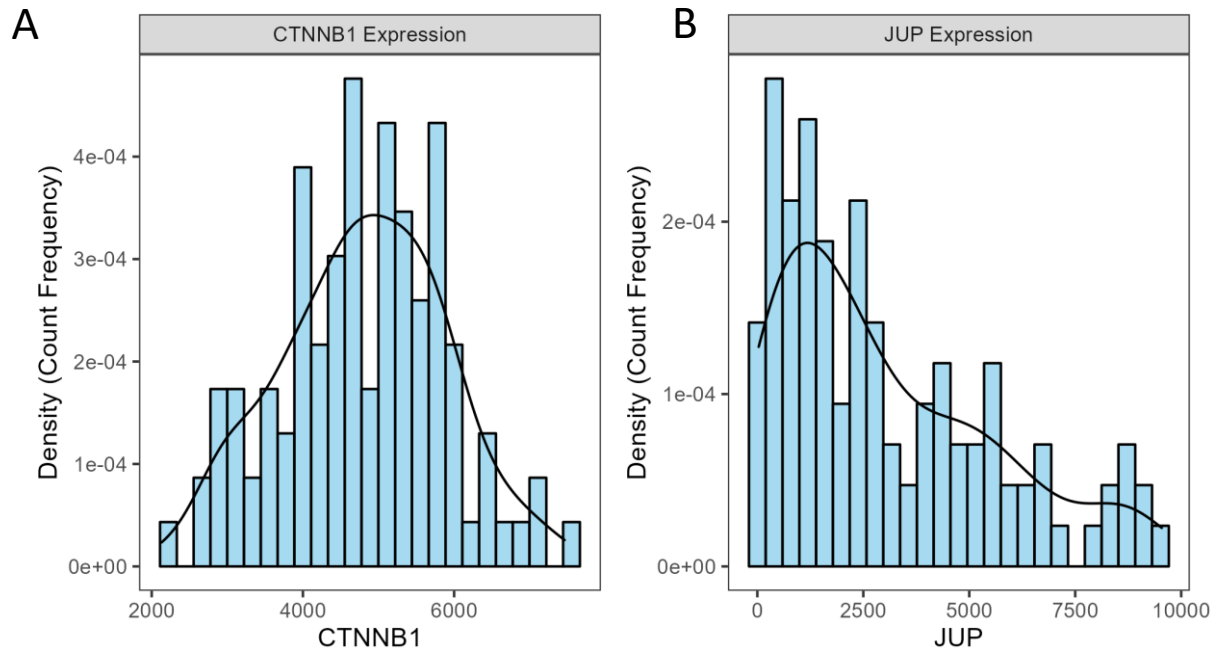


Figure S-6-3: Expression Patterns of *CTNNB1* and *JUP* in TCGA Patients

A) Histogram demonstrating the expression pattern of *CTNNB1* in the subset TCGA cohort of patients with AML. A gaussian distribution presents, with all patients expressing *CTNNB1*.

B) Histogram demonstrating the expression pattern of *JUP* in the subset TCGA cohort of patients with AML. *JUP* expression is absent or low in the majority of TCGA patients, with a small number of patients expressing a high level of *JUP* noted.

S2. Examining the Transcriptomic Profile of Responder AML

With the AML cell lines classified, it was possible to use the public CCLE RNA-seq data to further examine the transcriptomic profile of WNT/ β -catenin *responder* AML cell lines. Analysis of this data may reveal mechanisms by which WNT/ β -catenin is induced, β -catenin translocation partners, and mechanisms by which WNT/ β -catenin contributes to AML.

PCA revealed no clustering patterns on the basis of *responder* and *non-responder* status (**Figure S-6-4A**) These observations indicate responder status alone does not perturb the broad transcriptomic profile of AML. This is not unexpected, as the WNT/ β -catenin pathway represents only one of tens of signalling systems.

In an exploratory differential expression analysis, hundreds of transcripts were found to be overexpressed or repressed relative to the responder condition (**Figure S-6-4B**). Notably, numerous promoters or activation members of the WNT/ β -catenin signalling pathway were upregulated, whilst repressors were downregulated. *DACT3*, encoding Dishevelled Binding Antagonist of Beta Catenin 3, was significantly repressed in *responder* AML cells, and is an established epigenetic repressor of WNT/ β -catenin signalling with important roles in CRC progression (Jiang *et al.*, 2008). *DKK4*, encoding Dickkopf WNT Signalling Pathway Inhibitor 4 was also repressed, which inhibits β -catenin accumulation and self-renewal characteristics in CRC and HCC (Fatima *et al.*, 2012).

Contrarily, numerous WNT agonists were overexpressed in *responder* cell lines, including *WNT3* and *WNT5A*. *WNT3*, a close homolog of *WNT3a*, is recognised as the driver of WNT/ β -catenin signalling in APC^{MUT} CRC (Voloshanenko *et al.*, 2013). *WNT5a* is classically regarded as a prototypical non-canonical WNT ligand; however, *WNT5a* is overexpressed in CRC, and has been demonstrated to drive WNT/ β -catenin signalling via *FZD7*, suggesting context specific roles (Li *et al.*, 2018; Astudillo, 2021). Numerous WNT receptors were also found to be overexpressed in *responder* lines (**Figure S-6-4**). *FZD6* is a recognised WNT ligand receptor for WNT/ β -catenin signalling, though is classically considered a non-canonical receptor. *FZD6* was found significantly overexpressed in the *responder* cohort, an observation also documented for CRC and other cancers (Kim *et al.*, 2015). *LRP6*, encoding LDL Receptor Related Protein 6 is the main WNT/ β -catenin co-receptor, and levels were shown to be significantly higher in the *responder* population. *LRP6*

is frequently overexpressed in CRC (Astudillo, 2021), and was recently demonstrated to be the only co-receptor integrally required for WNT/ β -catenin signalling through CRISPR-Cas9 knockout in CRC (Chen *et al.*, 2021). *PTK7*, encoding Protein Tyrosine Kinase 7, was classically considered a non-canonical WNT pathway receptor, which repressed canonical WNT signalling (Peradziryi *et al.*, 2011; Hayes *et al.*, 2013); however, recent evidence has demonstrated *PTK7* increases the WNT/ β -catenin response to WNT3a, and this amplification is reliant upon the co-receptor LRP6 (Puppo *et al.*, 2011). *PTK7* is overexpressed in CRC and conveys a poor prognostic indication (Tian *et al.*, 2016). *PTK7* was proposed to act as a mechanistic switch by upregulating LRP6 to alternate between canonical and non-canonical WNT signalling (Bin-Nun *et al.*, 2014). A recent study has also reported *PTK7* can bind β -catenin directly to enhance WNT/ β -catenin target gene expression, with small molecule inhibitors blocking the association of these two members, capable of reducing WNT/ β -catenin activity and proliferation in CRC (Ganier *et al.*, 2021).

Additionally, several WNT/ β -catenin members were equally found to be overexpressed in the *responder* cohort. Notably, *CTNNB1* was abundantly expressed in both cohorts, though levels were comparable between conditions. Critically, *JUP* was overexpressed in the *responder* cohort, further suggesting involvement of γ -catenin in WNT/ β -catenin signalling. *LEF1* and *TCF7L2* (TCF4) were both significantly overexpressed in the *responder* cohort, whilst other TCF members were unaltered between the two conditions. When the hallmark WNT/ β -catenin target genes *MYC*, *POU5F1*, *PPARD*, *RUNX2*, *CCND1*, *MMP7*, *NANOG*, and *BIRC5* were considered, none were found significantly altered, although *CCND1* was trending towards significance. *NOTUM* is a WNT target gene classically reported to act as a negative WNT regulator by inactivating WNT ligands to cease excessive WNT/ β -catenin activity, which would suggest active WNT/ β -catenin signalling silencing via a negative feedback loop (Nusse, 2015). However, recent research in CRC has demonstrated *NOTUM* expression and secretion from CRC cells acts to disadvantage surrounding WT cells by conveying a clonal competition advantage to cancer cells (Flanagan *et al.*, 2021). *ABCB1* and *ABCB11* were significantly overexpressed in *responder* AML cells, with *ABCB1* a recognised WNT target gene regulated by WNT/ β -catenin and WNT5a (Corrêa, Binato, Du Rocher, Morgana T L Castelo-Branco, *et al.*, 2012; Hung *et al.*, 2014). The ABC family encodes ATP Binding Cassette Subfamily B members, also known as multidrug resistance genes. Taken together,

these results demonstrate that WNT/ β -catenin signalling is either active at modicum levels within *responder* cells at basal level or, alternatively, the heightened levels of core members facilitate a primed state from which further extrinsic activation would induce a response far greater than *non-responder* cells.

Whilst an overexpression of WNT ligands suggests an autocrine capacity to initiate WNT/ β -catenin signalling, this has not been documented *in vitro*. In the *in vivo* context, the surrounding stromal cells within the microenvironment are thought to secrete alternate WNT ligands and augmentative factors contributing to WNT/ β -catenin activation, which the cell line model cannot mimic. For instance, cancer-associated fibroblasts and tumour-associated macrophages secrete WNT3a, WNT5a, and components such as biglycan, which can act as a pericellular WNT ligand reservoir whilst also enhancing LRP6-ligand binding capacity (Berendsen *et al.*, 2011; Zhao *et al.*, 2013; Wang *et al.*, 2016).

Amongst the remaining most significantly differentially expressed genes, several notable candidates emerge which are not currently linked to WNT/ β -catenin signalling but convey mechanisms of drug resistance or present significantly poor prognostic indication. *SLC16A7*, a member of the monocarboxylate transporter family, has been demonstrated to convey resistance to methotrexate in rheumatoid arthritis, another disease involving WNT/ β -catenin signalling alterations (Fujii *et al.*, 2015). *SLC16A7* is an established poor prognostic indicator in AML, though sparse research exists in this context (Esteve *et al.*, 2007). *CRIMI* was found to be significantly overexpressed and has been demonstrated to facilitate resistance to DNR and Ara-c in AML (Prenekert *et al.*, 2010). Similarly, CD52 was significantly overexpressed, and has been established as an indicator of chemotherapy resistance by an unknown mechanism (Saito *et al.*, 2011). *RBM11* was significantly upregulated and is recognised as a poor prognostic indicator in ovarian cancer by positively regulating AKT/mTOR signalling (Fu *et al.*, 2021). In addition, numerous transcripts were identified as being repressed, relating to DNA damage response and differentiation drivers, which could relate to leukaemogenesis. *ZNF185* was significantly repressed in *responder* AML cell lines and has been established as a p53 target gene, upregulated in response to DNA damage. Reduced expression of *ZNF185* is a common early feature in numerous cancers, facilitating further mutational events (Smirnov *et al.*, 2018). *DPYSL2* was also significantly repressed, and has recently been demonstrated to be a master mediator of monocytic differentiation induction in AML with evidence supporting

it may be targetable (Kiyose *et al.*, 2016). Similarly, *UNC5C* and *MNDA* were significantly repressed in *responder* AML cell lines, with these encoding a dependence receptor and apoptotic regulator, respectively. *UNC5C* is frequently suppressed in cancer, with such cases documented in 80% of CRC patients, in which it conveys a poor prognostic outcome and is one of the earlier transcriptional events observed, suggesting a role in carcinogenesis (Wu *et al.*, 2017). *MNDA* is frequently reduced in high-grade MDS, conveying poor prognosis and elevated risk of AML transformation (Briggs *et al.*, 2006).

Pathway analysis was performed to examine whether a WNT/ β -catenin profile was revealed, alongside other pathways which could be of interest. ORA of significantly differentially expressed genes revealed a WNT profile within all pathway databases considered. The KEGG pathways included several diseases which are hallmarked by WNT signalling, including CRC, breast cancer, and HCC (**Figure S-6-5A**). GSEA revealed a negative profile for DNA repair pathways and the p53 pathway, whilst significant enrichment of the WNT, TGF β , RAS, PI3K-AKT, and mTOR signalling pathways was documented, with a particular focus on genes regulating pluripotency, all of which are involved in AML (**Figure S-6-5B**)

Together, these results demonstrate that the transcriptomic profile of *responder* AML is associated with an elevated WNT/ β -catenin profile and increased *JUP* expression, suggesting the involvement of γ -catenin, and multiple mechanisms by which differentiation block and drug resistance can occur. Further considerations of other pathways perturbed in WNT responder AML suggests that crosstalk between WNT/ β -catenin and TGF β , RAS, PI3K-AKT, and mTOR signalling exists. Such crosstalk is well documented with WNT signalling for TGF β , RAS, PI3K-AKT, and mTOR signalling, whilst suggestions exist for a WNT/RAP pathway (Habas *et al.*, 2007; Jeong *et al.*, 2018; Itatani *et al.*, 2019; Prossomariti *et al.*, 2020).

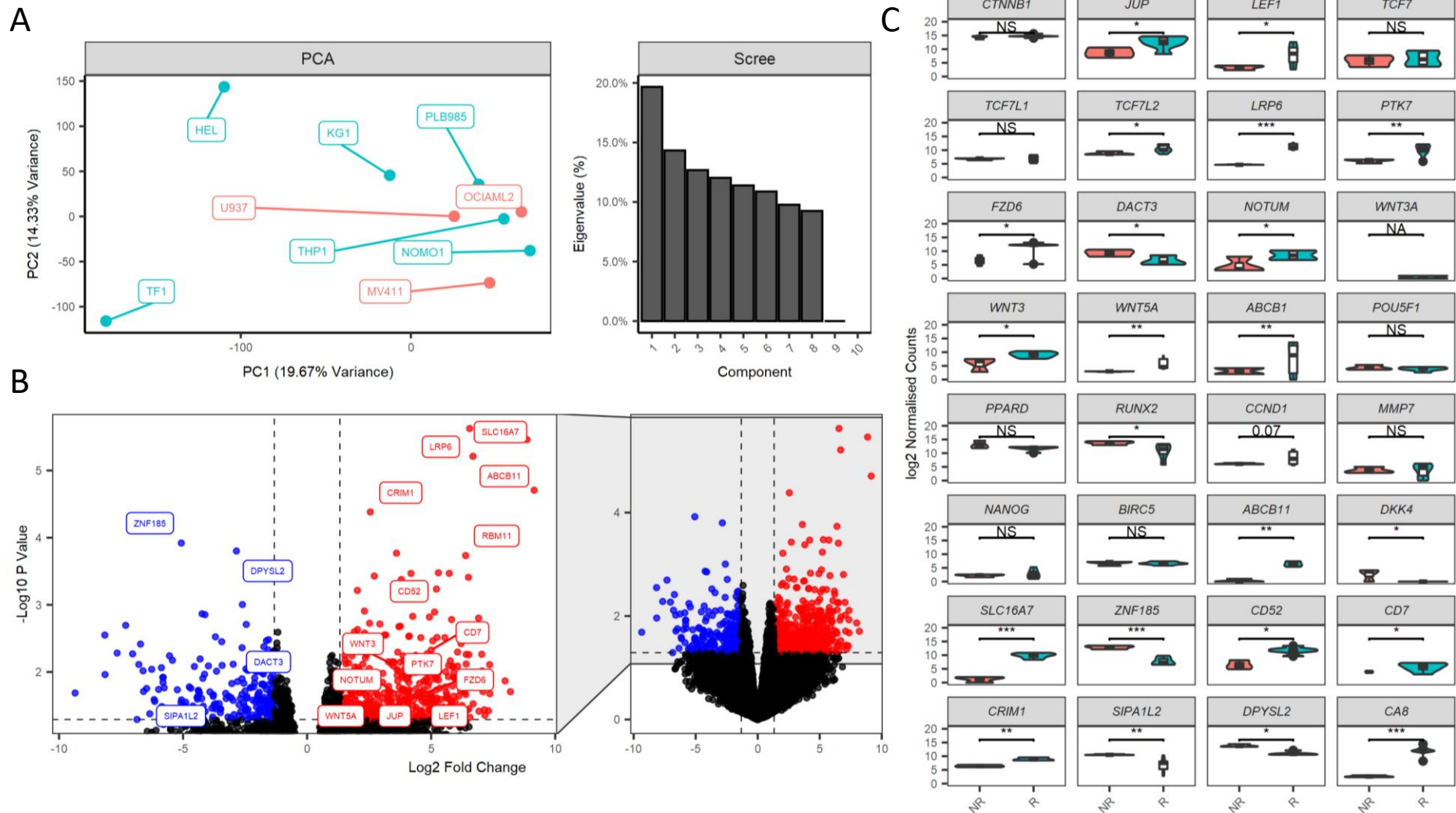


Figure S-6-4: Transcriptomic Profile Reveals Mechanisms of WNT/ β -catenin Activation and Prognostic Indicators

Analysis of CCLE data for responder and non-responder AML cell lines. **A**) Principal component analysis and scree plot based upon the entire transcriptomic profile. **B**) Volcano plot of responder contrasted with non-responder. Upregulated genes are coloured red, repressed genes are coloured blue. Horizontal dash represents significant p-value cut-off, vertical dash represents ± 1.5 -fold change. Targets of interest are annotated. **C**) Violin plots demonstrating expression levels between non-responder (NR) and responder (R) AML cell lines.

S3. Public Pooled CRISPR Data Suggests No Requirement for β -catenin or γ -catenin

The DEPMAP database of pooled single-cell CRISPR-Seq data in cancer cell lines from the Achilles, Sanger and GeCKO projects were examined to determine the predicted necessity of β -catenin and γ -catenin for AML maintenance (Dempster *et al.*, 2019). CRISPR-Seq was recently developed and has enabled mass screening of gene dependency. The dataset was generated by CRISPR-Cas9 knockout of numerous genes in parallel by applying a pool of gRNA, which are DNA barcoded. Cells were sequenced after several days with scRNA-seq enabling the detection of gRNA barcodes. Absent barcodes indicate that the gRNA targets a gene essential for cancer survival. If mechanisms of redundancy or compensation exist, deconvolution is capable of revealing gRNA partners which are only essential in concert. However, as the pooled population will not suffer complete knockout, the readout is not binary and instead presents as a spectrum.

As CRISPR-Seq represents a marrying of scRNA-seq and CRISPR-Cas9 genetic manipulation, it was unsurprising that the technique was simultaneously published by distinct groups. However, conceptually, distinctions present between the methods: some are feasible *in vivo*, others directly read gRNA levels and do not require DNA barcoding, whilst some are capable of massively parallel perturbation. The flexibility of each approach has enabled adaption to specific research questions (Adamson *et al.*, 2016; Dixit *et al.*, 2016; Jaitin *et al.*, 2016; Datlinger *et al.*, 2017).

If either catenin member was absolutely required for AML maintenance, this method would allow this detection; however, it is incapable of providing information on reduced drug resistance, proliferative, or clonogenicity characteristics, which is furthered by the constraint that limited cells with a functional gene may rescue other cells by extrinsic factors. To address this, CRC, which is well recognised for being a WNT/ β -catenin signalling driven cancer, was used as a reference (Morin *et al.*, 1997; Emons *et al.*, 2017). As expected, CRC demonstrated dependency upon β -catenin, with a small proportion of the cell lines also showing dependency for γ -catenin (**Figure S-6-6**). Within AML, no cell line demonstrated any dependency characteristics for β -catenin, with limited dependency in three AML cell lines for γ -catenin (KO52, HEL, CMK115). These data are indicative of β -catenin and γ -catenin being unnecessary for AML maintenance, which is supported by independent CRISPR-seq screens (Wang *et al.*, 2014; Tzelepis *et al.*, 2016; Meyers *et al.*, 2017; T. Wang *et al.*, 2017; Behan *et al.*, 2019; Chen *et al.*, 2019; Nechiporuk *et al.*, 2019; Sharon *et al.*, 2019; X. Wu *et al.*, 2020).

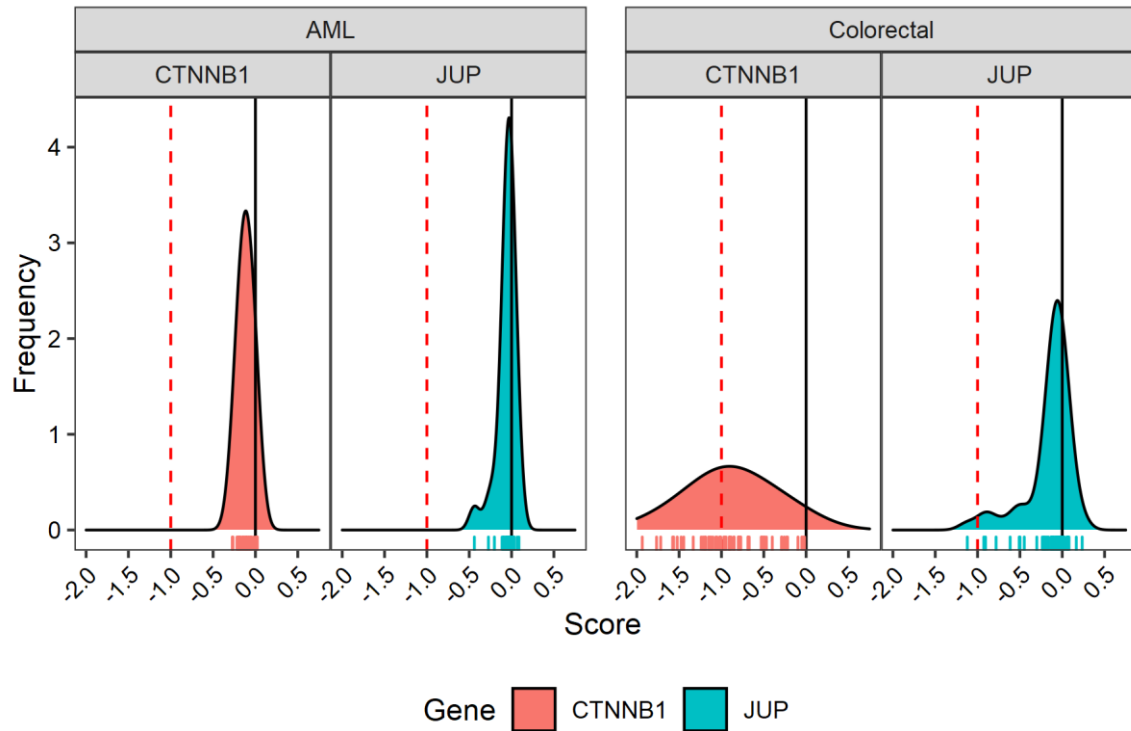


Figure S-6-6: β -catenin and γ -catenin Are Not Essential in AML.

Public CRISPR-Seq dependency data for AML and CRC cell lines from the DEPMAP database (2.13.4). Black vertical line at zero score represents a gene which is not essential, whilst a score of -1, indicated by a dashed red line, is comparable to the median of all pan-essential genes. A lower score means that a gene is more likely to be dependent in a given cell line. Individual cell lines are shown as marginal rug lines, from which the density histogram was generated. *CTNNB1* (β -catenin) is represented by red fill, whilst *JUP* (γ -catenin) is represented by blue fill.

S4. Master Regulator Analysis Identifies Factors of Interest

Whilst several interesting TF were found differentially expressed, this alone was incapable of revealing whether the associated interaction partners were affected. To determine whether dysregulated TF and co-TF were influencing downstream targets, MRA was performed, in the context of WNT-activation by rWNT3a treatment (5.3.2), in knockout (5.3.2), in the *LEF1*^{HIGH}, and in the five-year deceased group.

rWNT3a treated THP1 samples demonstrated a profile of positive TF and co-TF activity enrichment, including numerous factors centrally involved in AML (*NPM1*, *MAPK*, *KRAS*); however, due to low sample size, no statistical significance was achieved (**Figure S-6-7A**). Curiously, whilst *LEF1* was positively enriched, *TCF7L2* (encoding TCF4) was repressed; however, *TCF4* (encoding a WNT/ β -catenin unrelated TCF4) was positively enriched. *CEBPB* (TCF5) was negatively enriched and was also found repressed transcriptionally. In the knockout contrast, statistical significance was achieved and a profile of both activation and repression was noted, including negative enrichment of *CTNNB1* and *JUP*, as anticipated due to knockout (**Figure S-6-7B**). Notably, *ETV4*, *GLIS3*, *POU4F1*, *RBI*, and *RAPGEF4* (encoding EPAC2) were negatively enriched by knockout, whilst *HIVEP1*, *VDR*, and *BCL3* were positively enriched.

When repeating MRA in the context of patient samples, identification of comparable targets and thus, similar profiles, was of interest. In the comparison between *LEF1*^{HIGH} and *LEF1*^{LOW}, which was previously proposed as an approximation of WNT-active vs WNT-inactive contrast, *CTNNB1* was once again found negatively enriched further supporting the repression of β -catenin:TCF/LEF complex transcription effects. However, the remaining profile was largely positive as was the case with the rWNT3a treated samples. *LEF1*, *TCF7* (encoding TCF1), *GATA3*, *RUNX3*, *FZD6*, *WNT5a*, *JUP*, and *RAPGEF4* were notable factors which were enriched positively in *LEF1*^{HIGH} patients (**Figure S-6-8A**). When the contrast between five-year deceased and five-year survived was performed, *TCF4* was once again identified as positively enriched, alongside WNT/ β -catenin-repressor *RUNX3*, suggesting an element of excessive WNT/ β -catenin signalling control remains present (**Figure S-6-8B**). Further, *RAPGEF3* (encoding EPAC1) was identified as positively enriched. Together, these findings demonstrate the complex interplay between β -catenin, γ -catenin, LEF1, and the WNT/ β -catenin signalling pathway.

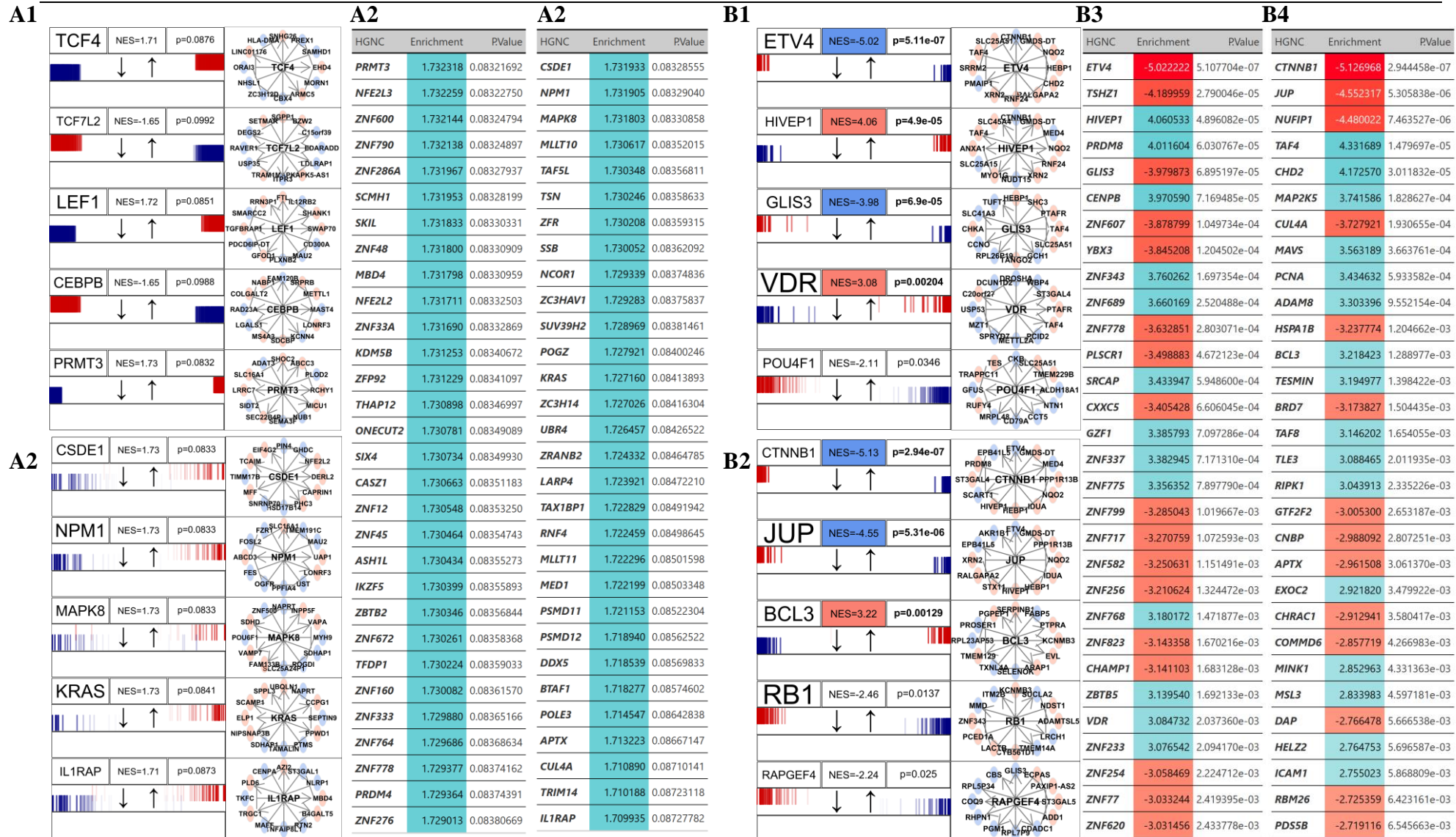


Figure S-6-7: Identified Master Regulator Transcription Factors Perturbed Within Generated Dataset

Transcription factors were identified with Corto. For the THP1 scrambled contrast with rWNT3a or vehicle treatment, transcription factor enrichment plots are shown (A1) alongside the associated top 30 (A3); enrichment plots are also shown for co-transcription factors (A2) and the top 30 tabled (A4). For the knockout versus scrambled contrast, transcription factor enrichment plots are shown (B1) and the associated top 30 (B3); enrichment plots are also shown for co-transcription factors (B2) and the top 30 tabled (B4). Enrichment values are coloured green blue for positive and red for negative.

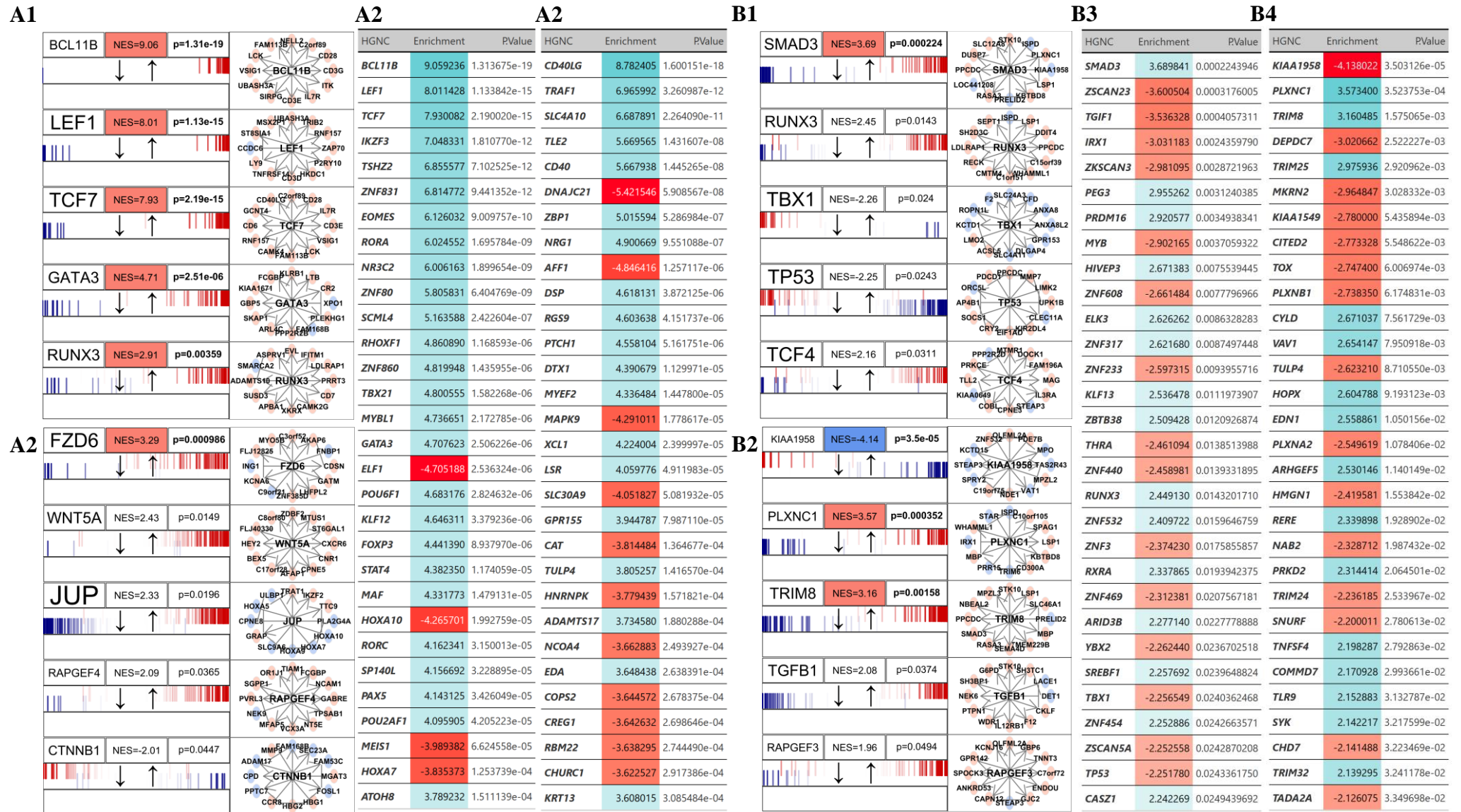


Figure S-6-8: Identified Master Regulator Transcription Factors Perturbed with *LEF1*^{HIGH} vs *LEF1*^{LOW} and five-year survival

Transcription factors were identified with Corto. For the *LEF1*^{HIGH} vs *LEF1*^{LOW} contrast, transcription factor enrichment plots are shown (A1) alongside the associated top 30 (A3); enrichment plots are also shown for co-transcription factors (A2) and the top 30 tabled (A4). For the five-year deceased vs survived contrast, transcription factor enrichment plots are shown (B1) and the associated top 30 (B3); enrichment plots are also shown for co-transcription factors (B2) and the top 30 tabled (B4). Enrichment values are coloured green blue for positive and red for negative.

S5. Examining the rWNT3a-induced WNT-active Transcriptomic Profile

Comparative integration of the two comparisons (WNT-active, WNT-knockout) enabled insights into gene and pathway expression shifts. The DET identified as upregulated with rWNT3a *MS4A3*, *SLC7A11*, *AKR1C1*, *IL1RAP*, and *TRGC1* were lost with knockout, whilst *ITGAL*, *BCL3*, and *RAB37* were upregulated with knockout and repressed with rWNT3a treatment.

It was only possible to examine the WNT-active profile of THP1 cells with rWNT3a treatment *versus* vehicle as HEL did not respond to rWNT3a. Whilst RAP1 signalling has been revealed to be a central mediator of stemness *in vitro* in *responder* AML lines, other genes regulated by WNT/ β -catenin, RAP1, or incompletely defined signalling pathways could contribute to stemness, cell cycle progression, proliferation, and other mechanisms beneficial to AML.

Notable genes identified as significantly upregulated included *TNFAIP8*, an anti-apoptotic regulator with a poor prognostic indication through chemoresistance derived from ERK signalling activation (Pang *et al.*, 2020). *MMP7*, a matrix metalloproteinase involved in breakdown of extracellular matrix (Yokoyama *et al.*, 2008) and well characterised as a poor indicator of survival in AML and other cancers was also identified (J. Wu *et al.*, 2018; Y. Wu *et al.*, 2019; R. Zhu *et al.*, 2020); further, *MMP7* is known to be regulated by WNT/ β -catenin signalling activity and is a biomarker for WNT/ β -catenin activity in several diseases (He *et al.*, 2012; Dey *et al.*, 2013). *ZBTB16* is a transcriptional repressor involved in cell cycle progression, HSC homeostasis, and apoptotic protection (Wasim *et al.*, 2010; Vincent-Fabert *et al.*, 2016) with evidence demonstrating WNT/ β -catenin modulates its levels (Marofi *et al.*, 2019). *ITGA9* is an integrin transmembrane protein which functions as a cell surface receptor and activates numerous processes, including ERK signalling and is a potential WNT/ β -catenin/ERK target in CRC (Xu *et al.*, 2021). *ITGA9* is known to be upregulated in LSC (Wesely *et al.*, 2020), enhances drug resistance (Yamakawa *et al.*, 2012), and has known interplay with WNT/ β -catenin (Z. Wang *et al.*, 2019). *MNDA*, myeloid nuclear differentiation antigen, has been shown to protect against programmed cell death and inflammation and is established for AML disease progression (Briggs *et al.*, 2006; van Galen *et al.*, 2019). *GPR160* is a member of the G protein-coupled receptor family and is a cell surface receptor that detects extracellular molecules and activates cellular responses by acting as guanine nucleotide exchange factors; overexpression of GPR160 provides an anti-apoptotic and proliferative benefit, with suppression linked to decreased survival in CRC and alteration of WNT/ β -catenin

suggesting co-involvement (Zhou *et al.*, 2016; W. Guo *et al.*, 2021). *ILIRAP* encodes Interleukin-1 receptor accessory protein and is classically recognised for inducing proinflammatory protein expression during stress, with recent researching expanding to incorporate oncogenic roles through multiple pathway potentiation (Mitchell *et al.*, 2018). *ILIRAP* is frequently overexpressed in AML, particularly in LSC, in which it proves a poor prognostic indicator, marker of self-renewal, and a potential therapeutic target (Barreyro *et al.*, 2012; Askmyr *et al.*, 2013b; de Boer *et al.*, 2020).

Secondly, numerous upregulated genes were identified which regulate energy metabolism, a feature often perturbed in AML which has recently received greater recognition as a target of interest (de Beauchamp *et al.*, 2021; Jones *et al.*, 2021; Kumar, 2021; Panina *et al.*, 2021; Mesbahi *et al.*, 2022). These include *PPARG*, which is involved in glucose metabolism, oxidative stress, and anti-inflammatory effects (Peluso *et al.*, 2012; Ahmadian *et al.*, 2013; Gruszka *et al.*, 2019), alongside known interplay with WNT/ β -catenin signalling (Lecarpentier *et al.*, 2017). *SLC35F1*, a glucose transporter, has been found upregulated in WNT-activated conditions (Goodchild *et al.*, 2019) and reduced levels in a CRISPR-Cas9 screen have sensitised AML cells to Venetoclax (Chen *et al.*, 2019). *SLC7A11* is a glutamate antiporter which regulates glutamine metabolism and glucose dependency, alongside roles in oxidative stress and ferroptotic death protection (Koppula *et al.*, 2018); further, *SLC7A11* is a known poor prognostic indicator in AML (Lin *et al.*, 2020). Whilst no link with WNT/ β -catenin signalling has been established in the literature, these findings and the discovery that close family members are established WNT targets in CRC (Sikder *et al.*, 2020) suggests WNT-derived regulation. *HSD11B1* is an enzyme which catalyses conversion of the stress hormone cortisol to an inactive metabolite and has roles in glucose metabolism; *ex vivo* culture of primary AML on mesenchymal stem cells (MSC) has demonstrated upregulation of *HSD11B1* perhaps due to MSC derived WNT promotion (Chowdhury *et al.*, 2020). *UGT3A2* is a glucuronosyltransferase which increases water solubility and enhances excretion to eliminate toxic accumulation of endogenous compounds and has recently been established for roles in drug resistance in AML (Zahreddine *et al.*, 2014). *AKR1C1* is a hydroxysteroid dehydrogenase which catalyses the reduction of progesterone and was found to promote AML survival and drug resistance alongside roles in IL-6, MCP, and G-CSF cytokine secretion and ERK activation (Matsunaga *et al.*, 2014; Jiang *et al.*, 2020). *B4GALT5* is a galactosyltransferase with roles in glucose metabolism, however, in addition to these roles, *B4GALT5* has been shown to generate drug resistance in HL-60 cells by promoting known multi-drug resistance genes PGP and MRP1 (Zhou *et al.*, 2013); further, in breast cancer, *B4GALT5* was found to promote

WNT/ β -catenin signalling and regulate breast cancer stemness (Tang *et al.*, 2020). *LPL*, a known WNT-related gene (Luo *et al.*, 2008), is a member of the lipase gene family and is involved in lipoprotein metabolism and is also recognised as an early differentiation marker; whilst little research exists in AML, *LPL* is a poor prognostic indicator in CML as *LPL* provides malignant cells with fatty acids as an energy source at the cost of reactive oxygen species production (Rozovski *et al.*, 2016).

Ca^{2+} signalling is potentially central to HSC maintenance and LSC self-renewal (Lewuillon *et al.*, 2022). Numerous upregulated genes relate to Ca^{2+} , such as *TRGC1*, which has established roles in Ca^{2+} mobilisation and ERK activation (Ribeiro *et al.*, 2015); further, *TRGC1* is established to be highly upregulated in LSC and conveys a poor prognostic outcome (Depreter, De Moerloose, *et al.*, 2020), with research demonstrating chemoresistance roles in a CRISPR-Cas9 screen and successes in therapeutic targeting (Chen *et al.*, 2019; Depreter, Weening, *et al.*, 2020). Further, *SI00A8* and *SI00A9* together form the Ca^{2+} binding complex Calprotectin (Lehmann *et al.*, 2015) which are known WNT/ β -catenin-modulated genes (Duan *et al.*, 2013) together incurring a poor prognosis (Hu *et al.*, 2013) by chemoresistance to Venetoclax (Karjalainen *et al.*, 2017). *CD300A*, a glycoprotein, is activated by inflammatory and high reactive oxygen species conditions to inhibit G-protein-coupled receptor (GPCR) signalling and Ca^{2+} influx when activated which in turn would inhibit RAS1 signalling (Alvarez *et al.*, 2008; Y *et al.*, 2008; Munitz, 2010). Further, *ADM2*, encoding a calcitonin family member, regulates fluid composition to reduce Ca^{2+} levels (Naot *et al.*, 2019). *PLCB2* is a phospholipase enzyme which utilises Ca^{2+} as a cofactor to transduce extracellular signals and modulate intracellular Ca^{2+} levels; downregulation is a poor prognostic indicator in AML (Park *et al.*, 2021). Further, *HRC* is a Ca^{2+} and lipoprotein binding protein responsible for Ca^{2+} homeostasis (Arvanitis *et al.*, 2011) *MYOF* has been demonstrated to be involved in Ca^{2+} -mediated membrane processes which could relate to the inability to divide properly (Harsini *et al.*, 2018; R. Zhu *et al.*, 2020).

Notable genes identified as significantly downregulated in response to rWNT3a treatment included *JUP*, which was not expected, as this study previously established that application of CHIR did not affect γ -catenin levels. Whilst reductions in γ -catenin also reduced β -catenin, enabling speculation that γ -catenin and β -catenin share a destruction process, the finding that WNT/ β -catenin signalling activity significantly reduces *JUP* levels suggests a direct mechanism of repression. As γ -catenin has been speculated to bind TCF/LEF in a suppressive

role, this suggests that inhibition of *JUP* expression may help to sustain β -catenin:TCF/LEF promotion.

As with the upregulated genes, notable repressed genes which relate to survival include *GAS7* which was recently identified for roles in cell cycle suppression (F. Wu *et al.*, 2020). *FGFR3* was repressed with loss linked to reprogramming of non-LSC into LSC-like cells with promoted self-renewal and has established interaction with WNT/ β -catenin signalling (Buchtova *et al.*, 2015; C. Guo *et al.*, 2021). The expression of *CSPG4* is controlled by inflammatory cytokines or hypoxic conditions, and is expressed in AML, but not HSPC, suggesting it promotes survival of AML (Hilden *et al.*, 1997; Wuchter *et al.*, 2000; Drake *et al.*, 2009; Fenton *et al.*, 2011, 2015; Ilieva *et al.*, 2018). *NFE2* was repressed, and is speculated to interact with WNT/ β -catenin signalling (D. Zhang *et al.*, 2020); furthermore, *NFE2* is frequently mutated in AML (Jutzi *et al.*, 2019) and impacts overall survival (Marcault *et al.*, 2020). *CDKN1A* (p21), a target of p53 linking DNA damage to cell cycle arrest (Gartel *et al.*, 2005) and a known β -catenin target gene (Xu *et al.*, 2016), was repressed suggesting evasion of DNA damage repair. *JDP2* is a positive prognostic indicator in AML as it regulates cell cycle arrest, apoptosis, and regulates reactive oxygen species levels; therefore, reduced levels of *JDP2* enables progression of AML (Boasman *et al.*, 2018, 2019). *CEBPB* (alias, *TCF5*) is a critical gene for normal macrophage function and is integral to differentiation in a murine model (Ruffell *et al.*, 2009); repression by WNT/ β -catenin signalling could enable a differentiation block. Furthermore, *DLL1*, a Notch delta ligand homolog, is recognised to mediate cell fate decisions in haematopoiesis and upregulation is associated with AML growth inhibition and apoptosis (Van De Walle *et al.*, 2011; Kannan *et al.*, 2013). *DACT3* was repressed, which is an established inhibitor of WNT/ β -catenin signalling in colon cancer (Jiang *et al.*, 2008). The related member *BNIP3* (BCL2) has pro-apoptotic roles and reduced levels are a poor prognostic indicator in AML (Lazarini *et al.*, 2012). Similarly, *RAB37* is a known GTPase and has established roles for repressing WNT activity and stemness in lung cancer patients (Cho *et al.*, 2018); *RAB37* has not been investigated in AML, but recent transcriptomic research has identified *RAB37* as a potential drug target (J. Wu *et al.*, 2020). Taken together, repression of these genes would maintain stemness.

Further, numerous genes with roles in energy metabolism were repressed, including *PDLIM1* which is a known β -catenin interacting target (L. M. Li *et al.*, 2020) that stimulates glycogenesis and regulates lipid metabolism (Y. Zhang *et al.*, 2017). *PFKFB4* was repressed and is another key enzyme in glycolysis which regulates the balance between energy needs and

free radical accumulation (Ros *et al.*, 2012), though contrastingly *PFKFB4* has recently been established as essential for AML cell survival (Wang *et al.*, 2020). The top genes induced by reactive oxygen species in AML, *ALDOC*, *SUNCNR1*, and *SLC6A8*, were repressed, suggesting levels are controlled; *SLC6A8* is involved in import of metabolic energy (Hopkins *et al.*, 2014; Chigaev, 2015), *SUNCNR1* protects cells from starvation-induced death (El-Masry *et al.*, 2020), and *ALDOC* is a key enzyme in glycolysis and ATP biosynthesis (Arakaki *et al.*, 2009), and is known to interact with WNT/ β -catenin signalling (Caspi *et al.*, 2014).

Additional indications of perturbed Ca^{2+} flux and speculative RAP1 activation are found in the repressed genes, such as *ITGAL* (CD11a) which, along with CD18, associate to form lymphocyte function-associated antigen-1 (LFA-1) (Bécharde *et al.*, 2001). LFA-1 is involved in migration, cell killing, and differentiation and is modulated by RAP1 signalling (Côte *et al.*, 2015; Ferreira *et al.*, 2017; Verma *et al.*, 2017). *RAP1GAP2*, a RAP GTPase which inactivates RAP1, was repressed (Steele *et al.*, 2012). *CD300A*, a glycoprotein, is activated by inflammatory and high reactive oxygen species conditions to inhibit GPCR signalling and Ca^{2+} influx when activated which in turn would inhibit RAP1 signalling (Alvarez *et al.*, 2008; Y *et al.*, 2008; Munitz, 2010). Further, *ADM2*, encoding a calcitonin family member, regulates fluid composition to reduce Ca^{2+} levels (Naot *et al.*, 2019). *PLCB2* is a phospholipase enzyme which utilises Ca^{2+} as a cofactor to transduce extracellular signals and modulate intracellular Ca^{2+} levels; downregulation is a poor prognostic indicator in AML (Park *et al.*, 2021). Further, *HRC* is a Ca^{2+} and lipoprotein binding protein responsible for Ca^{2+} homeostasis (Arvanitis *et al.*, 2011) *MYOF* has been demonstrated to be involved in Ca^{2+} -mediated membrane processes which could relate to the inability to divide properly (Harsini *et al.*, 2018; R. Zhu *et al.*, 2020).

S6. Examining the Effect of Dual Knockout Transcriptomic Profile

Genes found repressed in both cell lines upon dual gene knockout may prove to be required for clonal growth, survival, and evasion of apoptosis, and are possibly more relevant in this context than those found upregulated as loss of an effect could relate to loss of clonogenicity. Repressed genes included notable stemness markers, including the LSC stemness markers *CD7* (Haubner *et al.*, 2019), *CD109* (Emori *et al.*, 2013; S. Zhou *et al.*, 2017; Handschuh *et al.*, 2019), *IGFBP7* (Verhagen *et al.*, 2018), *IL1RAP* (Barreyro *et al.*, 2012; Askmyr *et al.*, 2013b; Mitchell *et al.*, 2018), the HSC markers *ALDH1L2* (Kastan *et al.*, 1990; Nakahata *et al.*, 2015; Tomita *et al.*, 2016), *CAMK4* (Kitsos *et al.*, 2005), the embryonic stem cell markers *ZIC2* (Luo *et al.*, 2015), *INHBE* (Spitzhorn *et al.*, 2019), and *ESRP1* (Fagoonee *et al.*, 2013), and the MSC markers *MCAM* (Covas *et al.*, 2008; Russell *et al.*, 2010) and *CD79a* (Chosa *et al.*, 2018). Further, these included *CCR7*, a chemokine receptor stemness marker in breast cancer (Boyle

et al., 2017; Yang *et al.*, 2020); *AKR1C1* (Chang *et al.*, 2019) an aldo-keto reductase stemness marker identified in head and neck squamous cell carcinoma (Pedemonte *et al.*, 2007; Hao *et al.*, 2018); as well as *CBS*, a stem related *LEF1* target gene (Park *et al.*, 2019).

Numerous genes involved in, or related to, Ca^{2+} influx were repressed and relate to RAP1 signalling. *AQP1* (Aquaporin 1), a water channel protein, is regulated by *RUNX1T1* via Ca^{2+} influx (Maltaneri *et al.*, 2020), with recent research finding direct interaction between AQP1 and β -catenin via competitive binding at the armadillo region usually bound by GSK3 β (Chong *et al.*, 2021), enabling AQP1-derived β -catenin accumulation. AQP1 promotes cell survival and is a stemness marker (Gao *et al.*, 2013; M. Chen *et al.*, 2020). *CAMK4* is a member of the Ca^{2+} /Calmodulin-dependent protein kinase family and is regulated by high intracellular Ca^{2+} levels and Calmodulin; *CAMK4* ablation in HSC results in haematopoietic failure and is required for AML leukaemogenesis (Kitsos *et al.*, 2005; Chan *et al.*, 2007; Si *et al.*, 2008; Ma *et al.*, 2011; Deng *et al.*, 2014; Monaco *et al.*, 2015). *CAMK4* promotes *CREB* family members, of which *CREB3L1* was also repressed (Kang *et al.*, 2018). *HRH2*, a histamine receptor, was found to be repressed and is a potent activator of cAMP, which classically regulates glycogen, sugar, and lipid metabolism via PKA, alongside activation of Ca^{2+} channels; furthermore, cAMP activates EPAC1 (*RAPGEF3*) and EPAC2 (*RAPGEF4*) which in turn activate RAP1 signalling and ERK (ES *et al.*, 2016; Martynov *et al.*, 2020). *RAPGEF4*, in turn, was significantly repressed with dual knockout of β -catenin and γ -catenin. EPAC2–RAP1 signalling is proposed to promote endoplasmic reticulum Ca^{2+} store release to increase intracellular Ca^{2+} levels (Dzhura *et al.*, 2011; Parnell *et al.*, 2015). Similarly, *RASGRP3*, a dual RAS and RAP pathway GEF, is positively controlled directly by intracellular Ca^{2+} levels and indirectly by diacylglycerol (DAG, signalling lipid) through PKC; *RASGRP3* has roles in inhibition of proinflammatory cytokine production in macrophages (Teixeira *et al.*, 2003; Stone, 2011; Tang *et al.*, 2014). *THBS1* is a glycoprotein which mediates cell-cell and cell-matrix interactions (L. Zhu *et al.*, 2020). Research indicates *THBS1* can enhance cell survival, therapy resistance and has known roles in leukaemogenesis (Isenberg *et al.*, 2008; Liu *et al.*, 2017; S. Chen *et al.*, 2020), however, it has also been demonstrated to reduce HSC repopulation when expressed (Liu *et al.*, 2017), explaining the positive impact upon patient survival. *THBS1* is also a WNT/ β -catenin signalling target gene suggesting complex modulation of *THBS1* in LSC (Jackson *et al.*, 2005; Pedemonte *et al.*, 2007).

Repression of genes relating to proliferation, anti-apoptotic effects, and cell cycling was observed in the dual knockout condition as compared to the scrambled control, which could

covey consequence to clonogenicity. These included the matrix metalloproteinases *MMP2* and *MMP17*, which have described roles in growth, proliferation, and apoptosis and convey prognostic value in AML (Chaudhary *et al.*, 2016; Si *et al.*, 2018; Pietrzak *et al.*, 2021). *CCND2* is mutated in AML (Eisfeld *et al.*, 2017), particularly frequently in *RUNX1::RUNX1T1* (Martinez-Soria *et al.*, 2018), and is a known contributor to leukaemogenesis, stemness, and proliferation of AML in addition to roles in glycolysis (Malumbres *et al.*, 2001; Deshpande *et al.*, 2005). Tumour necrosis factor receptor associated factor 1 (*TRAF1*) is a pro-survival signalling receptor which mediates the anti-apoptotic signals from TNF receptors (Edilova *et al.*, 2018). Toll-like receptor 4 (*TLR4*) is noted for activation of the MAPK and NF- κ B pathways, providing proliferation, anti-apoptotic, and stemness traits to AML cells; indeed, *TLR4* has prognostic consequence in AML (Rybka *et al.*, 2015; Ramzi *et al.*, 2018). *TP73*, encoding p73, induces apoptosis similarly to p53 through downstream target genes and is found mutated in AML frequently (Nishida *et al.*, 2019; Mims *et al.*, 2021); however, research on p73 is limited in the context of AML whilst in other diseases, p73 has been demonstrated to promote proliferation by regulating glucose metabolism, antioxidant capacity, and Ca²⁺-dependent apoptosis which could all prove relevant in AML (Al-Bahlani *et al.*, 2011; Fets *et al.*, 2013). *AIF1L* is a poorly researched gene, but roles in inflammation and survival are speculated, alongside findings of upregulation in primitive AML (Pei *et al.*, 2020); further, *AIF1L* contains a Ca²⁺ binding element, suggesting regulatory crosstalk with Ca²⁺ levels (Zhao *et al.*, 2017). *TPD52* and *TPD52L1* both represent poor prognostic markers in AML and were recently associated with maintenance of stemness, enabling AML to avoid control mechanisms (Ha *et al.*, 2019; Kang *et al.*, 2021). Similarly, *POU4F1* is regularly overexpressed in AML, particularly in *RUNX1::RUNX1T1*, but it has been established to be correlated with, rather than induced by, *RUNX1::RUNX1T1* and induced a similar expression profile, suggesting it is a cooperating factor and is able to produce similar stemness and survival traits (Hudson *et al.*, 2008; Fortier *et al.*, 2010; Dunne *et al.*, 2012).

Opposingly, genes found upregulated by knockout included several mechanisms by which stemness and survival is maintained despite loss of other elements, suggesting a differentiation pressure in the absence of WNT/ β -catenin signalling was being suppressed. These include leukaemia inhibitory factor (*LIF*), named for its ability to maintain stemness by inhibiting terminal differentiation and enabling the constitutive growth of myeloid leukaemic cells (Gearing *et al.*, 1987). *LIF* is a member of the pro-inflammatory IL-6 family, with established roles in maintaining LSC self-renewal (Takanashi *et al.*, 1993). A balance between apoptosis and survival was suggested to be in effect, as apoptosis-inducing factor 2 (*AIFM2*) which is

induced by p53 in colon cancer (Gong *et al.*, 2007; Navarrete-Meneses *et al.*, 2017; J. Li *et al.*, 2020), and anti-apoptotic genes such as *TERT* which enhances immortalisation (Nofrini *et al.*, 2021) were upregulated; the careful balance between pro- and anti-apoptotic regulation perhaps enables survival of knockout cells in the bulk condition. Further pro-apoptotic genes were found, including *VIM* and *AHNAK* (I. H. Lee *et al.*, 2014; Petti *et al.*, 2019). Critically, annexin family members are Ca^{2+} dependent inhibitors of inflammation and are induced by inflammatory stress, however, annexin members can also negatively regulate apoptosis; *ANXA1*, *ANXA2*, *ANXA5*, and *ANXA6* were upregulated in knockout and would provide anti-apoptotic effects, and are all negative prognostic indicators in AML (Niu *et al.*, 2019).

Stem cell growth factor receptor, encoded by *KIT*, was upregulated with knockout, and high *KIT* expression is a known indicator of LSC and conveys a poor prognosis in AML through enhancement of stemness and self-renewal capacity (Somerville *et al.*, 2006b; Knorr *et al.*, 2020; Velten *et al.*, 2021); however, activation requires binding of SCF, encoded by *KITLG*, which was found significantly repressed with knockout (Hassan *et al.*, 1996; Sands *et al.*, 2013; Thomas *et al.*, 2017). *ERG* is a known regulator of HSC and indicator of LSC and is a well-established poor prognostic indicator in AML. Upregulation of these genes with knockout suggests alternate pathways are activated to maintain AML without WNT/ β -catenin signalling activity, though these are incapable of compensating in regard to clonogenicity (Marcucci *et al.*, 2007; Eppert *et al.*, 2011; Hasan *et al.*, 2017; Yassin *et al.*, 2019). Similarly, genes relating to cell death signalling or evasion of death would provide an indication as to the mechanism by which dual knockout cells are maintained in bulk culture. C3, a central mediator in the complement system with known roles in regulation of inflammation and clearance of damaged cells, was upregulated. CD11b, complement receptor 3, was also upregulated and is a known binding partner to activate C3 (Lamers *et al.*, 2021). However, as the co-receptor CD18 was repressed, this activation is insufficient to induce death. *PIM1*, an established proto-oncogene, was upregulated with knockout and is involved in negative regulation of apoptosis and promotion of the cell cycle by which it conveys a poor prognosis in AML (Fathi *et al.*, 2012; Yu Wu *et al.*, 2015; Cheng *et al.*, 2017).

Alterations to Ca^{2+} -related genes were also found amongst the upregulated genes with knockout. Ca^{2+} homeostasis in the context of the body is controlled by three central hormones: parathyroid hormone (PTH), calcitonin, and calcitriol. In response to low intracellular calcium levels, PTH and Calcitriol serve to increase Ca^{2+} levels, whilst Calcitonin reduces Ca^{2+} influx to reduce calcium levels (Goltzman *et al.*, 2018). As metabolites, these are not captured by

RNA-seq technology, however, closely regulates genes would provide indication as to the regulation of these metabolites. *PTH2R*, a parathyroid hormone receptor, was upregulated, alongside the fact that calcitriol, the active metabolite form of vitamin D, is controlled by the PI3K family, of which *PIK3CD* was upregulated; together, these induce myeloid differentiation and expression of *ITGAM* and *VDR* which were both found upregulated, with the latter found as a positively enriched TF (Kurbel *et al.*, 2003; Moeenrezakhanlou *et al.*, 2008). Critically, *ITGAM* increases intracellular Ca^{2+} levels in immature THP1, but this effect is downmodulated with maturation of THP1 (Altieri *et al.*, 1992); secondly, *VDR* expression has been linked to loss of stemness and induced differentiation in AML (Paubelle *et al.*, 2020).

When studying the cell lines independently, several genes which are well established in the literature were identified and were found to either be opposingly expressed between cell lines, or not expressed in one of the two. These included *RUNX1*, *RUNX3*, and *RUNXIT1*, which were downregulated in HEL upon dual β -catenin and γ -catenin knockout, as compared to control scrambled cells, but not in THP1; alternatively, *RUNX2* was upregulated in THP1 with knockout compared to cells transduced with a scrambled vector, but not in HEL. Interplay between WNT/ β -catenin signalling and the *RUNX* family transcription factors is well established, and both are phosphorylated for destruction via GSK3 β (Sweeney *et al.*, 2020). *RUNX1* is known to activate WNT/ β -catenin signalling at several components (Sweeney *et al.*, 2020), which has been suggested to thereby generate the *RUNX1::RUNXIT1* translocation, thus leading to development of t(8;21) AML (Friedman, 2009; Wu *et al.*, 2012; Naillat *et al.*, 2015; Ugarte *et al.*, 2015). *RUNX2* is both a regulator and a downstream target of WNT/ β -catenin signalling; the fact that *RUNX2* was shown to be upregulated in knockout cells indicates a potential response to β -catenin knockout (Gaur *et al.*, 2005; Kawane *et al.*, 2014; Ferrari *et al.*, 2015). *RUNX3*, on the other hand, is an inhibitor of the β -catenin/TCF4 complex, thus attenuating WNT/ β -catenin signalling (Ito *et al.*, 2008, 2011); however, in specific contexts, it is recognised to paradoxically promote this signalling pathway (Ju *et al.*, 2014). *THY1* is recognised broadly as a stemness marker in HSC, but in AML it remains contentious; here, *THY1* was repressed with knockout in HEL, but upregulated with knockout in THP1, suggesting the alterations to *THY1* expression are perhaps subtype specific in AML (Blair *et al.*, 1997; Buccisano *et al.*, 2004). Similarly, *TCF7* was upregulated by rWNT3a in THP1, and repressed significantly in knockout; however, *TCF7* was not detected in HEL suggesting discrepancy between AML disease types. *TCF7* is recognised as a regulator switch of HSC

self-renewal (Wu *et al.*, 2012), and is upregulated in AML, suggesting HEL may not represent the patient condition with regard to *TCF7*.

S7. LEF1 Patient Context

As β -catenin is regulated post-translationally rather than transcriptionally, it was not suitable to utilise *CTNNB1* to classify patients; rather, *LEF1* was used as an indicator. *LEF1* has been established for roles in nuclear translocation of β -catenin and was found significantly upregulated in *responder* AML cell lines within this study, suggesting parallel between mRNA and protein levels (**Figure S-6-9**) (Morgan *et al.*, 2019). Comparison of patients based on *LEF1*^{HIGH} and *LEF1*^{LOW} expression was able to identify WNT/ β -catenin signalling as overrepresented. However, the ORA and GSEA were able to demonstrate downstream *MYC* target genes were negatively enriched; GSVA provided a potential explanation, as *RUNX3* regulation was enriched in *LEF1*^{HIGH} patients, with *RUNX3* repressing transcriptional activity of the β -catenin:TCF4/*LEF1* complex (Ito *et al.*, 2008; Sweeney *et al.*, 2020).

S8. Integrating Datasets

Integration of comparisons between public cell line data and data generated here-in with public patient data revealed a gene profile of upregulation of genes via WNT/ β -catenin that was found lost with knockout (**Table S-1**). The only exception to this profile was *MAFF*, however *MAFF* has been established to be a negative indicator of stemness with upregulation reducing colony formation and self-renewal, whilst promoting differentiation, explaining the discrepancy (Cheng *et al.*, 2016). Of the upregulated profile, *RAPGEF4*, an activator of RAP1 signalling, *CAMK4*, a stimulator of Ca^{2+} -dependent gene expression which is speculated to interact with RAP1 signalling, and *TRPC1* which was previously mentioned in relation to roles in mediating Ca^{2+} influx were noted (Grewal *et al.*, 2000; Anderson *et al.*, 2004; Si *et al.*, 2008). Other stemness-related genes include *ALPK3* which with knockdown in AML has been demonstrated to reduce colony forming efficiency (Meyer *et al.*, 2016). Similarly, *GLIS3* has been identified for providing stemness traits in HSC and leukaemia and was both upregulated at the mRNA level and negatively enriched by TF activity in knockout (Scoville *et al.*, 2017; Jetten, 2019). *NAPIL3* is highly expressed in HSC in which it is required for HSC proliferation, maintenance, and repopulation capacity *in vitro* and *in vivo* (Heshmati *et al.*, 2018). *CCR7*, *CD79a*, and *POU4F1* were previously mentioned for roles in breast cancer, ESC, and HSC stemness respectively, whilst *TRAF1* was previously mentioned for mediating anti-apoptotic signals. *CKB* is scarcely researched, but evidence suggests LSC upregulate *CKB* to enhance stem traits (Ishikawa *et al.*, 2005).

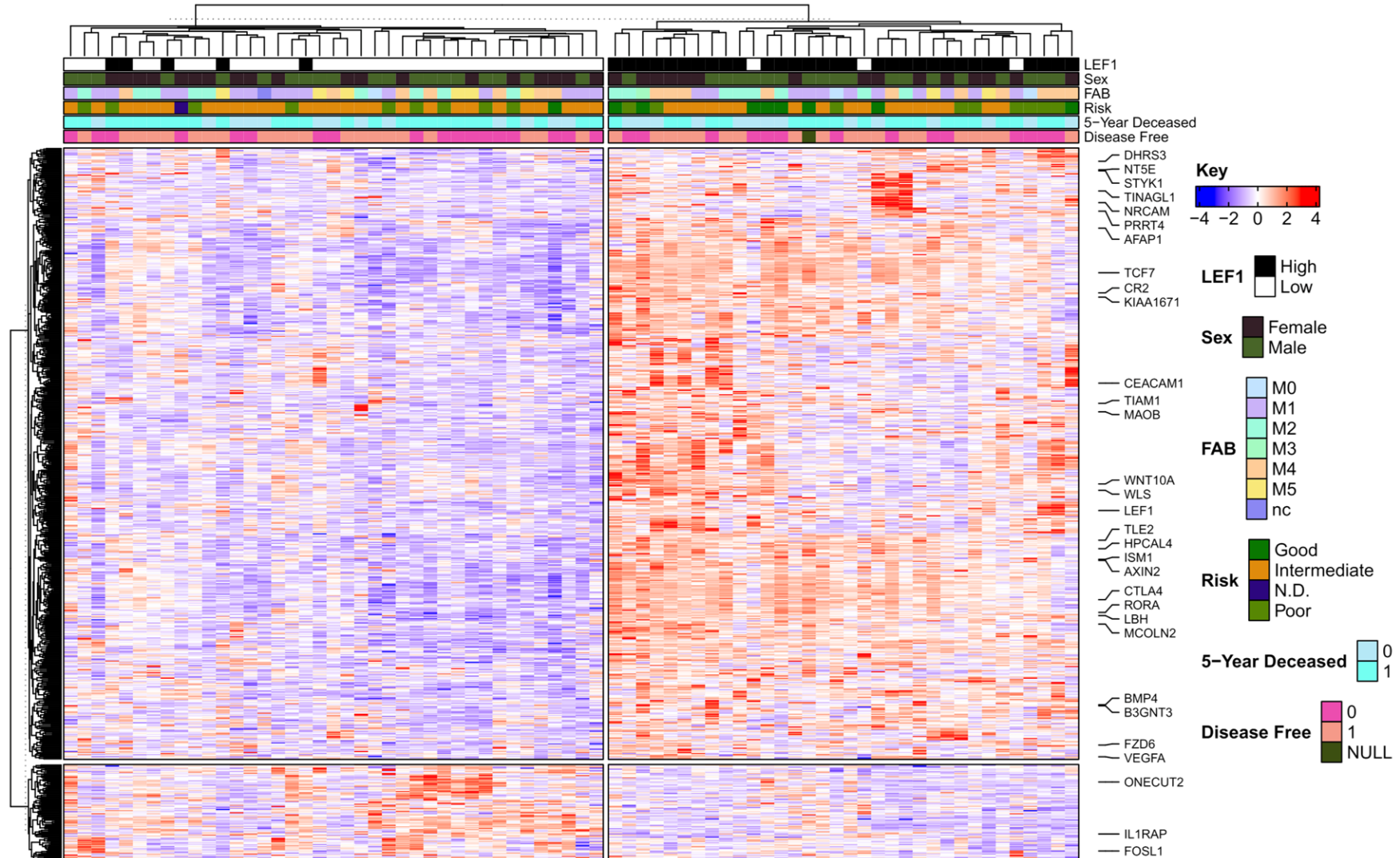


Figure S-6-9: Heatmap Demonstrating Transcript Expression Differences Between *LEF1*^{HIGH} and *LEF1*^{LOW}

Heatmap of the identified differentially expressed transcripts. Columns represent patient samples whilst rows are transcripts. Samples were z-score scaled around expression mean, with red and blue indicating high respectively. Samples segregated into two groups with k-means clustering. Annotation is provided on *LEF1* status, patient sex, FAB type, risk score, 5-year survival status (1=Deceased, 0=Living) and 5-year disease-free status (1=Event, 0=Event-free). WNT-related genes are annotated.

Table S-1: Integration of Patient and Cell Line Data Reveals Novel Insight into Directionally Changing Genes**A**

ENSG	HGNC	CCLE WNT-Active		Patient High LEF1		Description
		CCLLog2FC	CCLPAAdjusted	PatientLog2FC	PatientPAAdjusted	
ENSG00000096006	CRISP3	3.612677	0.01531101	2.392426	3.315358e-02	Cysteine rich secretory protein 3
ENSG00000164930	FZD6	4.092291	0.01688381	1.168917	2.960423e-02	Frizzled class receptor 6
ENSG00000176928	GCNT4	1.991005	0.03222325	2.157191	2.423734e-12	Glucosaminyl (n-acetyl) transferase 4
ENSG00000087495	PHACTR3	-5.351433	0.01412830	-3.094273	2.600468e-03	Phosphatase and actin regulator 3

B

ENSG	HGNC	Patient LEF1 High		THP1 WNT-Active		Description
		PatientLog2FC	PatientPAAdjusted	THPLog2FC	THPPAAdjusted	
ENSG00000224940	PRRT4	1.312523	3.111158e-02	1.0699126	3.369229e-02	Proline rich transmembrane protein 4
ENSG00000081059	TCF7	1.604628	1.064549e-15	0.9209377	9.240861e-06	Transcription factor 7

C

ENSG	HGNC	CCLE WNT-Active		THP1 WNT-Active		Description
		CCLLog2FC	CCLPAAdjusted	THPLog2FC	THPPAAdjusted	
ENSG00000125726	CD70	-5.664385	0.007103429	-0.6689278	0.0001293257	Cd70 molecule
ENSG00000181577	C6orf223	-3.699447	0.010347205	-1.1177406	0.0218725987	Chromosome 6 open reading frame 223
ENSG00000144668	ITGA9	2.410352	0.024739259	1.2912569	0.0336527404	Integrin subunit alpha 9

D

ENSG	HGNC	CCLE WNT-Active		Knockout		Description
		CCLLog2FC	CCLPAAdjusted	KOLog2FC	KOPAAdjusted	
ENSG00000078596	ITM2A	6.658153	0.010026978	-0.6145087	1.606857e-03	Integral membrane prot...
ENSG00000166165	CKB	5.045145	0.028933016	-0.7074758	2.204808e-16	Creatine kinase b
ENSG00000150637	CD226	4.464426	0.036230209	-1.0421195	4.725619e-02	Cd226 molecule
ENSG00000152952	PLOD2	3.824474	0.005122489	-0.7300188	1.700782e-04	Procollagen-lysine,2-o...

E

ENSG	HGNC	Patient LEF1 High		Knockout		Description
		PatientLog2FC	PatientPAAdjusted	KOLog2FC	KOPAAdjusted	
ENSG00000136383	ALPK3	1.0965708	1.729274e-02	-1.2608440	1.981629e-02	Alpha kinase 3
ENSG00000114529	C3orf52	0.8354843	1.323844e-02	-1.1006965	8.342793e-16	Chromosome 3 open read...
ENSG00000152495	CAMK4	2.1957223	3.963106e-16	-1.3203835	2.250679e-02	Calcium/calmodulin dep...
ENSG00000126353	CCR7	1.5717778	6.493642e-07	-2.2221080	5.273030e-08	C-c motif chemokine re...
ENSG00000105369	CD79A	1.0256080	3.766733e-03	-1.0264431	8.381845e-03	Cd79a molecule
ENSG00000021826	CPS1	1.9089993	3.436799e-02	-0.5873560	1.022506e-02	Carbamoyl-phosphate sy...
ENSG00000206052	DOK6	0.9215164	3.501021e-02	-1.6350400	1.307258e-05	Docking protein 6
ENSG00000107249	GLIS3	2.0989594	3.705192e-03	-1.1541340	5.560748e-03	Glis family zinc finge...
ENSG00000163328	GPR155	0.6856663	1.756886e-02	-0.5994596	2.188863e-02	G protein-coupled rece...
ENSG00000185022	MAFF	-1.2537067	6.710920e-04	0.5880859	1.277792e-02	Maf bzip transcription...
ENSG00000186310	NAP1L3	2.2685674	9.309879e-06	-1.3935244	2.828355e-02	Nucleosome assembly pr...
ENSG00000152192	POU4F1	6.2184471	5.136389e-16	-0.6993771	2.629011e-02	Pou class 4 homeobox 1
ENSG00000115828	QPCT	1.5270263	1.976751e-02	-0.6555211	1.474440e-02	Glutaminyl-peptide cyc...
ENSG00000091428	RAPGEF4	1.9829023	3.875282e-04	-0.9754197	1.790134e-02	Rap guanine nucleotide...
ENSG00000072195	SPEG	1.7179685	7.309862e-04	-0.7386299	2.931020e-02	Striated muscle enrich...
ENSG00000056558	TRAF1	0.7764354	1.795087e-05	-0.8977044	3.215131e-02	Tnf receptor associate...
ENSG00000144935	TRPC1	1.5800768	5.805887e-03	-0.6409744	3.991631e-03	Transient receptor pot...

Tables of genes found in concordance, or differentially expressed between comparison of determined contrasts. Genes are coloured by expression alterations in the respective contrast, with green representing overexpression and red representing repression. **A)** Intersecting genes in the contrast between WNT-active vs WNT-inactive lines, and Patient LEF1^{HIGH} and LEF1^{LOW}. **B)** Intersecting genes between the Patient LEF1^{HIGH} vs LEF1^{LOW} contrast and the THP1 scrambled rWNT3a treated and untreated samples. **C)** Intersecting genes between the CCLE WNT-Active versus WNT-inactive cell lines and the THP1 scrambled rWNT3a treated and untreated samples. **D)** Directionally opposing genes between CCLE WNT-Active versus WNT-inactive and the knockout versus scrambled contrast. **E)** Directionally opposing genes between the Patient LEF1^{HIGH} vs LEF1^{LOW} contrast and the knockout versus scrambled contrast.

References

- Abelson, S., Collord, G., Ng, S.W.K., Weissbrod, O., Mendelson Cohen, N., Niemeyer, E., *et al.* (2018) 'Prediction of acute myeloid leukaemia risk in healthy individuals', *Nature*, 559(7714), pp. 400–404. doi:10.1038/s41586-018-0317-6.
- Aberle, H., Bauer, A., Stappert, J., Kispert, A. and Kemler, R. (1997) ' β -catenin is a target for the ubiquitin–proteasome pathway', *The EMBO Journal*, 16(13), pp. 3797–3804. doi:10.1093/EMBOJ/16.13.3797.
- Abrahamsson, A.E., Geron, I., Gotlib, J., Dao, K.H.T., Barroga, C.F., Newton, I.G., *et al.* (2009) 'Glycogen synthase kinase 3 β missplicing contributes to leukemia stem cell generation', *Proceedings of the National Academy of Sciences of the United States of America*, 106(10), pp. 3925–3929. doi:10.1073/pnas.0900189106.
- Adams, G.B., Chabner, K.T., Alley, I.R., Olson, D.P., Szczepiorkowski, Z.M., Poznansky, M.C., *et al.* (2006) 'Stem cell engraftment at the endosteal niche is specified by the calcium-sensing receptor', *Nature*, 439(7076), pp. 599–603. doi:10.1038/nature04247.
- Adamson, B., Norman, T.M., Jost, M., Cho, M.Y., Nuñez, J.K., Chen, Y., *et al.* (2016) 'A Multiplexed Single-Cell CRISPR Screening Platform Enables Systematic Dissection of the Unfolded Protein Response.', *Cell*, 167(7), pp. 1867–1882.e21. doi:10.1016/j.cell.2016.11.048.
- Adati, N., Huang, M.C., Suzuki, T., Suzuki, H. and Kojima, T. (2009) 'High-resolution analysis of aberrant regions in autosomal chromosomes in human leukemia THP-1 cell line', *BMC Research Notes*, 2, p. 153. doi:10.1186/1756-0500-2-153.
- Ågerstam, H., Hansen, N., von Palffy, S., Sandén, C., Reckzeh, K., Karlsson, C., *et al.* (2016) 'IL1RAP antibodies block IL-1–induced expansion of candidate CML stem cells and mediate cell killing in xenograft models', *Blood*, 128(23), pp. 2683–2693. doi:10.1182/blood-2015-11-679985.
- Ahmadian, M., Suh, J.M., Hah, N., Liddle, C., Atkins, A.R., Downes, M., *et al.* (2013) 'Ppar γ signaling and metabolism: The good, the bad and the future', *Nature Medicine*, 19(5), pp. 557–566. doi:10.1038/nm.3159.
- Ahmed, A., Boulton, S., Shao, H., Akimoto, M., Natarajan, A., Cheng, X., *et al.* (2019) 'Recent Advances in EPAC-Targeted Therapies: A Biophysical Perspective', *Cells*. doi:10.3390/cells8111462.
- Ahmed, A., Jani, C., Bhatt, P., Singh, H., Jani, R., Shalhoub, J., *et al.* (2022) 'EPR22-104: A Comparison of the Burden of Leukemia Amongst Various Regions of the World, 1990-2019', *Journal of the National Comprehensive Cancer Network*, 20(3.5), pp. EPR22-104-EPR22-104. doi:10.6004/jnccn.2021.7211.
- Akagi, T., Ogawa, S., Dugas, M., Kawamata, N., Yamamoto, G., Nannya, Y., *et al.* (2009) 'Frequent genomic abnormalities in acute myeloid leukemia/myelodysplastic syndrome with normal karyotype', *Haematologica*, 94(2), pp. 213–223. doi:10.3324/haematol.13024.
- Aktary, Z., Kulak, S., Mackey, J., Jahroudi, N. and Pasdar, M. (2013) 'Plakoglobin interacts with the transcription factor p53 and regulates the expression of 14-3-3 σ ', *Journal of Cell Science*, 126(14), pp. 3031–3042. doi:10.1242/jcs.120642.
- Aktary, Z. and Pasdar, M. (2012) 'Plakoglobin: Role in tumorigenesis and metastasis', *International Journal of Cell Biology*, 2012, p. 14. doi:10.1155/2012/189521.
- Al-Bahlani, S., Fraser, M., Wong, A.Y.C., Sayan, B.S., Bergeron, R., Melino, G., *et al.* (2011) 'P73 regulates cisplatin-induced apoptosis in ovarian cancer cells via a calcium/calpain-dependent mechanism', *Oncogene*, 30(41), pp. 4219–4230. doi:10.1038/onc.2011.134.
- Alaee, M., Padda, A., Mehrabani, V., Churchill, L. and Pasdar, M. (2016) 'The physical interaction of

- p53 and plakoglobin is necessary for their synergistic inhibition of migration and invasion', *Oncotarget*, 7(18), pp. 26898–26915. doi:10.18632/oncotarget.8616.
- Alanazi, B., Munje, C., Rastogi, N., Williamson, A., Taylor, S., Hole, P., *et al.* (2020) 'Integrated nuclear proteomics and transcriptomics identifies S100A4 as a therapeutic target in acute myeloid leukemia', *Leukemia*, 34, pp. 1–14. doi:10.1038/s41375-019-0596-4.
- Alexandrov, L.B., Nik-Zainal, S., Wedge, D.C., Aparicio, S.A.J.R., Behjati, S., Biankin, A. V., *et al.* (2013) 'Signatures of mutational processes in human cancer', *Nature*, 500(7463), pp. 415–421. doi:10.1038/nature12477.
- Almahariq, M., Mei, F.C. and Cheng, X. (2014) 'Cyclic AMP sensor EPAC proteins and energy homeostasis', *Trends in Endocrinology and Metabolism*, 25(2), pp. 60–71. doi:10.1016/j.tem.2013.10.004.
- Almajali, B., Johan, M.F., Al-Wajeeh, A.S., Wan Taib, W.R., Ismail, I., Alhawamdeh, M., *et al.* (2022) 'Gene Expression Profiling and Protein Analysis Reveal Suppression of the C-Myc Oncogene and Inhibition JAK/STAT and PI3K/AKT/mTOR Signaling by Thymoquinone in Acute Myeloid Leukemia Cells', *Pharmaceuticals*. doi:10.3390/ph15030307.
- Altieri, D.C., Stamnes, S.J. and Gahmberg, C.G. (1992) 'Regulated Ca²⁺ signalling through leukocyte CD11b/CD18 integrin', *Biochemical Journal*, 288(2), pp. 465–473. doi:10.1042/bj2880465.
- Alvarez, Y., Tang, X., Coligan, J.E. and Borrego, F. (2008) 'The CD300a (IRp60) inhibitory receptor is rapidly up-regulated on human neutrophils in response to inflammatory stimuli and modulates CD32a (FcγRIIa) mediated signaling', *Molecular Immunology*, 45(1), pp. 253–258. doi:10.1016/j.molimm.2007.05.006.
- Aly, H., Rohatgi, N., Marshall, C.A., Grossenheider, T.C., Miyoshi, H., Stappenbeck, T.S., *et al.* (2013) 'A Novel Strategy to Increase the Proliferative Potential of Adult Human β-Cells While Maintaining Their Differentiated Phenotype', *PLoS ONE*. Edited by C. Liu, 8(6), p. e66131. doi:10.1371/journal.pone.0066131.
- Van Amerongen, R., Fuerer, C., Mizutani, M. and Nusse, R. (2012) 'Wnt5a can both activate and repress Wnt/B-catenin signaling during mouse embryonic development', *Developmental Biology*, 369(1), pp. 101–114. doi:10.1016/j.ydbio.2012.06.020.
- van Amerongen, R. and Nusse, R. (2009) 'Towards an integrated view of Wnt signaling in development', *Development*, 136(19), pp. 3205–3214. doi:10.1242/dev.033910.
- An, T., Gong, Y., Li, X., Kong, L., Ma, P., Gong, L., *et al.* (2017) 'USP7 inhibitor P5091 inhibits Wnt signaling and colorectal tumor growth', *Biochemical Pharmacology*, 131, pp. 29–39. doi:10.1016/j.bcp.2017.02.011.
- Anderson, K.A., Noeldner, P.H., Reece, K., Wadzinski, B.E. and Means, A.R. (2004) 'Regulation and function of the calcium/calmodulin-dependent protein kinase IV/protein serine/threonine phosphatase 2A signaling complex', *Journal of Biological Chemistry*, 279(30), pp. 31708–31716. doi:10.1074/jbc.M404523200.
- Anjos-Afonso, F., Buettner, F., Mian, S.A., Rhys, H., Perez-Lloret, J., Garcia-Albornoz, M., *et al.* (2022) 'Single cell analyses identify a highly regenerative and homogenous human CD34+ hematopoietic stem cell population', *Nature Communications* 2022 13:1, 13(1), pp. 1–13. doi:10.1038/s41467-022-29675-w.
- Anzalone, A. V., Randolph, P.B., Davis, J.R., Sousa, A.A., Koblan, L.W., Levy, J.M., *et al.* (2019) 'Search-and-replace genome editing without double-strand breaks or donor DNA', *Nature*, 576(7785), pp. 149–157. doi:10.1038/s41586-019-1711-4.
- Arai, F., Hirao, A., Ohmura, M., Sato, H., Matsuoka, S., Takubo, K., *et al.* (2004) 'Tie2/angiopoietin-1 signaling regulates hematopoietic stem cell quiescence in the bone marrow niche', *Cell*, 118(2), pp. 149–161. doi:10.1016/j.cell.2004.07.004.
- Arakaki, T.L., Pezza, J.A., Cronin, M.A., Hopkins, C.E., Zimmer, D.B., Tolan, D.R., *et al.* (2009) 'Structure of human brain fructose 1,6-(bis)phosphate aldolase: Linking isozyme structure with

- function', *Protein Science*, 13(12), pp. 3077–3084. doi:10.1110/ps.04915904.
- Aran, D., Hu, Z. and Butte, A.J. (2017) 'xCell: Digitally portraying the tissue cellular heterogeneity landscape', *Genome Biology*, 18(1), pp. 1–14. doi:10.1186/s13059-017-1349-1.
- Arber, N., Eagle, C.J., Spicak, J., Rácz, I., Dite, P., Hajer, J., *et al.* (2006) 'Celecoxib for the Prevention of Colorectal Adenomatous Polyps', *New England Journal of Medicine*, 355(9), pp. 885–895. doi:10.1056/nejmoa061652.
- Arora, S., Pattwell, S.S., Holland, E.C. and Bolouri, H. (2020) 'Variability in estimated gene expression among commonly used RNA-seq pipelines', *Scientific Reports*, 10(1), pp. 1–9. doi:10.1038/s41598-020-59516-z.
- Arvanitis, D.A., Vafiadaki, E., Sanoudou, D. and Kranias, E.G. (2011) 'Histidine-rich calcium binding protein: The new regulator of sarcoplasmic reticulum calcium cycling', *Journal of Molecular and Cellular Cardiology*, 50(1), pp. 43–49. doi:10.1016/j.yjmcc.2010.08.021.
- Ashmore, J., Olsen, H., Sørensen, N., Thrasivoulou, C. and Ahmed, A. (2019) 'Wnts control membrane potential in mammalian cancer cells', *Journal of Physiology*, 597(24), pp. 5899–5914. doi:10.1113/JP278661.
- Askmyr, M., Ågerstam, H., Hansen, N., Gordon, S., Arvanitakis, A., Rissler, M., *et al.* (2013a) 'Selective killing of candidate AML stem cells by antibody targeting of IL1RAP', *Blood*, 121(18), pp. 3709–3713. doi:10.1182/BLOOD-2012-09-458935.
- Askmyr, M., Ågerstam, H., Hansen, N., Gordon, S., Arvanitakis, A., Rissler, M., *et al.* (2013b) 'Selective killing of candidate AML stem cells by antibody targeting of IL1RAP', *Blood*, 121(18), pp. 3709–3713. doi:10.1182/blood-2012-09-458935.
- Astudillo, P. (2021) 'A Non-canonical Wnt Signature Correlates With Lower Survival in Gastric Cancer', *Frontiers in Cell and Developmental Biology*. Available at: <https://www.frontiersin.org/article/10.3389/fcell.2021.633675>.
- Asuri, S., Yan, J., Paronavitana, N.C. and Quilliam, L.A. (2008) 'E-cadherin dis-engagement activates the Rap1 GTPase', *Journal of Cellular Biochemistry*, 105(4), pp. 1027–1037. doi:10.1002/jcb.21902.
- Attisano, L. and Wrana, J.L. (2013) 'Signal integration in TGF- β , WNT, and Hippo pathways', *F1000Prime Reports*, 5. doi:10.12703/P5-17.
- Austin, T.W., Solar, G.P., Ziegler, F.C., Liem, L. and Matthews, W. (1997) 'A Role for the Wnt Gene Family in Hematopoiesis: Expansion of Multilineage Progenitor Cells', *Blood*, 89(10), pp. 3624–3635. doi:10.1182/blood.v89.10.3624.
- Avila, M.E., Sepúlveda, F.J., Burgos, C.F., Moraga-Cid, G., Parodi, J., Moon, R.T., *et al.* (2010) 'Canonical Wnt3a modulates intracellular calcium and enhances excitatory neurotransmission in hippocampal neurons', *Journal of Biological Chemistry*, 285(24), pp. 18939–18947. doi:10.1074/jbc.M110.103028.
- Azadniv, M., Myers, J.R., McMurray, H.R., Guo, N., Rock, P., Coppage, M.L., *et al.* (2020) 'Bone marrow mesenchymal stromal cells from acute myelogenous leukemia patients demonstrate adipogenic differentiation propensity with implications for leukemia cell support.', *Leukemia*, 34(2), pp. 391–403. doi:10.1038/s41375-019-0568-8.
- Aziz, H., Ping, C.Y., Alias, H., Ab Mutalib, N.S. and Jamal, R. (2017) 'Gene mutations as emerging biomarkers and therapeutic targets for relapsed acute myeloid leukemia', *Frontiers in Pharmacology*, 8(DEC), p. 897. doi:10.3389/fphar.2017.00897.
- Babushok, D. V., Bessler, M. and Olson, T.S. (2016) 'Genetic predisposition to myelodysplastic syndrome and acute myeloid leukemia in children and young adults', *Leukemia and Lymphoma*, 57(3), pp. 520–536. doi:10.3109/10428194.2015.1115041.
- Bagger, F.O., Kinalis, S. and Rapin, N. (2019) 'BloodSpot: a database of healthy and malignant haematopoiesis updated with purified and single cell mRNA sequencing profiles.', *Nucleic acids research*, 47(D1), pp. D881–D885. doi:10.1093/nar/gky1076.

- Bain, B.J. and Béné, M.C. (2019) 'Morphological and Immunophenotypic Clues to the WHO Categories of Acute Myeloid Leukaemia', *Acta Haematologica*, 141(4), pp. 232–244. doi:10.1159/000496097.
- Barbieri, E., Deflorian, G., Pezzimenti, F., Valli, D., Saia, M., Meani, N., *et al.* (2016) 'Nucleophosmin leukemogenic mutant activates Wnt signaling during zebrafish development', *Oncotarget*, 7(34), pp. 55302–55312. doi:10.18632/oncotarget.10878.
- Baron, J. and Wang, E.S. (2018) 'Gemtuzumab ozogamicin for the treatment of acute myeloid leukemia', *Expert Review of Clinical Pharmacology*, 11(6), pp. 549–559. doi:10.1080/17512433.2018.1478725.
- Barrangou, R., Fremaux, C., Deveau, H., Richards, M., Boyaval, P., Moineau, S., *et al.* (2007) 'CRISPR provides acquired resistance against viruses in prokaryotes', *Science*, 315(5819), pp. 1709–1712. doi:10.1126/science.1138140.
- Barrangou, R. (2015) 'The roles of CRISPR-Cas systems in adaptive immunity and beyond', *Current Opinion in Immunology*, 32, pp. 36–41. doi:10.1016/j.coi.2014.12.008.
- Barretina, J., Caponigro, G., Stransky, N., Venkatesan, K., Margolin, A.A., Kim, S., *et al.* (2012) 'The Cancer Cell Line Encyclopedia enables predictive modelling of anticancer drug sensitivity', *Nature*, 483(7391), pp. 603–607. doi:10.1038/nature11003.
- Barreyro, L., Will, B., Bartholdy, B., Zhou, L., Todorova, T.I., Stanley, R.F., *et al.* (2012) 'Overexpression of IL-1 receptor accessory protein in stem and progenitor cells and outcome correlation in AML and MDS', *Blood*, 120(6), pp. 1290–1298. doi:10.1182/blood-2012-01-404699.
- Basecke, J., Whelan, J.T., Griesinger, F. and Bertrand, F.E. (2006) 'The MLL partial tandem duplication in acute myeloid leukaemia', *British Journal of Haematology*. Br J Haematol, pp. 438–449. doi:10.1111/j.1365-2141.2006.06301.x.
- Basharat, M., Khan, S.A., Nasir Ud Din and Ahmed, D. (2019) 'Immunophenotypic characterisation of morphologically diagnosed cases of acute myeloid Leukaemia (AML)', *Pakistan Journal of Medical Sciences*, 35(2), pp. 470–476. doi:10.12669/pjms.35.2.614.
- Batista Napotnik, T., Polajžer, T. and Miklavčič, D. (2021) 'Cell death due to electroporation – A review', *Bioelectrochemistry*, 141, p. 107871. doi:10.1016/J.BIOELECTCHEM.2021.107871.
- Baum, C.M., Weissman, I.L., Tsukamoto, A.S., Buckle, A.M. and Peault, B. (1992) 'Isolation of a candidate human hematopoietic stem-cell population', *Proceedings of the National Academy of Sciences of the United States of America*, 89(7), pp. 2804–2808. doi:10.1073/pnas.89.7.2804.
- de Beauchamp, L., Himonas, E. and Helgason, G.V. (2021) 'Mitochondrial metabolism as a potential therapeutic target in myeloid leukaemia', *Leukemia* 2021 36:1, 36(1), pp. 1–12. doi:10.1038/s41375-021-01416-w.
- Béchar, D., Scherpereel, A., Hammad, H., Gentina, T., Tscopoulos, A., Aumercier, M., *et al.* (2001) 'Human Endothelial-Cell Specific Molecule-1 Binds Directly to the Integrin CD11a/CD18 (LFA-1) and Blocks Binding to Intercellular Adhesion Molecule-1', *The Journal of Immunology*, 167(6), pp. 3099–3106. doi:10.4049/jimmunol.167.6.3099.
- Behan, F.M., Iorio, F., Picco, G., Gonçalves, E., Beaver, C.M., Migliardi, G., *et al.* (2019) 'Prioritization of cancer therapeutic targets using CRISPR-Cas9 screens', *Nature*, 568(7753), pp. 511–516. doi:10.1038/S41586-019-1103-9.
- Ben-Ze'ev, A., Basu, S. and Haase, G. (2016) 'Wnt signaling in cancer stem cells and colon cancer metastasis', *F1000Research*, 5. doi:10.12688/f1000research.7579.1.
- Bennett, J.M., Catovsky, D., Daniel, M. -T, Flandrin, G., Galton, D.A.G., Gralnick, H.R., *et al.* (1976) 'Proposals for the Classification of the Acute Leukaemias French-American-British (FAB) Co-operative Group', *British Journal of Haematology*, 33(4), pp. 451–458. doi:10.1111/j.1365-2141.1976.tb03563.x.
- Benveniste, P., Frelin, C., Janmohamed, S., Barbara, M., Herrington, R., Hyam, D., *et al.* (2010)

- ‘Intermediate-Term Hematopoietic Stem Cells with Extended but Time-Limited Reconstitution Potential’, *Cell Stem Cell*, 6(1), pp. 48–58. doi:10.1016/j.stem.2009.11.014.
- Berendsen, A.D., Fisher, L.W., Kilts, T.M., Owens, R.T., Robey, P.G., Gutkind, J.S., *et al.* (2011) ‘Modulation of canonical Wnt signaling by the extracellular matrix component biglycan.’, *Proceedings of the National Academy of Sciences of the United States of America*, 108(41), pp. 17022–17027. doi:10.1073/pnas.1110629108.
- Berge, D., Ten, Kurek, D., Blauwkamp, T., Koole, W., Maas, A., Eroglu, E., *et al.* (2011) ‘Embryonic stem cells require Wnt proteins to prevent differentiation to epiblast stem cells’, *Nature Cell Biology*, 13(9), pp. 1070–1077. doi:10.1038/ncb2314.
- Bernitz, J.M., Kim, H.S., MacArthur, B., Sieburg, H. and Moore, K. (2016) ‘Hematopoietic Stem Cells Count and Remember Self-Renewal Divisions’, *Cell*, 167(5), pp. 1296–1309.e10. doi:10.1016/j.cell.2016.10.022.
- Bhatia, M., Wang, J.C.Y., Kapp, U., Bonnet, D. and Dick, J.E. (1997) ‘Purification of primitive human hematopoietic cells capable of repopulating immune-deficient mice’, *Proceedings of the National Academy of Sciences of the United States of America*, 94(10), pp. 5320–5325. doi:10.1073/pnas.94.10.5320.
- Bigas, A., Robert-Moreno, A. and Espinosa, L. (2010) ‘The Notch pathway in the developing hematopoietic system.’, *The International journal of developmental biology*, 54(6–7), pp. 1175–1188. doi:10.1387/ijdb.093049ab.
- Bilić, J., Huang, Y.L., Davidson, G., Zimmermann, T., Cruciat, C.M., Bienz, M., *et al.* (2007) ‘Wnt induces LRP6 signalosomes and promotes dishevelled-dependent LRP6 phosphorylation’, *Science*, 316(5831), pp. 1619–1622. doi:10.1126/science.1137065.
- Bin-Nun, N., Lichtig, H., Malyarova, A., Levy, M., Elias, S. and Frank, D. (2014) ‘PTK7 modulates Wnt signaling activity via LRP6’, *Development*, 141(2), pp. 410–421. doi:10.1242/dev.095984.
- Binder, S., Luciano, M. and Horejs-Hoeck, J. (2018) ‘The cytokine network in acute myeloid leukemia (AML): A focus on pro- and anti-inflammatory mediators’, *Cytokine and Growth Factor Reviews*. Elsevier Ltd, pp. 8–15. doi:10.1016/j.cytogfr.2018.08.004.
- Blair, A., Hogge, D.E., Ailles, L.E., Lansdorp, P.M. and Sutherland, H.J. (1997) ‘Lack of expression of Thy-1 (CD90) on acute myeloid leukemia cells with long-term proliferative ability in vitro and in vivo’, *Blood*, 89(9), pp. 3104–3112. doi:10.1182/blood.v89.9.3104.
- Blighe K, L.-S.J. (2021) *RegParallel: Standard regression functions in R enabled for parallel processing over large data-frames.*, *Bioconductor*. Available at: <https://bioconductor.org/packages/release/data/experiment/html/RegParallel.html> (Accessed: 21 July 2021).
- Bloh, K., Kanchana, R., Bialk, P., Banas, K., Zhang, Z., Yoo, B.C., *et al.* (2021) ‘Deconvolution of Complex DNA Repair (DECODR): Establishing a Novel Deconvolution Algorithm for Comprehensive Analysis of CRISPR-Edited Sanger Sequencing Data’, *The CRISPR Journal*, 4(1), p. 120. doi:10.1089/CRISPR.2020.0022.
- Boasman, K., Simmonds, M., Sauntharajah, Y. and Rinaldi, C.R. (2018) ‘PU.1 and JDP2 expression in myelodysplastic syndromes to predict treatment response and leukemia transformation.’, *Journal of Clinical Oncology*, 36(15_suppl), pp. 7065–7065. doi:10.1200/jco.2018.36.15_suppl.7065.
- Boasman, K., Simmonds, M.J., Graham, C., Sauntharajah, Y. and Rinaldi, C.R. (2019) ‘Using PU.1 and Jun dimerization protein 2 transcription factor expression in myelodysplastic syndromes to predict treatment response and leukaemia transformation’, *Annals of Hematology*, 98(6), pp. 1529–1531. doi:10.1007/s00277-019-03627-9.
- de Boer, B., Sheveleva, S., Apelt, K., Vellenga, E., Mulder, A.B., Huls, G., *et al.* (2020) ‘The IL1-IL1RAP axis plays an important role in the inflammatory leukemic niche that favors acute myeloid leukemia proliferation over normal hematopoiesis’, *Haematologica*, 106(12 SE-Articles), pp. 3067–3078. doi:10.3324/haematol.2020.254987.

- De Boer, B., Sheveleva, S., Apelt, K., Vellenga, E., Mulder, A.B., Huls, G., *et al.* (2021) 'The IL1-IL1RAP axis plays an important role in the inflammatory leukemic niche that favors acute myeloid leukemia proliferation over normal hematopoiesis.', *Haematologica*, 106(12), pp. 3067–3078. doi:10.3324/haematol.2020.254987.
- Boissel, N., Renneville, A., Leguay, T., Lefebvre, P.C., Recher, C., Lecerf, T., *et al.* (2015) 'Dasatinib in high-risk core binding factor acute myeloid leukemia in first complete remission: A french acute myeloid leukemia intergroup trial', *Haematologica*, 100(6), pp. 780–785. doi:10.3324/haematol.2014.114884.
- Bonnet, D. and Dick, J.E. (1997) 'Human acute myeloid leukemia is organized as a hierarchy that originates from a primitive hematopoietic cell', *Nature Medicine*, 3(7), pp. 730–737. doi:10.1038/nm0797-730.
- Boriack-Sjodin, P.A., Margarit, S.M., Bar-Sagi, D. and Kuriyan, J. (1998) 'The structural basis of the activation of Ras by Sos', *Nature*, 394(6691), pp. 337–343. doi:10.1038/28548.
- Bos, J.L. (2005) 'Linking Rap to cell adhesion', *Current Opinion in Cell Biology*, 17(2), pp. 123–128. doi:10.1016/j.ceb.2005.02.009.
- Boutros, M. and Niehrs, C. (2016) 'Sticking Around: Short-Range Activity of Wnt Ligands', *Developmental Cell*, 36(5), pp. 485–486. doi:10.1016/j.devcel.2016.02.018.
- Boyer, T., Gonzales, F., Barthélémy, A., Marceau-Renaut, A., Peyrouze, P., Guihard, S., *et al.* (2019) 'Clinical significance of ABCB1 in acute myeloid leukemia: A comprehensive study', *Cancers*, 11(9). doi:10.3390/cancers11091323.
- Boyle, E.I., Weng, S., Gollub, J., Jin, H., Botstein, D., Cherry, J.M., *et al.* (2004) 'GO::TermFinder - Open source software for accessing Gene Ontology information and finding significantly enriched Gene Ontology terms associated with a list of genes', *Bioinformatics*, 20(18), pp. 3710–3715. doi:10.1093/bioinformatics/bth456.
- Boyle, S.T., Gieniec, K.A., Gregor, C.E., Faulkner, J.W., McColl, S.R. and Kochetkova, M. (2017) 'Interplay between CCR7 and Notch1 axes promotes stemness in MMTV-PyMT mammary cancer cells', *Molecular Cancer*, 16(1), pp. 1–8. doi:10.1186/s12943-017-0592-0.
- Brandt, J.T., Tisone, J.A., Bohman, J.E. and Theil, K.S. (1997) 'Aberrant expression of CD19 as a marker of monocytic lineage in acute myelogenous leukemia', *American Journal of Clinical Pathology*, 107(3), pp. 283–291. doi:10.1093/ajcp/107.3.283.
- Bras, A.E., de Haas, V., van Stigt, A., Jongen-Lavrencic, M., Beverloo, H.B., te Marvelde, J.G., *et al.* (2019) 'CD123 expression levels in 846 acute leukemia patients based on standardized immunophenotyping', *Cytometry Part B - Clinical Cytometry*, 96(2), pp. 134–142. doi:10.1002/cyto.b.21745.
- Bray, L.J., Binner, M., Körner, Y., von Bonin, M., Bornhäuser, M. and Werner, C. (2017) 'A three-dimensional ex vivo tri-culture model mimics cell-cell interactions between acute myeloid leukemia and the vascular niche', *Haematologica*. 2017/03/30, 102(7), pp. 1215–1226. doi:10.3324/haematol.2016.157883.
- Breheny, P., Stromberg, A. and Lambert, J. (2018) 'p-Value Histograms: Inference and Diagnostics.', *High-throughput*, 7(3). doi:10.3390/ht7030023.
- Briggs, R.C., Shults, K.E., Flye, L.A., McClintock-Treep, S.A., Jagasia, M.H., Goodman, S.A., *et al.* (2006) 'Dysregulated human myeloid nuclear differentiation antigen expression in myelodysplastic syndromes: Evidence for a role in apoptosis', *Cancer Research*, 66(9), pp. 4645–4651. doi:10.1158/0008-5472.CAN-06-0229.
- Broudy, V.C. (1997) 'Stem cell factor and hematopoiesis', *Blood*, 90(4), pp. 1345–1364. doi:10.1182/blood.v90.4.1345.
- Brown, G., Ceredig, R. and Tsapogas, P. (2018) 'The making of hematopoiesis: Developmental ancestry and environmental nurture', *International Journal of Molecular Sciences*, 19(7), p. 2122. doi:10.3390/ijms19072122.

- Brown, G., Tsapogas, P. and Ceredig, R. (2018) 'The changing face of hematopoiesis: a spectrum of options is available to stem cells', *Immunology and Cell Biology*, 96(9), pp. 898–911. doi:10.1111/imcb.12055.
- Buccisano, F., Rossi, F.M., Venditti, A., Del Poeta, G., Cox, M.C., Abbruzzese, E., *et al.* (2004) 'CD90/Thy-1 is preferentially expressed on blast cells of high risk acute myeloid leukaemias', *British Journal of Haematology*, 125(2), pp. 203–212. doi:10.1111/j.1365-2141.2004.04883.x.
- Buchtova, M., Oralova, V., Aklian, A., Masek, J., Vesela, I., Ouyang, Z., *et al.* (2015) 'Fibroblast growth factor and canonical WNT/ β -catenin signaling cooperate in suppression of chondrocyte differentiation in experimental models of FGFR signaling in cartilage', *Biochimica et Biophysica Acta - Molecular Basis of Disease*, 1852(5), pp. 839–850. doi:10.1016/j.bbadis.2014.12.020.
- Burnett, A.K., Russell, N.H., Kell, J., Dennis, M., Milligan, D., Paolini, S., *et al.* (2010) 'European development of clofarabine as treatment for older patients with acute myeloid leukemia considered unsuitable for intensive chemotherapy', *Journal of Clinical Oncology*, 28(14), pp. 2389–2395. doi:10.1200/JCO.2009.26.4242.
- Burnett, A.K., Hills, R.K., Milligan, D., Kjeldsen, L., Kell, J., Russell, N.H., *et al.* (2011) 'Identification of Patients with Acute Myeloblastic Leukemia Who Benefit from the Addition of Gemtuzumab Ozogamicin: Results of the MRC AML15 Trial', *Journal of Clinical Oncology*, 29(4), pp. 369–377. doi:10.1200/JCO.2010.31.4310.
- Burock, S., Daum, S., Keilholz, U., Neumann, K., Walther, W. and Stein, U. (2018) 'Phase II trial to investigate the safety and efficacy of orally applied niclosamide in patients with metachronous or synchronous metastases of a colorectal cancer progressing after therapy: The NIKOLO trial', *BMC Cancer*, 18(1), pp. 1–7. doi:10.1186/s12885-018-4197-9.
- Calvi, L.M., Adams, G.B., Weibrecht, K.W., Weber, J.M., Olson, D.P., Knight, M.C., *et al.* (2003) 'Osteoblastic cells regulate the haematopoietic stem cell niche', *Nature*, 425(6960), pp. 841–846. doi:10.1038/nature02040.
- Carbon, S., Douglass, E., Dunn, N., Good, B., Harris, N.L., Lewis, S.E., *et al.* (2019) 'The Gene Ontology Resource: 20 years and still GOing strong', *Nucleic Acids Research*, 47(D1), pp. D330–D338. doi:10.1093/nar/gky1055.
- Cartel, M., Mouchel, P.L., Gotanègre, M., David, L., Bertoli, S., Mansat-De Mas, V., *et al.* (2021) 'Inhibition of ubiquitin-specific protease 7 sensitizes acute myeloid leukemia to chemotherapy', *Leukemia*, 35(2), pp. 417–432. doi:10.1038/s41375-020-0878-x.
- Caspi, M., Perry, G., Skalka, N., Meisel, S., Firsow, A., Amit, M., *et al.* (2014) 'Aldolase positively regulates of the canonical Wnt signaling pathway', *Molecular Cancer*, 13(1), p. 164. doi:10.1186/1476-4598-13-164.
- Cate, B., de Bruyn, M., Wei, Y., Bremer, E., Helfrich, W., Mourabet, M., *et al.* (2009) 'Targeted Elimination of Leukemia Stem Cells; a New Therapeutic Approach in Hemato-Oncology', *Current Drug Targets*, 11(1), pp. 95–110. doi:10.2174/138945010790031063.
- Catlin, S.N., Busque, L., Gale, R.E., Guttorp, P. and Abkowitz, J.L. (2011) 'The replication rate of human hematopoietic stem cells in vivo', *Blood*, 117(17), pp. 4460–4466. doi:10.1182/blood-2010-08-303537.
- Cha, P.H. and Choi, K.Y. (2016) 'Simultaneous destabilization of β -catenin and Ras via targeting of the axin-RGS domain as a potential therapeutic strategy for colorectal cancer', *BMB Reports*, 49(9), pp. 455–456. doi:10.5483/BMBRep.2016.49.9.125.
- Chakrabarti, A.M., Henser-Brownhill, T., Monserrat, J., Poetsch, A.R., Luscombe, N.M. and Scaffidi, P. (2019) 'Target-Specific Precision of CRISPR-Mediated Genome Editing', *Molecular Cell*, 73(4), p. 699. doi:10.1016/J.MOLCEL.2018.11.031.
- Chan, L.N., Fiji, H.D.G., Watanabe, M., Kwon, O. and Tamanoi, F. (2011) 'Identification and Characterization of Mechanism of Action of P61-E7, a Novel Phosphine Catalysis-Based Inhibitor of Geranylgeranyltransferase-I', *PLoS ONE*, 6(10). doi:10.1371/JOURNAL.PONE.0026135.

- Chan, R.J. and Feng, G.S. (2007) 'PTPN11 is the first identified proto-oncogene that encodes a tyrosine phosphatase', *Blood*, 109(3), pp. 862–867. doi:10.1182/blood-2006-07-028829.
- Chang, W.M., Chang, Y.C., Yang, Y.C., Lin, S.K., Chang, P.M.H. and Hsiao, M. (2019) 'AKR1C1 controls cisplatin-resistance in head and neck squamous cell carcinoma through cross-talk with the STAT1/3 signaling pathway', *Journal of Experimental and Clinical Cancer Research*, 38(1), pp. 1–14. doi:10.1186/s13046-019-1256-2.
- Chaudhary, A.K., Chaudhary, S., Ghosh, K., Shanmukaiah, C. and Nadkarni, A.H. (2016) 'Secretion and expression of matrix metalloproteinase-2 and 9 from bone marrow mononuclear cells in myelodysplastic syndrome and acute myeloid leukemia', *Asian Pacific Journal of Cancer Prevention*, 17(3), pp. 1519–1529. doi:10.7314/APJCP.2016.17.3.1519.
- Chen, C.G., Gau, J.P., You, J.Y., Lee, K. Der, Yu, A. Bin, Lu, C.H., *et al.* (2009) 'Prognostic significance of β -catenin and topoisomerase II α in de novo acute myeloid leukemia', *American Journal of Hematology*, 84(2), pp. 87–92. doi:10.1002/ajh.21334.
- Chen, G.T., Tifrea, D.F., Murad, R., Habowski, A.N., Lyou, Y., Duong, M.R., *et al.* (2021) 'Disruption of β -Catenin-Dependent Wnt Signaling in Colon Cancer Cells Remodels the Microenvironment to Promote Tumor Invasion', *Molecular Cancer Research* [Preprint]. doi:10.1158/1541-7786.MCR-21-0349.
- Chen, L., Hu, N., Wang, C. and Zhao, H. (2020) 'HOTAIRM1 knockdown enhances cytarabine-induced cytotoxicity by suppression of glycolysis through the Wnt/ β -catenin/PFKF pathway in acute myeloid leukemia cells', *Archives of Biochemistry and Biophysics*, 680. doi:10.1016/j.abb.2019.108244.
- Chen, M., Li, Y., Xiao, L., Dai, G., Lu, P., Wang, Y., *et al.* (2020) 'AQP1 modulates tendon stem/progenitor cells senescence during tendon aging', *Cell Death and Disease*, 11(3). doi:10.1038/s41419-020-2386-3.
- Chen, P., Huang, H., Wu, J., Lu, R., Wu, Y., Jiang, X., *et al.* (2015) 'Bone marrow stromal cells protect acute myeloid leukemia cells from anti-CD44 therapy partly through regulating PI3K/Akt-p27Kip1 axis', *Molecular Carcinogenesis*, 54(12), pp. 1678–1685. doi:10.1002/mc.22239.
- Chen, S., Chen, Y., Lu, J., Yuan, D., He, L., Tan, H., *et al.* (2020) 'Bioinformatics analysis identifies key genes and pathways in acute myeloid leukemia associated with DNMT3A mutation', *BioMed Research International*, 2020. doi:10.1155/2020/9321630.
- Chen, S. and Liu, Y. (2018) 'Battle in stem cell niches: Canonical versus noncanonical Wnt signaling', *Journal of Leukocyte Biology*, 103(3), pp. 377–379. doi:10.1002/JLB.2CE1117-453RR.
- Chen, W.-L., Wang, J.-H., Zhao, A.-H., Xu, X., Wang, Y.-H., Chen, T.-L., *et al.* (2014) 'A distinct glucose metabolism signature of acute myeloid leukemia with prognostic value.', *Blood*, 124(10), pp. 1645–1654. doi:10.1182/blood-2014-02-554204.
- Chen, X., Glytsou, C., Zhou, H., Narang, S., Reyna, D.E., Lopez, A., *et al.* (2019) 'Targeting mitochondrial structure sensitizes acute myeloid Leukemia to venetoclax treatment', *Cancer Discovery*, 9(7), pp. 890–909. doi:10.1158/2159-8290.CD-19-0117.
- Chen, Y. Bin, Li, S., Lane, A.A., Connolly, C., Del Rio, C., Valles, B., *et al.* (2014) 'Phase I trial of maintenance sorafenib after allogeneic hematopoietic stem cell transplantation for fms-like tyrosine kinase 3 internal tandem duplication acute myeloid leukemia', *Biology of Blood and Marrow Transplantation*, 20(12), pp. 2042–2048. doi:10.1016/j.bbmt.2014.09.007.
- Cheng, H., Liu, Y., Jia, Q., Ma, S., Yuan, W., Jia, H., *et al.* (2016) 'Novel regulators in hematopoietic stem cells can be revealed by a functional approach under leukemic condition', *Leukemia*, 30(10), pp. 2074–2077. doi:10.1038/leu.2016.118.
- Cheng, H., Huang, C., Xu, X., Hu, X., Gong, S., Tang, G., *et al.* (2017) 'PIM-1 mRNA expression is a potential prognostic biomarker in acute myeloid leukemia', *Journal of Translational Medicine*, 15(1), p. 179. doi:10.1186/s12967-017-1287-4.
- Cheng, H., Zheng, Z. and Cheng, T. (2020) 'New paradigms on hematopoietic stem cell

- differentiation', *Protein and Cell*, 11(1), pp. 34–44. doi:10.1007/s13238-019-0633-0.
- Cheng, X., Xu, X., Chen, D., Zhao, F. and Wang, W. (2019) 'Therapeutic potential of targeting the Wnt/ β -catenin signaling pathway in colorectal cancer', *Biomedicine & Pharmacotherapy*, 110, pp. 473–481. doi:10.1016/J.BIOPHA.2018.11.082.
- Cheruku, H.R., Mohamedali, A., Cantor, D.I., Tan, S.H., Nice, E.C. and Baker, M.S. (2015) 'Transforming growth factor- β , MAPK and Wnt signaling interactions in colorectal cancer', *EuPA Open Proteomics*, 8, pp. 104–115. doi:10.1016/j.euprot.2015.06.004.
- Chicaybam, L., Barcelos, C., Peixoto, B., Carneiro, M., Limia, C.G., Redondo, P., *et al.* (2017) 'An Efficient Electroporation Protocol for the Genetic Modification of Mammalian Cells', *Frontiers in Bioengineering and Biotechnology*, 4, p. 99. doi:10.3389/FBIOE.2016.00099/BIBTEX.
- Chigaev, A. (2015) 'Does aberrant membrane transport contribute to poor outcome in adult acute myeloid leukemia?', *Frontiers in Pharmacology*, 6(JUL). doi:10.3389/fphar.2015.00134.
- Cho, S.H., Kuo, I.Y., Lu, P.J.F., Tzeng, H.T., Lai, W.W., Su, W.C., *et al.* (2018) 'Rab37 mediates exocytosis of secreted frizzled-related protein 1 to inhibit Wnt signaling and thus suppress lung cancer stemness', *Cell Death and Disease*, 9(9), pp. 1–13. doi:10.1038/s41419-018-0915-0.
- Chong, P.S.Y., Zhou, J., Chooi, J.Y., Chan, Z.L., Toh, S.H.M., Tan, T.Z., *et al.* (2019) 'Non-canonical activation of β -catenin by PRL-3 phosphatase in acute myeloid leukemia', *Oncogene*, 38(9), pp. 1508–1519. doi:10.1038/s41388-018-0526-3.
- Chong, W., Zhang, H., Guo, Z., Yang, L., Shao, Y., Liu, X., *et al.* (2021) 'Aquaporin 1 promotes sensitivity of anthracycline chemotherapy in breast cancer by inhibiting β -catenin degradation to enhance TopoII α activity', *Cell Death and Differentiation*, 28(1), pp. 382–400. doi:10.1038/s41418-020-00607-9.
- Chosa, N. and Ishisaki, A. (2018) 'Two novel mechanisms for maintenance of stemness in mesenchymal stem cells: SCRG1/BST1 axis and cell–cell adhesion through N-cadherin', *Japanese Dental Science Review*, 54(1), pp. 37–44. doi:10.1016/j.jdsr.2017.10.001.
- Chowdhury, A., Loaiza, S., Yebra-Fernandez, E., Nadal-Melsio, E., Apperley, J.F. and Khorashad, J.S. (2020) 'An ex vivo investigation of interactions between primary acute myeloid leukaemia and mesenchymal stromal cells yields novel therapeutic targets', *British Journal of Haematology*, 190(4), pp. e236–e239. doi:10.1111/bjh.16810.
- Christie, K.A. and Kleinstiver, B.P. (2021) 'Making the cut with PAMless CRISPR-Cas enzymes', *Trends in Genetics*, 37(12), pp. 1053–1055. doi:10.1016/j.tig.2021.09.002.
- Cobas, M., Wilson, A., Ernst, B., Mancini, S.J.C., MacDonald, H.R., Kemler, R., *et al.* (2004a) ' β -Catenin Is Dispensable for Hematopoiesis and Lymphopoiesis', *Journal of Experimental Medicine*, 199(2), pp. 221–229. doi:10.1084/jem.20031615.
- Cobas, M., Wilson, A., Ernst, B., Mancini, S.J.C., MacDonald, H.R., Kemler, R., *et al.* (2004b) ' β -Catenin Is Dispensable for Hematopoiesis and Lymphopoiesis', *The Journal of Experimental Medicine*, 199(2), pp. 221–229. doi:10.1084/jem.20031615.
- Conant, D., Hsiao, T., Rossi, N., Oki, J., Maures, T., Waite, K., *et al.* (2022) 'Inference of CRISPR Edits from Sanger Trace Data', *The CRISPR journal*, 5(1), pp. 123–130. doi:10.1089/CRISPR.2021.0113.
- Conesa, A., Madrigal, P., Tarazona, S., Gomez-Cabrero, D., Cervera, A., McPherson, A., *et al.* (2016) 'A survey of best practices for RNA-seq data analysis', *Genome biology*, 17(1). doi:10.1186/S13059-016-0881-8.
- Conway O'Brien, E., Prideaux, S. and Chevassut, T. (2014) 'The epigenetic landscape of acute myeloid leukemia', *Advances in Hematology*, 2014. doi:10.1155/2014/103175.
- Corrêa, S., Binato, R., Du Rocher, B., Castelo-Branco, Morgana T.L., Pizzatti, L. and Abdelhay, E. (2012) 'Wnt/ β -catenin pathway regulates ABCB1 transcription in chronic myeloid leukemia', *BMC Cancer*, 12(1), p. 303. doi:10.1186/1471-2407-12-303.

- Corrêa, S., Binato, R., Du Rocher, B., Castelo-Branco, Morgana T L, Pizzatti, L. and Abdelhay, E. (2012) 'Wnt/ β -catenin pathway regulates ABCB1 transcription in chronic myeloid leukemia', *BMC cancer*, 12, p. 303. doi:10.1186/1471-2407-12-303.
- Corrêa, S., Abdelhay, E., Paschka, P., Gaidzik, V.I., Hassan, R., Claus, R., *et al.* (2014) 'ABCB1 Expression in Acute Myeloid Leukemia (AML): A Possible Predictive Value for Treatment Resistance?', *Blood*, 124(21), pp. 3618–3618. doi:10.1182/blood.v124.21.3618.3618.
- Cortes, J.E., Jonas, B.A., Graef, T., Luan, Y. and Stein, A.S. (2019) 'Clinical Experience With Ibrutinib Alone or in Combination With Either Cytarabine or Azacitidine in Patients With Acute Myeloid Leukemia', *Clinical Lymphoma, Myeloma and Leukemia*, 19(8), pp. 509-515.e1. doi:10.1016/j.clml.2019.05.008.
- Côte, M., Fos, C., Canonigo-Balancio, A.J., Ley, K., Bécart, S. and Altman, A. (2015) 'SLAT promotes TCR-mediated, Rap1-dependent LFA-1 activation and adhesion through interaction of its PH domain with Rap1', *Journal of Cell Science*, 128(23), pp. 4341–4352. doi:10.1242/jcs.172742.
- Covas, D.T., Panepucci, R.A., Fontes, A.M., Silva, W.A., Orellana, M.D., Freitas, M.C.C., *et al.* (2008) 'Multipotent mesenchymal stromal cells obtained from diverse human tissues share functional properties and gene-expression profile with CD146+ perivascular cells and fibroblasts', *Experimental Hematology*, 36(5), pp. 642–654. doi:10.1016/j.exphem.2007.12.015.
- Cozzio, A., Passegué, E., Ayton, P.M., Karsunky, H., Cleary, M.L. and Weissman, I.L. (2003) 'Similar MLL-associated leukemias arising from self-renewing stem cells and short-lived myeloid progenitors', *Genes & Development*, 17(24), p. 3029. doi:10.1101/GAD.1143403.
- Cripe, L.D., Uno, H., Paietta, E.M., Litzow, M.R., Ketterling, R.P., Bennett, J.M., *et al.* (2010) 'Zosuquidar, a novel modulator of P-glycoprotein, does not improve the outcome of older patients with newly diagnosed acute myeloid leukemia: A randomized, placebo-controlled trial of the Eastern Cooperative Oncology Group 3999', *Blood*, 116(20), pp. 4077–4085. doi:10.1182/blood-2010-04-277269.
- Croft, D., Mundo, A.F., Haw, R., Milacic, M., Weiser, J., Wu, G., *et al.* (2014) 'The Reactome pathway knowledgebase', *Nucleic Acids Research*, 42(D1), pp. D472–D477. doi:10.1093/nar/gkt1102.
- Cruciat, C.M., Dolde, C., De Groot, R.E.A., Ohkawara, B., Reinhard, C., Korswagen, H.C., *et al.* (2013) 'RNA helicase DDX3 is a regulatory subunit of casein kinase 1 in Wnt- β -catenin signaling', *Science*, 339(6126), pp. 1436–1441. doi:10.1126/science.1231499.
- Cruciat, C.M. (2014) 'Casein kinase 1 and Wnt/ β -catenin signaling', *Current Opinion in Cell Biology*, 31, pp. 46–55. doi:10.1016/j.ceb.2014.08.003.
- Cucchi, D.G.J., Groen, R.W.J., Janssen, J.J.W.M. and Cloos, J. (2020) 'Ex vivo cultures and drug testing of primary acute myeloid leukemia samples: Current techniques and implications for experimental design and outcome', *Drug Resistance Updates*, 53, p. 100730. doi:https://doi.org/10.1016/j.drug.2020.100730.
- Cui, C., Zhou, X., Zhang, W., Qu, Y. and Ke, X. (2018) 'Is β -Catenin a Druggable Target for Cancer Therapy?', *Trends in Biochemical Sciences*, 43(8), pp. 623–634. doi:10.1016/j.tibs.2018.06.003.
- Cuilliere-Dartigues, P., El-Bchiri, J., Krimi, A., Buhard, O., Fontanges, P., Fléjou, J.F., *et al.* (2006) 'TCF-4 isoforms absent in TCF-4 mutated MSI-H colorectal cancer cells colocalize with nuclear CtBP and repress TCF-4-mediated transcription', *Oncogene*, 25(32), pp. 4441–4448. doi:10.1038/sj.onc.1209471.
- Dahlman, J.E., Abudayyeh, O.O., Joung, J., Gootenberg, J.S., Zhang, F. and Konermann, S. (2015) 'Orthogonal gene knockout and activation with a catalytically active Cas9 nuclease', *Nature Biotechnology*, 33(11), pp. 1159–1161. doi:10.1038/nbt.3390.
- Dang, Y., Jia, G., Choi, J., Ma, H., Anaya, E., Ye, C., *et al.* (2015) 'Optimizing sgRNA structure to improve CRISPR-Cas9 knockout efficiency', *Genome Biology*, 16(1), pp. 1–10. doi:10.1186/S13059-015-0846-3/FIGURES/7.

- Daniels, D.L. and Weis, W.I. (2002) 'ICAT inhibits β -catenin binding to tcf/lef-family transcription factors and the general coactivator p300 using independent structural modules', *Molecular Cell*, 10(3), pp. 573–584. doi:10.1016/S1097-2765(02)00631-7.
- Datlinger, P., Rendeiro, A.F., Schmidl, C., Krausgruber, T., Traxler, P., Klughammer, J., *et al.* (2017) 'Pooled CRISPR screening with single-cell transcriptome readout.', *Nature methods*, 14(3), pp. 297–301. doi:10.1038/nmeth.4177.
- Daud, S.S., Pumford, S.L., Gilmour, M.N., Gilkes, A.F., Burnett, A.K., Hills, R., *et al.* (2012) 'Identification of the Wnt Signalling Protein, TCF7L2 As a Significantly Overexpressed Transcription Factor in AML', *Blood*, 120(21), pp. 1281–1281. doi:10.1182/blood.v120.21.1281.1281.
- Daver, N., Cortes, J., Ravandi, F., Patel, K.P., Burger, J.A., Konopleva, M., *et al.* (2015) 'Secondary mutations as mediators of resistance to targeted therapy in leukemia', *Blood*, 125(21), pp. 3236–3245. doi:10.1182/blood-2014-10-605808.
- DeBruine, Z.J., Xu, H.E. and Melcher, K. (2017) 'Assembly and architecture of the Wnt/ β -catenin signalosome at the membrane', *British Journal of Pharmacology*, 174(24), pp. 4564–4574. doi:10.1111/bph.14048.
- Degos, L. and Wang, Z.Y. (2001) 'All trans retinoic acid in acute promyelocytic leukemia', *Oncogene*, 20(49), pp. 7140–7145. doi:10.1038/sj.onc.1204763.
- Delaney, J.R., Patel, C.B., Willis, K.M.C., Haghghiabyaneh, M., Axelrod, J., Tancioni, I., *et al.* (2017) 'Haploinsufficiency networks identify targetable patterns of allelic deficiency in low mutation ovarian cancer', *Nature Communications*, 8(1), pp. 1–11. doi:10.1038/ncomms14423.
- Dempster, J.M., Pacini, C., Pantel, S., Behan, F.M., Green, T., Krill-Burger, J., *et al.* (2019) 'Agreement between two large pan-cancer CRISPR-Cas9 gene dependency data sets', *Nature Communications 2019 10:1*, 10(1), pp. 1–14. doi:10.1038/s41467-019-13805-y.
- Deng, M., Lu, Z., Zheng, J., Wan, X., Chen, X., Hirayasu, K., *et al.* (2014) 'A motif in LILRB2 critical for Angptl2 binding and activation', *Blood*, 124(6), pp. 924–935. doi:10.1182/blood-2014-01-549162.
- Depreter, B., De Moerloose, B., Vandepoele, K., Uyttebroeck, A., Van Damme, A., Denys, B., *et al.* (2020) 'Clinical Significance of TARP Expression in Pediatric Acute Myeloid Leukemia', *HemaSphere*, 4(2), p. e346. doi:10.1097/hs9.0000000000000346.
- Depreter, B., Weening, K.E., Vandepoele, K., Essand, M., De Moerloose, B., Themeli, M., *et al.* (2020) 'TARP is an immunotherapeutic target in acute myeloid leukemia expressed in the leukemic stem cell compartment', *Haematologica*, 105(5), pp. 1306–1316. doi:10.3324/HAEMATOL.2019.222612.
- Deshpande, A., Sicinski, P. and Hinds, P.W. (2005) 'Cyclins and cdks in development and cancer: A perspective', *Oncogene*, 24(17), pp. 2909–2915. doi:10.1038/sj.onc.1208618.
- Dey, N., Young, B., Abramovitz, M., Bouzyk, M., Barwick, B., De, P., *et al.* (2013) 'Differential Activation of Wnt- β -Catenin Pathway in Triple Negative Breast Cancer Increases MMP7 in a PTEN Dependent Manner', *PLoS ONE*, 8(10). doi:10.1371/journal.pone.0077425.
- Dhillon, S. (2018) 'Ivosidenib: First Global Approval', *Drugs*, 78(14), pp. 1509–1516. doi:10.1007/s40265-018-0978-3.
- Dietrich, P.A., Yang, C., Leung, H.H.L., Lynch, J.R., Gonzales, E., Liu, B., *et al.* (2014) 'GPR84 sustains aberrant β -catenin signaling in leukemic stem cells for maintenance of MLL leukemogenesis', *Blood*, 124(22), pp. 3284–3294. doi:10.1182/BLOOD-2013-10-532523.
- Dillies, M.A., Rau, A., Aubert, J., Hennequet-Antier, C., Jeanmougin, M., Servant, N., *et al.* (2013) 'A comprehensive evaluation of normalization methods for Illumina high-throughput RNA sequencing data analysis', *Briefings in bioinformatics*, 14(6), pp. 671–683. doi:10.1093/BIB/BBS046.
- DiNardo, C.D., Garcia-Manero, G., Pierce, S., Nazha, A., Bueso-Ramos, C., Jabbour, E., *et al.* (2016) 'Interactions and relevance of blast percentage and treatment strategy among younger and older

- patients with acute myeloid leukemia (AML) and myelodysplastic syndrome (MDS)', *American journal of hematology*, 91(2), pp. 227–232. doi:10.1002/ajh.24252.
- DiNardo, C.D., Pratz, K., Pullarkat, V., Jonas, B.A., Arellano, M., Becker, P.S., *et al.* (2019) 'Venetoclax combined with decitabine or azacitidine in treatment-naïve, elderly patients with acute myeloid leukemia', *Blood*, 133(1), pp. 7–17. doi:10.1182/blood-2018-08-868752.
- Ding, Y., Gao, H. and Zhang, Q. (2017) 'The biomarkers of leukemia stem cells in acute myeloid leukemia', *Stem Cell Investigation*, 2017(MAR). doi:10.21037/sci.2017.02.10.
- Dixit, A., Parnas, O., Li, B., Chen, J., Fulco, C.P., Jerby-Arnon, L., *et al.* (2016) 'Perturb-Seq: Dissecting Molecular Circuits with Scalable Single-Cell RNA Profiling of Pooled Genetic Screens', *Cell*, 167(7), pp. 1853–1866.e17. doi:10.1016/j.cell.2016.11.038.
- Dobrosotskaya, I.Y. and James, G.L. (2000) 'MAGI-1 interacts with β -catenin and is associated with cell-cell adhesion structures', *Biochemical and Biophysical Research Communications*, 270(3), pp. 903–909. doi:10.1006/bbrc.2000.2471.
- Doench, J.G., Fusi, N., Sullender, M., Hegde, M., Vaimberg, E.W., Donovan, K.F., *et al.* (2016) 'Optimized sgRNA design to maximize activity and minimize off-target effects of CRISPR-Cas9', *Nature biotechnology*, 34(2), pp. 184–191. doi:10.1038/nbt.3437.
- Döhner, H., Estey, E.H., Amadori, S., Appelbaum, F.R., Büchner, T., Burnett, A.K., *et al.* (2010) 'Diagnosis and management of acute myeloid leukemia in adults: Recommendations from an international expert panel, on behalf of the European LeukemiaNet', *Blood*, 115(3), pp. 453–474. doi:10.1182/blood-2009-07-235358.
- Döhner, H., Estey, E., Grimwade, D., Amadori, S., Appelbaum, F.R., Büchner, T., *et al.* (2017) 'Diagnosis and management of AML in adults: 2017 ELN recommendations from an international expert panel', *Blood*, 129(4), pp. 424–447. doi:10.1182/blood-2016-08-733196.
- Dombret, H., Seymour, J.F., Butrym, A., Wierzbowska, A., Selleslag, D., Jang, J.H., *et al.* (2015) 'International phase 3 study of azacitidine vs conventional care regimens in older patients with newly diagnosed AML with >30% blasts', *Blood*, 126(3), pp. 291–299. doi:10.1182/blood-2015-01-621664.
- Dombret, H. and Gardin, C. (2016) 'An update of current treatments for adult acute myeloid leukemia', *Blood*, 127(1), pp. 53–61. doi:10.1182/blood-2015-08-604520.
- Domingo-Fernández, D., Mubeen, S., Marín-Llaó, J., Hoyt, C.T. and Hofmann-Apitius, M. (2019a) 'PathMe: merging and exploring mechanistic pathway knowledge', *BMC Bioinformatics*, 20(1), p. 243. doi:10.1186/s12859-019-2863-9.
- Domingo-Fernández, D., Mubeen, S., Marín-Llaó, J., Hoyt, C.T. and Hofmann-Apitius, M. (2019b) 'PathMe: Merging and exploring mechanistic pathway knowledge', *BMC Bioinformatics*, 20(1), pp. 1–12. doi:10.1186/s12859-019-2863-9.
- Dong, X., Fang, Z., Yu, M., Zhang, L., Xiao, R., Li, X., *et al.* (2018) 'Knockdown of Long Noncoding RNA HOXA-AS2 Suppresses Chemoresistance of Acute Myeloid Leukemia via the miR-520c-3p/S100A4 Axis', *Cellular Physiology and Biochemistry*, 51(2), pp. 886–896. doi:10.1159/000495387.
- Doroshov, J.H. (2019) 'Mechanisms of Anthracycline-Enhanced Reactive Oxygen Metabolism in Tumor Cells', *Oxidative Medicine and Cellular Longevity*, 2019. doi:10.1155/2019/9474823.
- Drake, A.S., Brady, M.T., Wang, X.H., Sait, S.J.N., Earp, J.C., Ghoshal, S., *et al.* (2009) 'Targeting 11q23 positive acute leukemia cells with high molecular weight-melanoma associated antigen-specific monoclonal antibodies', *Cancer Immunology, Immunotherapy*, 58(3), pp. 415–427. doi:10.1007/s00262-008-0567-5.
- Du, W., Lu, C., Zhu, X., Hu, D., Chen, X., Li, J., *et al.* (2019) 'Prognostic significance of CXCR4 expression in acute myeloid leukemia', *Cancer Medicine*, 8(15), p. 6595. doi:10.1002/CAM4.2535.
- Duan, L., Wu, R., Ye, L., Wang, H., Yang, X., Zhang, Yunyuan, *et al.* (2013) 'S100A8 and S100A9 Are Associated with Colorectal Carcinoma Progression and Contribute to Colorectal Carcinoma Cell

Survival and Migration via Wnt/ β -Catenin Pathway', *PLoS ONE*, 8(4).

doi:10.1371/journal.pone.0062092.

Dugan, J. and Pollyea, D. (2018) 'Enasidenib for the treatment of acute myeloid leukemia', *Expert Review of Clinical Pharmacology*, 11(8), pp. 755–760. doi:10.1080/17512433.2018.1477585.

Duncavage, E.J., Schroeder, M.C., O'Laughlin, M., Wilson, R., MacMillan, S., Bohannon, A., *et al.* (2021) 'Genome Sequencing as an Alternative to Cytogenetic Analysis in Myeloid Cancers', *New England Journal of Medicine*, 384(10), pp. 924–935. doi:10.1056/nejmoa2024534.

Dunne, J., Mannari, D., Farzaneh, T., Gessner, A., Van Delft, F.W., Heidenreich, O., *et al.* (2012) 'AML1/ETO and POU4F1 synergy drives B-lymphoid gene expression typical of t(8;21) acute myeloid leukemia', *Leukemia*, 26(5), pp. 1131–1135. doi:10.1038/leu.2011.316.

Dzhura, I., Chepurny, O.G., Leech, C.A., Roe, M.W., Dzhura, E., Xu, X., *et al.* (2011) 'Phospholipase C- ϵ links Epac2 activation to the potentiation of glucose-stimulated insulin secretion from mouse islets of Langerhans', *Islets*, 3(3), pp. 121–128. doi:10.4161/isl.3.3.15507.

Ebert, B.L. (2009) 'Deletion 5q in myelodysplastic syndrome: A paradigm for the study of hemizygous deletions in cancer', *Leukemia*. Nature Publishing Group, pp. 1252–1256. doi:10.1038/leu.2009.53.

Ebert, B.L. (2011) 'Molecular Dissection of the 5q Deletion in Myelodysplastic Syndrome', *Seminars in Oncology*, 38(5), pp. 621–626. doi:10.1053/j.seminoncol.2011.04.010.

Edilova, M.I., Abdul-Sater, A.A. and Watts, T.H. (2018) 'TRAF1 Signaling in Human Health and Disease', *Frontiers in Immunology*, 9, p. 2969. doi:10.3389/fimmu.2018.02969.

Eisfeld, A.K., Kohlschmidt, J., Schwind, S., Nicolet, D., Blachly, J.S., Orwick, S., *et al.* (2017) 'Mutations in the CCND1 and CCND2 genes are frequent events in adult patients with t(8;21)(q22;q22) acute myeloid leukemia', *Leukemia*, 31(6), pp. 1278–1285. doi:10.1038/leu.2016.332.

El-Masry, O.S., Al-Amri, A.M., Alqatari, A. and Alsamman, K. (2020) 'RNA sequencing-based identification of potential targets in acute myeloid leukemia: A case report', *Biomedical Reports*, 13(5), pp. 1–7. doi:10.3892/br.2020.1349.

Emami, K.H., Nguyen, C., Ma, H., Kim, D.H., Jeong, K.W., Eguchi, M., *et al.* (2004) 'A small molecule inhibitor of β -catenin/cyclic AMP response element-binding protein transcription', *Proceedings of the National Academy of Sciences of the United States of America*, 101(34), pp. 12682–12687. doi:10.1073/pnas.0404875101.

Emons, G., Spitzner, M., Reineke, S., Möller, J., Auslander, N., Kramer, F., *et al.* (2017) 'Chemoradiotherapy resistance in colorectal cancer cells is mediated by Wnt/ β -catenin signaling', *Molecular Cancer Research*, 15(11), pp. 1481–1490. doi:10.1158/1541-7786.MCR-17-0205.

Emori, M., Tsukahara, T., Murase, M., Kano, M., Murata, K., Takahashi, A., *et al.* (2013) 'High expression of CD109 antigen regulates the phenotype of cancer stem-like cells/cancer-initiating cells in the novel epithelioid sarcoma cell line ESX and is related to poor prognosis of soft tissue sarcoma', *PLoS ONE*, 8(12). doi:10.1371/journal.pone.0084187.

Eppert, K., Takenaka, K., Lechman, E.R., Waldron, L., Nilsson, B., Van Galen, P., *et al.* (2011) 'Stem cell gene expression programs influence clinical outcome in human leukemia', *Nature Medicine*, 17(9), pp. 1086–1094. doi:10.1038/nm.2415.

ES, A., J, H., CH, W., GA, T., FH, Z., GY, R., *et al.* (2016) 'The glucagon-like peptide-1 analogue exendin-4 reverses impaired intracellular Ca(2+) signalling in steatotic hepatocytes', *Biochimica et biophysica acta*, 1863(9), pp. 2135–2146. doi:10.1016/J.BBAMCR.2016.05.006.

Esteve, J., Kalko, S., Torreadell, M., Camos, M., Jares, P., Rozman, M., *et al.* (2007) 'Molecular Markers Predicting Clinical Outcome in Patients with Intermediate-Risk Acute Myeloid Leukemia Receiving Autologous Stem Cell Transplantation.', *Blood*, 110(11), p. 604. doi:https://doi.org/10.1182/blood.V110.11.604.604.

- Estey, E.H. (2009) 'Treatment of acute myeloid leukemia', *Haematologica*, 94(1), pp. 10–16. doi:10.3324/haematol.2008.001263.
- Esvelt, K.M., Mali, P., Braff, J.L., Moosburner, M., Yaung, S.J. and Church, G.M. (2013) 'Orthogonal Cas9 proteins for RNA-guided gene regulation and editing', *Nature Methods*, 10(11), pp. 1116–1123. doi:10.1038/nmeth.2681.
- Fagoonee, S., Bearzi, C., Di Cunto, F., Clohessy, J.G., Rizzi, R., Reschke, M., *et al.* (2013) 'The RNA Binding Protein ESRP1 Fine-Tunes the Expression of Pluripotency-Related Factors in Mouse Embryonic Stem Cells', *PLoS ONE*, 8(8), p. e72300. doi:10.1371/journal.pone.0072300.
- Falini, B., Tiacci, E., Martelli, M.P., Ascani, S. and Pileri, S.A. (2010) 'New classification of acute myeloid leukemia and precursor-related neoplasms: changes and unsolved issues.', *Discovery medicine*, 10(53), pp. 281–292. Available at: <http://www.ncbi.nlm.nih.gov/pubmed/21034669> (Accessed: 24 April 2019).
- Fang, L., Zhu, Q., Neuenschwander, M., Specker, E., Wulf-Goldenberg, A., Weis, W.I., *et al.* (2016) 'A Small-Molecule Antagonist of the β -Catenin/TCF4 Interaction Blocks the Self-Renewal of Cancer Stem Cells and Suppresses Tumorigenesis', *Cancer research*, 76(4), pp. 891–901. doi:10.1158/0008-5472.CAN-15-1519.
- Farboud, B. and Meyer, B.J. (2015) 'Dramatic enhancement of genome editing by CRISPR/cas9 through improved guide RNA design', *Genetics*, 199(4), pp. 959–971. doi:10.1534/GENETICS.115.175166/-/DC1.
- Farin, H.F., Jordens, I., Mosa, M.H., Basak, O., Korving, J., Tauriello, D.V.F., *et al.* (2016) 'Visualization of a short-range Wnt gradient in the intestinal stem-cell niche', *Nature*, 530(7590), pp. 340–343. doi:10.1038/NATURE16937.
- Fathi, A.T., Arowojolu, O., Swinnen, I., Sato, T., Rajkhowa, T., Small, D., *et al.* (2012) 'A potential therapeutic target for FLT3-ITD AML: PIM1 kinase', *Leukemia Research*, 36(2), pp. 224–231. doi:10.1016/j.leukres.2011.07.011.
- Fathi, A.T., Blonquist, T.M., Hernandez, D., Amrein, P.C., Ballen, K.K., McMasters, M., *et al.* (2018) 'Cabozantinib is well tolerated in acute myeloid leukemia and effectively inhibits the resistance-conferring FLT3/tyrosine kinase domain/F691 mutation', *Cancer*, 124(2), pp. 306–314. doi:10.1002/cncr.31038.
- Fatima, S., Lee, N.P., Tsang, F.H., Kolligs, F.T., Ng, I.O.L., Poon, R.T.P., *et al.* (2012) 'Dickkopf 4 (DKK4) acts on Wnt/ β -catenin pathway by influencing β -catenin in hepatocellular carcinoma', *Oncogene*, 31(38), pp. 4233–4244. doi:10.1038/onc.2011.580.
- Fenton, M., Gasparetto, M., Hong, C.-S., Wang, X., Smith, C., Whiteside, T., *et al.* (2011) 'Identification of Chondroitin Sulfate Proteoglycan-4 In Acute Myeloid Leukemia Using Monoclonal Antibody 225.28', *Blood*, 118(21), pp. 4885–4885. doi:10.1182/blood.v118.21.4885.4885.
- Fenton, M., Whiteside, T.L., Ferrone, S. and Boyiadzis, M. (2015) 'Chondroitin sulfate proteoglycan-4 (CSPG4)-specific monoclonal antibody 225.28 in detection of acute myeloid leukemia blasts', *Oncology Research*, 22(2), pp. 117–121. doi:10.3727/096504014X14174484758503.
- Ferrari, N., Riggio, A.I., Mason, S., McDonald, L., King, A., Higgins, T., *et al.* (2015) 'Runx2 contributes to the regenerative potential of the mammary epithelium', *Scientific Reports*, 5. doi:10.1038/srep15658.
- Ferreira, C.P., Cariste, L.M., Virgílio, F.D.S., Moraschi, B.F., Monteiro, C.B., Machado, A.M.V., *et al.* (2017) 'LFA-1 mediates cytotoxicity and tissue migration of specific CD8+ T cells after heterologous prime-boost vaccination against *Trypanosoma cruzi* infection', *Frontiers in Immunology*, 8(OCT), p. 1291. doi:10.3389/fimmu.2017.01291.
- Fets, L. and Anastasiou, D. (2013) 'P73 keeps metabolic control in the family', *Nature Cell Biology*, 15(8), pp. 891–893. doi:10.1038/ncb2810.
- Fialkow, P.J. (1974) 'The Origin and Development of Human Tumors Studied with Cell Markers', *New England Journal of Medicine*, 291(1), pp. 26–35. doi:10.1056/nejm197407042910109.

- Finn, L., Dalovisio, A. and Foran, J. (2017) 'Older patients with acute myeloid leukemia: Treatment challenges and future directions', *Ochsner Journal*, 17(4), pp. 398–404. doi:10.1043/TOJ-17-0035.
- Fiskus, W., Sharma, S., Saha, S., Shah, B., Devaraj, S.G.T., Sun, B., *et al.* (2015) 'Pre-clinical efficacy of combined therapy with novel β -catenin antagonist BC2059 and histone deacetylase inhibitor against AML cells', *Leukemia*, 29(6), pp. 1267–1278. doi:10.1038/leu.2014.340.
- Flanagan, D.J., Pentimikko, N., Luopajarvi, K., Willis, N.J., Gilroy, K., Raven, A.P., *et al.* (2021) 'NOTUM from Apc-mutant cells biases clonal competition to initiate cancer', *Nature*, 594(7863), pp. 430–435. doi:10.1038/s41586-021-03525-z.
- Fleming, H.E., Janzen, V., Lo Celso, C., Guo, J., Leahy, K.M., Kronenberg, H.M., *et al.* (2008a) 'Wnt Signaling in the Niche Enforces Hematopoietic Stem Cell Quiescence and Is Necessary to Preserve Self-Renewal In Vivo', *Cell Stem Cell*, 2(3), pp. 274–283. doi:10.1016/j.stem.2008.01.003.
- Fleming, H.E., Janzen, V., Lo Celso, C., Guo, J., Leahy, K.M., Kronenberg, H.M., *et al.* (2008b) 'Wnt Signaling in the Niche Enforces Hematopoietic Stem Cell Quiescence and Is Necessary to Preserve Self-Renewal In Vivo', *Cell Stem Cell*, 2(3), pp. 274–283. doi:10.1016/j.stem.2008.01.003.
- Fortier, J.M., Payton, J.E., Cahan, P., Ley, T.J., Walter, M.J. and Graubert, T.A. (2010) 'POU4F1 is associated with t(8;21) acute myeloid leukemia and contributes directly to its unique transcriptional signature', *Leukemia*, 24(5), pp. 950–957. doi:10.1038/leu.2010.61.
- Frankish, A., Diekhans, M., Ferreira, A.M., Johnson, R., Jungreis, I., Loveland, J., *et al.* (2019) 'GENCODE reference annotation for the human and mouse genomes', *Nucleic Acids Research*, 47(D1), pp. D766–D773. doi:10.1093/nar/gky955.
- Frelin, C., Herrington, R., Janmohamed, S., Barbara, M., Tran, G., Paige, C.J., *et al.* (2013) 'GATA-3 regulates the self-renewal of long-term hematopoietic stem cells', *Nature Immunology*, 14(10), pp. 1037–1044. doi:10.1038/ni.2692.
- Friedland, A.E., Tzur, Y.B., Esvelt, K.M., Colaiácovo, M.P., Church, G.M. and Calarco, J.A. (2013) 'Heritable genome editing in *C. elegans* via a CRISPR-Cas9 system', *Nature methods*, 10(8), p. 741. doi:10.1038/NMETH.2532.
- Friedman, A.D. (2009) 'Cell cycle and developmental control of hematopoiesis by Runx1', *Journal of Cellular Physiology*. *J Cell Physiol*, pp. 520–524. doi:10.1002/jcp.21738.
- Fu, C., Yuan, M., Sun, J., Liu, G., Zhao, X., Chang, W., *et al.* (2021) 'RNA-Binding Motif Protein 11 (RBM11) Serves as a Prognostic Biomarker and Promotes Ovarian Cancer Progression', *Disease markers*, 2021, p. 3037337. doi:10.1155/2021/3037337.
- Fujii, N., You, L., Xu, Z., Uematsu, K., Shan, J., He, B., *et al.* (2007) 'An antagonist of dishevelled protein-protein interaction suppresses β -catenin-dependent tumor cell growth', *Cancer Research*, 67(2), pp. 573–579. doi:10.1158/0008-5472.CAN-06-2726.
- Fujii, W., Kawahito, Y., Nagahara, H., Kukida, Y., Seno, T., Yamamoto, A., *et al.* (2015) 'Monocarboxylate transporter 4, associated with the acidification of synovial fluid, is a novel therapeutic target for inflammatory arthritis.', *Arthritis & rheumatology (Hoboken, N.J.)*, 67(11), pp. 2888–2896. doi:10.1002/art.39270.
- Fujikura, K., Akita, M., Ajiki, T., Fukumoto, T., Itoh, T. and Zen, Y. (2018) 'Recurrent Mutations in APC and CTNNB1 and Activated Wnt/ β -catenin Signaling in Intraductal Papillary Neoplasms of the Bile Duct', *American Journal of Surgical Pathology*, 42(12), pp. 1674–1685. doi:10.1097/PAS.0000000000001155.
- Gabrilove, J.L., Jakubowski, A., Scher, H., Sternberg, C., Wong, G., Grous, J., *et al.* (1988) 'Effect of Granulocyte Colony-Stimulating Factor on Neutropenia and Associated Morbidity Due to Chemotherapy for Transitional-Cell Carcinoma of the Urothelium', *New England Journal of Medicine*, 318(22), pp. 1414–1422. doi:10.1056/nejm198806023182202.
- Gadhoun, S.Z., Gadhoun, N.Y., Abuelela, A.F. and Merzaban, J.S. (2016) 'Anti-CD44 antibodies inhibit both mTORC1 and mTORC2: A new rationale supporting CD44-induced AML differentiation therapy', *Leukemia*. Nature Publishing Group, pp. 2397–2401. doi:10.1038/leu.2016.221.

- Galán-Díez, M., Isa, A., Ponzetti, M., Nielsen, M.F., Kassem, M. and Kousteni, S. (2016) 'Normal hematopoiesis and lack of β -catenin activation in osteoblasts of patients and mice harboring Lrp5 gain-of-function mutations', *Biochimica et biophysica acta*, 2015/12/08, 1863(3), pp. 490–498. doi:10.1016/j.bbamcr.2015.11.037.
- Galanis, A., Ma, H., Rajkhowa, T., Ramachandran, A., Small, D., Cortes, J., *et al.* (2014) 'Crenolanib is a potent inhibitor of flt3 with activity against resistance-Confering point mutants', *Blood*, 123(1), pp. 94–100. doi:10.1182/blood-2013-10-529313.
- van Galen, P., Hovestadt, V., Wadsworth, M.H., Hughes, T.K., Griffin, G.K., Battaglia, S., *et al.* (2019) 'Single-Cell RNA-Seq Reveals AML Hierarchies Relevant to Disease Progression and Immunity', *Cell*, 176(6), pp. 1265-1281.e24. doi:10.1016/j.cell.2019.01.031.
- Galli, L.M., Barnes, T., Cheng, T., Acosta, L., Anglade, A., Willert, K., *et al.* (2006) 'Differential inhibition of Wnt-3a by Strp-1, Sfrp-2, and Sfrp-3', *Developmental Dynamics*, 235(3), pp. 681–690. doi:10.1002/dvdy.20681.
- Gandillet, A., Park, S., Lassailly, F., Griessinger, E., Vargaftig, J., Filby, A., *et al.* (2011a) 'Heterogeneous sensitivity of human acute myeloid leukemia to β -catenin down-modulation', *Leukemia*, 25(5), pp. 770–780. doi:10.1038/leu.2011.17.
- Gandillet, A., Park, S., Lassailly, F., Griessinger, E., Vargaftig, J., Filby, A., *et al.* (2011b) 'Heterogeneous sensitivity of human acute myeloid leukemia to β -catenin down-modulation', *Leukemia*, 25(5), pp. 770–780. doi:10.1038/leu.2011.17.
- Ganesh, K., Adam, S., Taylor, B., Simpson, P., Rada, C. and Neuberger, M. (2011) 'CTNNB1 is a novel nuclear localization sequence-binding protein that recognizes RNA-splicing factors CDC5L and Prp31', *Journal of Biological Chemistry*, 286(19), pp. 17091–17102. doi:10.1074/jbc.M110.208769.
- Ganier, L., Betzi, S., Derviaux, C., Roche, P., Muller, C., Hoffer, L., *et al.* (2021) 'Discovery of small molecule inhibitors of the PTK7/ β -catenin inter-action targeting the Wnt signaling pathway in colorectal cancer', *bioRxiv*, p. 2021.10.15.464507. doi:10.1101/2021.10.15.464507.
- Gao, L.R., Zhang, N.K., Ding, Q.A., Chen, H.Y., Hu, X., Jiang, S., *et al.* (2013) 'Common expression of stemness molecular markers and early cardiac transcription factors in human Wharton's jelly-derived mesenchymal stem cells and embryonic stem cells', *Cell Transplantation*, 22(10), pp. 1883–1900. doi:10.3727/096368912X662444.
- Gao, W., Ye, G., Liu, L. and Wei, L. (2018) 'The downregulation of Rap1 GTPase-activating protein is associated with a poor prognosis in colorectal cancer and may impact on tumor progression', *Oncol Lett*, 15(5), pp. 7661–7668. doi:10.3892/ol.2018.8305.
- Garbe, A., Spyridonidis, A., Möbest, D., Schmoor, C., Mertelsmann, R. and Henschler, R. (1997) 'Transforming growth factor-beta 1 delays formation of granulocyte- macrophage colony-forming cells, but spares more primitive progenitors during ex vivo expansion of CD34+ haemopoietic progenitor cells', *British Journal of Haematology*, 99(4), pp. 951–958. doi:10.1046/j.1365-2141.1997.4893291.x.
- Garcia-Gras, E., Lombardi, R., Giocondo, M.J., Willerson, J.T., Schneider, M.D., Khoury, D.S., *et al.* (2006) 'Suppression of canonical Wnt/ β -catenin signaling by nuclear plakoglobin recapitulates phenotype of arrhythmogenic right ventricular cardiomyopathy', *Journal of Clinical Investigation*, 116(7), pp. 2012–2021. doi:10.1172/JCI27751.
- García-Tuñón, I., Alonso-Pérez, V., Vuelta, E., Pérez-Ramos, S., Herrero, M., Méndez, L., *et al.* (2019) 'Splice donor site sgRNAs enhance CRISPR/ Cas9-mediated knockout efficiency', *PLoS ONE*. Edited by S. Maas, 14(5), p. e0216674. doi:10.1371/journal.pone.0216674.
- Gartel, A.L. and Radhakrishnan, S.K. (2005) 'Lost in transcription: p21 repression, mechanisms, and consequences', *Cancer Research*, 65(10), pp. 3980–3985. doi:10.1158/0008-5472.CAN-04-3995.
- Gary Gilliland, D. and Griffin, J.D. (2002) 'The roles of FLT3 in hematopoiesis and leukemia', *Blood*, 100(5), pp. 1532–1542. doi:10.1182/blood-2002-02-0492.
- Gaur, T., Lengner, C.J., Hovhannisyanyan, H., Bhat, R.A., Bodine, P.V.N., Komm, B.S., *et al.* (2005)

- 'Canonical WNT signaling promotes osteogenesis by directly stimulating Runx2 gene expression', *Journal of Biological Chemistry*, 280(39), pp. 33132–33140. doi:10.1074/jbc.M500608200.
- Gearing, D.P., Gough, N.M., King, J.A., Hilton, D.J., Nicola, N.A., Simpson, R.J., *et al.* (1987) 'Molecular cloning and expression of cDNA encoding a murine myeloid leukaemia inhibitory factor (LIF).', *The EMBO journal*, 6(13), pp. 3995–4002. doi:10.1002/j.1460-2075.1987.tb02742.x.
- Geistlinger, L., Csaba, G., Santarelli, M., Ramos, M., Schiffer, L., Turaga, N., *et al.* (2021) 'Toward a gold standard for benchmarking gene set enrichment analysis', *Briefings in Bioinformatics*, 22(1), pp. 545–556. doi:10.1093/bib/bbz158.
- Ghandi, M., Huang, F.W., Jané-Valbuena, J., Kryukov, G. V, Lo, C.C., McDonald 3rd, E.R., *et al.* (2019) 'Next-generation characterization of the Cancer Cell Line Encyclopedia', *Nature*. 2019/05/08, 569(7757), pp. 503–508. doi:10.1038/s41586-019-1186-3.
- Ghorashian, S., Kramer, A.M., Onuoha, S., Wright, G., Bartram, J., Richardson, R., *et al.* (2019) 'Enhanced CAR T cell expansion and prolonged persistence in pediatric patients with ALL treated with a low-affinity CD19 CAR', *Nature Medicine*, 25(9), pp. 1408–1414. doi:10.1038/s41591-019-0549-5.
- Ghosh, N., Hossain, U., Mandal, A. and Sil, P.C. (2019) 'The Wnt signaling pathway: a potential therapeutic target against cancer', *Annals of the New York Academy of Sciences*, 1443(1), pp. 54–74. doi:10.1111/nyas.14027.
- Giebel, B. and Punzel, M. (2008) 'Lineage development of hematopoietic stem and progenitor cells', *Biological Chemistry*, 389(7), pp. 813–824. doi:10.1515/BC.2008.092.
- Gilbert, L.A., Horlbeck, M.A., Adamson, B., Villalta, J.E., Chen, Y., Whitehead, E.H., *et al.* (2014) 'Genome-Scale CRISPR-Mediated Control of Gene Repression and Activation', *Cell*, 159(3), pp. 647–661. doi:10.1016/j.cell.2014.09.029.
- Gillet, L.C., Navarro, P., Tate, S., Röst, H., Selevsek, N., Reiter, L., *et al.* (2012) 'Targeted Data Extraction of the MS/MS Spectra Generated by Data-independent Acquisition: A New Concept for Consistent and Accurate Proteome Analysis', *Molecular & Cellular Proteomics : MCP*, 11(6). doi:10.1074/MCP.O111.016717.
- Glading, A.J. and Ginsberg, M.H. (2010) 'Rap1 and its effector KRIT1/CCM1 regulate β -catenin signaling', *DMM Disease Models and Mechanisms*, 3(1–2), pp. 73–83. doi:10.1242/dmm.003293.
- Godley, L.A. and Shimamura, A. (2017) 'Genetic predisposition to hematologic malignancies: management and surveillance.', *Blood*, 130(4), pp. 424–432. doi:10.1182/blood-2017-02-735290.
- Goltzman, D., Mannstadt, M. and Marcocci, C. (2018) 'Physiology of the Calcium-Parathyroid Hormone-Vitamin D Axis', *Frontiers of Hormone Research*, 50, pp. 1–13. doi:10.1159/000486060.
- Gomes-Silva, D., Atilla, E., Atilla, P.A., Mo, F., Tashiro, H., Srinivasan, M., *et al.* (2019) 'CD7 CAR T Cells for the Therapy of Acute Myeloid Leukemia', *Molecular Therapy*, 27(1), pp. 272–280. doi:10.1016/j.ymthe.2018.10.001.
- Gong, M., Hay, S., Marshall, K.R., Munro, A.W. and Scrutton, N.S. (2007) 'DNA binding suppresses human AIF-M2 activity and provides a connection between redox chemistry, reactive oxygen species, and apoptosis', *Journal of Biological Chemistry*, 282(41), pp. 30331–30340. doi:10.1074/jbc.M703713200.
- Gonsalves, F.C., Klein, K., Carson, B.B., Katz, S., Ekas, L.A., Evans, S., *et al.* (2011) 'An RNAi-based chemical genetic screen identifies three small-molecule inhibitors of the Wnt/wingless signaling pathway', *Proceedings of the National Academy of Sciences of the United States of America*, 108(15), pp. 5954–5963. doi:10.1073/pnas.1017496108.
- González-Romero, E., Martínez-Valiente, C., García-Ruiz, C., Vázquez-Manrique, R.P., Cervera, J. and Sanjuan-Pla, A. (2019) 'CRISPR to fix bad blood: A new tool in basic and clinical hematology', *Haematologica*, 104(5), pp. 881–893. doi:10.3324/haematol.2018.211359.
- Goodchild, E., Linton, K., Drake, W. and Brown, M. (2019) 'SLC35F1, a potential marker for

- aldosterone producing cell clusters', *Endocrine Abstracts*, 65. doi:10.1530/endoabs.65.oc5.6.
- Goto, M., Mitra, R.S., Liu, M., Lee, J., Henson, B.S., Carey, T., *et al.* (2010) 'Rap1 stabilizes β -catenin and enhances β -catenin-dependent transcription and invasion in squamous cell carcinoma of the head and neck', *Clinical Cancer Research*, 16(1), pp. 65–76. doi:10.1158/1078-0432.CCR-09-1122.
- De Graaf, E.L., Altelaar, A.F.M., Van Breukelen, B., Mohammed, S. and Heck, A.J.R. (2011) 'Improving SRM assay development: a global comparison between triple quadrupole, ion trap, and higher energy CID peptide fragmentation spectra', *Journal of proteome research*, 10(9), pp. 4334–4341. doi:10.1021/PR200156B.
- Gréen, H., Falk, I.J., Lotfi, K., Paul, E., Hermansson, M., Rosenquist, R., *et al.* (2012) 'Association of ABCB1 polymorphisms with survival and in vitro cytotoxicity in de novo acute myeloid leukemia with normal karyotype', *Pharmacogenomics Journal*, 12(2), pp. 111–118. doi:10.1038/tj.2010.79.
- Grewal, S.S., Fass, D.M., Yao, H., Ellig, C.L., Goodman, R.H. and Stork, P.J.S. (2000) 'Calcium and cAMP signals differentially regulate cAMP-responsive element-binding protein function via a Rap-1-extracellular signal-regulated kinase pathway', *Journal of Biological Chemistry*, 275(44), pp. 34433–34441. doi:10.1074/jbc.M004728200.
- Griffin, J.D. and Lowenberg, B. (1986) 'Clonogenic cells in acute myeloblastic leukemia', *Blood*, 68(6), pp. 1185–1195. doi:10.1182/blood.v68.6.1185.bloodjournal6861185.
- Griffin, J.N., del Viso, F., Duncan, A.R., Robson, A., Hwang, W., Kulkarni, S., *et al.* (2018) 'RAPGEF5 Regulates Nuclear Translocation of β -Catenin', *Developmental Cell*, 44(2), pp. 248–260.e4. doi:10.1016/j.devcel.2017.12.001.
- Griffiths, E.A., Gore, S.D., Hooker, C., McDevitt, M.A., Karp, J.E., Smith, B.D., *et al.* (2010a) 'Acute myeloid leukemia is characterized by Wnt pathway inhibitor promoter hypermethylation', *Leukemia and Lymphoma*, 51(9), pp. 1711–1719. doi:10.3109/10428194.2010.496505.
- Griffiths, E.A., Gore, S.D., Hooker, C., McDevitt, M.A., Karp, J.E., Smith, B.D., *et al.* (2010b) 'Acute myeloid leukemia is characterized by Wnt pathway inhibitor promoter hypermethylation', *Leukemia & lymphoma*, 51(9), p. 1711. doi:10.3109/10428194.2010.496505.
- Griffiths, E.A., Golding, M.C., Srivastava, P., Povinelli, B.J., James, S.R., Ford, L.A., *et al.* (2015) 'Pharmacological targeting of β -Catenin in normal karyotype acute myeloid leukemia blasts', *Haematologica*, 100(2), pp. e49–e52. doi:10.3324/haematol.2014.113118.
- Grimwade, D., Walker, H., Harrison, G., Oliver, F., Chatters, S., Harrison, C.J., *et al.* (2001) 'The predictive value of hierarchical cytogenetic classification in older adults with acute myeloid leukemia (AML): Analysis of 1065 patients entered into the United Kingdom Medical Research Council AML11 trial', *Blood*, 98(5), pp. 1312–1320. doi:10.1182/blood.V98.5.1312.
- Gross, J.C., Chaudhary, V., Bartscherer, K. and Boutros, M. (2012) 'Active Wnt proteins are secreted on exosomes', *Nature Cell Biology*, 14(10), pp. 1036–1045. doi:10.1038/ncb2574.
- Grove, C.S. and Vassiliou, G.S. (2014) 'Acute myeloid leukaemia: A paradigm for the clonal evolution of cancer?', *DMM Disease Models and Mechanisms*, 7(8), pp. 941–951. doi:10.1242/dmm.015974.
- Growney, J.D., Shigematsu, H., Li, Z., Lee, B.H., Adelsperger, J., Rowan, R., *et al.* (2005) 'Loss of Runx1 perturbs adult hematopoiesis and is associated with a myeloproliferative phenotype', *Blood*. 2005/03/22, 106(2), pp. 494–504. doi:10.1182/blood-2004-08-3280.
- Gruszka, A.M., Valli, D. and Alcalay, M. (2019) 'Wnt Signalling in Acute Myeloid Leukaemia', *Cells*, 8(11), p. 1403. doi:10.3390/cells8111403.
- Gu, L., Fullam, A., Brennan, R. and Schröder, M. (2013) 'Human DEAD Box Helicase 3 Couples I κ B Kinase ϵ to Interferon Regulatory Factor 3 Activation', *Molecular and Cellular Biology*, 33(10), pp. 2004–2015. doi:10.1128/mcb.01603-12.
- Gu, R., Yang, X. and Wei, H. (2018) 'Molecular landscape and targeted therapy of acute myeloid

leukemia', *Biomarker Research*, 6(1), pp. 1–8. doi:10.1186/s40364-018-0146-7.

Guan, L., Zhu, S., Han, Y., Yang, C., Liu, Y., Qiao, L., *et al.* (2018) 'Knockout of CTNNB1 by CRISPR-Cas9 technology inhibits cell proliferation through the Wnt/ β -catenin signaling pathway.', *Biotechnology Letters*, 40(3), pp. 501–508. doi:10.1007/s10529-017-2491-2.

Gunes, B.A., Ozkan, T., Gurel, A.K., Hekmatshoar, Y., Beksac, M. and Sunguroglu, A. (2020) ' β -catenin mutations in acute myeloid leukemia', *The Egyptian Journal of Haematology*, 45(2), p. 105. doi:10.4103/EJH.EJH_54_19.

Günschmann, C., Chiticariu, E., Garg, B., Hiz, M.M., Mostmans, Y., Wehner, M., *et al.* (2014) 'Transgenic mouse technology in skin biology: Inducible gene knockout in mice', *Journal of Investigative Dermatology*, 134(7), pp. 1–4. doi:10.1038/jid.2014.213.

Guo, C., Ran, Q., Sun, C., Zhou, T., Yang, X., Zhang, J., *et al.* (2021) 'Loss of FGFR3 Delays Acute Myeloid Leukemogenesis by Programming Weakly Pathogenic CD117-Positive Leukemia Stem-Like Cells', *Frontiers in Pharmacology*, 11, p. 2406. doi:10.3389/fphar.2020.632809.

Guo, H., Zhang, T. Juan, Wen, X. mei, Zhou, J. dong, Ma, J. chun, An, C., *et al.* (2017) 'Hypermethylation of secreted frizzled-related proteins predicts poor prognosis in non-M3 acute myeloid leukemia', *OncoTargets and Therapy*, 10, pp. 3635–3644. doi:10.2147/OTT.S136502.

Guo, W., Zhang, J., Zhou, Y., Zhou, C., Yang, Y., Cong, Z., *et al.* (2021) 'GPR160 is a potential biomarker associated with prostate cancer', *Signal Transduction and Targeted Therapy*, 6(1), pp. 1–3. doi:10.1038/s41392-021-00583-7.

Guo, X. and Wang, X.F. (2009) 'Signaling cross-talk between TGF- β /BMP and other pathways', *Cell Research*. Nature Publishing Group, pp. 71–88. doi:10.1038/cr.2008.302.

Gurney, A., Axelrod, F., Bond, C.J., Cain, J., Chartier, C., Donigan, L., *et al.* (2012) 'Wnt pathway inhibition via the targeting of Frizzled receptors results in decreased growth and tumorigenicity of human tumors', *Proceedings of the National Academy of Sciences of the United States of America*, 109(29), pp. 11717–11722. doi:10.1073/pnas.1120068109.

Gyan, E., Frew, M., Bowen, D., Beldjord, C., Preudhomme, C., Lacombe, C., *et al.* (2005) 'Mutation in RAP1 is a rare event in myelodysplastic syndromes', *Leukemia* 2005 19:9, 19(9), pp. 1678–1680. doi:10.1038/sj.leu.2403882.

Ha, M., Han, M.E., Kim, J.Y., Jeong, D.C., Oh, S.O. and Kim, Y.H. (2019) 'Prognostic role of TPD52 in acute myeloid leukemia: A retrospective multicohort analysis', *Journal of Cellular Biochemistry*, 120(3), pp. 3672–3678. doi:10.1002/jcb.27645.

Habas, R. and He, X. (2007) 'Cell Signaling: Moving to a Wnt-Rap', *Current Biology*, 17(12), pp. R474–R477. doi:10.1016/j.cub.2007.04.020.

Haegel, H., Larue, L., Ohsugi, M., Fedorov, L., Herrenknecht, K. and Kemler, R. (1995) 'Lack of β -catenin affects mouse development at gastrulation', *Development*, 121(11), pp. 3529–3537. doi:10.1242/dev.121.11.3529.

Hafner, M., Niepel, M., Chung, M. and Sorger, P.K. (2016) 'Growth rate inhibition metrics correct for confounders in measuring sensitivity to cancer drugs', *Nature Methods*, 13(6), pp. 521–527. doi:10.1038/nmeth.3853.

Hamidouche, Z., Haÿ, E., Vaudin, P., Charbord, P., Schüle, R., Marie, P.J., *et al.* (2008) 'FHL2 mediates dexamethasone-induced mesenchymal cell differentiation into osteoblasts by activating Wnt/ β -catenin signaling-dependent Runx2 expression', *The FASEB Journal*, 22(11), pp. 3813–3822. doi:10.1096/fj.08-106302.

Handschuh, L. and Lonetti, A. (2019) 'Not only Mutations Matter: Molecular Picture of Acute Myeloid Leukemia Emerging from Transcriptome Studies', *Journal of Oncology*, 2019. doi:10.1155/2019/7239206.

Hanekamp, D., Cloos, J. and Schuurhuis, G.J. (2017) 'Leukemic stem cells: identification and clinical application', *International Journal of Hematology*, 105(5), pp. 549–557. doi:10.1007/s12185-017-

- Hänzelmann, S., Castelo, R. and Guinney, J. (2013) 'GSVA: Gene set variation analysis for microarray and RNA-Seq data', *BMC Bioinformatics*, 14(1), pp. 1–15. doi:10.1186/1471-2105-14-7.
- Hao, J. and Yu, J.S. (2018) 'Semaphorin 3C and its receptors in cancer and cancer stem-like cells', *Biomedicines*, 6(2). doi:10.3390/biomedicines6020042.
- Harsini, F.M., Chebrolu, S., Fuson, K.L., White, M.A., Rice, A.M. and Sutton, R.B. (2018) 'FerA is a Membrane-Associating Four-Helix Bundle Domain in the Ferlin Family of Membrane-Fusion Proteins', *Scientific Reports*, 8(1). doi:10.1038/s41598-018-29184-1.
- Hartman, M.L., Piliponsky, A.M., Temkin, V. and Levi-Schaffer, F. (2001) 'Human peripheral blood eosinophils express stem cell factor', *Blood*, 97(4), pp. 1086–1091. doi:10.1182/blood.V97.4.1086.
- Hasan, S.K., Patkar, N., Vishwakarma, D., Rajamanickam, D., Gokarn, A., Sahu, A., *et al.* (2017) 'Over-Expression of ERG Predicts Poor Outcome in Acute Myeloid Leukemia', *Blood*, 130(Supplement 1), pp. 3920–3920. doi:10.1182/blood.V130.Suppl_1.3920.3920.
- Hassan, H.T. and Zander, A. (1996) 'Stem Cell Factor as a Survival and Growth Factor in Human Normal and Malignant Hematopoiesis', *Acta Haematologica*, 95(3–4), pp. 257–262. doi:10.1159/000203893.
- Haubner, S., Perna, F., Köhnke, T., Schmidt, C., Berman, S., Augsberger, C., *et al.* (2019) 'Coexpression profile of leukemic stem cell markers for combinatorial targeted therapy in AML', *Leukemia*, 33(1), pp. 64–74. doi:10.1038/s41375-018-0180-3.
- Hayes, M., Naito, M., Daulat, A., Angers, S. and Ciruna, B. (2013) 'Ptk7 promotes non-canonical Wnt/PCP-mediated morphogenesis and inhibits Wnt/ β -catenin-dependent cell fate decisions during vertebrate development', *Development*, 140(8), pp. 1807–1818. doi:10.1242/dev.090183.
- He, B., Reguart, N., You, L., Mazieres, J., Xu, Z., Lee, A.Y., *et al.* (2005) 'Blockade of Wnt-1 signaling induces apoptosis in human colorectal cancer cells containing downstream mutations', *Oncogene*, 24(18), pp. 3054–3058. doi:10.1038/sj.onc.1208511.
- He, J., Nguyen, A.T. and Zhang, Y. (2011) 'KDM2b/JHDM1b, an H3K36me2-specific demethylase, is required for initiation and maintenance of acute myeloid leukemia', *Blood*, 117(14), pp. 3869–3880. doi:10.1182/blood-2010-10-312736.
- He, M., Cai, X. and Zeng, Y. (2021) 'MAPK Signaling Pathway was Dysregulated in Acute Myeloid Leukemia with RUNX1 Mutations'. doi:10.21203/RS.3.RS-502740/V1.
- He, W., Tan, R.J., Li, Y., Wang, D., Nie, J., Hou, F.F., *et al.* (2012) 'Matrix metalloproteinase-7 as a surrogate marker predicts renal Wnt/ β -catenin activity in CKD', *Journal of the American Society of Nephrology*, 23(2), pp. 294–304. doi:10.1681/ASN.2011050490.
- Herbst, A., Jurinovic, V., Krebs, S., Thieme, S.E., Blum, H., Göke, B., *et al.* (2014) 'Comprehensive analysis of β -catenin target genes in colorectal carcinoma cell lines with deregulated Wnt/ β -catenin signaling', *BMC Genomics*, 15(1), pp. 1–15. doi:10.1186/1471-2164-15-74.
- Heshmati, Y., Kharazi, S., Türköz, G., Chang, D., Kamali Dolatabadi, E., Boström, J., *et al.* (2018) 'The histone chaperone NAP1L3 is required for haematopoietic stem cell maintenance and differentiation', *Scientific Reports*, 8(1), pp. 1–17. doi:10.1038/s41598-018-29518-z.
- Heuser, M., Freeman, S.D., Ossenkoppele, G.J., Buccisano, F., Hourigan, C.S., Ngai, L.L., *et al.* (2021) '2021 Update on MRD in acute myeloid leukemia: a consensus document from the European LeukemiaNet MRD Working Party', *Blood*, 138(26), pp. 2753–2767. doi:10.1182/BLOOD.2021013626.
- Heuser, M., Thol, F. and Ganser, A. (2016) 'Klonale Hämatopoese von unbestimmtem Potenzial', *Deutsches Arzteblatt International*, 113(18), pp. 317–322. doi:10.3238/arztebl.2016.0317.
- Hilden, J.M., Smith, F.O., Frestedt, J.L., McGlennen, R., Howells, W.B., Sorensen, P.H.B., *et al.* (1997) 'MLL gene rearrangement, cytogenetic 11q23 abnormalities, and expression of the NG2 molecule in infant acute myeloid leukemia', *Blood*, 89(10), pp. 3801–3805.

doi:10.1182/blood.v89.10.3801.

Hirschi, K.K., Nicoli, S. and Walsh, K. (2017) 'Hematopoiesis Lineage Tree Uprooted: Every Cell Is a Rainbow', *Developmental Cell*, 41(1), pp. 7–9. doi:10.1016/j.devcel.2017.03.020.

Ho, T.C., LaMere, M., Stevens, B.M., Ashton, J.M., Myers, J.R., O'Dwyer, K.M., *et al.* (2016) 'Evolution of acute myelogenous leukemia stem cell properties after treatment and progression', *Blood*, 128(13), pp. 1671–1678. doi:10.1182/blood-2016-02-695312.

Ho, T.C., Kim, H.S., Chen, Y., Li, Y., LaMere, M.W., Chen, C., *et al.* (2021) 'Scaffold-mediated crispr-cas9 delivery system for acute myeloid leukemia therapy', *Science Advances*, 7(21). doi:10.1126/sciadv.abg3217.

Hock, H., Hamblen, M.J., Rooke, H.M., Traver, D., Bronson, R.T., Cameron, S., *et al.* (2003) 'Intrinsic requirement for zinc finger transcription factor Gfi-1 in neutrophil differentiation', *Immunity*, 18(1), pp. 109–120. doi:10.1016/S1074-7613(02)00501-0.

Holmes, T., O'Brien, T.A., Knight, R., Lindeman, R., Shen, S., Song, E., *et al.* (2008) 'Glycogen Synthase Kinase-3 β Inhibition Preserves Hematopoietic Stem Cell Activity and Inhibits Leukemic Cell Growth', *Stem Cells*, 26(5), pp. 1288–1297. doi:10.1634/stemcells.2007-0600.

Holtshcke, T., Löhler, J., Kanno, Y., Fehr, T., Giese, N., Rosenbauer, F., *et al.* (1996) 'Immunodeficiency and chronic myelogenous leukemia-like syndrome in mice with a targeted mutation of the ICSBP gene', *Cell*, 87(2), pp. 307–317. doi:10.1016/S0092-8674(00)81348-3.

Hong, M., Wu, J., Ma, L., Han, X., Lu, T., Wang, Z., *et al.* (2021) 'Inflammation-related genes S100s, RNASE3, and CYBB and risk of leukemic transformation in patients with myelodysplastic syndrome with myelofibrosis', *Biomarker Research*, 9(1), p. 53. doi:10.1186/s40364-021-00304-w.

Hopkins, G.L., Robinson, A.J., Hole, P.S., Darley, R.L. and Tonks, A. (2014) 'Analysis of ROS-Responsive Genes in Mutant RAS Expressing Hematopoietic Progenitors Identifies the Glycolytic Pathway As a Major Target Promoting Both Proliferation and Survival', *Blood*, 124(21), pp. 2210–2210. doi:10.1182/blood.v124.21.2210.2210.

Horst, D., Chen, J., Morikawa, T., Ogino, S., Kirchner, T. and Shivdasani, R.A. (2012) 'Differential WNT activity in colorectal cancer confers limited tumorigenic potential and is regulated by MAPK signaling', *Cancer Research*, 72(6), pp. 1547–1556. doi:10.1158/0008-5472.CAN-11-3222.

Hosen, N., Park, C.Y., Tatsumi, N., Oji, Y., Sugiyama, H., Gramatzki, M., *et al.* (2007) 'CD96 is a leukemic stem cell-specific marker in human acute myeloid leukemia', *Proceedings of the National Academy of Sciences of the United States of America*, 104(26), pp. 11008–11013. doi:10.1073/pnas.0704271104.

Hou, H.A., Kuo, Y.Y., Liu, C.Y., Lee, M.C., Tang, J.L., Chen, C.Y., *et al.* (2011) 'Distinct association between aberrant methylation of Wnt inhibitors and genetic alterations in acute myeloid leukaemia', *British Journal of Cancer*, 105(12), pp. 1927–1933. doi:10.1038/bjc.2011.471.

Hsieh, E.M., Scherer, L.D. and Rouse, R.H. (2020) 'Replacing CAR-T cell resistance with persistence by changing a single residue', *Journal of Clinical Investigation*, 130(6), pp. 2806–2808. doi:10.1172/JCI136872.

Hsu, P.D., Lander, E.S. and Zhang, F. (2014) 'Development and applications of CRISPR-Cas9 for genome engineering', *Cell*, 157(6), pp. 1262–1278. doi:10.1016/j.cell.2014.05.010.

Hu, S., Zhang, M., Wu, S., Wu, D., Ashwani, N., Pan, J., *et al.* (2013) 'High Transcription Levels Of S100A8 and S100A9 In Acute Myeloid Leukemia Are Predictors For Poor Overall Survival', *Blood*, 122(21), pp. 2610–2610. doi:10.1182/blood.v122.21.2610.2610.

Hu, T. and Li, C. (2010) 'Convergence between Wnt- β -catenin and EGFR signaling in cancer', *Molecular Cancer*, 9, p. 236. doi:10.1186/1476-4598-9-236.

Hu, Y., Chen, Y., Douglas, L. and Li, S. (2009) ' β -Catenin is essential for survival of leukemic stem cells insensitive to kinase inhibition in mice with BCR-ABL-induced chronic myeloid leukemia', *Leukemia*, 23(1), pp. 109–116. doi:10.1038/leu.2008.262.

- Huang, R., Liao, X. and Li, Q. (2017) 'Identification of key pathways and genes in β -TP53 mutation acute myeloid leukemia: evidence from bioinformatics analysis', *OncoTargets and Therapy*, 11, pp. 163–173. doi:10.2147/OTT.S156003.
- Huang, S.M.A., Mishina, Y.M., Liu, S., Cheung, A., Stegmeier, F., Michaud, G.A., *et al.* (2009) 'Tankyrase inhibition stabilizes axin and antagonizes Wnt signalling', *Nature*, 461(7264), pp. 614–620. doi:10.1038/nature08356.
- Huber, O., Korn, R., McLaughlin, J., Ohsugi, M., Herrmann, B.G. and Kemler, R. (1996) 'Nuclear localization of β -catenin by interaction with transcription factor LEF-1', *Mechanisms of Development*, 59(1), pp. 3–10. doi:10.1016/0925-4773(96)00597-7.
- Hudson, C.D., Sayan, A.E., Melino, G., Knight, R.A., Latchman, D.S. and Budhram-Mahadeo, V. (2008) 'Brn-3a/POU4F1 interacts with and differentially affects p73-mediated transcription', *Cell Death and Differentiation*, 15(8), pp. 1266–1278. doi:10.1038/cdd.2008.45.
- Hultmark, S., Baudet, A., Schmiderer, L., Prabhala, P., Palma-Tortosa, S., Sandén, C., *et al.* (2021) 'Combinatorial molecule screening identified a novel diterpene and the BET inhibitor CPI-203 as differentiation inducers of primary acute myeloid leukemia cells', *Haematologica*, 106(10), p. 2566. doi:10.3324/HAEMATOL.2020.249177.
- Hung, T.-H., Hsu, S.-C., Cheng, C.-Y., Choo, K.-B., Tseng, C.-P., Chen, T.-C., *et al.* (2014) 'Wnt5A regulates ABCB1 expression in multidrug-resistant cancer cells through activation of the non-canonical PKA/ β -catenin pathway.', *Oncotarget*, 5(23), pp. 12273–12290. doi:10.18632/oncotarget.2631.
- Huntly, B.J.P., Shigematsu, H., Deguchi, K., Lee, B.H., Mizuno, S., Duclos, N., *et al.* (2004) 'MOZ-TIF2, but not BCR-ABL, confers properties of leukemic stem cells to committed murine hematopoietic progenitors', *Cancer cell*, 6(6), pp. 587–596. doi:10.1016/J.CCR.2004.10.015.
- Hwang, S.M. (2020) 'Classification of acute myeloid leukemia', *Blood Research*, 55(S1), pp. 1–4. doi:10.5045/br.2020.S001.
- Hwang, S.Y., Deng, X., Byun, S., Lee, C., Lee, S.J., Suh, H., *et al.* (2016) 'Direct Targeting of β -Catenin by a Small Molecule Stimulates Proteasomal Degradation and Suppresses Oncogenic Wnt/ β -Catenin Signaling', *Cell Reports*, 16(1), pp. 28–36. doi:10.1016/J.CELREP.2016.05.071.
- Hyodoh, F. (1987) 'Effects of retinoic acid on the differentiation of THP-1 cell lines containing aneuploid or diploid chromosomes.', *Cell structure and function*, 12(3), pp. 225–242. doi:10.1247/csf.12.225.
- Ichikawa, M., Asai, T., Saito, T., Yamamoto, G., Seo, S., Yamazaki, I., *et al.* (2004) 'AML-1 is required for megakaryocytic maturation and lymphocytic differentiation, but not for maintenance of hematopoietic stem cells in adult hematopoiesis', *Nature Medicine*, 10(3), pp. 299–304. doi:10.1038/nm997.
- Ihle, J.N. (1992) 'Interleukin-3 and hematopoiesis', *Chemical Immunology*, 51, pp. 65–106. doi:10.1159/000420755.
- Ilieva, K.M., Cheung, A., Mele, S., Chiaruttini, G., Crescioli, S., Griffin, M., *et al.* (2018) 'Chondroitin sulfate proteoglycan 4 and its potential as an antibody immunotherapy target across different tumor types', *Frontiers in Immunology*, 8(JAN), p. 1911. doi:10.3389/fimmu.2017.01911.
- Ilyas, A.M., Ahmad, S., Faheem, M., Naseer, M.I., Kumosani, T.A., Al-Qahtani, M.H., *et al.* (2015) 'Next Generation Sequencing of Acute Myeloid Leukemia: Influencing Prognosis', *BMC Genomics*, 16(1), p. S5. doi:10.1186/1471-2164-16-S1-S5.
- Imai, T., Tanaka, H., Hamazaki, Y. and Minato, N. (2019) 'Rap1 signal modulators control the maintenance of hematopoietic progenitors in bone marrow and adult long-term hematopoiesis', *Cancer science*, 110(4), pp. 1317–1330. doi:10.1111/CAS.13974.
- In't Hout, F.E.M., van der Reijden, B.A., Monteferrario, D., Jansen, J.H. and Huls, G. (2014) 'High expression of transcription factor 4 (TCF4) is an independent adverse prognostic factor in acute myeloid leukemia that could guide treatment decisions', *Haematologica*, 99(12), pp. e257–e259.

doi:10.3324/haematol.2014.110437.

Isenberg, J.S., Maxhimer, J.B., Hyodo, F., Pendrak, M.L., Ridnour, L.A., DeGraff, W.G., *et al.* (2008) 'Thrombospondin-1 and CD47 limit cell and tissue survival of radiation injury', *American Journal of Pathology*, 173(4), pp. 1100–1112. doi:10.2353/ajpath.2008.080237.

Ishida, D., Kometani, K., Yang, H., Kakugawa, K., Masuda, K., Iwai, K., *et al.* (2003) 'Myeloproliferative stem cell disorders by deregulated Rap1 activation in SPA-1-deficient mice', *Cancer Cell*, 4(1), pp. 55–65. doi:10.1016/S1535-6108(03)00163-6.

Ishikawa, J., Taniguchi, T., Takeshita, A. and Maekawa, M. (2005) 'Increased creatine kinase BB activity and CKB mRNA expression in patients with hematologic disorders: Relation to methylation status of the CKB promoter', *Clinica Chimica Acta*, 361(1–2), pp. 135–140. doi:10.1016/j.cccn.2005.05.028.

Ishino, Y., Krupovic, M. and Forterre, P. (2018) 'History of CRISPR-Cas from encounter with a mysterious repeated sequence to genome editing technology', *Journal of Bacteriology*, 200(7), pp. e00580-17. doi:10.1128/JB.00580-17.

Itatani, Y., Kawada, K. and Sakai, Y. (2019) 'Transforming Growth Factor- β Signaling Pathway in Colorectal Cancer and Its Tumor Microenvironment', *International journal of molecular sciences*, 20(23), p. 5822. doi:10.3390/ijms20235822.

Ito, K., Lim, A.C.B., Salto-Tellez, M., Motoda, L., Osato, M., Chuang, L.S.H., *et al.* (2008) 'RUNX3 Attenuates β -Catenin/T Cell Factors in Intestinal Tumorigenesis', *Cancer Cell*, 14(3), pp. 226–237. doi:10.1016/j.ccr.2008.08.004.

Ito, K., Chuang, L.S.H., Ito, T., Chang, T.L., Fukamachi, H., Saltotellez, M., *et al.* (2011) 'Loss of Runx3 is a key event in inducing precancerous state of the stomach', *Gastroenterology*, 140(5). doi:10.1053/j.gastro.2011.01.043.

Ito, M., Kawa, Y., Ono, H., Okura, M., Baba, T., Kubota, Y., *et al.* (1999) 'Removal of stem cell factor or addition of monoclonal anti-c-KIT antibody induces apoptosis in murine melanocyte precursors', *Journal of Investigative Dermatology*, 112(5), pp. 796–801. doi:10.1046/j.1523-1747.1999.00552.x.

Ivanovs, A., Rybtsov, S., Ng, E.S., Stanley, E.G., Elefanty, A.G. and Medvinsky, A. (2017) 'Human haematopoietic stem cell development: From the embryo to the dish', *Development (Cambridge)*, 144(13), pp. 2323–2337. doi:10.1242/dev.134866.

Jackson, A., Vayssière, B., Garcia, T., Newell, W., Baron, R., Roman-Roman, S., *et al.* (2005) 'Gene array analysis of Wnt-regulated genes in C3H10T1/2 cells', *Bone*, 36(4), pp. 585–598. doi:10.1016/j.bone.2005.01.007.

Jaitin, D.A., Weiner, A., Yofe, I., Lara-Astiaso, D., Keren-Shaul, H., David, E., *et al.* (2016) 'Dissecting Immune Circuits by Linking CRISPR-Pooled Screens with Single-Cell RNA-Seq.', *Cell*, 167(7), pp. 1883-1896.e15. doi:10.1016/j.cell.2016.11.039.

James, R.G., Davidson, K.C., Bosch, K.A., Biechele, T.L., Robin, N.C., Taylor, R.J., *et al.* (2012) 'WIKI4, a Novel Inhibitor of Tankyrase and Wnt/ β -Catenin Signaling', *PLoS ONE*. Edited by E. Morrisey, 7(12), p. e50457. doi:10.1371/journal.pone.0050457.

Jamieson, C., Sharma, M. and Henderson, B.R. (2014) 'Targeting the β -catenin nuclear transport pathway in cancer', *Seminars in Cancer Biology*, 27, pp. 20–29. doi:10.1016/j.semcancer.2014.04.012.

Jeannot, G., Scheller, M., Scarpellino, L., Duboux, S., Gardiol, N., Back, J., *et al.* (2008a) 'Long-term, multilineage hematopoiesis occurs in the combined absence of β -catenin and γ -catenin', *Blood*, 111(1), pp. 142–149. doi:10.1182/blood-2007-07-102558.

Jeannot, G., Scheller, M., Scarpellino, L., Duboux, S., Gardiol, N., Back, J., *et al.* (2008b) 'Long-term, multilineage hematopoiesis occurs in the combined absence of β -catenin and γ -catenin', *Blood*, 111(1), pp. 142–149. doi:10.1182/blood-2007-07-102558.

- Jeong, W. and Jho, E.H. (2021) 'Regulation of the Low-Density Lipoprotein Receptor-Related Protein LRP6 and Its Association With Disease: Wnt/ β -Catenin Signaling and Beyond', *Frontiers in Cell and Developmental Biology*, 9, p. 2559. doi:10.3389/FCELL.2021.714330/BIBTEX.
- Jeong, W.J., Ro, E.J. and Choi, K.Y. (2018) 'Interaction between Wnt/ β -catenin and RAS-ERK pathways and an anti-cancer strategy via degradations of β -catenin and RAS by targeting the Wnt/ β -catenin pathway', *npj Precision Oncology*, 2(1), pp. 1–10. doi:10.1038/s41698-018-0049-y.
- Jetten, A.M. (2019) 'Emerging Roles of GLI-Similar Krüppel-like Zinc Finger Transcription Factors in Leukemia and Other Cancers', *Trends in Cancer*, 5(9), pp. 547–557. doi:10.1016/j.trecan.2019.07.005.
- Jiang, S., Zhang, M., Sun, J. and Yang, X. (2018) 'Casein kinase 1 α : Biological mechanisms and theranostic potential', *Cell Communication and Signaling*, 16(1), pp. 1–24. doi:10.1186/s12964-018-0236-z.
- Jiang, X., Tan, J., Li, J., Kivimäe, S., Yang, X., Zhuang, L., *et al.* (2008) 'DACT3 Is an Epigenetic Regulator of Wnt/ β -Catenin Signaling in Colorectal Cancer and Is a Therapeutic Target of Histone Modifications', *Cancer Cell*, 13(6), pp. 529–541. doi:10.1016/j.ccr.2008.04.019.
- Jiang, X., Mak, P.Y., Mu, H., Tao, W., Mak, D.H., Kornblau, S., *et al.* (2018a) 'Disruption of wnt/ β -catenin exerts antileukemia activity and synergizes with flt3 inhibition in flt3-mutant acute myeloid leukemia', *Clinical Cancer Research*, 24(10), pp. 2417–2429. doi:10.1158/1078-0432.CCR-17-1556.
- Jiang, X., Mak, P.Y., Mu, H., Tao, W., Mak, D.H., Kornblau, S., *et al.* (2018b) 'Disruption of wnt/ β -catenin exerts antileukemia activity and synergizes with flt3 inhibition in flt3-mutant acute myeloid leukemia', *Clinical Cancer Research*, 24(10), pp. 2417–2429. doi:10.1158/1078-0432.CCR-17-1556.
- Jiang, Y., Li, Y., Cheng, J., Ma, J., Li, Q. and Pang, T. (2020) 'Upregulation of AKR1C1 in mesenchymal stromal cells promotes the survival of acute myeloid leukaemia cells', *British Journal of Haematology*, 189(4), pp. 694–706. doi:10.1111/bjh.16253.
- Jin, L., Hope, K.J., Zhai, Q., Smadja-Joffe, F. and Dick, J.E. (2006) 'Targeting of CD44 eradicates human acute myeloid leukemic stem cells', *Nature Medicine*, 12(10), pp. 1167–1174. doi:10.1038/nm1483.
- Joberty, G., Fälth-Savitski, M., Paulmann, M., Bösche, M., Doce, C., Cheng, A.T., *et al.* (2020) 'A Tandem Guide RNA-Based Strategy for Efficient CRISPR Gene Editing of Cell Populations with Low Heterogeneity of Edited Alleles', *The CRISPR Journal*, 3(2), p. 123. doi:10.1089/CRISPR.2019.0064.
- Johnson, R.W., Merkel, A.R., Page, J.M., Ruppender, N.S., Guelcher, S.A. and Sterling, J.A. (2014) 'Wnt signaling induces gene expression of factors associated with bone destruction in lung and breast cancer', *Clinical and Experimental Metastasis*, 31(8), pp. 945–959. doi:10.1007/s10585-014-9682-1.
- Johnson, V., Volikos, E., Halford, S.E., Sadat, E.T.E., Popat, S., Talbot, I., *et al.* (2005) 'Exon 3 β -catenin mutations are specifically associated with colorectal carcinomas in hereditary non-polyposis colorectal cancer syndrome', *Gut*, 54(2), pp. 264–267. doi:10.1136/gut.2004.048132.
- Jones, C.L., Inguva, A. and Jordan, C.T. (2021) 'Targeting Energy Metabolism in Cancer Stem Cells: Progress and Challenges in Leukemia and Solid Tumors', *Cell Stem Cell*, 28(3), pp. 378–393. doi:10.1016/J.STEM.2021.02.013.
- Jordan, C.T. (2007) 'The leukemic stem cell', *Best Practice and Research in Clinical Haematology*, 20(1), pp. 13–18. doi:10.1016/j.beha.2006.10.005.
- Jothimani, G., Di Liddo, R., Pathak, S., Piccione, M., Sriramulu, S. and Banerjee, A. (2020) 'Wnt signaling regulates the proliferation potential and lineage commitment of human umbilical cord derived mesenchymal stem cells', *Molecular biology reports*, 47(2), pp. 1293–1308. doi:10.1007/S11033-019-05232-5.
- Ju, X., Ishikawa, T. o., Naka, K., Ito, K., Ito, Y. and Oshima, M. (2014) 'Context-dependent activation of Wnt signaling by tumor suppressor RUNX3 in gastric cancer cells', *Cancer Science*, 105(4), pp. 418–424. doi:10.1111/cas.12356.

- Juliusson, G., Antunovic, P., Derolf, Å., Lehmann, S., Möllgård, L., Stockelberg, D., *et al.* (2009) 'Age and acute myeloid leukemia: Real world data on decision to treat and outcomes from the Swedish Acute Leukemia Registry', *Blood*, 113(18), pp. 4179–4187. doi:10.1182/blood-2008-07-172007.
- Jung, R.E., Cochran, D.L., Domken, O., Seibl, R., Jones, A.A., Buser, D., *et al.* (2007) 'The effect of matrix bound parathyroid hormone on bone regeneration', *Clinical Oral Implants Research*, 18(3), pp. 319–325. doi:10.1111/j.1600-0501.2007.01342.x.
- Jung, Y.S. and Park, J. Il (2020) 'Wnt signaling in cancer: therapeutic targeting of Wnt signaling beyond β -catenin and the destruction complex', *Experimental and Molecular Medicine*, 52(2), pp. 183–191. doi:10.1038/s12276-020-0380-6.
- Jutzi, J.S., Basu, T., Pellmann, M., Kaiser, S., Steinemann, D., Sanders, M.A., *et al.* (2019) 'Altered NFE2 activity predisposes to leukemic transformation and myelosarcoma with AML-specific aberrations', *Blood*, 133(16), pp. 1766–1777. doi:10.1182/blood-2018-09-875047.
- Kadekar, D., Kale, V. and Limaye, L. (2015) 'Differential ability of MSCs isolated from placenta and cord as feeders for supporting ex vivo expansion of umbilical cord blood derived CD34(+) cells.', *Stem cell research & therapy*, 6, p. 201. doi:10.1186/s13287-015-0194-y.
- Kahn, M. (2014) 'Can we safely target the WNT pathway?', *Nature Reviews Drug Discovery*, 13(7), pp. 513–532. doi:10.1038/nrd4233.
- Kajiguchi, T., Chung, E.J., Lee, S., Stine, A., Kiyoi, H., Naoe, T., *et al.* (2007) 'FLT3 regulates β -catenin tyrosine phosphorylation, nuclear localization, and transcriptional activity in acute myeloid leukemia cells', *Leukemia*, 21(12), pp. 2476–2484. doi:10.1038/sj.leu.2404923.
- Kamga, P.T., Collo, G.D., Cassaro, A., Bazzoni, R., Delfino, P., Adamo, A., *et al.* (2020) 'Small molecule inhibitors of microenvironmental wnt/ β -catenin signaling enhance the chemosensitivity of acute myeloid leukemia', *Cancers*, 12(9), pp. 1–16. doi:10.3390/cancers12092696.
- Kaneko, K., Xu, P., Cordonier, E.L., Chen, S.S., Ng, A., Xu, Y., *et al.* (2016) 'Neuronal Rap1 Regulates Energy Balance, Glucose Homeostasis, and Leptin Actions', *Cell Reports*, 16(11), pp. 3003–3015. doi:10.1016/j.celrep.2016.08.039.
- Kang, J.W., Kim, Y., Lee, Y., Myung, K., Kim, Y.H. and Oh, C.K. (2021) 'AML poor prognosis factor, TPD52, is associated with the maintenance of haematopoietic stem cells through regulation of cell proliferation', *Journal of Cellular Biochemistry*, 122(3–4), pp. 403–412. doi:10.1002/jcb.29869.
- Kang, X., Cui, C., Wang, C., Wu, G., Chen, H., Lu, Z., *et al.* (2018) 'CAMKs support development of acute myeloid leukemia', *Journal of Hematology and Oncology*, 11(1), pp. 1–12. doi:10.1186/s13045-018-0574-8.
- Kannan, S., Sutphin, R.M., Hall, M.G., Golfman, L.S., Fang, W., Nolo, R.M., *et al.* (2013) 'Notch activation inhibits AML growth and survival: A potential therapeutic approach', *Journal of Experimental Medicine*, 210(2), pp. 321–337. doi:10.1084/jem.20121527.
- Kantarjian, H., Kadia, T., DiNardo, C., Daver, N., Borthakur, G., Jabbour, E., *et al.* (2021) 'Acute myeloid leukemia: current progress and future directions', *Blood Cancer Journal*, 11(2), p. 41. doi:10.1038/s41408-021-00425-3.
- Karjalainen, R., Liu, M., Kumar, A., Parsons, A., Kontro, M., Porkka, K., *et al.* (2017) 'Elevated Expression of the S100A8/S100A9 Complex in AML Correlates with Reduced Sensitivity to the BCL2 Inhibitor Venetoclax', *Blood*, 130(Supplement 1), pp. 298–298. doi:10.1182/blood.V130.Suppl_1.298.298.
- Karjalainen, R., Liu, M., Kumar, A., He, L., Malani, D., Parsons, A., *et al.* (2019) 'Elevated expression of S100A8 and S100A9 correlates with resistance to the BCL-2 inhibitor venetoclax in AML', *Leukemia*, 33(10), pp. 2548–2553. doi:10.1038/s41375-019-0504-y.
- Kassambara, A., Kosinski, M., Biecek, P. and Fabian, S. (2017) 'Package "survminer". In Drawing Survival Curves Using "ggplot2".(R package version 0.3. 1.)', *R package version 0.4.3* [Preprint]. Comprehensive R Archive Network (CRAN). Available at: <https://cran.r->

project.org/package=survminer (Accessed: 21 July 2021).

Kastan, M.B., Schlaffer, E., Russo, J.E., Colvin, O.M., Civin, C.I. and Hilton, J. (1990) 'Direct demonstration of elevated aldehyde dehydrogenase in human hematopoietic progenitor cells', *Blood*, 75(10), pp. 1947–1950. doi:10.1182/blood.v75.10.1947.1947.

Kawaguchi-Ihara, N., Murohashi, I., Nara, N. and Tohda, S. (2008) 'Promotion of the self-renewal capacity of human acute leukemia cells by Wnt3A', *Anticancer Research*, 28(5 A), pp. 2701–2704. Available at: <https://pubmed.ncbi.nlm.nih.gov/19035298/> (Accessed: 27 February 2021).

Kawajiri, A., Itoh, N., Fukata, M., Nakagawa, M., Yamaga, M., Iwamatsu, A., *et al.* (2000) 'Identification of a novel β -catenin-interacting protein', *Biochemical and Biophysical Research Communications*, 273(2), pp. 712–717. doi:10.1006/bbrc.2000.3002.

Kawane, T., Komori, H., Liu, W., Moriishi, T., Miyazaki, T., Mori, M., *et al.* (2014) 'Dlx5 and Mef2 regulate a novel Runx2 enhancer for osteoblast-specific expression', *Journal of Bone and Mineral Research*, 29(9), pp. 1960–1969. doi:10.1002/jbmr.2240.

Kelly, L.M. and Gilliland, D.G. (2002) 'Genetics of myeloid leukemias', *Annual Review of Genomics and Human Genetics*, 3, pp. 179–198. doi:10.1146/annurev.genom.3.032802.115046.

Keyes, J., Ganesan, A., Molinar-Inglis, O., Hamidzadeh, A., Zhang, Jinfan, Ling, M., *et al.* (2020) 'Signaling diversity enabled by rap1-regulated plasma membrane ERK with distinct temporal dynamics', *eLife*, 9. doi:10.7554/ELIFE.57410.

Khwaja, A., Bjorkholm, M., Gale, R.E., Levine, R.L., Jordan, C.T., Ehninger, G., *et al.* (2016) 'Acute myeloid leukaemia', *Nature Reviews Disease Primers*, 2. doi:10.1038/nrdp.2016.10.

Kim, B.-K., Yoo, H.-I., Kim, I., Park, J. and Kim Yoon, S. (2015) 'FZD6 expression is negatively regulated by miR-199a-5p in human colorectal cancer', *BMB reports*, 48(6), pp. 360–366. doi:10.5483/bmbrep.2015.48.6.031.

Kim, C. (2010) 'Homeostatic and pathogenic extramedullary hematopoiesis', *Journal of Blood Medicine*, 1, p. 13. doi:10.2147/jbm.s7224.

Kim, H., Ishidate, T., Ghanta, K.S., Seth, M., Conte, D., Shirayama, M., *et al.* (2014) 'A co-CRISPR strategy for efficient genome editing in *Caenorhabditis elegans*', *Genetics*, 197(4), pp. 1069–1080. doi:10.1534/GENETICS.114.166389.

Kim, J.-Y., Lee, H.-Y., Park, K.-K., Choi, Y.-K., Nam, J.-S. and Hong, I.-S. (2016) 'CWP232228 targets liver cancer stem cells through Wnt/ β -catenin signaling: a novel therapeutic approach for liver cancer treatment.', *Oncotarget*, 7(15), pp. 20395–20409. doi:10.18632/oncotarget.7954.

Kim, J.S., Crooks, H., Foxworth, A. and Waldman, T. (2002) 'Proof-of-principle: Oncogenic β -catenin is a valid molecular target for the development of pharmacological inhibitors', *Molecular Cancer Therapeutics*, 1(14), pp. 1355–1359. Available at: <http://www.ncbi.nlm.nih.gov/pubmed/12516970> (Accessed: 21 April 2020).

Kim, Y., Thanendrarajan, S. and Schmidt-Wolf, I.G.H. (2011) 'Wnt/ β -Catenin: A New Therapeutic Approach to Acute Myeloid Leukemia', *Leukemia Research and Treatment*, 2011, pp. 1–4. doi:10.4061/2011/428960.

Kirstetter, P., Anderson, K., Porse, B.T., Jacobsen, S.E.W. and Nerlov, C. (2006) 'Activation of the canonical Wnt pathway leads to loss of hematopoietic stem cell repopulation and multilineage differentiation block', *Nature Immunology*, 7(10), pp. 1048–1056. doi:10.1038/ni1381.

Kirtane, K. and Lee, S.J. (2017) 'Racial and ethnic disparities in hematologic malignancies', *Blood*, 130(15), pp. 1699–1705. doi:10.1182/blood-2017-04-778225.

Kirton, H.M., Al-Owais, M., Peers, C. and Steele, D.S. (2018) 'The EPAC2 Inhibitor ESI-05 Prolongs the Action Potential and Increases Susceptibility to EAD Arrhythmias', *Biophysical Journal*, 114(3), p. 140a. doi:10.1016/j.bpj.2017.11.788.

Kitsos, C.M., Sankar, U., Illario, M., Colomer-Font, J.M., Duncan, A.W., Ribar, T.J., *et al.* (2005) 'Calmodulin-dependent protein kinase IV regulates hematopoietic stem cell maintenance', *Journal of*

Biological Chemistry, 280(39), pp. 33101–33108. doi:10.1074/jbc.M505208200.

Kiyose, H., Morita, K., Maeda, S., Suzuki, K., Adachi, S. and Kamikubo, Y. (2016) ‘Deciphering the Function of KLF4 as a Differentiation Inducer in Hematologic Malignancies’, *Blood*, 128(22), p. 1546. doi:10.1182/blood.V128.22.1546.1546.

Klymkowsky, M.W., Williams, B.O., Barish, G.D., Varmus, H.E. and Vourgourakis, Y.E. (1999) ‘Membrane-anchored plakoglobins have multiple mechanisms of action in Wnt signaling’, *Molecular Biology of the Cell*, 10(10), pp. 3151–3169. doi:10.1091/mbc.10.10.3151.

Knapp, D.J.H.F., Hammond, C.A., Hui, T., Van Loenhout, M.T.J., Wang, F., Aghaeepour, N., *et al.* (2018) ‘Single-cell analysis identifies a CD33 + subset of human cord blood cells with high regenerative potential’, *Nature Cell Biology*, 20(6), pp. 710–720. doi:10.1038/s41556-018-0104-5.

Knippschild, U., Krüger, M., Richter, J., Xu, P., Balbina García-Reyes, Peifer, C., *et al.* (2014) ‘The CK1 family: Contribution to cellular stress response and its role in carcinogenesis’, *Frontiers in Oncology*, 4 MAY. doi:10.3389/fonc.2014.00096.

Knorr, K.L.B. and Goldberg, A.D. (2020) ‘Leukemia stem cell gene expression signatures contribute to acute myeloid leukemia risk stratification’, *Haematologica*, 105(3), pp. 533–536. doi:10.3324/haematol.2019.241117.

Knudsen, K.A., Soler, A.P., Johnson, K.R. and Wheelock, M.J. (1995) ‘Interaction of α -actinin with the cadherin/catenin cell-cell adhesion complex via α -catenin’, *Journal of Cell Biology*, 130(1), pp. 67–77. doi:10.1083/jcb.130.1.67.

Koch, U., Wilson, A., Cobas, M., Kemler, R., MacDonald, H.R. and Radtke, F. (2008a) ‘Simultaneous loss of β - and γ -catenin does not perturb hematopoiesis or lymphopoiesis’, *Blood*, 111(1), pp. 160–164. doi:10.1182/blood-2007-07-099754.

Koch, U., Wilson, A., Cobas, M., Kemler, R., MacDonald, H.R. and Radtke, F. (2008b) ‘Simultaneous loss of β - and γ -catenin does not perturb hematopoiesis or lymphopoiesis’, *Blood*, 111(1), pp. 160–164. doi:10.1182/blood-2007-07-099754.

Kockeritz, L., Doble, B., Patel, S. and Woodgett, J. (2012) ‘Glycogen Synthase Kinase-3 - An Overview of An Over-Achieving Protein Kinase’, *Current Drug Targets*, 7(11), pp. 1377–1388. doi:10.2174/1389450110607011377.

Kode, A., Manavalan, J.S., Mosialou, I., Bhagat, G., Rathinam, C. V., Luo, N., *et al.* (2014) ‘Leukaemogenesis induced by an activating β -catenin mutation in osteoblasts’, *Nature*, 506(7487), pp. 240–244. doi:10.1038/nature12883.

Komiya, Y. and Habas, R. (2008) ‘Wnt signal transduction pathways’, *Organogenesis*, 4(2), pp. 68–75. doi:10.4161/org.4.2.5851.

Koppula, P., Zhang, Y., Zhuang, L. and Gan, B. (2018) ‘Amino acid transporter SLC7A11/xCT at the crossroads of regulating redox homeostasis and nutrient dependency of cancer’, *Cancer communications (London, England)*, 38(1), p. 12. doi:10.1186/s40880-018-0288-x.

Koreth, J., Schlenk, R., Kopecky, K.J., Honda, S., Sierra, J., Djulbegovic, B.J., *et al.* (2009) ‘Allogeneic stem cell transplantation for acute myeloid leukemia in first complete remission: Systematic review and meta-analysis of prospective clinical trials’, *JAMA - Journal of the American Medical Association*, 301(22), pp. 2349–2361. doi:10.1001/jama.2009.813.

Kosuru, R. and Chrzanowska, M. (2020) ‘Integration of rap1 and calcium signaling’, *International Journal of Molecular Sciences*, 21(5). doi:10.3390/ijms21051616.

De Kouchkovsky, I. and Abdul-Hay, M. (2016) ‘“Acute myeloid leukemia: A comprehensive review and 2016 update”’, *Blood Cancer Journal*, 6(7), pp. e441–e441. doi:10.1038/bcj.2016.50.

Koumakis, L., Kanterakis, A., Kartsaki, E., Chatzimina, M., Zervakis, M., Tsiknakis, M., *et al.* (2016) ‘MinePath: Mining for Phenotype Differential Sub-paths in Molecular Pathways’, *PLoS Computational Biology*, 12(11), p. e1005187. doi:10.1371/journal.pcbi.1005187.

Koury, M.J. and Bondurant, M.C. (1990) ‘Erythropoietin retards DNA breakdown and prevents

- programmed death in erythroid progenitor cells', *Science*, 248(4953), pp. 378–381. doi:10.1126/science.2326648.
- Krivtsov, A. V., Twomey, D., Feng, Z., Stubbs, M.C., Wang, Y., Faber, J., *et al.* (2006) 'Transformation from committed progenitor to leukaemia stem cell initiated by MLL-AF9', *Nature*, 442(7104), pp. 818–822. doi:10.1038/NATURE04980.
- Krupka, C., Kufer, P., Kischel, R., Zugmaier, G., Bögeholz, J., Köhnke, T., *et al.* (2014) 'CD33 target validation and sustained depletion of AML blasts in long-term cultures by the bispecific T-cell-engaging antibody AMG 330', *Blood*, 123(3), pp. 356–365. doi:10.1182/blood-2013-08-523548.
- Krupka, C., Lichtenegger, F.S., Köhnke, T., Bögeholz, J., Bücklein, V., Roiss, M., *et al.* (2017) 'Targeting CD157 in AML using a novel, Fc-engineered antibody construct', *Oncotarget*, 8(22), pp. 35707–35717. doi:10.18632/oncotarget.16060.
- Kulkarni, R. and Kale, V. (2020) 'Physiological Cues Involved in the Regulation of Adhesion Mechanisms in Hematopoietic Stem Cell Fate Decision', *Frontiers in Cell and Developmental Biology*, 8, p. 611. doi:10.3389/FCELL.2020.00611/BIBTEX.
- Kumar, B. (2021) 'Harnessing the Metabolic Vulnerabilities of Leukemia Stem Cells to Eradicate Acute Myeloid Leukemia', *Frontiers in Oncology*, 11, p. 766. doi:10.3389/FONC.2021.632789/BIBTEX.
- Kurbel, S., Radić, R., Kotromanović, Ž., Pušeljić, Ž. and Kratošil, B. (2003) 'A calcium homeostasis model: Orchestration of fast acting PTH and calcitonin with slow calcitriol', *Medical Hypotheses*, 61(3), pp. 346–350. doi:10.1016/S0306-9877(03)00107-5.
- Kusnadi, E.P., Trigos, A.S., Cullinane, C., Goode, D.L., Larsson, O., Devlin, J.R., *et al.* (2020) 'Reprogrammed mRNA translation drives resistance to therapeutic targeting of ribosome biogenesis', *The EMBO Journal*, 39(21), p. e105111. doi:10.15252/EMBJ.2020105111.
- Kutmon, M., Riutta, A., Nunes, N., Hanspers, K., Willighagen, E.L., Bohler, A., *et al.* (2016) 'WikiPathways: Capturing the full diversity of pathway knowledge', *Nucleic Acids Research*, 44(D1), pp. D488–D494. doi:10.1093/nar/gkv1024.
- Kwong, L.N. and Dove, W.F. (2009) 'APC and its modifiers in colon cancer', *Advances in Experimental Medicine and Biology*, 656, pp. 85–106. doi:10.1007/978-1-4419-1145-2_8.
- Laco, F., Woo, T.L., Zhong, Q., Szmyd, R., Ting, S., Khan, F.J., *et al.* (2018) 'Unraveling the Inconsistencies of Cardiac Differentiation Efficiency Induced by the GSK3 β Inhibitor CHIR99021 in Human Pluripotent Stem Cells', *Stem Cell Reports*, 10(6), pp. 1851–1866. doi:10.1016/J.STEMCR.2018.03.023.
- Ladines-Castro, W., Barragán-Ibañez, G., Luna-Pérez, M.A., Santoyo-Sánchez, A., Collazo-Jaloma, J., Mendoza-García, E., *et al.* (2016) 'Morphology of leukaemias', *Revista Médica del Hospital General de México*, 79(2), pp. 107–113. doi:10.1016/j.hgmx.2015.06.007.
- Lambert, S.A., Jolma, A., Campitelli, L.F., Das, P.K., Yin, Y., Albu, M., *et al.* (2018) 'The Human Transcription Factors', *Cell*, 172(4), pp. 650–665. doi:10.1016/j.cell.2018.01.029.
- Lamers, C., Plüss, C.J. and Ricklin, D. (2021) 'The Promiscuous Profile of Complement Receptor 3 in Ligand Binding, Immune Modulation, and Pathophysiology', *Frontiers in Immunology*, 12, p. 1483. doi:10.3389/fimmu.2021.662164.
- Lane, S.W., Wang, Y.J., Lo Celso, C., Ragu, C., Bullinger, L., Sykes, S.M., *et al.* (2011) 'Differential niche and Wnt requirements during acute myeloid leukemia progression', *Blood*, 118(10), pp. 2849–2856. doi:10.1182/blood-2011-03-345165.
- Lansdorp, P.M., Sutherland, H.J. and Eaves, C.J. (1990) 'Selective expression of CD45 isoforms on functional subpopulations of CD34+ hemopoietic cells from human bone marrow', *Journal of Experimental Medicine*, 172(1), pp. 363–366. doi:10.1084/jem.172.1.363.
- Lapidot, T., Sirard, C., Vormoor, J., Murdoch, B., Hoang, T., Caceres-Cortes, J., *et al.* (1994) 'A cell initiating human acute myeloid leukaemia after transplantation into SCID mice', *Nature*, 367(6464),

pp. 645–648. doi:10.1038/367645a0.

Larmonie, N.S.D., Arentsen-Peters, T.C.J.M., Obulkasim, A., Valerio, D., Sonneveld, E., Danen-Van Oorschot, A.A., *et al.* (2018) ‘MN1 overexpression is driven by loss of DNMT3B methylation activity in inv(16) pediatric AML’, *Oncogene*, 37(1), pp. 107–115. doi:10.1038/onc.2017.293.

Laurenti, E. and Göttgens, B. (2018) ‘From haematopoietic stem cells to complex differentiation landscapes’, *Nature*, 553(7689), pp. 418–426. doi:10.1038/nature25022.

Lazarini, M., Machado-Neto, J., Duarte, A.S.S., Pericole, F. V, Favaro, P., Barcellos, K.S.A., *et al.* (2012) ‘BNIP3 Is Downregulated in Myelodysplastic Syndromes and Acute Myeloid Leukemia and Is a Potential Molecular Target for Decitabine’, *Blood*, 120(21), pp. 1708–1708. doi:10.1182/blood.v120.21.1708.1708.

Lecarpentier, Y., Claes, V., Vallée, A. and Hébert, J.L. (2017) ‘Interactions between PPAR Gamma and the Canonical Wnt/Beta-Catenin Pathway in Type 2 Diabetes and Colon Cancer’, *PPAR Research*, 2017. doi:10.1155/2017/5879090.

Lee, E., Salic, A. and Kirschner, M.W. (2001) ‘Physiological regulation of β -catenin stability by Tcf3 and CK1 ϵ ’, *Journal of Cell Biology*, 154(5), pp. 983–993. doi:10.1083/jcb.200102074.

Lee, I.H., Sohn, M., Lim, H.J., Yoon, S., Oh, H., Shin, S., *et al.* (2014) ‘Ahnak functions as a tumor suppressor via modulation of TGF β /Smad signaling pathway’, *Oncogene*, 33(38), pp. 4675–4684. doi:10.1038/onc.2014.69.

Lee, J., Breton, G., Aljoufi, A., Zhou, Y.J., Puhr, S., Nussenzweig, M.C., *et al.* (2015) ‘Clonal analysis of human dendritic cell progenitor using a stromal cell culture’, *Journal of Immunological Methods*, 425, pp. 21–26. doi:10.1016/j.jim.2015.06.004.

Lee, J.H., Faderl, S., Pagel, J.M., Jung, C.W., Yoon, S.S., Pardnani, A.D., *et al.* (2020) ‘Phase 1 study of CWP232291 in patients with relapsed or refractory acute myeloid leukemia and myelodysplastic syndrome’, *Blood Advances*, 4(9), pp. 2032–2043. doi:10.1182/bloodadvances.2019000757.

Lee, M.A., Park, J.H., Rhyu, S.Y., Oh, S.T., Kang, W.K. and Kim, H.N. (2014) ‘Wnt3a expression is associated with MMP-9 expression in primary tumor and metastatic site in recurrent or stage IV colorectal cancer’, *BMC Cancer*, 14(1), pp. 1–7. doi:10.1186/1471-2407-14-125.

Legras, S., Günthert, U., Stauder, R., Curt, F., Oliferenko, S., Kluin-Nelemans, H.C., *et al.* (1998) ‘A Strong Expression of CD44-6v Correlates With Shorter Survival of Patients With Acute Myeloid Leukemia’, *Blood*, 91(9), pp. 3401–3413. doi:10.1182/blood.v91.9.3401.

Lehmann, F.S., Burri, E. and Beglinger, C. (2015) ‘The role and utility of faecal markers in inflammatory bowel disease’, *Therapeutic Advances in Gastroenterology*, 8(1), pp. 23–36. doi:10.1177/1756283X14553384.

Lehmann, M., Vilar, K.D.S.P., Franco, A., Reguly, M.L. and De Andrade, H.H.R. (2004) ‘Activity of topoisomerase inhibitors daunorubicin, idarubicin, and aclarubicin in the *Drosophila* somatic mutation and recombination test’, *Environmental and Molecular Mutagenesis*, 43(4), pp. 250–257. doi:10.1002/em.20023.

Leisch, M., Jansko, B., Zaborsky, N., Greil, R. and Pleyer, L. (2019) ‘Next generation sequencing in AML-on the way to becoming a new standard for treatment initiation and/or modulation?’, *Cancers*, 11(2). doi:10.3390/cancers11020252.

Lento, W., Ito, T., Zhao, C., Harris, J.R., Huang, W., Jiang, C., *et al.* (2014) ‘Loss of β -catenin triggers oxidative stress and impairs hematopoietic regeneration’, *Genes and Development*, 28(9), pp. 995–1004. doi:10.1101/gad.231944.113.

Lesueur, L.L., Mir, L.M. and André, F.M. (2016) ‘Overcoming the Specific Toxicity of Large Plasmids Electrotransfer in Primary Cells In Vitro’, *Molecular Therapy. Nucleic Acids*, 5(3), p. e291. doi:10.1038/MTNA.2016.4.

Lewuillon, C., Laguillaumie, M.-O., Quesnel, B., Idziorek, T., Touil, Y. and Lemonnier, L. (2022)

- 'Put in a Ca²⁺ to Acute Myeloid Leukemia', *Cells*. doi:10.3390/cells11030543.
- Ley, T.J. (2013) 'Genomic and Epigenomic Landscapes of Adult De Novo Acute Myeloid Leukemia', *New England Journal of Medicine*, 368(22), pp. 2059–2074. doi:10.1056/nejmoa1301689.
- Li, G., Su, Q., Liu, H., Wang, D., Zhang, W., Lu, Z., *et al.* (2018) 'Frizzled7 Promotes Epithelial-to-mesenchymal Transition and Stemness Via Activating Canonical Wnt/ β -catenin Pathway in Gastric Cancer.', *International journal of biological sciences*, 14(3), pp. 280–293. doi:10.7150/ijbs.23756.
- Li, H., Liang, J., Wang, J., Han, J., Li, S., Huang, K., *et al.* (2021) 'Mex3a promotes oncogenesis through the RAP1/MAPK signaling pathway in colorectal cancer and is inhibited by hsa-miR-6887-3p.', *Cancer communications (London, England)*, 41(6), pp. 472–491. doi:10.1002/cac2.12149.
- Li, J., Cao, F., Yin, H. liang, Huang, Z. jian, Lin, Z. tao, Mao, N., *et al.* (2020) 'Ferroptosis: past, present and future', *Cell Death and Disease*, 11(2), pp. 1–13. doi:10.1038/s41419-020-2298-2.
- Li, L., Wang, S., Jezierski, A., Moalim-Nour, L., Mohib, K., Parks, R.J., *et al.* (2010) 'A unique interplay between Rap1 and E-cadherin in the endocytic pathway regulates self-renewal of human embryonic stem cells', *Stem cells (Dayton, Ohio)*, 28(2), pp. 247–257. doi:10.1002/STEM.289.
- Li, L.M., Luo, F.J. and Song, X. (2020) 'MicroRNA-370-3p inhibits cell proliferation and induces chronic myelogenous leukemia cell apoptosis by suppressing PDLIM1/Wnt/ β -catenin signaling', *Neoplasma*, 67(3), pp. 509–518. doi:10.4149/neo_2020_190612N506.
- Li, Y., Wang, Jiying, Li, X., Jia, Y., Huai, L., He, K., *et al.* (2014) 'Role of the Wilms' tumor 1 gene in the aberrant biological behavior of leukemic cells and the related mechanisms', *Oncology Reports*, 32(6), pp. 2680–2686. doi:10.3892/OR.2014.3529/HTML.
- Li, Z., Guo, J.R., Chen, Q.Q., Wang, C.Y., Zhang, W.J., Yao, M.C., *et al.* (2017) 'Exploring the antitumor mechanism of high-dose cytarabine through the metabolic perturbations of ribonucleotide and deoxyribonucleotide in human promyelocytic Leukemia HL-60 Cells', *Molecules*, 22(3). doi:10.3390/molecules22030499.
- Liao, Y., Smyth, G.K. and Shi, W. (2019) 'The R package Rsubread is easier, faster, cheaper and better for alignment and quantification of RNA sequencing reads', *Nucleic Acids Research*, 47(8), pp. e47–e47. doi:10.1093/nar/gkz114.
- Liberzon, A., Birger, C., Thorvaldsdóttir, H., Ghandi, M., Mesirov, J.P. and Tamayo, P. (2015) 'The Molecular Signatures Database Hallmark Gene Set Collection', *Cell Systems*, 1(6), pp. 417–425. doi:10.1016/j.cels.2015.12.004.
- Lilien, J. and Balsamo, J. (2005) 'The regulation of cadherin-mediated adhesion by tyrosine phosphorylation/dephosphorylation of β -catenin', *Current Opinion in Cell Biology*, 17(5 SPEC. ISS.), pp. 459–465. doi:10.1016/j.ceb.2005.08.009.
- Lim, J.C., Kania, K.D., Wijesuriya, H., Chawla, S., Sethi, J.K., Pulaski, L., *et al.* (2008) 'Activation of β -catenin signalling by GSK-3 inhibition increases p-glycoprotein expression in brain endothelial cells', *Journal of neurochemistry*, 106(4), p. 1855. doi:10.1111/J.1471-4159.2008.05537.X.
- Lin, C.S., Lim, S.K., D'Agati, V. and Costantini, F. (1996) 'Differential effects of an erythropoietin receptor gene disruption on primitive and definitive erythropoiesis', *Genes and Development*, 10(2), pp. 154–164. doi:10.1101/gad.10.2.154.
- Lin, H. and Zelterman, D. (2002) 'Modeling Survival Data: Extending the Cox Model', *Technometrics*, 44(1), pp. 85–86. doi:10.1198/tech.2002.s656.
- Lin, W., Wang, C., Liu, G., Bi, C., Wang, X., Zhou, Q., *et al.* (2020) 'SLC7A11/xCT in cancer: biological functions and therapeutic implications.', *American journal of cancer research*, 10(10), pp. 3106–3126. Available at: <http://www.ncbi.nlm.nih.gov/pubmed/33163260> <http://www.pubmedcentral.nih.gov/articlerender.fcgi?artid=PMC7642655> (Accessed: 24 July 2021).
- Ling, Y. and Du, Q. (2022) 'FGF10/FGF17 as prognostic and drug response markers in acute myeloid leukemia', *Current Research in Translational Medicine*, 70(1), p. 103316.

doi:10.1016/J.RETRAM.2021.103316.

Liu, G., Zhang, Y. and Zhang, T. (2020) ‘Computational approaches for effective CRISPR guide RNA design and evaluation’, *Computational and Structural Biotechnology Journal*, 18, pp. 35–44. doi:10.1016/J.CSBJ.2019.11.006.

Liu, L.J., Xie, S.X., Chen, Y.T., Xue, J.L., Zhang, C.J. and Zhu, F. (2016) ‘Aberrant regulation of WNT signaling in hepatocellular carcinoma’, *World Journal of Gastroenterology*, 22(33), pp. 7486–7499. doi:10.3748/wjg.v22.i33.7486.

Liu, T., Ivaturi, V., Sabato, P., Gobburu, J.V.S., Greer, J.M., Wright, J.J., *et al.* (2018) ‘Sorafenib Dose Recommendation in Acute Myeloid Leukemia Based on Exposure-FLT3 Relationship’, *Clinical and Translational Science*, 11(4), pp. 435–443. doi:10.1111/cts.12555.

Liu, Y., Zhang, C., Li, Z., Wang, C., Jia, J., Gao, T., *et al.* (2017) ‘Latexin Inactivation Enhances Survival and Long-Term Engraftment of Hematopoietic Stem Cells and Expands the Entire Hematopoietic System in Mice’, *Stem Cell Reports*, 8(4), pp. 991–1004. doi:10.1016/j.stemcr.2017.02.009.

Liu, Y., Wang, G., Zhang, J., Chen, X., Xu, H., Heng, G., *et al.* (2021) ‘CD9, a potential leukemia stem cell marker, regulates drug resistance and leukemia development in acute myeloid leukemia’, *Stem Cell Research and Therapy*, 12(1), pp. 1–13. doi:10.1186/s13287-021-02155-6.

Lo-Coco, F., Avvisati, G., Vignetti, M., Thiede, C., Orlando, S.M., Iacobelli, S., *et al.* (2013) ‘Retinoic Acid and Arsenic Trioxide for Acute Promyelocytic Leukemia’, *New England Journal of Medicine*, 369(2), pp. 111–121. doi:10.1056/nejmoa1300874.

Löcken, H., Clamor, C. and Müller, K. (2018) ‘Napabucasin and Related Heterocycle-Fused Naphthoquinones as STAT3 Inhibitors with Antiproliferative Activity against Cancer Cells’, *Journal of Natural Products*, 81(7), pp. 1636–1644. doi:10.1021/ACS.JNATPROD.8B00247/SUPPL_FILE/NP8B00247_SI_001.PDF.

Logtenberg, M.E.W., Jansen, J.H.M., Raaben, M., Toebes, M., Franke, K., Brandsma, A.M., *et al.* (2019) ‘Glutaminy cyclase is an enzymatic modifier of the CD47- SIRP α axis and a target for cancer immunotherapy’, *Nature Medicine*, 25(4), pp. 612–619. doi:10.1038/s41591-019-0356-z.

Looi, C.-K., Hii, L.-W., Ngai, S.C., Leong, C.-O. and Mai, C.-W. (2020) ‘The Role of Ras-Associated Protein 1 (Rap1) in Cancer: Bad Actor or Good Player?’, *Biomedicines*, 8(9). doi:10.3390/biomedicines8090334.

Löwenberg, B., Suci, S., Archimbaud, E., Haak, H., Stryckmans, P., De Cataldo, R., *et al.* (1998) ‘Mitoxantrone versus daunorubicin in induction-consolidation chemotherapy - The value of low-dose cytarabine for maintenance of remission, and an assessment of prognostic factors in acute myeloid leukemia in the elderly’, *Journal of Clinical Oncology*, 16(3), pp. 872–881. doi:10.1200/JCO.1998.16.3.872.

Lowenberg, B. and Rowe, J.M. (2016) ‘Introduction to the review series on advances in acute myeloid leukemia (AML)’, *Blood*, 127(1), p. 1. doi:10.1182/blood-2015-10-662684.

Lu, J., Chen, S., Tan, H., Huang, Z., Li, B., Liu, L., *et al.* (2021) ‘Eukaryotic initiation factor-2, gamma subunit, suppresses proliferation and regulates the cell cycle via the MAPK/ERK signaling pathway in acute myeloid leukemia’, *Journal of Cancer Research and Clinical Oncology*, 147(11), pp. 3157–3168. doi:10.1007/S00432-021-03712-5/FIGURES/6.

Luis, Tiago C., Weerkamp, F., Naber, B.A.E., Baert, M.R.M., De Haas, E.F.E., Nikolic, T., *et al.* (2009) ‘Wnt3a deficiency irreversibly impairs hematopoietic stem cell self-renewal and leads to defects in progenitor cell differentiation’, *Blood*, 113(3), pp. 546–554. doi:10.1182/blood-2008-06-163774.

Luis, T. C., Weerkamp, F., Naber, B.A.E., Baert, M.R.M., de Haas, E.F.E., Nikolic, T., *et al.* (2009) ‘Wnt3a deficiency irreversibly impairs hematopoietic stem cell self-renewal and leads to defects in progenitor cell differentiation’, *Blood*, 113(3), pp. 546–554. doi:10.1182/blood-2008-06-163774.

Luis, T.C., Naber, B.A.E., Roozen, P.P.C., Brugman, M.H., De Haas, E.F.E., Ghazvini, M., *et al.*

- (2011) 'Canonical wnt signaling regulates hematopoiesis in a dosage-dependent fashion', *Cell Stem Cell*, 9(4), pp. 345–356. doi:10.1016/j.stem.2011.07.017.
- Luis, T.C., Ichii, M., Brugman, M.H., Kincade, P. and Staal, F.J.T. (2012) *Wnt signaling strength regulates normal hematopoiesis and its deregulation is involved in leukemia development*, *Leukemia*. NIH Public Access. doi:10.1038/leu.2011.387.
- Luna-Ulloa, L.B., Hernández-Maqueda, J.G., Castañeda-Patlán, M.C. and Robles-Flores, M. (2011) 'Protein kinase C in Wnt signaling: Implications in cancer initiation and progression', *IUBMB Life*, 63(10), pp. 915–921. doi:10.1002/iub.559.
- Luo, K. (2017) 'Signaling cross talk between TGF- β /Smad and other signaling pathways', *Cold Spring Harbor Perspectives in Biology*. Cold Spring Harbor Laboratory Press, p. a022137. doi:10.1101/cshperspect.a022137.
- Luo, X., Li, H. and Yang, G. (2008) 'Sequential Expression of Wnt/ β -catenin Signal Pathway Related Genes and Adipocyte Transcription Factors During Porcine Adipose Tissue Development', *Chinese Journal of Biotechnology*, 24(5), pp. 746–753. doi:10.1016/S1872-2075(08)60039-4.
- Luo, Z., Gao, X., Lin, C., Smith, E.R., Marshall, S.A., Swanson, S.K., *et al.* (2015) 'Zic2 is an enhancer-binding factor required for embryonic stem cell specification', *Molecular Cell*, 57(4), pp. 685–694. doi:10.1016/j.molcel.2015.01.007.
- Lv, C., Sun, L., Guo, Z., Li, H., Kong, D., Xu, B., *et al.* (2018) 'Circular RNA regulatory network reveals cell-cell crosstalk in acute myeloid leukemia extramedullary infiltration', *Journal of Translational Medicine*, 16(1), pp. 1–15. doi:10.1186/S12967-018-1726-X/FIGURES/8.
- Lyons, A.B. and Ashman, L.K. (1988) 'The effect of recombinant cytokines on the proliferative potential and phenotype of cells of the human myelomonocytic leukaemia line, RC-2A', *Leukemia Research*, 12(8), pp. 659–666. doi:10.1016/0145-2126(88)90100-2.
- Ma, G., Pan, P.Y., Eisenstein, S., Divino, C.M., Lowell, C.A., Takai, T., *et al.* (2011) 'Paired immunoglobulin-like receptor-B regulates the suppressive function and fate of myeloid-derived suppressor cells', *Immunity*, 34(3), pp. 385–395. doi:10.1016/j.immuni.2011.02.004.
- Ma, J., Shojaie, A. and Michailidis, G. (2019) 'A comparative study of topology-based pathway enrichment analysis methods', *BMC Bioinformatics*, 20(1), p. 546. doi:10.1186/s12859-019-3146-1.
- Ma, L., Wang, Y., Hui, Y., Du, Y., Chen, Z., Feng, H., *et al.* (2019) 'WNT/NOTCH Pathway Is Essential for the Maintenance and Expansion of Human MGE Progenitors', *Stem Cell Reports*, 12(5), pp. 934–949. doi:10.1016/j.stemcr.2019.04.007.
- Ma, Q., Yang, Y., Feng, D., Zheng, S., Meng, R., Fa, P., *et al.* (2015) 'MAGI3 negatively regulates Wnt/ β -catenin signaling and suppresses malignant phenotypes of glioma cells', *Oncotarget*, 6(34), pp. 35851–35865. doi:10.18632/oncotarget.5323.
- Ma, S., Yang, L.L., Niu, T., Cheng, C., Zhong, L., Zheng, M.W., *et al.* (2015) 'SKLB-677, an FLT3 and Wnt/ β -catenin signaling inhibitor, displays potent activity in models of FLT3-driven AML', *Scientific Reports*, 5(1), pp. 1–15. doi:10.1038/srep15646.
- MacDonald, B.T., Tamai, K. and He, X. (2009) 'Wnt/ β -Catenin Signaling: Components, Mechanisms, and Diseases', *Developmental Cell*, 17(1), pp. 9–26. doi:10.1016/j.devcel.2009.06.016.
- Mackarehtschian, K., Hardin, J.D., Moore, K.A., Boast, S., Goff, S.P. and Lemischka, I.R. (1995) 'Targeted disruption of the flk2/flt3 gene leads to deficiencies in primitive hematopoietic progenitors', *Immunity*, 3(1), pp. 147–161. doi:10.1016/1074-7613(95)90167-1.
- Mackinnon, R.N., Wall, M., Zordan, A., Nutalapati, S., Mercer, B., Peverall, J., *et al.* (2013) 'Genome organization and the role of centromeres in evolution of the erythroleukaemia cell line HEL', *Evolution, medicine, and public health*. 2013/10/01, 2013(1), pp. 225–240. doi:10.1093/emph/eot020.
- MacKinnon, R.N., Peverall, J., Campbell, L.J. and Wall, M. (2020) 'Detailed molecular cytogenetic characterisation of the myeloid cell line U937 reveals the fate of homologous chromosomes and shows that centromere capture is a feature of genome instability', *Molecular Cytogenetics*, 13(1), pp.

1–14. doi:10.1186/S13039-020-00517-Y/TABLES/3.

Magliozzi, R., Low, T.Y., Weijts, B.G.M.W., Cheng, T., Spanjaard, E., Mohammed, S., *et al.* (2013) ‘Control of epithelial cell migration and invasion by the IKK β - and CK1 α -mediated degradation of RAPGEF2’, *Developmental Cell*, 27(5), pp. 574–585. doi:10.1016/j.devcel.2013.10.023.

Majeti, R., Chao, M.P., Alizadeh, A.A., Pang, W.W., Jaiswal, S., Gibbs, K.D., *et al.* (2009) ‘CD47 Is an Adverse Prognostic Factor and Therapeutic Antibody Target on Human Acute Myeloid Leukemia Stem Cells’, *Cell*, 138(2), pp. 286–299. doi:10.1016/j.cell.2009.05.045.

Majeti, R., Becker, M.W., Tian, Q., Lee, T.L.M., Yan, X., Liu, R., *et al.* (2009) ‘Dysregulated gene expression networks in human acute myelogenous leukemia stem cells’, *Proceedings of the National Academy of Sciences of the United States of America*, 106(9), pp. 3396–3401. doi:10.1073/pnas.0900089106.

Majeti, R., Park, C.Y. and Weissman, I.L. (2007) ‘Identification of a Hierarchy of Multipotent Hematopoietic Progenitors in Human Cord Blood’, *Cell Stem Cell*, 1(6), pp. 635–645. doi:10.1016/j.stem.2007.10.001.

Malhotra, S., Baba, Y., Garrett, K.P., Staal, F.J.T., Gerstein, R. and Kincade, P.W. (2008) ‘Contrasting Responses of Lymphoid Progenitors to Canonical and Noncanonical Wnt Signals’, *The Journal of Immunology*, 181(6), pp. 3955–3964. doi:10.4049/jimmunol.181.6.3955.

Malhotra, S. and Kincade, P.W. (2009) ‘Wnt-related molecules and signaling pathway equilibrium in hematopoiesis’, *Cell stem cell*, 4(1), pp. 27–36. doi:10.1016/J.STEM.2008.12.004.

Maltaneri, R.E., Schiappacasse, A., Chamorro, M.E., Nesse, A.B. and Vittori, D.C. (2020) ‘Aquaporin-1 plays a key role in erythropoietin-induced endothelial cell migration’, *Biochimica et Biophysica Acta - Molecular Cell Research*, 1867(1), p. 118569. doi:10.1016/j.bbamcr.2019.118569.

Malumbres, M. and Barbacid, M. (2001) ‘To cycle or not to cycle: A critical decision in cancer’, *Nature Reviews Cancer*, 1(3), pp. 222–231. doi:10.1038/35106065.

Marcault, C., Zhao, L.-P., Daltro De Oliveira, R., Soret, J., Gauthier, N., Verger, E., *et al.* (2020) ‘NFE2 Mutations Impact AML Transformation and Overall Survival in Patients with Myeloproliferative Neoplasms (MPN)’, *Blood*, 136(Supplement 1), pp. 36–36. doi:10.1182/blood-2020-136177.

Marchand, T. and Pinho, S. (2021) ‘Leukemic Stem Cells: From Leukemic Niche Biology to Treatment Opportunities’, *Frontiers in Immunology*. Available at: <https://www.frontiersin.org/article/10.3389/fimmu.2021.775128>.

Marcucci, G., Maharry, K., Whitman, S.P., Vukosavljevic, T., Paschka, P., Langer, C., *et al.* (2007) ‘High expression levels of the ETS-related gene, ERG, predict adverse outcome and improve molecular risk-based classification of cytogenetically normal acute myeloid leukemia: A cancer and leukemia group B study’, *Journal of Clinical Oncology*, 25(22), pp. 3337–3343. doi:10.1200/JCO.2007.10.8720.

Marofi, F., Vahedi, G., Solali, S., Alivand, M., Salarinasab, S., Zadi Heydarabad, M., *et al.* (2019) ‘Gene expression of TWIST1 and ZBTB16 is regulated by methylation modifications during the osteoblastic differentiation of mesenchymal stem cells’, *Journal of Cellular Physiology*, 234(5), pp. 6230–6243. doi:10.1002/jcp.27352.

Marple, A.H. and DeZern, A.E. (2021) ‘Please “Eat me”: Can Magrolimab Put Higher-risk MDS Back on the Immunologic Menu?’, *The Hematologist*, 18(4). doi:10.1182/hem.v18.4.2021410.

Martella, A., Firth, M., Taylor, B.J.M., Göppert, A., Cuomo, E.M., Roth, R.G., *et al.* (2019) ‘Systematic Evaluation of CRISPRa and CRISPRi Modalities Enables Development of a Multiplexed, Orthogonal Gene Activation and Repression System’, *ACS Synthetic Biology*, 8(9), pp. 1998–2006. doi:10.1021/acssynbio.8b00527.

Martemyanov, K.A., Parameswaran, P., Aligianis, I., Handley, M., Gual-Soler, M., Taguchi, T., *et al.* (2012) ‘Rap GEF Family’, *Encyclopedia of Signaling Molecules*, pp. 1590–1596. doi:10.1007/978-1-4419-0461-4_274.

- Martin-Orozco, E., Sanchez-Fernandez, A., Ortiz-Parra, I. and Ayala-San Nicolas, M. (2019) *WNT Signaling in Tumors: The Way to Evade Drugs and Immunity*, *Frontiers in Immunology*. doi:10.3389/fimmu.2019.02854.
- Martinez-Soria, N., McKenzie, L., Draper, J., Ptasinska, A., Issa, H., Potluri, S., *et al.* (2018) 'The Oncogenic Transcription Factor RUNX1/ETO Corrupts Cell Cycle Regulation to Drive Leukemic Transformation', *Cancer Cell*, 34(4), pp. 626–642.e8. doi:10.1016/j.ccell.2018.08.015.
- Martynov, A., Bomko, T., Nosalskaya, T., Farber, B. and Brek, O. (2020) 'Non-classical effects of the cAMP accumulation activators in vivo', *Advanced Pharmaceutical Bulletin*, 10(3), pp. 477–481. doi:10.34172/apb.2020.059.
- Masetti, R., Pigazzi, M., Togni, M., Astolfi, A., Indio, V., Manara, E., *et al.* (2013) 'CBFA2T3-GLIS2 fusion transcript is a novel common feature in pediatric, cytogenetically normal AML, not restricted to FAB M7 subtype', *Blood*, 121(17), pp. 3469–3472. doi:10.1182/blood-2012-11-469825.
- Masetti, R., Togni, M., Astolfi, A., Pigazzi, M., Manara, E., Indio, V., *et al.* (2013) 'DHH-RHEBL1 fusion transcript: A novel recurrent feature in the new landscape of pediatric CBFA2T3-GLIS2-positive acute myeloid leukemia', *Oncotarget*, 4(10), pp. 1712–1720. doi:10.18632/oncotarget.1280.
- Matsoukas, I.G. (2020) 'Prime Editing: Genome Editing for Rare Genetic Diseases Without Double-Strand Breaks or Donor DNA', *Frontiers in Genetics*, p. 528. doi:10.3389/fgene.2020.00528.
- Matsunaga, T., Yamaguchi, A., Morikawa, Y., Kezuka, C., Takazawa, H., Endo, S., *et al.* (2014) 'Induction of aldo-keto reductases (AKR1C1 and AKR1C3) abolishes the efficacy of daunorubicin chemotherapy for leukemic U937 cells', *Anti-Cancer Drugs*, 25(8), pp. 868–877. doi:10.1097/CAD.0000000000000112.
- Matteucci, C., La Starza, R., Crescenzi, B., Falzetti, D., Romoli, S., Emiliani, C., *et al.* (2002) 'Interpretation of the complex karyotype and identification of a new 6p amplicon by integrated comparative genomic hybridization and fluorescence in situ hybridization on the U937-I cell line', *Cancer genetics and cytogenetics*, 135(1), pp. 28–34.
- McBride, J.D., Rodriguez-Menocal, L., Guzman, W., Candanedo, A., Garcia-Contreras, M. and Badiavas, E. V. (2017) 'Bone Marrow Mesenchymal Stem Cell-Derived CD63+ Exosomes Transport Wnt3a Exteriorly and Enhance Dermal Fibroblast Proliferation, Migration, and Angiogenesis In Vitro', <https://home.liebertpub.com/scd>, 26(19), pp. 1384–1398. doi:10.1089/SCD.2017.0087.
- McCarty, N.S., Graham, A.E., Studená, L. and Ledesma-Amaro, R. (2020) 'Multiplexed CRISPR technologies for gene editing and transcriptional regulation', *Nature Communications*, 11(1), p. 1281. doi:10.1038/s41467-020-15053-x.
- McKenzie, A.T., Katsyv, I., Song, W.M., Wang, M. and Zhang, B. (2016) 'DGCA: A comprehensive R package for Differential Gene Correlation Analysis', *BMC Systems Biology*, 10(1), pp. 1–25. doi:10.1186/s12918-016-0349-1.
- McNerney, M.E., Godley, L.A. and Le Beau, M.M. (2017) 'Therapy-related myeloid neoplasms: When genetics and environment collide', *Nature Reviews Cancer*, 17(9), pp. 513–527. doi:10.1038/nrc.2017.60.
- Medvinsky, A. and Dzierzak, E. (1999) 'Development of the hematopoietic stem cell: Can we describe it? [4] (multiple letters)', *Blood*, 94(10), pp. 3613–3614. doi:10.1182/blood.V94.10.3613.422a38d_3613_3614.
- Mercatelli, D., Lopez-Garcia, G. and Giorgi, F.M. (2020) 'Corto: A lightweight R package for gene network inference and master regulator analysis', *Bioinformatics*, 36(12), pp. 3916–3917. doi:10.1093/bioinformatics/btaa223.
- Merenda, A., Fenderico, N. and Maurice, M.M. (2020) 'Wnt Signaling in 3D: Recent Advances in the Applications of Intestinal Organoids', *Trends in Cell Biology*, 30(1), pp. 60–73. doi:10.1016/J.TCB.2019.10.003.
- Mesbahi, Y., Trahair, T.N., Lock, R.B. and Connerty, P. (2022) 'Exploring the Metabolic Landscape of AML: From Haematopoietic Stem Cells to Myeloblasts and Leukaemic Stem Cells', *Frontiers in*

Oncology, 12, p. 281. doi:10.3389/FONC.2022.807266/BIBTEX.

Metcalf, D. and Burgess, A.W. (1982) 'Clonal analysis of progenitor cell commitment to granulocyte or macrophage production', *Journal of Cellular Physiology*, 111(3), pp. 275–283. doi:10.1002/jcp.1041110308.

Metzeler, K.H., Heilmeier, B., Edmaier, K.E., Rawat, V.P.S., Dufour, A., Döhner, K., *et al.* (2012) 'High expression of lymphoid enhancer-binding factor-1 (LEF1) is a novel favorable prognostic factor in cytogenetically normal acute myeloid leukemia', *Blood*, 120(10), pp. 2118–2126. doi:10.1182/blood-2012-02-411827.

Meyer, S.E., Qin, T., Muench, D.E., Masuda, K., Venkatasubramanian, M., Orr, E., *et al.* (2016) 'DNMT3A haploinsufficiency transforms FLT3ITD myeloproliferative disease into a rapid, spontaneous, and fully penetrant acute myeloid leukemia', *Cancer Discovery*, 6(5), pp. 501–515. doi:10.1158/2159-8290.CD-16-0008.

Meyers, R.M., Bryan, J.G., McFarland, J.M., Weir, B.A., Sizemore, A.E., Xu, H., *et al.* (2017) 'Computational correction of copy number effect improves specificity of CRISPR-Cas9 essentiality screens in cancer cells.', *Nature genetics*, 49(12), pp. 1779–1784. doi:10.1038/ng.3984.

Mianné, J., Codner, G.F., Caulder, A., Fell, R., Hutchison, M., King, R., *et al.* (2017) 'Analysing the outcome of CRISPR-aided genome editing in embryos: Screening, genotyping and quality control', *Methods*. Academic Press Inc., pp. 68–76. doi:10.1016/j.ymeth.2017.03.016.

Miao, Y., Ha, A., de Lau, W., Yuki, K., Santos, A.J.M., You, C., *et al.* (2020) 'Next-Generation Surrogate Wnts Support Organoid Growth and Deconvolute Frizzled Pleiotropy In Vivo', *Cell Stem Cell*, 27(5), pp. 840–851.e6. doi:10.1016/J.STEM.2020.07.020/ATTACHMENT/E94F1082-B5CE-447A-85B3-0F07F6313AB9/MMC1.PDF.

Midic, D., Rinke, J., Perner, F., Müller, V., Hinze, A., Pester, F., *et al.* (2020) 'Prevalence and dynamics of clonal hematopoiesis caused by leukemia-associated mutations in elderly individuals without hematologic disorders', *Leukemia*, 34(8), pp. 2198–2205. doi:10.1038/s41375-020-0869-y.

Mikesch, J.H., Steffen, B., Berdel, W.E., Serve, H. and Müller-Tidow, C. (2007) 'The emerging role of Wnt signaling in the pathogenesis of acute myeloid leukemia', *Leukemia*, 21(8), pp. 1638–1647. doi:10.1038/sj.leu.2404732.

Miller, J.R. (2002) 'The Wnts', *Genome Biology*, 3(1), p. reviews3001.1. doi:10.1186/gb-2001-3-1-reviews3001.

Mims, A.S., Kohlschmidt, J., Einfeld, A.K., Mrózek, K., Blachly, J.S., Orwick, S., *et al.* (2021) 'Comparison of clinical and molecular characteristics of patients with acute myeloid leukemia and either TP73 or TP53 mutations', *Leukemia*, 35(4), pp. 1188–1192. doi:10.1038/s41375-020-1007-6.

Minato, N. (2013) 'Rap G protein signal in normal and disordered lymphohematopoiesis', *Experimental Cell Research*, 319(15), pp. 2323–2328. doi:10.1016/j.yexcr.2013.04.009.

Minke, K.S., Staib, P., Puetter, A., Gehrke, I., Gandhirajan, R.K., Schlösser, A., *et al.* (2009) 'Small molecule inhibitors of WNT signaling effectively induce apoptosis in acute myeloid leukemia cells', *European Journal of Haematology*, 82(3), pp. 165–175. doi:10.1111/j.1600-0609.2008.01188.x.

Miravet, S., Piedra, J., Miró, F., Itarte, E., De Herreros, A.G. and Duñach, M. (2002) 'The transcriptional factor Tcf-4 contains different binding sites for β -catenin and plakoglobin', *Journal of Biological Chemistry*, 277(3), pp. 1884–1891. doi:10.1074/jbc.M110248200.

Mitchell, E., Spencer Chapman, M., Williams, N., Dawson, K.J., Mende, N., Calderbank, E.F., *et al.* (2022) 'Clonal dynamics of haematopoiesis across the human lifespan', *Nature*, 606(7913), pp. 343–350. doi:10.1038/s41586-022-04786-y.

Mitchell, K., Barreyro, L., Todorova, T.I., Taylor, S.J., Antony-Debré, I., Narayanagari, S.R., *et al.* (2018) 'IL1RAP potentiates multiple oncogenic signaling pathways in AML', *Journal of Experimental Medicine*, 215(6), pp. 1709–1727. doi:10.1084/jem.20180147.

Mo, R., Chew, T.L., Maher, M.T., Bellipanni, G., Weinberg, E.S. and Gottardi, C.J. (2009) 'The

- Terminal Region of β -Catenin Promotes Stability by Shielding the Armadillo Repeats from the Axin-scaffold Destruction Complex', *The Journal of Biological Chemistry*, 284(41), p. 28222. doi:10.1074/JBC.M109.045039.
- Mo, S.J., Hou, X., Hao, X.Y., Cai, J.P., Liu, X., Chen, W., *et al.* (2018) 'EYA4 inhibits hepatocellular carcinoma growth and invasion by suppressing NF- κ B-dependent RAP1 transactivation', *Cancer communications (London, England)*, 38(1), p. 9. doi:10.1186/S40880-018-0276-1/FIGURES/6.
- Moeenzakhanlou, A., Shephard, L., Lam, L. and Reiner, N.E. (2008) 'Myeloid cell differentiation in response to calcitriol for expression CD11b and CD14 is regulated by myeloid zinc finger-1 protein downstream of phosphatidylinositol 3-kinase', *Journal of Leukocyte Biology*, 84(2), pp. 519–528. doi:10.1189/jlb.1207833.
- Monaco, S., Rusciano, M.R., Maione, A.S., Soprano, M., Gomathinayagam, R., Todd, L.R., *et al.* (2015) 'A novel crosstalk between calcium/calmodulin kinases II and IV regulates cell proliferation in myeloid leukemia cells', *Cellular Signalling*, 27(2), pp. 204–214. doi:10.1016/j.cellsig.2014.11.007.
- Monga, I., Kaur, K. and Dhanda, S.K. (2022) 'Revisiting hematopoiesis: applications of the bulk and single-cell transcriptomics dissecting transcriptional heterogeneity in hematopoietic stem cells', *Briefings in Functional Genomics*, 21(3), pp. 159–176. doi:10.1093/BFGP/ELAC002.
- Morgan, M.A., Wegner, J., Aydilek, E., Ganser, A. and Reuter, C.W.M. (2003) 'Synergistic cytotoxic effects in myeloid leukemia cells upon cotreatment with farnesyltransferase and geranylgeranyl transferase-I inhibitors', *Leukemia*, 17(8), pp. 1508–1520. doi:10.1038/sj.leu.2403022.
- Morgan, R.G., Pearn, L., Liddiard, K., Pumford, S.L., Burnett, A.K., Tonks, A., *et al.* (2013) ' γ -Catenin is overexpressed in acute myeloid leukemia and promotes the stabilization and nuclear localization of β -catenin', *Leukemia*, 27(2), pp. 336–343. doi:10.1038/leu.2012.221.
- Morgan, R.G., Ridsdale, J., Payne, M., Heesom, K.J., Wilson, M.C., Davidson, A., *et al.* (2019) 'LEF-1 drives aberrant β -catenin nuclear localization in myeloid leukemia cells', *Haematologica*, 104(7), pp. 1365–1377. doi:10.3324/haematol.2018.202846.
- Morin, P.J., Sparks, A.B., Korinek, V., Barker, N., Clevers, H., Vogelstein, B., *et al.* (1997) 'Activation of β -catenin-Tcf signaling in colon cancer by mutations in β -catenin or APC', *Science*, 275(5307), pp. 1787–1790. doi:10.1126/science.275.5307.1787.
- Morita, K., Wang, F., Jahn, K., Hu, T., Tanaka, T., Sasaki, Y., *et al.* (2020) 'Clonal evolution of acute myeloid leukemia revealed by high-throughput single-cell genomics', *Nature Communications*, 11(1), pp. 1–17. doi:10.1038/s41467-020-19119-8.
- Morris, A., Pagare, P.P., Li, J. and Zhang, Y. (2021) 'Drug discovery efforts toward inhibitors of canonical Wnt/ β -catenin signaling pathway in the treatment of cancer: A composition-of-matter review (2010–2020)', *Drug Discovery Today* [Preprint]. doi:10.1016/j.drudis.2021.11.014.
- Morrison, S.J. and Scadden, D.T. (2014) 'The bone marrow niche for haematopoietic stem cells', *Nature*, 505(7483), pp. 327–334. doi:10.1038/nature12984.
- Mortazavi, A., Williams, B.A., McCue, K., Schaeffer, L. and Wold, B. (2008) 'Mapping and quantifying mammalian transcriptomes by RNA-Seq', *Nature Methods*, 5(7), pp. 621–628. doi:10.1038/nmeth.1226.
- Mubeen, S., Hoyt, C.T., Gemünd, A., Hofmann-Apitius, M., Fröhlich, H. and Domingo-Fernández, D. (2019) 'The Impact of Pathway Database Choice on Statistical Enrichment Analysis and Predictive Modeling', *Frontiers in Genetics*, 10, p. 1203. doi:10.3389/fgene.2019.01203.
- Müller-Tidow, C., Steffen, B., Cauvet, T., Tickenbrock, L., Ji, P., Diederichs, S., *et al.* (2004) 'Translocation Products in Acute Myeloid Leukemia Activate the Wnt Signaling Pathway in Hematopoietic Cells', *Molecular and Cellular Biology*, 24(7), pp. 2890–2904. doi:10.1128/mcb.24.7.2890-2904.2004.
- Munitz, A. (2010) 'Inhibitory receptors on myeloid cells: New targets for therapy?', *Pharmacology and Therapeutics*, 125(1), pp. 128–137. doi:10.1016/j.pharmthera.2009.10.007.

- Naillat, F., Yan, W., Karjalainen, R., Liakhovitskaia, A., Samoylenko, A., Xu, Q., *et al.* (2015) 'Identification of the genes regulated by Wnt-4, a critical signal for commitment of the ovary', *Experimental Cell Research*, 332(2), pp. 163–178. doi:10.1016/j.yexcr.2015.01.010.
- Nakahata, K., Uehara, S., Nishikawa, S., Kawatsu, M., Zenitani, M., Oue, T., *et al.* (2015) 'Aldehyde dehydrogenase 1 (ALDH1) is a potential marker for cancer stem cells in embryonal rhabdomyosarcoma', *PLoS ONE*, 10(4). doi:10.1371/journal.pone.0125454.
- Naot, D., Musson, D.S. and Cornish, J. (2019) 'The activity of peptides of the calcitonin family in bone', *Physiological Reviews*, 99(1), pp. 781–805. doi:10.1152/physrev.00066.2017.
- Di Nardo, C.D. and Cortes, J.E. (2016) 'Mutations in AML: Prognostic and therapeutic implications', *Hematology*, 2016(1), pp. 348–355. doi:10.1182/asheducation-2016.1.348.
- Naujok, O., Lentjes, J., Diekmann, U., Davenport, C. and Lenzen, S. (2014) 'Cytotoxicity and activation of the Wnt/beta-catenin pathway in mouse embryonic stem cells treated with four GSK3 inhibitors', *BMC Research Notes*, 7(1), p. 273. doi:10.1186/1756-0500-7-273.
- Navarrete-Meneses, M. del P. and Pérez-Vera, P. (2017) 'Epigenetic alterations in acute lymphoblastic leukemia', *Boletín Médico Del Hospital Infantil de México (English Edition)*, 74(4), pp. 243–264. doi:10.1016/j.bmhime.2018.01.004.
- Nechiporuk, T., Kurtz, S.E., Nikolova, O., Liu, T., Jones, C.L., D'alessandro, A., *et al.* (2019) 'The TP53 Apoptotic Network Is a Primary Mediator of Resistance to BCL2 Inhibition in AML Cells', *Cancer discovery*, 9(7), pp. 910–925. doi:10.1158/2159-8290.CD-19-0125.
- Nelson, J.W., Randolph, P.B., Shen, S.P., Everette, K.A., Chen, P.J., Anzalone, A. V., *et al.* (2021) 'Engineered pegRNAs improve prime editing efficiency', *Nature Biotechnology* [Preprint]. doi:10.1038/s41587-021-01039-7.
- Nemeth, M.J., Topol, L., Anderson, S.M., Yang, Y. and Bodine, D.M. (2007) 'Wnt5a inhibits canonical Wnt signaling in hematopoietic stem cells and enhances repopulation', *Proceedings of the National Academy of Sciences of the United States of America*, 104(39), pp. 15436–15441. doi:10.1073/pnas.0704747104.
- Newton, A.C. (2010) 'Protein kinase C: Poised to signal', *American Journal of Physiology - Endocrinology and Metabolism*. Am J Physiol Endocrinol Metab. doi:10.1152/ajpendo.00477.2009.
- Ng, A.P. and Alexander, W.S. (2017) 'Haematopoietic stem cells: Past, present and future', *Cell Death Discovery*, 3, p. 17002. doi:10.1038/cddiscovery.2017.2.
- Ng, S.W.K., Mitchell, A., Kennedy, J.A., Chen, W.C., McLeod, J., Ibrahimova, N., *et al.* (2016) 'A 17-gene stemness score for rapid determination of risk in acute leukaemia', *Nature*, 540(7633), pp. 433–437. doi:10.1038/nature20598.
- Niida, A., Hiroko, T., Kasai, M., Furukawa, Y., Nakamura, Y., Suzuki, Y., *et al.* (2004) 'DKK1, a negative regulator of Wnt signaling, is a target of the β -catenin/TCF pathway', *Oncogene*, 23(52), pp. 8520–8526. doi:10.1038/sj.onc.1207892.
- Nishida, Y., Ishizawa, J., Ruvolo, V., Wang, F., Takahashi, K., Mak, P.Y., *et al.* (2019) 'TP73 As Novel Determinant of Resistance to BCL-2 Inhibition in Acute Myeloid Leukemia', *Blood*, 134(Supplement_1), pp. 1251–1251. doi:10.1182/blood-2019-127182.
- Nishimura, D. (2001) 'BioCarta', *Biotech Software & Internet Report*, 2(3), pp. 117–120. doi:10.1089/152791601750294344.
- Nishinakamura, R., Nakayama, N., Hirabayashi, Y., Inoue, T., Aud, D., Mcneil, T., *et al.* (1995) 'Mice deficient for the IL-3/GM-CSF/IL-5 β c receptor exhibit lung pathology and impaired immune response, while β IL3 receptor-deficient mice are normal', *Immunity*, 2(3), pp. 211–222. doi:10.1016/1074-7613(95)90046-2.
- Niu, Y., Yang, X., Chen, Y., Jin, X., Xie, Y., Tang, Y., *et al.* (2019) 'Distinct prognostic values of Annexin family members expression in acute myeloid leukemia', *Clinical and Translational Oncology*, 21(9), pp. 1186–1196. doi:10.1007/s12094-019-02045-7.

- Nofrini, V., Matteucci, C., Pellanera, F., Gorello, P., Di Giacomo, D., Lema Fernandez, A.G., *et al.* (2021) 'Activating somatic and germline TERT promoter variants in myeloid malignancies', *Leukemia*, 35(1), pp. 274–278. doi:10.1038/s41375-020-0837-6.
- Noone, A., Howlader, N., Krapcho, M., Miller, D., Brest, A., Yu, M., *et al.* (2018) 'Acute Myeloid Leukemia - Cancer Stat Facts', <https://seer.cancer.gov/statfacts/html/amyl.html>, pp. 1–3. Available at: <https://seer.cancer.gov/statfacts/html/amyl.html> (Accessed: 21 August 2022).
- Nopparat, J., Zhang, J., Lu, J.P., Chen, Y.H., Zheng, D., Neuffer, P.D., *et al.* (2015) 'δ-Catenin, a Wnt/β-catenin modulator, reveals inducible mutagenesis promoting cancer cell survival adaptation and metabolic reprogramming', *Oncogene*, 34(12), pp. 1542–1552. doi:10.1038/onc.2014.89.
- Normal, I.D. (2008) *Incidence Statistics, Leukemia*.
- Notta, F., Doulatov, S., Laurenti, E., Poepl, A., Jurisica, I. and Dick, J.E. (2011) 'Isolation of single human hematopoietic stem cells capable of long-term multilineage engraftment', *Science*, 333(6039), pp. 218–221. doi:10.1126/science.1201219.
- Novellasdemunt, L., Foglizzo, V., Cuadrado, L., Antas, P., Kucharska, A., Encheva, V., *et al.* (2017) 'USP7 Is a Tumor-Specific WNT Activator for APC-Mutated Colorectal Cancer by Mediating β-Catenin Deubiquitination', *Cell Reports*, 21(3), pp. 612–627. doi:10.1016/j.celrep.2017.09.072.
- Novellasdemunt, L., Antas, P. and Li, V.S.W. (2015) 'Targeting Wnt signaling in colorectal cancer. A review in the theme: Cell signaling: Proteins, pathways and mechanisms', *American Journal of Physiology - Cell Physiology*. 2015/08/19, 309(8), pp. C511–C521. doi:10.1152/ajpcell.00117.2015.
- Nusinow, D.P., Szpyt, J., Ghandi, M., Rose, C.M., McDonald, E.R., Kalocsay, M., *et al.* (2020) 'Quantitative Proteomics of the Cancer Cell Line Encyclopedia', *Cell*, 180(2), pp. 387–402.e16. doi:<https://doi.org/10.1016/j.cell.2019.12.023>.
- Nusse, R. (2015) 'Disarming Wnt', *Nature*, 519(7542), pp. 163–164. doi:10.1038/nature14208.
- De Obaldia, M.E., Bell, J.J., Wang, X., Harly, C., Yashiro-Ohtani, Y., DeLong, J.H., *et al.* (2013) 'T cell development requires constraint of the myeloid regulator C/EBP-α by the Notch target and transcriptional repressor Hes1.', *Nature immunology*, 14(12), pp. 1277–1284. doi:10.1038/ni.2760.
- Odero, M.D., Zeleznik-Le, N.J., Chinwalla, V. and Rowley, J.D. (2000) 'Cytogenetic and molecular analysis of the acute monocytic leukemia cell line THP-1 with an MLL-AF9 translocation.', *Genes, chromosomes & cancer*, 29(4), pp. 333–338.
- Ogata, H., Goto, S., Sato, K., Fujibuchi, W., Bono, H. and Kanehisa, M. (1999) 'KEGG: Kyoto encyclopedia of genes and genomes', *Nucleic Acids Research*, 27(1), pp. 29–34. doi:10.1093/nar/27.1.29.
- Ogawa, M., Matsuzaki, Y., Nishikawa, S., Hayashi, S.I., Kunisada, T., Sudo, T., *et al.* (1991) 'Expression and function of c-kit in hemopoietic progenitor cells', *Journal of Experimental Medicine*, 174(1), pp. 63–71. doi:10.1084/jem.174.1.63.
- Onai, N., Obata-Onai, A., Tussiwand, R., Lanzavecchia, A. and Manz, M.G. (2006) 'Activation of the Flt3 signal transduction cascade rescues and enhances type I interferon-producing and dendritic cell development', *Journal of Experimental Medicine*, 203(1), pp. 227–238. doi:10.1084/jem.20051645.
- Orkin, S.H. and Zon, L.I. (2008) 'Hematopoiesis: An Evolving Paradigm for Stem Cell Biology', *Cell*, 132(4), pp. 631–644. doi:10.1016/j.cell.2008.01.025.
- Páez, D., Gerger, A., Zhang, W., Yang, D., Labonte, M.J., Benhanim, L., *et al.* (2014) 'Association of common gene variants in the WNT/β-catenin pathway with colon cancer recurrence', *Pharmacogenomics Journal*, 14(2), pp. 142–150. doi:10.1038/tpj.2013.20.
- Pagella, P., Söderholm, S., Nordin, A., Zambanini, G., Jauregi-Miguel, A. and Cantù, C. (2022) 'Time-resolved analysis of Wnt-signaling reveals β-catenin temporal genomic repositioning and cell type-specific plastic or elastic chromatin responses', *bioRxiv*, p. 2022.08.05.502932. doi:10.1101/2022.08.05.502932.
- Pai, S.G., Carneiro, B.A., Mota, J.M., Costa, R., Leite, C.A., Barroso-Sousa, R., *et al.* (2017)

- ‘Wnt/beta-catenin pathway: Modulating anticancer immune response’, *Journal of Hematology and Oncology*, 10(1). doi:10.1186/s13045-017-0471-6.
- Paik, E.J. and Zon, L.I. (2010) ‘Hematopoietic development in the zebrafish’, *International Journal of Developmental Biology*, 54(6–7), pp. 1127–1137. doi:10.1387/ijdb.093042ep.
- Palva, I.P., Almqvist, A., Elonen, E., Hänninen, A., Jouppila, J., Järventie, G., *et al.* (1991) ‘Value of maintenance therapy with chemotherapy or interferon during remission of acute myeloid leukaemia’, *European Journal of Haematology*, 47(3), pp. 229–233. doi:10.1111/j.1600-0609.1991.tb01560.x.
- Pang, Y., Zhao, Y., Wang, Y., Wang, X., Wang, R., Liu, N., *et al.* (2020) ‘TNFAIP8 promotes AML chemoresistance by activating ERK signaling pathway through interaction with Rac1’, *Journal of Experimental and Clinical Cancer Research*, 39(1), pp. 1–18. doi:10.1186/s13046-020-01658-z.
- Panina, S.B., Pei, J. and Kirienko, N. V. (2021) ‘Mitochondrial metabolism as a target for acute myeloid leukemia treatment’, *Cancer & Metabolism 2021 9:1*, 9(1), pp. 1–25. doi:10.1186/S40170-021-00253-W.
- Papaemmanuil, E., Gerstung, M., Bullinger, L., Gaidzik, V.I., Paschka, P., Roberts, N.D., *et al.* (2016) ‘Genomic Classification and Prognosis in Acute Myeloid Leukemia’, *New England Journal of Medicine*, 374(23), pp. 2209–2221. doi:10.1056/nejmoa1516192.
- Park, M.S., Lee, Y.E., Kim, H.R., Shin, J.H., Cho, H.W., Lee, J.H., *et al.* (2021) ‘Phospholipase C Beta 2 Protein Overexpression Is a Favorable Prognostic Indicator in Newly Diagnosed Normal Karyotype Acute Myeloid Leukemia’, *Annals of laboratory medicine*, 41(4), pp. 409–413. doi:10.3343/alm.2021.41.4.409.
- Park, S.Y., Kim, J.Y., Choi, J.H., Kim, J.H., Lee, C.J., Singh, P., *et al.* (2019) ‘Inhibition of LEF1-mediated DCLK1 by niclosamide attenuates colorectal cancer stemness’, *Clinical Cancer Research*, 25(4), pp. 1415–1429. doi:10.1158/1078-0432.CCR-18-1232.
- Parnell, E., Palmer, T.M. and Yarwood, S.J. (2015) ‘The future of EPAC-targeted therapies: Agonism versus antagonism’, *Trends in Pharmacological Sciences*, 36(4), pp. 203–214. doi:10.1016/j.tips.2015.02.003.
- Patel, C., Stenke, L., Varma, S., Lindberg, M.L., Björkholm, M., Sjöberg, J., *et al.* (2013) ‘Multidrug resistance in relapsed acute myeloid leukemia: Evidence of biological heterogeneity’, *Cancer*, 119(16), pp. 3076–3083. doi:10.1002/cncr.28098.
- Pau, G., Fuchs, F., Sklyar, O., Boutros, M. and Huber, W. (2010) ‘EBImage—an R package for image processing with applications to cellular phenotypes’, *Bioinformatics*, 26(7), pp. 979–981. doi:10.1093/bioinformatics/btq046.
- Paubelle, E., Zylbersztejn, F., Maciel, T.T., Carvalho, C., Mupo, A., Cheok, M., *et al.* (2020) ‘Vitamin D Receptor Controls Cell Stemness in Acute Myeloid Leukemia and in Normal Bone Marrow’, *Cell Reports*, 30(3), pp. 739–754.e4. doi:10.1016/j.celrep.2019.12.055.
- Pedemonte, E., Benvenuto, F., Casazza, S., Mancardi, G., Oksenberg, J.R., Uccelli, A., *et al.* (2007) ‘The molecular signature of therapeutic mesenchymal stem cells exposes the architecture of the hematopoietic stem cell niche synapse’, *BMC Genomics*, 8(1), pp. 1–14. doi:10.1186/1471-2164-8-65.
- Pei, S., Pollyea, D.A., Gustafson, A., Stevens, B.M., Minhajuddin, M., Fu, R., *et al.* (2020) ‘Monocytic subclones confer resistance to venetoclax-based therapy in patients with acute myeloid leukemia’, *Cancer Discovery*, 10(4), pp. 536–551. doi:10.1158/2159-8290.CD-19-0710.
- Pelullo, M., Zema, S., Nardoza, F., Checquolo, S., Screpanti, I. and Bellavia, D. (2019) ‘Wnt, Notch, and TGF- β pathways impinge on hedgehog signaling complexity: An open window on cancer’, *Frontiers in Genetics*. Frontiers Media S.A., p. 711. doi:10.3389/fgene.2019.00711.
- Peluso, I., Morabito, G., Urban, L., Ioannone, F. and Serafi, M. (2012) ‘Oxidative Stress in Atherosclerosis Development: The Central Role of LDL and Oxidative Burst’, *Endocrine, Metabolic & Immune Disorders-Drug Targets*, 12(4), pp. 351–360. doi:10.2174/187153012803832602.
- Peng, X., Yang, L., Chang, H., Dai, G., Wang, F., Duan, X., *et al.* (2014) ‘Wnt/ β -catenin signaling

regulates the proliferation and differentiation of mesenchymal progenitor cells through the p53 pathway', *PLoS ONE*, 9(5), p. e97283. doi:10.1371/journal.pone.0097283.

Pepe, F., Bill, M., Papaioannou, D., Karunasiri, M., Walker, A., Naumann, E., *et al.* (2022) 'Targeting Wnt signaling in acute myeloid leukemia stem cells', *Haematologica*, 107(1), p. 307. doi:10.3324/HAEMATOL.2020.266155.

Peradziryi, H., Kaplan, N.A., Podleschny, M., Liu, X., Wehner, P., Borchers, A., *et al.* (2011) 'PTK7/Otk interacts with Wnts and inhibits canonical Wnt signalling', *The EMBO Journal*, 30(18), pp. 3729–3740. doi:https://doi.org/10.1038/emboj.2011.236.

Perez-Moreno, M., Davis, M.A., Wong, E., Pasolli, H.A., Reynolds, A.B. and Fuchs, E. (2006) 'P120-Catenin Mediates Inflammatory Responses in the Skin', *Cell*, 124(3), pp. 631–644. doi:10.1016/j.cell.2005.11.043.

Perry, J.M., Tao, F., Roy, A., Lin, T., He, X.C., Chen, S., *et al.* (2020) 'Overcoming Wnt- β -catenin dependent anticancer therapy resistance in leukaemia stem cells', *Nature Cell Biology*, 22(6), pp. 689–700. doi:10.1038/s41556-020-0507-y.

Petropoulos, K., Arseni, N., Schessl, C., Stadler, C.R., Rawat, V.P.S., Deshpande, A.J., *et al.* (2008) 'A novel role for Lef-1, a central transcription mediator of Wnt signaling, in leukemogenesis', *Journal of Experimental Medicine*, 205(3), pp. 515–522. doi:10.1084/jem.20071875.

Petti, A.A., Williams, S.R., Miller, C.A., Fiddes, I.T., Srivatsan, S.N., Chen, D.Y., *et al.* (2019) 'A general approach for detecting expressed mutations in AML cells using single cell RNA-sequencing', *Nature Communications*, 10(1), pp. 1–16. doi:10.1038/s41467-019-11591-1.

Peyrieras, N., Louvard, D. and Jacob, F. (1985) 'Characterization of antigens recognized by monoclonal and polyclonal antibodies directed against uvomorulin', *Proceedings of the National Academy of Sciences of the United States of America*, 82(23), pp. 8067–8071. doi:10.1073/pnas.82.23.8067.

Pietrzak, J., Mirowski, M., Świechowski, R., Wodziński, D., Wosiak, A., Michalska, K., *et al.* (2021) 'Importance of Altered Gene Expression of Metalloproteinases 2, 9, and 16 in Acute Myeloid Leukemia: Preliminary Study', *Journal of Oncology*, 2021. doi:10.1155/2021/6697975.

Pizzola, C.J., Rakszawski, K.L., Ehmann, W.C., Rybka, W.B., Wirk, B., Naik, S., *et al.* (2019) 'Non-Myeloablative Allogeneic Stem Cell Transplant in Acute Myeloid Leukemia: Graft-Versus-Host Disease Potentiates Graft-Versus-Leukemia Effect and Improves Overall Survival', *Blood*, 134(Supplement_1), pp. 5724–5724. doi:10.1182/blood-2019-128817.

Poeta, G. Del, Stasi, R., Venditti, A., Cox, C., Aronica, G., Masi, M., *et al.* (1995) 'CD7 expression in acute myeloid leukemia', *Leukemia and Lymphoma*, 17(1–2), pp. 111–119. doi:10.3109/10428199509051710.

Poggi, L., Casarosa, S. and Carl, M. (2018) 'An eye on the wnt inhibitory factor Wif1', *Frontiers in Cell and Developmental Biology*, 6(DEC), p. 167. doi:10.3389/fcell.2018.00167.

Polprasert, C., Schulze, I., Sekeres, M.A., Makishima, H., Przychodzen, B., Hosono, N., *et al.* (2015) 'Inherited and Somatic Defects in *DDX41* in Myeloid Neoplasms', *Cancer Cell*, 27(5), pp. 658–670. doi:10.1016/j.ccell.2015.03.017.

Pommier, Y., Leo, E., Zhang, H. and Marchand, C. (2010) 'DNA topoisomerases and their poisoning by anticancer and antibacterial drugs', *Chemistry and Biology*, 17(5), pp. 421–433. doi:10.1016/j.chembiol.2010.04.012.

Ponomaryov, T., Peled, A., Petit, I., Taichman, R.S., Habler, L., Sandbank, J., *et al.* (2000) 'Induction of the chemokine stromal-derived factor-1 following DNA damage improves human stem cell function', *Journal of Clinical Investigation*, 106(11), pp. 1331–1339. doi:10.1172/JCI10329.

Porteu, F., Rouyez, M.C., Cocault, L., Bénit, L., Charon, M., Picard, F., *et al.* (1996) 'Functional regions of the mouse thrombopoietin receptor cytoplasmic domain: evidence for a critical region which is involved in differentiation and can be complemented by erythropoietin', *Molecular and Cellular Biology*, 16(5), pp. 2473–2482. doi:10.1128/mcb.16.5.2473.

- Poulos, M.G., Crowley, M.J.P., Gutkin, M.C., Ramalingam, P., Schachterle, W., Thomas, J.L., *et al.* (2015) 'Vascular platform to define hematopoietic stem cell factors and enhance regenerative hematopoiesis', *Stem Cell Reports*, 5(5), pp. 881–894. doi:10.1016/j.stemcr.2015.08.018.
- Powell, R.H. and Behnke, M.S. (2017) 'WRN conditioned media is sufficient for in vitro propagation of intestinal organoids from large farm and small companion animals', *Biology Open*, 6(5), pp. 698–705. doi:10.1242/bio.021717.
- Prenkert, M., Uggla, B., Tidefelt, U.L.F. and Strid, H. (2010) 'CRIM1 is Expressed at Higher Levels in Drug-resistant than in Drug-sensitive Myeloid Leukemia HL60 Cells', *Anticancer Research*, 30(10), pp. 4157 LP – 4161. Available at: <http://ar.iiarjournals.org/content/30/10/4157.abstract>.
- Prossomariti, A., Piazzzi, G., Alquati, C. and Ricciardiello, L. (2020) 'Are Wnt/ β -Catenin and PI3K/AKT/mTORC1 Distinct Pathways in Colorectal Cancer?', *Cmgh*. Elsevier Inc, pp. 491–506. doi:10.1016/j.jcmgh.2020.04.007.
- Puppo, F., Thomé, V., Lhoumeau, A.-C., Cibois, M., Gangar, A., Lembo, F., *et al.* (2011) 'Protein tyrosine kinase 7 has a conserved role in Wnt/ β -catenin canonical signalling', *EMBO reports*, 12(1), pp. 43–49. doi:<https://doi.org/10.1038/embo.2010.185>.
- Qian, J., Huang, X., Zhang, Y., Ye, X. and Qian, W. (2020) ' γ -Catenin overexpression in AML Patients may promote tumor cell survival via activation of the Wnt/ β -catenin axis', *OncoTargets and Therapy*, 13, pp. 1265–1276. doi:10.2147/OTT.S230873.
- Qiu, T., Qi, X., Cen, J. and Chen, Z. (2012) 'Rap1GAP alters leukemia cell differentiation, apoptosis and invasion in vitro', *Oncology Reports*, 28(2), pp. 622–628. doi:10.3892/OR.2012.1825/HTML.
- Quillet-Mary, A., Mansat, V., Duchayne, E., Come, M.G., Allouche, M., Bailly, J.D., *et al.* (1996) 'Daunorubicin-induced internucleosomal DNA fragmentation in acute myeloid cell lines.', *Leukemia*, 10(3), pp. 417–425.
- Raaijmakers, M.H.G.P., Mukherjee, S., Guo, S., Zhang, S., Kobayashi, T., Schoonmaker, J.A., *et al.* (2010) 'Bone progenitor dysfunction induces myelodysplasia and secondary leukaemia', *Nature*, 464(7290), pp. 852–857. doi:10.1038/nature08851.
- Rahman, M., Jackson, L.K., Johnson, W.E., Li, D.Y., Bild, A.H. and Piccolo, S.R. (2015) 'Alternative preprocessing of RNA-Sequencing data in the Cancer Genome Atlas leads to improved analysis results', *Bioinformatics*, 31(22), pp. 3666–3672. doi:10.1093/bioinformatics/btv377.
- Ramos, C.J., Lin, C., Liu, X. and Antonetti, D.A. (2018) 'The EPAC–Rap1 pathway prevents and reverses cytokine-induced retinal vascular permeability', *The Journal of Biological Chemistry*, 293(2), p. 717. doi:10.1074/JBC.M117.815381.
- Ramzi, M., Khalafi-Nezhad, A., Saadi, M.I. and Jowkar, Z. (2018) 'Association between tlr2 and tlr4 expression and response to induction therapy in acute myeloid leukemia patients', *International Journal of Hematology-Oncology and Stem Cell Research*, 12(4), pp. 302–311. doi:10.18502/ijhoscr.v12i4.109.
- Ranes, M., Zaleska, M., Sakalas, S., Knight, R. and Guettler, S. (2021) 'Reconstitution of the destruction complex defines roles of AXIN polymers and APC in β -catenin capture, phosphorylation, and ubiquitylation', *Molecular Cell*, 81(16), pp. 3246–3261.e11. doi:10.1016/j.molcel.2021.07.013.
- Rao, D.M., Bordeaux, E.K., Yamamoto, T.M., Bitler, B.G. and Sikora, M.J. (2018) 'WNT4 and WNT3A activate cell autonomous Wnt signaling independent of PORCN or secretion', *bioRxiv*. bioRxiv, p. 333906. doi:10.1101/333906.
- Ratajczak, M.Z., Ratajczak, J., Marlicz, W., Pletcher, C.H., Machalinski, B., Moore, J., *et al.* (1997) 'Recombinant human thrombopoietin (TPO) stimulates erythropoiesis by inhibiting erythroid progenitor cell apoptosis', *British Journal of Haematology*, 98(1), pp. 8–17. doi:10.1046/j.1365-2141.1997.1802997.x.
- Raudvere, U., Kolberg, L., Kuzmin, I., Arak, T., Adler, P., Peterson, H., *et al.* (2019) 'G:Profiler: A web server for functional enrichment analysis and conversions of gene lists (2019 update)', *Nucleic Acids Research*, 47(W1), pp. W191–W198. doi:10.1093/nar/gkz369.

- Raut, L.S. (2015) 'Novel formulation of cytarabine and daunorubicin: A new hope in AML treatment', *South Asian Journal of Cancer*, 04(01), pp. 038–040. doi:10.4103/2278-330x.149950.
- Redman, M., King, A., Watson, C. and King, D. (2016) 'What is CRISPR/Cas9?', *Archives of Disease in Childhood: Education and Practice Edition*, 101(4), pp. 213–215. doi:10.1136/archdischild-2016-310459.
- Retta, S.F., Balzac, F. and Avolio, M. (2006) 'Rap1: A turnabout for the crosstalk between cadherins and integrins', *European Journal of Cell Biology*, 85(3–4), pp. 283–293. doi:10.1016/j.ejcb.2005.09.007.
- Reverter, A. and Chan, E.K.F. (2008) 'Combining partial correlation and an information theory approach to the reversed engineering of gene co-expression networks', *Bioinformatics*, 24(21), pp. 2491–2497. doi:10.1093/bioinformatics/btn482.
- Reya, T., Duncan, A.W., Ailles, L., Domen, J., Scherer, D.C., Willert, K., *et al.* (2003) 'A role for Wnt signalling in self-renewal of haematopoietic stem cells', *Nature*, 423(6938), pp. 409–414. doi:10.1038/nature01593.
- Ribeiro, S.T., Ribot, J.C. and Silva-Santos, B. (2015) 'Five layers of receptor signaling in $\gamma\delta$ T-cell differentiation and activation', *Frontiers in Immunology*, 6(JAN). doi:10.3389/fimmu.2015.00015.
- Richter, J., Traver, D. and Willert, K. (2017) 'The role of Wnt signaling in hematopoietic stem cell development', *Critical Reviews in Biochemistry and Molecular Biology*, 52(4), pp. 414–424. doi:10.1080/10409238.2017.1325828.
- Rieger, M.A., Hoppe, P.S., Smejkal, B.M., Eitelhuber, A.C. and Schroeder, T. (2009) 'Hematopoietic cytokines can instruct lineage choice', *Science (New York, N.Y.)*, 325(5937), pp. 217–218. doi:10.1126/SCIENCE.1171461.
- Riganti, C., Salaroglio, I.C., Caldera, V., Campia, I., Kopecka, J., Mellai, M., *et al.* (2013) 'Temozolomide downregulates P-glycoprotein expression in glioblastoma stem cells by interfering with the Wnt3a/glycogen synthase-3 kinase/ β -catenin pathway', *Neuro-oncology*, 15(11), pp. 1502–1517. doi:10.1093/NEUONC/NOT104.
- Rijsewijk, F., Schuermann, M., Wagenaar, E., Parren, P., Weigel, D. and Nusse, R. (1987) 'The Drosophila homology of the mouse mammary oncogene int-1 is identical to the segment polarity gene wingless', *Cell*, 50(4), pp. 649–657. doi:10.1016/0092-8674(87)90038-9.
- Rio-Machin, A., Vulliamy, T., Hug, N., Walne, A., Tawana, K., Cardoso, S., *et al.* (2020) 'The complex genetic landscape of familial MDS and AML reveals pathogenic germline variants', *Nature Communications*, 11(1), pp. 1–12. doi:10.1038/s41467-020-14829-5.
- Rodon, J., Argilés, G., Connolly, R.M., Vaishampayan, U., de Jonge, M., Garralda, E., *et al.* (2021) 'Phase 1 study of single-agent WNT974, a first-in-class Porcupine inhibitor, in patients with advanced solid tumours', *British Journal of Cancer*, 125(1), pp. 28–37. doi:10.1038/s41416-021-01389-8.
- Rodríguez González, A., Sahores, A., Díaz-Nebreda, A., Yaneff, A., Di Siervi, N., Gómez, N., *et al.* (2021) 'MRP4/ABCC4 expression is regulated by histamine in acute myeloid leukemia cells, determining cAMP efflux', *The FEBS Journal*, 288(1), pp. 229–243. doi:10.1111/FEBS.15344.
- Ros, S., Santos, C.R., Moco, S., Baenke, F., Kelly, G., Howell, M., *et al.* (2012) 'Functional metabolic screen identifies 6-phosphofructo-2-kinase/fructose-2, 6-biphosphatase 4 as an important regulator of prostate cancer cell survival', *Cancer Discovery*, 2(4), pp. 328–343. doi:10.1158/2159-8290.CD-11-0234.
- Rouillard, A.D., Gunderson, G.W., Fernandez, N.F., Wang, Z., Monteiro, C.D., McDermott, M.G., *et al.* (2016) 'The harmonizome: a collection of processed datasets gathered to serve and mine knowledge about genes and proteins', *Database*, 2016. doi:10.1093/DATABASE/BAW100.
- Rozovski, U., Hazan-Halevy, I., Barzilai, M., Keating, M.J. and Estrov, Z. (2016) 'Metabolism pathways in chronic lymphocytic leukemia', *Leukemia and Lymphoma*, 57(4), pp. 758–765. doi:10.3109/10428194.2015.1106533.

- Ruan, Y., Kim, H.N., Ogana, H. and Kim, Y.M. (2020) 'Wnt signaling in leukemia and its bone marrow microenvironment', *International Journal of Molecular Sciences*. MDPI AG, pp. 1–20. doi:10.3390/ijms21176247.
- Ruffell, D., Mourkioti, F., Gambardella, A., Kirstetter, P., Lopez, R.G., Rosenthal, N., *et al.* (2009) 'A CREB-C/EBP β cascade induces M2 macrophage-specific gene expression and promotes muscle injury repair', *Proceedings of the National Academy of Sciences of the United States of America*, 106(41), pp. 17475–17480. doi:10.1073/pnas.0908641106.
- Russell, K.C., Phinney, D.G., Lacey, M.R., Barrilleaux, B.L., Meyertholen, K.E. and O'Connor, K.C. (2010) 'In vitro high-capacity assay to quantify the clonal heterogeneity in trilineage potential of mesenchymal stem cells reveals a complex hierarchy of lineage commitment', *Stem Cells*, 28(4), pp. 788–798. doi:10.1002/stem.312.
- Russo, P.S.T., Ferreira, G.R., Cardozo, L.E., Bürger, M.C., Arias-Carrasco, R., Maruyama, S.R., *et al.* (2018) 'CEMiTool: A Bioconductor package for performing comprehensive modular co-expression analyses', *BMC Bioinformatics*, 19(1), p. 56. doi:10.1186/s12859-018-2053-1.
- Rybka, J., Butrym, A., Wróbel, T., Jaźwiec, B., Stefanko, E., Dobrzyńska, O., *et al.* (2015) 'The expression of Toll-like receptors in patients with acute myeloid leukemia treated with induction chemotherapy', *Leukemia Research*, 39(3), pp. 318–322. doi:10.1016/j.leukres.2015.01.002.
- Sadot, E., Simcha, I., Iwai, K., Ciechanover, A., Geiger, B. and Ben-Ze'ev, A. (2000) 'Differential interaction of plakoglobin and β -catenin with the ubiquitin-proteasome system', *Oncogene*, 19(16), pp. 1992–2001. doi:10.1038/sj.onc.1203519.
- Saenz, D.T., Fiskus, W., Manshour, T., Mill, C.P., Qian, Y., Raina, K., *et al.* (2019) 'Targeting nuclear β -catenin as therapy for post-myeloproliferative neoplasm secondary AML', *Leukemia*, 33(6), pp. 1373–1386. doi:10.1038/s41375-018-0334-3.
- Saito, Y., Nakahata, S., Yamakawa, N., Kaneda, K., Ichihara, E., Suekane, A., *et al.* (2011) 'CD52 as a molecular target for immunotherapy to treat acute myeloid leukemia with high EVI1 expression.', *Leukemia*, 25(6), pp. 921–931. doi:10.1038/leu.2011.36.
- Sales, G., Calura, E., Cavalieri, D. and Romualdi, C. (2012) 'Graphite - a Bioconductor package to convert pathway topology to gene network', *BMC Bioinformatics*, 13(1), pp. 1–12. doi:10.1186/1471-2105-13-20.
- Sallman, D.A., Al Malki, M., Asch, A.S., Lee, D.J., Kambhampati, S., Donnellan, W.B., *et al.* (2020) 'Tolerability and efficacy of the first-in-class anti-CD47 antibody magrolimab combined with azacitidine in MDS and AML patients: Phase Ib results.', *Journal of Clinical Oncology*, 38(15_suppl), pp. 7507–7507. doi:10.1200/jco.2020.38.15_suppl.7507.
- Salomon, D., Sacco, P.A., Roy, S.G., Simcha, I., Johnson, K.R., Wheelock, M.J., *et al.* (1997) 'Regulation of β -catenin levels and localization by overexpression of plakoglobin and inhibition of the ubiquitin-proteasome system', *Journal of Cell Biology*, 139(5), pp. 1325–1335. doi:10.1083/jcb.139.5.1325.
- Samra, B., Richard-Carpentier, G., Kadia, T.M., Ravandi, F., Daver, N., DiNardo, C.D., *et al.* (2020) 'Characteristics and outcomes of patients with therapy-related acute myeloid leukemia with normal karyotype', *Blood Cancer Journal*, 10(5), pp. 1–9. doi:10.1038/s41408-020-0316-3.
- Sanchez-Correa, B., Bergua, J.M., Campos, C., Gayoso, I., Arcos, M.J., Bañas, H., *et al.* (2013) 'Cytokine profiles in acute myeloid leukemia patients at diagnosis: Survival is inversely correlated with IL-6 and directly correlated with IL-10 levels', *Cytokine*, 61(3), pp. 885–891. doi:10.1016/j.cyto.2012.12.023.
- Sands, W.A., Copland, M. and Wheadon, H. (2013) 'Targeting self-renewal pathways in myeloid malignancies', *Cell Communication and Signaling*, 11(1), pp. 1–13. doi:10.1186/1478-811X-11-33.
- Sanz, M.A., Fenaux, P., Tallman, M.S., Estey, E.H., Löwenberg, B., Naoe, T., *et al.* (2019) 'Management of acute promyelocytic leukemia: Updated recommendations from an expert panel of the European LeukemiaNet', *Blood*, 133(15), pp. 1630–1643. doi:10.1182/blood-2019-01-894980.

- Saraceni, F., Bruno, B., Lemoli, R.M., Meloni, G., Arcese, W., Falda, M., *et al.* (2017) 'Autologous stem cell transplantation is still a valid option in good- and intermediate-risk AML: A GITMO survey on 809 patients autografted in first complete remission', *Bone Marrow Transplantation*, 52(1), pp. 163–166. doi:10.1038/bmt.2016.233.
- Sarry, J.E., Murphy, K., Perry, R., Sanchez, P. V., Secreto, A., Keefer, C., *et al.* (2011) 'Human acute myelogenous leukemia stem cells are rare and heterogeneous when assayed in NOD/SCID/IL2R γ -deficient mice', *Journal of Clinical Investigation*, 121(1), pp. 384–395. doi:10.1172/JCI41495.
- Satyanarayana, A., Gudmundsson, K.O., Chen, X., Coppola, V., Tessarollo, L., Keller, J.R., *et al.* (2010) 'RapGEF2 is essential for embryonic hematopoiesis but dispensable for adult hematopoiesis', *Blood*, 116(16), pp. 2921–2931. doi:10.1182/blood-2010-01-262964.
- Sauter, C., Fopp, M., Imbach, P., Tschopp, L., Berchtold, W., Gratwohl, A., *et al.* (1984) 'Acute Myelogenous Leukaemia: Maintenance Chemotherapy After Early Consolidation Treatment Does Not Prolong Survival', *The Lancet*, 323(8373), pp. 379–382. doi:10.1016/S0140-6736(84)90424-0.
- Scheller, M., Huelsken, J., Rosenbauer, F., Taketo, M.M., Birchmeier, W., Tenen, D.G., *et al.* (2006) 'Hematopoietic stem cell and multilineage defects generated by constitutive β -catenin activation', *Nature Immunology*, 7(10), pp. 1037–1047. doi:10.1038/ni1387.
- Schlenk, R.F., Jaramillo, S. and Müller-Tidow, C. (2018) 'Improving consolidation therapy in acute myeloid leukemia - A tough nut to crack', *Haematologica*, 103(10), pp. 1579–1581. doi:10.3324/haematol.2018.200485.
- Schmidlin, T., Garrigues, L., Lane, C.S., Mulder, T.C., van Doorn, S., Post, H., *et al.* (2016) 'Assessment of SRM, MRM(3), and DIA for the targeted analysis of phosphorylation dynamics in non-small cell lung cancer', *Proteomics*, 16(15–16), pp. 2193–2205. doi:10.1002/PMIC.201500453.
- Schmidt, E.E., Pelz, O., Buhlmann, S., Kerr, G., Horn, T. and Boutros, M. (2013) 'GenomeRNAi: a database for cell-based and in vivo RNAi phenotypes, 2013 update.', *Nucleic acids research*, 41(Database issue), pp. D1021–6. doi:10.1093/nar/gks1170.
- Schmitt, M., Metzger, M., Gradl, D., Davidson, G. and Orian-Rousseau, V. (2015) 'CD44 functions in Wnt signaling by regulating LRP6 localization and activation', *Cell Death and Differentiation*, 22(4), pp. 677–689. doi:10.1038/cdd.2014.156.
- Schoch, C., Kern, W., Schnittger, S., Hiddemann, W. and Haferlach, T. (2004) 'Karyotype is an independent prognostic parameter in therapy-related acute myeloid leukemia (t-AML): An analysis of 93 patients with t-AML in comparison to 1091 patients with de novo AML', *Leukemia*, 18(1), pp. 120–125. doi:10.1038/sj.leu.2403187.
- Schofield, R. (1978) 'The relationship between the spleen colony-forming cell and the haemopoietic stem cell. A hypothesis', *Blood Cells*, 4(1–2), pp. 7–25.
- Scholefield, J. and Harrison, P.T. (2021) 'Prime editing – an update on the field', *Gene Therapy*, 28(7–8), pp. 396–401. doi:10.1038/s41434-021-00263-9.
- Schubert, M., Colomé-Tatché, M. and Foijer, F. (2020) 'Gene networks in cancer are biased by aneuploidies and sample impurities', *Biochimica et Biophysica Acta - Gene Regulatory Mechanisms*, 1863(6). doi:10.1016/j.bbagr.2019.194444.
- Schwarer, A.P., Wight, J., Jackson, K., Beligaswatte, A.M., Butler, J.P., Kennedy, G., *et al.* (2016) 'High-Dose Cytarabine (HiDAC) Improves the Cure Rate of Patients with Newly Diagnosed Acute Myeloid Leukemia (AML): Is It Better to be Given As Induction Therapy or As Consolidation Therapy?', *Blood*, 128(22), pp. 3989–3989. doi:10.1182/blood.v128.22.3989.3989.
- Scoville, D.W., Kang, H.S. and Jetten, A.M. (2017) 'GLIS1-3: Emerging roles in reprogramming, stem and progenitor cell differentiation and maintenance', *Stem Cell Investigation*, 4(9). doi:10.21037/sci.2017.09.01.
- Seita, J. and Weissman, I.L. (2010) 'Hematopoietic stem cell: Self-renewal versus differentiation', *Wiley Interdisciplinary Reviews: Systems Biology and Medicine*, 2(6), pp. 640–653. doi:10.1002/wsbm.86.

- Serinsöz, E., Neusch, M., Büsche, G., Von Wasielewski, R., Kreipe, H. and Bock, O. (2004) 'Aberrant expression of β -catenin discriminates acute myeloid leukaemia from acute lymphoblastic leukaemia', *British Journal of Haematology*, 126(3), pp. 313–319. doi:10.1111/j.1365-2141.2004.05049.x.
- Seth, C., Mas, C., Conod, A., Mueller, J., Siems, K., Kuciak, M., *et al.* (2016) 'Long-Lasting WNT-TCF Response Blocking and Epigenetic Modifying Activities of Withanolide F in Human Cancer Cells', *PLOS ONE*, 11(12), p. e0168170. doi:10.1371/JOURNAL.PONE.0168170.
- Seymour, J.F., Döhner, H., Butrym, A., Wierzbowska, A., Selleslag, D., Jang, J.H., *et al.* (2017) 'Azacitidine improves clinical outcomes in older patients with acute myeloid leukaemia with myelodysplasia-related changes compared with conventional care regimens', *BMC Cancer*, 17(1), pp. 1–13. doi:10.1186/s12885-017-3803-6.
- Shaffer, B.C., Gillet, J.P., Patel, C., Baer, M.R., Bates, S.E. and Gottesman, M.M. (2012) 'Drug resistance: Still a daunting challenge to the successful treatment of AML', *Drug Resistance Updates*, 15(1–2), pp. 62–69. doi:10.1016/j.drug.2012.02.001.
- Shah, B. and Püschel, A.W. (2016) 'Regulation of Rap GTPases in mammalian neurons', *Biological Chemistry*, 397(10), pp. 1055–1069. doi:10.1515/hsz-2016-0165.
- Shahriyari, L. and Komarova, N.L. (2013) 'Symmetric vs. asymmetric stem cell divisions: an adaptation against cancer?', *PloS one*. Edited by A.B. Pant, 8(10), p. e76195. doi:10.1371/journal.pone.0076195.
- Shallis, R.M., Wang, R., Davidoff, A., Ma, X. and Zeidan, A.M. (2019) 'Epidemiology of acute myeloid leukemia: Recent progress and enduring challenges', *Blood reviews*, 36, pp. 70–87. doi:10.1016/J.BLRE.2019.04.005.
- Sharma, M., Jamieson, C., Lui, C. and Henderson, B.R. (2016) 'Distinct hydrophobic "patches" in the N- and C-tails of beta-catenin contribute to nuclear transport', *Experimental Cell Research*, 348(2), pp. 132–145. doi:10.1016/j.yexcr.2016.09.009.
- Sharma, M., Castro-Piedras, I., Simmons, G.E. and Pruitt, K. (2018) 'Dishevelled: A masterful conductor of complex Wnt signals', *Cellular Signalling*, 47, pp. 52–64. doi:10.1016/j.cellsig.2018.03.004.
- Sharon, D., Cathelin, S., Mirali, S., Di Trani, J.M., Yanofsky, D.J., Keon, K.A., *et al.* (2019) 'Inhibition of mitochondrial translation overcomes venetoclax resistance in AML through activation of the integrated stress response', *Science translational medicine*, 11(516). doi:10.1126/SCITRANSLMED.AAX2863.
- Sheldahl, L.C., Slusarski, D.C., Pandur, P., Miller, J.R., Kühl, M. and Moon, R.T. (2003) 'Dishevelled activates Ca²⁺ flux, PKC, and CamKII in vertebrate embryos', *Journal of Cell Biology*, 161(4), pp. 769–777. doi:10.1083/jcb.200211094.
- Shipley, J.M., Sheppard, D.M. and Sheer, D. (1988) 'Karyotypic analysis of the human monoblastic cell line U937', *Cancer genetics and cytogenetics*, 30(2), pp. 277–284.
- Short, N.J., Rytting, M.E. and Cortes, J.E. (2018) 'Acute myeloid leukaemia', *The Lancet*, 392(10147), pp. 593–606. doi:10.1016/S0140-6736(18)31041-9.
- Si, J. and Collins, S.J. (2008) 'Activated Ca²⁺/calmodulin-dependent protein kinase II γ is a critical regulator of myeloid leukemia cell proliferation', *Cancer Research*, 68(10), pp. 3733–3742. doi:10.1158/0008-5472.CAN-07-2509.
- Si, M. and Lang, J. (2018) 'The roles of metallothioneins in carcinogenesis', *Journal of Hematology and Oncology*, 11(1). doi:10.1186/s13045-018-0645-x.
- Siapati, E.K., Papadaki, M., Kozaou, Z., Rouka, E., Michali, E., Savvidou, I., *et al.* (2008) '649. Delineating the Beta Catenin Pathway in Acute Myeloid Leukemia', *Molecular Therapy*, 16, pp. S242–S243. doi:10.1016/s1525-0016(16)40052-3.
- Sidney, L.E., Branch, M.J., Dunphy, S.E., Dua, H.S. and Hopkinson, A. (2014) 'Concise review:

- Evidence for CD34 as a common marker for diverse progenitors', *Stem Cells*, 32(6), pp. 1380–1389. doi:10.1002/stem.1661.
- Signer, R.A.J., Magee, J.A., Salic, A. and Morrison, S.J. (2014) 'Haematopoietic stem cells require a highly regulated protein synthesis rate', *Nature*, 508(7498), pp. 49–54. doi:10.1038/nature13035.
- Sikder, M.O.F., Sivaprakasam, S., Brown, T.P., Thangaraju, M., Bhutia, Y.D. and Ganapathy, V. (2020) 'SLC6A14, a Na⁺/Cl⁻-coupled amino acid transporter, functions as a tumor promoter in colon and is a target for Wnt signaling', *Biochemical Journal*, 477(8), pp. 1409–1425. doi:10.1042/BCJ20200099.
- Simcha, I., Shtutman, M., Salomon, D., Zhurinsky, J., Sadot, E., Geiger, B., *et al.* (1998) 'Differential nuclear translocation and transactivation potential of β -Catenin and plakoglobin', *Journal of Cell Biology*, 141(6), pp. 1433–1448. doi:10.1083/jcb.141.6.1433.
- Simon, M., Grandage, V.L., Linch, D.C. and Khwaja, A. (2005a) 'Constitutive activation of the Wnt/ β -catenin signalling pathway in acute myeloid leukaemia', *Oncogene*, 24(14), pp. 2410–2420. doi:10.1038/sj.onc.1208431.
- Simon, M., Grandage, V.L., Linch, D.C. and Khwaja, A. (2005b) 'Constitutive activation of the Wnt/ β -catenin signalling pathway in acute myeloid leukaemia', *Oncogene*, 24(14), pp. 2410–2420. doi:10.1038/sj.onc.1208431.
- Simonetti, G., Padella, A., do Valle, I.F., Fontana, M.C., Fonzi, E., Bruno, S., *et al.* (2019) 'Aneuploid acute myeloid leukemia exhibits a signature of genomic alterations in the cell cycle and protein degradation machinery.', *Cancer*, 125(5), pp. 712–725. doi:10.1002/cncr.31837.
- Singh, A. and Settleman, J. (2010) 'EMT, cancer stem cells and drug resistance: An emerging axis of evil in the war on cancer', *Oncogene*. NIH Public Access, pp. 4741–4751. doi:10.1038/ncr.2010.215.
- Smirnov, A., Cappello, A., Lena, A.M., Anemona, L., Mauriello, A., Di Daniele, N., *et al.* (2018) 'ZNF185 is a p53 target gene following DNA damage', *Aging*, 10(11), pp. 3308–3326. doi:10.18632/aging.101639.
- Smith, C.C., Levis, M.J., Frankfurt, O., Pagel, J.M., Roboz, G.J., Stone, R.M., *et al.* (2020) 'A phase 1/2 study of the oral FLT3 inhibitor pexidartinib in relapsed/ refractory FLT3-ITD-mutant acute myeloid leukemia', *Blood Advances*, 4(8), pp. 1711–1721. doi:10.1182/bloodadvances.2020001449.
- Smith, I., Greenside, P.G., Natoli, T., Lahr, D.L., Wadden, D., Tirosh, I., *et al.* (2017) 'Evaluation of RNAi and CRISPR technologies by large-scale gene expression profiling in the Connectivity Map', *PLoS Biology*. Edited by T. Freeman, 15(11), p. e2003213. doi:10.1371/journal.pbio.2003213.
- Smith, S.M., Le Beau, M.M., Huo, D., Karrison, T., Sobecks, R.M., Anastasi, J., *et al.* (2003) 'Clinical-cytogenetic associations in 306 patients with therapy-related myelodysplasia and myeloid leukemia: The University of Chicago series', *Blood*, 102(1), pp. 43–52. doi:10.1182/blood-2002-11-3343.
- Smits, A.H., Ziebell, F., Joberty, G., Zinn, N., Mueller, W.F., Clauder-Münster, S., *et al.* (2019) 'Biological plasticity rescues target activity in CRISPR knock outs', *Nature Methods*, 16(11), pp. 1087–1093. doi:10.1038/s41592-019-0614-5.
- Somervaille, T.C.P. and Cleary, M.L. (2006a) 'Identification and characterization of leukemia stem cells in murine MLL-AF9 acute myeloid leukemia', *Cancer cell*, 10(4), pp. 257–268. doi:10.1016/J.CCR.2006.08.020.
- Somervaille, T.C.P. and Cleary, M.L. (2006b) 'Identification and characterization of leukemia stem cells in murine MLL-AF9 acute myeloid leukemia', *Cancer Cell*, 10(4), pp. 257–268. doi:10.1016/j.ccr.2006.08.020.
- Song, A.J. and Palmiter, R.D. (2018) 'Detecting and Avoiding Problems When Using the Cre-lox System', *Trends in Genetics*. Elsevier Ltd, pp. 333–340. doi:10.1016/j.tig.2017.12.008.
- Song, B., Chi, Y., Li, X., Du, W., Han, Z.-B., Tian, J., *et al.* (2015) 'Inhibition of Notch Signaling Promotes the Adipogenic Differentiation of Mesenchymal Stem Cells Through Autophagy Activation

and PTEN-PI3K/AKT/mTOR Pathway.’, *Cellular physiology and biochemistry : international journal of experimental cellular physiology, biochemistry, and pharmacology*, 36(5), pp. 1991–2002. doi:10.1159/000430167.

Song, Q., Zhang, W. and Sun, Y. (2017) ‘Haploinsufficiency and mutation are two sides of the cancer coin as cause and therapeutics target’, *Translational Cancer Research*, 6(3), pp. S590–S593. doi:10.21037/tcr.2017.05.12.

Sontakke, P., Carretta, M., Capala, M., Schepers, H. and Schuringa, J.J. (2014) ‘Ex Vivo Assays to Study Self-Renewal, Long-Term Expansion, and Leukemic Transformation of Genetically Modified Human Hematopoietic and Patient-Derived Leukemic Stem Cells BT - Hematopoietic Stem Cell Protocols’, in Bunting, K.D. and Qu, C.-K. (eds). New York, NY: Springer New York, pp. 195–210. doi:10.1007/978-1-4939-1133-2_13.

Sperling, A.S., Gibson, C.J. and Ebert, B.L. (2017) ‘The genetics of myelodysplastic syndrome: From clonal haematopoiesis to secondary leukaemia’, *Nature Reviews Cancer*. Nature Publishing Group, pp. 5–19. doi:10.1038/nrc.2016.112.

Spitzhorn, L.S., Megges, M., Wruck, W., Rahman, M.S., Otte, J., Degistirici, Ö., *et al.* (2019) ‘Human iPSC-derived MSCs (iMSCs) from aged individuals acquire a rejuvenation signature’, *Stem Cell Research and Therapy*, 10(1), pp. 1–18. doi:10.1186/s13287-019-1209-x.

Srivastava, M., Begovic, E., Chapman, J., Putnam, N.H., Hellsten, U., Kawashima, T., *et al.* (2008) ‘The Trichoplax genome and the nature of placozoans.’, *Nature*, 454(7207), pp. 955–960. doi:10.1038/nature07191.

Staal, F.J.T., Famili, F., Perez, L.G. and Pike-Overzet, K. (2016) ‘Aberrant Wnt Signaling in Leukemia’, *Cancers*, 8(9). doi:10.3390/CANCERS8090078.

Stamos, J.L. and Weis, W.I. (2013) ‘The β -catenin destruction complex’, *Cold Spring Harbor Perspectives in Biology*, 5(1), pp. a007898–a007898. doi:10.1101/cshperspect.a007898.

Stanley, E., Lieschke, G.J., Grail, D., Metcalf, D., Hodgson, G., Gall, J.A.M., *et al.* (1994) ‘Granulocyte/macrophage colony-stimulating factor-deficient mice show no major perturbation of hematopoiesis but develop a characteristic pulmonary pathology’, *Proceedings of the National Academy of Sciences of the United States of America*, 91(12), pp. 5592–5596. doi:10.1073/pnas.91.12.5592.

Steele, B.M., Harper, M.T., Smolenski, A.P., Alkazemi, N., Poole, A.W., Fitzgerald, D.J., *et al.* (2012) ‘WNT-3a modulates platelet function by regulating small GTPase activity’, *FEBS Letters*, 586(16), pp. 2267–2272. doi:10.1016/j.febslet.2012.05.060.

Steensma, D.P., Bejar, R., Jaiswal, S., Lindsley, R.C., Sekeres, M.A., Hasserjian, R.P., *et al.* (2015) ‘Clonal hematopoiesis of indeterminate potential and its distinction from myelodysplastic syndromes’, *Blood*, 126(1), pp. 9–16. doi:10.1182/blood-2015-03-631747.

Steinbichler, T.B., Dudás, J., Skvortsov, S., Ganswindt, U., Riechelmann, H. and Skvortsova, I.I. (2018) ‘Therapy resistance mediated by cancer stem cells’, *Seminars in Cancer Biology*. Academic Press, pp. 156–167. doi:10.1016/j.semcancer.2018.11.006.

Stewart, H.J.S., Chaudry, S., Crichlow, A., Feilding, F.L. and Chevassut, T.J.T. (2018) ‘BET Inhibition Suppresses S100A8 and S100A9 Expression in Acute Myeloid Leukemia Cells and Synergises with Daunorubicin in Causing Cell Death’. doi:10.1155/2018/5742954.

Stieglitz, E. and Loh, M.L. (2013) ‘Genetic predispositions to childhood leukemia’, *Therapeutic Advances in Hematology*, 4(4), pp. 270–290. doi:10.1177/2040620713498161.

Stier, S., Ko, Y., Forkert, R., Lutz, C., Neuhaus, T., Grünewald, E., *et al.* (2005) ‘Osteopontin is a hematopoietic stem cell niche component that negatively regulates stem cell pool size’, *Journal of Experimental Medicine*, 201(11), pp. 1781–1791. doi:10.1084/jem.20041992.

Stoddard, J. (2009) ‘Interpreting U.S. History: The Competing Roles of Race, Schools, and Communities’, *Theory & Research in Social Education*, 37(1), pp. 140–143. doi:10.1080/00933104.2009.10473391.

- Stoddart, A., Wang, J., Hu, C., Fernald, A.A., Davis, E.M., Cheng, J.X., *et al.* (2017) 'Inhibition of WNT signaling in the bone marrow niche prevents the development of MDS in the Apc del/1 MDS mouse model', *Blood*, 129(22), pp. 2959–2970. doi:10.1182/blood-2016-08.
- Stone, J.C. (2011) 'Regulation and function of the rasGRP family of ras activators in blood cells', *Genes and Cancer*, 2(3), pp. 320–334. doi:10.1177/1947601911408082.
- Stone, R.M., Mandrekar, S.J., Sanford, B.L., Laumann, K., Geyer, S., Bloomfield, C.D., *et al.* (2017) 'Midostaurin plus Chemotherapy for Acute Myeloid Leukemia with a FLT3 Mutation', *New England Journal of Medicine*, 377(5), pp. 454–464. doi:10.1056/nejmoa1614359.
- Stork, P.J.S. (2003) 'Does Rap1 deserve a bad Rap?', *Trends in biochemical sciences*, 28(5), pp. 267–275. doi:10.1016/S0968-0004(03)00087-2.
- Stork, P.J.S. and Dillon, T.J. (2005) 'Multiple roles of Rap1 in hematopoietic cells: complementary versus antagonistic functions', *Blood*, 106(9), p. 2952. doi:10.1182/BLOOD-2005-03-1062.
- Subramanian, A., Narayan, R., Corsello, S.M., Peck, D.D., Natoli, T.E., Lu, X., *et al.* (2017) 'A Next Generation Connectivity Map: L1000 Platform and the First 1,000,000 Profiles', *Cell*, 171(6), pp. 1437–1452.e17. doi:10.1016/j.cell.2017.10.049.
- Suela, J., Álvarez, S., Cifuentes, F., Largo, C., Ferreira, B.I., Blesa, D., *et al.* (2007) 'DNA profiling analysis of 100 consecutive de novo acute myeloid leukemia cases reveals patterns of genomic instability that affect all cytogenetic risk groups', *Leukemia*, 21(6), pp. 1224–1231. doi:10.1038/sj.leu.2404653.
- Sugimura, R., He, X.C., Venkatraman, A., Arai, F., Box, A., Semerad, C., *et al.* (2012) 'Noncanonical Wnt signaling maintains hematopoietic stem cells in the niche', *Cell*, 150(2), pp. 351–365. doi:10.1016/j.cell.2012.05.041.
- Suh, E.K. and Gumbiner, B.M. (2003) 'Translocation of β -catenin into the nucleus independent of interactions with FG-rich nucleoporins', *Experimental Cell Research*, 290(2), pp. 447–456. doi:10.1016/S0014-4827(03)00370-7.
- Sun, Y., Chen, B.R. and Deshpande, A. (2018) 'Epigenetic regulators in the development, maintenance, and therapeutic targeting of acute myeloid leukemia', *Frontiers in Oncology*, 8(FEB), p. 41. doi:10.3389/fonc.2018.00041.
- Sundstrom, C. (1976) 'Establishment and characterization of a human histiocytic lymphoma cell line (U-937)', *Int. J. Cancer*, 17, p. 565.
- Swart, L.E. and Heidenreich, O. (2021) 'The RUNX1/RUNX1T1 network: translating insights into therapeutic options', *Experimental Hematology*, 94, pp. 1–10. doi:10.1016/j.exphem.2020.11.005.
- Sweeney, K., Cameron, E.R. and Blyth, K. (2020) 'Complex Interplay between the RUNX Transcription Factors and Wnt/ β -Catenin Pathway in Cancer: A Tango in the Night', *Molecules and cells*, 43(2), pp. 188–197. doi:10.14348/molcells.2019.0310.
- Swiatek, W., Tsai, I.C., Klimowski, L., Pepler, A., Barnette, J., Yost, H.J., *et al.* (2004) 'Regulation of Casein Kinase I ϵ Activity by Wnt Signaling', *Journal of Biological Chemistry*, 279(13), pp. 13011–13017. doi:10.1074/jbc.M304682200.
- Swiatek, W., Kang, H., Garcia, B.A., Shabanowitz, J., Coombs, G.S., Hunt, D.F., *et al.* (2006) 'Negative regulation of LRP6 function by casein kinase I ϵ phosphorylation', *Journal of Biological Chemistry*, 281(18), pp. 12233–12241. doi:10.1074/jbc.M510580200.
- Syama, K., Hassan, E.M. and Zou, S. (2021) 'Advances in culture methods for acute myeloid leukemia research', *Oncoscience*, 8, pp. 82–90. doi:10.18632/oncoscience.540.
- Szade, K., Gulati, G.S., Chan, C.K.F., Kao, K.S., Miyanishi, M., Marjon, K.D., *et al.* (2018) 'Where Hematopoietic Stem Cells Live: The Bone Marrow Niche', *Antioxidants and Redox Signaling*, 29(2), pp. 191–204. doi:10.1089/ars.2017.7419.
- Taejoon, K., Sun, R.J., Soyoun, L., In-Joon, B., Woo, K.K., A, L.E., *et al.* (2022) 'Precision targeting tumor cells using cancer-specific InDel mutations with CRISPR-Cas9', *Proceedings of the*

National Academy of Sciences, 119(9), p. e2103532119. doi:10.1073/pnas.2103532119.

Tago, K.I., Nakamura, T., Nishita, M., Hyodo, J., Nagai, S.I., Murata, Y., *et al.* (2000) 'Inhibition of Wnt signaling by ICAT, a novel β -catenin-interacting protein', *Genes and Development*, 14(14), pp. 1741–1749. doi:10.1101/gad.14.14.1741.

Taichman, R.S. and Emerson, S.G. (1994) 'Human osteoblasts support hematopoiesis through the production of granulocyte colony-stimulating factor', *Journal of Experimental Medicine*, 179(5), pp. 1677–1682. doi:10.1084/jem.179.5.1677.

Takam Kanga, P., Bassi, G., Cassaro, A., Midolo, M., Di Trapani, M., Gatti, A., *et al.* (2016) 'Notch signalling drives bone marrow stromal cell-mediated chemoresistance in acute myeloid leukemia.', *Oncotarget*, 7(16), pp. 21713–21727. doi:10.18632/oncotarget.7964.

Takam Kanga, P., Cassaro, A., Dal Collo, G., Adamo, A., Gatti, A., Carusone, R., *et al.* (2016) 'Role of Wnt/ β -Catenin Signalling in Acute Myeloid Leukemia (AML) Cell Response to Chemotherapy', *Blood*, 128(22), p. 2753. doi:10.1182/blood.V128.22.2753.2753.

Takanashi, M., Motoji, T., Masuda, M., Oshimi, K. and Mizoguchi, H. (1993) 'The effects of leukemia inhibitory factor and interleukin 6 on the growth of acute myeloid leukemia cells', *Leukemia Research*, 17(3), pp. 217–222. doi:10.1016/0145-2126(93)90004-5.

Takubo, K., Goda, N., Yamada, W., Iriuchishima, H., Ikeda, E., Kubota, Y., *et al.* (2010) 'Regulation of the HIF-1 α level is essential for hematopoietic stem cells', *Cell Stem Cell*, 7(3), pp. 391–402. doi:10.1016/j.stem.2010.06.020.

Tallman, M.S., Gilliland, D.G. and Rowe, J.M. (2005) 'Drug therapy for acute myeloid leukemia', *Blood*, 106(4), pp. 1154–1163. doi:10.1182/blood-2005-01-0178.

Tamai, K., Zeng, X., Liu, C., Zhang, X., Harada, Y., Chang, Z., *et al.* (2004) 'A Mechanism for Wnt Coreceptor Activation', *Molecular Cell*, 13(1), pp. 149–156. doi:10.1016/S1097-2765(03)00484-2.

Tan, H.Y., Wang, N., Li, S., Hong, M., Guo, W., Man, K., *et al.* (2018) 'Repression of WT1-Mediated LEF1 Transcription by Mangiferin Governs β -Catenin-Independent Wnt Signalling Inactivation in Hepatocellular Carcinoma', *Cellular Physiology and Biochemistry*, 47(5), pp. 1819–1834. doi:10.1159/000491063.

Tanaka, T., Tanaka, K., Ogawa, S., Kurokawa, M., Mitani, K., Nishida, J., *et al.* (1995) 'An acute myeloid leukemia gene, AML 1, regulates hemopoietic myeloid cell differentiation and transcriptional activation antagonistically by two alternative spliced forms', *EMBO Journal*, 14(2), pp. 341–350. doi:10.1002/j.1460-2075.1995.tb07008.x.

Tang, R., Faussat, A.M., Perrot, J.Y., Marjanovic, Z., Cohen, S., Storme, T., *et al.* (2008) 'Zosuquidar restores drug sensitivity in P-glycoprotein expressing acute myeloid leukemia (AML)', *BMC Cancer*, 8(1), p. 51. doi:10.1186/1471-2407-8-51.

Tang, S., Chen, T., Yu, Z., Zhu, X., Yang, M., Xie, B., *et al.* (2014) 'RasGRP3 limits Toll-like receptor-triggered inflammatory response in macrophages by activating Rap1 small GTPase', *Nature Communications*, 5(1), pp. 1–14. doi:10.1038/ncomms5657.

Tang, W., Li, M., Qi, X. and Li, J. (2020) ' β 1,4-Galactosyltransferase V modulates breast cancer stem cells through Wnt/ β -catenin signaling pathway', *Cancer Research and Treatment*, 52(4), pp. 1084–1102. doi:10.4143/crt.2020.093.

Tarca, A.L., Draghici, S., Khatri, P., Hassan, S.S., Mittal, P., Kim, J.S., *et al.* (2009) 'A novel signaling pathway impact analysis', *Bioinformatics*, 25(1), pp. 75–82. doi:10.1093/bioinformatics/btn577.

Taussig, D.C., Vargaftig, J., Miraki-Moud, F., Griessinger, E., Sharrock, K., Luke, T., *et al.* (2010) 'Leukemia-initiating cells from some acute myeloid leukemia patients with mutated nucleophosmin reside in the CD34- fraction', *Blood*, 115(10), pp. 1976–1984. doi:10.1182/blood-2009-02-206565.

Teixeira, C., Stang, S.L., Zheng, Y., Beswick, N.S. and Stone, J.C. (2003) 'Integration of DAG signaling systems mediated by PKC-dependent phosphorylation of RasGRP3', *Blood*, 102(4), pp.

1414–1420. doi:10.1182/blood-2002-11-3621.

Tenen, D.G., Hromas, R., Licht, J.D. and Zhang, D.E. (1997) 'Transcription factors, normal myeloid development, and leukemia', *Blood*, 90(2), pp. 489–519. doi:10.1182/blood.v90.2.489.

Teulière, J., Faraldo, M.M., Shtutman, M., Birchmeier, W., Huelsken, J., Thiery, J.P., *et al.* (2004) 'β-Catenin-Dependent and -Independent Effects of ΔN-Plakoglobin on Epidermal Growth and Differentiation', *Molecular and Cellular Biology*, 24(19), pp. 8649–8661. doi:10.1128/mcb.24.19.8649-8661.2004.

Thambyrajah, R., Patel, R., Mazan, M., Lie-a-Ling, M., Lilly, A., Eliades, A., *et al.* (2016) 'New insights into the regulation by RUNX1 and GFI1(s) proteins of the endothelial to hematopoietic transition generating primordial hematopoietic cells', *Cell Cycle*. 2016/07/11, 15(16), pp. 2108–2114. doi:10.1080/15384101.2016.1203491.

Thol, F. and Ganser, A. (2020) 'Treatment of Relapsed Acute Myeloid Leukemia', *Current Treatment Options in Oncology*, 21(8), p. 66. doi:10.1007/s11864-020-00765-5.

Thomas, D. and Majeti, R. (2017) 'Biology and relevance of human acute myeloid leukemia stem cells', *Blood*, 129(12), pp. 1577–1585. doi:10.1182/blood-2016-10-696054.

Thrasivoulou, C., Millar, M. and Ahmed, A. (2013a) 'Activation of intracellular calcium by multiple Wnt ligands and translocation of β-catenin into the nucleus: A convergent model of Wnt/Ca²⁺ and Wnt/β-catenin pathways', *Journal of Biological Chemistry*, 288(50), pp. 35651–35659. doi:10.1074/jbc.M112.437913.

Thrasivoulou, C., Millar, M. and Ahmed, A. (2013b) 'Activation of intracellular calcium by multiple Wnt ligands and translocation of β-catenin into the nucleus: A convergent model of Wnt/Ca²⁺ and Wnt/β-catenin pathways', *Journal of Biological Chemistry*, 288(50), pp. 35651–35659. doi:10.1074/jbc.M112.437913.

Tian, H., Biehs, B., Chiu, C., Siebel, C.W., Wu, Y., Costa, M., *et al.* (2015) 'Opposing activities of notch and wnt signaling regulate intestinal stem cells and gut homeostasis', *Cell Reports*, 11(1), pp. 33–42. doi:10.1016/j.celrep.2015.03.007.

Tian, W., Han, Xiaofeng, Yan, M., Xu, Y., Duggineni, S., Lin, N., *et al.* (2012) 'Structure-based discovery of a novel inhibitor targeting the β-catenin/Tcf4 interaction', *Biochemistry*, 51(2), pp. 724–731. doi:10.1021/bi201428h.

Tian, X., Yan, L., Zhang, D., Guan, X., Dong, B., Zhao, M., *et al.* (2016) 'PTK7 overexpression in colorectal tumors: Clinicopathological correlation and prognosis relevance.', *Oncology reports*, 36(4), pp. 1829–1836. doi:10.3892/or.2016.4983.

Tickenbrock, L., Schwäble, J., Wiedehage, M., Steffen, B., Sargin, B., Choudhary, C., *et al.* (2005) 'Flt3 tandem duplication mutations cooperate with Wnt signaling in leukemic signal transduction', *Blood*, 105(9), pp. 3699–3706. doi:10.1182/blood-2004-07-2924.

Tickenbrock, L., Hehn, S., Sargin, B., Choudhary, C., Bäumer, N., Buerger, H., *et al.* (2008) 'Activation of Wnt signalling in acute myeloid leukemia by induction of Frizzled-4', *International Journal of Oncology*, 33(6), pp. 1215–1221. doi:10.3892/ijo_00000111.

Tomita, H., Tanaka, K., Tanaka, T. and Hara, A. (2016) 'Aldehyde dehydrogenase 1A1 in stem cells and cancer', *Oncotarget*, 7(10), pp. 11018–11032. doi:10.18632/oncotarget.6920.

Tonks, A., Pearn, L., Tonks, A.J., Pearce, L., Hoy, T., Phillips, S., *et al.* (2003) 'The AML1-ETO fusion gene promotes extensive self-renewal of human primary erythroid cells', *Blood*, 101(2), pp. 624–632. doi:10.1182/blood-2002-06-1732.

Triana, S., Vonficht, D., Jopp-Saile, L., Raffel, S., Lutz, R., Leonce, D., *et al.* (2021) 'Single-cell proteo-genomic reference maps of the hematopoietic system enable the purification and massive profiling of precisely defined cell states', *Nature Immunology*, 22(12), pp. 1577–1589. doi:10.1038/s41590-021-01059-0.

Trowbridge, J.J., Xenocostas, A., Moon, R.T. and Bhatia, M. (2006) 'Glycogen synthase kinase-3 is

- an in vivo regulator of hematopoietic stem cell repopulation', *Nature Medicine*, 12(1), pp. 89–98. doi:10.1038/nm1339.
- Tsai, I.C., Amack, J.D., Gao, Z.H., Band, V., Yost, H.J. and Virshup, D.M. (2007) 'A Wnt-CKI ϵ -Rap1 Pathway Regulates Gastrulation by Modulating SIPA1L1, a Rap GTPase Activating Protein', *Developmental Cell*, 12(3), pp. 335–347. doi:10.1016/j.devcel.2007.02.009.
- Tsapogas, P., Swee, L.K., Nusser, A., Nuber, N., Kreuzaler, M., Capoferri, G., *et al.* (2014) 'In vivo evidence for an instructive role of fms-like tyrosine kinase-3 (FLT3) ligand in hematopoietic development', *Haematologica*, 99(4), pp. 638–646. doi:10.3324/haematol.2013.089482.
- Tsherniak, A., Vazquez, F., Montgomery, P.G., Weir, B.A., Kryukov, G., Cowley, G.S., *et al.* (2017) 'Defining a Cancer Dependency Map', *Cell*, 170(3), pp. 564–576.e16. doi:https://doi.org/10.1016/j.cell.2017.06.010.
- Tsuchiya, S., Yamabe, M., Yamaguchi, Y., Kobayashi, Y., Konno, T. and Tada, K. (1980) 'Establishment and characterization of a human acute monocytic leukemia cell line (THP-1).', *International journal of cancer*, 26(2), pp. 171–176. doi:10.1002/ijc.2910260208.
- Tufail, M. (2022) 'Genome editing: An essential technology for cancer treatment', *Medicine in Omics*, 4, p. 100015. doi:https://doi.org/10.1016/j.meomic.2022.100015.
- Tyner, J.W., Tognon, C.E., Bottomly, D., Wilmot, B., Kurtz, S.E., Savage, S.L., *et al.* (2018) 'Functional genomic landscape of acute myeloid leukaemia', *Nature*, 562(7728), pp. 526–531. doi:10.1038/s41586-018-0623-z.
- Tzelepis, K., Koike-Yusa, H., De Braekeleer, E., Li, Y., Metzakopian, E., Dovey, O.M., *et al.* (2016) 'A CRISPR Dropout Screen Identifies Genetic Vulnerabilities and Therapeutic Targets in Acute Myeloid Leukemia.', *Cell reports*, 17(4), pp. 1193–1205. doi:10.1016/j.celrep.2016.09.079.
- Ueno, Y., Mori, M., Kamiyama, Y., Saito, R., Kaneko, N., Isshiki, E., *et al.* (2019) 'Evaluation of gilteritinib in combination with chemotherapy in preclinical models of FLT3-ITD+ acute myeloid leukemia', *Oncotarget*, 10(26), pp. 2530–2545. doi:10.18632/oncotarget.26811.
- Ugarte, G.D., Vargas, M.F., Medina, M.A., León, P., Necuñir, D., Elorza, A.A., *et al.* (2015) 'Wnt signaling induces transcription, spatial proximity, and translocation of fusion gene partners in human hematopoietic cells', *Blood*, 126(15), pp. 1785–1789. doi:10.1182/blood-2015-04-638494.
- Ulgen, E., Ozisik, O. and Sezerman, O.U. (2019) 'PathfindR: An R package for comprehensive identification of enriched pathways in omics data through active subnetworks', *Frontiers in Genetics*, 10(SEP), p. 858. doi:10.3389/fgene.2019.00858.
- Upadhyay, G., Goessling, W., North, T.E., Xavier, R., Zon, L.I. and Yajnik, V. (2008) 'Molecular association between β -catenin degradation complex and Rac guanine exchange factor DOCK4 is essential for Wnt/ β -catenin signaling', *Oncogene*, 27(44), pp. 5845–5855. doi:10.1038/onc.2008.202.
- Valencia, A., Román-Gómez, J., Cervera, J., Such, E., Barragán, E., Bolufer, P., *et al.* (2009) 'Wnt signaling pathway is epigenetically regulated by methylation of Wnt antagonists in acute myeloid leukemia', *Leukemia*, 23(9), pp. 1658–1666. doi:10.1038/leu.2009.86.
- del Valle-Perez, B., Arques, O., Vinyoles, M., de Herreros, A.G. and Dunach, M. (2011) 'Coordinated Action of CK1 Isoforms in Canonical Wnt Signaling', *Molecular and Cellular Biology*, 31(14), pp. 2877–2888. doi:10.1128/mcb.01466-10.
- Valle-Pérez, B. del, Arqués, O., Vinyoles, M., Herreros, A.G. de and Duñach, M. (2011) 'Coordinated Action of CK1 Isoforms in Canonical Wnt Signaling', *Molecular and Cellular Biology*, 31(14), p. 2877. doi:10.1128/MCB.01466-10.
- VanDussen, K.L., Sonnek, N.M. and Stappenbeck, T.S. (2019) 'L-WRN conditioned medium for gastrointestinal epithelial stem cell culture shows replicable batch-to-batch activity levels across multiple research teams', *Stem Cell Research*, 37, p. 101430. doi:10.1016/j.scr.2019.101430.
- Vannini, N., Girotra, M., Naveiras, O., Nikitin, G., Campos, V., Giger, S., *et al.* (2016) 'Specification of haematopoietic stem cell fate via modulation of mitochondrial activity', *Nature Communications*,

7(1), pp. 1–9. doi:10.1038/ncomms13125.

Varnum-Finney, B., Wu, L., Yu, M., Brashem-Stein, C., Staats, S., Flowers, D., *et al.* (2000) ‘Immobilization of Notch ligand, Delta-1, is required for induction of Notch signaling’, *Journal of Cell Science*, 113(23), pp. 4313–4318. doi:10.1242/jcs.113.23.4313.

Velten, L., Haas, S.F., Raffel, S., Blaszkiewicz, S., Islam, S., Hennig, B.P., *et al.* (2017) ‘Human haematopoietic stem cell lineage commitment is a continuous process’, *Nature Cell Biology*, 19(4), pp. 271–281. doi:10.1038/ncb3493.

Velten, L., Story, B.A., Hernández-Malmierca, P., Raffel, S., Leonce, D.R., Milbank, J., *et al.* (2021) ‘Identification of leukemic and pre-leukemic stem cells by clonal tracking from single-cell transcriptomics’, *Nature Communications*, 12(1), pp. 1–13. doi:10.1038/s41467-021-21650-1.

Verhagen, H.J.M.P., van Gils, N., Martiáñez, T., van Rhenen, A., Rutten, A., Denkers, F., *et al.* (2018) ‘IGFBP7 Induces Differentiation and Loss of Survival of Human Acute Myeloid Leukemia Stem Cells without Affecting Normal Hematopoiesis’, *Cell Reports*, 25(11), pp. 3021–3035.e5. doi:10.1016/j.celrep.2018.11.062.

Verma, N.K. and Kelleher, D. (2017) ‘Not Just an Adhesion Molecule: LFA-1 Contact Tunes the T Lymphocyte Program’, *The Journal of Immunology*, 199(4), pp. 1213–1221. doi:10.4049/jimmunol.1700495.

Vetter, I.R. and Wittinghofer, A. (2001) ‘The guanine nucleotide-binding switch in three dimensions’, *Science (New York, N.Y.)*, 294(5545), pp. 1299–1304. doi:10.1126/SCIENCE.1062023.

Villatoro, A., Konieczny, J., Cuminetti, V. and Arranz, L. (2020) ‘Leukemia Stem Cell Release From the Stem Cell Niche to Treat Acute Myeloid Leukemia’, *Frontiers in Cell and Developmental Biology*, 8, p. 607. doi:10.3389/fcell.2020.00607.

Vincent-Fabert, C., Platet, N., Vandeveld, A., Poplineau, M., Koubi, M., Finetti, P., *et al.* (2016) ‘PLZF mutation alters mouse hematopoietic stem cell function and cell cycle progression’, *Blood*, 127(15), pp. 1881–1885. doi:10.1182/blood-2015-09-666974.

Vinyoles, M., Del Valle-Pérez, B., Curto, J., Padilla, M., Villarroel, A., Yang, J., *et al.* (2017) ‘Activation of CK1 ϵ by PP2A/PR61 ϵ is required for the initiation of Wnt signaling’, *Oncogene*, 36(3), pp. 429–438. doi:10.1038/onc.2016.209.

Vlaminckx, K., Kemler, R. and Hecht, A. (1999) ‘The C-terminal transactivation domain of β -catenin is necessary and sufficient for signaling by the LEF-1/ β -catenin complex in *Xenopus laevis*’, *Mechanisms of Development*, 81(1–2), pp. 65–74. doi:10.1016/S0925-4773(98)00225-1.

Voloshanenko, O., Erdmann, G., Dubash, T.D., Augustin, I., Metzger, M., Moffa, G., *et al.* (2013) ‘Wnt secretion is required to maintain high levels of Wnt activity in colon cancer cells.’, *Nature communications*, 4, p. 2610. doi:10.1038/ncomms3610.

Waaijers, S., Portegijs, V., Kerver, J., Lemmens, B.B.L.G., Tijsterman, M., van den Heuvel, S., *et al.* (2013) ‘CRISPR/Cas9-targeted mutagenesis in *Caenorhabditis elegans*’, *Genetics*, 195(3), pp. 1187–1191. doi:10.1534/GENETICS.113.156299/-/DC1/GENETICS.113.156299-3.PDF.

Waalder, J., Machon, O., Von Kries, J.P., Wilson, S.R., Lundenes, E., Wedlich, D., *et al.* (2011) ‘Novel synthetic antagonists of canonical Wnt signaling inhibit colorectal cancer cell growth’, *Cancer Research*, 71(1), pp. 197–205. doi:10.1158/0008-5472.CAN-10-1282.

Waalder, J., Machon, O., Tumova, L., Dinh, H., Korinek, V., Wilson, S.R., *et al.* (2012) ‘A novel tankyrase inhibitor decreases canonical Wnt signaling in colon carcinoma cells and reduces tumor growth in conditional APC mutant mice’, *Cancer Research*, 72(11), pp. 2822–2832. doi:10.1158/0008-5472.CAN-11-3336.

Wagner, G.P., Kin, K. and Lynch, V.J. (2012) ‘Measurement of mRNA abundance using RNA-seq data: RPKM measure is inconsistent among samples’, *Theory in Biosciences*, 131(4), pp. 281–285. doi:10.1007/s12064-012-0162-3.

Wagstaff, M., Tsaponina, O., Caalim, G., Greenfield, H., Milton-Harris, L., Mancini, E.J., *et al.*

- (2022) 'Crosstalk between β -catenin and WT1 signalling activity in acute myeloid leukemia.', *Haematologica* [Preprint]. doi:10.3324/haematol.2021.280294.
- Van De Walle, I., De Smet, G., Gärtner, M., De Smedt, M., Waegemans, E., Vandekerckhove, B., *et al.* (2011) 'Jagged2 acts as a Delta-like Notch ligand during early hematopoietic cell fate decisions', *Blood*, 117(17), pp. 4449–4459. doi:10.1182/blood-2010-06-290049.
- Wang, B., Wang, Z., Wang, D., Zhang, B., Ong, S.G., Li, M., *et al.* (2019) 'KrCRISPR: An easy and efficient strategy for generating conditional knockout of essential genes in cells', *Journal of Biological Engineering*, 13(1), p. 35. doi:10.1186/s13036-019-0150-y.
- Wang, B., Yang, B., Ling, Y., Zhang, J., Hua, X., Gu, W., *et al.* (2021) 'Role of CD19 and specific KIT-D816 on risk stratification refinement in t(8;21) acute myeloid leukemia induced with different cytarabine intensities', *Cancer Medicine*, 10(3), pp. 1091–1102. doi:https://doi.org/10.1002/cam4.3705.
- Wang, G., Li, S., Xue, K. and Dong, S. (2020) 'PFKFB4 is critical for the survival of acute monocytic leukemia cells', *Biochemical and Biophysical Research Communications*, 526(4), pp. 978–985. doi:10.1016/j.bbrc.2020.03.174.
- Wang, L., Steele, I., Kumar, J.D., Dimaline, R., Jithesh, P. V, Tiszlavicz, L., *et al.* (2016) 'Distinct miRNA profiles in normal and gastric cancer myofibroblasts and significance in Wnt signaling.', *American journal of physiology. Gastrointestinal and liver physiology*, 310(9), pp. G696-704. doi:10.1152/ajpgi.00443.2015.
- Wang, N., Tan, H.-Y., Chan, Y.-T., Guo, W., Li, S., Feng, Y., *et al.* (2017) 'Identification of WT1 as determinant of hepatocellular carcinoma and its inhibition by Chinese herbal medicine *Salvia chinensis* Benth and its active ingredient protocatechualdehyde', *Oncotarget*, 8(62), pp. 105848–105859. doi:10.18632/ONCOTARGET.22406.
- Wang, Q.S., Wang, Y., Lv, H.Y., Han, Q.W., Fan, H., Guo, B., *et al.* (2015) 'Treatment of CD33-directed chimeric antigen receptor-modified T cells in one patient with relapsed and refractory acute myeloid leukemia', *Molecular Therapy*, 23(1), pp. 184–191. doi:10.1038/mt.2014.164.
- Wang, T., Wei, J.J., Sabatini, D.M. and Lander, E.S. (2014) 'Genetic screens in human cells using the CRISPR-Cas9 system.', *Science (New York, N.Y.)*, 343(6166), pp. 80–84. doi:10.1126/science.1246981.
- Wang, T., Yu, H., Hughes, N.W., Liu, B., Kendirli, A., Klein, K., *et al.* (2017) 'Gene Essentiality Profiling Reveals Gene Networks and Synthetic Lethal Interactions with Oncogenic Ras.', *Cell*, 168(5), pp. 890-903.e15. doi:10.1016/j.cell.2017.01.013.
- Wang, Y., Krivtsov, A. V., Sinha, A.U., North, T.E., Goessling, W., Feng, Z., *et al.* (2010) 'The wnt/ β -catenin pathway is required for the development of leukemia stem cells in AML', *Science*, 327(5973), pp. 1650–1653. doi:10.1126/science.1186624.
- Wang, Y.H., Imai, Y., Shiseki, M., Tanaka, J. and Motoji, T. (2018) 'Knockdown of the Wnt receptor Frizzled-1 (FZD1) reduces MDR1/P-glycoprotein expression in multidrug resistant leukemic cells and inhibits leukemic cell proliferation', *Leukemia Research*, 67, pp. 99–108. doi:10.1016/j.leukres.2018.01.020.
- Wang, Z., Li, Y., Xiao, Y., Lin, H.P., Yang, P., Humphries, B., *et al.* (2019) 'Integrin α 9 depletion promotes β -catenin degradation to suppress triple-negative breast cancer tumor growth and metastasis', *International Journal of Cancer*, 145(10), pp. 2767–2780. doi:10.1002/ijc.32359.
- Wasim, M., Carlet, M., Mansha, M., Greil, R., Ploner, C., Trockenbacher, A., *et al.* (2010) 'PLZF/ZBTB16, a glucocorticoid response gene in acute lymphoblastic leukemia, interferes with glucocorticoid-induced apoptosis', *Journal of Steroid Biochemistry and Molecular Biology*, 120(4–5), pp. 218–227. doi:10.1016/j.jsbmb.2010.04.019.
- Watts, J. and Nimer, S. (2018) 'Recent advances in the understanding and treatment of acute myeloid leukemia', *F1000Research*, 7. doi:10.12688/f1000research.14116.1.
- Wei, A.H., Döhner, H., Pocock, C., Montesinos, P., Afanasyev, B., Dombret, H., *et al.* (2019) 'The

QUAZAR AML-001 Maintenance Trial: Results of a Phase III International, Randomized, Double-Blind, Placebo-Controlled Study of CC-486 (Oral Formulation of Azacitidine) in Patients with Acute Myeloid Leukemia (AML) in First Remission', *Blood*, 134(Supplement_2), p. LBA-3-LBA-3. doi:10.1182/blood-2019-132405.

Welch, John S, Ley, T.J., Link, D.C., Miller, C.A., Larson, D.E., Koboldt, D.C., *et al.* (2012) 'The origin and evolution of mutations in acute myeloid leukemia.', *Cell*, 150(2), pp. 264–78. doi:10.1016/j.cell.2012.06.023.

Welch, John S., Ley, T.J., Link, D.C., Miller, C.A., Larson, D.E., Koboldt, D.C., *et al.* (2012) 'The origin and evolution of mutations in acute myeloid leukemia', *Cell*, 150(2), pp. 264–278. doi:10.1016/J.CELL.2012.06.023.

Wen, H., Li, Y., Malek, S.N., Kim, Y.C., Xu, J., Chen, P., *et al.* (2012) 'New Fusion Transcripts Identified in Normal Karyotype Acute Myeloid Leukemia', *PLoS ONE*, 7(12). doi:10.1371/journal.pone.0051203.

Wesely, J., Kotini, A.G., Izzo, F., Luo, H., Yuan, H., Sun, J., *et al.* (2020) 'Acute Myeloid Leukemia iPSCs Reveal a Role for RUNX1 in the Maintenance of Human Leukemia Stem Cells', *Cell Reports*, 31(9). doi:10.1016/j.celrep.2020.107688.

Whitlock, N., Jeady, R.A. and A.mcgrath, J. (2000) 'Genomic organization and amplification of the human plakoglobin gene (JUP)', *Experimental Dermatology*, 9(5), pp. 323–326. doi:10.1034/j.1600-0625.2000.009005323.x.

Wickline, E.D., Awuah, P.K., Behari, J., Ross, M., Stolz, D.B. and Monga, S.P.S. (2011) 'Hepatocyte γ -catenin compensates for conditionally deleted β -catenin at adherens junctions.', *Journal of hepatology*, 55(6), pp. 1256–1262. doi:10.1016/j.jhep.2011.03.014.

Wickline, E.D., Du, Y., Stolz, Donna B, Kahn, M. and Monga, S.P.S. (2013) ' γ -Catenin at adherens junctions: mechanism and biologic implications in hepatocellular cancer after β -catenin knockdown', *Neoplasia (New York, N.Y.)*, 15(4), pp. 421–434. doi:10.1593/neo.122098.

Wickline, E.D., Du, Y., Stolz, Donna B., Kahn, M. and Monga, S.P.S. (2013) ' γ -Catenin at adherens junctions: Mechanism and biologic implications in hepatocellular cancer after β -Catenin knockdown', *Neoplasia (United States)*, 15(4), pp. 421–434. doi:10.1593/neo.122098.

Willert, K., Brown, J.D., Danenberg, E., Duncan, A.W., Weissman, I.L., Reya, T., *et al.* (2003) 'Wnt proteins are lipid-modified and can act as stem cell growth factors', *Nature*, 423(6938), pp. 448–452. doi:10.1038/nature01611.

Williams, B.A., Law, A., Hunyadkurti, J., Desilets, S., Leyton, J. V. and Keating, A. (2019) 'Antibody therapies for acute myeloid leukemia: Unconjugated, toxin-conjugated, radio-conjugated and multivalent formats', *Journal of Clinical Medicine*, 8(8). doi:10.3390/jcm8081261.

Williamson, L., Raess, N.A., Caldelari, R., Zakher, A., De Bruin, A., Posthaus, H., *et al.* (2006) 'Pemphigus vulgaris identifies plakoglobin as key suppressor of c-Myc in the skin', *EMBO Journal*, 25(14), pp. 3298–3309. doi:10.1038/sj.emboj.7601224.

Wilson, L.O.W., O'Brien, A.R. and Bauer, D.C. (2018) 'The current state and future of CRISPR-Cas9 gRNA design tools', *Frontiers in Pharmacology*, 9(JUN), p. 749. doi:10.3389/FPHAR.2018.00749/BIBTEX.

Wong, H.C., Bourdelas, A., Krauss, A., Lee, H.J., Shao, Y., Wu, D., *et al.* (2003) 'Direct binding of the PDZ domain of Dishevelled to a conserved internal sequence in the C-terminal region of Frizzled', *Molecular Cell*, 12(5), pp. 1251–1260. doi:10.1016/S1097-2765(03)00427-1.

Wong, J.C., Weinfurter, K.M., del pilar Alzamora, M., Kogan, S.C., Burgess, M.R., Zhang, Y., *et al.* (2015) 'Functional evidence implicating chromosome 7q22 haploinsufficiency in myelodysplastic syndrome pathogenesis', *eLife*, 4(JULY2015). doi:10.7554/eLife.07839.001.

Wong, T.N., Ramsingh, G., Young, A.L., Miller, C.A., Touma, W., Welch, J.S., *et al.* (2015) 'Role of TP53 mutations in the origin and evolution of therapy-related acute myeloid leukaemia', *Nature*, 518(7540), pp. 552–555. doi:10.1038/nature13968.

- Woodgett, J.R. and Cormier, K.W. (2017) 'Recent advances in understanding the cellular roles of GSK-3', *F1000Research*, 6. doi:10.12688/f1000research.10557.1.
- Wu, F., Yin, C., Qi, J., Duan, D., Jiang, X., Yu, J., *et al.* (2020) 'miR-362-5p promotes cell proliferation and cell cycle progression by targeting GAS7 in acute myeloid leukemia', *Human Cell*, 33(2), pp. 405–415. doi:10.1007/s13577-019-00319-4.
- Wu, F., Yang, J., Liu, J., Wang, Y., Mu, J., Zeng, Q., *et al.* (2021) 'Signaling pathways in cancer-associated fibroblasts and targeted therapy for cancer', *Signal Transduction and Targeted Therapy* 2021 6:1, 6(1), pp. 1–35. doi:10.1038/s41392-021-00641-0.
- Wu, H., Liu, X., Jaenisch, R. and Lodish, H.F. (1995) 'Generation of committed erythroid BFU-E and CFU-E progenitors does not require erythropoietin or the erythropoietin receptor', *Cell*, 83(1), pp. 59–67. doi:10.1016/0092-8674(95)90234-1.
- Wu, H.H., Cao, H., Wang, Y.Z., Wang, D.X., Lin, H.R., Qin, Y.Z., *et al.* (2009) '[Expression of 5 genes in CD7 positive acute myeloid leukemia stem/progenitor cells from bone marrow].', *Zhongguo shi yan xue ye xue za zhi / Zhongguo bing li sheng li xue hui = Journal of experimental hematology / Chinese Association of Pathophysiology*, 17(2), pp. 298–303.
- Wu, J., Wang, G., He, B., Chen, X. and An, Y. (2017) 'Methylation of the UNC5C gene and its protein expression in colorectal cancer.', *Tumour biology : the journal of the International Society for Oncodevelopmental Biology and Medicine*, 39(4), p. 1010428317697564. doi:10.1177/1010428317697564.
- Wu, J., Xiao, Y., Sun, J., Sun, H., Chen, H., Zhu, Y., *et al.* (2020) 'A single-cell survey of cellular hierarchy in acute myeloid leukemia', *Journal of Hematology and Oncology*, 13(1), pp. 1–19. doi:10.1186/s13045-020-00941-y.
- Wu, J., Song, M.-Z., Deng, L.-J. and Ye, Q.-L. (2021) 'Comprehensive DNA Methylation-transcriptome Profiles Association Analysis During the Treatment of Acute Myelocytic Leukemia', *Current Pharmaceutical Design*, pp. 2817–2826. doi:http://dx.doi.org/10.2174/1381612827666210603165253.
- Wu, J. and Song, Y. (2018) 'Expression and clinical significance of serum MMP-7 and PTEN levels in patients with acute myeloid leukemia', *Oncology Letters*, 15(3), pp. 3447–3452. doi:10.3892/ol.2018.7799.
- Wu, J.Q., Seay, M., Schulz, V.P., Hariharan, M., Tuck, D., Lian, J., *et al.* (2012) 'Tcf7 is an important regulator of the switch of self-renewal and differentiation in a multipotential hematopoietic cell line', *PLoS Genetics*, 8(3). doi:10.1371/journal.pgen.1002565.
- Wu, M., Li, C. and Zhu, X. (2018) 'FLT3 inhibitors in acute myeloid leukemia', *Journal of Hematology and Oncology*, 11(1), pp. 1–11. doi:10.1186/s13045-018-0675-4.
- Wu, P.Y., Phan, J.H. and Wang, M.D. (2013) 'Assessing the impact of human genome annotation choice on RNA-seq expression estimates.', *BMC bioinformatics*, 14 Suppl 1(11), pp. 1–13. doi:10.1186/1471-2105-14-S11-S8.
- Wu, S., Zhang, W., Shen, D., Lu, J. and Zhao, L. (2019) 'PLCB4 upregulation is associated with unfavorable prognosis in pediatric acute myeloid leukemia', *Oncology Letters*, 18(6), pp. 6057–6065. doi:10.3892/OL.2019.10921/HTML.
- Wu, X., Schnitzler, G.R., Gao, G.F., Diamond, B., Baker, A.R., Kaplan, B., *et al.* (2020) 'Mechanistic insights into cancer cell killing through interaction of phosphodiesterase 3A and schlafen family member 12', *The Journal of biological chemistry*, 295(11), pp. 3431–3446. doi:10.1074/JBC.RA119.011191.
- Wu, Yougen, Zhou, J., Li, Y., Zhou, Y., Cui, Y., Yang, G., *et al.* (2015) 'Rap1A Regulates Osteoblastic Differentiation via the ERK and p38 Mediated Signaling', *PLoS ONE*, 10(11). doi:10.1371/JOURNAL.PONE.0143777.
- Wu, Y., Pan, S., Leng, J., Xie, T., Jamal, M., Yin, Q., *et al.* (2019) 'The prognostic value of matrix metalloproteinase-7 and matrix metalloproteinase-15 in acute myeloid leukemia', *Journal of Cellular*

Biochemistry, 120(6), pp. 10613–10624. doi:10.1002/jcb.28351.

Wu, Yu, Sun, R. and Lun, Y. (2015) ‘Pim-1, Beyond an Oncogene, in Acute Myeloid Leukemia’, *Blood*, 126(23), pp. 4979–4979. doi:10.1182/blood.v126.23.4979.4979.

Wuchter, C., Harbott, J., Schoch, C., Schnittger, S., Borkhardt, A., Karawajew, L., *et al.* (2000) ‘Detection of acute leukemia cells with mixed lineage leukemia (MLL) gene rearrangements by flow cytometry using monoclonal antibody 7.1’, *Leukemia*, 14(7), pp. 1232–1238. doi:10.1038/sj.leu.2401840.

Xiao, Y., Hsiao, T.H., Suresh, U., Chen, H.I.H., Wu, X., Wolf, S.E., *et al.* (2014) ‘A novel significance score for gene selection and ranking’, *Bioinformatics*, 30(6), pp. 801–807. doi:10.1093/bioinformatics/btr671.

Xiao, Y., Deng, T., Ming, X. and Xu, J. (2020) ‘TRIM31 promotes acute myeloid leukemia progression and sensitivity to daunorubicin through the Wnt/ β -catenin signaling’, *Bioscience Reports*, 40(4). doi:10.1042/BSR20194334.

Xie, J., Xiang, D.B., Wang, H., Zhao, C., Chen, J., Xiong, F., *et al.* (2012) ‘Inhibition of Tcf-4 Induces Apoptosis and Enhances Chemosensitivity of Colon Cancer Cells’, *PLoS ONE*, 7(9), p. e45617. doi:10.1371/journal.pone.0045617.

Xin, H., Li, C. and Wang, M. (2018) ‘DIXDC1 promotes the growth of acute myeloid leukemia cells by upregulating the Wnt/ β -catenin signaling pathway’, *Biomedicine and Pharmacotherapy*, 107, pp. 1548–1555. doi:10.1016/j.biopha.2018.08.144.

Xu, J., Chen, Y., Huo, D., Khramtsov, A., Khramtsova, G., Zhang, C., *et al.* (2016) ‘ β -catenin regulates c-Myc and CDKN1A expression in breast cancer cells’, *Molecular Carcinogenesis*, 55(5), pp. 431–439. doi:10.1002/mc.22292.

Xu, S., Zhang, T., Cao, Z., Zhong, W., Zhang, C., Li, H., *et al.* (2021) ‘Integrin- α 9 β 1 as a Novel Therapeutic Target for Refractory Diseases: Recent Progress and Insights’, *Frontiers in Immunology*, 12, p. 767. doi:10.3389/fimmu.2021.638400.

Xu, W. and Kimelman, D. (2007) ‘Mechanistic insights from structural studies of β -catenin and its binding partners’, *Journal of Cell Science*, 120(19), pp. 3337–3344. doi:10.1242/jcs.013771.

Y, A., X, T., JE, C. and F, B. (2008) ‘The CD300a (IRp60) inhibitory receptor is rapidly up-regulated on human neutrophils in response to inflammatory stimuli and modulates CD32a (Fc γ RIIIa) mediated signaling’, *Molecular immunology*, 45(1), pp. 253–258. doi:10.1016/J.MOLIMM.2007.05.006.

Yajnik, V., Paulding, C., Sordella, R., McClatchey, A.I., Saito, M., Wahrer, D.C.R., *et al.* (2003) ‘DOCK4, a GTPase activator, is disrupted during tumorigenesis’, *Cell*, 112(5), pp. 673–684. doi:10.1016/S0092-8674(03)00155-7.

Yamakawa, N., Kaneda, K., Saito, Y., Ichihara, E. and Morishita, K. (2012) ‘The increased expression of integrin α 6 (itga6) enhances drug resistance in evi1 high leukemia’, *PLoS ONE*, 7(1), p. 30706. doi:10.1371/journal.pone.0030706.

Yamanaka, R., Kim, G. Do, Radomska, H.S., Lekstrom-Himes, J., Smith, L.T., Antonson, P., *et al.* (1997) ‘CCAAT/enhancer binding protein ϵ is preferentially up-regulated during granulocytic differentiation and its functional versatility is determined by alternative use of promoters and differential splicing’, *Proceedings of the National Academy of Sciences of the United States of America*, 94(12), pp. 6462–6467. doi:10.1073/pnas.94.12.6462.

Yamane, T., Kunisada, T., Tsukamoto, H., Yamazaki, H., Niwa, H., Takada, S., *et al.* (2001) ‘Wnt Signaling Regulates Hemopoiesis Through Stromal Cells’, *The Journal of Immunology*, 167(2), pp. 765–772. doi:10.4049/jimmunol.167.2.765.

Yan, X., Ait-Oudhia, S. and Krzyzanski, W. (2013) ‘Erythropoietin-induced erythroid precursor pool depletion causes erythropoietin hyporesponsiveness’, *Pharmaceutical Research*, 30(4), pp. 1026–1036. doi:10.1007/s11095-012-0938-7.

- Yang, L., Yang, M., Zhang, H., Wang, Z., Yu, Y., Xie, M., *et al.* (2012a) 'S100A8-targeting siRNA enhances arsenic trioxide-induced myeloid leukemia cell death by down-regulating autophagy', *International Journal of Molecular Medicine*, 29(1), pp. 65–72. doi:10.3892/IJMM.2011.806/HTML.
- Yang, L., Yang, M., Zhang, H., Wang, Z., Yu, Y., Xie, M., *et al.* (2012b) 'S100A8-targeting siRNA enhances arsenic trioxide-induced myeloid leukemia cell death by down-regulating autophagy', *International journal of molecular medicine*, 29(1), pp. 65–72. doi:10.3892/IJMM.2011.806.
- Yang, L., Shi, P., Zhao, G., Xu, J., Peng, W., Zhang, J., *et al.* (2020) 'Targeting cancer stem cell pathways for cancer therapy', *Signal Transduction and Targeted Therapy*, 5(1), pp. 1–35. doi:10.1038/s41392-020-0110-5.
- Yang, Q., Wang, S., Dai, E., Zhou, S., Liu, D., Liu, H., *et al.* (2019) 'Pathway enrichment analysis approach based on topological structure and updated annotation of pathway', *Briefings in Bioinformatics*, 20(1), pp. 168–177. doi:10.1093/bib/bbx091.
- Yang, X.Y., Zhang, M.Y., Zhou, Q., Wu, S.Y., Gu, W.Y., Zhao, Y., *et al.* (2016) 'High expression of S100A8 gene is associated with drug resistance to etoposide and poor prognosis in acute myeloid leukemia through influencing the apoptosis pathway', *OncoTargets and therapy*, 9, p. 4887. doi:10.2147/OTT.S101594.
- Yassin, M., Aqaq, N., Yassin, A.A., van Galen, P., Kugler, E., Bernstein, B.E., *et al.* (2019) 'A novel method for detecting the cellular stemness state in normal and leukemic human hematopoietic cells can predict disease outcome and drug sensitivity', *Leukemia*, 33(8), pp. 2061–2077. doi:10.1038/s41375-019-0386-z.
- Ye, M., Zhang, H., Yang, H., Koche, R., Staber, P.B., Cusan, M., *et al.* (2015) 'Hematopoietic Differentiation Is Required for Initiation of Acute Myeloid Leukemia', *Cell Stem Cell*, 17(5), pp. 611–623. doi:10.1016/j.stem.2015.08.011.
- Yeung, J., Esposito, M.T., Gandillet, A., Zeisig, B.B., Griessinger, E., Bonnet, D., *et al.* (2010) 'β-Catenin Mediates the Establishment and Drug Resistance of MLL Leukemic Stem Cells', *Cancer Cell*, 18(6), pp. 606–618. doi:10.1016/j.ccr.2010.10.032.
- Yokoyama, Y., Grünebach, F., Schmidt, S.M., Heine, A., Häntschel, M., Stevanovic, S., *et al.* (2008) 'Matrilysin (MMP-7) is a novel broadly expressed tumor antigen recognized by antigen-specific T cells', *Clinical Cancer Research*, 14(17), pp. 5503–5511. doi:10.1158/1078-0432.CCR-07-4041.
- Yoshihara, H., Arai, F., Hosokawa, K., Hagiwara, T., Takubo, K., Nakamura, Y., *et al.* (2007) 'Thrombopoietin/MPL Signaling Regulates Hematopoietic Stem Cell Quiescence and Interaction with the Osteoblastic Niche', *Cell Stem Cell*, 1(6), pp. 685–697. doi:10.1016/j.stem.2007.10.020.
- Ysebaert, L., Chicanne, G., Demur, C., De Toni, F., Prade-Houdellier, N., Ruidavets, J.B., *et al.* (2006) 'Expression of β-catenin by acute myeloid leukemia cells predicts enhanced clonogenic capacities and poor prognosis', *Leukemia*, 20(7), pp. 1211–1216. doi:10.1038/sj.leu.2404239.
- Yu, F., Yu, C., Li, F., Zuo, Y., Wang, Y., Yao, L., *et al.* (2021) 'Wnt/β-catenin signaling in cancers and targeted therapies', *Signal Transduction and Targeted Therapy*, 6(1), pp. 1–24. doi:10.1038/s41392-021-00701-5.
- Yu, G., Wang, L.G., Han, Y. and He, Q.Y. (2012) 'ClusterProfiler: An R package for comparing biological themes among gene clusters', *OMICS A Journal of Integrative Biology*, 16(5), pp. 284–287. doi:10.1089/omi.2011.0118.
- Yu, J., Jiang, P.Y.Z., Sun, H., Zhang, X., Jiang, Z., Li, Y., *et al.* (2020) 'Advances in targeted therapy for acute myeloid leukemia', *Biomarker Research*, 8(1), pp. 1–11. doi:10.1186/s40364-020-00196-2.
- Zahreddine, H.A., Culjkovic-Kraljacic, B., Assouline, S., Gendron, P., Romeo, A.A., Morris, S.J., *et al.* (2014) 'The sonic hedgehog factor GLI1 imparts drug resistance through inducible glucuronidation', *Nature*, 511(7507), pp. 90–93. doi:10.1038/nature13283.
- Zalatan, J.G., Lee, M.E., Almeida, R., Gilbert, L.A., Whitehead, E.H., La Russa, M., *et al.* (2015) 'Engineering complex synthetic transcriptional programs with CRISPR RNA scaffolds', *Cell*, 160(1–2), pp. 339–350. doi:10.1016/j.cell.2014.11.052.

- Zambanini, G., Nordin, A., Jonasson, M., Pagella, P. and Cantù, C. (2022) 'A New CUT&RUN Low Volume-Urea (LoV-U) protocol uncovers Wnt/ β -catenin tissue-specific genomic targets', *bioRxiv*, p. 2022.07.06.498999. doi:10.1101/2022.07.06.498999.
- Zarrinkar, P.P., Gunawardane, R.N., Cramer, M.D., Gardner, M.F., Brigham, D., Belli, B., *et al.* (2009) 'AC220 is a uniquely potent and selective inhibitor of FLT3 for the treatment of acute myeloid leukemia (AML)', *Blood*, 114(14), pp. 2984–2992. doi:10.1182/blood-2009-05-222034.
- Zeng, H., Lu, B., Zamponi, R., Yang, Z., Wetzel, K., Loureiro, J., *et al.* (2018) 'MTORC1 signaling suppresses Wnt/ β -catenin signaling through DVL-dependent regulation of Wnt receptor FZD level', *Proceedings of the National Academy of Sciences of the United States of America*, 115(44), pp. E10362–E10369. doi:10.1073/pnas.1808575115.
- Zeng, X., Huang, H., Tamai, K., Zhang, X., Harada, Y., Yokota, C., *et al.* (2008) 'Initiation of Wnt signaling: control of Wnt coreceptor Lrp6 phosphorylation/activation via frizzled, dishevelled and axin functions', *Development (Cambridge, England)*, 135(2), pp. 367–375. doi:10.1242/DEV.013540.
- zhang, xinwen, Xiong, H., Duan, J., Chen, X., Liu, Y., Huang, C., *et al.* (2021) 'High Expression of PXN Predicts a Poor Prognosis in Acute myeloid leukemia'. doi:10.21203/RS.3.RS-847908/V1.
- Zhang, D., Iwabuchi, S., Baba, T., Hashimoto, S.I., Mukaida, N. and Sasaki, S.I. (2020) 'Involvement of a transcription factor, nfe2, in breast cancer metastasis to bone', *Cancers*, 12(10), pp. 1–18. doi:10.3390/cancers12103003.
- Zhang, F., Wen, Y. and Guo, X. (2014) 'CRISPR/Cas9 for genome editing: Progress, implications and challenges', *Human Molecular Genetics*, 23(R1), pp. R40–R46. doi:10.1093/hmg/ddu125.
- Zhang, G., Zeng, T., Dai, Z. and Dai, X. (2021) 'Prediction of CRISPR/Cas9 single guide RNA cleavage efficiency and specificity by attention-based convolutional neural networks', *Computational and Structural Biotechnology Journal*, 19, pp. 1445–1457. doi:10.1016/J.CSBJ.2021.03.001.
- Zhang, H., Bi, Y., Wei, Y., Liu, J., Kuerban, K. and Ye, L. (2021) 'Blocking Wnt/ β -catenin signal amplifies anti-PD-1 therapeutic efficacy by inhibiting tumor growth, migration, and promoting immune infiltration in glioblastomas', *Molecular Cancer Therapeutics*, 20(7), pp. 1305–1315. doi:10.1158/1535-7163.MCT-20-0825.
- Zhang, Y., Gu, J., Wang, L., Zhao, Z., Pan, Y. and Chen, Y. (2017) 'Ablation of PPP1R3G reduces glycogen deposition and mitigates high-fat diet induced obesity', *Molecular and Cellular Endocrinology*, 439, pp. 133–140. doi:10.1016/j.mce.2016.10.036.
- Zhang, Y., Huang, Y., Hu, L. and Cheng, T. (2022) 'New insights into Human Hematopoietic Stem and Progenitor Cells via Single-Cell Omics', *Stem Cell Reviews and Reports*, 18(4), pp. 1322–1336. doi:10.1007/S12015-022-10330-2/TABLES/1.
- Zhang, Y. and Wang, X. (2020a) 'Targeting the Wnt/ β -catenin signaling pathway in cancer', *Journal of Hematology & Oncology 2020 13:1*, 13(1), pp. 1–16. doi:10.1186/S13045-020-00990-3.
- Zhang, Y. and Wang, X. (2020b) 'Targeting the Wnt/ β -catenin signaling pathway in cancer', *Journal of Hematology and Oncology*, 13(1), pp. 1–16. doi:10.1186/s13045-020-00990-3.
- Zhang, Y.L., Wang, R.C., Cheng, K., Ring, B.Z. and Su, L. (2017) 'Roles of Rap1 signaling in tumor cell migration and invasion', *Cancer Biology & Medicine*, 14(1), p. 90. doi:10.20892/J.ISSN.2095-3941.2016.0086.
- Zhao, C., Blum, J., Chen, A., Kwon, H.Y., Jung, S.H., Cook, J.M., *et al.* (2007) 'Loss of β -Catenin Impairs the Renewal of Normal and CML Stem Cells In Vivo', *Cancer Cell*, 12(6), pp. 528–541. doi:10.1016/j.ccr.2007.11.003.
- Zhao, C., Ma, H., Bu, X., Wang, W. and Zhang, N. (2013) 'SFRP5 inhibits gastric epithelial cell migration induced by macrophage-derived Wnt5a.', *Carcinogenesis*, 34(1), pp. 146–152. doi:10.1093/carcin/bgs309.
- Zhao, S., Ye, Z. and Stanton, R. (2020) 'Misuse of RPKM or TPM normalization when comparing across samples and sequencing protocols', *RNA*, 26(8), p. 903. doi:10.1261/RNA.074922.120.

- Zhao, W., Kitidis, C., Fleming, M.D., Lodish, H.F. and Ghaffari, S. (2006) 'Erythropoietin stimulates phosphorylation and activation of GATA-1 via the PI3-kinase/AKT signaling pathway', *Blood*, 107(3), pp. 907–915. doi:10.1182/BLOOD-2005-06-2516.
- Zhao, X., Shao, P., Gai, K., Li, F., Shan, Q. and Xue, H.H. (2020) ' β -catenin and γ -catenin are dispensable for T lymphocytes and AML leukemic stem cells', *eLife*, 9, pp. 1–18. doi:10.7554/ELIFE.55360.
- Zhao, Y., Tao, L., Yi, J., Song, H. and Chen, L. (2018) 'The Role of Canonical Wnt Signaling in Regulating Radioresistance', *Cellular Physiology and Biochemistry*. S. Karger AG, pp. 419–432. doi:10.1159/000491774.
- Zhao, Y., Li, M.-C., Konaté, M.M., Chen, L., Das, B., Karlovich, C., *et al.* (2021) 'TPM, FPKM, or Normalized Counts? A Comparative Study of Quantification Measures for the Analysis of RNA-seq Data from the NCI Patient-Derived Models Repository', *Journal of Translational Medicine*, 19(1), p. 269. doi:10.1186/s12967-021-02936-w.
- Zhao, Y. ying, Lin, Y. qiu and Xu, Y. ou (2017) 'Functional Identification of Allograft Inflammatory Factor 1-Like Gene in Luning Chicken', *Animal Biotechnology*, 29(3), pp. 234–240. doi:10.1080/10495398.2017.1369096.
- Zheng, X., Beissert, T., Kukoc-Zivojnov, N., Puccetti, E., Altschmied, J., Strolz, C., *et al.* (2004) ' γ -Catenin contributes to leukemogenesis induced by AML-associated translocation products by increasing the self-renewal of very primitive progenitor cells', *Blood*, 103(9), pp. 3535–3543. doi:10.1182/BLOOD-2003-09-3335.
- Zhou, B., Jin, X., Jin, W., Huang, X., Wu, Y., Li, H., *et al.* (2020) 'WT1 facilitates the self-renewal of leukemia-initiating cells through the upregulation of BCL2L2: WT1-BCL2L2 axis as a new acute myeloid leukemia therapy target', *Journal of Translational Medicine*, 18(1), p. 254. doi:10.1186/s12967-020-02384-y.
- Zhou, C., Dai, X., Chen, Y., Shen, Y., Lei, S., Xiao, T., *et al.* (2016) 'G protein-coupled receptor GPR160 is associated with apoptosis and cell cycle arrest of prostate cancer cells', *Oncotarget*, 7(11), p. 12823. doi:10.18632/ONCOTARGET.7313.
- Zhou, H., Ma, H., Wei, W., Ji, D., Song, X., Sun, J., *et al.* (2013) 'B4GALT family mediates the multidrug resistance of human leukemia cells by regulating the hedgehog pathway and the expression of p-glycoprotein and multidrug resistance-associated protein 1', *Cell Death & Disease* 2013 4:6, 4(6), pp. e654–e654. doi:10.1038/cddis.2013.186.
- Zhou, J., Bi, C., Chng, W.J., Cheong, L.L., Liu, S.C., Mahara, S., *et al.* (2011) 'PRL-3, a Metastasis Associated Tyrosine Phosphatase, Is Involved in FLT3-ITD Signaling and Implicated in Anti-AML Therapy', *PLOS ONE*, 6(5), p. e19798. doi:10.1371/JOURNAL.PONE.0019798.
- Zhou, J., Chan, Z.L., Bi, C., Lu, X., Chong, P.S.Y., Chooi, J.Y., *et al.* (2017) 'LIN28B Activation by PRL-3 Promotes Leukemogenesis and a Stem Cell-like Transcriptional Program in AML', *Molecular cancer research : MCR*, 15(3), pp. 294–303. doi:10.1158/1541-7786.MCR-16-0275-T.
- Zhou, S., Cecere, R. and Philip, A. (2017) 'CD109 released from human bone marrow mesenchymal stem cells attenuates TGF- β -induced epithelial to mesenchymal transition and stemness of squamous cell carcinoma', *Oncotarget*, 8(56), p. 95632. doi:10.18632/ONCOTARGET.21067.
- Zhu, L., Li, Q., Wang, X., Liao, J., Zhang, W., Gao, L., *et al.* (2020) 'THBS1 Is a Novel Serum Prognostic Factors of Acute Myeloid Leukemia', *Frontiers in Oncology*, 9. doi:10.3389/fonc.2019.01567.
- Zhu, R., Tao, H., Lin, W., Tang, L. and Hu, Y. (2020) 'Identification of an Immune-Related Gene Signature Based on Immunogenomic Landscape Analysis to Predict the Prognosis of Adult Acute Myeloid Leukemia Patients', *Frontiers in Oncology*, 0, p. 2453. doi:10.3389/FONC.2020.574939.
- Zhu, Y., Chen, H., Boulton, S., Mei, F., Ye, N., Melacini, G., *et al.* (2015) 'Biochemical and Pharmacological Characterizations of ESI-09 Based EPAC Inhibitors: Defining the ESI-09 "Therapeutic Window"', *Scientific Reports* 2015 5:1, 5(1), pp. 1–8. doi:10.1038/srep09344.

Zhurinsky, J., Shtutman, M. and Ben-Ze'ev, A. (2000) 'Differential mechanisms of LEF/TCF family-dependent transcriptional activation by beta-catenin and plakoglobin', *Molecular and cellular biology*, 20(12), pp. 4238–4252. doi:10.1128/MCB.20.12.4238-4252.2000.

Zon, L.I. (2008) 'Intrinsic and extrinsic control of haematopoietic stem-cell self-renewal', *Nature*, 453(7193), pp. 306–313. doi:10.1038/nature07038.